

VOL. 516 NO. 1 SEPTEMBER 7, 1990

2nd Int. Symp. on High Performance
Capillary Electrophoresis
San Francisco, CA
January 29-31, 1990

JOURNAL OF

CHROMATOGRAPHY

INTERNATIONAL JOURNAL ON CHROMATOGRAPHY, ELECTROPHORESIS AND RELATED METHODS

EDITORS

R. W. Giese (Boston, MA)
J. K. Haken (Kensington, N.S.W.)
K. Macek (Prague)
L. R. Snyder (Orinda, CA)

EDITOR, SPECIAL ELECTROPHORESIS VOLUMES

Z. Deyl (Prague)

EDITOR, SYMPOSIUM VOLUMES, E. Heftmann (Orinda, CA)

EDITORIAL BOARD

D. W. Armstrong (Rolla, MO)
W. A. Aue (Halifax)
P. Boček (Brno)
A. A. Boulton (Saskatoon)
P. W. Carr (Minneapolis, MN)
N. H. C. Cooke (San Ramon, CA)
V. A. Davankov (Moscow)
Z. Deyl (Prague)
S. Dilli (Kensington, N.S.W.)
H. Engelhardt (Saarbrücken)
F. Erni (Basle)
M. B. Evans (Hatfield)
J. L. Glajch (N. Billerica, MA)
G. A. Guiochon (Knoxville, TN)
P. R. Haddad (Kensington, N.S.W.)
I. M. Hais (Hradec Králové)
W. S. Hancock (San Francisco, CA)
S. Hjertén (Uppsala)
Cs. Horváth (New Haven, CT)
J. F. K. Huber (Vienna)
K.-P. Hupe (Waldbronn)
T. W. Hutchens (Houston, TX)
J. Janák (Brno)
P. Jandera (Pardubice)
B. L. Karger (Boston, MA)
E. sz. Kováts (Lausanne)
A. J. P. Martin (Cambridge)
L. W. McLaughlin (Chestnut Hill, MA)
E. D. Morgan (Keele)
J. D. Pearson (Kalamazoo, MI)
H. Poppe (Amsterdam)
F. E. Regnier (West Lafayette, IN)
P. G. Righetti (Milan)
P. Schoenmakers (Eindhoven)
G. Schomburg (Mülheim/Ruhr)
R. Schwarzenbach (Dübendorf)
R. E. Shoup (West Lafayette, IN)
A. M. Siouffi (Marseille)
D. J. Strydom (Boston, MA)
K. K. Unger (Mainz)
R. Verpoorte (Leiden)
Gy. Vigh (College Station, TX)
J. T. Watson (East Lansing, MI)
B. D. Westerlund (Uppsala)

EDITORS, BIBLIOGRAPHY SECTION

Z. Deyl (Prague), J. Janák (Brno), V. Schwarz (Prague), K. Macek (Prague)

ELSEVIER

JOURNAL OF CHROMATOGRAPHY

Scope. The *Journal of Chromatography* publishes papers on all aspects of chromatography, electrophoresis and related methods. Contributions consist mainly of research papers dealing with chromatographic theory, instrumental development and their applications. The section *Biomedical Applications*, which is under separate editorship, deals with the following aspects: developments in and applications of chromatographic and electrophoretic techniques related to clinical diagnosis or alterations during medical treatment; screening and profiling of body fluids or tissues with special reference to metabolic disorders; results from basic medical research with direct consequences in clinical practice; drug level monitoring and pharmacokinetic studies; clinical toxicology; analytical studies in occupational medicine.

Submission of Papers. Manuscripts (in English; four copies are required) should be submitted to: The Editor of *Journal of Chromatography*, P.O. Box 681, 1000 AR Amsterdam, The Netherlands, or to: The Editor of *Journal of Chromatography, Biomedical Applications*, P.O. Box 681, 1000 AR Amsterdam, The Netherlands. Review articles are invited or proposed by letter to the Editors. An outline of the proposed review should first be forwarded to the Editors for preliminary discussion prior to preparation. Submission of an article is understood to imply that the article is original and unpublished and is not being considered for publication elsewhere. For copyright regulations, see below.

Subscription Orders. Subscription orders should be sent to: Elsevier Science Publishers B.V., P.O. Box 211, 1000 AE Amsterdam, The Netherlands, Tel. 5803 911, Telex 18582 ESPA NL. The *Journal of Chromatography* and the *Biomedical Applications* section can be subscribed to separately.

Publication. The *Journal of Chromatography* (incl. *Biomedical Applications*) has 37 volumes in 1990. The subscription prices for 1990 are:

J. Chromatogr. (incl. *Cum. Indexes, Vols. 451–500*) + *Biomed. Appl.* (Vols. 498–534):

Dfl. 6734.00 plus Dfl. 1036.00 (p.p.h.) (total ca. US\$ 3885.00)

J. Chromatogr. (incl. *Cum. Indexes, Vols. 451–500*) only (Vols. 498–524):

Dfl. 5616.00 plus Dfl. 756.00 (p.p.h.) (total ca. US\$ 3186.00)

Biomed. Appl. only (Vols. 525–534):

Dfl. 2080.00 plus Dfl. 280.00 (p.p.h.) (total ca. US\$ 1180.00).

Our p.p.h. (postage, package and handling) charge includes surface delivery of all issues, except to subscribers in Argentina, Australia, Brasil, Canada, China, Hong Kong, India, Israel, Malaysia, Mexico, New Zealand, Pakistan, Singapore, South Africa, South Korea, Taiwan, Thailand and the U.S.A. who receive all issues by air delivery (S.A.L. — Surface Air Lifted) at no extra cost. For Japan, air delivery requires 50% additional charge; for all other countries airmail and S.A.L. charges are available upon request. Back volumes of the *Journal of Chromatography* (Vols. 1–497) are available at Dfl. 195.00 (plus postage). Claims for missing issues will be honoured, free of charge, within three months after publication of the issue. Customers in the U.S.A. and Canada wishing information on this and other Elsevier journals, please contact Journal Information Center, Elsevier Science Publishing Co. Inc., 655 Avenue of the Americas, New York, NY 10010. Tel. (212) 633-3750.

Abstracts/Contents Lists published in Analytical Abstracts, ASCA, Biochemical Abstracts, Biological Abstracts, Chemical Abstracts, Chemical Titles, Chromatography Abstracts, Clinical Chemistry Lookout, Current Contents/Life Sciences, Current Contents/Physical, Chemical & Earth Sciences, Deep-Sea Research/Part B: Oceanographic Literature Review, Excerpta Medica, Index Medicus, Mass Spectrometry Bulletin, PASCAL-CNRS, Pharmaceutical Abstracts, Referativnyi Zhurnal, Science Citation Index and Trends in Biotechnology.

See inside back cover for Publication Schedule, Information for Authors and information on Advertisements.

© ELSEVIER SCIENCE PUBLISHERS B.V. — 1990

0021-9673/90/\$03.50

All rights reserved. No part of this publication may be reproduced, stored in a retrieval system or transmitted in any form or by any means, electronic, mechanical, photocopying, recording or otherwise, without the prior written permission of the publisher, Elsevier Science Publishers B.V., P.O. Box 330, 1000 AH Amsterdam, The Netherlands.

Upon acceptance of an article by the journal, the author(s) will be asked to transfer copyright of the article to the publisher. The transfer will ensure the widest possible dissemination of information.

Submission of an article for publication entails the authors' irrevocable and exclusive authorization of the publisher to collect any sums or considerations for copying or reproduction payable by third parties (as mentioned in article 17 paragraph 2 of the Dutch Copyright Act of 1912 and the Royal Decree of June 20, 1974 (S. 351) pursuant to article 16 b of the Dutch Copyright Act of 1912) and/or to act in or out of Court in connection therewith.

Special regulations for readers in the U.S.A. This journal has been registered with the Copyright Clearance Center, Inc. Consent is given for copying of articles for personal or internal use, or for the personal use of specific clients. This consent is given on the condition that the copier pays through the Center the per-copy fee stated in the code on the first page of each article for copying beyond that permitted by Sections 107 or 108 of the U.S. Copyright Law. The appropriate fee should be forwarded with a copy of the first page of the article to the Copyright Clearance Center, Inc., 27 Congress Street, Salem, MA 01970, U.S.A. If no code appears in an article, the author has not given broad consent to copy and permission to copy must be obtained directly from the author. All articles published prior to 1980 may be copied for a per-copy fee of US\$ 2.25, also payable through the Center. This consent does not extend to other kinds of copying, such as for general distribution, resale, advertising and promotion purposes, or for creating new collective works. Special written permission must be obtained from the publisher for such copying.

No responsibility is assumed by the Publisher for any injury and/or damage to persons or property as a matter of products liability, negligence or otherwise, or from any use or operation of any methods, products, instructions or ideas contained in the materials herein. Because of rapid advances in the medical sciences, the Publisher recommends that independent verification of diagnoses and drug dosages should be made.

Although all advertising material is expected to conform to ethical (medical) standards, inclusion in this publication does not constitute a guarantee or endorsement of the quality or value of such product or of the claims made of it by its manufacturer.

This issue is printed on acid-free paper.

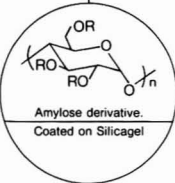
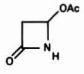
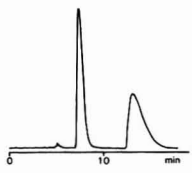
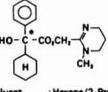
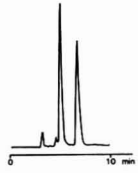
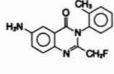
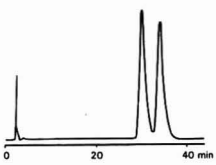
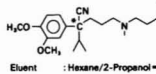
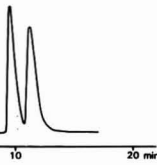
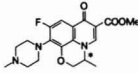
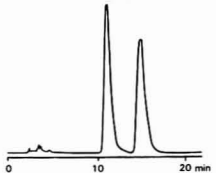
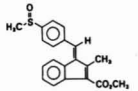
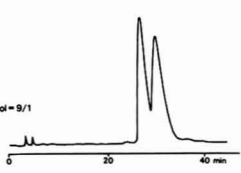
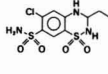
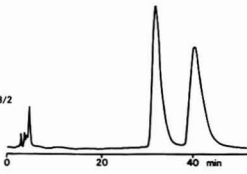
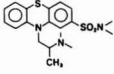
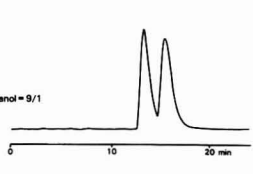
Printed in The Netherlands

For contents see p. VII

For Superior Chiral Separation

The finest from DAICEL.....

Why look beyond DAICEL? We have developed the finest CHIRALCEL, CHIRALPAK and CROWNPAK with up to 17 types of HPLC columns, all providing superior resolution of racemic compounds.

NEW CHIRALPAK AS		NEW CHIRALPAK AD	
<p>• CHIRALPAK AS</p> <p>R: <chem>CC(=O)N[C@H](C)C1=CC=CC=C1</chem></p> <p>* : S*</p> <p>for β-Lactam antibiotics</p>	 <p>Amylose derivative. Coated on Silicagel</p>	<p>• CHIRALPAK AD</p> <p>R: <chem>CC(=O)Nc1cc(C)c(C)cc1</chem></p>	
<p>4-Acetoxy-2-azetidine</p>  <p>Eluent : Hexane/Ethanol = 8/2 Flow rate : 1.0 ml/min Temperature : r.t. Detection : UV254 nm</p> 		<p>Oxyphenacycline</p>  <p>Eluent : Hexane/2-Propanol = 9/1 Flow rate : 1.0 ml/min Temperature : r.t. Detection : UV254 nm</p> 	
<p>Afloqualone</p>  <p>Eluent : Hexane/EtOH = 95/5 Flow rate : 1.3 ml/min Temperature : 50°C Detection : UV254 nm</p> 		<p>Verapamil</p>  <p>Eluent : Hexane/2-Propanol = 9/1 Flow rate : 1.0 ml/min Temperature : r.t. Detection : UV254 nm</p> 	
<p>Ofloxacin methyl ester</p>  <p>Eluent : Hexane/EtOH = 8/2 Flow rate : 1.2 ml/min Temperature : 40°C Detection : UV254 nm</p> 		<p>Salindac methyl ester</p>  <p>Eluent : Hexane/2-Propanol = 9/1 Flow rate : 1.0 ml/min Temperature : r.t. Detection : UV254 nm</p> 	
<p>Ethiazide</p>  <p>Eluent : Hexane/Ethanol = 8/2 Flow rate : 1.0 ml/min Temperature : 40°C Detection : UV254 nm</p> 		<p>Dimethiazine</p>  <p>Eluent : Hexane/2-Propanol = 9/1 Flow rate : 1.0 ml/min Temperature : r.t. Detection : UV254 nm</p> 	

■ Separation Service

- A pure enantiomer separation in the amount of 100g~10kg is now available.
- Please contact us for additional information regarding the manner of use and application of our chiral columns and how to procure our separation service.



DAICEL CHEMICAL INDUSTRIES, LTD.

8-1, Kasumigaseki 3-chome, Chiyoda-ku, Tokyo 100, Japan Phone: 03 (507) 3151 FAX: 03 (507) 3193

DAICEL (U.S.A.), INC.

Fort Lee Executive Park
Two Executive Drive, Fort Lee,
New Jersey 07024
Phone: (201) 461-4466
FAX: (201) 461-2776

DAICEL (U.S.A.), INC.

23456 Hawthorne Blvd.
Bldg. 5, Suit 130
Torrance, CA 90505
Phone: (213) 791-2030
FAX: (213) 791-2031

DAICEL (EUROPA) GmbH

Oststr. 22
4000 Düsseldorf 1, F.R. Germany
Phone: (211) 369848
Telex: (411) 8588042 DCEL D
FAX: (211) 364429

DAICEL CHEMICAL (ASIA) PTE. LTD.

65 Chulia Street #40-07
OCBC Centre, Singapore 0104
Phone: 5332511
FAX: 5326454

15th International

Symposium

on Column Liquid

Chromatography

Convention Center

Basel, Switzerland

June 3-7, 1991

HPLC '91 Basel



Chairman

Dr. Fritz Erni

Secretariat

Swiss Industries Fair

Congress Department

P. O. Box

CH-4021 Basel

Switzerland

Telephone

++ 41 61/686 28 28

Telefax

++ 41 61/691 80 49

Chromatography and Modification of Nucleosides

edited by C.W. Gehrke and K.C.T. Kuo, Department of Biochemistry, University of Missouri-Columbia, and Cancer Research Center, P.O. Box 1268, Columbia, MO, U.S.A.

Part A

Analytical Methods for Major and Modified Nucleosides - HPLC, GC, MS, NMR, UV and FT-IR

Chromatography and Modification of Nucleosides is a four-volume work which provides state-of-the-art chromatography and analytical methods for use in a wide spectrum of nucleic acid modification research.

The focus of Part A, is the presentation of advanced methods for modification research on tRNAs, mRNAs, mtRNAs, rRNAs and DNAs. HPLC-UV, GC-MS, NMR, FT-IR and affinity chromatography approaches to nucleic acid modification studies are presented, as are nucleoside, oligonucleotide and nucleic acid isolation techniques.

Contents: Introduction and Overview (C.W. Gehrke, K.C. Kuo). 1. Ribonucleoside analysis by reversed-phase high performance liquid chromatography (C.W. Gehrke, K.C. Kuo). 2. HPLC of transfer RNAs using ionic-hydrophobic mixed-mode and hydrophobic-interaction chromatography (R. Bischoff, L.W. McLaughlin). 3. Nucleic acid chromatographic isolation and sequence methods (G. Keith). 4. Affinity chromatography of mammalian tRNAs on immobilized elongation factor Tu from *Thermus thermophilus* (M. Sprinzl, K.-H. Derwenskus). 5. Structural elucidation of nucleosides in nucleic acids (C.W. Gehrke et al.). 6. Three dimensional dynamic structure of tRNAs by nuclear magnetic resonance spectroscopy (P.F. Agris, H. Sierzputowska-Gracz). 7. Codon recognition: evaluation of the effects of modified bases in the anticodon loop of tRNA using the temperature-jump relaxation method (H. Grosjean, C. Houssier). 8. High-performance liquid chromatography of Cap structures and nucleoside composition in mRNAs (K.C. Kuo et al.). 9. Immunoassays for modified nucleosides of ribonucleic acids (B.S. Vold). 10. Chromatography of synthetic and natural oligonucleotides (H. Eckstein, H. Schott). Subject Index.

1990 liii + 400 pages, ISBN 0-444-88540-4
Price: US\$ 141.00 / Dfl. 275.00

Part B

Biological Roles and Function of Modification

Part B, the second of the four-volume work *Chromatography and Modification of Nucleosides*, has as its central theme the modified nucleosides of tRNA and the current analytical means for studying rRNA modifications. Modified nucleoside synthesis, function, structural conformation, biological regulation, and occurrence of modification in a wide range of tRNAs are presented, as is a chapter on DNA modification and a chapter on solid phase immunoassay for determining a particular modification.

The chapters are written by leading scientists in their respective fields and present an up-to-date review on the roles of modified nucleosides in nucleic acids which will be extremely useful for workers in chromatography, molecular biology, genetics, biochemistry, biotechnology and the pharmaceutical industry.

Contents: Introduction and Overview (D.G. Söll). 1. Synthesis and function of modified nucleosides (G.R. Björk, J. Kohli). 2. Biosynthesis and function of queuine and queuosine (H. Kersten, W. Kersten). 3. Codon usage and Q-base modification in *Drosophila melanogaster* (E. Kubli). 4. Solid phase immunoassay for determining the inosine content in transfer RNA (E.F. Yamasaki, A.A. Wani, R.W. Trewyn). 5. Site directed replacement of nucleotides in the anticodon loop of tRNA: application to the study of inosine biosynthesis in yeast tRNA^{Ala} (K.A. Kretz, R.W. Trewyn, G. Keith, H. Grosjean). 6. tRNA and tRNA-like molecules: structural peculiarities and biological recognition (R.L. Joshi, A.L. Haenni). 7. Mitochondrial tRNAs-structure, modified nucleosides and codon reading patterns (G. Dirheimer, R.P. Martin). 8. The modified nucleotides in ribosomal RNA from man and other eukaryotes (B.E.H. Maden). Modified uridines in the first positions of anticodons of tRNAs and mechanisms of codon recognition (S. Yokoyama, T. Miyazawa). 10. Natural occurring modified nucleosides in DNA (M. Ehrlich, X.Y. Zhang). Subject Index.

1990 xliiv + 370 pages, ISBN 0-444-88505-6
Price: US\$ 153.75 / Dfl. 300.00



Selective Sample Handling and Detection in High-Performance Liquid Chromatography

Journal of Chromatography Library, 39

part A

edited by **R.W. Frei**[†], *Free University, Amsterdam, The Netherlands*, and **K. Zech**, *Byk Gulden Pharmaceuticals, Konstanz, FRG*

Part A of this two-volume project attempts to treat the sample handling and detection processes in a liquid chromatographic system in an integrated fashion. The need for more selective and sensitive chromatographic methods to help solve the numerous trace analysis problems in complex samples is undisputed. However, few workers realize the strong interdependence of the various steps - sample handling, separation and detection - which must be considered if one wants to arrive at an optimal solution. By introducing a strong element of selectivity and trace enrichment in the sample preparation step, fewer demands are placed on the quality of the chromatography and often a simple UV detector can be used. By using a selective detection mode, i.e. a reaction detector, the sample handling step can frequently be simplified and more easily automated. The impact of such a "total system" approach on handling series of highly complex samples such as environmental specimens or biological fluids can be easily imagined.

Contents: 1. On-line sample handling and trace enrichment in liquid chromatography. The determination of organic compounds in water samples. 2. Determination of drugs and their metabolites in biological samples by fully automated HPLC with on-line solid-liquid extraction and pre-column switching. 3. Immobilization of compounds for selective interaction with analytes in liquid chromatography. 4. Design and choice of suitable labelling reagents for liquid chromatography. 5. Photodiode array detection and recognition in high-performance liquid chromatography. 6. Electrochemical techniques for detection in HPLC. 7. Solid-phase reactors in high-performance liquid chromatography. 8. Commercial aspects of post-column reaction detectors for liquid chromatography. Subject Index.

1988 xii + 458 pages
US\$ 123.00 / Dfl. 240.00
ISBN 0-444-42881-X

part B

edited by **K. Zech**, *Byk Gulden Pharmaceuticals, Konstanz, FRG*, and **R.W. Frei**[†], *Free University, Amsterdam, The Netherlands*

Part B completes the treatment of the handling, separation and detection of complex samples as an integrated, interconnected process. On the basis of this philosophy the editors have selected those contributions which demonstrate that optimal sample preparation leads to a simplification of detection or reduced demands on the separation process. Throughout the book emphasis is on chemical principles with minimum discussion of the equipment required - an approach which reflects the editors' view that the limiting factor in the analysis of complex samples is an incomplete knowledge of the underlying chemistry rather than the hardware available. This lack of knowledge becomes more evident as the demands for lower detection limits grow, as solving complex matrix problems requires a greater understanding of the chemical interaction between the substance to be analysed and the stationary phase.

Contents: I. Preconcentration and Chromatography on Chemically Modified Silicas with Complexation Properties. II. Sample Handling in Ion Chromatography. III. Whole Blood Sample Clean-Up for Chromatographic Analysis. IV. Radio-Column Liquid Chromatography. V. Modern Post-Column Reaction Detection in High-Performance Liquid Chromatography. VI. New Luminescence Detection Techniques. VII. Continuous Separation Techniques in Flow-Injection Analysis. Subject Index.

1989 xii + 394 pages
US\$ 136.00 / Dfl. 265.00
ISBN 0-444-88327-4

Written by experienced practitioners, these volumes will be of interest to investigators in many areas of application, including environmental scientists and those active in the clinical, pharmaceutical and bioanalytical fields.

For more information, please write to:



Elsevier Science Publishers

P.O. Box 211, 1000 AE Amsterdam, The Netherlands
P.O. Box 882, Madison Square Station, New York, NY 10159, USA

JOURNAL OF CHROMATOGRAPHY

VOL. 516 (1990)

JOURNAL *of* CHROMATOGRAPHY

INTERNATIONAL JOURNAL ON CHROMATOGRAPHY,
ELECTROPHORESIS AND RELATED METHODS

EDITORS

R. W. GIESE (Boston, MA), J. K. HAKEN (Kensington, N.S.W.), K. MACEK (Prague),
L. R. SNYDER (Orinda, CA)

EDITOR, SPECIAL ELECTROPHORESIS VOLUMES

Z. DEYL (Prague).

EDITOR, SYMPOSIUM VOLUMES

E. HEFTMANN (Orinda, CA)

EDITORIAL BOARD

D. W. Armstrong (Rolla, MO), W. A. Aue (Halifax), P. Boček (Brno), A. A. Boulton (Saskatoon), P. W. Carr (Minneapolis, MN), N. H. C. Cooke (San Ramon, CA), V. A. Davankov (Moscow), Z. Deyl (Prague), S. Dilli (Kensington, N.S.W.), H. Engelhardt (Saarbrücken), F. Erni (Basle), M. B. Evans (Hatfield), J. L. Glajch (N. Billerica, MA), G. A. Guiochon (Knoxville, TN), P. R. Haddad (Kensington, N.S.W.), I. M. Hais (Hradec Králové), W. S. Hancock (San Francisco, CA), S. Hjertén (Uppsala), Cs. Horváth (New Haven, CT), J. F. K. Huber (Vienna), K.-P. Hupe (Waldbronn), T. W. Hutchens (Houston, TX), J. Janák (Brno), P. Jandera (Pardubice), B. L. Karger (Boston, MA), E. sz. Kováts (Lausanne), A. J. P. Martin (Cambridge), L. W. McLaughlin (Chestnut Hill, MA), E. D. Morgan (Keele), J. D. Pearson (Kalamazoo, MI), H. Poppe (Amsterdam), F. E. Regnier (West Lafayette, IN), P. G. Righetti (Milan), P. Schoenmakers (Eindhoven), G. Schomburg (Mülheim/Ruhr), R. Schwarzenbach (Dübendorf), R. E. Shoup (West Lafayette, IN), A. M. Siouffi (Marseille), D. J. Strydom (Boston, MA), K. K. Unger (Mainz), R. Verpoorte (Leiden), Gy. Vigh (College Station, TX), J. T. Watson (East Lansing, MI), B. D. Westerlund (Uppsala)

EDITORS, BIBLIOGRAPHY SECTION

Z. Deyl (Prague), J. Janák (Brno), V. Schwarz (Prague), K. Macek (Prague)



ELSEVIER
AMSTERDAM — OXFORD — NEW YORK — TOKYO

J. Chromatogr., Vol. 516 (1990)

All rights reserved. No part of this publication may be reproduced, stored in a retrieval system or transmitted in any form or by any means, electronic, mechanical, photocopying, recording or otherwise, without the prior written permission of the publisher, Elsevier Science Publishers B.V., P.O. Box 330, 1000 AH Amsterdam, The Netherlands.

Upon acceptance of an article by the journal, the author(s) will be asked to transfer copyright of the article to the publisher. The transfer will ensure the widest possible dissemination of information.

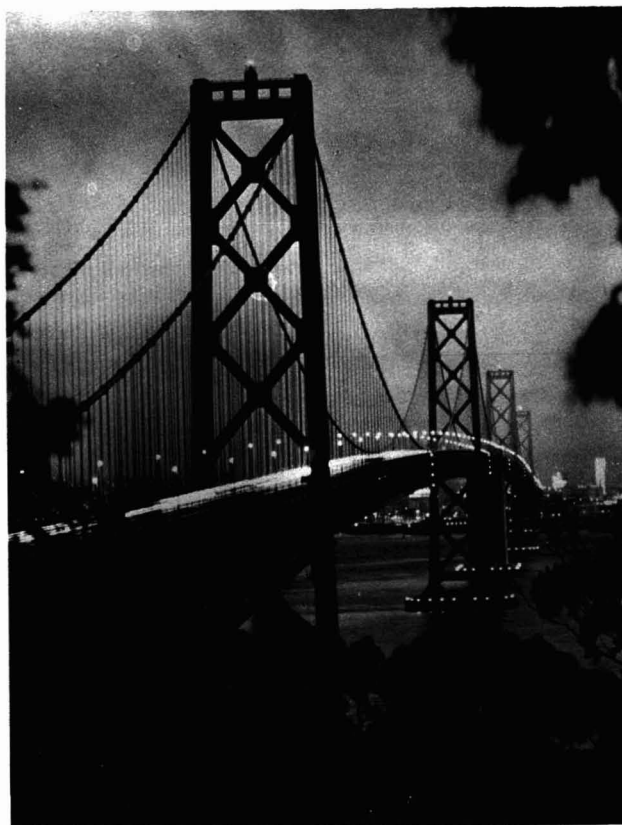
Submission of an article for publication entails the authors' irrevocable and exclusive authorization of the publisher to collect any sums or considerations for copying or reproduction payable by third parties (as mentioned in article 17 paragraph 2 of the Dutch Copyright Act of 1912 and the Royal Decree of June 20, 1974 (S. 351) pursuant to article 16 b of the Dutch Copyright Act of 1912) and/or to act in or out of Court in connection therewith.

Special regulations for readers in the U.S.A. This journal has been registered with the Copyright Clearance Center, Inc. Consent is given for copying of articles for personal or internal use, or for the personal use of specific clients. This consent is given on the condition that the copier pays through the Center the per-copy fee stated in the code on the first page of each article for copying beyond that permitted by Sections 107 or 108 of the U.S. Copyright Law. The appropriate fee should be forwarded with a copy of the first page of the article to the Copyright Clearance Center, Inc., 27 Congress Street, Salem, MA 01970, U.S.A. If no code appears in an article, the author has not given broad consent to copy and permission to copy must be obtained directly from the author. All articles published prior to 1980 may be copied for a per-copy fee of US\$ 2.25, also payable through the Center. This consent does not extend to other kinds of copying, such as for general distribution, resale, advertising and promotion purposes, or for creating new collective works. Special written permission must be obtained from the publisher for such copying.

No responsibility is assumed by the Publisher for any injury and/or damage to persons or property as a matter of products liability, negligence or otherwise, or from any use or operation of any methods, products, instructions or ideas contained in the materials herein. Because of rapid advances in the medical sciences, the Publisher recommends that independent verification of diagnoses and drug dosages should be made. Although all advertising material is expected to conform to ethical (medical) standards, inclusion in this publication does not constitute a guarantee or endorsement of the quality or value of such product or of the claims made of it by its manufacturer.

This issue is printed on acid-free paper.

SPECIAL ISSUE



**SECOND INTERNATIONAL SYMPOSIUM ON
HIGH PERFORMANCE CAPILLARY ELECTROPHORESIS**

San Francisco, CA (U.S.A.), January 29–31, 1990

Guest Editor

B. L. KARGER

(Boston, MA)

CONTENTS

2ND INTERNATIONAL SYMPOSIUM ON HIGH PERFORMANCE CAPILLARY ELECTROPHORESIS, SAN FRANCISCO, CA, JANUARY 29-31, 1990

In memoriam: Vern Berry	1
Foreword	
by B. L. Karger (Boston, MA, U.S.A.)	2
Recent developments in electrophoretic methods (Review)	
by P. G. Righetti (Milan, Italy)	3
Separation of highly hydrophobic compounds by cyclodextrin-modified micellar electrokinetic chromatography	
by S. Terabe, Y. Miyashita and O. Shibata (Kyoto, Japan), E. R. Barnhart, L. R. Alexander and D. G. Patterson (Atlanta, GA, U.S.A.), B. L. Karger (Boston, MA, U.S.A.) and K. Hosoya and N. Tanaka (Kyoto, Japan)	23
Separation of DNA restriction fragments by high performance capillary electrophoresis with low and zero crosslinked polyacrylamide using continuous and pulsed electric fields	
by D. N. Heiger, A. S. Cohen and B. L. Karger (Boston, MA, U.S.A.)	33
Separation and analysis of DNA sequence reaction products by capillary gel electrophoresis	
by A. S. Cohen, D. R. Najarian and B. L. Karger (Boston, MA, U.S.A.)	49
Capillary gel electrophoresis for DNA sequencing. Laser-induced fluorescence detection with the sheath flow cuvette	
by H. Swerdlow (Salt Lake City, UT, U.S.A.) and S. Wu, H. Harke and N. J. Dovichi (Edmonton, Canada)	61
Polyethyleneimine-bonded phases in the separation of proteins by capillary electrophoresis	
by J. K. Towns and F. E. Regnier (West Lafayette, IN, U.S.A.)	69
Analysis of dilute peptide samples by capillary zone electrophoresis	
by R. Aebersold and H. D. Morrison (Vancouver, Canada)	79
High-performance capillary electrophoresis of hydrophobic membrane proteins	
by D. Josić, K. Zeilinger and W. Reutter (Berlin, F.R.G.) and A. Böttcher and G. Schmitz (Münster, F.R.G.)	89
Method optimization in capillary zone electrophoretic analysis of hGH tryptic digest fragments	
by R. G. Nielsen and E. C. Rickard (Indianapolis, IN, U.S.A.)	99
Use of high-performance capillary electrophoresis to monitor charge heterogeneity in recombinant-DNA derived proteins	
by S.-L. Wu, G. Teshima, J. Cacia and W. S. Hancock (South San Francisco, CA, U.S.A.)	115
Capillary electrophoresis of proteins under alkaline conditions	
by M. Zhu, R. Rodriguez, D. Hansen and T. Wehr (Richmond, CA, U.S.A.)	123
Capillary zone electrophoresis for monitoring r-DNA protein purification in multi-compartment electrolyzers with immobiline membranes	
by E. Wenisch, C. Tauer, A. Jungbauer and H. Katinger (Vienna, Austria), M. Faupel (Basle, Switzerland) and P. G. Righetti (Milan, Italy)	133
Static and scanning array detection in capillary electrophoresis-mass spectrometry	
by N. J. Reinhoud (Leiden, The Netherlands), E. Schröder (Bremen, F.R.G.), U. R. Tjaden and W. M. A. Niessen (Leiden, The Netherlands), M. C. ten Noever de Brauw and J. van der Greef (Zeist, The Netherlands)	147

Sensitivity considerations for large molecule detection by capillary electrophoresis–electrospray ionization mass spectrometry by R. D. Smith, J. A. Loo, C. G. Edmonds, C. J. Barinaga and H. R. Udseth (Richland, WA, U.S.A.)	157
Capillary zone electrophoresis–mass spectrometry using a coaxial continuous-flow fast atom bombardment interface by M. A. Moseley (Research Triangle Park and Chapel Hill, NC, U.S.A.), L. J. Deterding and K. B. Tomer (Research Triangle Park, NC, U.S.A.) and J. W. Jorgenson (Chapel Hill, NC, U.S.A.)	167
Identification of aprotinin degradation products by the use of high-performance capillary electrophoresis, high-pressure liquid chromatography and mass spectrometry by A. Vinther (Gentofte, Denmark), S. E. Bjørn (Bagsværd, Denmark), H. H. Sørensen (Gentofte, Denmark) and H. Sæberg (Lyngby, Denmark)	175
Continuous sample collection in capillary zone electrophoresis by coupling the outlet of a capillary to a moving surface by X. Huang and R. N. Zare (Stanford, CA, U.S.A.)	185
Thermal model of capillary electrophoresis and a method for counteracting thermal band broadening by W. A. Gobie and C. F. Ivory (Pullman, WA, U.S.A.)	191
Isotachopheresis in open-tubular fused-silica capillaries. Impact of electroosmosis on zone formation and displacement by W. Thormann (Berne, Switzerland)	211
Applicability of dynamic change of pH in the capillary zone electrophoresis of proteins by F. Foret (Brno, Czechoslovakia), S. Fanali (Monterotondo Scalo, Italy) and P. Boček (Brno, Czechoslovakia)	219
Influence of buffer concentration, capillary internal diameter and forced convection on resolution in capillary zone electrophoresis by H. T. Rasmussen and H. M. McNair (Blacksburg, VA, U.S.A.)	223
Non-uniform electrical field effect caused by different concentrations of electrolyte in capillary zone electrophoresis by X. Huang and J. I. Ohms (Palo Alto, CA, U.S.A.)	233
Free solution capillary electrophoresis and micellar electrokinetic resolution of amino acid enantiomers and peptide isomers with L- and D-Marfey's reagents by A. D. Tran and T. Blanc (Raritan, NJ, U.S.A.) and E. J. Leopold (Palo Alto, CA, U.S.A.)	241
Isotachopheretic separation of organic acids in biological fluids by P. Oefner, R. Häfele, G. Bartsch and G. Bonn (Innsbruck, Austria)	251
Retention of eleven priority phenols using micellar electrokinetic chromatography by C. P. Ong, C. L. Ng, N. C. Chong, H. K. Lee and S. F. Y. Li (Kent Ridge, Singapore)	263
Capillary electrophoresis of urinary porphyrins with absorbance and fluorescence detection by R. Weinberger and E. Sapp (Ramsey, NJ, U.S.A.) and S. Moring (San Jose, CA, U.S.A.)	271
Separation and partial characterization of Maillard reaction products by capillary zone electrophoresis by Z. Deyl, I. Miksik and R. Struzinsky (Prague, Czechoslovakia)	287

 * In articles with more than one author, the name of the author to whom correspondence should be addressed is indicated in the *
 * article heading by a 6-pointed asterisk (*) *

IN MEMORIAM: VERN BERRY

On July 20, 1990, Vern Berry passed away after a short illness. Given his enthusiasm for separation science, this symposium volume is dedicated to his memory. Indeed, his final article was a summary of this meeting [*LC · GC*, 8 (1990) 485 (Part I) and 546 (Part II)].

Vern Berry received his Ph.D. under my direction in 1972, the title of his thesis being "Development and Application of High-Performance Liquid Chromatographic Instrumentation to Complex Mixtures". He then conducted post-doctoral research with Heinz Engelhardt and Istvan Halasz in Saarbrücken. Upon returning to the U.S.A., he was employed by Polaroid Corporation for a number of years. He then moved to Salem State College to practice his first love, teaching. Concurrently, he was the head of SepCon Separations Consultants.

Vern was well-known in the separations community. He was at most of the major chromatographic (and recently electrophoretic) international meetings. Many of us vividly recall his uncanny ability to enliven discussion sessions at these meetings. Recently, he has written excellent summaries of these meetings for *LC · GC*.

The Vern Berry Memorial Foundation has been established in Vern's memory. The purpose of the fund will be to provide an internal annual award for excellence in chromatographic research by a graduate student. The awardee will be selected by an independent scientific committee, and the first presentation will be made at HPLC'91, June, 1991, Basel, Switzerland. Contributions can be made to The Vern Berry Foundation, c/o Austin Wentworth, 326 Reservoir Road, Boston, MA 02167, U.S.A. The contributions will be tax deductible.

In his career, Vern helped to advance the art and science of separations. His engaging personality was very much appreciated. It is difficult to believe he is no longer with us, given his energy and enthusiasm. He will be sorely missed.

BARRY L. KARGER

FOREWORD

The *2nd International Symposium on High Performance Capillary Electrophoresis* (HPCE '90) was held in San Francisco, CA on January 29–31, 1990. While the meeting was only 10 months after the first one in Boston, HPCE '90 can be judged a major success. There were approximately 550 participants from all over the world, close to 100 presentations and an instrument exhibit of 10 companies. Many new advances were presented including DNA sequencing, restriction fragment separations, new approaches to protein separations, innovative detector design, new sample handling techniques and broad areas of application. The enthusiasm of researchers for this new methodology was quite evident, and many expressed their belief that full exploitation will take place after a short development time span.

The success of the meeting is largely due to the efforts of Tom Gilbert, Vice Chairman, and Shirley Schlessinger, Symposium Manager, who duplicated their achievements of HPCE '89. The assistance of the Scientific Committee in assembling the program is also gratefully acknowledged. Zdenek Deyl is thanked for his excellent editorial efforts in organizing this volume in rapid time. Finally, the Bay Area Colloquium Committee and the Barnett Institute are acknowledged for their sponsorship of student travel grants to this meeting.

All participants eagerly await HPCE '91 in San Diego, February 2–4, 1991 under the Chairmanship of Jim Jorgenson.

Boston, MA (U.S.A.)

B. L. KARGER

Review

Recent developments in electrophoretic methods

PIER GIORGIO RIGHETTI

Department of Biomedical Sciences and Technologies, University of Milan, Via Celoria 2, Milan 20133 (Italy)

CONTENTS

1. Introduction	3
2. Nucleic acid electrophoresis	4
3. DNA sequence analysis	4
4. Separation of mega-DNA fragments	5
5. Electrophoresis as a probe of macromolecular structure	11
6. Two-dimensional maps	12
7. Immobilized pH gradients	14
8. Capillary zone electrophoresis	16
9. Chromatophoresis	17
10. Conclusion	18
11. Abbreviations	19
12. Acknowledgements	20
13. Abstract	20
References	20

1. INTRODUCTION

At the first International Symposium on High Performance Capillary Zone Electrophoresis (CZE) in Boston, Vesterberg¹ gave a comprehensive account of the history of electrophoretic methods, including the pioneering work of the nineteenth-century physicists. His survey correctly emphasized the importance of the Uppsala School of Separation Science, where most of developments in both chromatography and electrophoresis have been initiated. He also extensively covered the field of isoelectric focusing (IEF), to which he has made some fundamental contributions. In addition, there has been a recent historical survey^{2,3} of electrophoresis based on the development of gel matrices, the latter playing a fundamental role in many electrokinetic techniques. In this review, it was therefore decided to concentrate on the last 10 years of electrophoresis, and to give particular emphasis to nucleic acid separations, often overlooked at electrophoresis meetings, still frequented by numerous protein chemists. The review includes recent developments in two-dimensional (2D) maps and their coupling to blotting techniques, which allow direct sequencing and fingerprinting of polypeptides from complex samples without a need for prior chromatographic steps. Some of the improvements in 2D techniques have been obtained

through the use of immobilized pH gradients (IPGs), which currently offer the highest resolving power in electrophoresis. An alternative approach to 2D mapping (which generates a pure charge/mass fractionation) is chromatofocusing, which separates polypeptides on a 2D plane having hydrophobicity and mass as coordinates. This is achieved by running directly the eluate from a reversed-phase high-performance liquid chromatographic (HPLC) column into a sodium dodecyl sulphate (SDS) gel. The two techniques are clearly complementary and could help in creating a three-dimensional map of polypeptides, having charge, hydrophobicity and mass as coordinates. The review ends with a brief discussion of CZE.

2. NUCLEIC ACID ELECTROPHORESIS

The revolution in modern biology over the past decade has been driven largely by the development of an array of new methods for the isolation, analysis and manipulation of DNA molecules. One of the key areas has been the ability to determine the precise chemical structure of large DNA molecules, *i.e.*, the sequence of the four bases on the DNA strand. The last step in this process is an electrophoretic analysis by which a series of oligonucleotides, differing in length by a single nucleotide, are separated, detected and read in order of sequence. The other major breakthrough has been the ability to separate very large DNA fragments, in the mega-base pair range, by a technique generally known as pulsed-field gel electrophoresis (PFGE). Both developments have opened up new dimensions in the field of electrophoretic DNA analysis, which previously was mostly dominated by electrophoretic separations in "submarine" gels, *i.e.*, dilute agarose gels run under a thin veil of buffer, for the analysis of restriction fragments of DNA. Such analyses, coupled to probing with radioactive or biotinylated probes, is routine in, *e.g.*, screening of defective human genes and parentage testing.

3. DNA SEQUENCE ANALYSIS

In the early 1970s, two groups developed rapid methods for sequencing DNA: the enzymatic method, proposed by Sanger *et al.*⁴ at the Medical Research Council in England, and the chemical method, described by Maxam and Gilbert⁵ at Harvard, work for which they shared the Nobel Prize. In enzymatic sequencing, a cloned copy of the DNA region to be sequenced is used as the template for an enzymatic reaction which copies the DNA sequence into a new strand. Four separate incubations are prepared, each containing a dideoxy nucleotide, which will act as chain terminator on incorporation at one end of the growing oligonucleotide. In the chemical sequencing method, four base-specific chemical reactions generate four sets of DNA fragments. In both instances, the key that permits DNA sequencing is the ability, by electrophoresis on very thin (*e.g.*, 200–400 μm thick) denaturing polyacrylamide gels, to separate DNA fragments differing by size increments of one nucleotide each, with extremely high resolution. In conventional DNA sequencing, the DNA fragments are labelled with radioisotopes, separated on the sequencing gel and visualized by the image they generate on a radiographic film in contact with the dried gel. This generates a "snapshot" image of the gel at the time at which power was disconnected.

The enzymatic sequencing method seems to be the predominant one, as it has

been adopted for the two largest sequencing projects presently reported, the analysis of the 172 000-base Epstein-Barr viral genome⁶ and the 48 000-base λ genome⁷. Nevertheless, neither method could be of any practical use for very large-scale sequencing projects, such as the analysis of the human genome, which is encoded in $3 \cdot 10^9$ bases of DNA. At this level of complexity, automation is strongly desirable. This has been made possible by abandoning radioactive tags in favour of fluorescent probes, which allow direct data acquisition in real time during the electrophoretic separation. This also has the added advantage of increased sensitivity, which is greatly needed, as there are only of the order of 10^{-15} – 10^{-16} mol of DNA in each band in the gel⁸. There are essentially three methods available: (a) use of four fluorophores linked to the primer (*i.e.*, to the short DNA fragment which serves as starting point for the enzymatic synthesis, by annealing to the template DNA molecule)^{8,9}; (b) use of four fluorophores linked to the chain-terminating dideoxy nucleotides¹⁰; and (c) use of a single fluorophore¹¹. The first two methods allow electrophoresis in a single lane, whereas the last still requires four separate electrophoretic lanes, as is customary in radioactive labelling (*i.e.*, one for each of the four terminating nucleotide analogues).

Fig. 1A and B shows the set-up developed by Smith and co-workers^{8,9} and introduced commercially by Applied Biosystems (Fig. 1C). Basically, four different fluorescent dyes (fluorescein, NBD, tetramethylrhodamine and Texas red) are linked to the primer and used for four different incubation reactions for A, C, G and T. The products of each reaction are then combined and co-electrophoresed on a single lane of a polyacrylamide gel. A fluorescence detector near the bottom of the gel reveals the fluorescent bands of DNA as they pass by during electrophoresis, and determines their colour. In the system of Prober *et al.*¹⁰ (adopted by DuPont in the Genesis 2000 DNA sequencer) the four fluorescent tags, instead of being attached to the primer, are linked to the chain-terminating base analogue itself. This accomplishes two operations in one step: first, it terminates the synthesis on dye-analogue incorporation, just as in conventional enzymatic sequencing, and second, it attaches a fluorophore to the end of the DNA molecule at the same time.

The optical instrumentation in the DuPont instrument is shown in Fig. 2. As the fluorophores are much more closely spaced, the ratio of the fluorescence emission at two wavelengths is measured, thus identifying the fluorophore on the basis of its spectral fingerprint. In the single fluorophore system developed by Anson *et al.*¹¹ (and introduced commercialized by Pharmacia-LKB Biotechnology), tetramethylrhodamine is bound to the primer and four electrophoretic lanes are probed by a laser beam entering through the gel from the side.

The limit of the above techniques still rests on the fact that, in a single run, it is impossible to obtain sequence data longer than *ca.* 400 nucleotides. Above this limit, there is not enough spacing among the different bands, which migrate almost as a continuum. By using a novel matrix, HydroLink¹², having properties intermediate between those of agarose and polyacrylamide, as shown in a Ferguson plot, we have been able to extend this upper limit to at least 600 bases¹³. It appears that also CZE could hold a major promise for DNA sequencing¹⁴.

4. SEPARATION OF MEGA-DNA FRAGMENTS

Conventional agarose gel electrophoresis separates native DNA molecules,

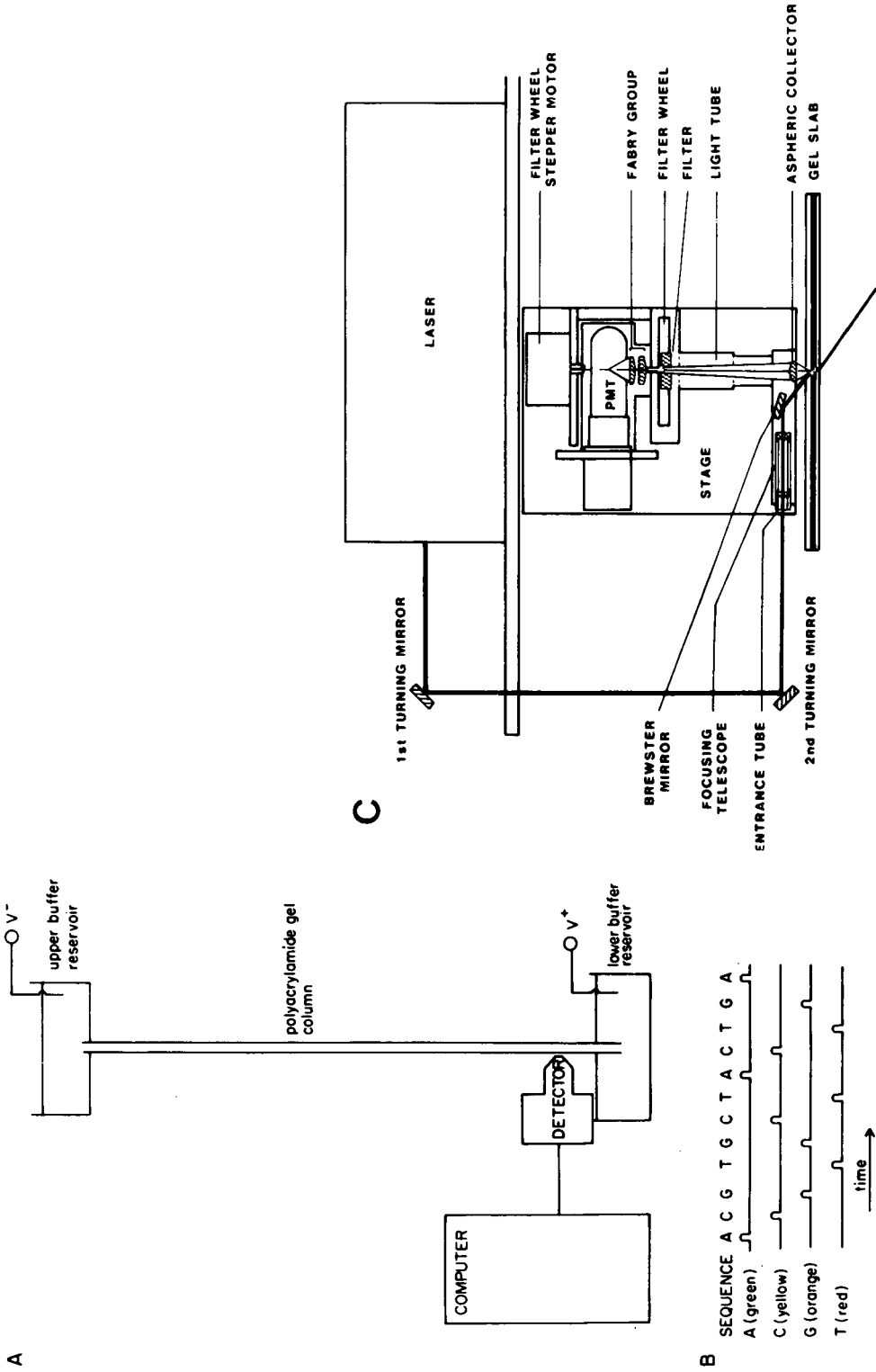


Fig. 1. Schematic diagram of the strategy used in automated fluorescence-based DNA sequence analysis according to Smith *et al.*⁸. (A) Schematic diagram of the prototype apparatus; (B) idealized representation of the data and the manner in which the measured fluorescence corresponds to the DNA sequence; (C) block diagram of the Model 370A fluorescence-based automated DNA sequencer of Applied Biosystems. Reproduced by permission from Smith and co-workers^{8,9}.

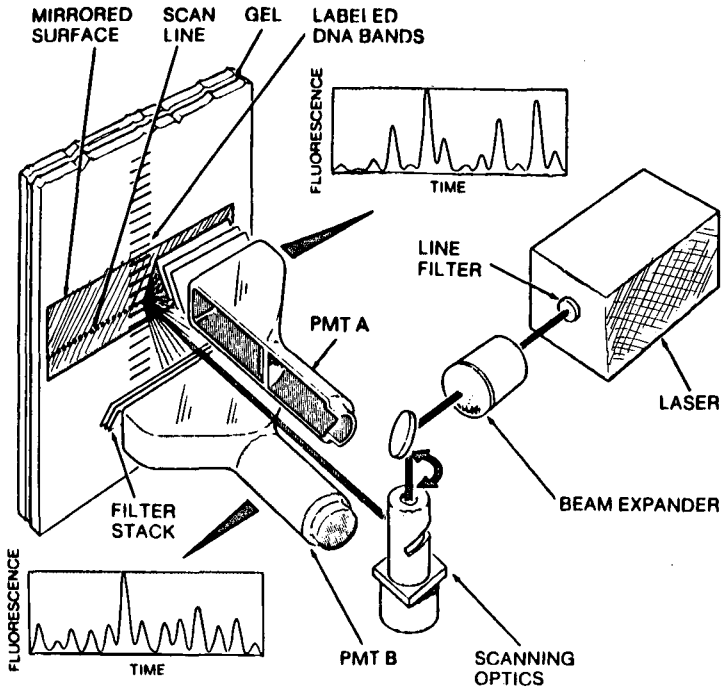


Fig. 2. Fluorescent detection system of the Genesis 2000. Schematic diagram of the optical system used for scanning excitation and for measurements of fluorescence from multiple sequencing lanes in an electrophoresis gel. The light from the argon ion laser is filtered to isolate the 488-nm emission line. The beam is deflected by a mirror into the scanning optics which are mounted on the shaft of digitally controlled stepping motor. A lens focuses the beam into a spot in the plane of the gel. A second mirror directs the beam to a position on the scan line defined by the rotational position of the motor shaft. Sequencing of multiple samples is achieved by directing the beam sequentially to each of the sequencing lanes on the gel. On entering the gel, the beam excites fluorescence in the terminator-labelled DNA. Fluorescence is detected by two elongated, stationary photomultiplier tubes (PMT A and B) which span the width of the gel. In front of each PMT, a filter stack is placed with one of the complementary transmission functions. Baseline-corrected ratios of signals in the PMTs are used to identify the labelled DNA fragments currently in the excitation region. Excitation efficiency and fluorescence collection are increased by the mirrored outer surface of the glass plate in the electrophoresis gel assembly. Reproduced by permission from Prober *et al.*¹⁰.

within the range 1000–40 000 bases, on the basis of molecular mass. Above this threshold, DNA molecules exhibit size-independent mobilities and co-migrate in an agarose gel matrix¹⁵. As the average pore size of a 1% agarose gel is *ca.* 90–120 nm¹⁶ and as, *e.g.*, the length of a small-size DNA, like the λ phage, is *ca.* 16 μm ¹⁷, with a radius, as an extended random coil, of *ca.* 500 nm, it would seem that for entering the gel these molecules must orient longitudinally with respect to the gel pores. Hence, the forward motion of the large DNA molecules is thought to be serpentine in nature, as they migrate through the gel pores, much as the movement of a snake in a field of grass. With the beginning of serpentine motion (called reptation)¹⁸, the capacity for the gel matrix to sieve large DNA molecules is lost because the charge on the DNA and the friction exerted on the moving molecules are both proportional to size.

In 1983, Schwartz *et al.*¹⁹ addressed the problem of separating large DNA molecules based on data from viscoelastic techniques for DNA molecular size determinations. They reasoned that, by forcing large molecules to change direction periodically and taking into account the strongly size-dependent relaxation time of large DNA, it might be possible to obtain size-dependent DNA separations. By arranging for a complex electrophoresis tank electrode geometry in conjunction with an electric switching unit, they were able to apply periodically across the gel two different electric fields at right-angles to each other in the horizontal plane²⁰, and large DNAs were again resolved on the basis of molecular mass. PFGE was thus introduced, and was shown to be able to separate DNAs in the 20 000–2 000 000-base size range. Subsequently, variations of the PFGE method were introduced, including orthogonal-field-alternation gel electrophoresis (O-FAGE)²¹, field-inversion gel electrophoresis (FIGE)²², electrophoresis using a contour-clamped homogeneous electric field (CHEF)²³, transverse alternating-field electrophoresis (TAFE)²⁴ and rotating-gel electrophoresis (RGE)^{25–27}. Intact chromosomal DNA molecules have been resolved on these gel systems from a number of lower eukaryotes, including *Saccharomyces cerevisiae*^{20,21,24} and several parasitic protozoa^{26,27}. Such electrophoretic karyotypes have complemented classical genetic mapping in *S. cerevisiae* and have facilitated the study of karyotype^{28,29}, ploidy³⁰, gene location³¹, chromosome polymorphism³² and chromosomal rearrangements^{33,34} in parasitic protozoa which are not amenable to genetic or cytogenetic analysis. PFGE methods have also been used for the separation of large human chromosomal DNA fragments generated with restriction enzymes that cleave the DNA infrequently³⁵, and in the analysis of amplified DNA in cell lines containing double minute chromosomes and homogeneously staining regions³⁶.

There are some basic problems with the first systems used (PFGE and O-FAGE), however. Owing to the non-uniformity of the electric field across the gel, the speed and migration path of DNA would vary from lane to lane and with distance from the wells, along curved trajectories, rendering comparison very poor. In CHEF²³, where the electrodes are clamped around the gel in a hexagonal array (see Fig. 3), the resulting field geometry allows migration of the DNA bands in a straight path towards the opposite gel extreme. The same applies to FIGE²² (Fig. 4) and to TAFE²⁴ (Fig. 5). In fact, with the advent of these systems, it became clear that the term O-FAGE was a misnomer: for optimum separation and performance, the two alternating electric fields did not have to be orthogonal, but at a rather obtuse angle (*ca.* 120°)³⁷. FIGE is in reality an extreme case, where the two electric fields are coupled at 180°, net forward migration being achieved either by employing longer switching intervals between the periodic inversion of the uniform electric field, or higher field strengths in the forward than in the reverse direction³⁸. In a 2D O-FAGE/FIGE run, an unexpected phenomenon of parabolic migration of DNA fragments is experienced, by which small and large DNAs move forward, whereas some intermediate sizes (depending on the pulse frequencies) are arrested in the application well. For this reason Olson³⁸ proposed a three-state model (see Fig. 4) in which some DNA fragments could resonate with given field frequencies, thus spending all their time dwelling in the application slots. The latest version of PFGE is rotating-gel electrophoresis, by which a conventional, continuous electric field is applied and pulsing is obtained by rotating the gel platform (Fig. 6).

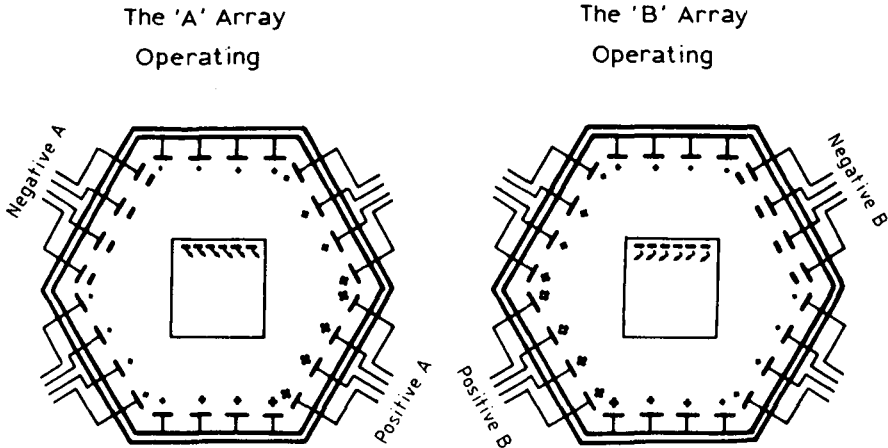


Fig. 3. Diagrammatic representation of the contour-clamped homogeneous electric field (CHEF) electrode format showing the clamped potentials at each electrode (represented by the size of the positive sign) when the A and B electrodes are in operation. The central square represents the agarose gel and the arrows indicate the direction of movement of the DNA out of the wells on activation of the A (right-pointing arrows) or B (left-pointing arrows) electrode couples. This electrode array has been adopted by Pharmacia-LKB to transform the Pulsephor (an O-FAGE-type apparatus) into a CHEF-type instrument. The clamped electrode potentials produce a homogeneous electric field throughout the gel and a field alternation angle of 120° . Reprinted by permission from Dawkins³⁷.

Whereas it appears that PFGE instrumentation has advanced considerably, at the theoretical level the mechanism of DNA migration is still not fully understood. Recent work by Stellwagen and Stellwagen³⁹ has shed more light on PFGE. It appears that, when the DNA molecule is much smaller than the median gel pore diameter, the DNA coil does not have to stretch or to orient. However, when the median pore diameter of the gel is smaller than the contour length of DNA, the DNA molecule becomes both stretched and oriented. However, whereas molecules smaller than *ca.* 4000 bases become completely stretched, larger molecules are only partially stretched. The orientation and stretching of DNA molecules in the gel matrix indicate that end-on migration, or reptation, is a likely mechanism for DNA electrophoresis in agarose. A unique finding³⁹ is that the effect of the pulsed electric field is exerted not

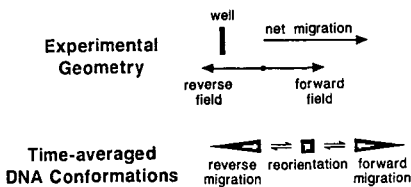


Fig. 4. Scheme of field-inversion gel electrophoresis (FIGE). The top of the diagram indicates the simple electrophoretic geometry. Note that the forward and reverse fields can be of equal strength with longer forward than reverse switching intervals, or the switching intervals can be equal with a higher forward than reverse field, or some combination of inequalities in the field strengths and the switching intervals can be used to achieve net forward migration. The bottom of the diagram presents a simple three-state model for the conformational changes that accompany the field-inversion events. Reproduced by permission from Olson³⁸.

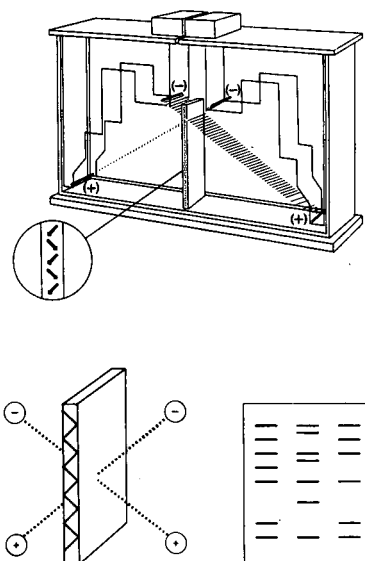


Fig. 5. Schematic diagram of transverse alternating-field electrophoresis (TAFE). The electrodes (+ and -) are wires stretched across the width of the box parallel to the gel faces (note that the gel is standing vertically and that both sides are exposed to the current). The angle formed at the sample loading wells between the fields generated by the electrodes is 115° . TAFE works like other pulsed-field techniques by causing periodic reorientation of DNA molecules under the influence of two alternating electric fields. The technique employs a three-dimensional geometry, causing DNA to zig-zag through the thickness of the gel (see the inset). The result of this movement is that the face of the gel displays perfectly straight migration paths (see lower part of the drawing). Reproduced by kind permission from Beckman Instruments, Palo Alto, CA, U.S.A.

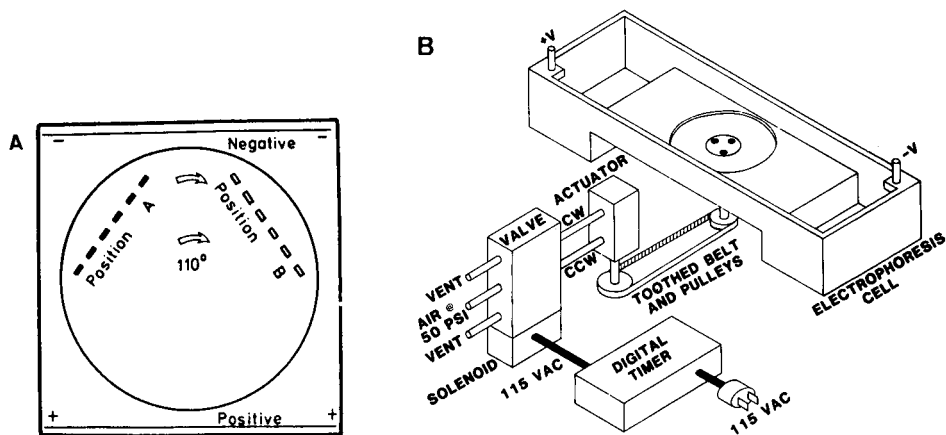


Fig. 6. (A) Diagrammatic representation of the rotating-gel electrophoresis (RGE) apparatus. The gel is subjected to a homogeneous electric field, but the circular gel rotation between positions A and B produces a field alternation on the samples. The optimum angle of the gel rotation is between 110 and 120° . The electric field is interrupted only for the few seconds it takes the gel to rotate to its new position. (B) Schematic diagram of the pneumatic apparatus of Sutherland *et al.*³⁴. The rotating platform holding the gel inside the electrophoresis cell is coupled via a toothed belt and pulleys to a pneumatically driven rotary actuator. Reproduced by permission from Sutherland *et al.*³⁴.

only on the DNA molecules, but also on the gel matrix. It appears that with very short pulses of high amplitude, individual agarose chains or bundles of chains, or dangling ends of the matrix, could be oriented in the field. At longer pulse times and at lower voltages, yet another phenomenon is apparent: larger sections of the agarose gel (microdomains) become oriented in the field. The entire matrix becomes in a way more “fluid”, and this could explain why very large DNA molecules can migrate through the gel. This is a fascinating new finding, and this effect will have to be taken into consideration in all theories of DNA migration under pulsed fields.

5. ELECTROPHORESIS AS A PROBE OF MACROMOLECULAR STRUCTURE

We are all used to the idea of electrophoresis as a powerful tool for macromolecular separation and characterization. However, recent work on DNA electrophoresis has proved that this technique is also a fine probe of structural conformation of this macromolecule. Some striking examples can be given. It is known that DNA molecules of the same size may assume different topologies, including supercoiled, bent, branched or cruciform structures. Recent work with CHEF has shown that such molecules exhibit anomalous shifts in mobility with respect to linear DNA in response to changes in electric field strength⁴⁰. A case in point is shown in Fig. 7: in lane 2, a mixture of linear and supercoiled DNAs, applied in the same sample slot, are

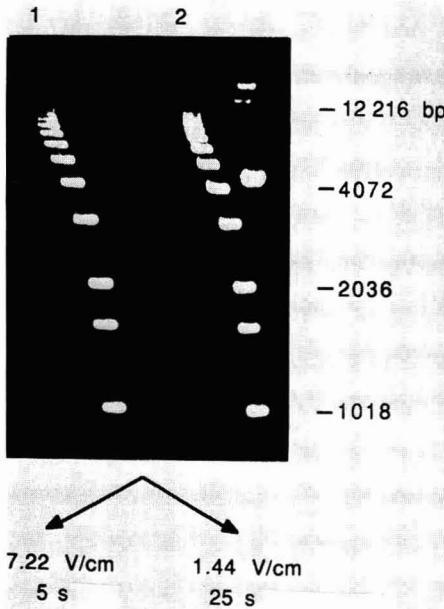


Fig. 7. Separation of DNA by topology. Lane 1 contains linear DNA markers (Bethesda Research Labs. 5615 SA/SB). Lane 2 contains a mixture of the linear DNA markers and pRSV cat plasmid DNA purified by equilibrium centrifugation in caesium chloride. The 5027-base pair (bp) supercoiled plasmid forms the major band that is displaced from the arc of linear molecules. The fainter bands (upper right corner) correspond to the nicked plasmid and supercoiled and nicked dimers. Electrophoresis was performed through a 1% agarose gel in Tris-borate-EDTA buffer (pH 8.3) at 9°C for 22 h. The field strength alternated between 7.22 V/m for 5 s and 1.44 V/cm for 25 s. Reprinted by permission from Chu⁴⁰.

seen to be separated along the migration path. The supercoiled 5027-base pair plasmid (and its dimer) are displaced from the arc of linear DNA molecules and resolved from fragments of the same size by a lateral displacement. This is a unique effect of the CHEF technique; previously, for resolving such topologies, a 2D method had to be employed, as follows.

Electrophoresis was performed under standard conditions in the first dimension. Then the gel was soaked in a DNA intercalating agent such as chloroquine to alter supercoiling. Finally, the gel was rotated by 90° with respect to the electrodes, and subjected to electrophoresis in the second dimension^{41,42}, where the topoisomers would ultimately be resolved.

Even in the absence of a pulsed electric field, conventional electrophoretic analysis can yield a wealth of information on DNA molecular structure. For instance, in the case of branched DNA, Ferguson plot analysis has given excellent information about junction structure, formation, stoichiometry, supramolecular assembly and accessibility to chemical attack⁴³. According to Seeman *et al.*⁴³, gel electrophoresis has been a valid substitute for NMR spectroscopy and crystallography in DNA analysis, even though the two latter techniques can be expected to yield eventually the conformational details of junction structure at higher resolution. According to Fried⁴⁴, measurement of protein–DNA interaction parameters can be performed by electrophoretic mobility shift assays. Under appropriate conditions, both equilibrium constants and rate constants for binding reactions can be obtained through analysis of electrophoretic patterns.

In addition, by performing electrophoresis in gradients of denaturants (*e.g.*, temperature-gradient gel electrophoresis, TGGE), it is possible to analyse conformational transitions and sequence variations of nucleic acids, as well as protein–nucleic acid interactions⁴⁵. For example, when analysing these thermal transition curves under electrophoresis, it is possible to detect point mutations induced in cDNA clones by site-directed mutagenesis⁴⁵. Moreover, the effects of a single amino acid exchange on the thermal stability of a protein–DNA complex can easily be assessed by TGGE. Thus, in the case of the Tet repressor from *E. coli*, containing a Trp → Phe mutation at positions 43 and/or 75, by TGGE analysis it was found that no alteration in binding was induced in the Trp₄₃ mutant, whereas the Trp₇₅ mutation strongly affected the complex DNA–tetracycline (Tet) repressor. Other types of denaturing gradients (urea and formamide) have been used to screen for DNA sequence polymorphism in the human factor VIII gene⁴⁶. These are just some examples of the power of electrophoresis in elucidating some complex structural variations in macromolecules.

6. TWO-DIMENSIONAL MAPS

2D Protein maps have also shown a marked growth. By coupling sequentially a pure charge (IEF) to a pure size [SDS–polyacrylamide gel electrophoresis (SDS-PAGE); the latter orthogonal to the first] fractionation, one can distribute the polypeptide chains on a surface having as coordinates charge and mass (IEF-SDS or ISO-DALT, according to the Andersons' nomenclature)⁴⁷. When the first dimension is performed in immobilized pH gradients, the technique is called IPG-DALT⁴⁸. Fig. 8 gives an example of a 2D map of [³⁵S]methionine-labelled proteins from human

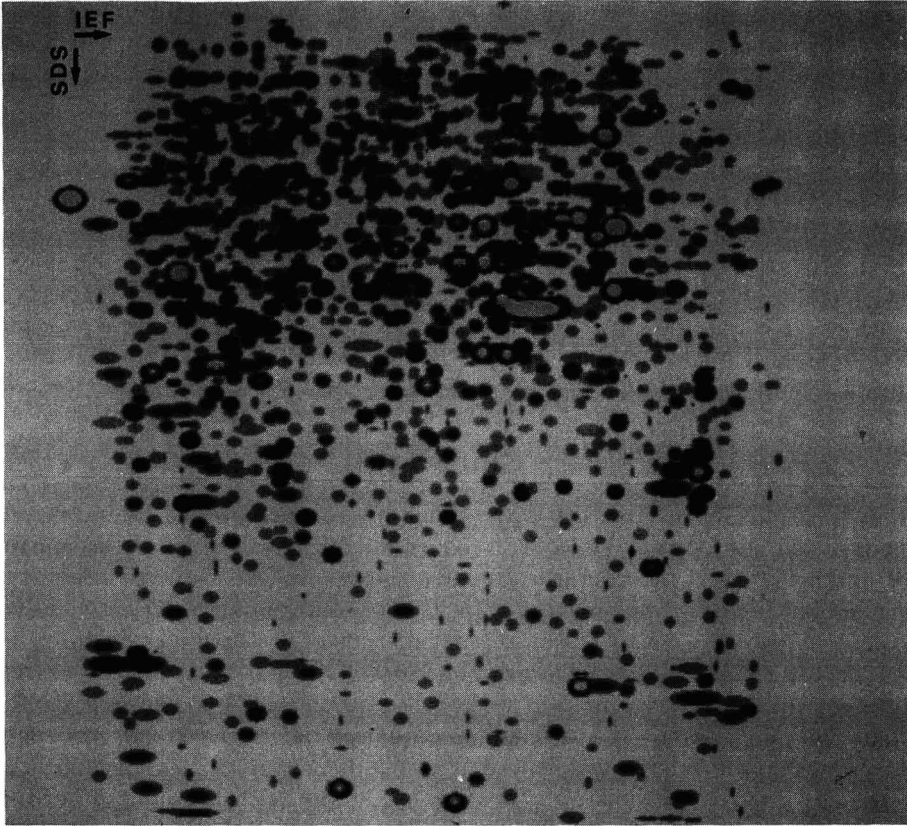


Fig. 8. Synthetic image of the two-dimensional (ISO-DALT) fluorogram of [^{35}S]methionine-labelled proteins from human epithelial amnion cells. There are 1244 spots in this map. Reproduced by permission from Celis *et al.*⁴⁹.

epithelial amnion cells⁴⁹: there is almost an artistic beauty to it, even though the image shown here is synthetic, *i.e.*, it has been redrawn by a computer after digitizing the experimental 2D map and cleaning the background, etc. The technique was reported for the first time by Barrett and Gould⁵⁰ and then described more extensively in 1975 by at least three workers: O'Farrell⁵¹, Klose⁵² and Scheele⁵³.

What is the value of 2D maps? In giant gels (*e.g.*, 30 × 40 cm size)⁵⁴ and on prolonged exposure of radiolabelled material (up to 2 months), the technique is capable of resolving as many as 12 000 spots in a total mammalian cell lysate. Hence it is likely that, in a properly run 2D map, a spot will represent an individual polypeptide chain, uncontaminated by other material co-migrating in the same gel area. On this assumption, and provided that enough material is present in an individual spot (about 1 μg), it is possible to elute it on a glass-fibre filter and to do microsequencing on it⁵⁵.

There are in fact two different strategies. According to Choli *et al.*⁵⁶, without removing the proteins from the membrane, direct microsequencing, enzymatic or chemical fragmentation or hydrolysis for amino acid analysis can be carried out. Simpson *et al.*⁵⁷, however, preferred to extract the Coomassie-stained polypeptides

from the blotting membrane in which they are trapped [usually poly(divinylidene difluoride) membranes] by using a mixture of SDS and Triton X-100. The proteins are then separated from the surfactant mixture by a chromatographic procedure on reversed-phase sorbents at high organic solvent concentration, *i.e.*, under conditions that prevent detergent binding. The proteins are then recovered from the sorbent by adding trifluoroacetic acid and by a decreasing gradient of organic solvent. After proteolytic fragmentation the peptides are analysed on a microbore column and, if needed, eluted for microsequence analysis.

In both instances a general strategy seems to be emerging: owing to the extremely high resolving power of 2D techniques, the possibility of blotting, the ease of the methodology and the availability of unsophisticated and inexpensive equipment, this methodology might replace HPLC techniques for the isolation and microsequencing of proteins.

7. IMMOBILIZED pH GRADIENTS

In 1982, IPGs were introduced, resulting in an increase in resolution of one order of magnitude when compared with conventional IEF⁵⁸. By 1980, it was apparent to many IEF users that there were some inherent problems with the technique, which had not been corrected in more than 20 years of use and were not likely to be solved. In particular, a major phenomenon was the near-isoelectric precipitation of samples of low solubility at the isoelectric point (*pI*) or of components present in large amounts in heterogeneous samples. The inability to reach stable steady-state conditions (resulting in a slow pH gradient loss at the cathodic gel end) and to obtain narrow and ultra-narrow pH gradients, aggravated the situation. Perhaps most annoying was the unreproducibility and non-linearity of pH gradients produced by the so-called "carrier ampholyte" buffers⁵⁹. IPGs proved to be able to abolish all these undesirable phenomena.

IPGs are based on the principle that the pH gradient, which exists prior to the IEF run itself, is copolymerized, and thus insolubilized, within the fibres of a polyacrylamide matrix. This is achieved by using, as buffers, a set of six commercial chemicals (called Immobiline, by analogy with Ampholine) having *pK* values distributed in the pH range 3.6–9.3. Previously, not much was known about the Immobiline chemicals, except that they are acrylamido derivatives, with the general formula $\text{CH}_2=\text{CHCONHR}$, where R denotes a set of two weak carboxyls, with *pK* 3.6 and 4.6, for the acidic compounds, and a set of four tertiary amino groups, with *pK* 6.2, 7.0, 8.5 and 9.3, for the basic buffers. We have recently been able to decode these structures and to give their synthetic routes and purification protocol^{60,61}. We have reported a total of ten such buffers: eight are weak acids and bases, with *pK*s covering the pH range 3.1–10.3, and the other two are a strongly acidic (*pK* 1.0) and a strongly basic (*pK* > 12) titrant which were introduced in 1984 by Gianazza *et al.*⁶² for producing linear pH gradients covering the entire pH 3–10 range (computer simulations had shown that, in the absence of these two titrants, extended pH intervals would exhibit strong deviations from linearity at the two extremes, as the most acidic and most basic of the commercial Immobilines would act simultaneously as buffers and titrants)⁶³.

With these additional Immobilines, it has been possible to extend the fraction-

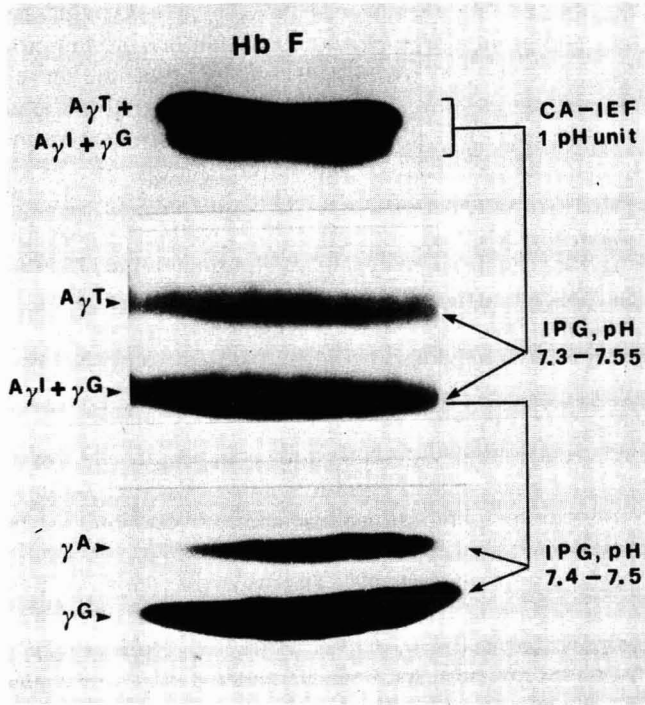


Fig. 9. Focusing of umbilical cord lysates from an individual heterozygous for foetal haemoglobin (Hb F) Sardinia (for simplicity, only the HbF bands are shown, and not the two other major components of cord blood, *i.e.*, Hb A and Hb F_{ac}). Top: focusing performed in a 1 pH unit span in the presence of carrier ampholytes (CA-IEF). Note that broadening of the Hb F zone occurs, but not splitting into well defined zones. Centre: same sample, but focused over an IPG range spanning 0.25 pH unit. Bottom: focusing of the lower band in central panel, but in an IPG gel spanning 0.1 pH unit. The resolved A γ /G γ bands are in a 20:80 ratio, as theoretically predicted from gene expression. Their identity was ascertained by eluting the two zones and fingerprinting the γ chains. Modified from Cossu and Righetti⁷⁶; reproduced by permission of Elsevier.

ation capability to strongly acidic proteins⁶⁴, as the pH gradient could be extended to as low as pH 2.5, and to strongly alkaline species⁶⁵. Given the evenly spaced pK values along the pH scale, it is clear that the set of ten chemicals proposed (eight buffers and two titrants) is adequate to ensure linear pH gradients along the pH 2.5–11 axis (the ideal ΔpK for linearity would be 1 pH unit between two adjacent buffers). For a more detailed treatise on how to run an IPG gel and how to use IPG recipes, the reader is referred to an extensive manual⁶⁶ and to a recent review⁶⁷.

Owing to the much increased resolution of IPGs, a number of so-called “electrophoretically silent” mutations (bearing amino acid replacements with no ionizable groups in the side-chains) have now been fully resolved. An illustration is shown in Fig. 9: two foetal human haemoglobin (Hb F) phenotypes, A γ and G γ , with an Ala \rightarrow Gly substitution in residue 136 of the γ chains, are fully resolved in IPGs, although their difference in surface charge (ΔpI) is barely 0.003 pH unit. This is an exceptional separation: in reality, what we are showing is that IPGs are able to detect not just a

difference of a single amino acid (out of a total of *ca.* 600), but a difference of one carbon atom out of total of >2000 in the haemoglobin molecule (disregarding the three protons of the methyl group).

8. CAPILLARY ZONE ELECTROPHORESIS

It is proposed not to elaborate extensively on this technique, and only a brief discussion will be presented. CZE appears to be a most powerful technique, perhaps equalling the resolving power of IPG. If one assumes that longitudinal diffusion is the only significant source of zone broadening, then the number of theoretical plates (N) in CZE is given by⁶⁸

$$N = \mu V / 2D$$

where μ and D are the electrophoretic mobility and diffusion coefficient, respectively, of the analyte and V is the applied voltage. This equation shows that high voltage gradients are the most direct route to high separation efficiencies. For proteins, it has been calculated that N could be as high as 10^6 theoretical plates.

Fig. 10 is a schematic diagram of a CZE system⁶⁹. The fused-silica capillary has a diameter of 50–80 μm and a length up to 1 m. It is suspended between two reservoirs, connected to a power supply that is able to deliver up to 30 kV (typical operating currents being of the order of 10–100 μA). One of the simplest ways of introducing the sample into the capillary is by electromigration, *i.e.*, by dipping the capillary extremity into the sample reservoir, under voltage, for a few seconds.

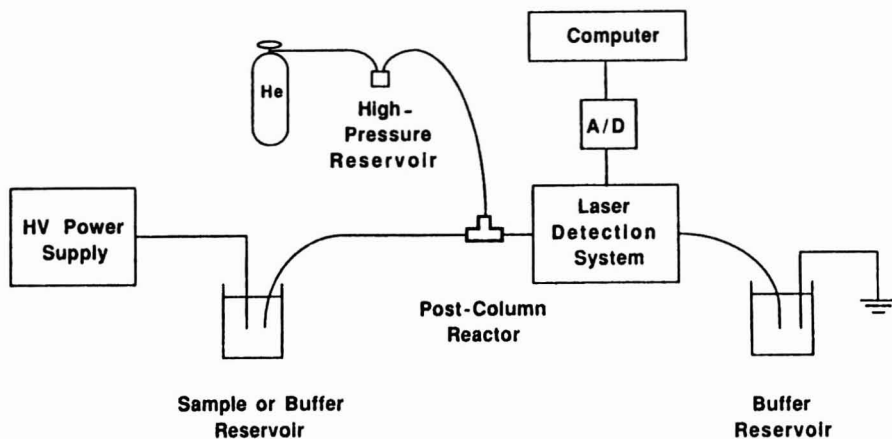


Fig. 10. Scheme of a CZE apparatus. The high-voltage (HV) power supply can deliver up to 30 kV. The fused-quartz capillary generally has an I.D. of 50–80 μm . The detector consists of a beam from a high-pressure mercury–xenon arc lamp source oriented perpendicular to the electric migration path, at the end of the capillary. The sample signal (generally emitted fluorescence) is measured with a photomultiplier and a photometer connected to the analogue–digital converter of a multi-function interface board mounted on a microcomputer. In the scheme reproduced here, postcolumn sample derivatization is obtained by reacting the sample zones with *o*-phthalaldehyde. A/D = Analog-to-digital converter. Reproduced by permission from Rose and Jorgenson⁶⁹.

Detection is usually accomplished by on-column fluorescence and/or UV absorption. Conductivity and thermal detectors, as employed in isotachopheresis, exhibit too low a sensitivity in CZE. The reason for this stems from the fact that the flow cell where sample monitoring occurs has a volume of only *ca.* 0.5 nl, allowing sensitivities down to the femtomole level. In fact, with the postcolumn derivatization method in Fig. 10, a detection limit for amino acids of the order of femtograms is claimed, which means working in the attomole range⁶⁹.

By forming a chiral complex with a component of the background electrolyte (Cu aspartame), it is possible to resolve racemates of amino acids⁷⁰. Even neutral organic molecules can be made to migrate in CZE by complexing them with charged ligands, such as SDS. This introduces a new parameter, a hydrophobicity scale, in electrokinetic migrations. For more on CZE, readers are referred to the Proceedings of the First International Symposium on High-Performance Capillary Electrophoresis⁷¹ and to other papers presented at this meeting. Review papers have also appeared recently^{14,72,73}.

However, it should not be thought that there are no problems with CZE. According to Pickering⁷⁴, CZE is a good complement to HPLC, but not without its own problems. To quote: "in absolute terms, mass sensitivity is good, but relatively high sample concentrations are needed, which means that reports of femtomoles analysed must be taken with some reservations. Selectivity is not outstanding, and reproducibility and quantitation raise questions that need to be addressed".

9. CHROMATOPHORESIS

This survey concludes by mentioning the latest development, chromatopheresis⁷⁵. In a way, this is a variant of 2D techniques, but it is unique under many respects. Classical 2D maps couple a charge (IEF) to a mass (SDS-PAGE) fractionation, whereas in this new analytical technology, reversed-phase HPLC is coupled in a real-time automated system to SDS-PAGE.

Fig. 11 gives an example of how this is achieved: proteins eluting from the HPLC column pass through a UV detector (UV) to a heated micromixing chamber (protein reaction system, PRS). Polypeptides in the eluate are denatured and complexed with SDS on mixing with the standard protein reaction cocktail (PRC) containing SDS, 2-mercaptoethanol and buffer. The SDS-protein complexes reach the SDS gel slab through an outlet lying flush on the surface of the stacking gel of a discontinuous polyacrylamide gradient gel. The capillary delivering the column eluate is moved across the gel surface by a computer-controlled tracking system, in such a way that the entire gel width accommodates, by the end of this sweeping process, the entire column eluate. Eluate delivery to the SDS-gel slab is performed under a moderate voltage gradient, so that each liquid element dispenses immediately its protein content to the stacking gel, thus minimizing side diffusion (there are no sample application slots). The height of the stacking gel is in general higher than in conventional gels, so that the stacking process can be continued for up to 1 h, if needed; hence, by the time the entire column eluate reaches the interface of the running gel, all the protein zones are aligned horizontally.

This seems to be a useful approach and it could provide a clue as to where the field of electrophoresis is moving: perhaps toward a more intense integration with

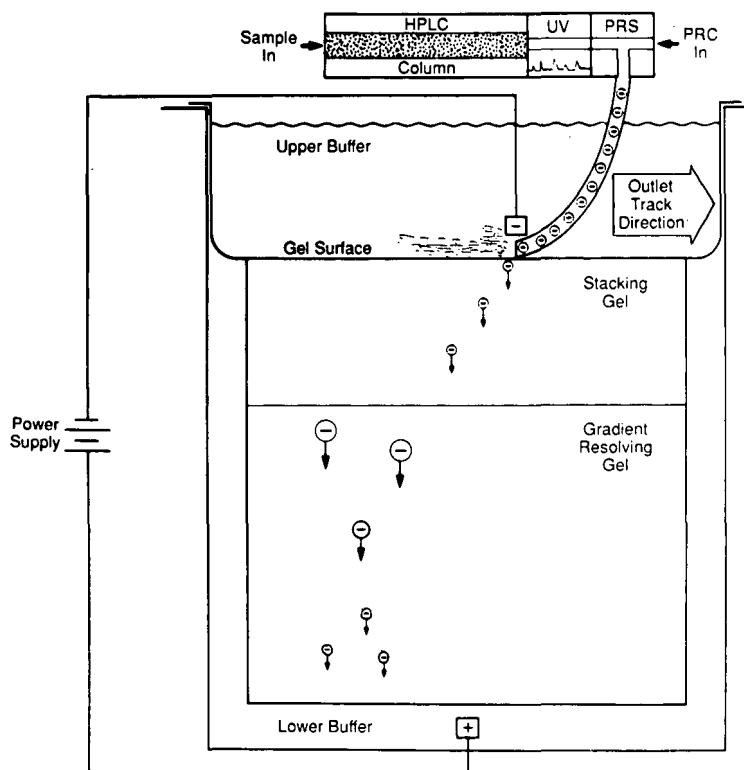


Fig. 11. Schematic illustration of the electrophoretic transfer of proteins in the chromatophoresis process. For details, see text. Reproduced by permission from Burton *et al.*⁷⁵.

chromatography. It now appears that the circle is closing: we are going back to moving boundary electrophoresis, as Tiselius, when starting electrophoresis at the Faculty of Science in Uppsala, also greatly encouraged work in chromatography. The two sciences started together then, divorced on the way and might end up united again.

10. CONCLUSION

A review in any field is always a damnation and a blessing: a damnation for the reviewer, who will come under attack by those scientists not mentioned, and a blessing for the reader, who will greatly benefit from a well written and well organized review. It is hoped that this review will prove useful, but I am willing to be damned, as I am sure I have unjustly left out many good articles which had to be sacrificed for lack of space or personal ignorance. A review also runs often the risk of being a personal recollection of the author's own experience and developments in a given field. In order to avoid that, I have on purpose expanded the field of nucleic acid electrophoresis, as I can claim no contributions in this field, in the hope also of focusing on this fascinating field.

Finally, some recent, special volumes of *Journal of Chromatography, Biomedical Applications*⁷⁷⁻⁷⁹, dedicated to selected topics in biomedical chromatography and electrophoresis can be mentioned, where readers will find ample additional information.

11. ABBREVIATIONS

A	adenine
A/D	analog-to-digital converter
bp	base pairs
C	cytosine
CA	carrier ampholytes (Ampholine)
CHEF	contour-clamped homogeneous electric field
CZE	capillary zone electrophoresis
2D	two-dimensional
DNA	deoxyribonucleic acid
FIGE	field-inversion gel electrophoresis
G	guanine
Hb	haemoglobin
Hb A	human adult haemoglobin
Hb F _{ac}	human acetylated foetal hemoglobin
HPLC	high-performance liquid chromatography
HV	high voltage
IEF	isoelectric focusing
IEF-SDS	same as ISO-DALT
IPG	immobilized pH gradient
IPG-DALT	same as ISO-DALT except that immobilized pH gradients are used for the first dimension
ISO-DALT	isoelectric focusing followed by sodium dodecyl sulphate electrophoresis at right-angles
<i>N</i>	number of theoretical plates
NBD	4-chloro-7-nitrobenzo-2-oxa-1-diazole
NMR	nuclear magnetic resonance
O-FAGE	orthogonal field-alternation gel electrophoresis
PAGE	polyacrylamide gel electrophoresis
PFGE	pulsed-field gel electrophoresis
PMT	photomultiplier tube
RGE	rotating-gel electrophoresis
SDS	sodium dodecyl sulphate
T	thymine
TAFE	transverse alternating field electrophoresis
TGGE	temperature-gradient gel electrophoresis
Trp	tryptophan
UV	ultraviolet

12. ACKNOWLEDGEMENTS

The author's research quoted here has been supported over the years by grants from Consiglio Nazionale delle Ricerche (CNR), Progetti Finalizzati Biotecnologie and Chimica Fine II, and by Ministero della Pubblica Istruzione (MPI), Rome, Italy.

ABSTRACT

13. Given the recent extended review by Vesterberg [*J. Chromatogr.*, 480 (1989) 3–19] of electrokinetic methods, this survey has been restricted to the last decade, which has seen tremendous progress in several fields. DNA electrophoresis has experienced strong developments, both in the sequencing strategies (which have been largely automated with the use of fluorescent probes) and in pulsed field analysis of mega-DNA fragments, which has seen such developments as inverse-field, contour-clamped and rotating gel platforms, all allowing for straight band migration in each lane. Chromosome size mapping has now become a reality. Two-dimensional (2D) maps have also shown a dramatic improvement in performance, largely through the development of immobilized pH gradients, giving highly reproducible protein spots in the 2D plane and allowing the exploration of very narrow pH regions. Blotting techniques, combined with 2D mapping, allow sequence analysis and fingerprinting of a single polypeptide spot in a complex sample without resorting to lengthy chromatographic purification steps. Chromatophoresis generates a novel type of 2D mapping, based on hydrophobicity vs. size, rather than on charge vs. size, by direct coupling of a reversed-phase high-performance liquid chromatographic (HPLC) eluate to sodium dodecyl sulphate electrophoresis. The new rising star, capillary zone electrophoresis, offers speed, a large number of theoretical plates, selectivity and small sample requirements in a highly automated equipment.

REFERENCES

- 1 O. Vesterberg, *J. Chromatogr.*, 480 (1989) 3–19.
- 2 P. G. Righetti, *J. Biochem. Biophys. Methods*, 19 (1989) 1–20.
- 3 E. Boschetti, *J. Biochem. Biophys. Methods*, 19 (1989) 21–30.
- 4 F. Sanger, S. Nicklen and A. R. Coulson, *Proc. Natl. Acad. Sci. U.S.A.*, 74 (1977) 5463–5467.
- 5 A. M. Maxam and W. Gilbert, *Proc. Natl. Acad. Sci. U.S.A.*, 74 (1977) 560–564.
- 6 R. Baer, A. T. Bankier, M. Biffin, P. L. Deininger, P. J. Farrel, T. J. Gibson, G. Hatfull, G. S. Hudson and S. C. Satchwell, *Nature (London)*, 310 (1984) 207–211.
- 7 F. Sanger, G. F. Hong, D. F. Hill and G. B. Petersen, *J. Mol. Biol.*, 162 (1982) 729–773.
- 8 L. M. Smith, J. Z. Sanders, R. J. Kaiser, P. Hughes, C. Dodd, C. R. Connel, C. Heiner, S. B. H. Kent and L. E. Hood, *Nature (London)*, 321 (1986) 674–679.
- 9 L. M. Smit, S. Fung, M. W. Hunkapillar, T. J. Hunkapillar and L. Hood, *Nucleic Acid Res.*, 13 (1985) 2399–2412.
- 10 J. M. Prober, G. L. Trainor, R. J. Dam, F. W. Hobbs, C. W. Robertson, R. J. Zagursky, A. J. Cocuzza, M. A. Jensen and K. Baumeister, *Science (Washington, D. C.)*, 238 (1987) 336–341.
- 11 W. Ansorge, B. S. Sproat, J. Stegemann and C. Schwager, *J. Biochem. Biophys. Methods*, 13 (1986) 315–323.
- 12 P. G. Righetti, M. Chiari, E. Casale, C. Chiesa, T. Jain and R. Shorr, *J. Biochem. Biophys. Methods*, 19 (1989) 37–50.
- 13 C. Gelfi, A. Canali, P. G. Righetti, P. Vezzoni, C. Smith, M. Mellon, T. Jain and R. Shorr, *Electrophoresis*, 11 (1990) in press.
- 14 B. L. Karger, A. S. Cohen and A. Guttman, *J. Chromatogr.*, 492 (1989) 585–614.

- 15 O. J. Lumpking and B. H. Zimm, *Biopolymers*, 11 (1982) 2315–2316.
- 16 P. G. Righetti, B. C. W. Brost and R. S. Snyder, *J. Biochem. Biophys. Methods*, 4 (1981) 347–363.
- 17 M. Davidson and W. Szybalski, in A. D. Hershey (Editor), *The Bacteriophage Lambda*, Cold Spring Harbour Laboratory, New York, 1971, pp. 45–50.
- 18 L. S. Lerman and H. L. Frisch, *Biopolymers*, 21 (1982) 995–997.
- 19 D. C. Schwartz, W. Saffran, J. Welsh, R. Haas, M. Goldenberg and C. R. Cantor, *Cold Spring Harbour Symp. Quant. Biol.*, 47 (1983) 189–195.
- 20 D. C. Schwartz and C. R. Cantor, *Cell*, 37 (1984) 67–75.
- 21 G. F. Carle and M. V. Olson, *Nucleic Acid Res.*, 12 (1984) 5647–5664.
- 22 G. F. Carle, M. Frank and M. V. Olson, *Science (Washington, D. C.)*, 232 (1986) 65–68.
- 23 G. Chu, D. Vollrath and R. W. Davis, *Science (Washington, D. C.)*, 234 (1986) 1582–1585.
- 29 K. Gardiner, W. Laas and D. Patterson, *Somatic Cell Mol. Genet.*, 12 (1986) 185–195.
- 25 R. Anand, *Trends Genet.*, 2 (1986) 278–283.
- 26 E. M. Southern, R. Anand, W. R. A. Brown and D. S. Fletcher, *Nucleic Acid Res.*, 15 (1987) 5925–5943.
- 27 P. Serwer, *Electrophoresis*, 8 (1987) 301–304.
- 28 I. Bancroft and C. P. Wolk, *Nucleic Acid Res.*, 16 (1988) 7405–7418.
- 29 S. M. Clark, E. Lai, B. W. Birren and L. Hood, *Science (Washington, D. C.)*, 241 (1988) 1203–1205.
- 30 B. W. Birren, E. Lai, S. M. Clark, L. Hood and M. I. Simon, *Nucleic Acid Res.*, 16 (1988) 7563–7582.
- 31 P. G. Watebury and M. J. Lane, *Nucleic Acid Res.*, 15 (1987) 3930–3935.
- 32 D. Vollrath and R. W. Davis, *Nucleic Acid Res.*, 15 (1987) 7865–7876.
- 33 M. Y. Graham, I. Otani, T. Boime, M. V. Olson, G. F. Carle and D. D. Chaplin, *Nucleic Acid Res.*, 15 (1987) 4437–4448.
- 34 J. Sutherland, D. Monteleone, J. Mugavero and J. Trunk, *Anal. Biochem.*, 162 (1987) 511–520.
- 35 C. L. Smith, T. Matsumoto, O. Niwa, S. Kico, J. B. Fan, M. Yanagida and C. R. Cantor, *Nucleic Acid Res.*, 15 (1987) 4481–4689.
- 36 C. L. Smith, P. E., Warburton, A. Gaal and C. R. Cantor, in J. K. Setlow and A. Hollaender (Editors), *Genetic Engineering*, 8 (1986) 45–70.
- 37 H. J. S. Dawkins, *J. Chromatogr.*, 492 (1989) 615–639.
- 38 M. V. Olson, *J. Chromatogr.*, 470 (1989) 377–383.
- 39 N. C. Stellwagen and J. Stellwagen, *Electrophoresis*, 10 (1989) 332–334.
- 40 G. Chu, *Electrophoresis*, 10 (1989) 290–295.
- 41 S. K. Brahmachari, R. K. Mishra, R. Bagga and N. Ramesh, *Nucleic Acid Res.*, 17 (1989) 7273–7281.
- 42 N. Ranesh and S. K. Brahmachari, *Indian J. Biochem. Biophys.*, 25 (1988) 542–547.
- 43 N. C. Seeman, J. H. Chen and N. R. Kallenbach, *Electrophoresis*, 10 (1989) 345–354.
- 44 M. G. Fried, *Electrophoresis*, 10 (1989) 366–376.
- 45 D. Riesner, G. Steger, R. Zimmat, R. A. Owens, M. Wagenhöfer, W. Hillen, S. Vollbach and K. Henco, *Electrophoresis*, 10 (1989) 377–389.
- 46 M. Collins, S. F. Wolf, L. L. Haines and L. Mitscock, *Electrophoresis*, 10 (1989) 390–396.
- 47 N. G. Anderson and N. L. Anderson, *Clin. Chem.*, 28 (1982) 739–748.
- 48 E. Gianazza, S. Astrua-Testori, P. Giacon and P. G. Righetti, *Electrophoresis*, 6 (1985) 332–339.
- 49 J. E. Celis, G. P. Ratz, A. Celis, P. Madsen, B. Gessen, S. Kwell, H. V. Nielsen, H. Ydel, J. B. Lauridsen and B. Basse, *Leukemia*, 2 (1988) 561–601.
- 50 T. Barret and H. J. Gould, *Biochim. Biophys. Acta*, 294 (1973) 165–170.
- 51 P. O'Farrell, *J. Biol. Chem.*, 250 (1975) 4007–4021.
- 52 J. Klose, *Humangenetik*, 26 (1975) 231–243.
- 53 G. A. Scheele, *J. Biol. Chem.*, 250 (1975) 5375–5385.
- 54 R. A. Colbert, J. M. Amatruda and D. S. Young, *Clin Chem.*, 30 (1984) 2053–2058.
- 55 R. H. Aebersold, J. Leavitt, L. E. Hood and S. B. H. Kent, in K. Walsh (Editor), *Methods in Protein Sequence Analysis*, Humana Press, Clifton, NJ, 1987, pp. 277–294.
- 56 T. Choli, U. Kapp, and B. Wittmann-Liebold, *J. Chromatogr.*, 476 (1989) 59–72.
- 57 R. J. Simpson, L. D. Ward, G. E. Reid, M. P. Batterham and R. L. Moritz, *J. Chromatogr.*, 476 (1989) 345–361.
- 58 B. Bjellqvist, K. Ek, P. G. Righetti, E. Gianazza, A. Görg, W. Postel and R. Westermeier, *J. Biochem. Biophys. Methods*, 6 (1982) 317–339.
- 59 P. G. Righetti, *Isoelectric Focusing: Theory, Methodology and Applications*, Elsevier, Amsterdam, 1983.
- 60 M. Chiari, E. Casale, E. Santaniello and P. G. Righetti, *Appl. Theor. Electrophoresis*, 1 (1989) 99–102.

- 61 M. Chiari, E. Casale, E. Santaniello and P. G. Righetti, *Appl. Theor. Electrophoresis*, 1 (1989) 103–107.
- 62 E. Gianazza, F. Celéntano, G. Dossi, B. Bjellqvist and P. G. Righetti, *Electrophoresis*, 5 (1984) 88–97.
- 63 G. Dossi, F. Celéntano, E. Gianazza and P. G. Righetti, *J. Biochem. Biophys. Methods*, 7 (1983) 123–142.
- 64 P. G. Righetti, M. Chiari, P. K. Sinha and E. Santaniello, *J. Biochem. Biophys. Methods*, 16 (1988) 185–192.
- 65 C. Gelfi, M. L. Bossi, B. Bjellqvist and P. G. Righetti, *J. Biochem. Biophys. Methods*, 15 (1987) 41–48.
- 66 P. G. Righetti, *Immobilized pH Gradients: Theory and Methodology*, Elsevier, Amsterdam, 1990.
- 67 P. G. Righetti, E. Gianazza, C. Gelfi, M. Chiari and P. K. Sinha, *Anal. Chem.*, 61 (1989) 1602–1612.
- 68 J. W. Jorgenson, in J. W. Jorgenson and M. Phillips (Editors), *New Directions in Electrophoretic Methods (ACS Symposium Series, Vol. 335)*, American Chemical Society, Washington, DC, 1987, pp. 70–93.
- 69 D. J. Rose, Jr. and J. W. Jorgenson, *J. Chromatogr.*, 447 (1988) 117–131.
- 70 P. Gozel, E. Gassmann, H. Michelsen and R. N. Zare, *Anal. Chem.*, 59 (1987) 44–49.
- 71 B. L. Karger (Guest Editor), *1st International Symposium on High-Performance Capillary Electrophoresis; J. Chromatogr.*, 480 (1989) 1–435.
- 72 M. J. Gordon, X. Hung, S. L. Pentaney, Jr. and R. N. Zare, *Science (Washington, D. C.)*, 242 (1988) 224–229.
- 73 R. A. Wallingford and A. G. Ewing, *Adv. Chromatogr.*, 25 (1989) 1–76.
- 74 M. V. Pickering, *LC-GC Int.*, 2 (1989) 20–26.
- 75 W. G. Burton, K. D. Nugent, T. K. Slattery, B. R. Summers and R. L. Snyder, *J. Chromatogr.*, 443 (1988) 363–379.
- 76 G. Cossu and P. G. Righetti, *J. Chromatogr.*, 398 (1987) 211–216.
- 77 Z. Deyl and M. T. W. Hearn (Guest Editors), *Separation of Biopolymers and Supramolecular Structures; J. Chromatogr.*, 418 (1987) 1–392.
- 78 Z. Deyl and P. M. Kabra (Guest Editors), *Chromatography and Electrophoresis in Routine Clinical Analysis; J. Chromatogr.*, 429 (1988) 1–452.
- 79 Z. Deyl and U. A. Th. Brinkman (Guest Editors), *Special Topics in Biomedical Chromatography and Electrophoresis; J. Chromatogr.*, 492 (1989) 1–662.

CHROM. 22 561

Separation of highly hydrophobic compounds by cyclodextrin-modified micellar electrokinetic chromatography

SHIGERU TERABE*^a, YOSUKE MIYASHITA and OSAMU SHIBATA

Department of Industrial Chemistry, Faculty of Engineering, Kyoto University, Sakyo-ku, Kyoto 606 (Japan)

ELIZABETH R. BARNHART, LOUIS R. ALEXANDER and DONALD G. PATTERSON

Toxicology Branch, Center for Disease Control, Public Health Service, Atlanta, GA 30333 (U.S.A.)

BARRY L. KARGER

Barnett Institute, Northeastern University, Boston, MA 02115 (U.S.A.)

and

KEN HOSOYA and NOBUO TANAKA

Department of Polymer Science and Engineering, Kyoto Institute of Technology, Sakyo-ku, Kyoto 606 (Japan)

ABSTRACT

Cyclodextrin-modified micellar electrokinetic chromatography (CD-MEKC), in which CD is added to the micellar solution, was developed for the separation of electrically neutral, highly hydrophobic compounds. The separation of such substances is generally difficult by electrophoretic techniques. In CD-MEKC, a water-insoluble hydrophobic solute is partitioned between the micelle and CD. When the solute is included in the CD cavity it migrates with the electroosmotic velocity, and when it is incorporated into the micelle it migrates with the micellar velocity. Accordingly, the differential partition of the solute between CD and the micelle enables a separation to be achieved. Highly hydrophobic and closely related compounds such as chlorinated benzene congeners, polychlorinated biphenyl congeners, tetrachlorodibenzo-*p*-dioxin isomers and polycyclic aromatic hydrocarbons have been successfully separated.

INTRODUCTION

Electrokinetic chromatography (EKC)¹ is a branch of both high-performance capillary electrophoresis (HPCE) and high-performance liquid chromatography (HPLC). From the viewpoint of electrophoresis, EKC is especially effective for the

^a Present address: Department of Material Science, Faculty of Science, Himeji Institute of Technology, 2167 Shosha, Himeji, Hyogo 671-22 Japan.

separation of electrically neutral substances, which cannot be separated in principle by conventional HPCE. Micellar EKC (MEKC)²⁻⁴, in which an ionic micelle migrates electrophoretically with a different velocity from that of the bulk solution, is the most popular technique among various forms of EKC. The separation principle of MEKC is based on the differential partition of the solute between the micelle and the surrounding aqueous phase, as micellar chromatography, but it has an extremely high efficiency in comparison with HPLC. Therefore, MEKC is a powerful technique for the separation of various neutral substances⁵⁻⁹; further, it also improves the selectivity of ionic substances in contrast with conventional HPCE¹⁰⁻¹⁴. Another useful application of MEKC is optical resolution with a mixed micelle of a chiral compound^{15,16} or with a chiral micelle^{17,18}.

In addition to MEKC, cyclodextrin (CD) EKC^{1,19}, ligand-exchange EKC²⁰, borate-complex EKC^{21,22} and ion-exchange EKC^{1,23} have been reported. Each of these methods has extended the applicability of HPCE to the analysis of various types of compounds. However, the separation of non-polar and highly hydrophobic compounds has not been reported, except for one paper²⁴, in which a tetraalkyl-ammonium ion was used as a carrier of EKC (electrophoretically migrating phase)¹ in an aqueous organic solvent to separate some aromatic hydrocarbons.

As a preliminary experiment, we tried to separate polycyclic aromatic hydrocarbons (PAHs) by MEKC at the early stage of the development of EKC²⁵, but PAHs were so hydrophobic that they were almost totally incorporated into the micelle. The use of aqueous organic solvents increased the distribution of PAHs to the aqueous phase but still the resolution was not very successful because of tailed peaks²⁵.

Some PAHs whose molecular weights were less than 200 were successfully separated by CD-EKC with a β -CD derivative having a 2-amino ethylamino group^{1,26}, but aqueous organic solvents such as 50% aqueous methanol had to be used in order to increase the solubility of the PAHs. The separation of larger PAHs seemed difficult because of the extremely low solubility into solvents compatible with CD-EKC.

This paper describes CD-modified MEKC (CD-MEKC), in which a neutral CD is added to the micellar solution. CD itself is electrically neutral and its outside surface is hydrophilic; accordingly, it will not interact with the micelle. Therefore, CD in the micellar solution should behave as another phase against the micelle, and migrate with an identical velocity with the bulk solution. When a highly hydrophobic substance, which is insoluble in water, is injected into the CD-MEKC system, it will distribute itself between the micelle and CD, as shown in Fig. 1. Such a hydrophobic solute is incorporated by either the micelle or CD, but it does not exist in the aqueous medium. It should be noted that the aqueous phase in MEKC is seemingly displaced by CD in CD-MEKC for hydrophobic compounds and that water is an inert solvent only for the micelle and CD and not for the analytes.

The capacity factor, \tilde{k}' , of a highly hydrophobic solute in CD-MEKC is given by

$$\tilde{k}' = \frac{n_{mc}}{n_{CD}} = K \cdot \frac{V_{mc}}{V_{CD}} \quad (1)$$

where n_{CD} and n_{mc} are the total amounts of the solute included by CD and those of the solutes incorporated by the micelle, respectively, V_{CD} and V_{mc} are the volumes of CD

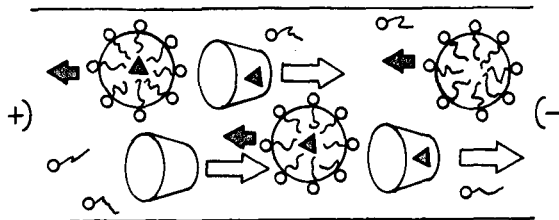


Fig. 1. Schematic illustration of the separation principle of CD-MEKC. Filled arrows indicate the electrophoretic migration of the micelle and open arrows the electroosmotic migration of CD.

and the micelle, respectively, and K is the distribution coefficient. The capacity factor is proportional to the phase (volume) ratio of the micelle to CD. The distribution coefficient means the relative affinity of the solute between CD and the micelle. The ratio of the solute incorporated in the micelle depends on its hydrophobicity but the inclusion-complex formation of the solute with CD depends on the concordance of the solute molecular size with the cavity diameter of CD in addition to the hydrophobicity. Consequently, the selectivity in CD-MEKC will be mostly determined by the tendency of the solute to form an inclusion complex with CD.

The purpose of this study was to explore the applicability of CD-MEKC to the separation of highly hydrophobic and closely related compounds, such as polychlorinated biphenyls (PCBs), tetrachlorodibenzo-*p*-dioxin (TCDD) isomers and PAHs. These compounds are generally separated by capillary gas chromatography (GC) or by HPLC. HPCE and EKC have advantages common to either of capillary GC or HPLC: (1) they require small amounts of samples as in capillary GC; (2) they give highly efficient resolution as in capillary GC; and (3) they are compatible with the analysis of biological fluids as in HPLC. Consequently, HPCE and EKC are considered to be very useful techniques for the analysis of minute amounts of biological fluids or environmental samples if sensitive detectors such as mass spectrometers or laser-induced fluorescence spectrophotometers become readily available.

EXPERIMENTAL

Apparatus

Fused-silica capillary tubes from two different commercial sources were employed to obtain different electroosmotic velocities: Scientific Glass Engineering (Ringwood, Victoria, Australia) (0.05 mm I.D., 0.25 mm O.D.) and Polymicro Technologies (Phoenix, AZ, U.S.A.) (0.05 mm I.D., 0.37 mm O.D.). The total length was 650 or 700 mm and the effective length to the detector was 500 mm for either tube.

The separation of PCBs and TCDD isomers was exclusively performed at the Toxicology Branch of the Center for Disease Control (CDC) on Chamblee Campus. A regulated high-voltage power supply laboratory-made in Northeastern University, which was operated under either constant voltage or current conditions, an ISCO (Lincoln, NE, U.S.A.) V⁴ spectrophotometric detector, the cell holder of which was modified to accommodate the capillary tube for on-column detection, and a Shimadzu (Columbia, MD, U.S.A.) C-R3A data processor were employed to build an HPCE

instrument. The detector was operated at 220 nm. An HPLC system, which consisted of a Waters Assoc. (Milford, MA, U.S.A.) Model 6000A pump, a Rheodyne (Cotati, CA, U.S.A.) Model 7125 injector and a Waters Assoc. Model 990 multi-channel absorbance detector, was used for the HPLC separation of trichlorobiphenyl isomers with Cyclobond I (β -CD bonded phase) and Cyclobond II (γ -CD bonded phase) (Advanced Separation Technologies, Whippany, NJ, U.S.A.).

The EKC separation of chlorinated benzenes and PAHs was mainly performed at Kyoto University using essentially the same apparatus as described previously^{2,3}. UVIDEC-100-IV and V spectrophotometric detectors (JASCO, Tokyo, Japan), which were operated at 210 nm, and HRS-24p and HeppLL-30N regulated high-voltage power supplies (Matsusada Precision Devices, Kusatsu, Shiga, Japan), which were operated under constant-voltage conditions, were employed to construct the apparatus.

Reagents

All of the PCB congeners employed were purchased from Ultra Scientific (Kingstown, RI, U.S.A.) and used without further purification. TCDD isomers were synthesized at the Toxicology Branch of CDC²⁷. Chlorinated benzene congeners and CDs from Nacalai Tesque (Kyoto, Japan) were used as received. PAHs were obtained from Accustandard (New Haven, CT, U.S.A.). Other reagents used for the preparation of the separation solutions or as solvents for the samples were of analytical-reagent grade. All of the micellar solutions were filtered through a membrane filter of 0.45- μ m pore size prior to use.

Procedure

Most solutes were injected as methanol solutions by the siphoning method. When a sample was poorly soluble in methanol, tetrahydrofuran (THF) or dimethyl sulphoxide (DMSO) was added to methanol in an appropriate proportion to give a sample solution. Hexachlorobenzene was dissolved in ethanol. The capillaries were washed with DMSO or THF and with borate buffer that was used for the preparation of the micellar solution when the peaks became broad and tailed.

RESULTS AND DISCUSSION

Separation of chlorinated benzene congeners

The total number of chlorinated benzene congeners is twelve: three each for di-, tri- and tetrachlorobenzene isomers and one each for mono-, penta- and hexachlorobenzene. Mono-, di- and trichlorobenzenes were not very hydrophobic and consequently they were not totally incorporated into the sodium dodecyl sulphate (SDS) micelle as shown in Fig. 2. Three isomers of dichlorobenzenes were partially resolved, but those of trichlorobenzenes were not, although they were separated from other polychlorinated benzenes. Tetra-, penta- and hexachlorobenzenes were eluted at migration times similar to that of the micelle. The slightly lower efficiencies observed in Fig. 2, except for chlorobenzene, can probably be ascribed to slow kinetics in the partition equilibrium of the solutes⁴.

The addition of 40 mM γ -CD to the separation solution employed in Fig. 2 permitted the separation of all of the chlorinated benzene congeners, as shown in Fig.

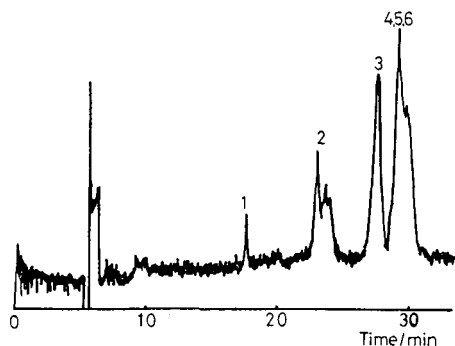


Fig. 2. MEKC separation of chlorinated benzene congeners: 1 = mono-, 2 = di-, 3 = tri-, 4 = tetra-, 5 = penta- and 6 = hexachlorobenzene. Capillary, 700 mm (Scientific Glass Engineering); separation solution, 100 mM SDS in 100 mM borate buffer (pH 8.0) containing 2 M urea; applied voltage, 18 kV; current 30 μ A.

3. The difference in electroosmotic velocities between Fig. 2 (1.6 mm s^{-1}) and Fig. 3 (0.93 mm s^{-1}) was due to both applied voltages and fused-silica materials. Capillary tubes from Polymicro Technologies usually generated a weaker electroosmotic flow than those from Scientific Glass Engineering. When the former tubes were used under the conditions shown in Fig. 2, the migration times increased significantly and elution of peaks 3–6 was hardly observed.

The isomer separation shown in Fig. 3 can evidently be ascribed to the differential partition of the isomers to the γ -CD cavity, because these isomers are not resolved in the absence of γ -CD, as shown in Fig. 2. An isomer having a shorter migration time is included more strongly in the CD cavity than an isomer having a longer migration time, *e.g.*, 1,2,3,5-tetrachlorobenzene forms the most stable complex among the three tetrachlorobenzene isomers. As all of the congeners are not totally incorporated into the SDS micelle, the migration order observed in Fig. 3 does not always agree with the order of the stability of the inclusion complexes.

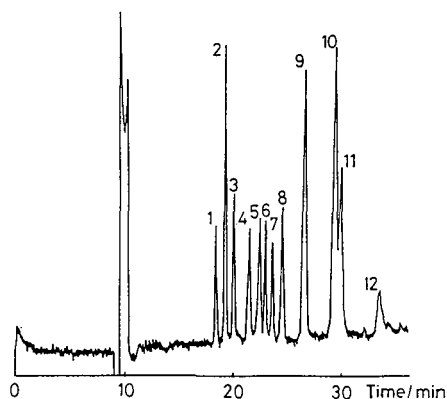


Fig. 3. γ -CD-MEKC separation of chlorinated benzene congeners: 1 = 1,2,3,5-tetra-, 2 = 1,2,3-tri-, 3 = 1,3,5-tri-, 4 = 1,2-di-, 5 = 1,2,4,5-tetra-, 6 = mono-, 7 = 1,3-di-, 8 = 1,2,4-tri-, 9 = 1,2,3,4-tetra-, 10 = penta-, 11 = 1,4-di- and 12 = hexachlorobenzene. Capillary, 700 mm (Polymicro Technologies); separation solution, as in Fig. 1 but containing an additional 40 mM γ -CD; applied voltage, 15 kV; current, 23 μ A.

Although the cavity diameter (0.95 nm)²⁸ of γ -CD seems slightly too large for chlorinated benzenes, all of the congeners are included by γ -CD. In particular, tetra- and trichlorobenzenes are strongly included. The discrepancy between the cavity and molecular sizes is explained by taking into consideration that an SDS molecule is probably co-included with a chlorobenzene congener. Hexachlorobenzene, which should have the largest molecular size among the congeners, migrates with the slowest velocity, but is still included to a considerable extent, as easily judged from the fact that it was not eluted in the absence of γ -CD, as mentioned above.

Separation of trichlorobiphenyl isomers

Among 24 possible isomers of trichlorobiphenyls, eleven isomers were available at CDC for the preparation of sample solutions for this study. Although HPCE and EKC have high mass sensitivities even with a UV detector, their concentration sensitivities are not very high because of the small detection volume. Therefore, concentrations higher than 0.1 mg ml⁻¹ are required for each solute.

All of the isomers of trichlorobiphenyls migrated with the same velocity as that of the micelle in MEKC. In other words, trichlorobiphenyls were too hydrophobic to be separated by MEKC. γ -CD-MEKC allowed the complete separation of the eleven isomers, as shown in Fig. 4. The separation using β -CD instead of γ -CD was not very successful, but the HPLC separation of the isomers was better with a β -CD bonded phase column (Cyclobond I) than with a γ -CD bonded phase column (Cyclobond II). A chromatogram with Cyclobond I is shown in Fig. 5, under which conditions biphenyl had a similar retention time to peak 35 at 36.5 min.

In CD-MEKC, the elution order should agree with the tendency of the isomers to form inclusion complexes with CD in the presence of SDS; on the other hand, in HPLC using a CD-bonded phase, the isomer that interacts more strongly with CD should have a longer retention time. Consequently, the elution order must be reversed between the two separation methods. However, the observed orders are not exactly reversed between Figs. 4 and 5. This can probably be explained in terms of three factors: the difference in the cavity size of the CDs, the presence of SDS in EKC and methanol in HPLC and possible extra retention mechanisms in HPLC such as hydrophobic interactions with the spacer or linkage part of CD.

Other PCBs such as mono-, di- and tetrachlorobiphenyls and commercial PCB products were also subjected to the γ -CD-MEKC separation under the same

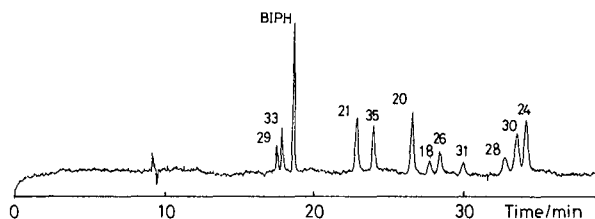


Fig. 4. Separation of eleven trichlorobiphenyl isomers by γ -CD-MEKC. Peaks are identified with the IUPAC number: 18 = 2,2',5-, 20 = 2,3,3'-, 21 = 2,3,4-, 24 = 2,3,6-, 26 = 2,3',5-, 28 = 2,4,4'-, 29 = 2,4,5-, 30 = 2,4,6-, 31 = 2,4',5-, 33 = 2',3,4- and 35 = 3,3',4-trichlorobiphenyl; BIPH = biphenyl. Capillary, 650 mm (Scientific Glass Engineering); separation solution, 60 mM γ -CD, 100 mM SDS and 2 M urea in 100 mM borate-50 mM phosphate buffer (pH 8.0); applied voltage, 15.4 kV; current, 50 μ A.

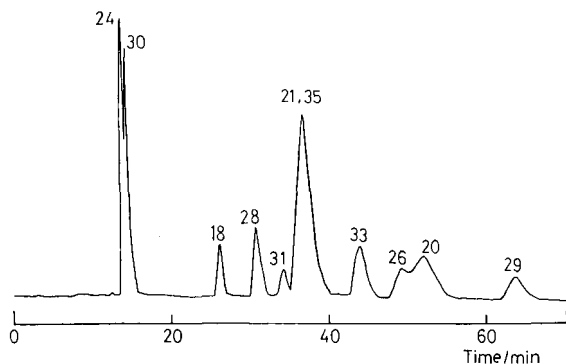


Fig. 5. HPLC separation of the trichlorobiphenyl isomers with a β -CD bonded phase column. See Fig. 4 for peak identification. Column, Cyclobond I (250 m \times 4.6 mm I.D.); mobile phase, 50% (v/v) aqueous methanol; flow-rate, 0.5 ml min⁻¹; detection wavelength, 210 nm.

conditions and excellent resolution was achieved, although each peak was not identified. As the purpose of this work was to confirm the applicability of the proposed method to the separation of highly hydrophobic and closely related compounds such as PCBs, we did not study extensively PCB analysis by CD-MEKC.

Separation of tetrachlorodibenzo-p-dioxin isomers

Three pairs of TCDD isomers that were hardly resolved even by capillary GC were employed as samples together with some other TCDD isomers to investigate the selectivity of closely related compounds by CD-MEKC. Examples of the TCDD pair separations are shown in Fig. 6. The complete separation of each pair was easily achieved under the same conditions as employed for the PCB analysis. In particular, 1,2,4,6- and 1,2,4,9-TCDD isomers were extremely difficult to resolve by capillary GC. Although the peaks are broad and tailed in Fig. 6c, sharp and symmetrical peaks were obtained when the capillary was washed with THF. The washing with THF increased the electroosmotic velocity and hence reduced the migration times but with slightly poorer resolution.

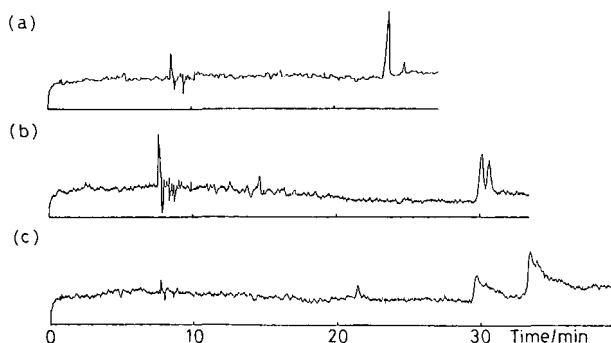


Fig. 6. γ -CD-MEKC separation of three pairs of closely related TCDD isomers: (a) 1,2,3,6- and 1,2,3,7-TCDD; (b) 1,2,6,7- and 1,2,8,9-TCDD; (c) 1,2,4,6- and 1,2,4,9-TCDD. Each peak was not identified. Conditions as in Fig. 4.

The identification of each peak was impossible because one or other compound of each pair was not available in an isolated form. 1,2,3,4- and 1,4,7,8-TCDD isomers were eluted at close migration times of 27.0 and 27.7 min under the conditions shown in Fig. 6. The most toxic isomer of TCDD, 2,3,7,8-TCDD, was poorly soluble in most organic solvents that were miscible with water, such as methanol, DMSO and THF, and therefore it was impossible to analyse it by CD-MEKC.

Some polychlorinated naphthalenes were also subjected to CD-MEKC, although extensive analyses were not performed. With TCDD isomers or polychlorinated naphthalenes, γ -CD generally gave better results than β -CD.

Separation of polycyclic aromatic hydrocarbons

Preliminary experiments on the separation by CD-MEKC of sixteen PAHs included in the list of priority pollutants showed a chromatogram which had more than fourteen peaks. Fig. 7 shows the separation of a mixture of naphthalene and four tricyclic and three tetracyclic aromatic hydrocarbons by γ -CD-MEKC. The elution order means that smaller PAHs are more easily included in the CD cavity or the larger PAHs are incorporated by the SDS micelle to a greater extent.

CONCLUSION

As this is preliminary work, we have not yet extensively studied the separation conditions for optimizing the resolution. The separations shown are not always satisfactory for the purpose of environmental or biological analysis. However, the results strongly suggest the potential of CD-MEKC as a microanalytical method for highly hydrophobic compounds.

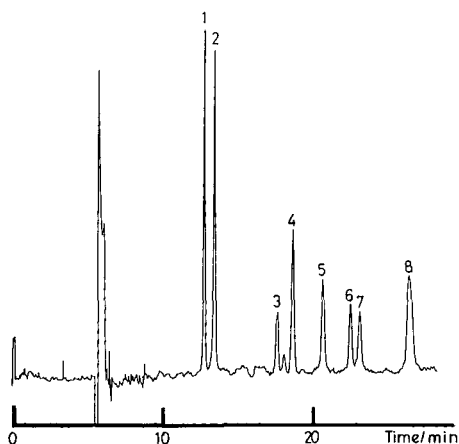


Fig. 7. γ -CD-MEKC separation of a mixture of naphthalene and four tricyclic and three tetracyclic aromatic hydrocarbons: 1 = naphthalene; 2 = acenaphthene; 3 = anthracene; 4 = fluorene; 5 = phenanthrene; 6 = chrysene; 7 = pyrene; 8 = fluoranthene. Capillary, 700 mm (Polymicro Technologies); separation solution, 30 mM γ -CD, 100 mM SDS and 5 M urea in 100 mM borate buffer (pH 9.0); applied voltage, 20 kV; current, 41 μ A.

ACKNOWLEDGEMENTS

This work was supported in part by a grant under the Monbusho International Scientific Research Program (01044081). S.T. is grateful to Yokogawa Electric and Shimadzu for research funds.

REFERENCES

- 1 S. Terabe, *Trends Anal. Chem.*, 8 (1989) 129.
- 2 S. Terabe, K. Otsuka, K. Ichikawa, A. Tsuchiya and T. Ando, *Anal. Chem.*, 56 (1984) 111.
- 3 S. Terabe, K. Otsuka and T. Ando, *Anal. Chem.*, 57 (1985) 834.
- 4 S. Terabe, K. Otsuka and T. Ando, *Anal. Chem.*, 61 (1989) 251.
- 5 K. Otsuka, S. Terabe and T. Ando, *J. Chromatogr.*, 332 (1985) 219.
- 6 K. Otsuka, S. Terabe and T. Ando, *Nippon Kagaku Kaishi*, (1986) 950.
- 7 D. E. Burton, M. J. Sepaniak and M. P. Maskarinec, *J. Chromatogr. Sci.*, 24 (1986) 347.
- 8 M. M. Bushey and J. W. Jorgenson, *Anal. Chem.*, 61 (1989) 491.
- 9 H. Nishi, T. Fukuyama, M. Matsuo and S. Terabe, *J. Chromatogr.*, 498 (1990) 313.
- 10 A. S. Cohen, S. Terabe, J. A. Smith and B. L. Karger, *Anal. Chem.*, 59 (1987) 1021.
- 11 K. Otsuka, S. Terabe and T. Ando, *J. Chromatogr.*, 348 (1985) 39.
- 12 S. Fujiwara, S. Iwase and S. Honda, *J. Chromatogr.*, 447 (1988) 133.
- 13 H. Nishi, N. Tsumagari, T. Kakimoto and S. Terabe, *J. Chromatogr.*, 465 (1989) 331.
- 14 H. Nishi, N. Tsumagari and S. Terabe, *Anal. Chem.*, 61 (1989) 2434.
- 15 A. S. Cohen, A. Paulus and B. L. Karger, *Chromatographia*, 24 (1987) 15.
- 16 A. Dobashi, T. Ono, S. Hara and J. Yamaguchi, *Anal. Chem.*, 61 (1989) 1984.
- 17 S. Terabe, M. Shibata and Y. Miyashita, *J. Chromatogr.*, 480 (1989) 403.
- 18 A. Dobashi, T. Ono, S. Hara and J. Yamaguchi, *J. Chromatogr.*, 480 (1989) 413.
- 19 S. Terabe, H. Ozaki, K. Otsuka and T. Ando, *J. Chromatogr.*, 332 (1985) 211.
- 20 P. Gozel, E. Gassman, H. Michelsen and R. N. Zare, *Anal. Chem.*, 59 (1987) 44.
- 21 R. A. Walingford and A. G. Ewing, *J. Chromatogr.*, 441 (1988) 299.
- 22 S. Honda, S. Iwase, A. Makino and S. Fujiwara, *Anal. Biochem.*, 176 (1989) 72.
- 23 S. Terabe and T. Isemura, *Anal. Chem.*, 62 (1990) 650.
- 24 Y. Walbrochl and J. W. Jorgenson, *Anal. Chem.*, 58 (1986) 479.
- 25 K. Otsuka and S. Terabe, unpublished data.
- 26 Y. Miyashita and S. Terabe, unpublished data.
- 27 E. R. Barnhart, D. G. Patterson, N. Tanaka and M. Araki, *J. Chromatogr.*, 445 (1988) 145.
- 28 J. Szejtli, B. Zsardon and T. Cserhati, in W. L. Hinze and D. W. Armstrong (Editors), *Ordered Media in Chemical Separations (ACS Symposium Series, Vol. 342)*, American Chemical Society, Washington, DC, 1987, pp. 200–217.

CHROM. 22 609

Separation of DNA restriction fragments by high performance capillary electrophoresis with low and zero crosslinked polyacrylamide using continuous and pulsed electric fields

DAVID N. HEIGER, AHARON S. COHEN and BARRY L. KARGER*

Barnett Institute, Northeastern University, Boston, MA 02115 (U.S.A.)

ABSTRACT

This paper presents results on the separation of DNA restriction fragments by high performance capillary electrophoresis (HPCE). Capillaries containing polyacrylamide with low amounts of crosslinking agent (*i.e.* 0.5% C) were first studied. The greater molecular accessibility offered with columns of low crosslinking, relative to higher crosslinked gels (*e.g.* 5% C), permitted high efficiency separations of double stranded DNA fragments up to 12 000 base pairs in length. Capillaries containing no crosslinking agent, *i.e.* linear polyacrylamide, were then examined. Ferguson plots (*i.e.* log mobility vs. %T) were used to assess the size selectivity of linear polyacrylamide capillaries. In another study, it was determined that the relative migration of DNA species was a strong function of applied electric field and molecular size. Lower fields yielded better resolution than higher fields for DNA molecules larger than about 1000 base pairs, albeit at the expense of longer separation time. Based on these results, we have examined pulsed field HPCE and have demonstrated the use of this approach to enhance separation.

INTRODUCTION

The separation of DNA species by high performance capillary electrophoresis (HPCE) is an area of growing activity. This interest follows from the use of polyacrylamide or agarose slab gel electrophoresis as a standard method for this field¹. Slab gel electrophoresis, however, is slow, difficult to quantitate, and not easily amenable to automation. HPCE, an instrumental approach to electrophoresis, is able to overcome many of these problems^{2–5}.

When separating oligonucleotides or DNA restriction fragments, a sieving medium is most often employed since it is known that mobility of these species is nearly independent of molecular size in free solution⁶. While open-tube HPCE has been examined^{7,8}, high-resolution separation of nucleic acids by this approach is limited. Accordingly, we have examined polyacrylamide gel-filled capillaries for the separation

of oligonucleotides^{9,10}. These capillaries have been shown to yield ultra-high efficiency, in excess of $30 \cdot 10^6$ theoretical plates/m (ref. 10). Capillaries with relatively large amounts of crosslinking agent (*e.g.* 5% C) yield stable columns with good size selectivity for single stranded oligonucleotides and DNA sequencing reaction products. (See ref. 11 for definition of %T and %C.)

As a continuation of this work, we describe the application of low or zero crosslinked polyacrylamide filled capillaries for the separation of DNA restriction fragments up to 12 000 base pairs. The analysis of such species is important, for example, in restriction fragment mapping¹², in analysis of restriction fragment length polymorphisms (RFLPs) for diagnostic¹³, clinical¹⁴ and forensic¹⁵ assays, in polymerase chain reaction (PCR) product applications¹⁶ and in genomic mapping¹⁷.

Linear polyacrylamide has been employed for the separation of proteins in the slab gel format¹⁸⁻²¹; however, the minimum monomer concentration required to achieve sufficient anticonvective character for slab operation was approximately 10 %T²¹. The anticonvective properties of the narrow capillaries in HPCE²² permit use of a much broader range of linear polyacrylamide compositions. While dissolution of hydrophilic polymers has been used in HPCE to improve DNA fragment separations^{23,24}, polymerization within the capillary will be shown to offer advantages in terms of size selectivity. Finally, we will demonstrate the influence of the applied electric field on the mobility of DNA fragments and the use of pulsed field²⁵⁻²⁷ HPCE to enhance separation.

EXPERIMENTAL

Apparatus

The basic HPCE instrumentation has been previously described in detail¹⁰. A 60-kV direct-current power supply (Model PS/MK 60; Glassman, Whitehouse Station, NJ, U.S.A.) was used to generate a potential drop across the capillary for continuous field electrophoresis. For pulsed field experiments a 20-kV operational amplifier (Model PO434; Trek, Medina, NY, U.S.A.) controlled with a function generator (Model 185; Wavetek, San Diego, CA, U.S.A.) was employed. A UV-VIS spectrophotometer (Model 100; Spectra-Physics, San Jose, CA, U.S.A.) was used at 260 nm to detect the DNA fragments. Column cooling was achieved by air convection using a laboratory fan. Each end of the capillary was placed in buffer reservoirs (3 ml) with platinum wire electrodes. In some cases, placing polyacrylamide in the reservoirs was found to be beneficial in extending column lifetime. Electrophoresis was performed in fused-silica tubing (Polymicro Technologies, Phoenix, AZ, U.S.A.) of 75 μm I.D. and 375 μm O.D., which had a 2-4-mm portion of the polyimide coating removed for spectroscopic detection. The electropherograms were acquired and stored on an IBM PC/XT (Boca Raton, FL, U.S.A.) via an analog-to-digital converter interface (Model 762SB; PE/Nelson, Cupertino, CA, U.S.A.).

Procedures

Capillary preparation followed procedures previously described^{9,10}. Methacryloxypropyltrimethoxy silane (Petrarch Systems, Bristol, PA, U.S.A.) was first covalently bound to the fused-silica capillary walls. Polymerization of polyacrylamide was next accomplished by filling the capillary with degassed, low viscosity acrylamide solution.

Polymerization was initiated using ammonium persulfate (APS) and N,N,N',N'-tetramethylethylenediamine (TEMED). Columns containing linear polyacrylamide concentrations between 3 and 14% T were prepared for study. Polyacrylamide gels crosslinked with N,N'-methylenebisacrylamide (bis) were used at compositions 3% T, 5% C and 3% T, 0.5% C. Acrylamide solutions were prepared in a buffer of 100 mM Tris base, 100 mM boric acid, 2 mM EDTA, pH 8.3. For single-stranded oligonucleotide separations the buffer also contained 7 M urea. Samples were injected electrophoretically with specific injection conditions provided in the figure captions.

Chemicals

Samples of ϕ X174 DNA digested with restriction enzyme *Hae* III were obtained from Pharmacia (Piscataway, NJ, U.S.A.) and New England Biolabs. (Beverly, MA, U.S.A.), and were used at a sample concentration of 500 μ g/ml in 10 mM Tris-HCl (pH 8.0) and 0.1 mM EDTA. Vectors M13mp18 and dephosphorylated pBR322, both digested with *Eco*R I, were obtained from New England Biolabs. These samples were used at a concentration of 100 μ g/ml in 10 mM Tris-HCl (pH 7.5) and 1 mM EDTA. Polydeoxyadenylic acids, p(dA)₂₀ and p(dA)₄₀₋₆₀, purchased from Pharmacia, were dissolved in water and used at 1 μ g/ml and 30 μ g/ml, respectively. A 1000-base pair ladder (up to 12000 base pairs) was supplied by Bethesda Research Labs. (Gaithersburg, MD, U.S.A.). This sample was used at a concentration of 920 μ g/ml in 10 mM Tris-HCl (pH 7.6), 50 mM NaCl and 1 mM EDTA. Ultra-pure Tris base, urea and EDTA were obtained from Schwartz/Mann Biotech (Cleveland, OH, U.S.A.). Acrylamide, bis, TEMED and APS were purchased from Bio-Rad (Richmond, CA, U.S.A.). All buffer and acrylamide solutions were filtered through a 0.2- μ m pore size filter (Schleicher and Schuell, Keene, NH, U.S.A.).

Each fragment of the *Hae* III digest of ϕ X174 was isolated from 1.8% SeaKem GTG agarose (FMC, Rockland, ME, U.S.A.) slab gels by standard methods¹ and were spiked into the mixture of HPCE peak identification. Similar isolation of the 1000-base pair ladder fragments was performed using 0.45% and 0.8% agarose slab gels. PCR was conducted using a thermal cycler (Perkin-Elmer Cetus, Norwalk, CT, U.S.A.). Twenty five cycles were run using the buffers, primers, λ DNA template, Taq polymerase, and protocol as supplied by Perkin-Elmer Cetus²⁸.

RESULTS AND DISCUSSION

3% T, 0.5% C polyacrylamide capillary columns

Previous work from this laboratory has concentrated on the use of crosslinked polyacrylamide gels for the HPCE separation of oligonucleotides^{9,10}. Gels of composition 3% T, 5% C were demonstrated to be particularly well suited to the high resolution separation of single stranded oligonucleotides. However, the pores were generally too small for restriction fragments to migrate efficiently. Specifically, introduction of fragments larger than about 700 base pairs resulted in distorted peak shapes and poor resolution.

The separation of DNA fragments would appear to require a more open pore structure of the gel. An increase in the pore size can be achieved by reducing the amount of crosslinking agent for a given percentage T²⁹. We have found that a ten-fold reduction in the percentage of bis crosslinker (*i.e.* from 5 to 0.5% C) resulted

in good resolution of DNA restriction fragments, as illustrated in Fig. 1. This electropherogram shows the separation of the *Hae* III restriction digest of ϕ X174 DNA and *Eco*R I digests of both pBR322 DNA and M13mp18 DNA. The ϕ X174 digest consisted of eleven fragments ranging from 72 to 1353 base pairs, and the pBR322 and M13mp18 digests consisted of single fragments of 4363 and 7250 base pairs, respectively. All thirteen fragments are well-resolved in less than 18 min. Peak identification was made by spiking each peak with slab gel-isolated fragments and, as expected, size-dependent migration was achieved. The separation power of this polyacrylamide capillary is evidenced by the resolution of species 5 and 6, which differ in length by only 10 base pairs (*i.e.* 271 and 281 base pairs). Efficiency is further noted

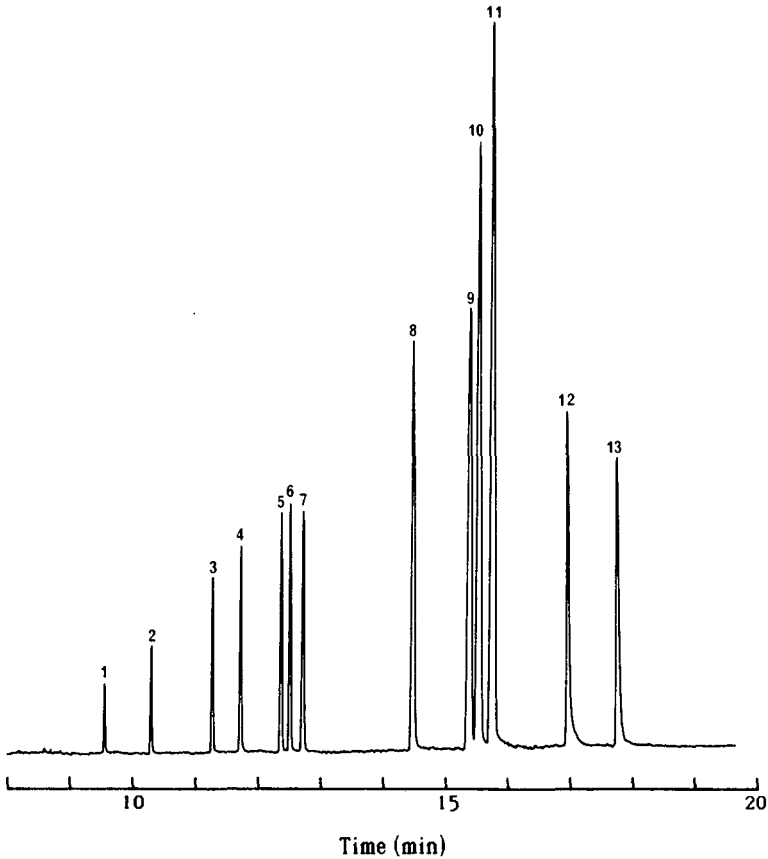


Fig. 1. Separation of *Hae* III digest of ϕ X174 DNA, *Eco*R I digest of pBR322 and *Eco*R I digest of M13mp18 on a 3% T, 0.5% C polyacrylamide capillary column. The 11 fragments of the ϕ X174 digest have been identified as the first 11 peaks in the electropherogram, followed by pBR322 and M13mp18. Identification was made by spiking each peak with slab gel isolated species. Peaks: 1 = 72; 2 = 118; 3 = 194; 4 = 234; 5 = 271; 6 = 281; 7 = 310; 8 = 603; 9 = 872; 10 = 1078; 11 = 1353; 12 = 4363 and 13 = 7253 base pairs. Conditions: effective length, l , was 30 cm, total length, L , was 40 cm, applied field, E , was 250 V/cm, current generated, i , was 12.5 μ A, and sample was injected electrophoretically at 10 kV for 0.5 s. Buffer: 100 mM Tris-borate (pH 8.3), 2 mM EDTA.

by the large number of theoretical plates per meter: $5 \cdot 10^6$ for the first peak (72 base pairs) and $1 \cdot 10^6$ for the last peak (7250 base pairs). The theoretical plates were calculated using the appropriate expressions which take into account peak asymmetry³⁰.

We next examined the performance of a 3% T, 0.5% C capillary for the separation of DNA restriction fragments up 12 000 base pairs. The electropherogram shown in Fig. 2 demonstrates the rapid separation of a 1000-base pair DNA ladder up

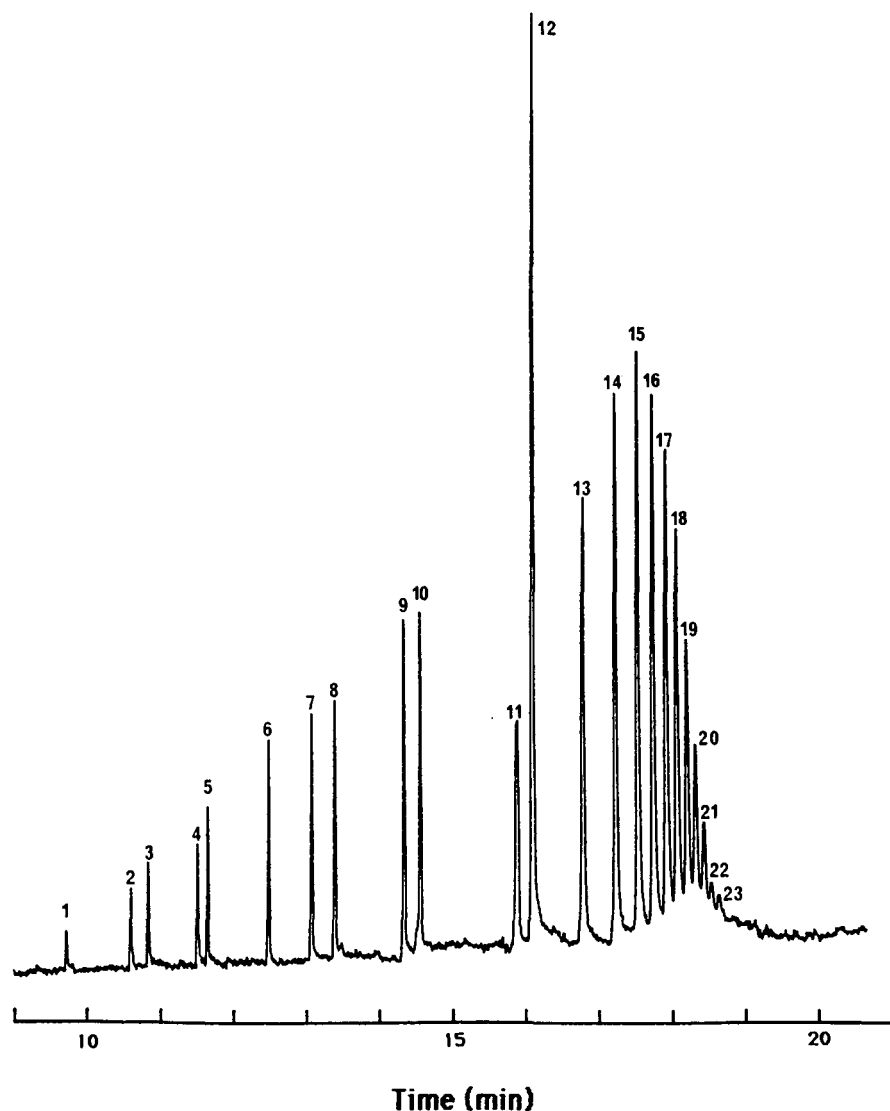


Fig. 2. Separation of 1000-base pair DNA ladder on a 3% T, 0.5% C polyacrylamide capillary. Fragment lengths range from 75 to 12 216 base pairs. All peaks were identified by spiking with slab gel isolated species. Peak legend: 1 = 75; 2 = 142; 3 = 154; 4 = 200; 5 = 220; 6 = 298; 7 = 344; 8 = 394; 9 = 506; 10 = 516; 11 = 1018; 12 = 1635; 13 = 2036; 14 = 3054; 15 = 4072; 16 = 5090; 17 = 6108; 18 = 7126; 19 = 8144; 20 = 9162; 21 = 10 180; 22 = 11 198; 23 = 12 216 base pairs. All conditions as in Fig. 1.

to 12 000 base pairs (*i.e.*, *ca.* 1000, *ca.* 2000, *ca.* 3000, ... *ca.* 12 000 base pairs). This complex mixture consisted of 11 species in addition to the 12 species from the ladder. The additional fragments, ranging from 75 to 1636 base pairs arise from enzymatic digestion of the cloning vector which was used in the preparation of the sample. A total of 23 fragments ranging from 75 to 12 216 base pairs were thus expected and were observed. Peak identification was again made by spiking all the peaks with slab gel isolated fragments. Notably, the electropherogram from slab gel electrophoresis, except fragments 9 and 10, which differ by only 10 base pairs, are usually not separated on the slab³¹.

Linear polyacrylamide capillary columns

With the success of low crosslinked polyacrylamide capillaries, we next turned to linear polyacrylamide (*i.e.* no crosslinking) in the composition range of 3% T to

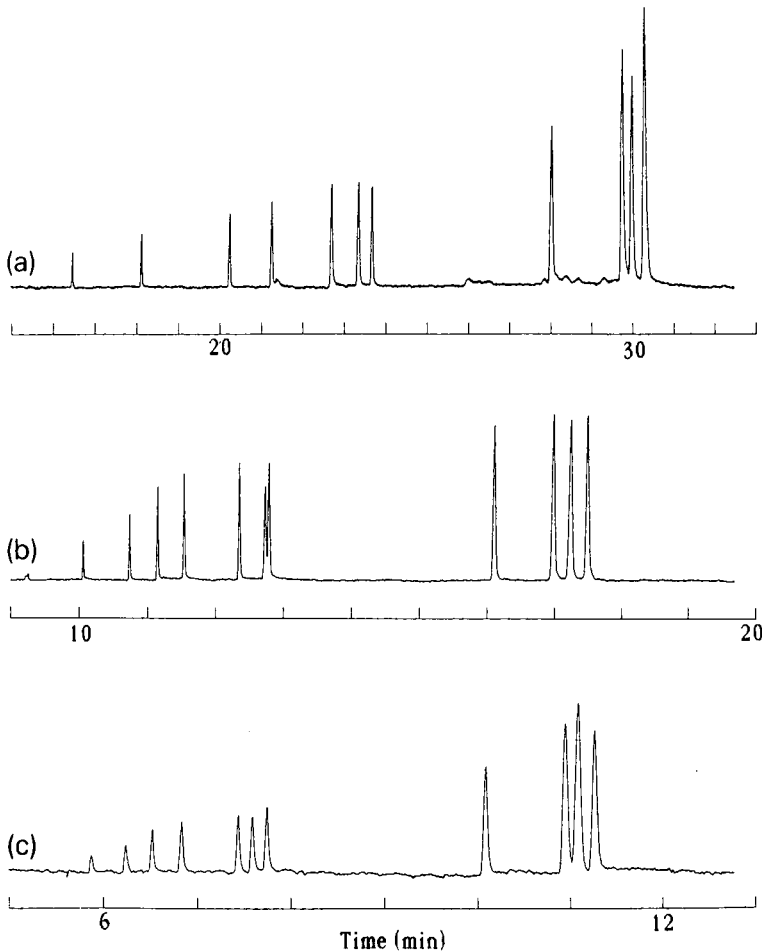


Fig. 3. Separation of *Hae* III restriction fragment digest of ϕ X174 DNA on linear polyacrylamide columns of composition: (a) 6, (b) 9 and (c) 12% T. Effective lengths of these capillaries were 35 cm, 15 cm and 10 cm, respectively. $E = 300$ V/cm, injection at 150 V/cm for 3 s. Currents generated were (a) $10.5 \mu\text{A}$, (b) $9.1 \mu\text{A}$, and, (c) $7.8 \mu\text{A}$. All other conditions as in Fig. 1.

14% T. The viscous character of such compositions range from nearly liquid-like at 3% T to that of a gelatinous material at 14% T. The separation performance of several different linear polyacrylamide compositions (*i.e.* 6, 9 and 12% T) is shown in Fig. 3, using the ϕ X174 *Hae* III digest as a test mixture. These electropherograms indicate that size selectivity is a function of polymer concentration. For a given electric field and base pair size range, shorter column lengths can be utilized with increasing acrylamide concentration due to the greater sieving capability of the higher percentage T. On the other hand, as described previously for crosslinked capillaries gels¹⁰, the reduced sieving power at lower polyacrylamide concentrations can be compensated by increasing the effective length of the capillary. This approach can result in a broader molecular size range, encompassing larger kilo base pair fragment sizes.

The currents generated at 300 V/cm in the 6, 9 and 12% T capillaries were, respectively, 10.5 μ A, 9.1 μ A and 7.8 μ A. These low currents are a direct consequence of the high viscosity of the polyacrylamide media. The power generated in a typical capillary (total length 40–80 cm) at 300 V/cm is well below 0.5 W/m, and significant Joule heating of the column is not expected³². As seen in Fig. 3, high fields and short effective length columns can be employed for rapid analysis.

The mechanism of sieving in linear polyacrylamide has been suggested to be similar to that occurring in crosslinked polyacrylamide gels^{18,19,33}. This model views the molecules migrating through “dynamic pores” which are formed by the fluctuating polymer chain network. As shown both here and by others^{19,21}, the extent of sieving is greater with increased polymer content. Since viscosity is proportional to polymer content, a system which polymerizes inside the column is advantageous relative to that obtained by simple dissolution of a polymer in a buffer. The viscosities of the medium can be much greater with *in situ* polymerization. Further, the difficulties of handling viscous solutions are minimized.

The linear polyacrylamide capillaries described here were stable for at least several weeks without degradation of performance. In addition, the 9% T linear polyacrylamide capillaries exhibited an absolute day-to-day reproducibility in migration time (for the 1358-base pair species from the ϕ X174 *Hae* III mixture) of 1.7% ($n = 10$) and a capillary-to-capillary reproducibility of 2.3% ($n = 21$). The day-to-day variation in the relative migration time for the 1358-base pair using the 72-base pair species as an internal standard was 0.9% ($n = 10$).

We have found the higher %T linear polyacrylamide capillaries also useful for single stranded oligonucleotide separations, as illustrated in Fig. 4 with a 9% T column. The sample in this figure consisted of a polydeoxyadenylic acid 20-mer [p(dA)₂₀] spiked into a mixture of polydeoxyadenylic acids ranging from 40 to 60 bases [p(dA)_{40–60}], each differing in length by a single residue. The high resolving power of this capillary is evidenced not only by the separation of each oligonucleotide, but also by the appearance of shoulders on the major peaks which have been identified as the dephosphorylated form of each oligonucleotide³⁴. While comparable resolution in shorter time has been previously achieved for these species on 3% T, 5% C gel columns¹⁰, the linear polyacrylamide is useful for resolving a broader range of fragment sizes.

Ferguson plot

The size selectivity of linear polyacrylamide capillaries can be characterized by

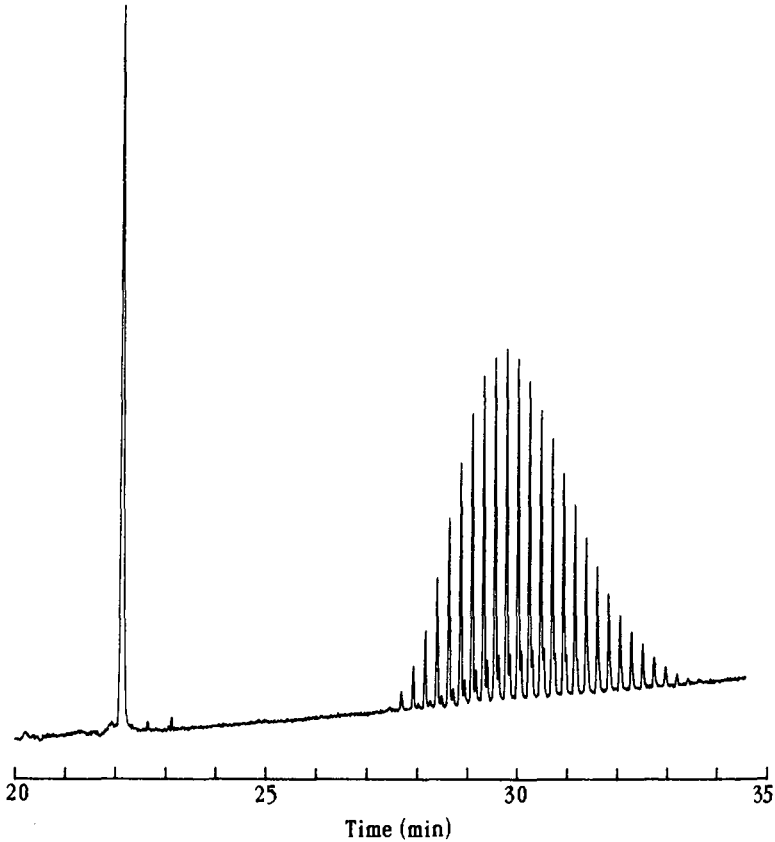


Fig. 4. Single base resolution of deoxyoligonucleotides on 9% T linear polyacrylamide. Sample mixture: p(dA)₂₀ and p(dA)₄₀₋₆₀. Conditions: $E = 308$ V/cm, $i = 8.8$ μ A, $l = 45$ cm, $L = 60$ cm, injection at 10 kV for 2 s. Buffer contained 7 M urea. All other conditions as in Fig. 1.

means of a Ferguson plot^{35,36}. This plot of log mobility *versus* %T at constant %C is a linear function as follows:

$$\log \mu = \log \mu_0 - k_R (\%T) \quad (1)$$

where μ is the measured mobility ($\text{cm}^2/\text{V s}$), μ_0 is the mobility in free solution, k_R is the retardation coefficient, and %T is the acrylamide concentration. Fig. 5 shows the Ferguson plots for ϕ X174 *Hae* III fragments from 273 to 1358 base pairs on capillaries containing between 6 and 14% T. The slope and intercept for each fragment was calculated by least squares analysis. As expected, the intercept (*i.e.* 0% T) of each line is essentially identical since, as noted earlier, the mobility of DNA molecules becomes increasingly independent of molecular size in free solution⁶. It is interesting to note that the measured free solution mobility of all fragments in the same buffer was $3.56 \cdot 10^{-4} \text{ cm}^2/\text{V} \cdot \text{s}$ ($\log \mu = -3.45$). This value is roughly 35% higher than the intercept of the Ferguson plot. It appears that the Ferguson plot may exhibit upward curvature at

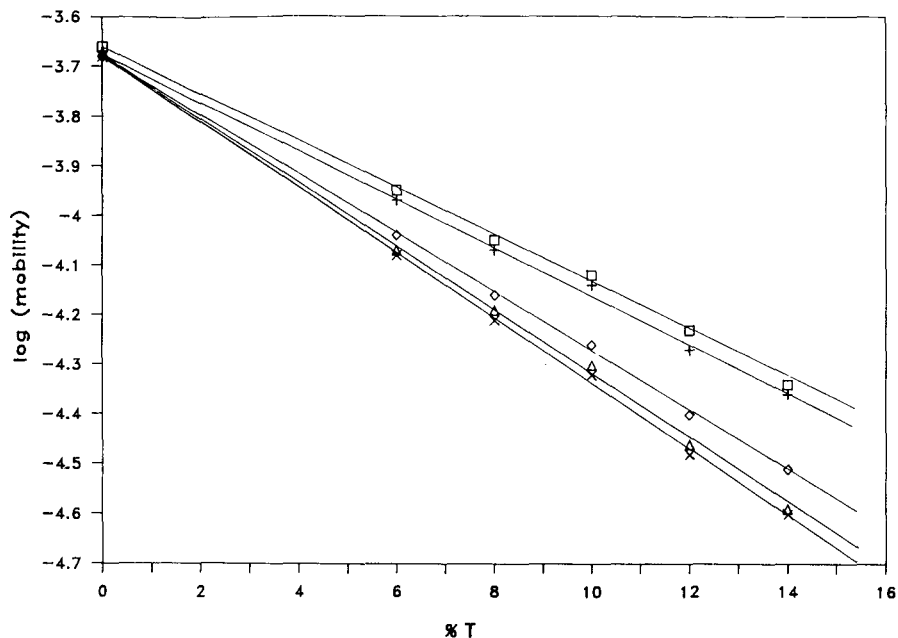


Fig. 5. Ferguson plots for linear polyacrylamide. The lines represent the log mobility of various ϕ X174 *Hae* III fragments as a function of monomer composition. \square = 273; + = 310; \diamond = 603; \triangle = 872; and \times = 1358 base pairs. Conditions: $E = 300$ V/cm, $l = 15$ cm, injection at 5 kV for 3 s. All other conditions as in Fig. 1.

low %T. Such non-linearity has already been described on slab²¹. The values of the retardation coefficient, k_R , range from $-4.6 \cdot 10^{-2}$ for the 273-base pair fragment to $-6.6 \cdot 10^{-2}$ for the 1358-base pair fragment. The steeper slope for the largest fragment is expected in the sieving mechanism. Caution must be exercised in the quantitative application of the Ferguson plot to the determination of fragment size dimensions and matrix structure, since, as shown below, the mobility of DNA species can be field dependent.

Polymerase chain reaction product analysis

One potential use for linear polyacrylamide HPCE is the fast analysis of PCR products¹⁶. The PCR method is capable of rapidly increasing the concentration of the target DNA 10^5 times or more. Since this method is susceptible to errors, such as amplification of spurious segments of DNA¹⁶, a method of analysis and possible purification is necessary. Currently, the predominant method is slab gel electrophoresis; however, capillary electrophoresis can be advantageously exploited as well.

Following standard protocols²⁸, we used PCR to amplify a 500-base region of λ DNA from an initial template concentration of 0.001 ng/ μ l. The electropherogram in Fig. 6 was obtained by direct injection of the PCR reaction mixture without further sample treatment. The separation reveals several peaks, with a major band appearing at 19 min. This band migrates at the expected velocity of a 500-base pair fragment, as shown in the inset of Fig. 6. Here, a calibration curve of migration time *versus* fragment size is presented, using the previously identified ϕ X174 *Hae* III fragments as

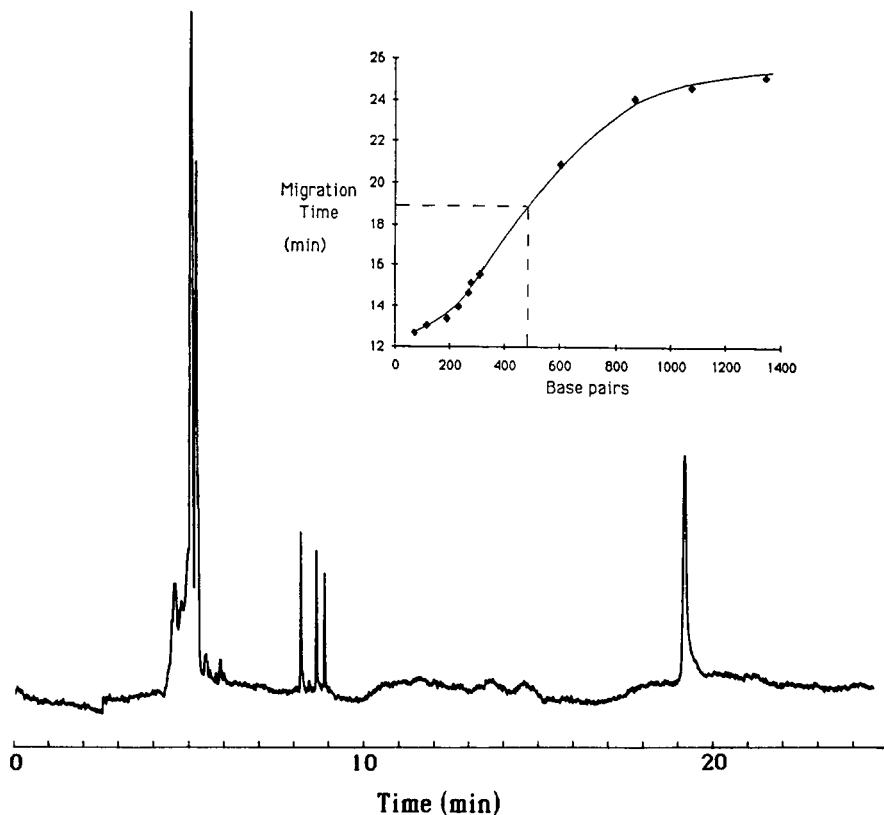


Fig. 6. Polymerase chain reaction (PCR) product analysis. Injection of PCR amplified 500-base pair fragment directly from reaction mixture onto a 9% T linear polyacrylamide column. Conditions: $E = 300$ V/cm, $i = 9.0 \mu\text{A}$, $l = 15$ cm, $L = 40$ cm, and injection at 300 V/cm for 10 s. All other conditions as in Fig. 1. Inset: size calibration curve for identification of PCR product. The fragments of the ϕX174 *Hae* III digest were electrophoresed as above, and migration time plotted as a function of fragment length. The dashed line indicates size of PCR product.

size standards. As noted by the dashed line, the migration time of the peak at 19 min compares well to a 500-base pair fragment. It is interesting to note that the shape of the calibration curve is similar to that found for DNA fragments in slab gels³⁷.

The fastest migrating species in Fig. 6, eluting at 5 min, are believed to be unincorporated nucleotides. The other peaks at 8–9 min are thought to be primers and possibly dimers of the primers which are known to form²⁸. Absolute identification requires further study. Nonetheless, the results in Fig. 6 demonstrate the potential of polyacrylamide HPCE for PCR product assignment and purity analysis. It is apparent that direct injection of PCR products is possible. Sample desalting to increase electrophoretic injection and preconcentration by isotachophoresis^{38,39} for analysis of sample concentrations more dilute than in this example can be used. Moreover, micropreparative collection of purified material can be achieved, if desired¹⁰.

Effect of applied electric field on mobility

The magnitude of the applied electric field is known to influence migration of DNA species in slab gels, particularly species larger than 15 000–20 000 base pairs²⁶.

While the causes of this phenomenon are not completely understood at present, it is known that DNA molecules can align parallel to the applied field, depending on the size of the fragment and the magnitude of the field⁴⁰. Migration of aligned species is thought to lead to a snake-like motion, called reptation⁴¹, which often results in movement in the gel matrix of fragments much larger than expected from the sieving mechanism of Ogston⁴². Reptation of aligned species also leads to size-independent mobilities.

In this work, we examined the influence of the applied field on the mobility of the DNA fragments shown in Figs. 1 and 2. The plot in Fig. 7 shows the electrophoretic velocity as a function of field for the 75- and 11 000-base pair fragments from the 1000-base pair ladder, on a 3% T, 0.5% C capillary column. The small fragment shows

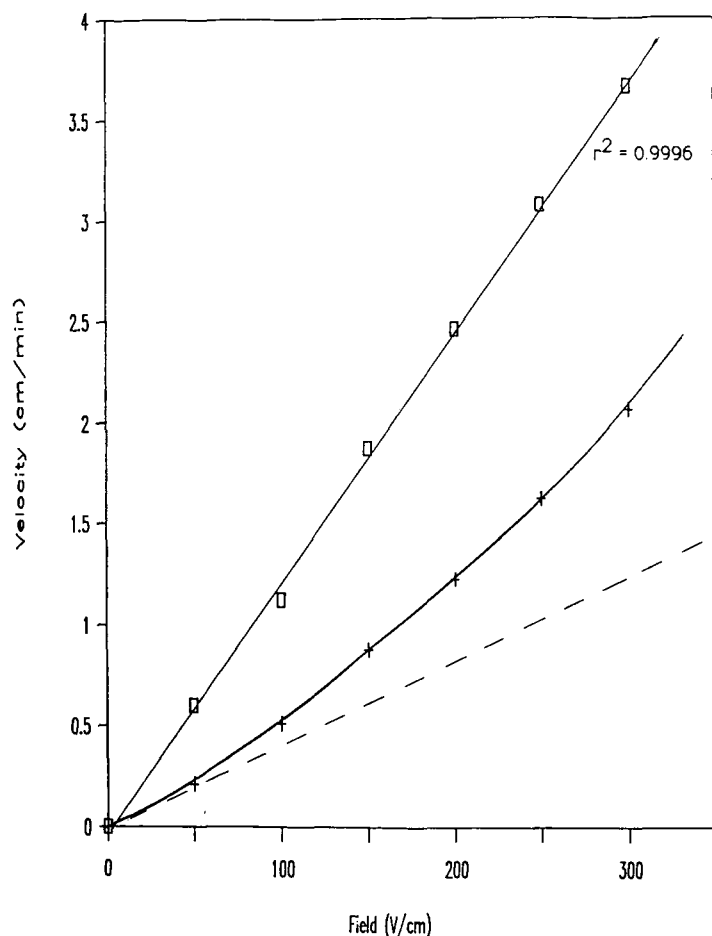


Fig. 7. Effect of applied electric field on linear velocity of various DNA fragments. □ = 75-base pair fragment; + = 11 198-base pair fragment. Solid line denotes experimental curve, dashed line denotes expected curve. Conditions: 3% T, 0.5% C polyacrylamide, $l = 30$ cm, $L = 40$ cm, injection at 10 kV for 0.5 s. Power generation at 300 V/cm was 0.37 W/m. All other conditions as in Fig. 1.

the expected linear trend with field^2 ; however, a non-linear behavior is observed for the large fragment, with higher than expected velocity at elevated fields. This latter behavior is consistent with known field effects on mobility of DNA molecules²⁶. Joule heating within the capillary can be eliminated as the cause of this behavior since only the largest fragment exhibits anomalous behavior and the power generated at the highest field is less than 0.4 W/m^2 . The upward curvature in velocity exhibited by the larger DNA molecules can eventually result in faster migration of the larger species than smaller ones²⁶. Such anomalous migration would be most prominent at both high electric fields and high %T.

Field effects were also found on a 12% T linear polyacrylamide capillary for the largest fragments of the *Hae* III digest of ϕX174 . Fig. 8 shows the separation of this mixture at 250 V/cm (Fig. 8a) and 125 V/cm (Fig. 8b). The smaller fragments are observed to have lower resolution at 125 V/cm, probably as a consequence of

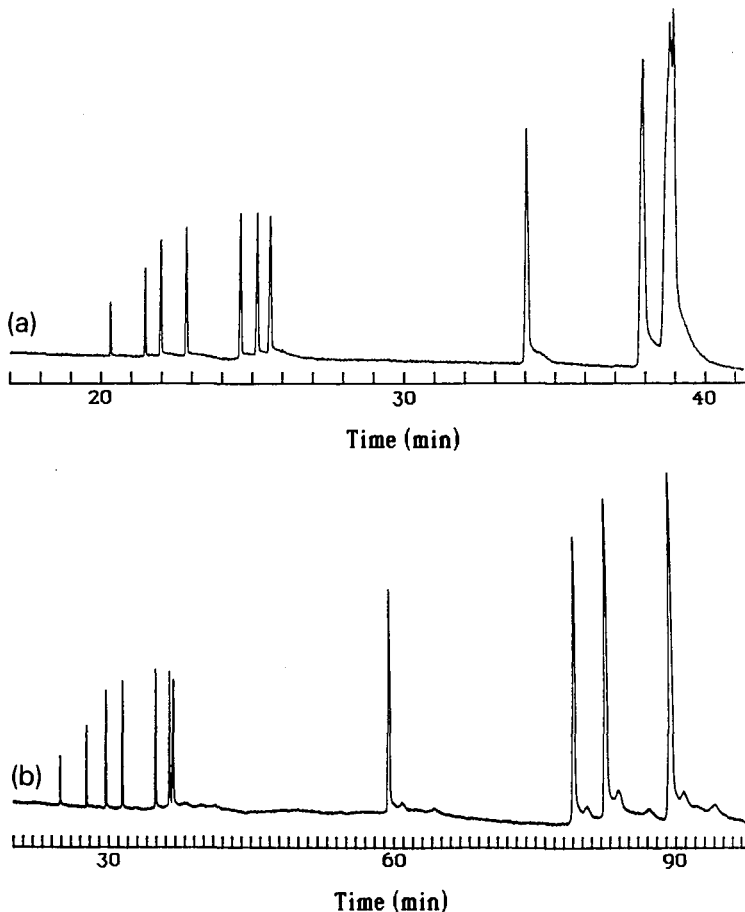


Fig. 8. Effect of applied electric field on separation of *Hae* III digest of ϕX174 DNA. (a) 250 V/cm. (b) 125 V/cm. Note loss of resolution at high field for the largest fragments. Conditions: 12% T linear polyacrylamide, $l = 20 \text{ cm}$, $L = 40 \text{ cm}$, injection at 10 kV for 1 s. Current: (a) $5.4 \mu\text{A}$, (b) $2.9 \mu\text{A}$. Power generated: (a) 0.14 W/m , (b) 0.04 W/m . All other conditions as in Fig. 1.

diffusional band broadening; however, a dramatic increase in resolution is seen for the largest fragments of roughly 1000 base pairs. It is believed that these species are less aligned at the lower applied field and as the molecules adopt a more random coil structure, size discrimination is increased.

Another manifestation of the influence of the applied field on resolution is shown in Fig. 9 for the 4363 and 7253-base pair species (see Fig. 1) on a 6% T, 0% C capillary. Calculation of resolution (R_s) for the two fragments was based on the standard equation, $R_s = 2[(t_2 - t_1)/(w_1 + w_2)]$, where t is the migration time at the peak height maximum and w is the baseline peak width in time units. The subscripts 1 and 2 denote the two species in question. As can be seen, there is a substantial improvement in resolution at lower fields, albeit at the expense of analysis time. Again, the low currents in the polyacrylamide capillary columns used in these studies result in minimal power generation and thus minimal Joule heating.

The field effects on mobility observed in Figs. 7-9 are occurring at much smaller fragment sizes than generally found in slab gel operation. A significant difference between the capillary and slab procedures, however, is the use of an applied field that is at least an order of magnitude higher in the capillary format. Since alignment is field dependent, it is not surprising that these effects are observed for molecules only a few thousand base pairs in length. Thus, manipulation of the applied field and proper selection of polyacrylamide composition are important parameters in the optimization of DNA separations.

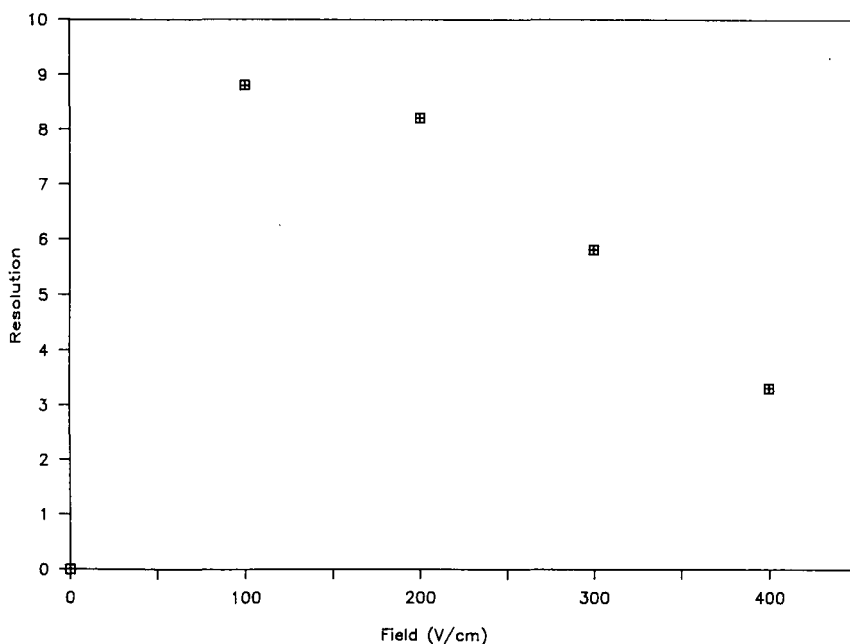


Fig. 9. Effect of applied electric field on resolution. Resolution calculated for DNA fragments 4363 and 7253 base pairs in length on a 6% T linear polyacrylamide capillary. Conditions: $l = 15$ cm, $L = 28$ cm, injection at 7.4 kV for 0.5 s. Current at 400 V/cm was 13 μ A. All other conditions as in Fig. 1.

Pulsed field HPCE

One approach to manage the loss of size dependent mobility, manifested in Figs. 7–9, is electric field programming. This discontinuous electric field method, originally described for sample collection¹⁰ and for enhancing sensitivity of radioactive detection⁴³, can be used to optimize separation of appropriate mixtures. For example, for the separation of Fig. 8, one could employ a high field initially to separate the small species with high efficiency, followed by a step or continuous gradient decrease in applied field to separate the larger species. While high resolution of both small and large species can be obtained using this approach, this benefit is offset by longer analysis time.

An alternative and more general method for optimization of DNA separations is the use of pulsed field electrophoresis^{25–27}. This technique is used to confer size-dependent mobility by periodically changing the direction and magnitude of the applied field, essentially relaxing molecular elongation. Both unidirectional⁴⁴ and field-inversion methods²⁷ are compatible with the capillary format. In this work we have examined the use of unidirectional pulsing to increase separation of the 4363- and 7253-base pair fragments of Fig. 1. With the apparatus described in the experimental section, a waveform consisting of a symmetric square wave between 0 and 300 V/cm was applied across a 6% T linear polyacrylamide capillary. Waveform frequency was varied incrementally between 0.1 and 1000 Hz.

Fig. 10 shows a plot of peak separation of the two species as a function of frequency. Here, a maximum was observed at 100 Hz; an optimum in frequency specific to the molecular size of the analyte is well expected⁴⁴. Interestingly, frequencies of 0.1 and 1 Hz resulted in the same separation as continuous field operation. The data points in Fig. 10 were independent of the sequence of measurements, *i.e.* no hysteresis in the curve was observed when pulsing frequencies were chosen in random order.

A 20% increase in peak separation was observed in pulsed-field (100-Hz) operation relative to continuous field operation. It is anticipated that greater

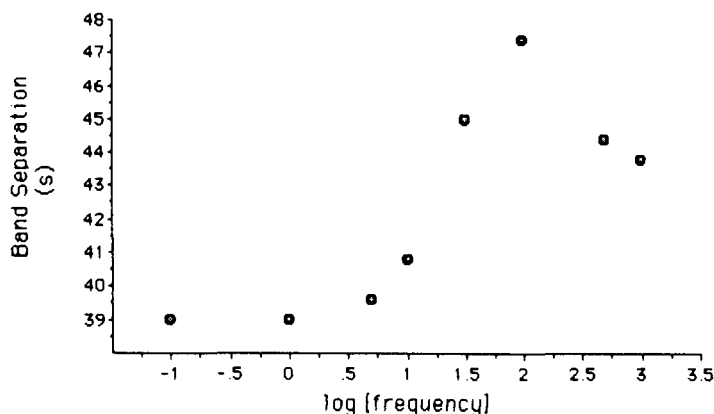


Fig. 10. Pulsed field HPCE of 4363- and 7253-base pair fragments. Plot of peak separation as a function of frequency of unidirectional pulse waveform. Maximum represents optimum frequency for separation of these species. Conditions: symmetric square wave of amplitude 0 to 300 V/cm, 6% T linear polyacrylamide, $l = 30$ cm, $L = 50$ cm. All other conditions as in Fig. 1.

variations will result when larger DNA species are studied²⁶. Further, as in slab gel operation, separation of larger species may only be achievable by employing pulsed fields. In addition to frequency, a number of other parameters can be manipulated to optimize separations, including field amplitude, type of waveform (e.g. field inversion or combination waveforms) and separation medium. These parameters are currently under investigation.

CONCLUSION

We have demonstrated the resolving power of polyacrylamide capillary columns with little or no crosslinking agent. The columns were stable and could be used repeatedly for long periods of time. The manipulation of monomer concentration permitted optimization of separation with respect to resolution and speed. Analysis of PCR products and restriction fragment mapping are applications well suited to these capillaries. Finally, pulsed field HPCE was shown to be feasible, and it is expected that this method will prove useful for the separation of DNA fragments.

ACKNOWLEDGEMENTS

This work was supported by Beckman Instruments. The authors thank Dr. Diana Najarian for the helping with the PCR experiment, and Dr. Jiun-Wei Chen and Ms. Maria Vilenchik for isolating the DNA fragments used for spiking. Stimulating discussions with Dr. Najarian, Dr. Chen, and also Dr. Andras Guttman are appreciated. Contribution No. 420 from the Barnett Institute.

REFERENCES

- 1 *Current Protocols in Molecular Biology*, Green Publishing and Wiley-Interscience, New York, 1988.
- 2 J. W. Jorgenson and K. D. Lukacs, *Science (Washington, D.C.)*, 222 (1983) 266.
- 3 B. L. Karger, A. S. Cohen and A. Guttman, *J. Chromatogr.*, 492 (1989) 585.
- 4 M. J. Gordon, X. Huang, S. L. Pentoney and R. N. Zare, *Science (Washington, D.C.)*, 242 (1988) 224.
- 5 A. G. Ewing, R. A. Wallingford and T. M. Olefirowicz, *Anal. Chem.*, 61 (1989) 292A.
- 6 B. M. Olivera, P. Baine and N. Davidson, *Biopolymers*, 2 (1984) 245.
- 7 A. S. Cohen, D. Najarian, J. A. Smith and B. L. Karger, *J. Chromatogr.*, 458 (1988) 303.
- 8 T. J. Kasper, M. Melera, P. Gozel and R. G. Brownlee, *J. Chromatogr.*, 458 (1988) 303.
- 9 A. S. Cohen, D. R. Najarian, A. Paulus, A. Guttman, J. A. Smith and B. L. Karger, *Proc. Natl. Acad. Sci. U.S.A.*, 85 (1988) 9660.
- 10 A. Guttman, A. S. Cohen, D. N. Heiger and B. L. Karger, *Anal. Chem.*, 62 (1990) 137.
- 11 S. Hjertén, *Arch. Biochem. Biophys.*, Suppl. 1 (1962) 147.
- 12 J. G. Chirikjian (Editor), *Restriction Endonucleases and Methylases*, Elsevier, New York, 1987.
- 13 H. H. Kazarian, in H. A. Erlich (Editor), *PCR Technology*, Stockton Press, New York, 1989.
- 14 M. Burmeister and H. Lehrach, *Nature (London)*, 324 (1986) 582.
- 15 J. Ballantyne, G. Sensabaugh and J. A. Witkowski, *DNA Technology and Forensic Science; Banbury Center Report No. 33*, Cold Spring Harbor Press, New York, 1989.
- 16 H. A. Erlich (Editor), *PCR Technology*, Stockton Press, New York, 1989.
- 17 R. White and J. M. Lalovel, *Adv. Human Genetics*, 16 (1987) 121.
- 18 H. J. Bode, *Anal. Biochem.*, 83 (1977) 204.
- 19 H. J. Bode, *Anal. Biochem.*, 83 (1977) 364.
- 20 B. G. Johansson and S. Hjerten, *Anal. Biochem.*, 59 (1974) 200.
- 21 D. Tietz, M. H. Gottlieb, J. S. Fawcett and A. Chrambach, *Electrophoresis*, 7 (1986) 217.
- 22 F. E. P. Mikkers, F. M. Everaerts and Th. P. E. M. Verheggen, *J. Chromatogr.*, 169 (1979) 11.

- 23 M. Zhu, D. L. Hansen, S. Burd and F. Gannon, *J. Chromatogr.*, 480 (1989) 311.
- 24 A. M. Chin and J. C. Colburn, *Am. Biotech. Lab.*, Dec. (1989) 16.
- 25 D. C. Schwartz and C. R. Cantor, *Cell*, 37 (1984) 67.
- 26 C. R. Cantor, C. L. Smith and M. K. Mathew, *Ann. Rev. Biophys. Chem.*, 17 (1988) 287.
- 27 G. F. Carle, M. Frank and M. V. Olson, *Science (Washington, D.C.)*, 232 (1986) 65.
- 28 *Protocol for GeneAmp DNA Amplification Reagent Kit*, Perkin-Elmer Cetus, Norwalk, CT, 1989.
- 29 A. Chrambach, *The Practice of Quantitative Gel Electrophoresis*, VCH, Deerfield Beach, FL, 1985.
- 30 J. P. Foley and J. G. Dorsey, *Anal. Chem.*, 55 (1983) 730.
- 31 *1 kb DNA Ladder Product Information*, Bethesda Research Laboratories, Gaithersburg, MD, 1990.
- 32 R. J. Nelson, A. Paulus, A. S. Cohen, A. Guttman and B. L. Karger, *J. Chromatogr.*, 480 (1989) 111.
- 33 H. J. Bode, *Electrophoresis '79*, Walter de Gruyter & Co., New York, 1980.
- 34 R. S. Dubrow, *2nd International Symposium on High Performance Capillary Electrophoresis, San Francisco, CA, January 1990*, paper P-208.
- 35 K. A. Ferguson, *Metabolism*, 13 (1964) 1985.
- 36 A. T. Andrews, *Electrophoresis*, Clarendon Press, Oxford, 2nd ed., 1986.
- 37 J. K. Elder and E. M. Southern, *Anal. Biochem.*, 128 (1983) 227.
- 38 P. Bocek, M. Deml, P. Gebauer and V. Dolnik, in B. J. Radola (Editor), *Analytical Isotachopheresis*, VCH Publishers, New York, 1988.
- 39 S. J. Hjerten, K. Elenbring, F. Kilar, J. Liao, A. J. C. Chen, C. J. Siebert and M. Zhu, *J. Chromatogr.*, 403 (1987) 47.
- 40 D. L. Holmes and N. C. Stellwagen, *Electrophoresis*, 11 (1990) 5.
- 41 G. W. Slater and J. Noolandi, *Biopolymers*, 28 (1989) 1781.
- 42 A. G. Ogston, *Trans. Faraday Soc.*, 54 (1958) 1754.
- 43 S. L. Pentoney, R. N. Zare and J. F. Quint, *Anal. Chem.*, 61 (1989) 1642.
- 44 J. C. Southerland, D. C. Monteleone, J. H. Mugavero and J. Trunk, *Anal. Biochem.*, 162 (1987) 511.

Separation and analysis of DNA sequence reaction products by capillary gel electrophoresis

A. S. COHEN, D. R. NAJARIAN and B. L. KARGER*

Barnett Institute, Northeastern University, Boston, MA 02115 (U.S.A.)

ABSTRACT

This paper demonstrates the potential of capillary gel electrophoresis with laser induced fluorescence detection as a tool for DNA sequence determination. Both synthetic oligonucleotides and single-stranded phage DNA were utilized as templates in the standard chain termination procedure. Primer molecules were tagged at the 5' end with the fluorescent dye, JOE. First, baseline resolution of a dA extended primer from 18 to 81 bases long, a total of 64 fragments, was observed. A second synthetic template was designed to yield alternating stretches of dA and dT extensions of the primer. Thirdly, the sequence reaction products from a synthetic oligonucleotide template containing all four bases was analyzed in four independent runs, one for each of the four base-specific reactions. In all cases, the expected number and patterns of peaks were observed by capillary gel electrophoretic analysis. Finally, separation of sequence reaction products generated with single-strand M13mp18 phage DNA as template exhibited baseline resolution of fragments differing in length by a single nucleotide and from 18 to greater than 330 bases total length.

INTRODUCTION

High performance capillary electrophoresis (HPCE) has become an important separation tool as a result of its high resolving power and speed^{1–4}. The technique has been applied in the open tube capillary format for separation of a wide variety of compounds including large biomolecules such as proteins and nucleic acids.

This laboratory has developed polyacrylamide gel-filled capillaries for the ultra-high resolution of nucleic acids^{5–7}. Efficiencies for separation of single stranded fragments up to at least 160 bases in length were found to be as high as $30 \cdot 10^6$ plates/m, with separation complete in under 30 min. In addition, the columns were shown to be stable for well in excess of 150 injections⁶. Such performance makes these columns very attractive for DNA sequence analysis which relies on the separation and identification of fragments having one common endpoint and differing in length by a single nucleotide. These fragments can be generated by base-specific chemical degradation⁸ or, more commonly, by the chain-termination method⁹. In either case, correlation of

the size of each fragment with a base-specific reaction allows the order of the nucleotides to be determined.

At present, separation of the DNA sequencing fragments is conventionally achieved by electrophoresis on high-resolution denaturing polyacrylamide slab gels¹⁰. The migration rate of a single-stranded DNA molecule is primarily dependent on chain length in these systems. It is routine to obtain sequence information for fragments greater than 400 bases in length in a single slab gel run. In conventional sequencing, radioisotopes are incorporated into the analyte during chain elongation, and detection is accomplished by autoradiography. In addition, automated systems using either radioisotopic¹¹ or laser-induced fluorescence detection¹²⁻¹⁶ have been developed to detect the products of Sanger sequencing reactions⁹ on slab gels.

DNA sequencing methodologies are currently under intense evaluation as a result of the Human Genome Project¹⁷. The goal of this program is to sequence the haploid human genome within 15 years. This effort involves the determination of roughly $3 \cdot 10^9$ base pairs, and with present slab gel technology, 100 of the most advanced automated slab gel systems operating for 60 years would be required¹⁸. Clearly, methodologies for much higher throughput are necessary.

Relative to slab gel operation, polyacrylamide gel HPCE offers more rapid separation, higher resolving power, and with appropriate instruments, subattomole level of detection. Ultimately, with columns operating in a parallel processing mode, throughputs as high as $1 \cdot 10^5$ base pairs per hour may be envisioned [*i.e.* 100 columns \times 1000 (bases/h/column)]. With such high throughputs, costs will easily be contained at levels well below the current US\$ 2-5 per base¹⁷. The first step in transforming this potential into reality is the development of gel HPCE for separation and detection of DNA sequence reaction products.

This paper demonstrates the use of gel-filled capillaries with laser-induced fluorescence for the separation and subattomole detection of DNA sequence reaction products. In addition, in approximately 1 h, baseline resolution of fragments greater than 330 bases long and differing in length by a single nucleotide can be achieved. The columns are useable for multiple injections. Other researchers are also investigating HPCE for the analysis of DNA sequence reaction products^{19,20}.

EXPERIMENTAL

Apparatus

The HPCE system used in this work was configured as described previously⁵ except that a 60 kV high voltage d.c. power supply (Model PS/MK30, Glassman, Whitehouse Station, NJ, U.S.A.) was used to generate the potential across the gel-filled capillary. The laser detection system employed is presented schematically in Fig. 1 and is similar to that described previously²¹. An argon ion laser (Model 532 AT, Omnichrom, Chino, CA, U.S.A.) mounted on a 4 \times 6 ft. optical table (Model 10531/13825, Oriel, Stamford, CT, U.S.A.), was operated in the light-regulated mode at 0.03-0.05 W. The laser light was passed through a narrow band filter (Model D1-488, Corion, Holliston, MA, U.S.A.), directed by reflection using a beam steerer (Model M670, Newport) and focused into the capillary with a 25-mm focal length lens (Model KBX043, Newport). Fluorescence from the sample was collected with a 40 \times microscope objective (Model M-Set, Newport) and passed through an interference filter

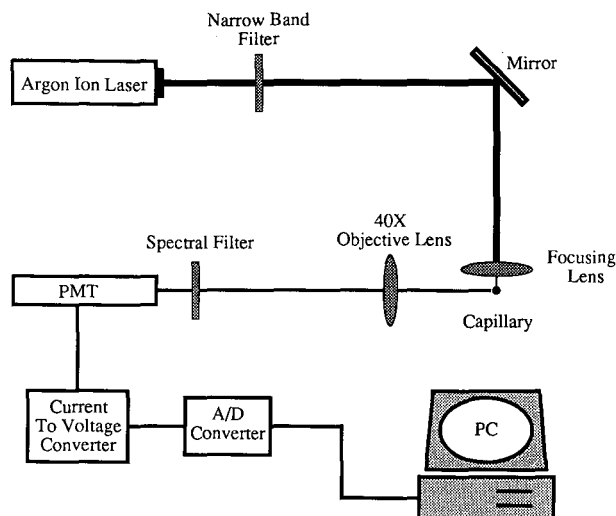


Fig. 1. Laser-induced fluorescence detection system for HPCE. The instrument consists of three major components: a detection system (laser, PMT = photomultiplier tube and accessories), a separation system (gel-filled capillary and power supply), and a data acquisition/analysis system (A/D interface and computer). See Experimental for complete details.

(Model S10-520-R, Corion) and a colored glass filter (Model OG520, Schott Glass Technol., Duryea, PA, U.S.A.). A photomultiplier tube (Model R928, Hamamatsu, San Jose, CA, U.S.A.) operated at 700 V and a photomultiplier readout (Model 7070, Oriel) were used to detect fluorescence. The resulting voltage output was displayed on a strip chart recorder and was simultaneously transmitted to an analog-to-digital (A/D) interface (Model 760 SB, Nelson Analytical, Cupertino, CA, U.S.A.) for transfer to a PC (Model ZBF-2526-EK, Zenith Data Systems).

Capillary columns

Polyacrylamide gel HPCE was performed in fused-silica tubing (Polymicro Technologies, Phoenix, AZ, U.S.A.), 75 μm I.D., 375 μm O.D., effective length (l) = 500–750 mm, total length (L) = 750–940 mm. Capillaries were prepared as described^{5,6}. Columns were first treated with methacryloxypropyltrimethoxysilane (Petrarch, Bristol, PA, U.S.A.). A solution of acrylamide (3% T/5% C)²² in 0.1 M Tris-borate, pH 7.6, 2.5 mM EDTA and 7 M urea was prepared, degassed, and introduced into the treated capillary column after adding ammonium persulfate and N,N,N',N'-tetramethylethylenediamine (TEMED).

Samples were injected into the column by dipping the cathodic end of the capillary into the sample solution and applying a voltage of 10 kV for 10–30 s. Separation was achieved at a typical applied field of 300 V/cm. Each column was used for multiple injections. Periodically, a short section of the capillary at the injection end was trimmed.

Sample preparation

Sequences for all oligonucleotides are given in the figure legends. All synthetic oligonucleotides except TEM80.1 and TEM80.2 were synthesized on a Cyclone DNA synthesizer (Milligen/Biosearch, Burlington, MA, U.S.A.). The two oligonucleotides, TEM80.1 and TEM80.2, were purchased from the Protein Chemistry Facility at Tufts Medical School, Boston, MA, U.S.A. Oligonucleotides to be fluorescently tagged were synthesized with a modified 5' end using N-TFA-C₆ Aminomodifier (CLONTECH, Labs, Palo Alto, CA, U.S.A.). Dye attachment reactions were performed with the fluorescein-based "JOE" dye purchased as the N-succinimide ester (Applied Biosystems, Foster City, CA, U.S.A.)²³. JOE-labelled DNA was purified by Sepharose G-25 chromatography followed by reversed-phase high-performance liquid chromatography²⁴. Single-stranded M13mp18 DNA was purchased from New England Biolabs, Beverly, MA, U.S.A. Deoxy- and dideoxynucleoside triphosphates were purchased from Pharmacia, Piscataway, NJ, U.S.A.; the Klenow fragment of DNA polymerase I and Sequenase 2.0 were obtained from U.S. Biochemical Corp., Cleveland, OH, U.S.A.

Sequence reactions performed with the Klenow enzyme contained 5 pmoles template, 20 pmoles primer and 60 units Klenow in 187 μ l of 10 mM Tris · HCl pH 7.5, 10 mM MgCl₂, 50 mM NaCl, 3.3 μ M dATP, 60 μ M ddATP and 33 μ M each of dCTP, dTTP and dGTP. After incubation at 37°C for 30 min, the reaction was stopped by heating to 65°C for 10 min. DNA was recovered by ethanol precipitation. For sequencing reactions performed with Sequenase 2.0, 4 pmoles each of template and primer in 25 μ l 10 mM Tris · HCl pH 7.5, 10 mM MgCl₂ and 50 mM NaCl were annealed by heating to 55°C for 2 min, followed by cooling to 37°C for 30 min. The mixture was adjusted to 37.5 μ l and made 200 μ M in dATP, dGTP, dCTP and dTTP, 7 mM in dithiothreitol and 5 μ M in the appropriate dideoxynucleotide. After addition of 7 units of Sequenase 2.0, the mixture was incubated at 37°C for 5 min, then stopped by heating to 65°C for 10 min. DNA was recovered by ethanol precipitation. All samples were stored in the dark at -20°C until use. Immediately prior to analysis the sample was resuspended in 2-5 μ l of 80% (v/v) formamide, 8 mM EDTA, heated to 90°C for 2 min and placed on ice.

RESULTS AND DISCUSSION

Our goal in pursuing this research was to demonstrate the feasibility of capillary gel electrophoresis as a tool in DNA sequencing. Our initial strategy was to examine products of a standard enzymatic DNA sequence reaction performed using synthetic oligonucleotides as both primer and template. This approach allowed us to predict exactly each product, while limiting the number and length of the resulting fragments.

TEM80.1 was sequenced using JOE-PRM18.1 as primer (see caption of Fig. 2 for oligonucleotide sequences). When annealed, these two oligonucleotides formed a double-stranded region of 17 base pairs. The Klenow fragment of DNA polymerase I was used to extend the primer in the presence of ddATP, and the electropherogram of the reaction products is presented in Fig. 2. Sixty-four baseline resolved peaks were observed in a time interval of less than 8 min, out of a total of 30 min run time. Based on the migration time separately determined for the primer, JOE-PRM18.1, the earli-

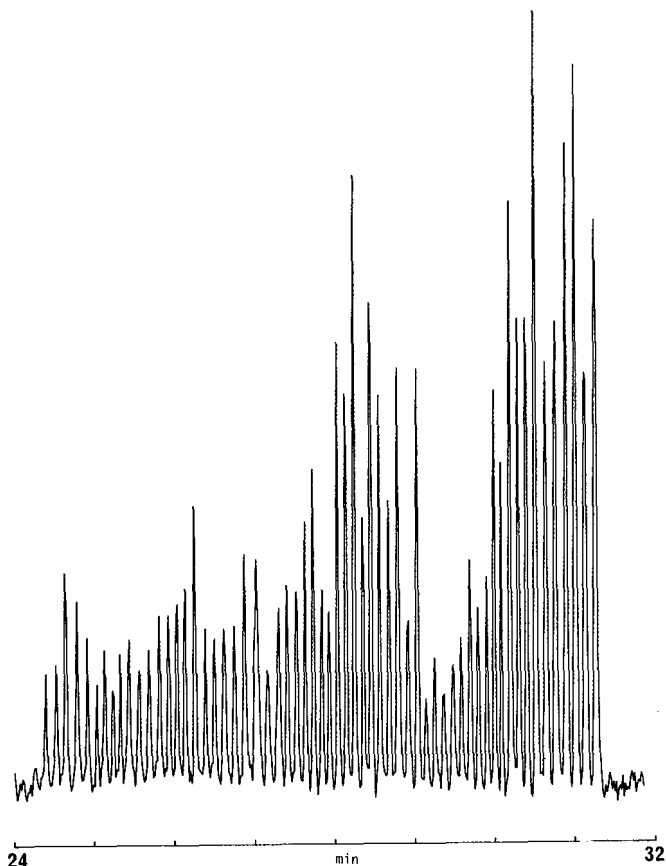


Fig. 2. Electropherogram of chain-termination sequencing reaction products. Template, TEM80.1 = 5'-T₆₃ACAACGTCGTGACTGGG-3'. Primer JOE-PRM18.1 = 5'-JOE-TCCCAGTCACGACGTTGT-3'. Primer was extended by the Klenow fragment of DNA polymerase I in the presence of ddATP. Sequence reactions and electrophoretic conditions are described in the Experimental section. Running conditions: $l = 540$ mm, $L = 680$ mm, $E = 300$ V/cm, injection = 10 kV, 30 s, buffer = 0.1 M Tris-borate, 2.5 mM EDTA, 7 M urea, pH 7.6.

est peak in the electropherogram was the unextended primer. The other peaks represented primer extended by 1, 2, 3 ... 63 residues and terminated by ddA. Upon examination, the migration time for each fragment was found to be a linear function of length with a correlation coefficient of better than 0.999. We interpreted this to mean that the contribution of the JOE dye moiety to each fragment added a constant increment to the mobility of fragments in this size range.

It can be observed that peak heights in Fig. 1 varied by up to six-fold. This variation was a consequence of the enzymatic nature of the Klenow fragment in which the relative rates of incorporation of dideoxy- and deoxynucleotides are sequence dependent⁹. Sequenase 2.0 has been shown to be superior to the Klenow fragment²⁵ and was used in all other experiments described in this report.

We next increased the complexity of the sequencing sample by using TEM80.2

as template (see caption of Fig. 3 for sequence). Two independent reactions were performed, one in the presence of ddATP and the second in the presence of ddTTP. Fig. 3 presents the electropherograms for the two reactions. The reaction containing ddATP was expected to generate a set of fragments all of which begin with Joe-PRM18.1 primer and which end at any position corresponding to dT in the template. The predicted pattern for the 34 expected products of this reaction was: sextet (un-extended primer plus 5 ddA-terminated fragments), space (no dT residues at these positions), quintet (5 ddA-terminated fragments), space, quintet, space ... triplet (final 3 ddA-terminated fragments). In an analogous manner, 31 peaks having a pattern of

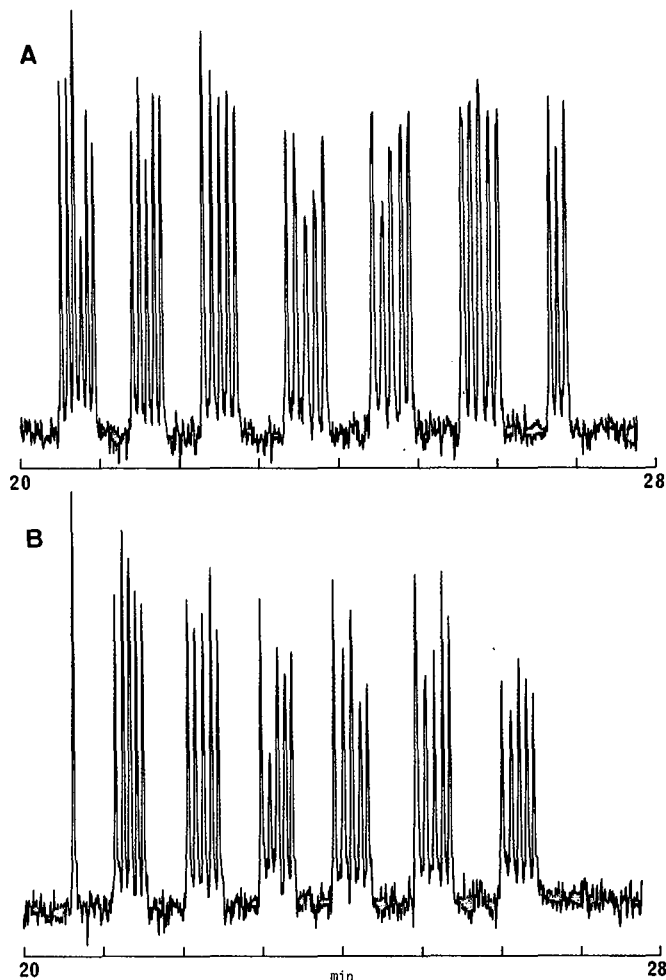


Fig. 3. Electropherogram of chain-termination sequencing reaction products. Template, TEM80.2 = 5'-T₃A₅T₅A₅T₅A₅T₅A₅T₅A₅T₅A₅T₅ACAACGTCGTGACTGGG-3'. Primer, JOE-PRM18.1 = 5'-JOE-TCCCAGTCACGACGTTGT-3'. (A) dA reaction: primer was extended by Sequenase 2.0 in the presence of ddATP. (B) dT reaction: primer was extended by Sequenase 2.0 in the presence of ddTTP. Sequence reaction and electrophoretic conditions are described in the Experimental section. Running conditions: see Fig. 2.

singlet (unextended primer), space, quintet, space ... quintet were predicted for extensions in the presence of ddTTP. The electropherograms in Fig. 3A and B depict exactly the expected patterns with baseline resolution of all fragments and with a run time of less than 30 min. It can also be noted that peak height variation in Fig. 3 was significantly less than that in Fig. 2, a direct consequence of replacing the Klenow fragment with Sequenase 2.0.

With the successful correlation between predicted and observed peak patterns for the synthetic templates in Figs. 2 and 3, we next investigated a more realistic template, TEM80.3. This DNA represented the sequence of the polylinker cloning site of the phagemid pBluescript SK(+) from positions 585 to 664 and contained all four nucleotides (see caption of Fig. 4 for sequence). Four separate base-specific reactions were performed, and the products of each reaction were independently analyzed three times.

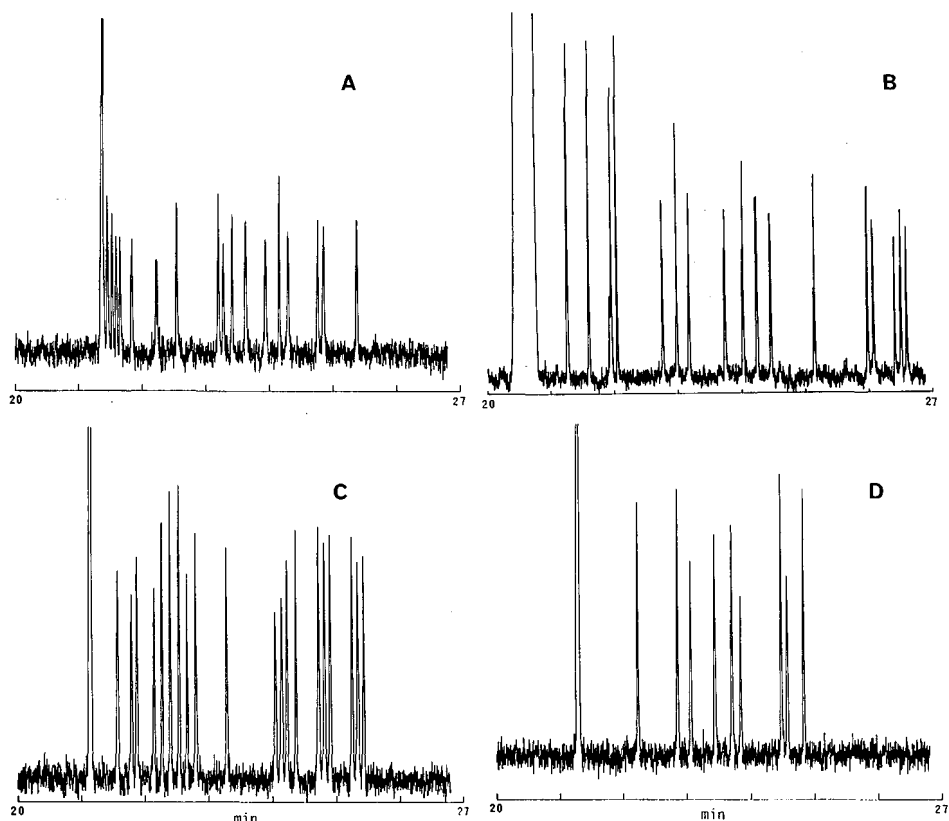
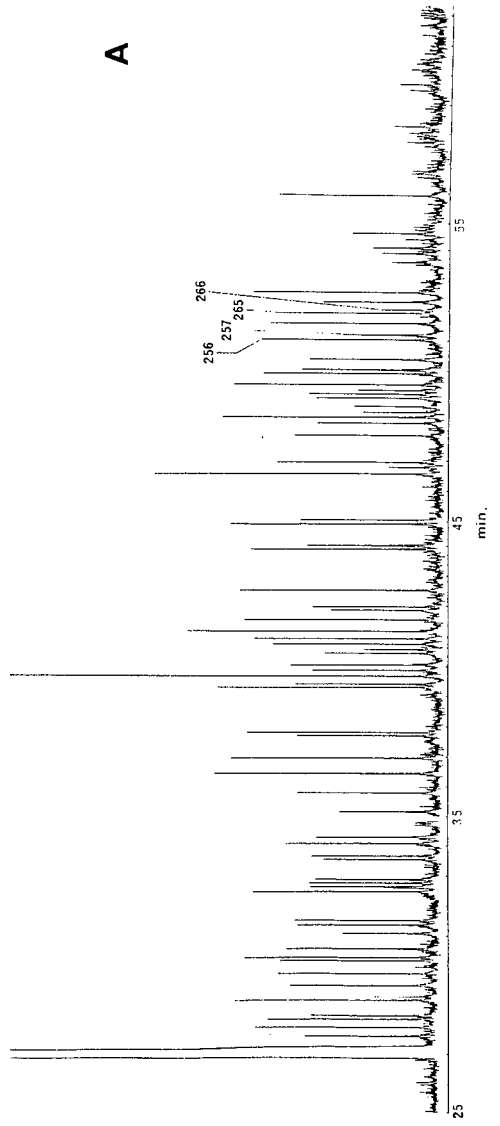


Fig. 4. Electropherogram of chain-termination sequencing reaction products. Template, TEM80.3 = 5'-GGGCCCCGGTACCCAATTTCGCCCTATAGTGAGTCGTATTACGCGCGCTCACTGGCCGT-CGTTTACAACGTCGTGACTGGG-3'. Primer, JOE-PRM18.1 = 5'-JOE-TCCCAGTCACGAC-GTTGT-3'. (A) dA reaction: primer was extended in the presence of ddATP. (B) dC reaction: primer was extended in the presence of ddCTP. (C) dG reaction: primer was extended in the presence of ddGTP. (D) dT reaction: primer was extended in the presence of ddTTP. Sequencing reactions were performed using Sequenase 2.0. Sequence reaction and electrophoretic conditions are described in the Experimental section. Running conditions: see Fig. 2.



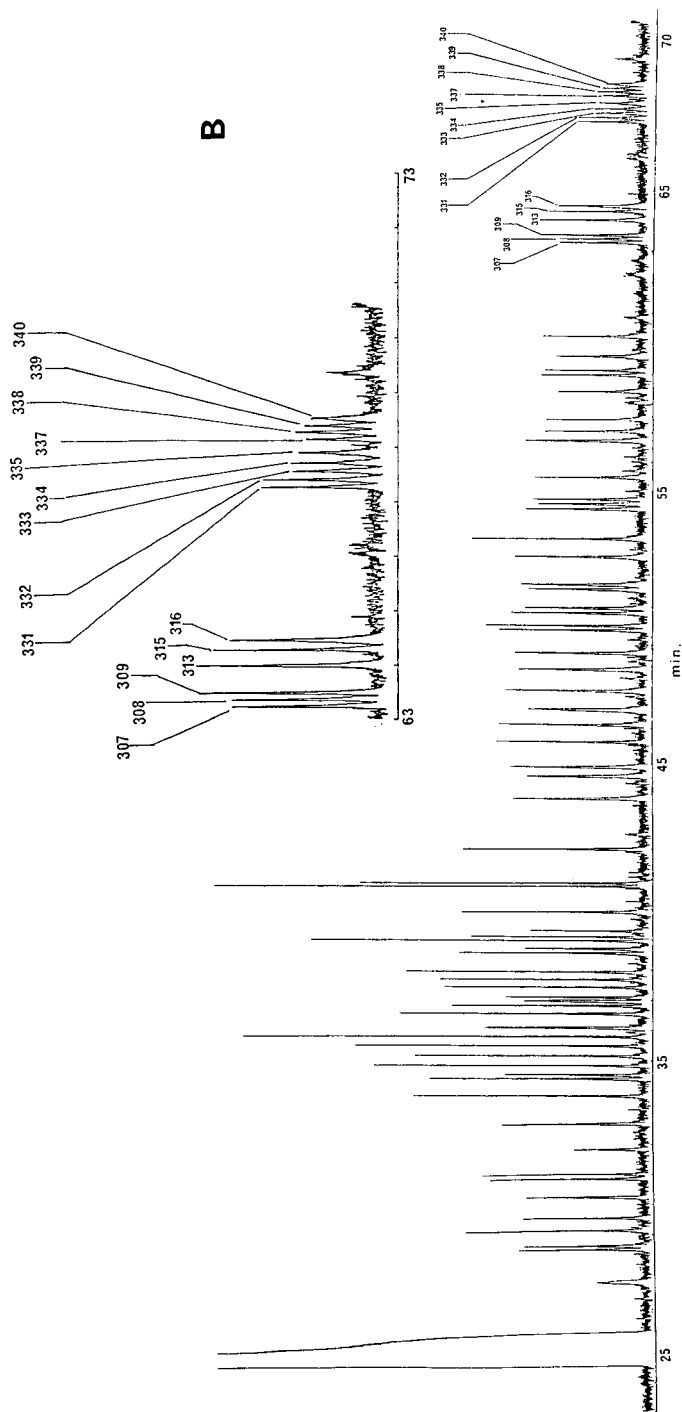


Fig. 5. Electropherogram of chain-termination sequencing reaction products. Template: single stranded M13mp18. Primer, JOE-PRM18.1 = 5'-JOE-TCCCAGT-CACGACGTTGT-3'. (A) dC reaction: primer was extended by Sequenase 2.0 in the presence of ddCTP. (B) dT reaction: primer was extended by Sequenase 2.0 in the presence of ddTTP. Sequence reactions and electrophoretic conditions are described in the Experimental section. Running conditions: (A) $l = 500$ mm, $L = 650$ mm, $E = 350$ V/cm, buffer = 0.1 M Tris-borate, 2.5 mM EDTA, 7 M urea, pH = 8.0 ; (B) $l = 750$ mm, $L = 920$ mm, $E = 310$ V/cm, pH = 8.0 , injection = 10 kV, 15 s.

The data from representative runs of each sample are shown in Fig. 4A–D. The number and pattern of peaks in each electropherogram were as predicted. For example, the reaction in the presence of ddATP, Fig. 4A, was expected to produce five peaks at the earliest migration time: the unextended primer plus primer extended by 1, 2, 3 and 4 residues and terminated with ddA. Second, for the reaction containing ddCTP (complementary to dG, Fig. 4B), it was predicted that a doublet, space, triplet would occur at the longest migration time. Third, in Fig. 4C, the expected pattern –triplet, singlet, triplet, triplet– was observed at the end of the run for the reaction containing ddGTP. Finally, in Fig. 4D, the expected total of 10 peaks was found, 9 from the reaction with ddTTP and one from the unextended primer. In all four electropherograms, baseline resolution was observed even when fragments differed in length by a single nucleotide.

A preliminary investigation of proper peak alignment in Fig. 4A–D was undertaken. In this work, relative migration, using the primer as internal standard, was determined for all 63 bands. The relative migration of the bands occurred in the proper sequence order; however, in some cases the experimental error of 0.2% R.S.D. was greater than the increment from one base to the next. With proper care, nevertheless, this result suggests that four separate runs might be utilized for sequence determination. However, a better approach is to employ one column run with four different fluorescently tagged primers, as currently used in slab gels¹⁸. This strategy for capillary gel electrophoresis is under study in our laboratory.

M13 DNA sequence reactions

To evaluate the performance of gel-filled capillaries for separation of longer sequencing fragments, single-stranded M13mp18 DNA was utilized as template. JOE-PRM18.1 was again used as primer, and reaction conditions were identical to those used when synthetic templates were employed. The electropherogram of the reaction products obtained in the presence of ddCTP is displayed in Fig. 5A. In 1 h, a large number of peaks were resolved which were identified based on the known sequence of M13mp18. It can be observed that baseline resolution of fragments 256–257 and 265–266 was readily achieved. Clearly, gel-filled capillary columns provide sufficient resolution to separate fragments as large as 300 nucleotides and differing in length only by one residue. Signal intensity decreased rapidly for fragments longer than 300 bases. This effect was probably a consequence of reaction conditions and sample matrix. The exact causes are currently under investigation.

The electropherogram of reaction products obtained in the presence of ddTTP is displayed in Fig. 5B. Separation of fragments up to 340 bases long was achieved in approximately 1 h with high resolution. Identification of peaks was again made from the known sequence of M13mp18. The clusters of fragments from 331–355 and 337–340 bases long, shown in the inset of Fig. 5B, demonstrate clearly the resolution of large fragments which differ in length by a single nucleotide. In addition, the temporal distance between peaks 335 and 337 was sufficient to accommodate a fragment 336 bases long which was not a predicted product of the ddTTP reaction. Also, a peak corresponding to a fragment 328 bases long was predicted but not observed. This was most likely due to a loss in signal intensity specific for this fragment coupled to the decreased signal generally seen for larger fragments in both electropherograms of Fig. 5. When migration time is examined with respect to fragment length, a linear relation-

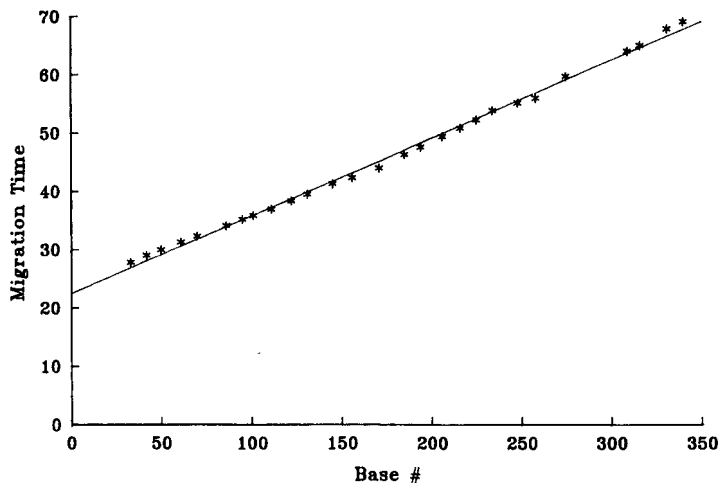


Fig. 6. Plot of migration time vs. fragment length. Values for migration time were taken from the electropherogram presented in Fig. 5B (dT reaction for M13mp18). Migration time of peaks representing ddT-terminated fragments approximately 10n bases long (where n is an integer from 2 to 36) were selected. Peaks were assigned fragment lengths based on the known sequence of M13mp18.

ship (correlation coefficient = 0.997) is observed (Fig. 6). This linear behavior is an important feature for DNA sequencing. It is important to recognize that no peak compression⁹ has been observed in the samples we have examined. Nevertheless, further studies of this point are necessary.

Detection limits

A preliminary assessment of detection limits was made in this work. We first determined the detection level in the open tube by examining the signal-to-noise ratio of various concentrations of fluorescein flowing by the detector. A 10^{-11} M solution yielded a signal-to-noise ratio greater than 5:1, using the apparatus described in Fig. 1. If we assume a detection cell volume of low pl, this signal represents approximately 0.001 attomole of mass determined at the detection zone. Next we examined the gel column. An aqueous solution of $1.5 \cdot 10^{-10}$ M JOE-PRM18.1 (10 kV, 2 s) yielded a signal-to-noise ratio of greater than 5:1. It is difficult to quantify the actual amount injected through the gel capillary, given such factors as sample focusing upon injection; however, a reasonable estimate would be 0.1 attomole or less, based on a comparison of the open tube to gel results.

CONCLUSIONS

The results of this work demonstrate the potential of polyacrylamide gel capillary electrophoresis and laser-induced fluorescence detection for DNA sequencing. The features of this approach include (1) very high resolution, (2) rapid separation, (3) high sensitivity, (4) multiple injections on a given column and (5) automation. Baseline resolution of fragments one base different in length is presented for fragments up to 340 bases in length, and detection limits are estimated to be subattomole.

Current studies include extending resolution to well in excess of 300 bases, exploring reaction and sample handling conditions and developing a single column instrument for detection of four different fluorescent dyes in one separation.

Ultimately, single column operation could be quite satisfactory for general laboratory sequencing needs. However, in the case of the Human Genome Project, a bank of columns would be required, so that multiple sequences can be analyzed simultaneously. In such an approach, each gel capillary column would represent a single lane in the current automated approaches to slab gel electrophoresis.

ACKNOWLEDGEMENTS

The authors gratefully acknowledge Beckman Instruments for support of this work. The authors further acknowledge Dr. Robert Rush for assistance in purification procedures. This is Paper No. 416 from the Barnett Institute.

REFERENCES

- 1 J. W. Jorgenson and K. D. Lukacs, *Science (Washington, D.C.)*, 222 (1983) 266.
- 2 A. G. Ewing, R. A. Wallingford and T. J. Olefirowicz, *Anal. Chem.*, 61 (1989) 292A.
- 3 M. J. Gordon, X. Huang, S. L. Pentoney and R. N. Zare, *Science (Washington, D.C.)*, 242 (1988) 224.
- 4 B. L. Karger, A. S. Cohen and A. Guttman, *J. Chromatogr.*, 492 (1989) 585.
- 5 A. S. Cohen, D. R. Najarian, A. Paulus, A. Guttman, J. A. Smith and B. L. Karger, *Proc. Natl. Acad. Sci. U.S.A.*, 85 (1988) 9660.
- 6 A. Guttman, A. S. Cohen, D. N. Heiger and B. L. Karger, *Anal. Chem.*, 62 (1990) 137.
- 7 A. Guttman, A. S. Cohen, A. Paulus, B. L. Karger, H. Rodriguez and W. S. Hancock, in C. Shaefer-Nielsen (Editor), *Electrophoresis '88*, VCH, New York, 1988, p. 151.
- 8 A. Maxam and W. Gilbert, *Proc. Natl. Acad. Sci. U.S.A.*, 74 (1977) 560.
- 9 F. Sanger, S. Nicklen and A. R. Coulson, *Proc. Natl. Acad. Sci. U.S.A.*, 74 (1977) 5463.
- 10 *Current Protocols in Molecular Biology*, Green Publishing and Wiley-Interscience, New York, 1988.
- 11 *Acugen 402 Sequencer*, EG & G Biomolecular, Natick, MA.
- 12 L. M. Smith, J. Z. Sanders, R. J. Kaiser, P. Hughes, C. Dodd, C. R. Connell, C. Heiner, S. B. H. Kent and L. E. Hood, *Nature (London)*, 321 (1986) 674.
- 13 J. M. Prober, G. L. Trainor, R. J. Dam, F. W. Hobbs, C. W. Robertson, R. J. Zagursky, A. J. Cocuzza, M. A. Jensen and K. Baumeister, *Science (Washington, D.C.)*, 238 (1987) 336.
- 14 W. Ansorge, B. Sproat, J. Stegemann, C. Schwager and M. Zenke, *Nucl. Acids Res.*, 15 (1987) 4593.
- 15 H. Kambara, T. Nishikawa, Y. Katayama and T. Yamaguchi, *BioTechnology*, 6 (1988) 816.
- 16 J. A. Brumbaugh, L. R. Middendorf, D. L. Grone and J. L. Ruth, *Proc. Natl. Acad. Sci. U.S.A.*, 85 (1988) 5610.
- 17 *Understanding Our Genetic Inheritance: The U.S. Human Genome Project. The First Five Years, 1991-1995*, Publication DOE/ER-0452P, U.S. Department of Health and Human Services and U.S. Department of Energy.
- 18 G. L. Trainor, *Anal. Chem.*, 62 (1990) 418.
- 19 H. Drossman, J. A. Luckey, A. J. Kostichka, J. D'Cunha and L. M. Smith, *Anal. Chem.*, 62 (1990) 900.
- 20 H. Swerdlow and R. Gesteland, *Nucl. Acids Res.*, 18 (1990) 1415.
- 21 W. G. Kuhr and E. S. Yeung, *Anal. Chem.*, 60 (1988) 2642.
- 22 B. G. Johansson and S. Hjerten, *Anal. Biochem.*, 59 (1974) 200.
- 23 *DNA Modification Reagents for Use in Automated DNA Synthesis: A User's Manual*, CLONTECH Laboratories, Palo Alto, CA.
- 24 *Synthesis of Fluorescent Dye-labelled Oligonucleotides for Use as Primers in Fluorescent-based DNA Sequencing*, User Bulletin 11, Applied Biosystems, Foster City, CA.
- 25 S. Tabor and C. C. Richardson, *Proc. Natl. Acad. Sci. U.S.A.*, 84 (1987) 4767.
- 26 D. Heiger, A. S. Cohen and B. L. Karger, unpublished results.

Capillary gel electrophoresis for DNA sequencing

Laser-induced fluorescence detection with the sheath flow cuvette

HAROLD SWERDLOW*

Howard Hughes Medical Institute, 743 Wintrobe Bldg., University of Utah, Salt Lake City, UT 84132 (U.S.A.)

and

SHAOLE WU, HEATHER HARKE and NORMAN J. DOVICH

Department of Chemistry, University of Alberta, Edmonton, Alberta T6G 2G2 (Canada)

ABSTRACT

Capillary polyacrylamide gel electrophoresis separation of dideoxycytidine chain-terminated DNA fragments is reported. A post-column laser-induced fluorescence detector based on the sheath flow cuvette was used to minimize background signals due to light scatter from the gel and capillary. A preliminary mass detection limit of 10^{-20} mol of fluorescein-labeled DNA fragments was obtained. The system was used to analyze an actual DNA sequencing sample. Theoretical plate counts of $2 \cdot 10^6$ were produced. Gel stability limits the performance of the current system.

INTRODUCTION

Capillary gel electrophoresis promises significant performance improvements when compared with conventional slab-gel electrophoresis. These advantages arise from the large surface-to-volume ratio of capillaries, providing rapid dissipation of Joule heat generated during electrophoresis. This efficient heat transfer allows use of high electric field strengths to generate fast, efficient separations. Early work with capillary-dimension electrophoresis media was performed by Edstrom^{1,2}, in the 1950s, who described the use of very fine cellulose fibers (5- μm diameter) for electrophoresis of nucleic acids from single cells at an electric-field gradient of 125 V/cm. In 1965, Matioli and Niewisch³ studied hemoglobin from single cells on fine polyacrylamide fibers of 50- μm diameter. Grossbach⁴ reported the use of gel-filled glass capillaries of 50- μm diameter in 1974. Slightly larger scale capillary polyacrylamide gel electrophoresis was reported in 1970 by Neuhoff *et al.*⁵ who used 5- μl capillaries for the study of ribonucleic acid polymerase. In 1983, Hjertén⁶ reported the use of a 150- μm I.D. capillary polyacrylamide electrophoresis separation of several samples

derived from bovine serum albumin. Beginning in 1987, Karger and co-workers⁷⁻¹⁰ have reported capillary polyacrylamide gel electrophoresis for the separation of proteins, chiral amino acids and polydeoxyadenylic acid fragments. Karger and Cohen^{11,12} received two patents describing both the use of a bifunctional reagent to chemically bind polyacrylamide to the capillary surface and the use of a polymeric additive to enhance the stability of gel-filled capillaries. Swerdlow and Gesteland¹³ have described the use of capillary polyacrylamide gel electrophoresis with on-column fluorescence detection to analyze actual DNA sequencing samples.

Recently, interest in the Human Genome Project has led to the study of more rapid DNA analysis. The application of capillary polyacrylamide gel electrophoresis to DNA sequencing appears to offer three advantages compared with conventional slab-gel electrophoresis. First, and most importantly, the high electric field that can be applied to the capillary system should increase the resolution of the separation, allowing longer segments of DNA to be analyzed in a single run. Second, the capillary electrophoresis instrument offers improved potential for automation. Third, the high electric field strength utilized in the capillary system should increase the speed of separating DNA sequencing samples. However, this last advantage can only be exploited if multiple capillary gels can be simultaneously run in the same instrument.

The application of capillary polyacrylamide gel electrophoresis to DNA analysis is currently limited by two problems. First, although partially addressed by Karger and Cohen^{11,12}, the routine production of reliable, bubble-free gels that can be operated at high electric field strength remains problematic. Second, the nature of the DNA sequencing reactions requires a high-sensitivity detection system¹⁴. Recent advances in automated DNA sequencing rely on fluorescence of labeled DNA fragments that have been separated by slab-gel electrophoresis^{14,15}. However, application of laser-induced fluorescence detection to capillary gel electrophoresis is not trivial. On-column fluorescence detection apparently suffers from a significant component of scattered light generated both in the gel and from the capillary walls¹⁵.

To overcome these detector limitations, we have turned to the sheath flow cuvette, commonly employed as a detection chamber in the biomedical technique of flow cytometry¹⁶ and proven as a high-sensitivity fluorescence detector for capillary zone electrophoresis¹⁷⁻¹⁹. In the cuvette, a sample stream is injected, under laminar flow conditions, in the center of a surrounding sheath stream, generally of the same refractive index. Our cuvette, taken from an Ortho cytofluorograph, is made of quartz, has optically flat windows and has a 250- μm square inner cross-section. Because the sample stream flows in the center of the sheath fluid in the high-optical-quality flow chamber, the contribution to the background signal due to light scatter from the windows is negligible. Extremely high-sensitivity fluorescence detection has been produced with the cuvette approaching single molecule detection²⁰⁻²⁴.

Application of the sheath flow cuvette to capillary polyacrylamide gel electrophoresis could suffer from a subtle problem. In capillary zone electrophoresis, the electroosmotic mobility of the solvent is normally significantly greater than the electrophoretic mobility of the analytes. As a result, the analytes are swept from the capillary to the cathodic detector by the solvent flow produced by electroosmosis. In gel-filled capillaries, by comparison, electroosmosis is greatly reduced; the electrophoretic mobility of the analyte is appreciably larger than the electroosmotic mobility of the solvent. Furthermore, in the application of capillary gel electrophoresis to

DNA separations, the polarity of the power supply is reversed compared with conventional zone electrophoresis; bulk solvent flow is directed from the detector (anode) toward the injection end (cathode). This bulk flow from the detection cuvette could distort the hydrodynamic characteristics of the sheath flow cuvette²⁵. It is not at all clear that the sheath flow cuvette will work well when used with capillary gel electrophoresis.

This paper demonstrates that the sheath flow cuvette functions well as a detector for capillary gel electrophoresis, independent of the relative magnitudes of electroosmosis and electrophoresis and independent of the direction of electroosmosis. Sheath flow cuvette-based fluorescence detection is employed for the analysis of an actual DNA sequencing sample.

EXPERIMENTAL

Materials

All solutions were prepared in filtered HPLC-grade water. Capillaries, 50 μm I.D. and 200 μm O.D. from Polymicro Technologies (Phoenix, AZ, U.S.A.) were used as received with no pre-treatment. Acrylamide, N,N'-methylenebisacrylamide (Bis) and N,N,N',N'-tetramethylethylenediamine (TEMED) were electrophoresis-purity reagents from Bio-Rad (Mississauga, Canada). Tris base and urea were ultrapure reagents (ICN, Montreal, Canada). Boric acid and EDTA were analytical-reagent grade (BDH, Edmonton, Canada) and ammonium persulfate was ultrapure electrophoresis grade (Boehringer Mannheim, Laval, Canada).

The DNA sequencing sample was prepared as described previously¹³. The 20-, 21-, 100- and 101-nucleotide long oligodeoxythymidylic acid marker DNAs were prepared on a Model 380A DNA synthesizer (Applied Biosystems, Foster City, CA, U.S.A.) using amino link 2 dye attachment reagent (Applied Biosystems) as the 5'-terminal monomer. Fluorescein isothiocyanate (400 μg) was reacted with 100 μg of the deprotected oligomer in 25 μl of 50 mM carbonate buffer at pH 9. The labeled oligonucleotides were purified chromatographically on a Sephadex G-25 column and by electrophoresis on a conventional 10% sequencing gel. Bands on the gel were identified by their fluorescence, eluted from the gel, concentrated by ethanol precipitation, and concentration determined in a fluorimeter.

Methods

A stock $10 \times$ TBE (pH 8.3) solution was prepared by dissolving 108 g Tris, 55 g boric acid and 40 ml of 0.5 M EDTA in water to a final volume of 1 l. Capillaries (50 cm long) were filled with a degassed 6% T, 5% C^a acrylamide/Bis, 8 M urea, 0.07% (w/v) ammonium persulfate, 0.07% (v/v) TEMED, solution prepared in a 1- to 10-dilution of the stock TBE buffer ($1 \times$ TBE final), and allowed to polymerize¹³.

Electrophoresis was driven by a 30-kV power supply (Spellman, Plainview, NY, U.S.A.). The laser-induced fluorescence detector, based on a sheath flow cuvette, was identical to that described previously, except that the sheath fluid was $1 \times$ TBE at a

^a C = g N,N'-methylenebisacrylamide Bis/(g Bis + g acrylamide); T = g acrylamide + g Bis/100 ml solution.

flow-rate of 0.5 ml/h¹⁷. Samples were loaded on the capillary electrophoretically as described previously¹³.

RESULTS AND DISCUSSION

In capillary gel electrophoresis, as applied to DNA sequencing, the electroosmotically induced bulk flow is directed from the detection cuvette to the injector. Thus it is not clear that the sheath flow cuvette will operate effectively. To test this possibility a mixture of fluorescein and fluorescein-labeled 20-, 21-, 100- and 101-nucleotide long oligodeoxythymidylic acid marker DNAs was injected onto a 50-cm long 6% T, 5% C, 8 M urea, polyacrylamide gel-filled capillary and electrophoresed at 200 V/cm. The instrument performed well; the electropherogram is displayed in Fig. 1. The first peak, at 35 min, is due to fluorescein, followed by the 20- and 21-mer doublet, and the 100- and 101-mer doublet. It appears that the electrophoretic velocity of the analyte is sufficiently high to inject the eluted sample quantitatively into the sheath stream, in spite of the fact that for the same sample electroosmotic mobility dominates over electrophoretic mobility in capillary zone electrophoresis (CZE; data not shown). Although these peaks are nearly baseline resolved, the plate count for the separation is rather low, about $1 \cdot 10^6$. We believe this is due to chemical inhomogeneity in the synthesized marker DNAs and not to inherent limitations of the system.

We estimated the mass detection limit for the 20-nucleotide long marker by two methods; the first based on the calculated injection volume and the known concentration of the sample, the second based on the signal observed for a standard solution of fluorescein and the area of the eluted peak. The detection limit of the sheath flow cuvette-based detector by both methods is about 10^{-20} mol of DNA injected on the capillary. This mass detection limit is about an order of magnitude poorer than that obtained for fluorescein thiocarbamyl derivatives of amino acids, but significantly better than other reported limits for fluorescent DNA sequencing¹³⁻¹⁵. The poor detection limit may arise from two sources. First, the fluorescence detection electronics were operated with a short time-constant, about 0.3 s, which was optimized for CZE separations. The time constant should be increased by about an order of magnitude to match the peak widths of the slower DNA analyses. Second, the low sample stream flow-rate, and its retrograde direction, results in a smaller sample-stream

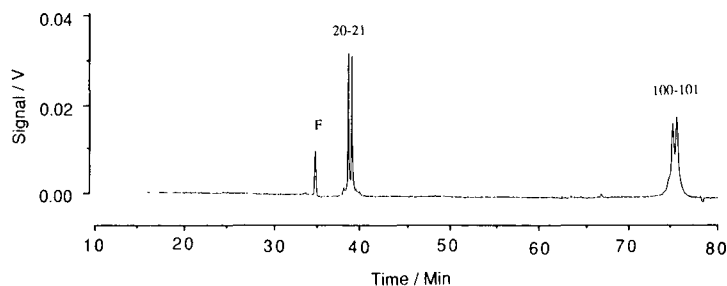


Fig. 1. Capillary gel electropherogram of synthetic fluorescently labelled oligodeoxythymidylic acid marker DNA molecules. F = Fluorescein. The other four peaks are oligodeoxythymidylic acid; numbering corresponds to the length in nucleotides.

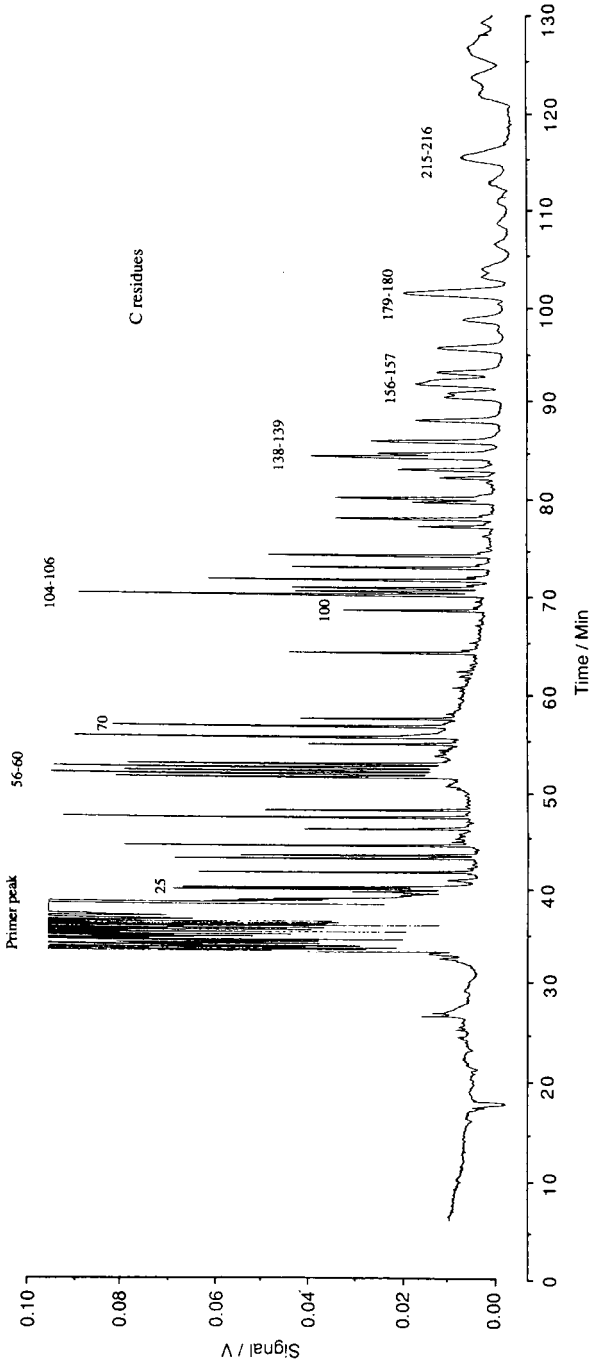


Fig. 2. Capillary gel electropherogram of a DNA sequencing reaction terminated with dideoxycytidine triphosphate. Each peak following the peak labeled 25 corresponds one-to-one to a C residue in the known DNA sequence. Peak numbering is according to total length of oligonucleotide fragments.

diameter passing through the detection region. Improved detection limits should follow by optimizing the sheath flow-rate to match the size of the image of the sample stream to the size of the pinhole in the collection optical train.

To assess the capabilities of our system for DNA sequencing, an actual DNA sequencing sample was run on a gel-filled capillary and visualized with the sheath flow cuvette-based detector (Fig. 2). A fluorescently labeled 18-nucleotide primer was chain extended, on a complementary template, in the presence of dideoxy cytidine triphosphate¹³. The resulting C-terminated oligonucleotides were electrophoresed in an identical manner to the separation of Fig. 1; the electropherogram is displayed in Fig. 2. The pattern of peaks at the beginning of the electropherogram are associated with the fluorescently labeled primer, it appears that this commercially produced primer is not pure but instead contains at least 25 minor components. The remaining peaks in Fig. 2 correspond directly to C residues in the known DNA sequence. The separation of DNA fragments is quite good in the region 25–140 bases. In particular, five consecutive cytidine residues, 56–60 nucleotides in length, are very well resolved in this analysis. The number of theoretical plates in the separation maximizes at about $2 \cdot 10^6$ in the range 25–100 bases.

Two rather significant problems appear to limit resolution of DNA oligomers in our system. First, the chemical inhomogeneity in the primer peak probably contributes significantly to broadening of the other peaks; the expected 25-nucleotide long oligonucleotide appears as a multiplet, although for larger peaks the subspecies do not resolve. Second, the separation degrades very rapidly for fragments longer than 140 bases. The origin of this degradation has been correlated with formation of one or more small bubbles at the injection end of the capillary during the separation run. This bubble formed after the start of the separation. Analytes that had passed the region where the bubble formed were not affected by its presence, whereas slower analytes suffered from reduced plate count due to eddy diffusion. Curiously, Guttman *et al.*¹⁰ has observed poor resolution past 150 nucleotides, also on a 6% T, 5% C column. He attributes this effect to restricted migration through the gel matrix for large-molecular-weight DNA molecules. Restricted migration cannot explain the observation, however, as separations performed on 6% T, 5% C gels in both capillary and slab-gel electrophoresis, yield satisfactory resolution to at least 300 bases^{13–15}.

The separations reported in this paper did not use gels that had been covalently attached to the walls. Karger's results with bifunctional silane reagents offer an excellent example of the potential of capillary gel techniques. Hopefully, by increasing the stability of the gel-filled capillaries, DNA sequence analysis that exploits the full separation properties of capillary gel electrophoresis will become a reality.

ACKNOWLEDGEMENTS

This work was funded by the Natural Sciences and Engineering Research Council of Canada and by the Department of Energy United States of America (Grant No. DE-FG02-88ER60700). H.S. gratefully acknowledges a fellowship from the National Science Foundation of the United States of America.

REFERENCES

- 1 J. E. Edstrom, *Nature (London)*, 172 (1953) 809.
- 2 J. E. Edstrom, *Biochim. Biophys. Acta*, 22 (1956) 378–388.
- 3 G. T. Matioli and H. B. Niewisch, *Science (Washington, D.C.)*, 150 (1965) 1824–1826.
- 4 U. Grossbach, in R. C. Allen and H. R. Maurer (Editors), *Electrophoresis and Isoelectric Focusing in Polyacrylamide Gel*, Walter de Gruyter, Berlin, 1974, p. 207.
- 5 V. Neuhoff, W. B. Schill, and H. Sternbach, *Biochem. J.*, 117 (1970) 623–631.
- 6 S. Hjertén, *J. Chromatogr.*, 270 (1983) 1–6.
- 7 A. S. Cohen and B. L. Karger, *J. Chromatogr.*, 397 (1987) 409–417.
- 8 A. Guttman, A. Paulus, A. S. Cohen, N. Grinberg and B. L. Karger, *J. Chromatogr.*, 488 (1988) 41–53.
- 9 A. S. Cohen, D. R. Najarian, A. Paulus, A. Guttman, J. A. Smith and B. L. Karger, *Proc. Natl. Acad. Sci. U.S.A.*, 85 (1988) 9660–9663.
- 10 A. Guttman, A. S. Cohen, D. N. Heiger and B. L. Karger, *Anal. Chem.*, 62 (1990) 137–141.
- 11 B. L. Karger and A. S. Cohen, *U.S. Pat.*, 4 865 706 (1989).
- 12 B. L. Karger and A. S. Cohen, *U.S. Pat.*, 4 865 707 (1989).
- 13 H. Swerdlow and R. Gesteland, *Nucleic Acids Res.*, 18 (1990) 1415–1419.
- 14 J. M. Prober, G. L. Trainor, R. J. Dam, F. W. Hobbs, C. W. Robertson, R. J. Zagursky, A. J. Cocuzza, M. A. Jensen and K. Baumeister, *Science (Washington, D.C.)*, 238 (1987) 336–341.
- 15 L. M. Smith, J. Z. Sanders, R. J. Kaiser, P. Hughes, C. Dodd, C. R. Connell, C. Heiner, S. B. H. Kent and L. E. Hood, *Nature (London)*, 321 (1986) 674–679.
- 16 D. Pinkel, *Anal. Chem.*, 54 (1982) 503A–508A.
- 17 Y. F. Cheng and N. J. Dovichi, *Science (Washington, D.C.)*, 242 (1988) 562–564.
- 18 S. Wu and N. J. Dovichi, *J. Chromatogr.*, 480 (1989) 141–155.
- 19 Y. F. Cheng, S. Wu, D. Y. Chen and N. J. Dovichi, *Anal. Chem.*, 62 (1990) 496–503.
- 20 L. W. Hershberger, J. B. Callis and G. D. Christian, *Anal. Chem.*, 51 (1979) 1444–1446.
- 21 N. J. Dovichi, J. C. Martin, J. H. Jett and R. A. Keller, *Science (Washington, D.C.)*, 219 (1983) 845–847.
- 22 N. J. Dovichi, J. C. Martin, J. H. Jett, M. Trkula and R. A. Keller, *Anal. Chem.*, 56 (1984) 348–354.
- 23 D. C. Nguyen, R. A. Keller, J. H. Jett and J. C. Martin, *Anal. Chem.*, 59 (1987) 2158–2160.
- 24 K. Peck, L. Stryer, A. N. Glazer and R. A. Mathies, *Proc. Natl. Acad. Sci. U.S.A.*, 86 (1989) 4087–4091.
- 25 F. Zarrin and N. J. Dovichi, *Anal. Chem.*, 57 (1985) 2690–2692.

Polyethyleneimine-bonded phases in the separation of proteins by capillary electrophoresis

JOHN K. TOWNS and FRED E. REGNIER*

Department of Chemistry, Purdue University, West Lafayette, IN 47907 (U.S.A.)

ABSTRACT

A hydrophilic, positively charged, durable coating has been developed for capillary electrophoresis of macromolecules. Polyethyleneimine is adsorbed to the inner wall of fused silica capillaries and the adsorbed coating cross-linked into a stable layer. Capillaries of polyethyleneimine-coated silica gave unique separations owing to the reversal of electro-osmotic flow caused by the positively charged coating. The resulting coating was stable from pH 2–12 and could be used over a wide pH range without substantial change in electro-osmotic flow. High-molecular-weight polymers were needed to give thick coatings which mask silanol groups on the wall. Proteins were resolved quickly and efficiently with good recovery using capillaries of 50 cm in length.

INTRODUCTION

Adsorption of positively charged species onto the walls of fused-silica capillaries is a problem in capillary zone electrophoresis. This is particularly true in the case of basic proteins and peptides where adsorption diminishes solute recovery and resolution. Therefore, in order to optimize the separation of basic solutes, adsorption to the capillary wall must be kept to a minimum.

Electro-osmotic flow is another issue that must be considered in fused-silica capillaries. Ionization of surface silanols generates an electrical double layer which migrates toward the cathode when an electric potential is applied to the capillary. Migration of positive ions in this double layer pulls the solution through the capillary, producing the phenomenon known as electro-osmotic flow. The rate of this flow is related to charge density and increases with the ionization of surface silanols from pH 3 to 9. The net velocity of a charged solute in a fused silica capillary is the sum of the rates of both convective and electrophoretic transport. Ideally, the convective component of transport should remain constant while the electrophoretic component is being varied with pH to optimize selectivity in a separation. This would only be possible in capillaries with no charge or constant charge at the surface.

To this end, modification of capillaries by either masking or deactivating surface silanol groups has been performed by physically coating capillary walls with

methylcellulose^{1,2} and by silane derivatization³⁻⁵, respectively. Although these coatings reduce both adsorption and electro-osmotic flow, they do not solve these problems. Residual silanols still diminish the recovery of basic proteins and cause electro-osmotic flow to vary widely with pH. Coating stability is also a problem. Hydrophilic organosilanes can erode from columns in a matter of days⁴.

This paper focuses on the preparation of fused-silica capillaries with a positively charged polymer coating. The function of this bonded phase is to enhance the separation and recovery of positively charged species, to stabilize electro-osmotic flow across the pH range from 5 to 11 and to extend the useful life of capillaries.

EXPERIMENTAL

Chemicals

Polyethyleneimine (PEI) 6 (average rel. mol. mass, $M_r = 600$) was purchased from Polysciences (Warrington, PA., U.S.A.). PEI 18 and 200 were gifts from Dow Chemical (Midland, MI, U.S.A.). Ethyleneglycol diglycidyl ether (EDGE) and triethylamine (TEA) were purchased from Aldrich (Milwaukee, WI, U.S.A.). All other reagents were commercially obtained, reagent grade if available or the purest grade obtainable if not.

Lysozyme (egg white), cytochrome *c* (horse heart), chymotrypsinogen A (bovine pancreas), ribonuclease A (bovine pancreas), and myoglobin (horse heart) were purchased from Sigma (St. Louis, MO, U.S.A.). The neutral markers, mesityl oxide and dextran blue (M_r 2000 000), were purchased from Aldrich.

Instrumentation

Capillary electrophoresis was performed on an instrument based on an in-house design. All high-voltage components of the system were contained in a Lucite cabinet fitted with a safety interlock that would interrupt the line voltage to the transformer in the power supply when the cabinet door was opened. A Spellman Model FHR 30P 60/EI (Spellman High Voltage Electronics, Plainview, NY, U.S.A.) power supply was used to apply the electric field across the capillary. The power supply output was connected to 22-gauge platinum-wire electrodes immersed in 3-ml buffer reservoirs along with the capillary ends. Polyimine-coated fused-silica capillaries (Polymicro Technologies, Phoenix, AZ, U.S.A.) of 50 and 75 μm I.D., 200 μm O.D. were used with the total length varying between 50 and 100 cm and the separation length from 35 to 85 cm. On-line detection was performed with a variable-wavelength UV absorbance detector (Model V4; Isco, Lincoln, NE, U.S.A.). Detection was monitored at 200 nm for the proteins and peptides and 254 nm for the mesityl oxide. The signal from the detector was fed to a Linear 2000 (Linear, Reno, NV, U.S.A.) strip chart recorder.

Electrophoresis

Protein solutions of a concentration of 1–5 mg/ml were injected into the capillary by syphoning for a fixed time (1–3 s) at a fixed height (5–8 cm). Mesityl oxide was used as the neutral marker along with dextran blue to determine any sizing differences in the coating. Several buffer solutions were used over the pH range of 3 to 11: 0.01 *M* acetate at pH 3 and 5, 0.01 *M* hydroxylamine-HCl at pH 7, 0.01 *M* diaminopropane at pH 9 and 11. Salt was added to each buffer to give comparable ionic strengths and

currents. During electrophoresis, current through the capillary never exceeded $50 \mu\text{A}$ with all analyses being run at ambient temperature. No temperature control of the capillary was employed. Between analyses, the capillary was flushed with 1% TFA in propanol, deionized water and the separation buffer for 1 min.

Capillary coating

Capillaries were first treated with 1.0 *M* NaOH for 15 min. followed by 15 min. of washing with deionized water. Residual water was evaporated from the capillaries by connecting the capillaries to a gas chromatography oven at 80°C for 1 h under a nitrogen pressure of 400 kPa. The methanolic solution of polyethyleneimine was then pulled through the capillary by syringe and allowed to sit for 8 h. The methanol-PEI solution was removed from the capillary by pushing nitrogen through the capillary. Nitrogen flow was continued through the capillary for 2 h to evaporate the methanol. In the case of PEI 200, which has water added to reduce the viscosity, the capillary was heated at 80°C for 4 h to remove the 33% water. Next, a 70% solution of EDGE in TEA was pulled into the capillary and allowed to sit for 1 h. This solution was then pushed out with nitrogen. Nitrogen flow through the capillary was continued at 400 kPa for 3 h. The capillary was then heated at 80°C for 30 min.

Picric acid assay

A $2 \text{ m} \times 100 \mu\text{m}$ I.D. PEI-coated capillary was washed with methylene chloride for 30 min followed by 0.2 *M* picric acid in methylene chloride. Unbound picric acid was removed with an additional methylene chloride wash. Bound picric acid was then released with 5% (v/v) TEA in methylene chloride into a 1-mm cuvette. Washing with the amine solution was continued until the solution eluting from the capillary was colorless. The eluent was then diluted to 0.1 ml and the triethylamine picrate assayed spectrophotometrically. The molar extinction coefficient of TEA picrate in methylene chloride is 14 500 at 358 nm.

RESULTS AND DISCUSSION

Surface derivatization

The synthetic route (Fig. 1) used to prepare positively charged capillaries in these studies was derived from techniques used in liquid chromatography to prepare silica-based anion-exchange packing materials. It has been shown⁶⁻⁸ that PEI is strongly adsorbed from organic solvents onto a silica surface where it may subsequently be cross-linked with a multifunctional oxirane into a continuous film. This cross-linked layer is held in place by electrostatic adsorption at many sites and cannot be eluted from the silica surface with solvents used in chromatography. Coating thickness is a function of both M_r and concentration of PEI in the coating solution⁸. EDGE was chosen as the cross-linking agent because it was of sufficient length to bridge between adjacent adsorbed PEI molecules and would contribute to the hydrophilicity of the coating. EDGE can react with a polyamine by either an intra- or intermolecular mechanism. The intermolecular reaction serves the purpose of crosslinking the coating into place as shown in Fig 1. In contrast, intramolecular reactions (not shown) can either cross-link within a polyamine molecule or more generally derivatize the polyamine with free oxiranes. These oxiranes are subsequently

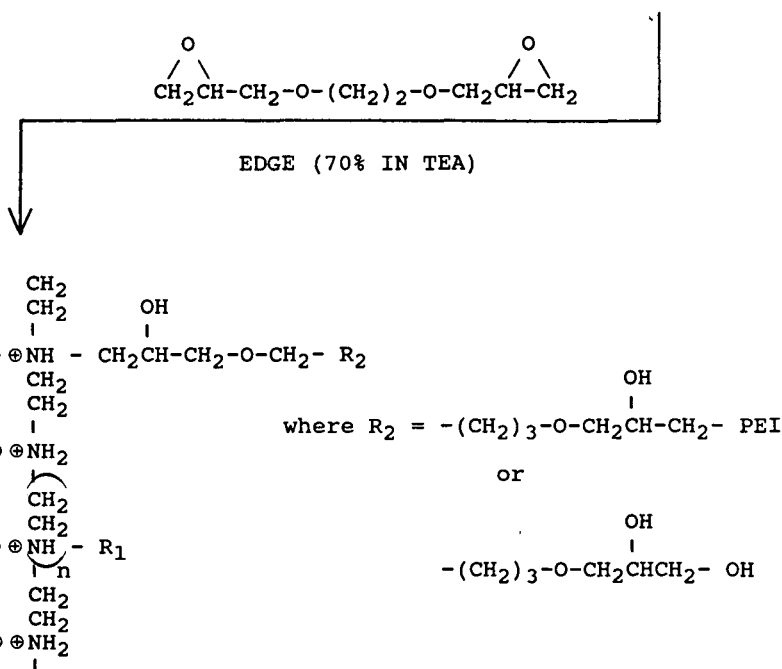
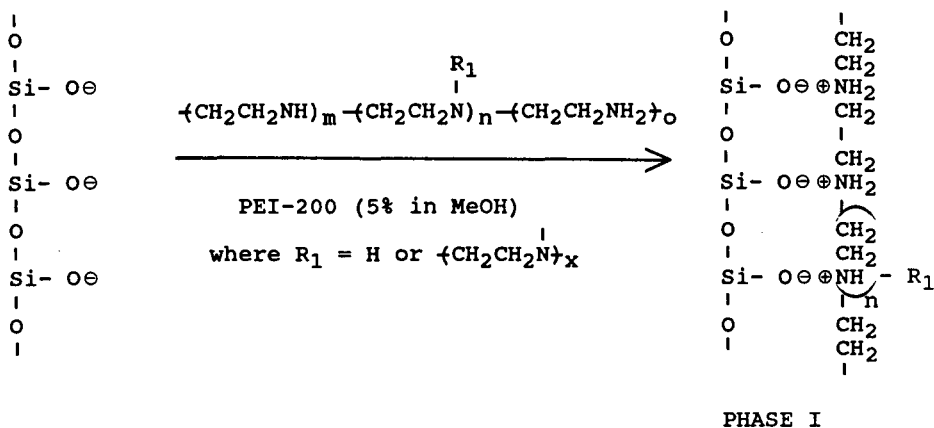


Fig. 1. Synthetic route to an adsorbed PEI-bonded phase. The coating process is two step: (1) adsorption of PEI 200 onto the fused-silica capillary, and (2) cross-linking of the PEI 200 polymer in order to stabilize the coating further.

hydrolyzed to produce a diol-rich coating⁸. Polyethyleneimines are known to be branched polymers with a primary:secondary:tertiary amino group ratio of approximately 1:2:1 (ref. 8). Since the tertiary amino groups are sterically hindered and non-reactive, the primary and secondary amino groups both dominate the electrostatic interaction of the coating with the capillary wall and react with the EDGE.

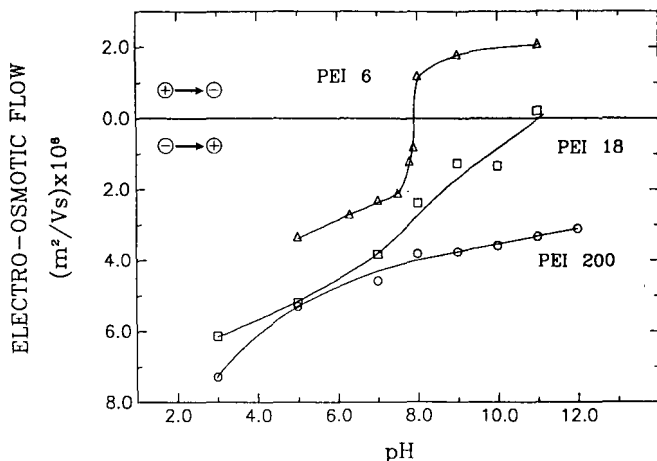


Fig. 2. Plot of electro-osmotic flow as a function of pH for three sizes of polyethyleneimine: PEI 6 (M_r 600); PEI 18 (M_r 1800); PEI 200 (M_r 20 000).

Influence of polymer size on electro-osmotic flow

The influence of polyamine molecular mass on electro-osmotic flow over the pH range from 3 to 11 is shown in Fig. 2. There is a strong correlation between the electro-osmotic flow-rate, direction of flow and polymer size. For low-molecular-mass polymer (PEI 6), the electro-osmotic flow moves from the negative to the positive electrode at low pH, indicating a positively charged wall. However, as the pH is increased, there is a sharp reversal in direction of the flow between pH 7.9 and 8.0. Flow reversal is the result of a switch in the net charge on the wall from positive to negative within that very small pH range. This is unusual in that the change occurs abruptly over a small pH range and the magnitude of the change (as expressed in flow-rate) is large on either side of this small range. These observations may be explained in the following way. It is known that the ionization of primary, secondary and tertiary amines in PEI is almost linearly related to pH between pH 4 and 10, *i.e.* PEI is not totally ionized until pH is dropped to 4 or less⁶. This is the result of the very high charge density in the polymer and electronic interaction between adjacent amine groups. In contrast, ionization of surface silanols begins at pH 3 and is not complete until the solution pH is raised to greater than 8. Again the broad titration curve is due to high charge density and electronic effects occurring at the surface. Below pH 7.9, positively charged amine groups dominate at the surface of the capillary causing the zeta potential to be positive. Above pH 8.0, surface silanol groups are more abundant than amine groups and the negative electrical potential of the silica surface projects through the polyamine coating into the solution and establishes a positively charged double layer. Between pH 7.9 and 8.0, the surface is isoelectric and electro-osmotic flow is zero. Although surface charge density is changing substantially on either side of this isoelectric point, electro-osmotic flow is almost constant. This shows that electro-osmotic flow is only weakly coupled to charge density.

As the molecular mass of the polymer is increased to 1800, electro-osmotic flow at low pH is faster than with PEI 6. This is due either to an increase in the positive

charge that a larger polymer would possess, or to a more efficient masking of the negative groups on the fused silica. However, this coating apparently does not completely mask all surface silanols. An increase in pH still results in a significant decrease in electro-osmotic flow. This decrease continues until at pH 11 the negative silanol groups once again predominate and push the electro-osmotic flow in the opposite direction (positive to negative electrode). When an even larger molecular mass polymer is coated onto the capillary (PEI 200), the electro-osmotic flow is further increased. However as the pH is increased, the electro-osmotic flow stays relatively constant, decreasing only slightly from pH 3 to 8 and almost staying constant from pH 8 to 12. This makes it possible to run a PEI 200-coated capillary between pH 3 and 12 without a significant change in electro-osmotic flow. Over this range, pH conditions can be employed to give the best selectivity without adversely effecting the analysis time. Uncoated fused silica capillaries are very different in contrast. Silanol ionization begins at pH 3 and continues to increase through pH 8. This means that electro-osmotic flow is extremely pH dependent^{10,11}.

Estimation of coating thickness

Polymer thickness influences the electro-osmotic flow by masking the deprotonated silanol groups on the capillary wall. The thicker the coating, the greater the masking of negative charges on the wall and the greater the electro-osmotic flow. To determine the thickness of the organic layer, a modification of the picric acid assay for ion-pairing capacity was employed¹². Assuming a density of 0.9 g/ml for ethyleneimine and that approximately one third of the total nitrogen bound in the organic coating is at the surface and accessible to picric acid⁷, a rough estimation of the coating thickness can be made from the picric-acid ion-pairing capacity. Table I shows surface nitrogen amounts and coating thickness estimates as a function of polymer molecular mass for 1, 5, and 25% PEI 200 in the methanol coating solution. As expected, the larger the molecular mass of polymer, the thicker the coating. In the case of PEI 200, a coating thickness estimated to be 30 Å results in a significant masking of the negative capillary wall charges.

TABLE I

SURFACE NITROGEN CONCENTRATION AND ESTIMATION OF COATING THICKNESS FOR POLYETHYLENEIMINE CAPILLARIES

<i>Polymer size</i>	<i>PET in methanol (%)</i>	<i>Concentration of surface nitrogens ($\mu\text{moles}/\text{m}^2$)</i>	<i>Estimation of coating thickness^a (Å)</i>
PEI 200	25	46.8	70
($M_r = 20\,000$)	5	16.2	24
	1	11.8	17
PEI 18	5	8.7	13
($M_r = 1800$)			
PEI 6	5	6.7	10
($M_r = 600$)			

^a Assuming 33% of bulk nitrogens are surface nitrogens⁷ and an ethyleneimine density of 0.9 g/ml.

The migration reproducibility was studied using the PEI-200 coating on $50 \text{ cm} \times 75 \mu\text{m}$ capillaries. It was found that the run to run reproducibility was 0.9% relative standard deviation (R.S.D.) ($n=6$), while the day to day reproducibility was 2.4% R.S.D. ($n=5$). A section to section reproducibility of 3.1% R.S.D. ($n=6$) was determined by cutting a three-meter-long coated capillary into six segments. The column-to-column migration reproducibility was examined over a three-month period and found to be 4.7% R.S.D. ($n=14$).

The stability of the coating was tested using a $50 \text{ cm} \times 75 \mu\text{m}$ coated capillary over an eight-day period. The total electrophoresis running time was 100 h or approximately 12 h a day for 8 days. After the neutral marker migration time increased slightly (12 s) over the first three hours, the migration times stayed steady for the next 6 days to the 84-h mark. The migration time then increased a total of 5 s to the 100-h mark where upon the experiment was terminated.

Influence of polymer concentration on electro-osmotic flow

The concentration of PEI 200 in the methanol coating solution was increased from 1 to 25% in order to determine the optimum polymer concentration that would maximize electro-osmotic flow over a wide pH range. The results are plotted in Fig. 3. As expected, electro-osmotic flow decreases for all five concentrations as the pH is increased from 3 to 11. This is the result of a gradual deprotonation of PEI between pH

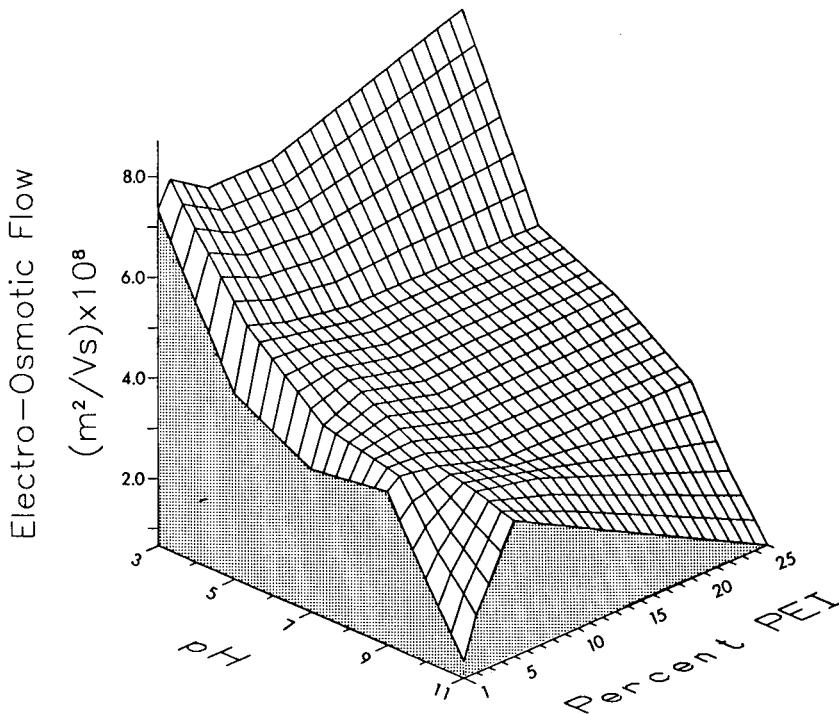


Fig. 3. Three-dimensional plot of electro-osmotic flow as a function of polymer concentration in methanol (1, 2, 5, 10 and 25%) for a given pH.

4 and 11. The fact that substantial electro-osmotic flow occurs at pH 11 indicates that the polyamine coating is still charged. This is probably due to quaternization of the amine during the cross-linking reaction⁸. It is to be expected that an increase of polymer concentration from 1 to 25% would result in a larger suppression of charge from the silica capillary and an increase in electro-osmotic flow. This is not strictly the case. Electro-osmotic flow is maximum with 5% PEI in all cases. This effect is largest at pH 11. The increase in electro-osmotic flow from 1 to 5% can be attributed to an increase in the coating thickness which is estimated to increase from 17 to 24 Å over this concentration range. This results in a more complete suppression of the negative charge on the capillary column. However, the opposite is observed as the PEI concentration is increased further; then the electro-osmotic flow decreases. Coating thickness is estimated to increase from 24 to 70 Å over this range. A satisfactory explanation for this phenomenon has not been developed.

Applications

Electrophoresis has been a valuable analytical technique for large, biological molecules such as proteins. This is why major emphasis is being placed on developing capillary electrophoresis for the separation of proteins. It has been demonstrated above that surface charges on the PEI (200)/EDGE coating do not change significantly over the pH range 3–12, *i.e.* fluctuation in electro-osmotic flow is minimal over this range. This uncoupling of electro-osmotic flow and pH allows pH manipulation of selectivity^{9,13}. In the separation of amphoteric compounds such as peptides and proteins, net charge and electrophoretic mobility can vary significantly with pH^{14,15}. Fig. 4 shows how variations in pH from 3 to 11 can optimize the separation of five proteins. At low and high pH, two sets of proteins (lysozyme/cytochrome *c* and chymotrypsinogen A/ribonuclease A) have similar migration rates and are therefore not well resolved. At pH 7, the migration rates are far enough apart so that these

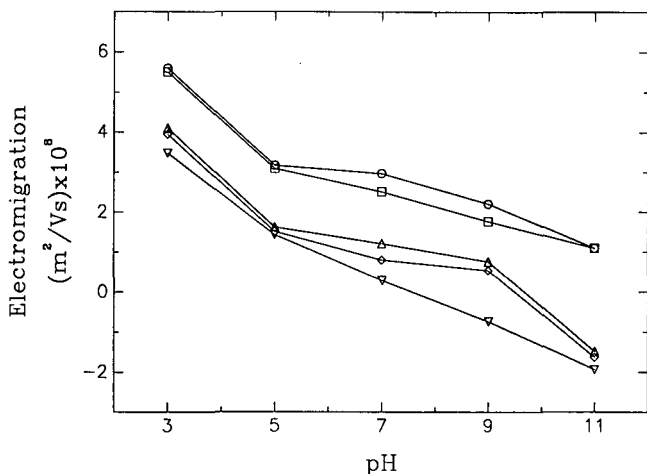


Fig. 4. Plot of electromigration for five proteins as a function of pH. ○ = Hen-egg lysozyme, pI 11.1; □ = horse-heart cytochrome *c*, pI 9.4; △ = bovine chymotrypsinogen A, pI 8.8; ◇ = bovine ribonuclease A, pI 8.7; ▽ = horse-heart myoglobin, pI = 7.3.

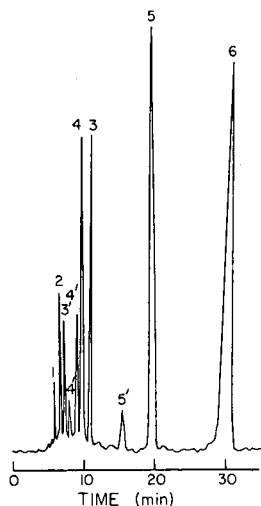


Fig. 5. Capillary electrophoretic separation of mode proteins on a PEI-200-EDGE coated capillary. Conditions: capillary length, 50 cm; separation length, 35 cm; I.D., 75 μm ; buffer, 0.02 *M* hydroxylamine-HCl at pH 7.0; separation potential, 12.5 kV. Peaks: 1 = Mesityl oxide (neutral marker); 2 = horse-heart myoglobin; 3 = bovine ribonuclease A; 4 = bovine chymotrypsinogen A; 5 = horse heart cytochrome *c*; 6 = hen-egg lysozyme. Peaks 3', 4' and 5' are impurities in 3, 4 and 5, respectively.

proteins can be well separated. This is demonstrated in Fig. 5 which shows the separation of the five proteins using a PEI(200)-EDGE capillary of 50 cm in length. The coating reversed the electro-osmotic flow so the polarity of the power supply must be switched from that used on uncoated fused-silica capillaries. The reversed flow results in lysozyme (pI 11.1) arriving at the detector last as compared to using uncoated capillaries where it would be the first to arrive. The pI values for the proteins range from 7.3 for myoglobin to 11.1 for lysozyme. Thus by using a buffer at pH 7, the coulombic repulsion of proteins from the positively charged capillary surface overcomes any solute-wall adsorption.

CONCLUSION

Adsorbed polyamine coatings on fused-silica capillaries may be cross-linked to give a thick, reproducible positive layer. This coating has the advantage that it is stable from pH 2 to 12 and does not adsorb positively charged proteins. Thick coatings of approximately 30 \AA are needed to effectively mask the underlying negative silanol groups.

The most notable advantage of this coating lies in its ability to retain a relatively constant positive surface charge over a wide pH range. This makes it possible to vary the pH to optimize selectivity without significantly affecting the rate of electro-osmotic flow.

ACKNOWLEDGEMENTS

The authors thank James R. Gord for his help in the graphical presentation of the data. Funds for this research were provided by Pfizer, Inc. and a research grant from the National Institute of Health (GM 25431).

REFERENCES

- 1 S.Hjerten, *J. Chromatogr. Rev.*, 9 (1967) 122.
- 2 B. J. Herren, S. G. Shafer, J. V. Alstine, J. M. Harris and R. S. Snyder, *J. Colloid Interface Sci.*, 115 (1987) 46.
- 3 J. W. Jorgenson and K. D. Lukacs, *Anal. Chem.*, 53(1981) 1298.
- 4 J. W. Jorgenson and K. D. Lukacs, *Science (Washington, D.C.)*, 222 (1983) 266.
- 5 S. H. Chang, K. M. Gooding and F. E. Regnier, *J. Chromatogr.*, 120 (1976) 321.
- 6 A. J. Alpert and F. E. Regnier, *J. Chromatogr.*, 185(1979) 375.
- 7 G. Vanecek and F. E. Regnier, *Anal. Biochem.*, 121 (1982) 156.
- 8 R. M. Chicz, Z. Shi and F. E. Regnier, *J. Chromatogr.*, 359(1986) 121.
- 9 V. Pretorius, B. J. Hopkins and J. D. Schieke, *J. Chromatogr.*, 264(1974) 385.
- 10 K. A. Cobb, J. Liu and M. Novotny, presented at 40th Pittsburgh Conference and Exposition on Analytical Chemistry and Applied Spectroscopy, Atlanta, GA, March 6-10, 1989, Abstract 1422.
- 11 R. M. McCormick, *Anal. Chem.*, 60 (1988) 2322.
- 12 W. S. Hancock, J. E. Battersby and D. R. K. Harding, *Anal. Biochem.*, 69 (1975) 497.
- 13 J. W. Jorgenson and K. D. Lukacs, *Clin. Chem.*, 27 1981) 1551.
- 14 S. Hjerten and M. D. Zhu, *J. Chromatogr.*, 346 (1985) 265.
- 15 R. J. Wieme, in E. Heftman (Editor), *Chromatography—A Laboratory Handbook of Chromatographic and Electrophoretic Methods*, Van Nostrand-Reinhold, New York, 3rd ed, 1975, Ch. 10.

CHROM. 22 554

Analysis of dilute peptide samples by capillary zone electrophoresis

RUEDI AEBERSOLD* and HAMISH D. MORRISON

Biomedical Research Centre, 2222 Health Sciences Mall, University of British Columbia, Vancouver, B.C. V6T 1W5 (Canada)

ABSTRACT

We report a method for the analysis of dilute peptide solutions by capillary zone electrophoresis. The procedure is based on an electrophoretic concentration step of the applied peptide solution in the capillary (stacking) prior to separation, thus allowing the application of increased sample volumes without a breakdown in resolution. Given a constant configuration of the hardware, the method permits the analysis of peptide solutions of an at least 5 times lower concentration than previously possible. The method was applied to the direct analysis of peptide samples separated by narrow-bore reversed-phase high-performance liquid chromatography for high-sensitivity peptide-sequence analysis.

INTRODUCTION

Capillary zone electrophoresis (CZE) is among the methods with the highest resolving power in a single dimension for charged molecules. Separations with several hundred thousand theoretical plates have already been achieved^{1,2}. In addition, the basis of separation is different from popular chromatographic methods such as reversed-phase high-performance liquid chromatography (RP-HPLC). The concentration of the analyte in a small detection volume gives CZE a high intrinsic sensitivity. High resolution, high sensitivity and orthogonal selectivity make CZE an ideal method for the further characterization of HPLC fractions.

In spite of the high intrinsic detection sensitivity, the usefulness of CZE for the analysis of dilute samples is limited. Sample volumes bigger than the 5–10 nl typically applied to the capillary lead to a dramatic breakdown in resolution.

Currently, automated high-sensitivity methods allow the sequence determination of peptide samples at the 10–20 pmole level³. The preparation and isolation of such small amounts of peptides in a form compatible with sequence analysis represents a considerable technical challenge. The most successful methods rely on the separation of proteolytic cleavage fragments by narrow-bore RP-HPLC^{4,5}. For a successful sequence determination it is of extreme importance to verify that the sample applied to the sequenator contains but a single peptide species. Multiple peptides simultaneously

applied to the sequenator generally make the sequence uninterpretable. Furthermore, peptides applied to the sequenator cartridge cannot be recovered for further separation.

The analysis of HPLC fractions which contain peptides at a concentration of 0.5–5 ng/ μ l in an essentially non-destructive way is therefore a common problem in high-sensitivity protein-sequence analysis. To date, no satisfactory method has been available to perform this task.

We have evaluated the potential of CZE for the analysis of dilute peptide solutions. In agreement with other groups we found that even with high-quality equipment, the detection limit imposed by the application volume is reached at sample concentrations in the order of 5–20 ng/ μ l.

We have developed a simple and fast procedure for the analysis of peptide solutions too dilute to be analyzed in the standard CZE operating mode. The method is based on the electrophoretic concentration of peptides in the capillary before the separation is started. In the concentrating mode significantly higher sample volumes can be applied without breakdown in resolution. We demonstrate the successful use of the method for the analysis of peptide fractions collected from narrow-bore HPLC systems prior to sequence analysis and discuss implications of this method for other analytical problems as well as for further developments in CZE methodology.

MATERIALS AND METHODS

Capillary electrophoresis

In this study we used an ABI Model 270A (Applied Biosystems, Foster City, CA, U.S.A.) capillary electrophoresis instrument. Materials and reagent for CZE, including capillaries, electrophoresis buffers and a calibrated mixture of three synthetic peptides (performance evaluation standard) were purchased from the manufacturer of the instrument.

UV absorption was measured at 215 nm. In the standard and concentrating operating mode, samples were loaded to the capillary by applying a reduced pressure to the cathodic electrode reservoir for a specified time, while the anodic end of the capillary was immersed in the sample solution. After sample application, the anodic end of the capillary was placed back into the electrophoresis buffer, along with the anodic electrode and electrophoresis was started. The temperature was maintained at 30°C for all experiments and electrophoresis was performed at 30 kV.

In the concentrating operating mode, the pH of the sample solution was raised to pH > 10 by the addition of small volumes of ammonia. The volume of ammonia required to raise the pH of a given sample volume was determined by direct measurement of the pH value of a scaled-up volume of sample buffer only.

Synthesis and purification of model decapeptide

The peptide NH₂-Val-Gln-Ala-Ala-Ile-Asn-Tyr-Ile-Asn-Gly-COOH was chemically synthesized using an Applied Biosystems Model 430 A peptide synthesizer. The crude peptide (50–100 mg) was dissolved in dilute acetic acid containing 6 M guanidine hydrochloride and injected into an Altex HPLC system equipped with a Waters 440A detector and a Vydac C4 column (250 × 4.6 mm I.D., 5 μ m). Fractions containing the pure peptide were collected, pooled and lyophilized. Chromatographic

conditions were the following: buffer A: 0.1% trifluoroacetic acid (TFA) in water; buffer B: 0.1% TFA in acetonitrile–water (60:40, v/v); column temperature: 50°C; flow-rate: 1.2 ml/min. A linear gradient of 0–100% buffer B over 90 min was applied.

Proteolytic cleavage and peptide isolation

The 85000-dalton protein used for the generation of tryptic cleavage fragments was isolated and processed as described before⁴. Approximately 5 µg of protein was separated from contaminating bands by sodium dodecyl sulfate–polyacrylamide gel electrophoresis. Proteins were electrophoretically transferred to nitrocellulose and cleaved on the matrix by trypsin. Resulting cleavage fragments were released into the supernatant and separated on a Vydac C4 narrow-bore (250 × 2.1 mm I.D.) reversed-phase column on a Waters peptide analyzer (Waters Associates, Milford, MA, U.S.A.). The system was equipped with a 200-µl sample-injector loop. Digestion mixture was acidified with 10 µl of 10% TFA, vortexed quickly and centrifuged for 1 min in a microfuge at high speed. The supernatant was removed and immediately injected into the HPLC unit. The following buffer system was used: buffer A: 0.1% TFA (Sequenal grade, Pierce, Rockford, IL, U.S.A.) in water; buffer B: 0.08–0.095% TFA in acetonitrile–water (70:30, v/v). The optical densities of buffers A and B were matched at 215 nm by titrating the TFA concentration in buffer B. Both buffers were continuously degassed with a stream of helium. All experiments were carried out with the column at 50°C at a flow-rate of 100 µl/min. Following sample injection, buffer A was pumped through the column for 5 min at a flow-rate of 200 µl/min before the gradient was started.

Peptides were detected with a Waters Model 900E photodiode array detector. The leading wavelength was 215 nm. Peptide-containing fractions were collected manually into microfuge tubes.

Buffers, HPLC solvents and other reagents were of analytical or HPLC grade. All aqueous solutions were prepared with deionized ultrafiltered water.

RESULTS AND DISCUSSION

Sensitivity limit of peptide analysis by CZE in the standard operating mode

We first determined the lower concentration limit for peptide analysis by CZE in the standard operating mode in the given hardware configuration of an Applied Biosystems Model 270A Instrument. The sample was the performance evaluation standard supplied by the manufacturer of the instrument. The three synthetic peptides were dissolved at an initial concentration of 100 ng/µl and then serially diluted two-fold in 10 mM citrate buffer, pH 2.5. Electrophoresis was performed in the same buffer and the peptides were detected at 215 nm. Samples were loaded to the capillary by applying reduced pressure at the cathodic end of the capillary for 5 s. To minimize the reduction of the apparent detection sensitivity by peak broadening, the loading time was kept constant and the sample concentration was varied.

The results are shown in Fig. 1. The lower concentration limit with this sample was reached at a sample concentration of 5–10 ng/µl. The application of larger sample volumes lead to significant peak broadening and did not improve on the detection limit as judged by the signal to noise ratio. The required minimal sample concentration for operation in the standard operating mode is about 10 ng/µl. This value is ap-

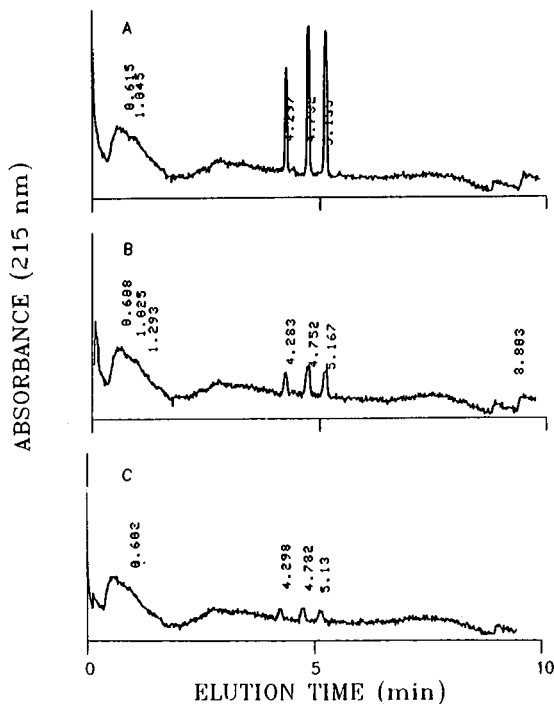


Fig. 1. Sensitivity of CZE in standard operating mode. A calibrated mixture of three synthetic peptides (performance evaluation standard) was dissolved in 10 mM citrate buffer, pH 2.5. Samples were loaded to the capillary by applying reduced pressure to the cathodic end of the capillary for 5 s. Electrophoresis carried out at 30 kV. Detector setting 0.005 a.u.f.s. at 215 nm. Sample concentration: (A) 25 ng/ μ l; (B) 12.5 ng/ μ l; (C) 6.25 ng/ μ l.

proximately 5–10-fold higher than actual peptide concentrations in typical peptide fractions collected for high-sensitivity sequence analysis from a narrow-bore HPLC system.

Electrophoretic concentration of dilute peptide samples in the capillary

The sensitivity of CZE in the standard operating mode is not sufficient for the analysis of peptide samples collected from narrow-bore HPLC columns for high-sensitivity sequence analysis. One way to overcome this limitation is to apply higher sample volumes to the capillary and to avoid the breakdown in resolution.

We attempted to concentrate the applied peptide solution electrophoretically in the capillary into a narrow zone before the separation was started. This was achieved by electrophoretic stacking of the peptides at the interface between the sample application solution and the electrophoresis buffer. The procedure is schematically illustrated in Fig. 2. The pH of the sample solution was raised to a value well above the isoelectric point (*pI*) of the peptides by the addition of base. The basic sample solution was then applied to the capillary previously filled with low-pH electrophoresis buffer (citrate buffer, pH 2.5). Immediately after sample application, the anodic end of the

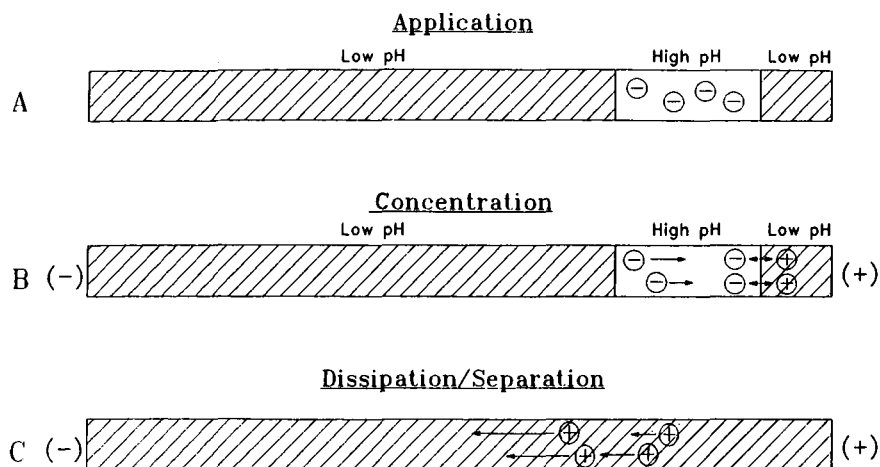


Fig. 2. Schematic illustration of electrophoretic stacking. (A) Samples are applied to the capillary in a solution with a pH value higher than the pI of the peptides, resulting in deprotonated, negatively charged peptides. (B) Application of a potential gradient over the capillary leads to concentration of the peptides at the electrophoresis buffer–sample interface. (C) After dissipation of the pH-step gradient, peptides resume mobility towards the cathode and are separated in the electric field.

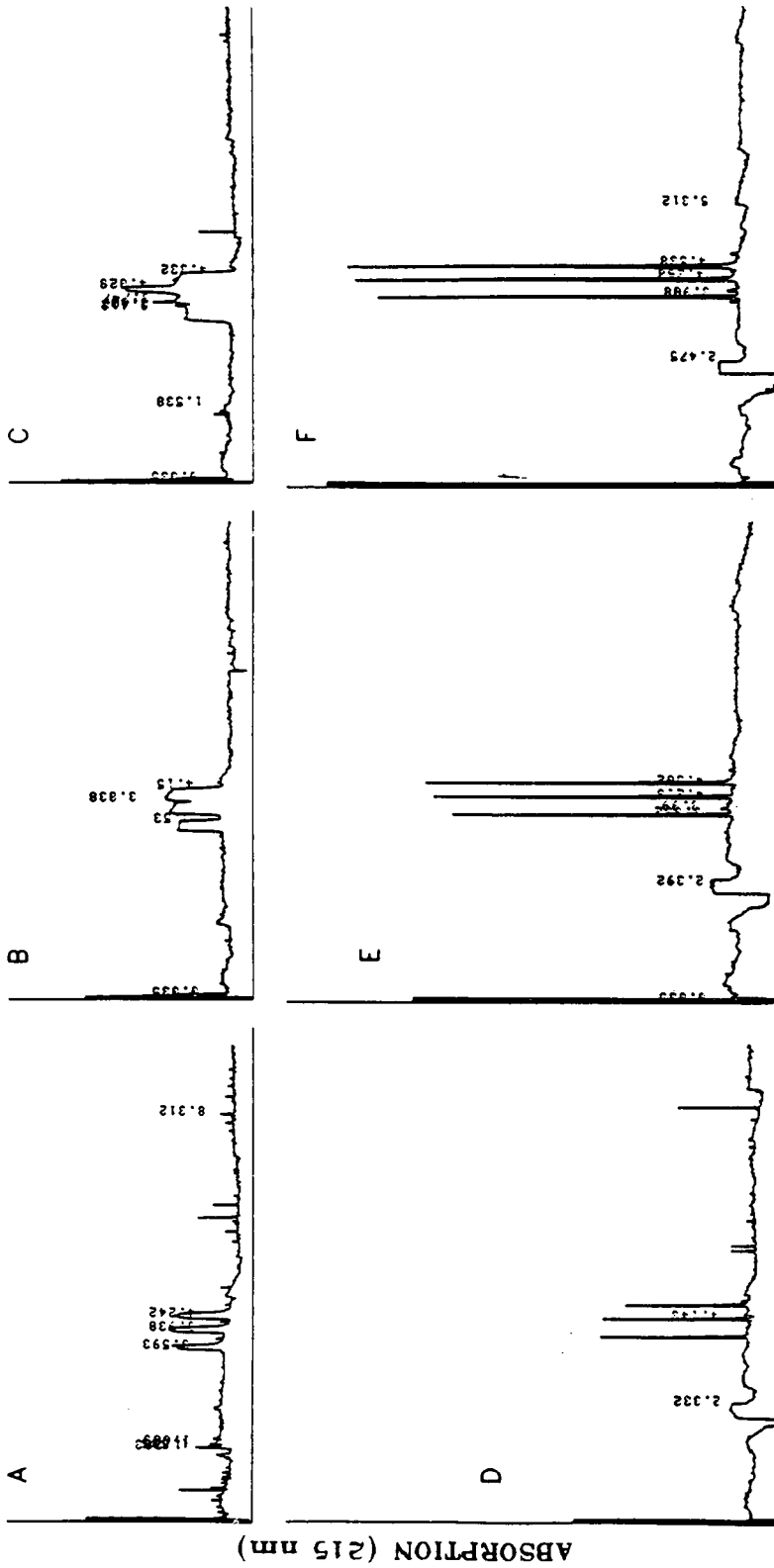
capillary was immersed into low-pH electrophoresis buffer. This procedure resulted in a pH-step gradient at the interface of the electrophoresis buffer and the applied sample.

Application of a potential gradient over the capillary initiated the movement of the peptides towards the anode (Fig. 2B). The direction of electrophoretic mobility was reversed, as soon as the peptides migrated into the acidic milieu of the electrophoresis buffer, leading to the concentration of the applied peptides at the sample solution–electrophoresis buffer interface.

If the potential gradient was maintained over the capillary, the pH step rapidly dissipated and peptides started to move from the concentrating zone towards the cathode.

The effect of the electrophoretic concentration procedure is shown in Fig. 3. Aliquots of the performance evaluation standard were dissolved at $10 \text{ ng}/\mu\text{l}$ in either 10 mM citrate buffer (pH 2.5) or in 20 mM NH_4OH . Both samples were applied to the capillary by applying negative pressure to the cathodic end of the capillary for 10, 20 or 30 s (Fig. 3). In the normal operating mode, severe peak broadening and a concurrent breakdown in resolution was observed at an application time as short as 10 s (Fig. 3A–C). In the concentrating mode, loading times in excess of 30 s were easily tolerated with minimal peak broadening and loss of resolution (Fig. 3D–F).

We next attempted to determine the minimal sample concentration required for peptide analysis by CZE in the concentrating mode. Aliquots of the performance evaluation standard were dissolved in 20 mM citrate buffer (pH 2.5) at concentrations ranging from 1 – $50 \text{ ng}/\mu\text{l}$. The pH of the sample solutions was raised by the addition of concentrated ammonia and the samples were loaded into the capillary by applying negative pressure at the cathodic end of the capillary for 60 s before electrophoresis was started (data not shown).



RETENTION TIME (min)

Fig. 3. Effect of the concentrating procedure. Performance evaluation standard was dissolved at 10 ng/ μ l in either 10 mM citrate buffer, pH 2.5 (A, B, C) or in 10 mM NH₄OH (D, E, F). Samples were loaded to the capillary by applying reduced pressure at the cathodic end of the capillary for 10 s (A, D) 20 s (B, E) or 30 s (C, F). Electrophoresis was performed at 30 kV. Peptides were detected at 215 nm at a detector setting of 0.005 a.u.f.s.

These results, together with the results shown in Fig. 3D–F and Fig. 4, showed that the minimal concentration required for analysis of performance evaluation standard by CZE in the concentrating mode was below 1 ng/ml. This represented a significant improvement over the limits observed in the same instrument in the same configuration with the same sample using the standard operating mode. Furthermore, the ability to successfully analyze samples at the 1–2-ng/ μ l level raised the possibility to directly analyze peptide fractions collected from narrow-bore HPLC prior to high-sensitivity sequence analysis.

CZE of peptide fractions separated by narrow-bore HPLC

We next determined whether the conditions for the electrophoretic concentration of dilute peptide samples in the capillary were applicable to the analysis of peptide fractions collected from a narrow-bore HPLC system.

Aliquots of 60–500 ng of the synthetic decapeptide $\text{NH}_2\text{-Val-Gln-Ala-Ala-Ile-Asn-Tyr-Ile-Asn-Gly-COOH}$ were applied to a C_4 HPLC column. The column was developed with an acetonitrile gradient in 0.1% TFA and the peptides were detected by UV absorbance at 215 nm. Peptides were collected manually into a microfuge tube. The fraction volume was 80 μ l. Two identical samples were collected at each concentration. One sample was directly applied to the capillary of the CZE

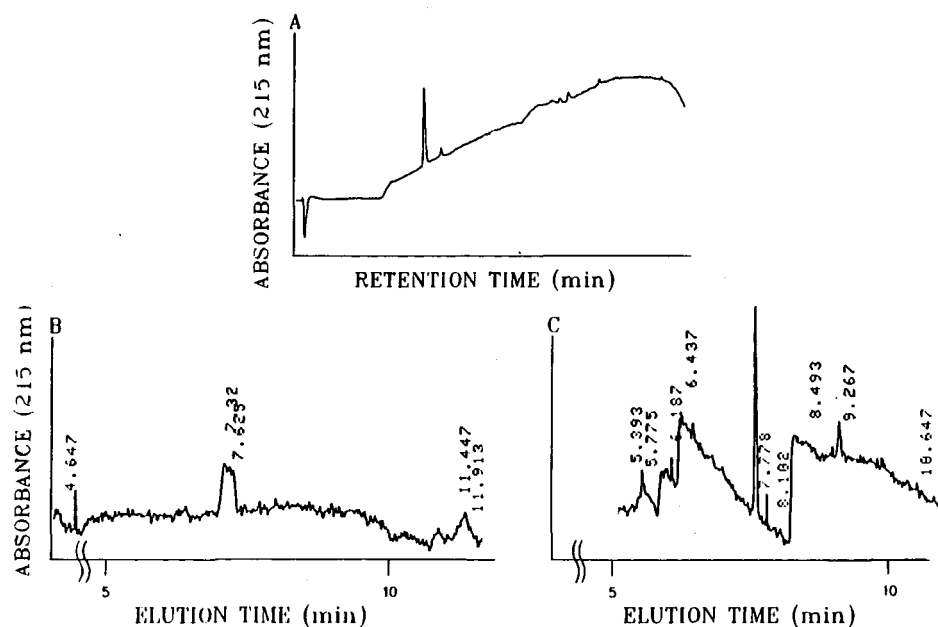


Fig. 4. Analysis of HPLC peptide fractions by CZE. Aliquots of 60 ng of the decapeptide $\text{NH}_2\text{-Val-Gln-Ala-Ala-Ile-Asn-Tyr-Ile-Asn-Gly-COOH}$ were applied to a narrow-bore RP-HPLC column. Eluting peptides, as detected by UV absorption at 215 nm (A), were manually collected in a fraction volume of 80 μ l. Collected peptide samples were either directly applied to the capillary of a CZE instrument for separation in the standard operating mode (B) or added with 2 μ l of concentrated NH_4OH for separation in the concentrating mode (C). Application time: 30 s. Electrophoresis was carried out at 30 kV at 30°C, CZE detector setting 0.005 a.u.f.s. at 215 nm.

system for analysis in the standard operating mode. The second sample was added with 2 μl of concentrated NH_4OH to raise the pH of the sample solution well above the pI of the peptide. Aliquots of the basic peptide solution were then applied to the capillary for analysis in the concentrating mode. Results shown in Fig. 4 demonstrated that the concentrating mode was applicable to the analysis of peptides collected directly from narrow-bore HPLC systems. As little as 60 ng of the decapeptide applied to a HPLC column could be successfully analyzed by CZE in the concentrating mode (Fig. 4). Assuming a typical recovery of 70–80% of the peptide applied to the HPLC system and a fraction volume of 80 μl , the analyte concentration was in the range of 0.52–0.6 ng/ μl . These results also indicated that the presence of small amounts of TFA and variable concentrations of acetonitrile in the peptide fractions collected from the HPLC system did not interfere with the concentrating process. These factors might however contribute to baseline noise in the CZE separation.

We then applied CZE in the concentrating mode to the analysis of selected peptides derived from the tryptic digestion of an estimated 5- μg aliquot of a 85 000-dalton protein. Fractions were collected from a narrow-bore HPLC system. We were able to resolve peptides coeluting from the HPLC system into several peaks by CZE analysis in the concentrating operating mode but not in the standard operating mode (Fig. 5). Subsequent sequence analysis of the peptide fraction analyzed in Fig. 5 revealed the presence of three different peptide species. Once detected, fractions containing more than one peptide species can be further separated under chromatographic conditions with different selectivity before their application to the sequenator⁵.

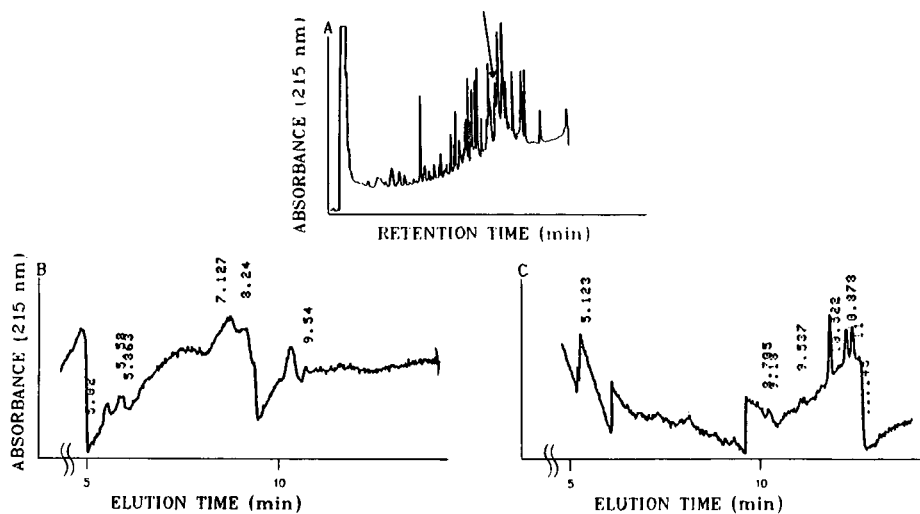


Fig. 5. Analysis of HPLC peptide fractions by CZE. An estimated 5 μg of a 85 000-dalton protein were electroblotted from a polyacrylamide gel onto nitrocellulose and cleaved with trypsin on the matrix. Resulting peptides were released and separated by RP-HPLC (A). Fractions were collected manually. The marked peak (|) was subjected to CZE analysis in the standard operating mode (B) or, after the addition of 2 μl of concentrated NH_4OH , in the concentrating mode (C). Electrophoresis was carried out at 30 kV at 30°C. Sample was applied for 30 s. Detector settings: HPLC: 0.1 a.u.f.s. at 215 nm; CZE: 0.005 a.u.f.s. at 215 nm.

DISCUSSION

We describe a simple method for the analysis by CZE of peptide samples too dilute to be detected after separation by CZE in the standard operating mode. It consists of an electrophoretic concentration (stacking) of the applied sample at the sample-electrophoresis buffer interface prior to the separation and therefore permits the application of increased sample volumes without a breakdown in resolution. This procedure allowed the analysis of peptide samples at lower concentrations compared to standard operating conditions in the same hardware configuration. With this improvement, peptide fractions separated by narrow-bore HPLC for high-sensitivity peptide-sequence analysis could be monitored without additional manipulations. As very small sample volumes are applied ($\ll 1 \mu\text{l}$), this procedure is essentially non-destructive.

This method currently represents the most effective way to monitor the purity of peptide fractions collected from HPLC columns at the submicrogram level. Alternative methods include spectral analysis of the HPLC effluent using a photodiode-array detector^{6,7}, the systematic rechromatography of peptides under conditions of different selectivity⁵ and the concentration of peptide solutions followed by mass-spectrometric analysis⁸ or separation by CZE in the standard operating mode.

The assessment of the peak purity by spectral analysis of HPLC effluents using a photodiode-array detector is based on the assumption that different peptides vary in the composition of aromatic amino acids and therefore show differences in their UV-absorption spectra in the range of 250–280 nm. The UV spectra of the ascending and descending slopes as well as at the apex of peptide peaks eluting from HPLC columns are compared with the expectation that peaks containing a single peptide would show identical spectra irrespective of the point of measurement whereas peaks containing more than one peptide slightly differing in chromatographic mobility and aromatic amino acids composition would show differences in the spectra as a function of the retention time. This method has been successfully used with microgram amounts of peptides^{6,7}. Relatively weak UV absorption of aromatic amino acids in the 250–280 nm range prevents the successful use of the method for the analysis of submicrogram amounts of peptide samples. Furthermore, peptides containing equal amounts and compositions of aromatic amino acids or no aromatic amino acids at all cannot be discriminated.

The systematic rechromatography of peptide fractions under conditions of different selectivity is cumbersome, time consuming and associated with a systematic loss of approximately 20–40% of the sample per round of rechromatography (chromatography conditions reviewed in ref. 5). Mass spectrometry as a tool for the analysis of HPLC fractions holds tremendous promise for the future. Currently, the usefulness of mass spectrometry for this application is still restricted by limited sensitivity. Furthermore, for most laboratories the cost of mass spectrometric equipment is prohibitively high.

Concentration of HPLC effluents prior to analysis by CZE is associated with significant loss of samples and therefore no viable alternative to the electrophoretic concentration in the capillary. Peptides are eluted from the HPLC column under conditions of good solubility in a mixture of aqueous phase and acetonitrile. If the peptide solution is concentrated under reduced pressure or by lyophilization, an

over-proportional fraction of acetonitrile will evaporate, making the solvent more polar. As a consequence, initially dissolved more hydrophilic peptides frequently precipitate during concentration and are lost for further analysis.

Recently an alternative procedure for the electrophoretic stacking of samples in capillaries was described. Samples were applied in a buffer of lower conductivity than the electrophoresis buffer. The higher resistance in the dilute sample buffer led to a disproportionate voltage drop over the applied sample. The resulting higher electric field induced analytes to move faster and to stack up at the buffer interface⁹. This procedure requires the dilution and/or solvent change of the sample to be analyzed and is therefore less suitable for the separation of HPLC fractions.

The method has some limitations. Even with electrophoretic concentration, the sample volume which can be loaded into the capillary is limited. We found that the upper loading limit was reached after approximately 1 min of sample application under reduced pressure. For even more extensive sample loads, the concentration effect was still very efficient, but strong UV-absorption discontinuities lead to a very noisy baseline and made interpretation of the results difficult. For situations requiring the application of even larger volumes, alternative approaches for the sample concentration need to be developed.

The use of the described electrophoretic stacking procedure is not limited to the separation of dilute samples. Even if small sample volumes are applied, the peaks are sharpened and therefore the resolving power of the separation is dramatically increased (Fig. 3D).

Furthermore the described method is not limited to the separation of peptide solutions, but should be generally applicable for the analysis of dilute samples by CZE and is therefore an important contribution to the analysis of dilute solutions of ionic compounds.

ACKNOWLEDGEMENT

The help of Divesh Sisodraker in preparing this manuscript is gratefully acknowledged.

REFERENCES

- 1 J. W. Jorgenson and K. D. Lukacs, *Science (Washington, D.C.)*, 222 (1983) 266.
- 2 H. H. Lauer and D. McManigill, *Anal. Chem.*, 58 (1986) 166.
- 3 R. M. Hewick, M. W. Hunkapiller, L. E. Hood and W. J. Dreyer, *J. Biol. Chem.*, 256 (1981) 7990.
- 4 R. Aebersold, J. Leavitt, R. A. Saavedra, L. E. Hood and S. B. H. Kent, *Proc. Natl. Acad. Sci. U.S.A.*, 84 (1987) 6970.
- 5 R. J. Simpson, R. L. Moritz, G. S. Begg, M. R. Rubira and E. C. Nice, *Anal. Biochem.*, 177 (1989) 221.
- 6 A. F. Fell, *Trends Anal. Chem.*, 2 (1983) 63.
- 7 B. Grego, I. R. Von Driel, J. W. Goding, E. C. Nice and R. J. Simpson, *Int. J. Peptide Protein Res.*, 27 (1986) 201.
- 8 E. D. Lee, T. R. Covey, W. Mück and J. D. Henion, *J. Chromatogr.*, 458 (1988) 313.
- 9 *Model 270A Application Update No. 6*, Applied Biosystems, Foster City, CA, 1989.

CHROM. 22 559

High-performance capillary electrophoresis of hydrophobic membrane proteins

DJURO JOSIĆ*, KATRIN ZEILINGER and WERNER REUTTER

Institut für Molekularbiologie und Biochemie, Freie Universität Berlin, Arnimallee 22, D-1000 Berlin 33 (F.R.G.)

and

ALFRED BÖTTCHER and GERD SCHMITZ

Institut für Klinische Chemie und Laboratoriumsmedizin, Westfälische Wilhelms-Universität, Albert-Schweitzer-Str. 33, D-4400 Münster (F.R.G.)

ABSTRACT

Hydrophobic membrane proteins, extrinsic and intrinsic ones, were separated by high-performance capillary zone electrophoresis (HPCZE) and high-performance capillary isotachopheresis (HPCITP). In the case of HPCZE with both coated and uncoated quartz capillaries the addition of 7 M urea to the separation buffers was necessary to achieve reproducible results. In the HPCITP experiments PTFE capillaries were used. When spacers were used, *e.g.*, ampholytes, additional splitting of peaks was observed. The splitting was caused by the microheterogeneity of the investigated proteins, which are differently glycosylated and/or phosphorylated.

INTRODUCTION

High-performance capillary electrophoresis (HPCE) has been established in many fields as a separation method for small molecules^{1–3}. Good progress has been made also with regard to high-molecular-mass polymers, such as proteins and nucleic acids. For their separation free-flow capillary electrophoresis was mainly used^{4,5}, but separation in prepacked capillaries has also been attempted^{6,7} (for a review, see ref. 8). At a time when other methods were being developed for the same purpose, capillary isotachopheresis (HPCITP) was used for the separation of biopolymers from complex mixtures, such as serum⁹ and protein mixtures¹⁰, and also for the separation of small molecules¹¹.

The separation of hydrophobic proteins in aqueous solutions is very difficult. Experience gained from high-performance liquid chromatographic (HPLC) experiments shows that solubility problems can occur during the separation, owing to a tendency for these proteins to undergo aggregation and self-aggregation. In addition, undesirable, non-specific interactions with the support frequently appear, leading to poor recovery of the sample and results which are no longer adequately repro-

ducible¹². These effects can be avoided or at least controlled by the addition of detergents¹² and/or other denaturing agents such as urea or formic acid¹³.

In this work we investigated the separation of membrane proteins by different HPCE methods. For the experiments we used two groups of model membrane proteins, intrinsic and extrinsic.

EXPERIMENTAL

Chemicals

All chemicals were of analytical-reagent grade from Merck (Darmstadt, F.R.G.) or Sigma (Munich, F.R.G.). Liver and Morris hepatoma membrane proteins were isolated as described elsewhere^{14,15}.

Apparatus

For all separations by high-performance capillary zone electrophoresis (HPCZE) and ITP, a Beckmann (Munich, F.R.G.) system was used. In ITP separations the capillary cassette contained the PTFE capillary. The ITP experiments on the Beckmann system were also carried out with a system developed by Schmitz and co-workers^{9,16}.

Capillaries

For HPCZE uncoated quartz capillaries (20 cm × 25 μm I.D.) (Beckmann and Bio-Rad Labs. Munich, F.R.G.) and coated capillaries (20 cm × 50 μm I.D.) (Bio-Rad Labs.) were used. According to information provided by the manufacturer, the coated capillaries contain a hydrophilic polymer which is covalently bound on the inner surface. PTFE capillaries (20 cm × 250–400 μm I.D.) (Labochron, Sinsheim, F. R. G.) were used for HPCITP.

Buffers

Sodium borate buffer (0.2 M, pH 9.2) was used for HPCZE, with or without the addition of 7 M urea. As the leading electrolyte in ITP, 5 mM H₃PO₄ was used. The electrolyte contained 0.25% (w/v) hydroxypropylmethylcellulose (HPMC) in order to increase the viscosity and to suppress electroosmotic movement in the capillary. Ammediol (2-amino-2-methyl-1,3-propanediol) was added as a counter ion to achieve pH 9.2. The terminating electrolyte contained 100 mM valine and was adjusted with ammediol to pH 9.4.

Separation conditions

HPCZE was carried out at a constant voltage of 30 kV and a current between 80 and 180 μA.

HPCITP experiments with the system from Beckmann were carried out at a voltage of 5–6 kV, the current being 240 μA (beginning) to 50 μA (end of separation). With the system developed by Schmitz and co-workers, the separation was started with a constant current of 150 μA and during the 10-min run the current was reduced to 100 μA (the corresponding voltage was 7 kV), and subsequently to 50 μA (6 kV) before detection.

The proteins were monitored spectrophotometrically at 280 nm. The tem-

perature during the separation was kept constant at 20°C (Beckmann apparatus) or 10°C (Schmitz and co-workers' system).

Gel electrophoretic methods

Sodium dodecyl sulphate–polyacrylamide gel electrophoresis (SDS-PAGE) of proteins was performed by the Laemmli method¹⁷, using a mini-system (Bio-Rad Labs). Two-dimensional electrophoresis was performed according to the method described by O'Farrel¹⁸.

RESULTS AND DISCUSSION

High-performance capillary zone electrophoresis

HPCZE separations were carried out with calcium-binding proteins from liver plasma membranes and Morris hepatoma 7777 plasma membranes, and also with a mixture consisting of three different intrinsic membrane glycoproteins, dipeptidyl peptidase IV (DPPIV), cell-CAM and a glycoprotein with an apparent molecular weight in SDS-PAGE of 95 000 dalton. The CBP solutions contained 0.1% (w/v) of CHAPS detergent; with the intrinsic membrane proteins the detergent Triton X-100 (0.1%, w/v) was used.

When the membrane proteins were separated in an uncoated fused-silica capillary using a buffer without denaturing reagents, no sample recovery was achieved (not shown). This result can be compared with those obtained by HPLC. When, in the course of separating hydrophobic proteins, non-specific interactions with the matrix could not be prevented, the proteins were only partly or were not eluted from the column¹². In HPLC these difficulties can be avoided by coating the silica gel matrix or by introducing hydrophilic groups into the polymer supports. With coated silica capillaries some substances showed a modest improvement in terms of their peak surface. However, the time for the appearance of single peaks was not reproducible (not shown). This suggests that the coated capillaries that are commercially available at present do not allow a satisfactory separation of membrane proteins under the described conditions. Only after addition of 7 mol/l urea, a denaturing reagent, are reproducible results obtained in terms of peak height and running time for single substances.

HPCZE of calcium-binding proteins with the addition of a denaturing reagent is shown in Fig. 1. The low-molecular-mass proteins CBP 33 and CBP 35, which in Morris hepatoma 7777 plasma membranes appear at much higher concentrations than in liver plasma membranes (*cf.*, SDS-PAGE in Fig. 1), are seen as additional, separate peaks (*cf.* Fig. 1b).

The separation of intrinsic membrane proteins, which were solubilized and kept in solution by means of the non-ionic detergent Triton X-100, requires more complicated conditions. If the separation is carried out without urea, a single peak is detected at 280 nm. A run with injection of a 1% solution Triton X-100 without protein showed that this peak could not be attributed to the protein, but to the detergent (not shown). Under these conditions, the detergent is separated from the proteins, which consequently aggregate and are precipitated. Fig. 2 shows a separation of intrinsic membrane proteins after 7 M urea has been added. The detergent, or at least part of it, is again separated, but the proteins are kept in solution all the same by the urea and can

be recovered. The first peak in the electropherogram in Fig. 2 has to be attributed to the Triton X-100. The additional peaks are due to the membrane proteins.

The results shown in Figs. 1 and 2 illustrate the guidelines that have to be followed in the separation of hydrophobic proteins by HPCZE. It is to be expected that the separation and recovery can be improved through adequate derivatization of the surface of the capillaries. However, the experiments with coated capillaries have shown that precipitation of the proteins occurs, because during the separation process the detergent is itself separated (data not shown). It can be avoided only by adding denaturing reagents to the separation buffer. The strongly denaturing 7 M urea solution that has been used so far can probably be replaced with more adequate reagents.

High-performance capillary isotachopheresis

The experiments on membrane protein separation by HPCITP were based on

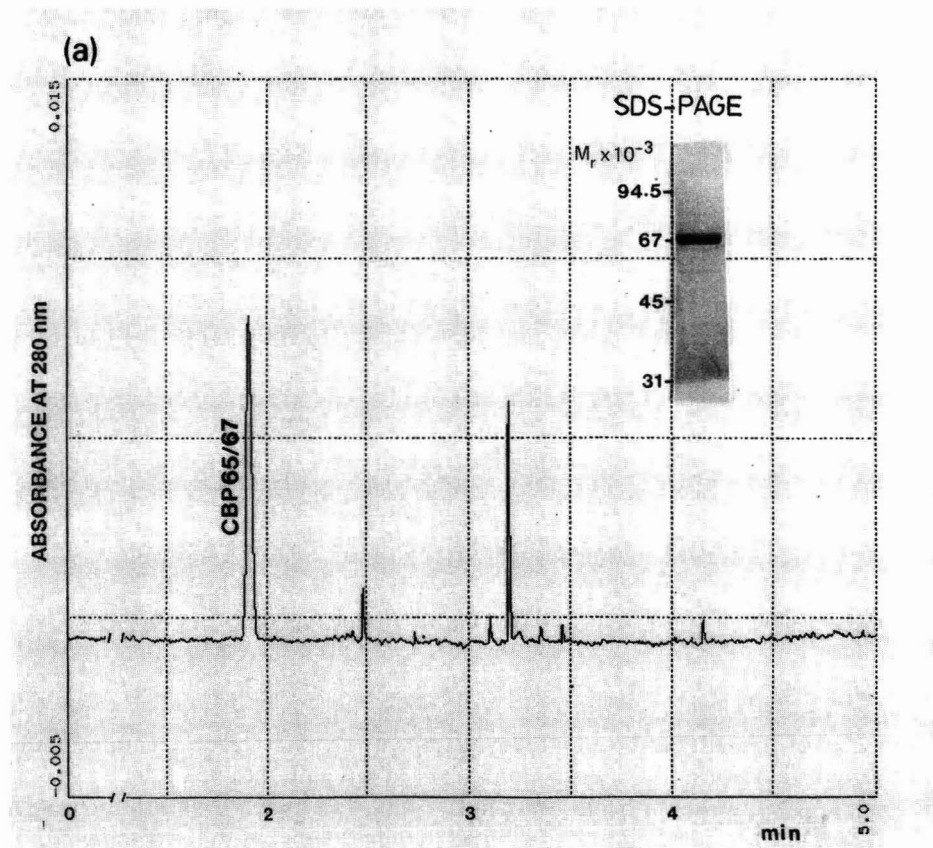


Fig. 1.

experience gained with the separation of serum lipoproteins^{9,16}. The buffer systems that were optimized for the separation of lipoproteins can also be used for the separation of hydrophobic membrane proteins. Fig. 3 shows the separation of calcium-binding proteins by HPCITP. In preliminary experiments that were carried out chiefly in order to check reproducibility, the influence of spacers on the separation process was not investigated. The CBP from liver and also from Morris hepatoma 7777 plasma membranes could be separated and recovered by HPCITP (see Fig. 3). An additional splitting of single peaks occurred through the use of spacers, as shown in Fig. 4. In the case of CBP, ampholytes in the pH range 5–7 were chosen.

The intrinsic membrane proteins DPP IV, cell-CAM and the 95 000-dalton protein could be separated very well by HPITP, as shown in Fig. 5. Through the addition of spacers, in this instance ampholytes in the pH range 4–6, an additional splitting of single peaks also occurred (see Fig. 6). Cell-CAM (the first peak in Fig. 5) consists of two isoforms, which can be separated in two-dimensional electrophoresis.

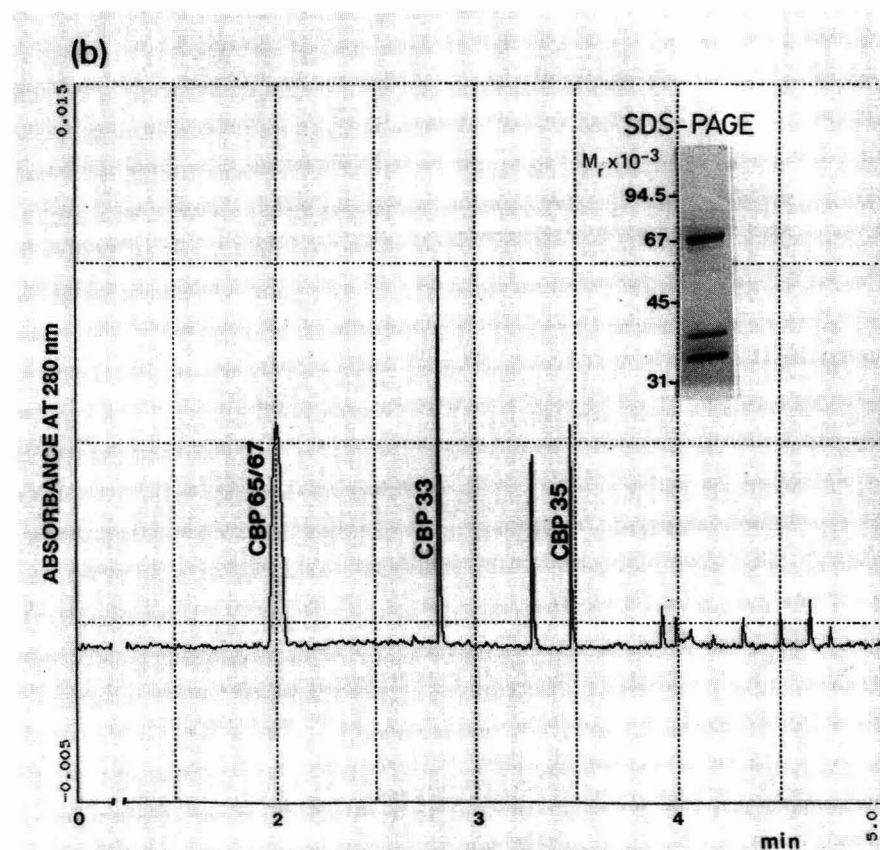


Fig. 1. Separation of calcium-binding proteins from (a) liver and (b) Morris hepatoma 7777 plasma membranes by HPCZE with addition of 7 M urea. The isolated membrane proteins (SDS-PAGE is shown in the inset) were injected into the capillary by pressure (0.5 bar). Injection time, 3 s. Other conditions are given under Experimental. M_r = Molecular mass.

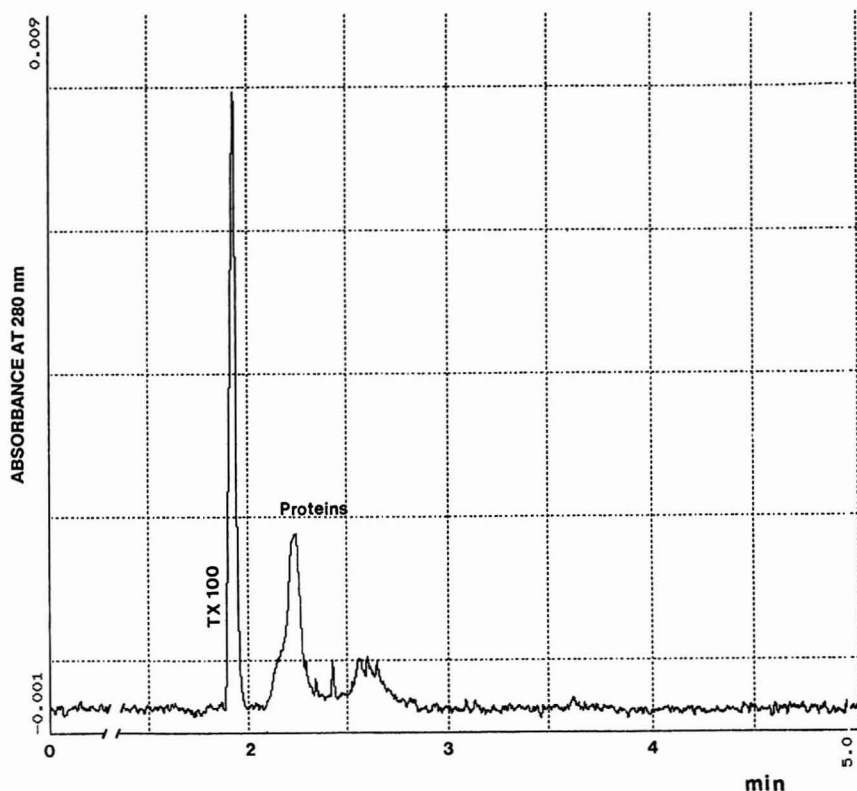


Fig. 2. Separation of intrinsic membrane proteins from liver by HPCZE with addition of 7 M urea. The proteins with an apparent molecular mass between 95 000 and 120 000 dalton in SDS-PAGE were injected under the same conditions as in Fig. 1 and separated. The first peak in the electropherogram was attributed to the detergent Triton X-100. The other peaks result from separated proteins.

Moreover, the protein is highly glycosylated and contains more than 50% carbohydrate. The carbohydrate part consists of at least twelve chains, which terminally contain sialic acid¹⁹. Different amounts of sialic acid can lead to further differences in the mobility of the isoforms of this protein. DPP IV contains about 24% carbohydrate in at least six chains²⁰. Therefore, microheterogeneity in this glycoprotein also can be assumed, owing a different sialic acid content. The third protein (95 000 dalton) is probably an enzymatically inactive form of DPP IV, which is glycosylated in another way²¹.

In all the separations of model membrane proteins that were carried out with HPCITP, both the peak size and running time were reproducible, because of two factors. First the non-specific interactions of the sample with the walls of the PTFE capillary are minimal, and second the HPMC that is added to the leading electrolyte to increase the viscosity also acts as a detergent and helps to keep the proteins in solution during separation.

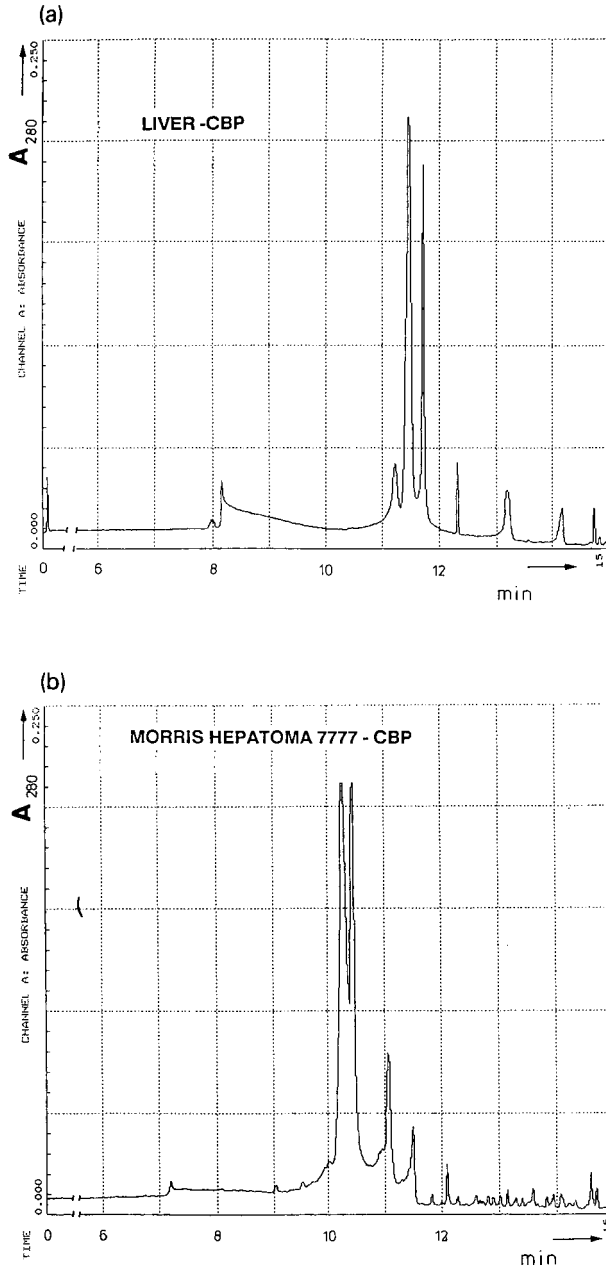


Fig. 3. Separation of calcium-binding membrane proteins from (a) liver and (b) Morris hepatoma 7777 by HPCITP without addition of spacers. The separation was carried out on a Beckmann HPCE system. Injection conditions as in Figs. 1 and 2. For SDS-PAGE, see Fig. 1b. Other conditions are given under Experimental.

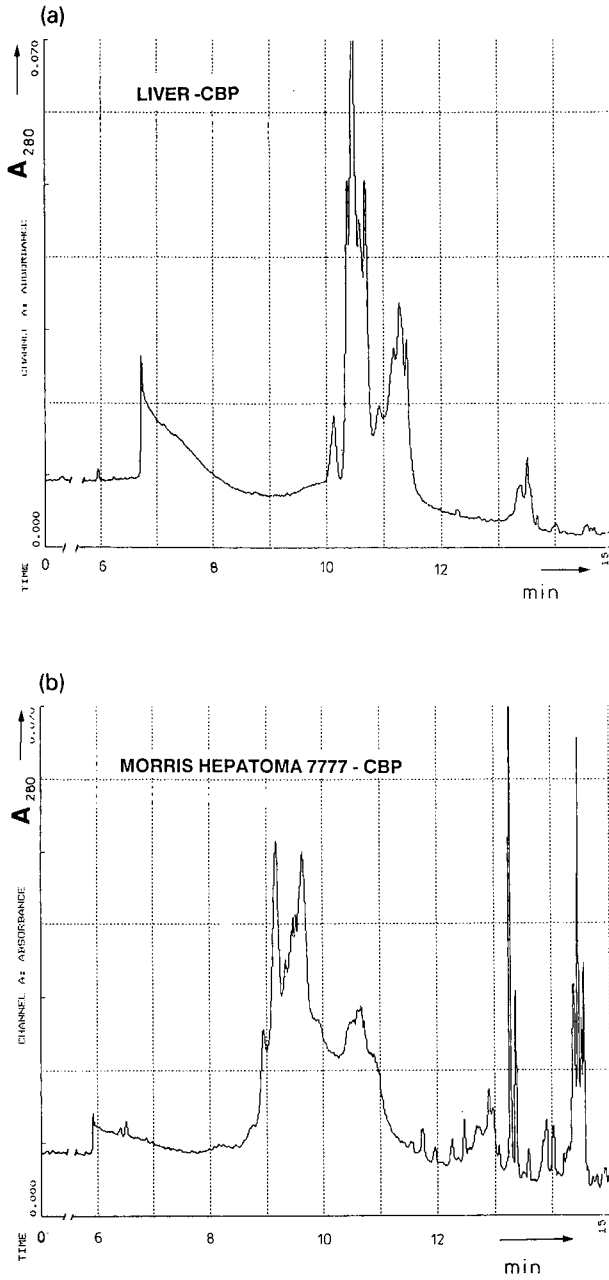


Fig. 4. Separation of calcium-binding membrane proteins from (a) liver and (b) Morris hepatoma 7777 by HPLCZE with addition of ampholytes as spacers in the pH range 5–7. Other conditions as in Fig. 3.

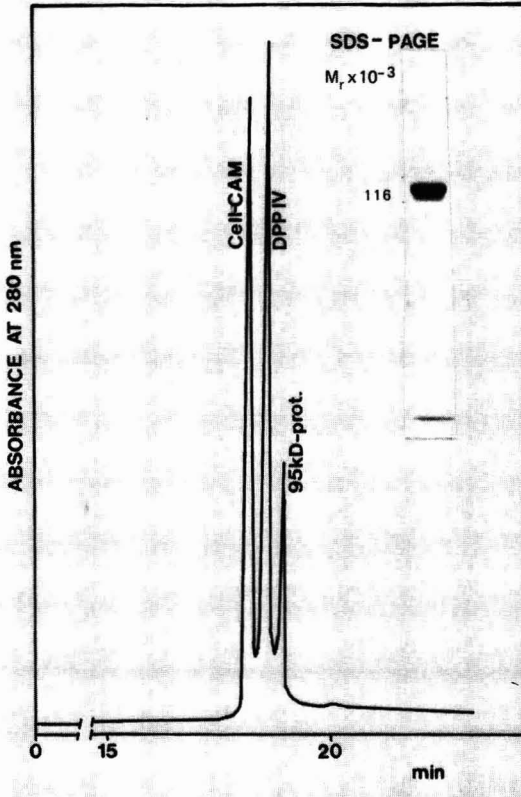


Fig. 5. Separation of intrinsic membrane proteins from liver by HPCITP without spacers. The three peaks belong to the three main components in the mixture, DPP IV, cell-CAM and 95 000-dalton protein (95kD-prot.)¹². One dimensional SDS-PAGE is shown in the inset. Other conditions as in Fig. 3.

CONCLUSIONS

The HPCZE and HPCITP methods described can be applied to the separation of membrane proteins. Precipitation of the proteins, which can occur during separation either on reaching the isoelectric point or through the separation of detergents, must be avoided. This can be achieved by applying detergents and/or denaturing reagents in HPCZE and HPCITP. The non-specific interactions with the surface of the capillary have to be suppressed. In this respect the nature of the capillary walls (PTFE or coated capillaries) plays an important role.

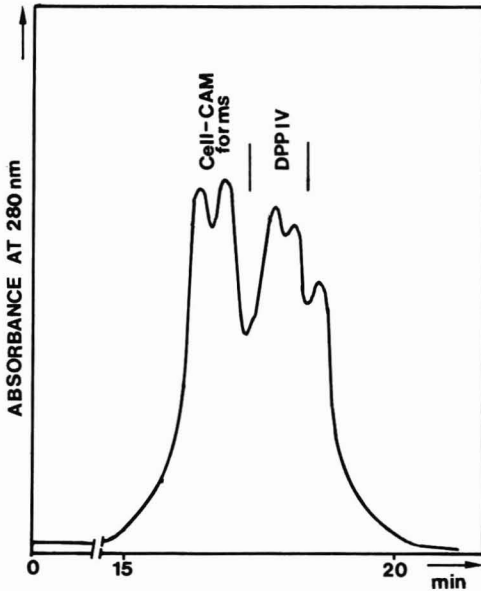


Fig. 6. Separation of intrinsic membrane proteins from liver by HPCITP with addition of ampholytes as spacers in the pH range 4–6. The same mixture as in Figs. 2 and 5 was separated. The splitting of single peaks is due to the microheterogeneity of these glycoproteins.

REFERENCES

- 1 Y. F. Chung and N. J. Dovichi, *Science (Washington, D.C.)*, 242 (1988) 562.
- 2 S. Honda, S. Iwase, A. Makino and S. Fujiwara, *Anal. Biochem.*, 176 (1989) 72.
- 3 J. P. Advis, L. Hernandez and N. A. Guzman, *Pept. Res.*, 2 (1989) 389.
- 4 J. W. Jorgenson and K. D. Lukacs, *Science (Washington, D.C.)*, 222 (1983) 266.
- 5 F. Kilár and S. Hjertén, *Electrophoresis*, 10 (1989) 23.
- 6 A. S. Cohen, A. Paulus and B. L. Karger, *Chromatographia*, 24 (1987) 224.
- 7 A. S. Cohen, D. R. Najarian, A. Paulus, A. Guttman, J. A. Smith and B. L. Karger, *Proc. Natl. Acad. Sci. U.S.A.*, 85 (1988) 9660.
- 8 B. L. Karger, A. S. Cohen and A. Guttman, *J. Chromatogr.*, 492 (1989) 585.
- 9 G. Schmitz, U. Borgmann and G. Assmann, *J. Chromatogr.*, 320 (1985) 253.
- 10 F. S. Stover, *J. Chromatogr.*, 470 (1989) 201.
- 11 M. M. Gladdines, J. C. Reijenga, R. G. Tieling, M. J. S. van Thiel and F. M. Everaerts, *J. Chromatogr.*, 470 (1989) 105.
- 12 Dj. Josić, Y.-P. Lim, K. Zeilinger, M. Raps, S. Hartel and W. Reutter, *J. Chromatogr.*, 484 (1989) 327.
- 13 R. M. Kamp, A. Bosserhoff, D. Kamp and B. Wittmann-Liebold, *J. Chromatogr.*, 317 (1984) 181.
- 14 R. Tauber and W. Reutter, *Eur. J. Biochem.*, 83 (1978) 37.
- 15 Dj. Josić, W. Schütt, R. Neumeier and W. Reutter, *FEBS Lett.*, 185 (1985) 182.
- 16 G. Nowicka, T. Brüning, B. Grothaus, G. Kahl and G. Schmitz, *J. Lipid Res.*, in press.
- 17 U. K. Laemmli, *Nature (London)*, 277 (1970) 680.
- 18 P. H. O'Farrel, *J. Biol. Chem.*, 250 (1975) 4007.
- 19 A. Becker, *Ph.D. Thesis*, Freie Universität, Berlin, 1989.
- 20 S. Hartel, *Ph.D. Thesis*, Freie Universität, Berlin, 1988.
- 21 N. Thompson and D. C. Hixson, *Biochem. J.*, in press.

Method optimization in capillary zone electrophoretic analysis of hGH tryptic digest fragments

R. G. NIELSEN*^a and E. C. RICKARD

Eli Lilly and Company, Lilly Research Laboratories, Lilly Corporate Center, Indianapolis, IN 46285 (U.S.A.)

ABSTRACT

The mobile phase composition was optimized for the separation of tryptic digest fragments of human growth hormone by capillary zone electrophoresis. The effect of pH (pH 2.4, 6.1, 8.1 and 10.4) was evaluated since pH determines the relative charge of species, the prime contributor to selectivity; pH 8.1 was selected for the optimization studies. Tricine (buffer), sodium chloride (ionic strength adjustor), and morpholine (mobile phase additive) concentrations were systematically varied at pH 8.1. All three exhibited major effects on the electroosmotic flow velocity and current, and minor effects on selectivity. Tricine was the most crucial for good resolution, although addition of morpholine helped to resolve closely eluting species. The optimum separation conditions were found to be pH 8.1 with 0.1 M tricine, 0.02 M morpholine and no salt.

INTRODUCTION

Capillary electrophoresis has been used in a variety of modes to separate and characterize diverse molecules, especially biomolecules^{1–4}. The open tubular mode is referred to as capillary zone electrophoresis (CZE), high-performance capillary electrophoresis, or free solution capillary electrophoresis. CZE has been widely used for separations due to its simplicity, high separative power, ease of quantitation, and ability to perform rapid, automated analyses. It has been applied to numerous polypeptide and protein molecules^{5–9}. One area of particular interest to us was the characterization of the identity and purity of proteins used as drugs. We reported separations of biosynthetic human insulin (BHI) and human growth hormone (hGH) from closely related species that could originate as impurities or as degradation products¹⁰. That paper also demonstrated that the results for the quantitation of the desamido-A21 BHI degradation product in BHI by CZE were equivalent to results obtained from reversed-phase high-performance liquid chromatography (RP-HPLC)

^a Present address: Process Development, Hybritech, Inc., P.O. Box 269006, San Diego, CA 92126-9006, U.S.A.

and polyacrylamide gel electrophoresis. Other papers have reported the separation of peptide mixtures such as the 19 peptide fragments produced from an enzymatic (trypsin) digest of human growth hormone^{11,12} and a series of synthetic peptides¹³. However, relatively few reports of a systematic approach to the selection of CZE operating conditions to achieve optimum separations have been given. This paper will describe the optimization of the separation of components in the complex tryptic digest of hGH.

The selectivity achieved in CZE separations is determined by differences in electrophoretic mobilities of the analytes. Mobility in the open tubular mode is predominantly related to charge, shape and size of the analyte as well as to the properties of the eluting solvent^{2,13,14}. For impurities and degradation products, which usually have shapes and sizes similar to that of the main component, adjustment of pH to a value near the midpoint of the isoelectric point (pI) range of the analytes will tend to maximize their net charge differences⁷. However, digest fragments generally consist of a rather heterogeneous mixture of peptide fragments such that the pH value that will maximize selectivity may not be easily predictable.

In addition to differences in selectivity, efficiency also plays an important role in the separation process. The efficiency (or number of theoretical plates) can be quite large if processes that lead to band broadening can be minimized^{5,15-18}. Some of the major processes that contribute to band broadening include interactions of the analyte with the capillary wall^{6,8,15-19}, temperature gradients (which affect viscosity and electrophoretic mobility)^{5,17,18,20}, sample loading (sample introduction technique, volume and amount)^{17,18}, sample solvent^{5,15,17,20}, and detector design¹⁷. The rate of electroosmotic flow also affects the efficiency since it decreases the amount of time that species are separated under the influence of the electric field but does not contribute to the separation²¹.

Although each of the above processes that lead to decreased efficiency can be addressed, they are generally not independent of the parameters that affect selectivity. For example, variation of pH to achieve optimum selectivity based on charge differences will also affect efficiency by changing the rate of electroosmotic flow in fused-silica capillaries. Furthermore, the net charge on the protein relative to that on the silica surface, which are both determined by pH, is one of the primary factors that determines the amount of analyte interaction with fused silica.

In addition to the pH effects described above, the buffer composition will affect the ionic strength and conductivity. Other additives may be included in the mobile phase. For example, the ionic strength may be adjusted with salts, and organic modifiers may be added to reduce wall interactions or to maintain analyte solubility. It is obvious that the effect on operating performance due to the interaction of the experimental parameters is complex. The effects of the most important parameters are reported herein: pH, tricine (buffer) concentration, sodium chloride (ionic strength adjustor) concentration, and morpholine (mobile phase modifier) concentration.

EXPERIMENTAL

Reagents and materials

Biosynthetic hGH was obtained from Eli Lilly and Co. (Lilly Research Labs., Indianapolis, IN, U.S.A.). Morpholine and glycine were purchased from Fisher Sci-

entific (Pittsburgh, PA, U.S.A.); tricine, 2-[N-morpholino]ethanesulfonic acid (MES), and 3-[cyclohexylamino]-1-propane-sulfonic acid (CAPS) were purchased from Sigma (St. Louis, MO, U.S.A.). Tris(hydroxymethyl)aminomethane (Tris) was purchased from Bio-Rad Labs. (Richmond, CA, U.S.A.). Trypsin (TPCK, 267 units/mg protein, 98% protein) was purchased from Cooper Biomedical (Malvern, PA, U.S.A.). Reagent-grade water obtained from a Milli-Q purification system from Millipore (Bedford, MA, U.S.A.) was used to prepare all solutions. All other reagents were analytical grade and were used without further purification. Polyimide-coated, fused-silica capillaries, 50 μm internal diameter and 360 μm outside diameter, were purchased from Polymicro Technol., (Phoenix, AZ, U.S.A.).

Tris-acetate buffer was prepared by adjusting the pH of a 0.05 *M* Tris solution to pH 7.5 with acetic acid. The pH 2.4 buffer was prepared from a 0.1 *M* glycine solution. The pH 6.1 buffer contained 0.1 *M* MES and 0.0363 *M* sodium chloride. The pH 8.1 buffer contained 0.1 *M* tricine and 0.0343 *M* sodium chloride. The pH 10.4 buffer contained 0.1 *M* CAPS and 0.0381 *M* sodium chloride. Minor adjustments of the pH of the latter four buffers were made with 0.1 *M* hydrochloric acid or 0.1 *M* sodium hydroxide as necessary.

Methods

The trypsin digestion was carried out according to reported methods using non-reducing conditions so that both the correct amino acid sequence and the presence of the correct disulfide linkages could be confirmed²². Aliquots of the digest mixture were frozen (-20°C) for use at a later time. The thawed digest mixture was injected directly. The concentration of the analyte in all studies was about 2 mg/ml total protein or 90 μM for each digest fragment except for fragments 17–19 which will be present at lower concentrations since fragments 17 and 19 derive from cleavage of fragment 18.

The mobile phase used in the initial CZE separations was 0.01 *M* tricine, 0.02 *M* sodium chloride, and 0.045 *M* morpholine adjusted to pH 8.0. The four buffers described above were used as mobile phases in the pH optimization study; the mobile phases used in the pH 8.1 optimization experiments are described below. The column was rinsed with mobile phase between injections or successively with 0.1 *M* sodium hydroxide and mobile phase when the mobile phase composition was changed.

Preliminary data were obtained using the CZE instrumentation previously described¹⁰ except that both CZE instruments now include vacuum injection devices and a constant temperature environment. The data presented in the figures were obtained on an Applied Biosystems (Santa Clara, CA, U.S.A.) Model 270A instrument. Sample (approximately 10 nl as estimated from the Poiseuille equation for a 3-s injection) was introduced by applying vacuum (127 mmHg) to a capillary that was approximately 100 cm in length with 80 cm to the detector. Separation conditions were: 30 kV applied voltage and 30°C . The components were detected by UV absorbance at 200 nm. Analog data were collected directly from the absorbance detector on an in-house centralized chromatography computer system based on the Hewlett-Packard Model 1000 minicomputer that has storage, manipulation, and graphics capabilities.

The electrophoretic separations were evaluated for selectivity, efficiency and resolution. Selectivity was determined by identification of peaks under selected condi-

tions. Efficiency was qualitatively judged by the peak sharpness. Overall resolution was qualitatively judged by the number of peaks which could be observed and the spacing between peaks.

The buffer capacity²³ and ionic strength of the buffers were calculated from the following values: glycine, $pK_{a1} = 2.35$ (carboxylate), $pK_{a2} = 9.78$ (amine); MES, $pK_a = 6.10$; tricine, $pK_{a1} = 2.33$ (carboxylate), $pK_{a2} = 8.15$ (amine); CAPS, $pK_a = 10.40$; morpholine, $pK_a = 8.40$. The buffer capacity is defined as the amount of acid or base required to change the pH by one unit. The calculated ionic strength includes contributions from all species with a net charge; concentrations of buffer components were determined using the acid dissociation constants given above without consideration of activity effects.

RESULTS AND DISCUSSION

The large number of hGH cleavage fragments and their diverse structure contribute to the complexity of designing an acceptable separation. The structure of the individual fragments and their RP-HPLC behavior were described by Becker *et al.*²². The properties of the fragments that are relevant to CZE and RP-HPLC separations are listed in Table I. Note that the fragments range from highly basic (*e.g.*, fragments

TABLE I
FRAGMENTS FROM ENZYMATIC DIGEST OF HUMAN GROWTH HORMONE

Fragment number	Isoelectric point ^a	Hydrophobicity ^b	Molecular weight	Amino acid residues	Amino acid sequence ^c
1	10.1	18.1	930	8	FPTIPLSR
2	5.8	17.5	978	8	LFDNAMLR
3	10.4	-12.3	382	3	AHR
4	4.2	45.5	2343	19	LHQLAFDITYQEFEEAYIPK
5	6.4	-15.7	404	3	EQK
6-16	7.3	74.8	3763	32	6: YSFLQNPQTSLCFSES IPTPSNR 16: NYGLLYCFR
7	4.5	-19.0	762	6	EETQQK
8	5.9	9.4	844	7	SNLELLR
9	6.4	72.1	2056	17	ISLLLIQSWLEPVQFLR
10	3.5	33.3	2263	21	SVFANSLVYGASDSNVYDLLK
11	4.0	13.0	1362	12	DLEEGIQTLMGR
12	4.0	-3.4	773	7	LEDGSPR
13	9.2	0.4	693	6	TGQIFK
14	9.0	-14.2	626	5	QTYSK
15	3.8	0.9	1490	13	FDTNSHNDDALLK
17	9.0	-13.9	146	1	K
18	6.1	10.5	1382	11	KDMDKVETFLR
19	4.0	12.1	1253	10	DMDKVETFLR
20-21	5.9	19.9	1401	13	20: IVQCR 21: SVEGSCGF

^a Calculated from a computer program based on Skoog and Wichman²⁷.

^b Calculated according to Meek and Rossetti²⁸.

^c Single-letter code for amino acids used.

1 and 3) that will be positively charged at neutral pH values to highly acidic (e.g., fragments 10 and 15) that will be negatively charged at neutral pH values. They also differ significantly in size, from fragment 17 that is a single amino acid residue (lysine) to fragment 6–16 that contains 32 amino acid residues in two chains linked by a disulfide bond. (Fragment 20–21 also consists of two chains connected by a disulfide bond.) Finally, the fragments range from hydrophobic (e.g., fragments 6–16, 9, 4 and 10) to hydrophilic (e.g., fragments 7, 5, 14, 17 and 3).

In previously reported data, the peaks in the electropherogram of the hGH digest were identified using the pH 8.0 CZE mobile phase described for the initial CZE separations¹¹. Identification was accomplished by spiking individual fragments isolated by RP-HPLC or, in cases where RP-HPLC did not produce a complete separation, material that was further fractionated by anion-exchange chromatography. The integrity of the isolated material was verified by reinjection on RP-HPLC; the identity of the material isolated by anion exchange was confirmed by amino acid analysis.

Note that fragment 14 gives more than one peak following isolation by RP-HPLC and solvent evaporation. Authentic fragment 14 elutes early in the electropherograms at pH 8.1 as labeled in Figs. 2 and 8. A degradation product of this fragment, labeled 14*, elutes much later. Therefore, fragment 14* must be more negatively charged than fragment 14; it probably arises from a spontaneous cyclization of the N-terminal glutamine (sequence, QTYSK) to give pyrrolidone carboxylic acid at the N-terminal. However, this postulated structure has not been confirmed. The subtle rearrangement of fragment 14* was missed in the preliminary peak assignments for the digest⁹. Fragment 11 also yields fragment 11* (of unknown composition), which is resolved only under the optimum separation conditions at pH 8.15 (Fig. 8).

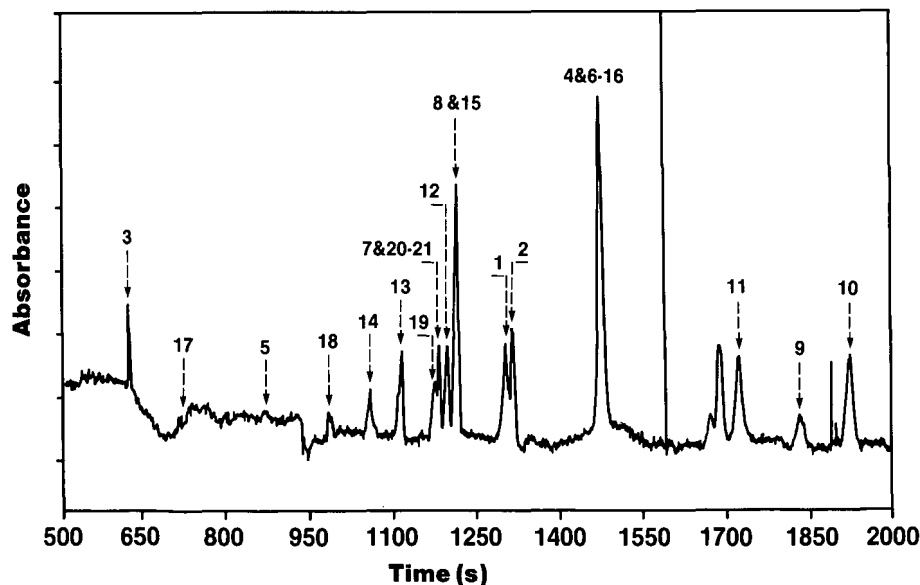


Fig. 1. Electropherogram of hGH digest in 0.1 M glycine buffer, pH 2.4.

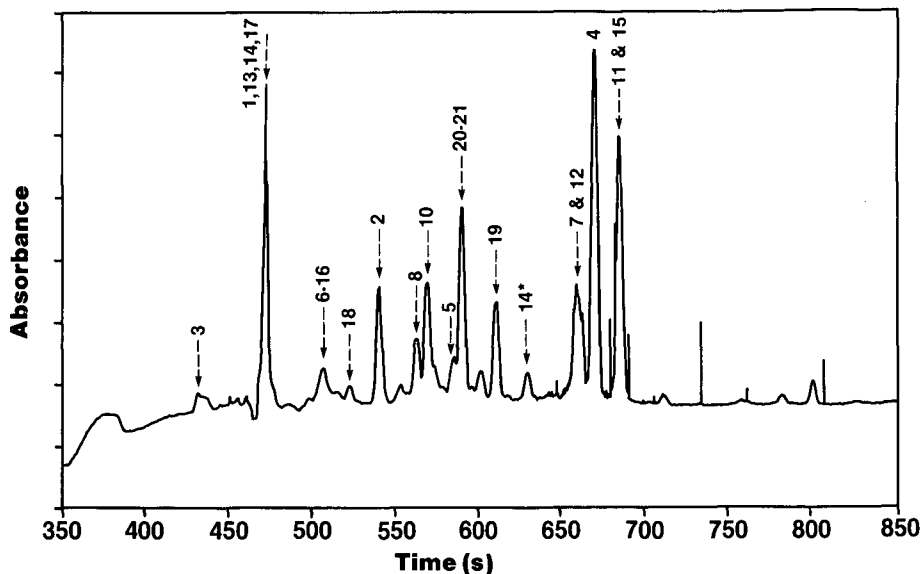


Fig. 2. Electropherogram of hGH digest in 0.1 *M* tricine buffer containing 0.0343 *M* sodium chloride, pH 8.1.

Fragment 9 also exhibits anomalous behavior. At low pH, it is soluble and migrates as labeled in Fig. 1. At high pH, more than one peak is associated with this fragment. The very limited solubility of fragment 9 at high pH produces insoluble particles that elute near fragment 4, usually as sharp spikes with variable migration times that are not representative of its true mobility. The soluble portion of fragment 9 is present at such low concentrations that it cannot be reliably observed, although it should elute near the position of fragment 6–16. Therefore, the identity of fragment 9 is not indicated on Figs. 2 and 8.

pH optimization

Various strategies have been used for selection of the pH of the mobile phase to minimize the interaction of proteins with the silica surface. These strategies are based on the reduced electrostatic interactions between the protein and the silica when they have charges of the same sign (compared to pH regions where they are oppositely charged). When the pH is greater than the *pI* of the protein, the protein will carry a net negative charge and, thus, be repelled from the negatively charged silica wall^{6,16}. Others have used low pH values to minimize wall interactions^{7,8,13} since the proteins are positively charged while the silica is relatively uncharged at pH values below about 2 (refs. 6, 8). Low pH also produces a drastic reduction in the electroosmotic flow velocity that will give greater efficiency (when other factors are maintained constant) at the cost of longer elution times. However, both of these strategies dictate that the pH value be chosen by factors other than optimization of selectivity. It is obvious that it would be better to minimize the interaction of the analyte with the silica by other means (buffer strength, mobile phase additives, ionic strength, coating

of capillaries, etc.) so that the pH of the mobile phase may be chosen to give optimum separations.

Four pH values over the range of 2.4 to 10.4 were selected for this study. These values encompass the extremes in the above two approaches and cover the *pI* range of the digest fragments (see Table I). A high buffer strength was used to maintain a constant pH within the analyte zone; the buffer capacity for all four buffers was about 52 mM or approximately 600 times the analyte concentration. The conductivity of the three higher pH buffers was empirically adjusted to be approximately equal to that of the pH 2.4 buffer by the addition of sodium chloride. This procedure resulted in approximately equal ionic strengths except for the pH 2.4 buffer where the hydrogen ion contributes disproportionately to the conductivity (calculated ionic strengths about 28, 61, 59 and 63 mM for pH 2.4, 6.1, 8.1 and 10.4 buffers, respectively). The high ionic strengths should minimize analyte interactions with the silica and maintain constant conductivity within the analyte zone.

The identities of the individual peaks in the electropherograms were assigned for pH 2.4 and 8.1 (Figs. 1 and 2; sequences given in Table I). The peak identification strategy was similar to that used in the earlier work and described briefly above. For pH 6.1 and 10.4, the efficiency and resolution were poorer than those at other pH values (data not shown). Since these conditions are not commonly used, no additional work was performed at these pH values.

The separation at pH 2.4 required a somewhat longer time (about 30 min) than the separations at higher pH values (about 18 min). There are two effects that contribute to the separation time. First, the electroosmotic flow is drastically reduced at low pH so that elution times are lengthened. Second, the electrophoretic velocity (which is proportional to the charge) is higher at low pH since the species carry a high net positive charge; this shortens the elution time and partially offsets the reduction in electroosmotic flow velocity.

Overall, the selectivity observed at pH 2.4 was different, but not necessarily better, than that at pH 8.1. For example, fragments 7 and 20–21, fragments 8 and 15, and fragments 4 and 6–16 overlap at pH 2.4; several other pairs migrate at very similar velocities. Note that fragments 5 and 17 show very low absorbance in the pH 2.4 glycine buffer since they have very similar absorptivities to the mobile phase. The separation in the glycine buffer is very similar to that obtained with another commonly used low pH buffer, pH 2.5 citrate (data not shown; peaks 5 and 17 have greater relative peak height in the citrate buffer).

At pH 8.1, fragments 7 and 12, fragments 11 and 15, and fragments 1, 13, 14 and 17 co-migrate. However, the separation previously reported for pH 8.0 (refs. 9, 11) is superior to either Fig. 1 or 2. The addition of morpholine in the previous report is important to achieve the best resolution because of combined changes in selectivity and efficiency. The changes in selectivity between the previous work at pH 8.0 and pH 8.1 in this work seem to be minor since the peak order is preserved, although fewer peaks overlap for the pH 8.0 conditions. The changes in efficiency are apparently the result of a reduction of the electroosmotic velocity due to morpholine (which coats the capillary walls) and the higher buffer strength; both contribute to a greater effective separation time. Additives such as morpholine may also interact with other species in ways that are only poorly understood as discussed below.

Although pH 8.1 is not the midpoint of the *pI* range of the fragments (average

pI, 6.3; median *pI*, 5.9), previous empirical data suggested that it would give a good separation. Thus, the remainder of the optimization was performed at pH 8.1.

Tricine (buffer) optimization

It is well known that the buffer concentration must be sufficiently high to maintain a constant conductivity and pH within the analyte zone to prevent band broadening^{5,6,15,24}. Buffer concentrations at least 100 times that of the sample may be necessary to meet this requirement. However, high concentrations of ionic buffers produce high conductivity, and therefore high currents and high heat loads. Use of a zwitterionic buffer allows one to adjust pH with only a minimal effect on conductivity^{6,25}. For the optimization at pH 8.1, tricine was chosen after examination of a number of possible buffer systems since it met all of the above criteria and gave reproducible electropherograms.

The initial concentration of tricine was 0.01 *M*, which gives a buffer capacity of about 5 mM at pH 8.1. Thus, the buffer capacity was about 50 times the concentration of the individual fragments. The upper tricine concentration value of 0.1 *M* gave a ten-fold increase in buffer capacity. Morpholine also contributed to the buffer capacity when it was present, *e.g.*, 0.01 *M* morpholine has a buffer capacity of about 5 mM at pH 8.1. The total buffer capacity (range of 5 to 78 mM) and approximate ionic strengths are given in Table II.

TABLE II
OPTIMIZATION OF CZE MOBILE PHASE COMPOSITION AT pH 8.1

Concentrations, buffer capacity and ionic strength are given as mmol/l.

Condition	Mobile phase concentration			Buffer capacity	Ionic strength
	Tricine	Sodium chloride	Morpholine		
A	10	0	0	5	2
B	50	0	0	26	12
C	100	0	0	52	25
D	10	20	0	5	22
E	10	40	0	5	42
F	10	0	5	8	4
G	10	0	15	13	7
H	10	0	45	27	17
I	10	20	45	27	37
J	10	40	45	27	57
K	50	0	45	48	27
L	50	20	30	41	42
M	100	40	0	52	65
N	100	0	20	62	31
P	100	0	30	67	35
Q	100	0	45	74	39
R	100	40	45	74	79
S	100	20	0	52	45
T	100	0	10	57	28
U	150	0	0	78	38

An increase in the tricine concentration from 0.01 to 0.1 *M* in the absence of morpholine and sodium chloride produced increased current (approximately 3 μA to 28 μA , conditions A and E, respectively) and a decreased electroosmotic flow (approximately 2.4 mm/s to 1.6 mm/s under the same conditions). However, the greatest

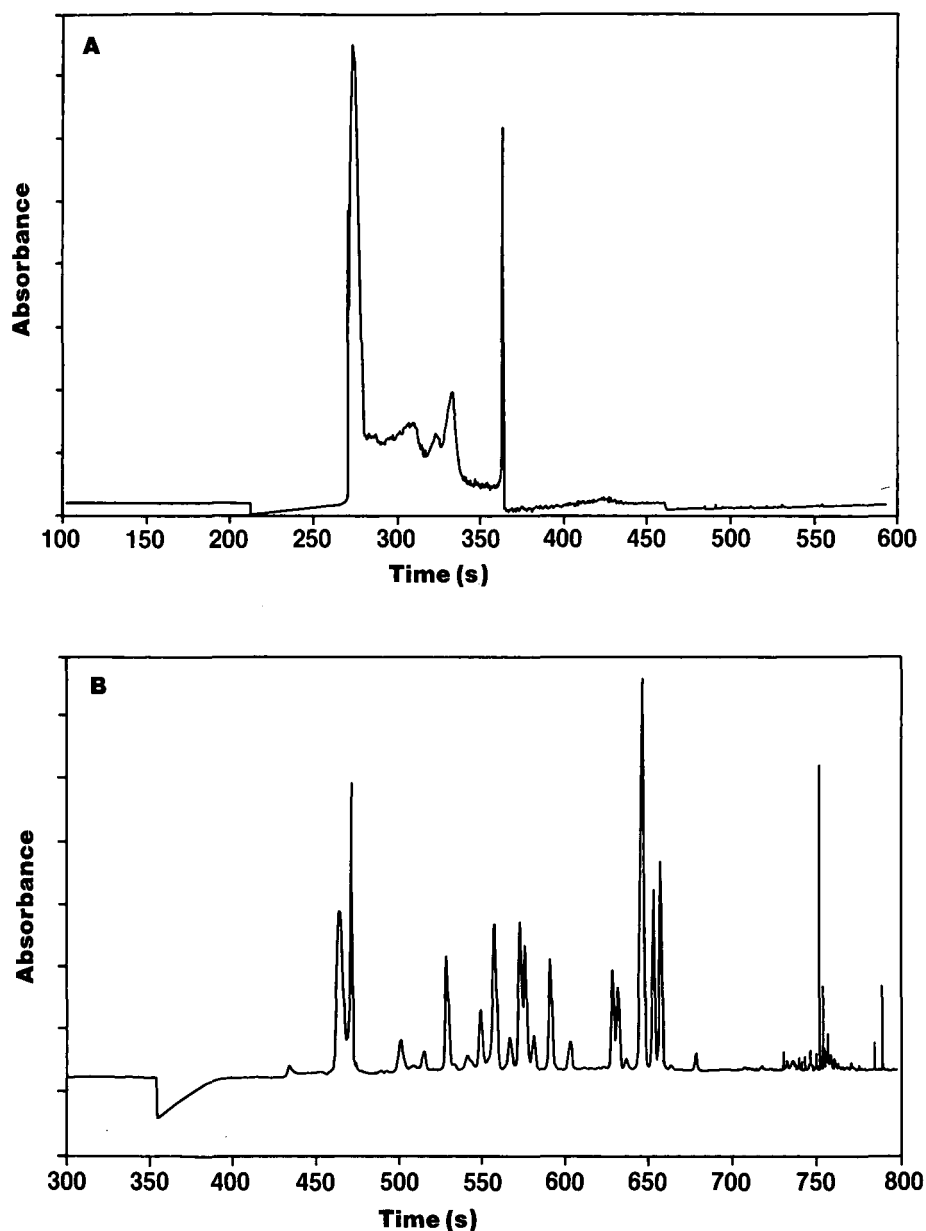


Fig. 3. Electropherogram of hGH digest in pH 8.1 tricine buffer. (A) 0.01 *M* tricine (condition A); (B) 0.1 *M* tricine (condition C).

effect of increased tricine concentration was the greatly improved efficiency and resolution (Fig. 3). The efficiency and resolution were improved by increasing the buffer concentration whether or not salt or morpholine was present (see Fig. 4; other data not shown). The increased efficiency was apparently due to the increased buffer capacity rather than ionic strength (see below). This result demonstrates the necessity of

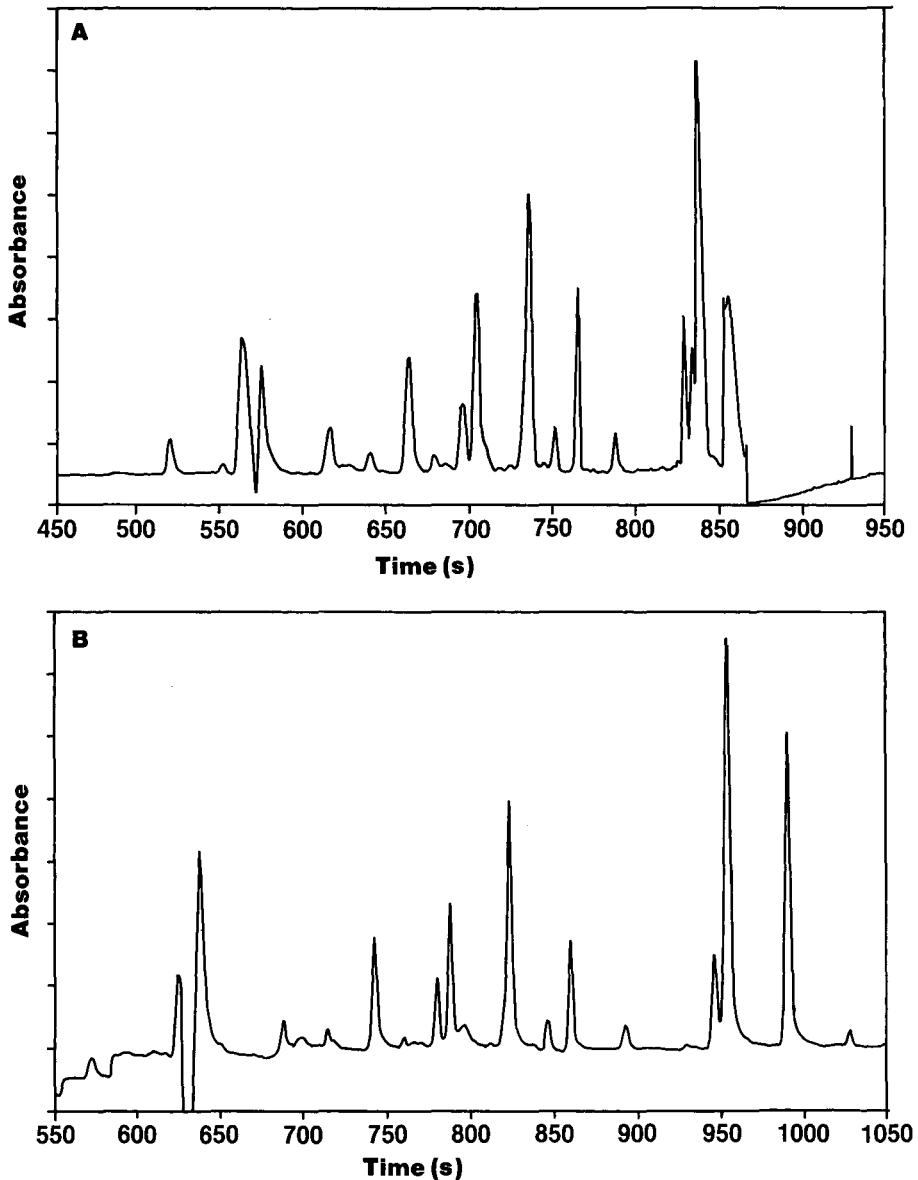


Fig. 4. Electropherogram of hGH digest in pH 8.1 tricine buffer. (A) 0.01 *M* tricine, 0.04 *M* sodium chloride, and 0.045 *M* morpholine (condition J); (B) 0.1 *M* tricine, 0.04 *M* sodium chloride, and 0.045 *M* morpholine (condition R).

maintaining a large excess of buffer to prevent distortions in the electric field gradient and pH within the sample zone and the resulting loss of resolution. Based on data for this system, at least 0.05 M tricine (*i.e.*, buffer capacity about 300 times the analyte concentration) is required for optimum resolution.

Other effects due to the increased tricine concentration need to be discussed. First, the higher ionic strength reduces the zeta potential which causes a lower electroosmotic flow velocity. (Other effects due to a higher ionic strength include a reduced thickness of the double layer, and changes in the dielectric constant and viscosity¹⁹). Therefore, the analyte effectively sees a reduced charge on the capillary surface at high buffer concentrations. The increased buffer concentration also competes for ion-exchange sites on the capillary as discussed in the next section. Thus, increasing the buffer concentration will minimize wall interactions by two mechanisms, a decrease in the zeta potential and saturation of ion exchange sites. Minimizing the wall interaction will allow analyte species that interact with free silanols (at low buffer strengths) to move at rates more consistent with their inherent electrophoretic mobility (*e.g.*, size and charge). Third, it is possible that at high ionic strengths, the charge on the analyte is more effectively shielded from the electrostatic field by its surrounding ionic environment. Finally, zwitterions such as tricine should not directly interact with the sample to produce species of different charge⁶.

Sodium chloride (ionic strength adjustor) optimization

Earlier work by Jorgenson¹⁵ and Lauer and McManigill⁶ suggested that one source of wall interaction was due to exposed silanols that act as cation-exchange sites for positively charged regions of the analyte. This type of interaction could be minimized by the addition of inert salts (to increase the ionic strength) or other cations (to compete for the exchange sites). Initial experiments in our laboratory suggested that resolution of the digest fragments might be dependent upon the ionic strength. Thus, the effect of ionic strength was investigated by the addition of 0–0.04 M salt.

The total ionic strength, including contributions from the buffer and morpholine, is given in Table II (range of 2 to 79 mM). At 0.01 M tricine and 0.04 M sodium chloride, the current was about 36 μA (condition E) compared to 3 μA without sodium chloride (condition A). Note that increased salt concentration affects the double layer structure and reduces the electroosmotic flow in a manner analogous to that produced by increased buffer concentrations (electroosmotic flow velocity 1.6 mm/s compared to 2.4 mm/s for conditions E and A, respectively). In addition to the changes in double layer structure, the sodium ion should compete with the sample for cation-exchange sites on the silica surface.

In this systematic study, the overall resolution was poorer in the presence of salt, as apparent in Fig. 5 compared to Fig. 3B (other data not shown). Based on our observations, it was concluded that there was no obvious advantage from increasing the ionic strength by the addition of sodium chloride.

Morpholine (mobile phase additive) optimization

In RP-HPLC, mobile phase additives are frequently employed to minimize the interaction of cationic analytes, especially amines, with exposed silanols. When used in CZE, these additives will have a similar effect in coating the free silanols. However, they have the additional major effect of modifying the interfacial double-layer struc-

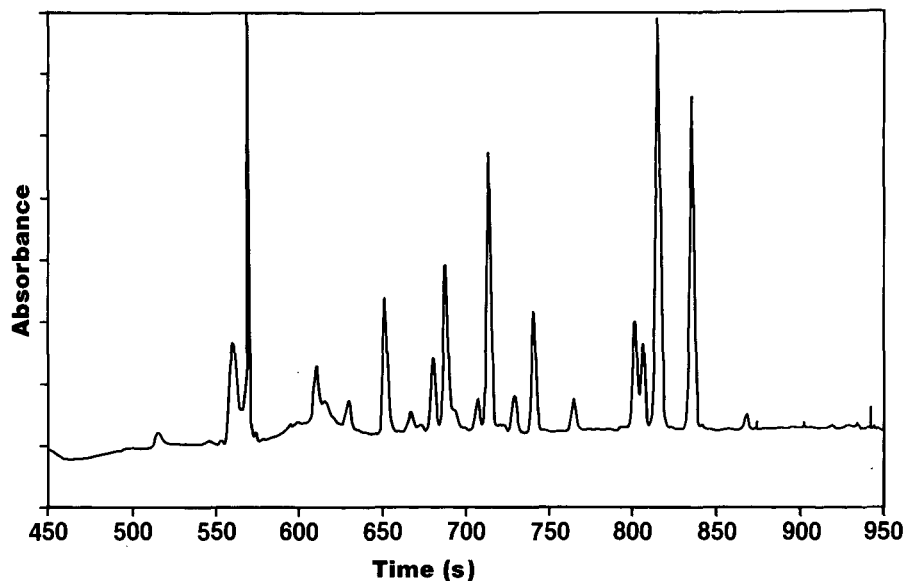


Fig. 5. Electropherogram of hGH digest in pH 8.1 tricine buffer, 0.1 *M* tricine and 0.04 *M* sodium chloride (condition M).

ture and reducing the zeta potential. Thus, they will reduce the electroosmotic flow as well as change the nature of the exposed surface. The effect of morpholine, a common additive for RP-HPLC, was investigated in CZE separations over a concentration range of 0 to 0.045 *M*. As mentioned above, morpholine will also increase the ionic strength and buffer capacity.

Addition of morpholine produced a lower electroosmotic flow and higher current as expected. For example, the current with 0.01 *M* tricine and 0.045 *M* morpholine was about 27 μA (condition H) compared to 3 μA without morpholine (condition A); the corresponding electroosmotic flows were about 1.3 mm/s and 2.4 mm/s, respectively. Both values are similar to that produced by changing the tricine concentration to 0.1 *M* in the absence of morpholine. However, morpholine also produced different resolution for the fragments (see Fig. 6 compared to Fig. 3A). Without any direct evidence, one can only speculate that it is either reducing the interaction of the analyte with the wall (as desired) and/or that it is changing the charge of the species in solution. In either case, there seems to be some advantage with using small amounts of morpholine (about 0.02 *M*), especially at low buffer concentrations.

Mobile phase interactions at pH 8.1

Additional mobile phase compositions were examined to validate the above observations and to uncover any interaction of variables. For example, condition Q (Fig. 7) represents a major increase in buffer concentration from condition H (Fig. 6) and shows improved resolution. This result is consistent with that expected from extrapolation of Figs. 3 and 4 as well as for other cases (data not shown) where the

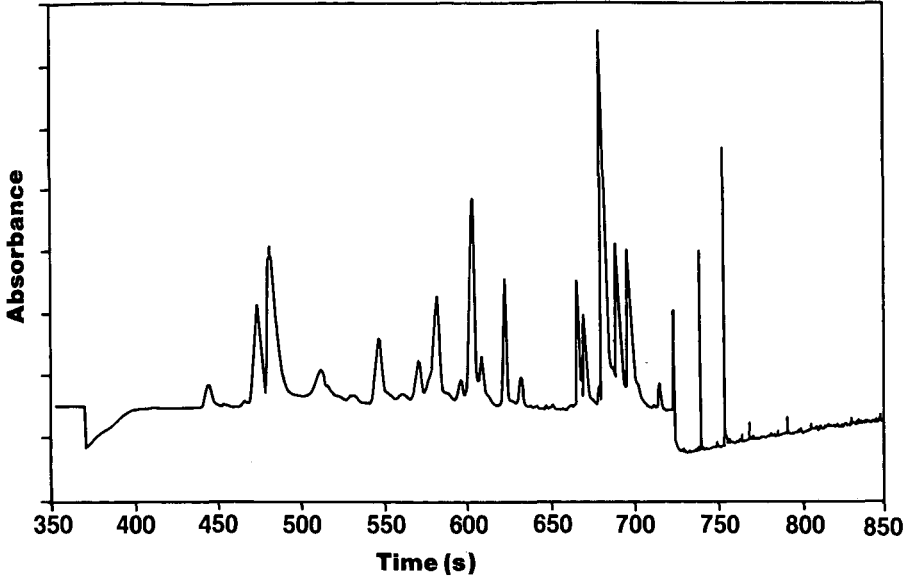


Fig. 6. Electropherogram of hGH digest in pH 8.1 tricine buffer, 0.01 M tricine and 0.045 M morpholine (condition H).

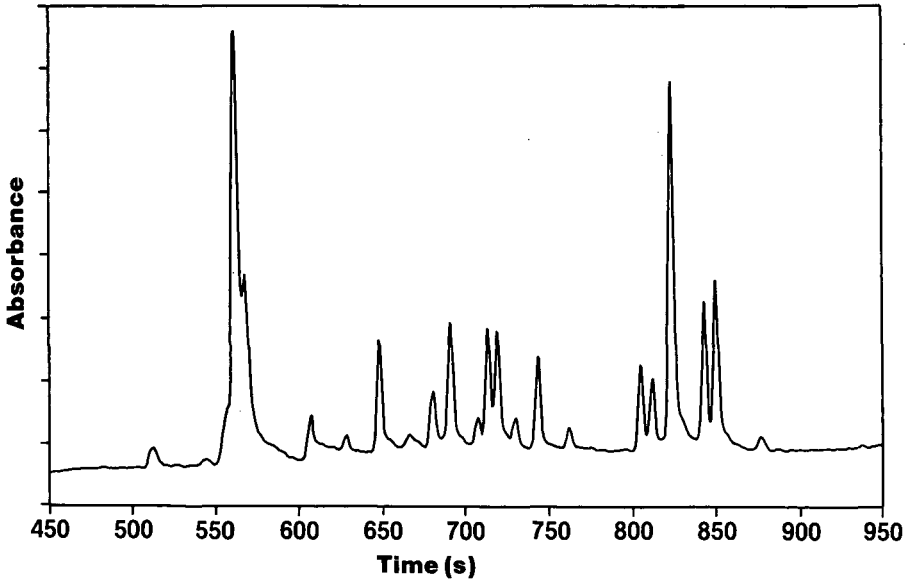


Fig. 7. Electropherogram of hGH digest in pH 8.1 tricine buffer, 0.1 M tricine and 0.045 M morpholine (condition Q).

tricine concentration was increased while the concentrations of the other components were kept approximately constant.

Similar comparisons can be made for the effect of added salt from condition H to condition J and from condition Q to condition R (Figs. 6 to 4A and 7 to 4B, respectively). No obvious advantage from increased sodium chloride concentration is observed regardless of the tricine or morpholine concentration levels.

The effect from addition of morpholine at high buffer levels (condition C to condition Q; Fig. 3B to 7) or with high salt and high buffer levels (condition M to condition R; Fig. 5 to 4B) is less obvious. Inspection of the electropherograms indicates some differences in resolution but no definite trends.

The observation that the optimum separation is obtained with a mobile phase that contains a high buffer concentration, no salt, and possibly some morpholine, was confirmed by running several additional conditions. These include conditions T, N, and P (0.1 *M* tricine, no salt, and increasing amounts of morpholine), condition S (0.1 *M* tricine, no morpholine and 0.02 *M* sodium chloride, an intermediate salt concentration), and condition U (0.15 *M* tricine, an increased buffer concentration, with no sodium chloride or morpholine). These data indicated that condition N (0.1 *M* tricine, 0.02 *M* morpholine and no salt) produced the optimum separation (Fig. 8).

In summary, the results of the mobile phase optimization at pH 8.1 are as follows: (1) increasing either tricine, sodium chloride or morpholine concentrations increased the current and reduced the electroosmotic flow velocity (all three species increase the ionic strength; only tricine and morpholine contribute to the buffer capacity), (2) a high buffer capacity, about 300 times the concentration of the analyte, was required to maintain high efficiency and good resolution, (3) added sodium chlo-

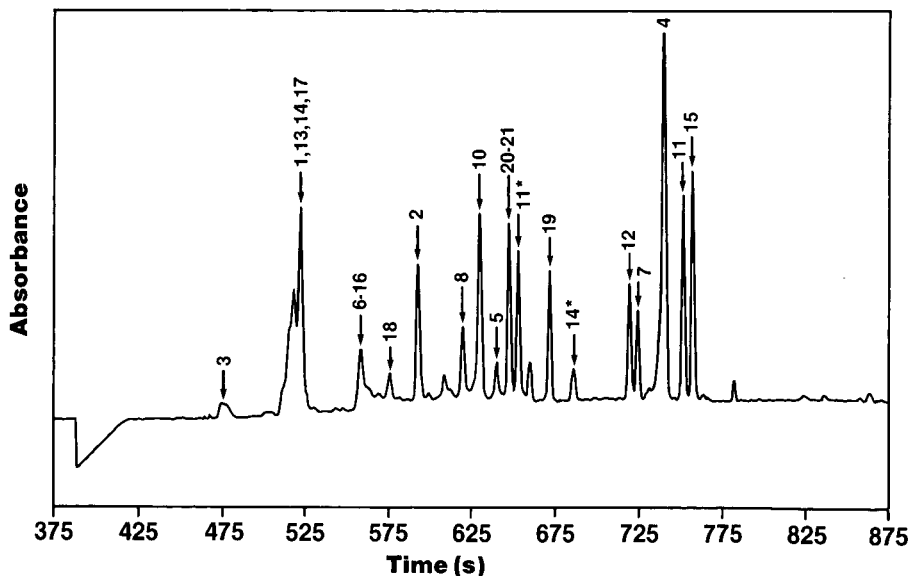


Fig. 8. Electropherogram of hGH digest in pH 8.1 tricine buffer, 0.1 *M* tricine and 0.02 *M* morpholine (condition N).

ride tended to decrease the resolution, and (4) small concentrations of morpholine improved the resolution.

Comparison of separation strategies

The initial separation at pH 8.0 (0.01 *M* tricine, 0.045 *M* morpholine, and 0.02 *M* sodium chloride) apparently has a high enough buffer capacity (25 mM) and ionic strength (38 mM) with an acceptable morpholine concentration to produce a good separation. However, the optimized separation (condition N, Fig. 8) is better for the mid-range and later eluting peaks with a minimal sacrifice in resolution for the three earliest eluting peaks. In contrast, the optimized separation is much better than the preliminary separation at pH 8.1 obtained in this work (Fig. 2) even though the change in mobile phase composition is relatively minor (replacement of 0.0343 *M* sodium chloride with 0.02 *M* morpholine). The optimized separation also is much better than that at pH 2.4 (Fig. 1), although the latter has not been optimized. Finally, it is important to note that the earlier eluting fragments (fragments 1, 13, 14 and 17) that are poorly resolved in the optimum separation are somewhat better resolved in the pH 8.0 system and are well resolved in the pH 2.4 system (although other peaks overlap).

Complete separation of all of the digest fragments was not achieved by any single elution condition in CZE. However, it appears that if two values of pH are used, then a more complete identification of all species in a complex mixture can be achieved. This is analogous to the use of two-dimensional techniques or coupled chromatographic conditions except that CZE is simpler since only the mobile phase composition needs to be changed. It is important to note that RP-HPLC does not achieve complete resolution of fragments even when a lengthy (1–2 h), complex gradient elution is used^{22,26}. (Fragments 3, 5, 7 and 17 co-elute as do fragments 2 and 19; several other pairs of fragments closely elute.) As noted previously¹¹, CZE is a powerful complement to RP-HPLC for the characterization of the tryptic digest of hGH.

CONCLUSION

Adjustment of the composition of the mobile phase has been demonstrated to be crucial to obtaining optimum efficiency and resolution for the CZE separation of the tryptic digest of hGH. The optimum conditions will be achieved when the interaction of the analyte with the silica can be decoupled from the mobile phase pH so that the pH can be chosen to maximize the differences in charges between the species. A high buffer capacity appears to be one of the most important variables for this approach to succeed. However, mobile phase additives such as morpholine may be important, partly due to the reduction in electroosmotic flow in their presence. It is obvious that there is no simple set of rules that will produce the optimum separation, although a process similar to the one we have followed should be useful. The key variables were identified and the effects of changes in variables were found to be approximately additive.

For the tryptic digest of hGH, a mobile phase composition of 0.1 *M* tricine and 0.02 *M* morpholine at pH 8.1 appears to be optimum. This separation is slightly better overall than our previously reported data. Fragments that overlap under the optimum separation conditions may be separated by performing a second separation at a different pH.

ACKNOWLEDGEMENTS

We thank Drs. J. W. Jorgenson, R. M. Riggin, G. W. Becker and G. S. Sittampalam for helpful discussions and encouragement. We acknowledge ISCO, for the donation of a detector. We are grateful for the technical assistance given by D. S. LeFeber and P. A. Farb.

REFERENCES

- 1 J. W. Jorgenson, *Anal. Chem.*, 58 (1986) 743A–758A.
- 2 M. J. Gorden, X. Huang, S. L. Pentoney and R. N. Zare, *Science (Washington, D.C.)*, 242 (1988) 224–228.
- 3 S. W. Compton and R. G. Brownlee, *Biotechniques*, 6 (1988) 432–440.
- 4 A. G. Ewing, R. A. Wallingford and T. M. Olefirowicz, *Anal. Chem.*, 61 (1989) 292A–303A.
- 5 J. W. Jorgenson and K. D. Lukacs, *Science (Washington, D.C.)*, 222 (1983) 266–272.
- 6 H. H. Lauer and D. McManigill, *Anal. Chem.*, 58 (1986) 166–170.
- 7 J. J. Kirkland and R. M. McCormick, *Chromatographia*, 24 (1987) 58–76.
- 8 R. M. McCormick, *Anal. Chem.*, 60 (1988) 2322–2328.
- 9 P. D. Grossman, J. C. Colburn, H. H. Lauer, R. G. Nielsen, R. M. Riggin, G. S. Sittampalam and E. C. Rickard, *Anal. Chem.*, 61 (1989) 1186–1194.
- 10 R. G. Nielsen, G. S. Sittampalam and E. C. Rickard, *Anal. Biochem.*, 177 (1989) 20–26.
- 11 R. G. Nielsen, R. M. Riggin and E. C. Rickard, *J. Chromatogr.*, 480 (1989) 393–401.
- 12 J. Frenz, S. Wu and W. S. Hancock, *J. Chromatogr.*, 480 (1989), 379–391.
- 13 P. D. Grossman, K. J. Wilson, G. Petrie and H. H. Lauer, *Anal. Biochem.*, 173 (1988) 265–270.
- 14 P. D. Grossman, J. C. Colburn and H. H. Lauer, *Anal. Biochem.*, 179 (1989) 28–33.
- 15 J. W. Jorgenson, in J. W. Jorgenson and M. Phillips (Editors), *New Directions in Electrophoretic Methods*, (ACS Symposium Series, Vol. 335), American Chemical Society, Washington, DC, 1987, Ch. 13.
- 16 H. H. Lauer and D. McManigill, *Trends Anal. Chem.*, 5 (1986) 11–15.
- 17 X. Huang, W. F. Coleman and R. N. Zare, *J. Chromatogr.*, 480 (1989) 95–110.
- 18 G. O. Roberts, P. H. Rhodes and R. S. Snyder, *J. Chromatogr.*, 480 (1989) 35–67.
- 19 T. S. Stevens and H. J. Cortes, *Anal. Chem.*, 55 (1983) 1365–1370.
- 20 E. Grushka, R. M. McCormick and J. J. Kirkland, *Anal. Chem.*, 61 (1989) 241–246.
- 21 J. W. Jorgenson and K. D. Lukacs, *Anal. Chem.*, 53 (1981) 1298–1302.
- 22 G. W. Becker, P. M. Tackitt, W. W. Bromer, D. S. LeFeber and R. M. Riggin, *Biotechnol. Appl. Biochem.*, 10 (1988) 326–337.
- 23 H. A. Laitinen, *Chemical Analysis*, McGraw-Hill, New York, 1960, Ch. 3.
- 24 R. A. Mosher, D. Dewey, W. Thormann, D. A. Saville and M. Bier, *Anal. Chem.*, 61 (1989) 362–366.
- 25 M. M. Bushey and J. W. Jorgenson, *J. Chromatogr.*, 480 (1989) 301–310.
- 26 E. Conova-Davis, R. C. Chloupek, I. P. Baldonado, J. E. Battersby, M. W. Spellman, L. J. Basa, B. O'Connor, R. Pearlman, C. Quan, J. A. Chakel, J. T. Stults and W. S. Hancock, *Am. Biotechnol. Lab.*, 6 (May) (1988) 8–17.
- 27 B. Skoog and A. Wichman, *Trends Anal. Chem.*, 5 (1986) 82–83.
- 28 J. L. Meek and Z. L. Rossetti, *J. Chromatogr.*, 211 (1981) 15–28.

Use of high-performance capillary electrophoresis to monitor charge heterogeneity in recombinant-DNA derived proteins

SHIAW-LIN WU, GLEN TESHIMA, JERRY CACIA and WILLIAM S. HANCOCK*

Genentech, Inc., Medicinal and Analytical Chemistry, 460 Point San Bruno Boulevard, South San Francisco, CA 94080 (U.S.A.)

ABSTRACT

The separation of charge variants of recombinant DNA-derived (rDNA) proteins by high-performance capillary electrophoresis (HPCE) has been explored with the following examples: human growth hormone (rhGH), a soluble form of a T4 receptor protein (rCD4) and tissue plasminogen activator (rt-PA). The separation of rhGH and deamidated variants were examined over the range of low pH (<2.5) to high pH (8.0) on a coated silica capillary. No resolution was observed at pH 2.5 while at pH values of 6.5 or greater the deamidated species were separated. At pH 3.5 the variant was partially resolved but no detector signal was observed at pH 4.5 and 5.0. HPCE was also used to monitor a glycoprotein (rt-PA) with charge heterogeneity presumably due to variable sialic acid content. At a pH value of 4.5, the charge heterogeneity was only observed as peak broadening. For rCD4 multiple peaks were observed at pH 5.5 but no signal was observed at pH 6.5 or above (the pI of rCD4 is 8). These results suggest that HPCE will prove to be a valuable technique for the analysis of charged variants present in rDNA products either as a consequence of natural microheterogeneity or due to degradative processes such as deamidation.

INTRODUCTION

Recently high-performance capillary zone electrophoresis (HPCE) has been applied to the analysis of polypeptide samples^{1–6}. While most of the applications have been directed at peptide samples several examples of protein separations have been reported such as adrenocorticotropin (ACTH)², ribonuclease A⁶, insulin⁶, growth hormone^{4–6}, transferrin² and albumin⁴. With the advent of protein pharmaceuticals produced by recombinant-DNA (rDNA) technology there has been a resurgence in analytical protein chemistry. The early potential of HPCE in this field has been demonstrated with the successful analysis of biosynthetic human growth hormone (rhGH)^{5–7}. HPCE has considerable potential to monitor charged variants of proteins as shown by the separation of deamidated rhGH^{5,6}, deamidated insulin⁶ and human transferrin isoforms³. Since HPCE has significant potential in drug development with applications as diverse as fermentation control to stability monitoring,

we decided to further investigate the separation of charged variants at different pH values. Deamidation has been chosen as an example of charge heterogeneity caused by degradative reactions, while sialic acid isoforms was used as illustrative of carbohydrate microheterogeneity. The rDNA-derived proteins included in this study range from a non-glycosylated protein (rhGH, mol.wt. 22 000 dalton) to a glycoprotein of moderate complexity (soluble human CD4, mol.wt. 40 000 dalton) to a glycoprotein of considerable microheterogeneity tissue plasminogen activator (rt-PA, mol.wt. 66 000 dalton). The separations were carried out on a coated capillary that is commercially available and the importance of pH on both the recovery and resolution of the charged variants was investigated.

METHODS

Capillary zone electrophoresis

All capillary electrophoresis was performed using the HPE 100 high-performance capillary electrophoresis system from Bio-Rad Labs. The capillaries used were enclosed in cartridges and coated on their internal surfaces with a covalently bonded linear polymer, significantly reducing both adsorption and electroosmosis⁴. The cartridges used were 20 cm × 25 μ m I.D.

Free zone capillary electrophoresis was carried out with the polarity of the internal power supply of the instrument set such that the sample components would migrate toward the detector, *i.e.*, the cathode was at the detector end of the capillary for the lower pH runs (*e.g.*, pH 2.5 for rhGH), and at the inlet end for the higher pH runs (*e.g.*, pH 6.5 for rhGH). At the start of an analysis the capillary and the electrode reservoir at the detector end of the capillary were filled with phosphate buffer, and the inlet-side electrode reservoir was flushed with distilled water. A 10- μ l volume of the sample solution (0.5 to 1.0 mg/ml) with an ionic strength approximately one-tenth that of the electrophoresis buffer was then placed by syringe into the reservoir just ahead of the inlet of the capillary. The power supply was turned on, and the sample electrophoresed into the capillary for 5 s at 8 kV. The inlet electrode reservoir was then flushed with the electrophoresis buffer, and the power supply turned back on at a constant voltage of 8 or 12 kV. Electropherograms were made by monitoring absorbance at 200 nm. Following a run, the capillary was flushed with buffer to remove uneluted components. Samples isolated from ion exchange chromatography were diluted 1:5 or 1:10 with distilled water depending on the ionic strength of the sample. Each analysis was performed a minimum of five times to demonstrate a reproducible electropherogram.

RESULTS

Fig. 1 shows the effect of pH on the separation of deamidated variants of rhGH. The sample used in this study contained approximately 10% deamidated material resulting from an incubation of rhGH in 10 mM sodium phosphate, pH 7.4 for 2 weeks at 4°C. The identification of the species observed in the HPCE separation was achieved by injection of standards isolated from ion-exchange chromatography (IEX)⁵. At pH 2.5 no separation was observed (A), while at pH 3.5 (B) the deamidated species was partially resolved as a shoulder (at approximately 4.5 min). No peaks

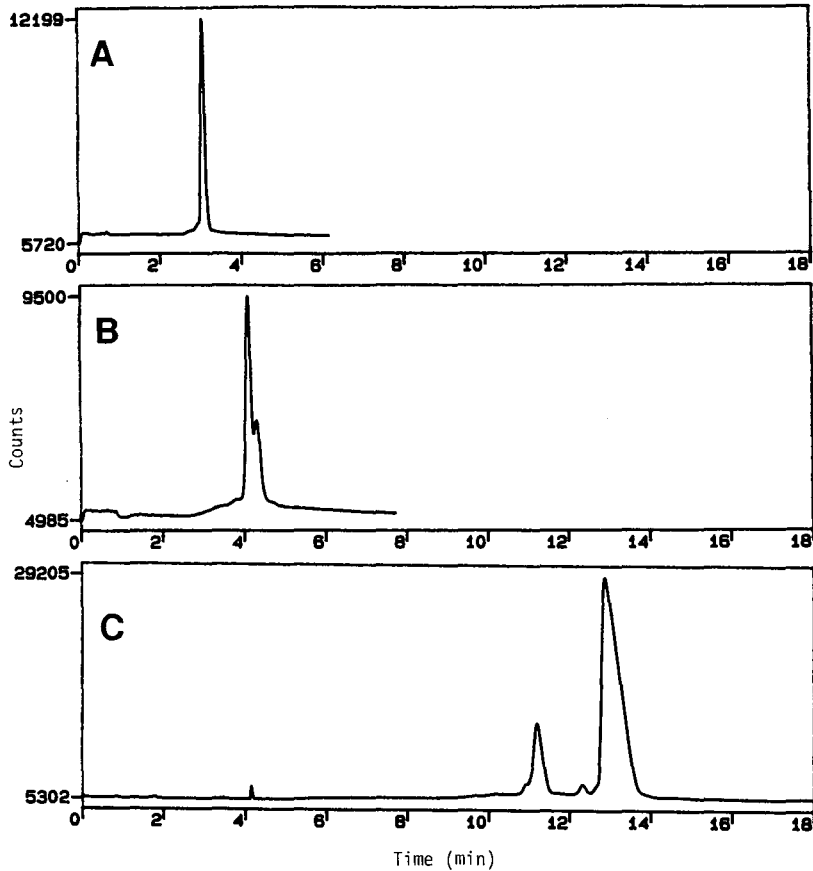


Fig. 1. Effect of pH on the separation of charged variants in degraded rhGH. The separation was carried out on a Bio-Rad coated silica capillary column (20 cm \times 25 μ m) at 8 kV using the conditions described in the Methods section. The earlier eluted fraction at pH 6.5 or later eluted fraction at pH 3.5 was identified as deamidated material. The pH conditions were 2.5 (A), 3.5 (B), and 6.5 (C). rhGH concentration 0.5 μ g/ μ l.

were observed when the separation was run at pH 4.5 or 5.5 (data not shown). In Fig. 1C at pH 6.5 the deamidated species was well resolved from native material (11.3 vs. 13.5 min). The reversal in migration order was caused by reversal in polarity of the capillary system to compensate for change in charge of the protein from a cationic to an anionic species at pH values above the *pI* of the protein.

Fig. 2 shows the effect of pH on the separation of charged variants of a highly purified sample of rCD4 (ref. 8). At pH 2.5 (A) only a single peak was observed, while at pH 3.5 (B) partial resolution was observed. The charged variants were well resolved at pH 4.5 (C) and almost baseline resolved at pH 5.5 (D). No signals were observed for separations carried out at pH 6.5 and above. Fig. 3 shows the results of analysis of the charge heterogeneity of rCD4 by HPCE after removal of sialic acid with neuraminidase⁹.

Fig. 4 shows the analysis of a sample of rt-PA by HPCE (A) and of a sample

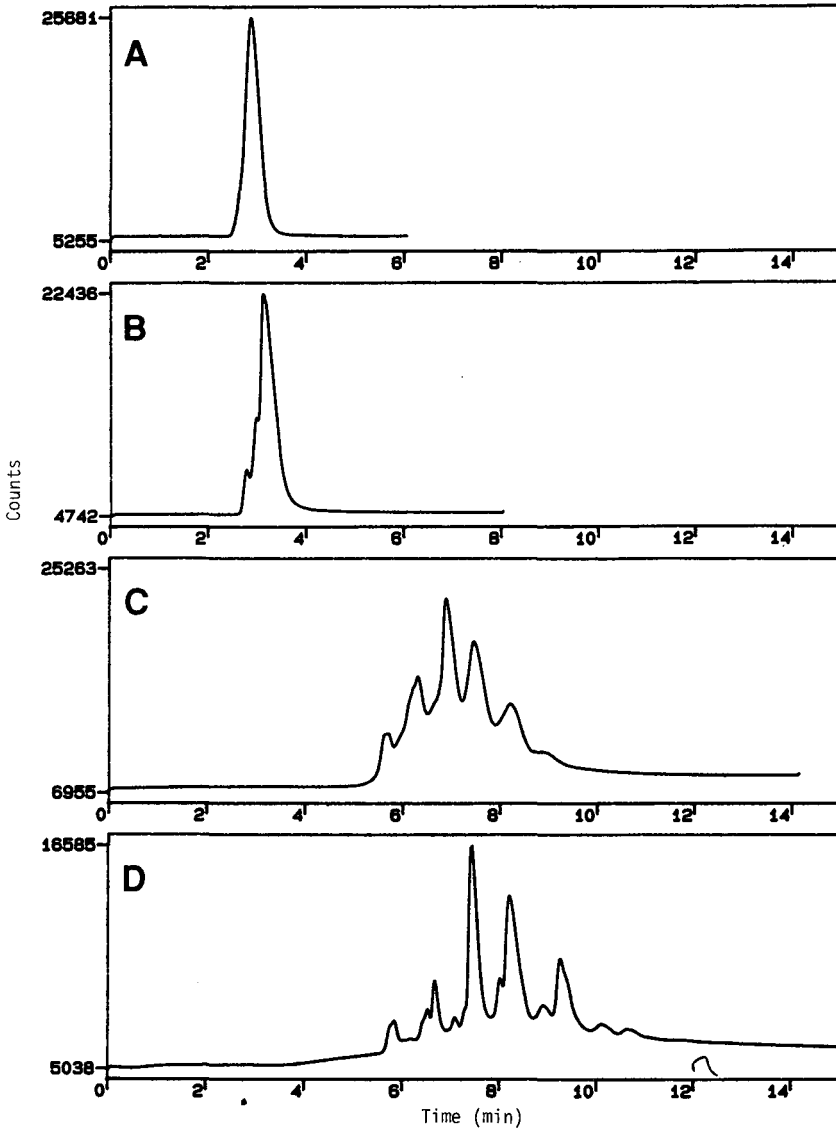


Fig. 2. Effect of pH on the separation of charged variants of rCD4. The separation was carried out on a Bio-Rad coated silica capillary column (20 cm \times 25 μ m) at 12 kV using the conditions described in the Methods section. The pH conditions were 2.5 (A), 3.5 (B), 4.5 (C) and 5.5 (D). rCD4 concentration was 0.5 μ g/ μ l.

after removal of sialic acid residues with the enzyme neuraminidase⁹ (B). The early eluting peak (2.5 min) was shown to be excipient related by a blank run (data not shown). Fig. 4B shows a much sharper peak profile which can be attributed to removal of the extensive charge heterogeneity due to the sialic acids.

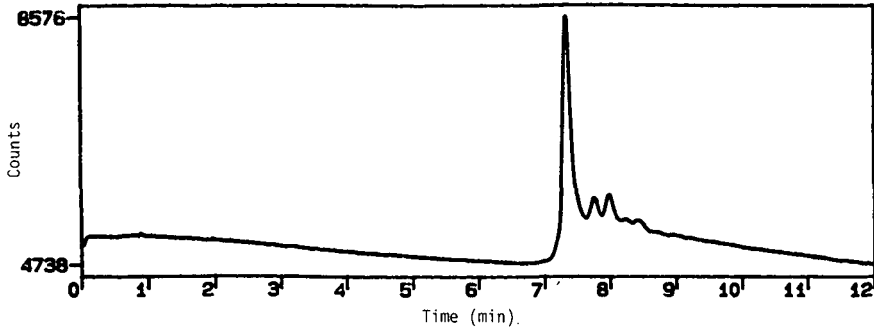


Fig. 3. The effect of sialic acid removal (neuraminidase treatment) on the electrophoretic pattern observed for rCD4. The analysis of rCD4 on the Bio-Rad coated capillary column (20 cm \times 25 μ m) was at 12 kV and at pH 4.5.

DISCUSSION

A major degradative pathway of recombinant DNA-derived human growth hormone (rhGH) has been identified as deamidation¹⁰. The site of deamidation was identified as asparagine (residue 149) which is converted to an aspartic acid (Asp). Since Asp has a pK_a of approximately 4.0 when incorporated into a polypeptide chain, we would expect that use of a buffer with a pH above this value would allow a

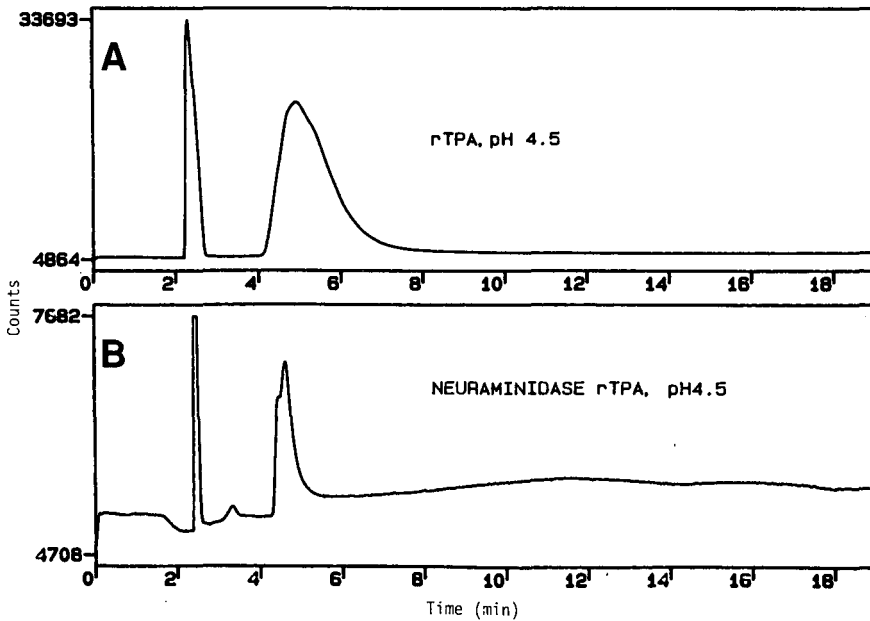


Fig. 4. The analysis of rt-PA by a Bio-Rad coated silica capillary column (20 cm \times 2.5 μ m) at 12 kV and pH 4.5 (A). (B) Analysis of a sample of rt-PA that has been treated with neuraminidase. rt-PA concentration was 1 μ g/ μ l.

TABLE I
MOLECULAR WEIGHT HETEROGENEITY OF rt-PA

These molecular weight values were calculated from a recent study (see ref. 9).

		<i>Molecular weight</i>
Amino acid residues		59 008
Carbohydrates		
Amino acid residue ^a		
117	(Type of glycan: high mannose)	1200–1600
184	(Type of glycan: complex)	2000–3600
448	(Type of glycan: complex)	2000–3600
Type I (three carbohydrate chains)	Total mol.wt. of rt-PA variants:	64 000–68 000
Type II (two carbohydrate chains)	Total mol.wt. of rt-PA variants:	62 000–64 000

^a Site of attachment of carbohydrate chain.

charge-based separation. However, the *pI* of rhGH and the presence of any free silanols on the walls of the capillary are important considerations in developing the HPCE separation. Previously the effect of pH on the analysis of rhGH by IEX was studied and the separation of charged variants was shown to be dependent on subtle changes in pH¹¹. In the HPCE separation the use of pH values below the pK_a value of Asp resulted in little separation of the deamidated variant. No peaks were detected at pH 4.5 and pH 5.5 and since the *pI* of rhGH is 5.0, this negative result could be attributed to lack of migration or loss of sample due to adsorption on the walls of the capillary. This separation was carried out on a coated capillary, however, such a coating does not completely inactivate reactive silanols and protein adsorption is possible, particularly under conditions where sample aggregation is promoted by an isoionic species¹². At pH values substantially above the *pI* of the sample and pK_a of the silanol groups, for example pH 6.5, both aggregation of the sample and protein/wall interactions are minimized due to charge repulsion and excellent separations were achieved (Fig. 1C). The rapid electrophoretic separation of variants produced by a major degradative pathway of rhGH illustrate the potential of HPCE in monitoring of the stability of protein pharmaceuticals. Such monitoring can have significant applications in areas of biotechnology such as quality control testing, formulation development and optimization of the fermentation process.

The recent introduction of large scale mammalian cell culture has allowed the production of rDNA derived glycoproteins as potential therapeutic agents¹³. However, the presence of sialic acid on the complex-type oligosaccharides introduces considerable charge as well as mass heterogeneity into the product. Table I lists the sites of N-linked glycosylation of rt-PA as residues 117, 184 and 448 with the two latter sites consisting of bi-, tri- and tetraantennary structures that contain sialic acid. Residue 184 is an optional glycosylation site and approximately 50% of the molecules contain two instead of three carbohydrate chains. This heterogeneity in addition to the microheterogeneity of each of the carbohydrate chains results in rt-PA containing a range of isoforms ranging in molecular weight from approximately 64 000 to 68 000 dalton. In Fig. 4A it can be seen that HPCE is unable to separate these isoforms and

a broad peak is observed. The type I variant (see Table I) was found to migrate at the front part of the broad peak, while the type II variant was concentrated at the back of the peak (data not shown). A 1:1 mixture of the two variants gave same profile as seen in Fig. 4A. However, removal of sialic acids by treatment of rt-PA with neuraminidase resulted in significant sharpening of the peak (Fig. 4B). This result might suggest that much of the peak broadening was caused by charge heterogeneity in the N-linked oligosaccharides. However an empirical relationship between electrophoretic mobility and molecular weight was reported⁴ and extended to the tryptic peptides of rhGH⁵. In a separate study Grossman *et al.*⁶ related mobility to molecular size of proteins. Thus it is likely that the molecular weight heterogeneity of rt-PA also contributes to the broad peak observed in Fig. 4A.

Despite a relatively high isoelectric point of rt-PA (in the range of 7.0 to 8.0) it was not possible to analyze samples above pH 4.5. This behavior parallels previous experience with reserved-phase HPLC on both silica and polymer based supports where we found that rt-PA could not be eluted from the column at pH values above 4.0¹⁴. In this study we used a coated capillary in an effort to reduce interactions between the sample and the capillary wall. Other authors have investigated a variety of approaches to minimize this problem such as the use of alkali metal salts¹⁵ zwitterionic reagents¹⁶, protein denaturants⁴, putrescine¹⁷ and the use of other coatings¹⁸ in an attempt to improve both peak shapes and recoveries. Currently we are investigating the use of zwitterionic reagents and detergents in an effort to improve this separation. It has been reported that temperature gradients can severely reduce separation efficiencies¹⁹. In this study we used unthermostatted capillaries although the use of small diameters (25 μm) and low voltages minimized this potential problem⁴.

CD4 is a glycoprotein expressed on the surface of a variety of cells of the immune system and binding of gp 120 to CD4 mediates the infectivity of the HIV virus²⁰. Recombinant soluble CD4 (rCD4) is a truncated form of human CD4 that is secreted from transfected Chinese hamster ovary cells. This 368-amino acid glycoprotein contains two potential sites of N-linked glycosylation (Asn-271 and Asn-300^{8,21}). The first site contains complex-type oligosaccharides, while Asn-300 has attached high-mannose or hybrid structures in addition to complex-type oligosaccharides. It was decided to investigate the potential of HPCE to monitor the charge variants of rCD4 due to variable sialic acid content. Since the sialic acid group has a pK_a value of 3.5 to 4.5 the effect of a range of pH values on the separation was investigated. From the results shown in Fig. 2A–D it can be seen that the optimal separation of rCD4 is around pH 5.5. The improved resolution observed for the charged variants of rCD4 relative to that of rt-PA may be related to the lower degree of sialylation with rCD4⁸ as well as less molecular weight heterogeneity as rCD4 unlike rt-PA does not contain an optional glycosylation site. No signals were detected at pH 6.5 or above. Since the pI of CD4 is approximately 8.0, the loss of sample may be associated with protein adsorption on the capillary wall. As was observed in the analysis of rt-PA, sample loss can occur at pH values well below the isoelectric point. Fig. 3 shows the analysis of a sample of rCD4 that has been treated with neuraminidase to remove sialic acid. As in the case of rt-PA, the electropherogram of rCD4 is significantly sharpened (compare Fig. 3 with Fig. 2C) and indicates that much of the charge heterogeneity is due to sialic acid microheterogeneity.

In conclusion, HPCE has been shown to be a valuable new analytical method

for the monitoring of charged variants that can occur during the production of a biosynthetic protein pharmaceutical. However the pH studies indicate that a successful electrophoretic analysis requires careful optimization of the separation conditions.

ACKNOWLEDGEMENTS

We wish to express our gratitude to Dr. M. Spellman and T. Gregory for the CD4 samples, Mr. A Guzetta for neuraminidase digested samples and Mr. Roger Tim and Dr. M. D. Zhu (Bio-Rad) for assistance in developing the HPCE conditions. Finally, we would like to thank our colleagues Dr. John O'Connor, John Frenz, Eleanor Canova-Davis, Mike Spellman and Matt Field for valuable scientific discussions.

REFERENCES

- 1 A. S. Cohen and B. L. Karger, *J. Chromatogr.*, 397 (1987) 409.
- 2 A. Guttman, A. Paulus, A. S. Cohen, B. L. Karger, H. Rodriguez and W. S. Hancock, in *Electrophoresis* 88, 1988, pp. 151–160.
- 3 F. Kilar and S. Hjertén, *J. Chromatogr.*, 480 (1989) 351.
- 4 M. Zhu, D. L. Hansen, S. Burd and F. Gannon, *J. Chromatogr.*, 480 (1989) 311.
- 5 J. Frenz, S.-L. Wu and W. S. Hancock, *J. Chromatogr.*, 480 (1989) 379.
- 6 P. D. Grossman, J. C. Colburn, H. H. Lauer, R. G. Nielsen, R. M. Riggan and E. C. Rickard, *Anal. Chem.*, 61 (1989) 1186.
- 7 R. G. Nielsen, R. M. Riggan and E. C. Rickard, *J. Chromatogr.*, 480 (1989) 393.
- 8 R. J. Harris, S. M. Chamow, T. J. Gregory and M. W. Spellman, *Eur. J. Biochem.*, 188 (1990) 291.
- 9 M. W. Spellman, L. J. Basa, C. K. Leonard, J. A. Chakel, J. V. O'Connor, S. Wilson and H. VanHalbeek, *J. Biol. Chem.*, 264 (1989) 14100.
- 10 W. S. Hancock, E. Canova-Davis, R. C. Chloupek, S.-L. Wu, I. P. Baldonado, J. E. Battersby, M. W. Spellman, L. J. Basa and J. A. Chakel, in J. L. Gueriguian, V. Fattorusso and D. Poggiolini *Therapeutic Peptides and Proteins: Assessing the New Technologies, Banbury Report 29*, Cold Spring Harbor Laboratory, Cold Spring Harbor, 1988, pp. 95–117.
- 11 G. Teshima, S.-L. Wu, W. Henzel and W. S. Hancock, Presented at *9th International Symposium on HPLC of Proteins, Peptides and Polynucleotides, Philadelphia, PA, November 6–8, 1989*, poster No. 210.
- 12 A. Sillero and J. M. Ribeiro, *Anal. Biochem.*, 179 (1989) 319.
- 13 S. E. Builder and E. Grossbard, in *Transfusion Medicine: Recent Technological Advances*, 1986, pp. 303–313.
- 14 S.-L. Wu, G. Teshima, J. Cacia and W. S. Hancock, in preparation.
- 15 J. S. Green and J. W. Jorgensen, *J. Chromatogr.*, 478 (1989) 63.
- 16 M. M. Bushey and J. W. Jorgensen, *J. Chromatogr.*, 480 (1989) 301.
- 17 F. S. Stover, B. L. Haymore and R. J. McBeath, *J. Chromatogr.*, 470 (1989) 241.
- 18 G. J. M. Bruin, R. Huisden, J. C. Kraak and H. Poppe, *J. Chromatogr.*, 480 (1989) 339.
- 19 S. Hjertén, *Chromatogr. Rev.*, 9 (1967) 122.
- 20 A. G. Dalgleish, P. C. L. Beverley, P. R. Clapham, D. H. Crawford, M. F. Greaves and R. A. Weiss, *Nature (London)*, 312 (1984) 763.
- 21 D. H. Smith, R. A. Byrn, S. A. Marsters, T. Gregory, J. E. Groopman and D. J. Capon, *Science (Washington, D.C.)*, 238 (1987) 1704.

Capillary electrophoresis of proteins under alkaline conditions

MINGDE ZHU, ROBERTO RODRIGUEZ, DAVE HANSEN and TIM WEHR*
Bio-Rad Laboratories, 3300 Regatta Boulevard, Richmond, CA 94804 (U.S.A.)

ABSTRACT

Successful separations of proteins by capillary electrophoresis in uncoated fused-silica capillaries is limited by adsorption and variable rates of electroendosmosis, which can compromise quantitative accuracy and precision. Operation at extremes of pH to minimize these problems is useful in special cases but is not a general strategy for protein separations. Three alternative strategies are described: use of capillaries coated with a linear hydrophilic polymer, the use of acidic solutions to wash the capillary between runs, and the incorporation of additives into the electrophoresis buffer to minimize adsorption during analysis. Applications of these techniques to protein samples is demonstrated.

INTRODUCTION

Migration in capillary electrophoresis is governed primarily by solute charge, so manipulation of the electrophoresis buffer pH is the most direct strategy in optimizing a separation¹. However, performing free zone separations at elevated pH values can introduce two complications in achieving good resolution and quantitative detector response. First, the increased rate of electroendosmosis can adversely effect resolution and reproducibility. Second, solute adsorption can cause poor peak shape, reduced response, and in worst cases, no elution. Adsorption is a particularly serious problem in the case of proteins because of the multiplicity of polar, charged, and hydrophobic sites on the molecular surface². Acceptable protein separations are typically more difficult to achieve compared to peptides and small molecules. Loss of protein due to adsorption can prevent accurate quantitation, particularly at low sample concentrations. In addition, protein adsorption can change the capillary surface characteristics, affecting results in subsequent runs. When electroendosmosis is used as a transport mechanism during loading and separation, the magnitude of electroendosmosis can drift as the capillary surface is modified by adsorption. Consequently, reproducibility of both migration times and peak areas could be reduced in repetitive analysis of complex mixtures.

A number of strategies have been adopted to minimize problems caused by electroendosmosis and adsorption. First, to achieve good resolution in the presence of

high rates of osmotic flow, long capillaries are typically used. Unfortunately, the increased surface area of the longer tube exacerbates the problem of adsorption. Second, separations can be performed at pH values where electroendosmosis and adsorption are minimized³⁻⁵. At pH values below 3 where silanols are fully protonated, both osmotic flow and electrostatic interactions with proteinaceous solutes are reduced. Although some proteins can be separated at low pH, many proteins aggregate and precipitate under acidic conditions, or there may be insufficient difference in their mass-to-charge ratios to achieve good separation. At pH values above 9, it is assumed that both proteins and the silica surface exhibit high negative charge density, and adsorption through electrostatic interaction should be reduced. Unfortunately, some basic amino acid side chains are partially protonated at high pH so some proteins can adsorb, and very high rates of osmotic flow under these conditions may reduce resolution.

Three alternative strategies to minimize adsorption and osmotic flow are the use of coated capillaries, the use of wash solutions to purge the capillary between runs, and the incorporation of additives to the electrophoresis buffer. We wish to report results using these approaches for free zone electrophoresis of proteins.

EXPERIMENTAL

Materials

The following proteins were obtained from Sigma (St. Louis, MO, U.S.A.): albumin (bovine), carbonic anhydrase (bovine erythrocytes), a chymotrypsinogen A (bovine pancreas), cytochrome *c* (horse heart), γ -globulins (human), β -lactoglobulin (bovine milk), lysozyme (chicken egg white), myoglobin (horse heart), ribonuclease A (bovine pancreas). Hemoglobin AFSC electrophoresis standard was obtained from Isolab (Akron, OH, U.S.A.) Methylcellulose (4000 cP at 25°C for 2% solution) was obtained from Sigma. Triton X-100 reduced was obtained from Aldrich (Milwaukee, WI, U.S.A.) Z4A, Z6C, and Z60 are experimental multicomponent mixtures of zwitterionic species.

All capillary electrophoresis was performed using the HPETM-100 high-performance capillary electrophoresis system from Bio-Rad Labs. The capillaries were enclosed in cartridges and, where indicated, were coated on their internal surfaces with a covalently bonded linear polymer. Capillary dimensions were 25 μ m I.D. and 20 cm or 50 cm length. Electropherograms were recorded using a Model 804 PC integrator (Bio-Rad Labs.).

Methods

To study the effect of electrophoresis buffers, wash procedures, and sample type on non-specific adsorption, we have used a flow injection procedure in which sample was introduced into the capillary by vacuum displacement and the amount of protein in the capillary or adsorbed onto the tube wall was estimated by the UV absorbance at 200 nm. Following an initial prewash of the capillary, buffer was drawn into the capillary and the detector was zeroed. Buffer was then displaced by buffer containing protein, and UV absorbance recorded after 1 min. To measure residual adsorption of protein to the capillary, the tube was then washed with 20 volumes of buffer and remaining UV absorption recorded. To measure the effectiveness of wash solutions,

the protein sample was displaced with 20 tube volumes of wash solution, followed by 20 tube volumes of buffer before recording remaining UV absorbance.

Electroendosmosis was measured by filling the capillary with a 0.05 *M* sodium borate buffer (pH 9) and placing 0.2 *M* sodium borate buffer (pH 9) in the inlet and outlet reservoirs of the instrument. When voltage is applied using positive-to-negative polarity, electroendosmosis will sweep buffer ions into the tube and monitored current will double at the time when 67% of the tube volume is filled with concentrated buffer; we define this as the osmosis time. This method is simple in that a UV detector is not required, and we use it for assessing coating chemistries and for monitoring capillary lifetime.

RESULTS AND DISCUSSION

Protein adsorption on an uncoated fused-silica capillary is illustrated in Fig. 1. Myoglobin (*pI* 7.0) and serum albumin (*pI* 4.8) were separated under alkaline conditions using an uncoated capillary. At low sample concentration, response for the more basic protein is severely reduced, demonstrating that loss of protein due to

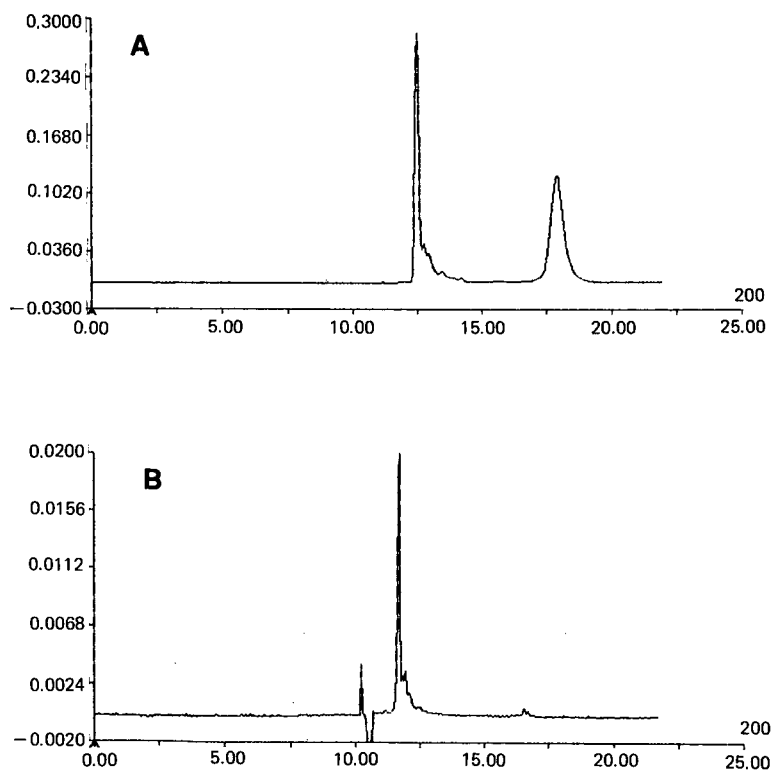


Fig. 1. Protein adsorption on a fused-silica capillary. Electrophoresis was performed in a 50 cm \times 50 μ m I.D. uncoated capillary at 8 kV using a 0.1 *M* sodium phosphate buffer (pH 8). Bovine serum albumin (first peak) and horse heart myoglobin (second peak) were prepared in 0.01 *M* sodium phosphate (pH 8.0) at (A) 5 mg/ml and (B) 0.5 mg/ml. Ordinate-axis values indicate absorbance at 200 nm. Retention times in min.

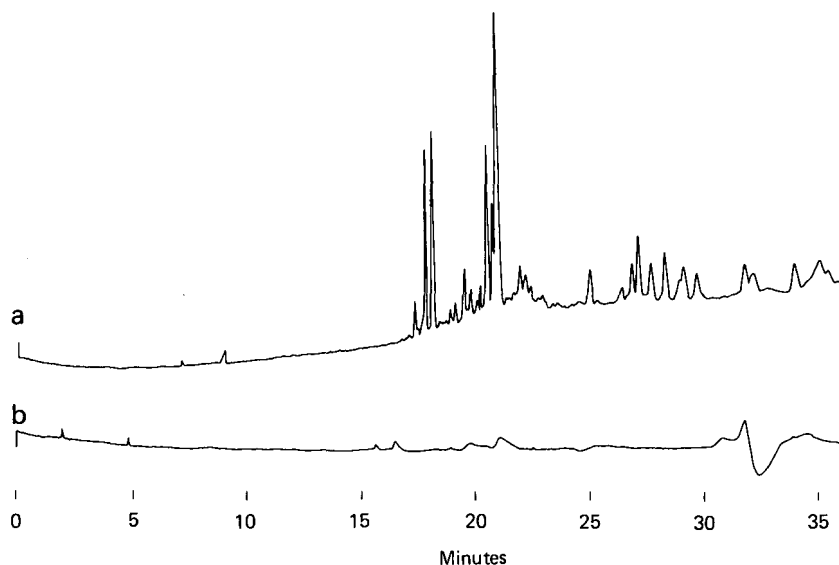


Fig. 2. Separation of a tryptic digest of bovine serum albumin on (a) coated and (b) uncoated 50 cm \times 50 μ m I.D. capillaries. Albumin (1 mg/ml) was digested with trypsin for 4 h at 37°C in 10 mM Tris chloride (pH 8). Electrophoresis was performed in 0.1 M potassium borate (pH 8.5)–0.2% methylcellulose–Z60 at 8 kV. Detection was at 200 nm. (a) Negative to positive polarity; (b) positive to negative polarity.

adsorption can prevent accurate quantitation. Protein adsorption will also reduce the rate of electroendosmosis from 10.83 cm/min for a fresh 50 cm \times 50 μ m I.D. uncoated capillary to 2.76 cm/min for a capillary washed with 10 mg/ml cytochrome *c* in 0.1 M phosphate buffer (pH 8), suggesting that quantitative precision can be compromised by a drift in the electroendosmotic flow during analysis of protein-containing samples. The problems of adsorption and variable electroendosmosis should be minimized using coated capillaries.

The use of polymer-coated tubes for capillary electrophoresis was first described by Hjertén⁶, who demonstrated that a linear hydrophilic polymer attached to the

TABLE I

NON-SPECIFIC ADSORPTION OF HEMOGLOBIN TO AN UNCOATED CAPILLARY

50 cm \times 50 μ m I.D. uncoated capillary; column B, capillary prewashed before introduction of 10 mg/ml hemoglobin with 20 mM sodium hydroxide; column A, capillary prewashed with 0.1 M phosphate (pH 2.5).

Testing buffer	Hemoglobin absorbance (mAU, 200 nm)	Remaining absorbance (mAU, 200 nm)	
		B	A
0.1 M boric (pH 9.0)	668	3.5	2.5
0.1 M phosphate (pH 7.0)	654	9.5	9.5
0.1 M acetate (pH 4.8)	658	30.5	7.5
0.1 M phosphate (pH 2.5)	666	0	0

capillary surface reduced electroendosmosis. His patented procedure employs linear polyacrylamide as the coating; we have modified this procedure to produce a coating which exhibits enhanced stability at alkaline pH. As seen in Fig. 2, a capillary coated with this technique exhibits good performance in electrophoresis of a tryptic digest of bovine serum albumin using tris-borate buffer at pH 8.3. Under the same conditions most of the peptide components are strongly adsorbed to the capillary surface when an uncoated tube is used. In addition to reducing solute adsorption, it can be shown that coating the capillary greatly diminishes electroendosmosis. This permits separations to be performed in short capillaries with low total voltages. Coated capillaries typically exhibit a 40-fold reduction in electroendosmosis, *viz.* 0.25 cm/min for a coated capillary and 10.0 cm/min for an uncoated capillary at the following conditions: 20 × 25 μ m I.D. capillary; 0.1 M borate buffer (pH 8.5); 400 V/cm.

Run-to-run reproducibility of migration time and peak area should be improved by washing the capillary between analyses to remove adsorbed protein. We have used the flow injection technique to evaluate between-run wash procedures. In Table I, non-specific adsorption of hemoglobin to an uncoated capillary is compared for acidic or basic prewash solutions and for hemoglobin solutions prepared in different test buffers (hemoglobin was purged from the capillary with 20 tube volumes of test buffer prior to reading residual absorbance). Non-specific adsorption was observed for hemoglobin prepared in pH 4.8, pH 7 and pH 9 buffers, but not for hemoglobin prepared in pH 2.5 phosphate buffer. Also, prewashing the capillary with pH 2.5 phosphate buffer reduced non-specific adsorption in two cases (hemoglobin in pH 4.8 and pH 9 test buffers). Table II summarizes the results for a similar experiment using a coated capillary. In all cases using coated capillaries, non-specific adsorption was reduced. Note that prewashing the tube with pH 2.5 phosphate was more effective than base (as observed for the uncoated tube) for hemoglobin in pH 4.8 and pH 9 buffers but the opposite was seen for hemoglobin in pH 7 buffer. These results indicate that prewashing the tube with acidic phosphate is generally more effective than base prewashes in preventing adsorption of hemoglobin to the capillary wall.

The use of additives to the electrophoresis buffer has been suggested for reducing protein adsorption^{7,8}. The effect of different test buffer additives on non-specific adsorption is shown in Table III. For this study, hemoglobin was prepared in pH 4.8

TABLE II

NON-SPECIFIC ADSORPTION OF HEMOGLOBIN TO A COATED CAPILLARY

50 cm × 50 μ m I.D. coated capillary; column B, capillary prewashed before introduction of 10 mg/ml hemoglobin with 20 mM sodium hydroxide; column A, capillary prewashed with 0.1 M phosphate (pH 2.5).

Testing buffer	Hemoglobin absorbance (mAU, 200 nm)	Remaining absorbance (mAU, 200 nm)	
		B	A
0.1 M boric (pH 9.0)	598	1.5	0.1
0.1 M phosphate (pH 7.0)	597	3.5	6.5
0.1 M acetate (pH 4.8)	562	26.5	6
0.1 M phosphate (pH 2.5)	608	0	0

TABLE III

EFFECT OF BUFFER ADDITIVES ON NON-SPECIFIC ADSORPTION OF HEMOGLOBIN

50 cm \times 50 μ m I.D. capillary; 0.1 M acetate (pH 4.8) buffer supplemented with additives as shown; capillary prewashed with 20 mM sodium hydroxide before introduction of 10 mg/ml hemoglobin.

<i>Additive</i>	<i>Remaining absorbance (mAU at 200 nm)</i>
0.05% Methylcellulose	30.5
0.25% Z60 zwitterion solution	6.0
0.25% Z4A zwitterion solution	29.5
1% Ethylene glycol	27.0
0.05% Triton X-100 R	27.0
None	30.5

acetate buffer supplemented with the different additives; an uncoated tube prewashed with 20 mM sodium hydroxide was used. Only the addition of the Z60 zwitterionic solution significantly reduced non-specific adsorption. This and the observation that detergents or methylcellulose had no effect suggests that non-specific adsorption is due primarily to electrostatic interactions.

Non-specific adsorption of acidic (β -lactoglobulin, *pI* 5.1) and basic proteins (bovine pancreatic α -chymotrypsinogen A, *pI* 9, and horse heart cytochrome *c*, *pI* 9) was investigated using uncoated and coated capillaries (Tables IV and V). Proteins prepared at 10 mg/ml in phosphate buffers ranging in pH from 2 to 10 were introduced into a base-prewashed capillary, then the tube was purged with phosphate buffer of the same pH. This study demonstrates that adsorption was higher for basic proteins as compared to acidic proteins, that adsorption was reduced using a coated capillary, and that adsorption increased for all proteins above pH 4. Capillary wash procedures were also compared for a variety of acidic and basic proteins (Table VI). The data in Table VI indicate that both sodium hydroxide and pH 2.5 phosphate buffer washes are effective in removing adsorbed proteins. However, we have observed that adsorption in subsequent protein injections is higher in base-washed tubes, suggesting that the state of the silica surface following protein removal affects nonspecific adsorption.

The results of these studies demonstrate that most proteins exhibit some degree of non-specific adsorption to capillary walls, and that the level of adsorption is dependent upon the pH of the buffer, the nature of the protein, and the previous history of the tube. Coating the internal surface of the capillary with a linear hydrophilic polymer reduces adsorption. Washing the capillary following a separation is necessary to remove adsorbed protein prior to a subsequent analysis, and acidic phosphate buffers were shown to be most effective in prewash and between-run wash steps. The observations are consistent with the report by McCormick⁵ that phosphate forms complexes with silanols on the silica surface, reducing electroendosmosis and protein-silica interaction. In cases where proteins adsorb to coated capillaries and can not be effectively removed by post-run washes, addition of zwitterionic species to the electrophoresis buffer can reduce adsorption during separation. Using the techniques reported here, we were able to obtain improved results with proteins separated under alkaline conditions (Fig. 3). We observed good reproducibility of peak height, peak

TABLE IV

ADSORPTION OF PROTEINS TO AN UNCOATED CAPILLARY AT DIFFERENT pH VALUES

50 cm \times 50 μ m uncoated capillary; proteins prepared in 0.1 M phosphate buffer at the designated pH; following protein introduction, capillary washed with phosphate buffer of the designated pH.

Protein	Remaining absorbance (mAU at 200 nm)									
	pH 2.0	pH 2.5	pH 3.0	pH 4.0	pH 5.0	pH 6.0	pH 7.0	pH 8.0	pH 9.0	pH 10.0
Chymotrypsinogen	0	0	0	5	11	18	14	11	8	1
Cytochrome <i>c</i>	0	0	0	3	11	24	20	20	15	5
β -Lactoglobulin	0	0	^a	^a	9	8	6	5	3	4

^a Precipitation.

TABLE V

ADSORPTION OF PROTEINS TO A COATED CAPILLARY AT DIFFERENT pH VALUES

50 cm \times 50 μ m coated capillary; proteins prepared in 0.1 M phosphate buffer at the designated pH; following protein introduction, capillary washed with phosphate buffer of the designated pH.

Protein	Remaining absorbance (mAU at 200 nm)									
	pH 2.0	pH 2.5	pH 3.0	pH 4.0	pH 5.0	pH 6.0	pH 7.0	pH 8.0	pH 9.0	pH 10.0
Chymotrypsinogen	0	0	1	0	1	1	1	2	2	4
Cytochrome <i>c</i>	0	0	0	1	2	6	6	6	9	
β -Lactoglobulin	0	0	0	0	2	2	2	3	2	2

TABLE VI

NON-SPECIFIC ADSORPTION UNDER ALKALINE CONDITIONS

50 cm × 50 μm uncoated capillary; proteins prepared at 1.0 mg/ml concentrations in 0.1 M phosphate buffer pH 8; following protein introduction, capillary washed with the designated rinse. Data in mAU.

Proteins	<i>pI</i>	Remaining absorbance (mAU at 200 nm)		
		Washing solution		
		Phosphate <i>pH</i> 8.0	Phosphate <i>pH</i> 2.5	Sodium hydroxide 20 mM
BSA	5.07	0	0	0
β-Lactoglobulin	5.14	7	0	0
Hemoglobin AFSC	6.9–7.41	7	0	0
Horse myoglobin	7.33	14	0	0
Chymotrypsinogen	8.8	11	0	0
Ribonuclease A	8.88	12	0	0
Cytochrome <i>c</i>	9.28	20	0	0
Lysozyme	10–11	10	0	0
Human γ-globulins	^a	21	0	0

^a Wide range.

shape, and migration time for a human red blood cell lysate in 49 consecutive separations using pH 9 borate as the electrophoresis buffer (Fig. 4). We conclude that the combined strategies of using coated capillaries, purging the capillary between runs, and adding zwitterionic species to the electrophoresis buffer can improve performance in capillary electrophoresis of proteinaceous samples.

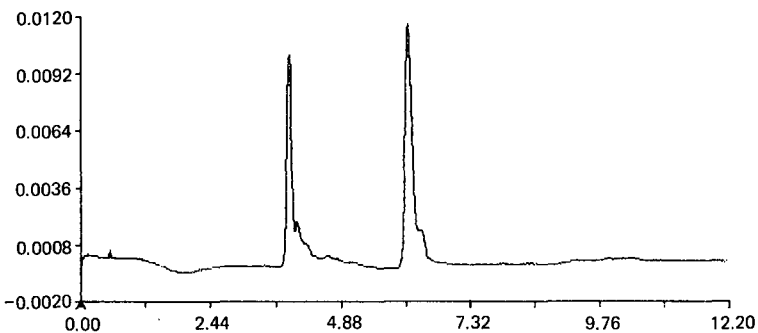


Fig. 3. Separation of cytochrome *c* (*pI* 9.3, first peak) and lysozyme (*pI* 10, second peak). Proteins were prepared at 0.1 mg/ml in a 1:10 dilution of the electrophoresis buffer. Electrophoresis was performed in a 12 cm × 25 μm I.D. coated capillary at 6 kV using a 0.05 M phosphate buffer (pH 8.0)-Z6C. Detection was at 200 nm. Retention times in minutes.

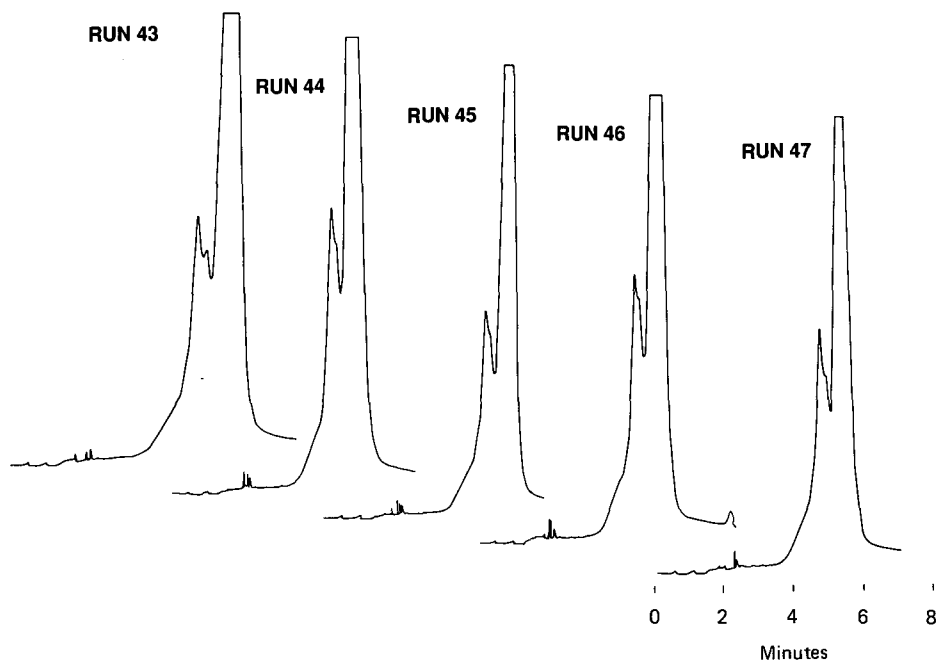


Fig. 4. Repetitive analyses of a human red blood cell lysate. Electrophoresis was performed in a 20 cm \times 25 μ m I.D. coated capillary at 8 kV using a 0.1 M phosphate buffer (pH 9.0)-Z60. Detection was at 200 nm.

REFERENCES

- 1 J. J. Kirkland and R. M. McCormick, *Chromatographia*, 24 (1987) 58.
- 2 J. W. Jorgenson and K. D. Lukacs, *Science (Washington, D.C.)*, 222 (1983) 266.
- 3 H. H. Lauer and D. McManigill, *Anal. Chem.*, 58 (1986) 166.
- 4 Y. Walbroehl and J. W. Jorgenson, *J. Microcolumn Sep.*, 1(1989) 4.
- 5 R. M. McCormick, *Anal. Chem.*, 60 (1988) 2322.
- 6 S. Hjertén, *J. Chromatogr.*, 347 (1985) 191.
- 7 J. S. Green and J. W. Jorgenson, *J. Chromatogr.*, 478 (1989) 63.
- 8 M. M. Bushey and J. W. Jorgenson, *J. Chromatogr.*, 480 (1989) 301.

CHROM. 22 564

Capillary zone electrophoresis for monitoring r-DNA protein purification in multi-compartment electrolyser with immobiline membranes

ELISABETH WENISCH, CHRISTA TAUER, ALOIS JUNGBAUER and HERMANN KATINGER
Institute of Applied Microbiology, University of Agriculture and Forestry, Peter-Jordanstrasse 82, A-1190 Vienna (Austria)

MICHEL FAUPEL

Exploratory Research and Services, Chromatographie Labor, Pharmaceutical Division, Ciba Geigy Ltd., Basle (Switzerland)

and

PIER GIORGIO RIGHETTI*

Department of Biomedical Sciences and Technologies, University of Milan, Via Celoria 2, Milan 20133 (Italy)

ABSTRACT

Isoforms of human monoclonal antibodies against the gp-41 of AIDS virus and of human recombinant superoxide dismutase have been purified to homogeneity by isoelectric focusing (IEF) in a multi-compartment electrolyser with isoelectric, immobiline membranes. This system allows the processing of large sample volumes and gram-scale protein loads and can resolve isoforms as close as 0.001 in *pI* difference. The purification progress was usually monitored by analytical IEF in immobilized pH gradients (IPG). Capillary zone electrophoresis (CZE) was applied to the monitoring of the content of each chamber of the electrolyser. CZE was found to be superior in terms of speed of analysis and quantification (but only by UV reading at 200–210 nm, *i.e.*, in the region of the peptide bond) but, notwithstanding the millions of theoretical plates reported, was no match for the resolving power of IPGs, at least for protein analysis. When compared also with chromatofocusing, the resolving power decreases in the order IPG > CZE \gg chromatofocusing.

INTRODUCTION

Capillary zone electrophoresis (CZE) is rapidly becoming a method with great potential for high-speed and high-sensitivity analysis of biological substances, including proteins produced by recombinant-DNA (r-DNA) techniques and targeted for human consumption as pharmaceuticals. Review papers on CZE have already appeared^{1–3}, and an international meeting has recently been held⁴.

In reality, the CZE technique has been extensively used for producing peptide maps and in general for peptide analysis, as the conditions adopted (typically high-molarity buffers at low pH) greatly help in quenching electrosmosis and reducing potential adsorption to the capillary wall. For proteins, CZE separations are more difficult, because in untreated capillaries a substantial fraction of the protein macroion can be adsorbed in the Debye–Hückel layer of the silica wall⁵. Even though some proteins have been analysed in the same buffer used for peptide fractionations⁶ (100 mM phosphate, pH 2.5), it should be borne in mind that this pH is denaturing for most proteins. As an alternative method one could use alkaline buffers, at pH higher than the isoelectric point (*pI*) of the sample proteins: as the capillary wall and the protein will bear a net negative charge, adsorption will be minimized^{7,8}. This problem is particularly severe with basic proteins, as the buffer pH would have to be so high as to destroy the silica capillary. For this particular problem Green and Jorgenson⁹ advocated the use of moderately alkaline buffers (pH 9.0) supplemented by high concentrations (0.25 M) of potassium sulphate, which minimized most efficiently protein adsorption, and least interfered with UV readings. More recently, Bushey and Jorgenson¹⁰ suggested the use of buffers containing high concentrations of zwitterions, as these compounds should not contribute to the conductivity of the operating buffer, but should be able to associate with the negatively charged capillary surface on the one side, and with the charged protein sites on the other, thus minimizing protein adsorption in the Debye–Hückel layer. The other alternative, as proposed by Hjertén's group¹¹, is to coat the capillary wall with a viscous agent (generally methylcellulose or bonded linear polyacrylamide) able to minimize the zeta potential at the wall. In coated capillaries, Kilar and Hjertén¹² were able to separate by zone electrophoresis and isoelectric focusing (IEF) transferrin isoforms and many other proteins.

Based on an original idea of Faupel *et al.*¹³ and Righetti *et al.*¹⁴, we have recently developed a multi-compartment electrolyser, able to purify to homogeneity large amounts of proteins (on the gram scale), particularly useful for removing the most tenacious contaminants from r-DNA proteins^{15,16}. In this apparatus, a single protein is kept isoelectric in each chamber of the electrolyser by two flanking membranes, able to titrate continuously the macroion to its *pI* value. By carefully engineering the different membranes, ideally in each compartment one can isolate a pure protein species. The membranes are made with the Immobiline technology, *i.e.*, they consist of neutral monomers [acrylamide and N,N'-methylenebisacrylamide (Bis)] and charged acrylamido derivatives (known as Immobilines) mixed in such ratios as to determine unequivocally and very precisely a given *pI* value. If the *pI* values of the two flanking membranes encompass the *pI* value of a given protein component, this species will be kept isoelectric in such a chamber (the membranes, by virtue of their high buffering capacity, act as pH-stat units) and will not be able to leave it even in the presence of a strong electrosmotic flow. We have purified by this technique large amounts of r-DNA proteins, including eglin C, monoclonal antibodies (Mab) against the gp-41 of AIDS virus, human growth hormone and superoxide dismutase (SOD). The rate-limiting step in monitoring the purification progress (which could be rapid if the contaminants have very different *pI* values, but slow with very small ΔpI) is the analytical method itself, which is IEF in immobilized pH gradients (IPG). Because in general the contaminants have small ΔpI , and thus focus over a narrow pH range, the analytical IPG step is generally performed over 1 pH unit (and sometimes even less).

In such ultra-narrow ranges, long focusing times are required¹⁷, so that it might well take 10–12 h before the results of the purification progress are available. Meanwhile, the purification will have further progressed in the electrolyser, so that the “picture” obtained has already aged. With CZE, owing to the short analysis time (usually 15–30 min even with protein mixtures), one could hope to monitor the progress of purification in real time. We have applied CZE to such analytical problems and compared its resolving power with that of IPGs and of chromatofocusing in resolving the same protein mixtures. In addition, we had an interesting problem to solve, as one of our proteins (the anti-gp-41 monoclonal antibody) was resolved into a series of bands with very high *pI* values (in the pH range 9.0–9.6).

EXPERIMENTAL

Instrumentation

CZE analysis of the basic monoclonal antibodies (Mab) anti-gp-41 was performed in a Bio-Rad Labs. (Richmond, CA, U.S.A.) HPE 100 unit. Capillaries were supplied mounted in cartridges with an integral flow cell for on-column optical detection. All capillaries were covalently coated at the internal wall with a hydrophilic polymer. Detection was by UV absorbance at 200 nm and the capillary was not thermostated. For human superoxide dismutase (hSOD), CZE analysis was performed in an Applied Biosystems (Foster City, CA, U.S.A.) Model 270A unit, equipped with an uncoated, air-cooled capillary. Chromatofocusing was carried out on a Mono P column (Pharmacia–LKB, Uppsala, Sweden) connected to a fast protein liquid chromatographic (FPLC) system and to an on-line pH monitor. Analytical IEF in IPGs was operated in a Multiphor II chamber, connected to a Macrodrive power supply and to a Multitemp Thermostat (Pharmacia–LKB). Preparative protein purification in a multi-compartment electrolyser equipped with isoelectric immobiline membranes was executed in the apparatus designed by Faupel¹³ and Righetti¹⁴.

Materials

Anti gp-41 Mabs were prepared according to Jungbauer *et al.*¹⁸. Recombinant human (r-h) SOD was produced as described by Weselake *et al.*¹⁹. All samples were lyophilized from volatile buffers (10 mM ammonium formate). Immobilines and carrier ampholytes were purchased from Pharmacia–LKB. The membranes for the multi-compartment electrolysers were made and used according to Righetti *et al.*¹⁵.

Capillary zone electrophoresis

Analysis of Mabs in the Bio-Rad HPE 100 unit was carried out in 100 mM phosphate buffer (pH 5.8), generally at 10 kV, 20 μ A, 20 mAU full-scale (200 nm). For sample loading, a 10- μ l volume of the sample (with an ionic strength about one tenth that of the electrophoresis buffer) was injected into the anodic reservoir just ahead of the capillary inlet. The power supply was then turned on and the sample electrophoresed into the capillary for 6–8 s at 8 kV. The anodic reservoir was then flushed with the electrophoresis buffer, and the CZE run made at 10 kV. For analysis of r-hSOD, CZE was performed in the Applied Biosystems apparatus (Model 270CE, standard 72-cm capillary) in 20 mM citrate buffer (pH 4.0). The conditions for sample loading were a 2-s vacuum injection, run at 21 kV, 21 μ A.

Analytical IPGs

Mab analysis was done in IPG gels in the pH range 8.5–10. The samples were loaded in slots preformed at the anodic side, in a pH 8.0 plateau gel segment (2-cm long). About 20 μ l, containing up to 50 μ g of protein, were loaded and focusing was continued for up to 30 000 V h; r-hSOD analysis was made in IPG pH 4.5–5.5 gels, using the above conditions (except for the cathodic sample application). All gels were stained with Coomassie Brilliant Blue R-250 in Cu^{2+} , according to Righetti and Drysdale²⁰.

Chromatofocusing

Mono P chromatofocusing columns (Mono HR5/20 and HR10/30) from Pharmacia–LKB were connected to an FPLC system equipped with an on-line pH flow electrode. The columns were operated at a flow-rate of 0.1 ml/min. About 1 mg of lyophilized monoclonal antibodies was dissolved in 500 μ l of equilibration buffer and loaded onto a 3.4-ml column. Elution was performed at a flow-rate of 0.1 ml/min in a linear pH gradient from 9.5 to 7.0.

Preparative IPGs

Preparative IPGs in multi-compartment electrolyzers were run according to Righetti and co-workers^{15,16}. For Mab purification, the electrolyser was assembled with six flow chambers (two electrodic and four sample chambers). The compartments were separated by five Immobiline membranes (supported by Whatman GF/D microfibre filters) having *pI* values of 9.11, 9.25, 9.36, 9.49 and 9.64. The membranes facing the cathodic and anodic reservoirs were made more robust (10% T, 4% C)^a, whereas the membranes in between the sample flow chambers were more porous (5% T, 8% C), so as to allow passage of the large Mab molecules (molecular mass 150 000). For r-hSOD purification, the electrolyser was assembled with eight chambers (two electrodic and six sample chambers), delimited by seven isoelectric membranes having *pI* values of 4.60, 4.82, 4.90, 4.94, 5.05, 5.09 and 5.30. The anodic and cathodic membranes were made 12% T, 5% C, whereas the sample membranes contained 5% T, 5% C gel matrix. The content of each chamber was analysed by CZE and by analytical IPGs.

RESULTS

Fig. 1A and B compares the pattern of isoforms of purified human Mab against the gp-41 of AIDS virus. It is seen that, notwithstanding the fact that the antibodies produced are monoclonal, and purified to homogeneity, they are resolved in a narrow IPG interval (pH 8.5–10) into a fine spectrum of as many as 21 bands (B). The IPG profile agrees fairly well with the CZE peak spectrum, except that the resolution is much lower (at best fifteen peaks can be counted) and that in the central portion, where three major components are present, no baseline resolution can be obtained in CZE (whereas ample, empty gel space can be seen among the same zones in the IPG profile). As a comparison, Fig. 1C shows the chromatofocusing chromatogram of the same preparation; even under the best conditions and by applying a shallow pH

^a C = g Bis/% T; T = (g acrylamide + g Bis)/100 ml solution.

gradient, not more than ten peaks are resolved and again no baseline resolution is achieved in the region of the most abundant Mab isoforms.

This Mab preparation has been subjected to purification in a multi-compartment electrolyser^{15,16}, equipped with isoelectric membranes able to define isoelectric conditions for a single species in each chamber. The purification progress has been monitored in parallel with CZE and IPGs. Fig. 2A-C compares the results of the two techniques in analysing the content of chambers 2, 3 and 4, respectively, of the electrolyser. Here too the two techniques compare fairly well except that, in cases in which a few large peaks are present, small zones in between tend to disappear in the CZE profile. This is clearly illustrated in Fig. 2B; as there is no baseline resolution

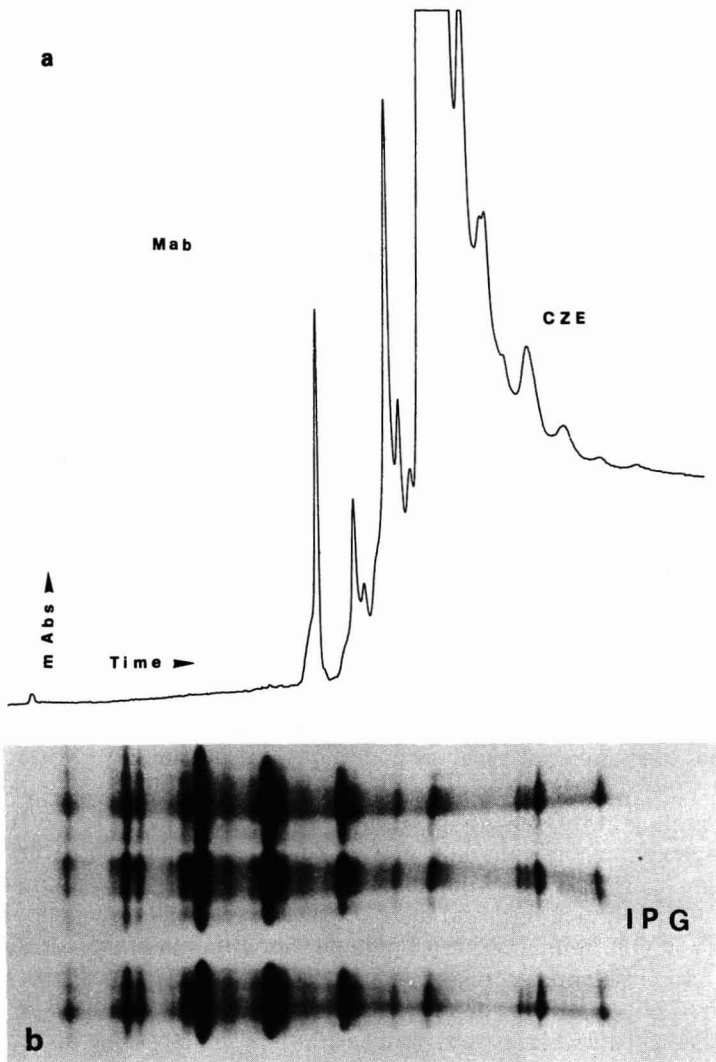


Fig. 1.

(Continued on p. 138)

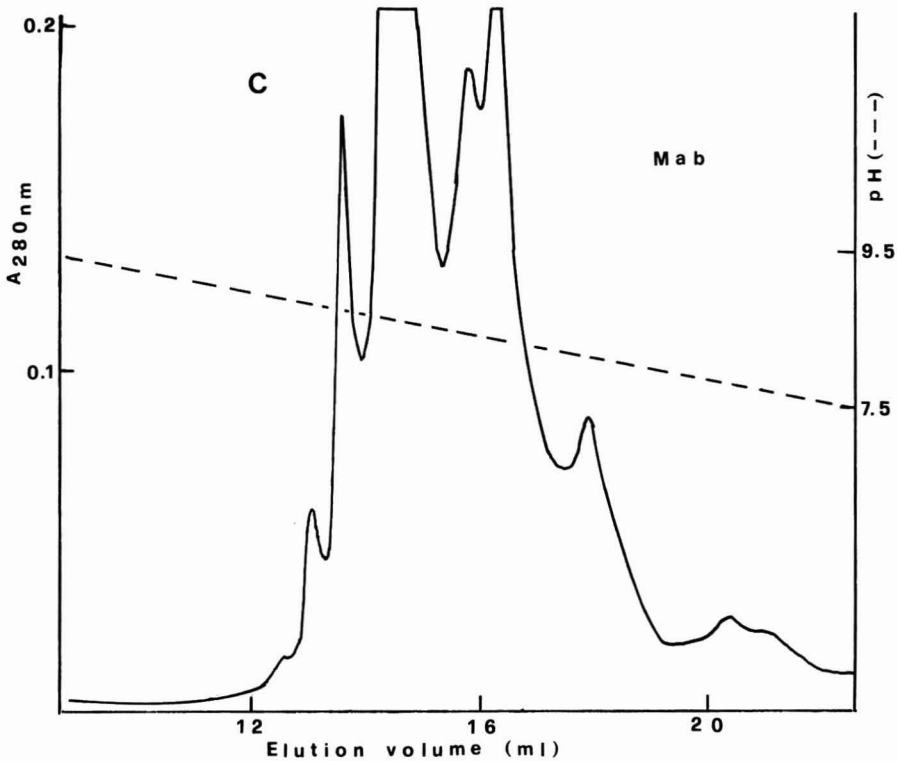


Fig. 1. Comparison among CZE, IPG and chromatofocusing. A pure preparation of human monoclonal antibody isoforms against the gp-41 of AIDS virus was analysed by (a) CZE, (b) IPG and (c) chromatofocusing. (A) CZE with the Bio-Rad HPE 100 unit in 100 mM phosphate buffer (pH 5.8). Sample loading: 8 s at 8 kV. Run: 20 kV, 20 μ A, 20 mAU full-scale. (B) IPG in the pH range 8.5–10. The sample was loaded in a pH 8.0 plateau in slots precast in the gel. Run: 30 000 V h at 10°C. Staining with Coomassie Brilliant Blue R-250 in Cu^{2+} . Three sample tracks are shown, for a visual assessment of pattern reproducibility in IPGs. (C) Chromatofocusing in a Mono P column; elution with a linear pH 9.5–7.0 gradient. Sample flow-rate: 0.1 ml/min.

between the two major peaks, the intermediate proteins bands are lost in the CZE profile but are clearly seen in the IPG pattern. This is possibly due to the fact that, in all focusing techniques, even under overloading conditions (often necessary to detect minor contaminants), there is a built-in force counteracting diffusion, whereas this mechanism is not operating in CZE.

We next investigated the purification progress of r-hSOD, produced in *Escherichia coli*. The protein was purified in a multi-chamber apparatus assembled with eight chambers (six for sample collection and two electrolyte reservoirs). Fig. 3 shows the isoform profile of r-hSOD, as analysed in a 1 pH unit wide IPG gel, of the starting material (control) and of the zones collected in each chamber. Fig. 4A–C shows representative runs in CZE vs. IPG of the contents of chambers 2, 3 and 4, respectively. Here too it is seen that, whereas the overall pattern is similar, some protein zones tend to disappear from the CZE profile. For example in Fig. 4C the spectrum of fine bands (as many as four) between the two major SOD zones, clearly visible in the

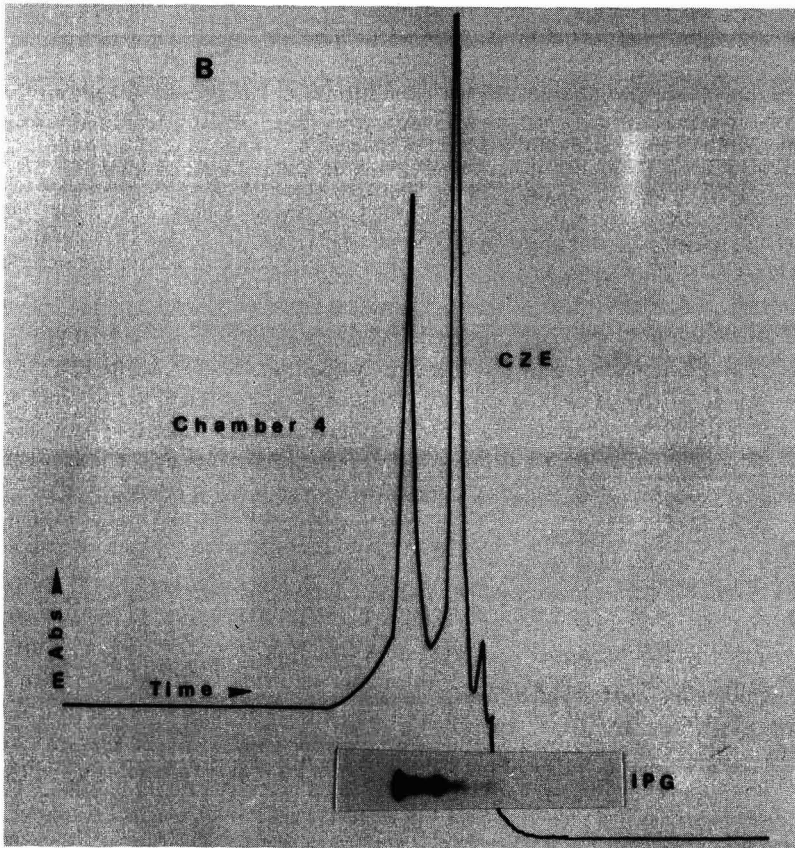
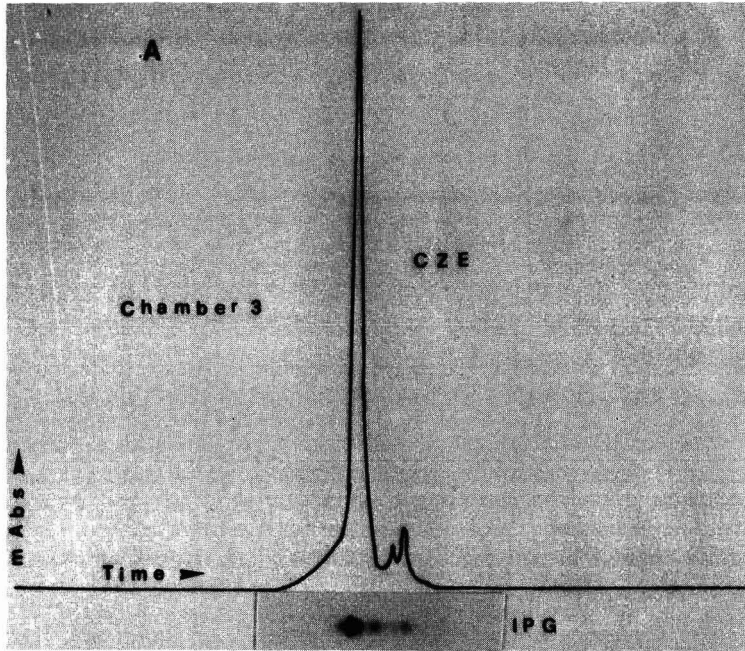


Fig. 2.

(Continued on p. 140)

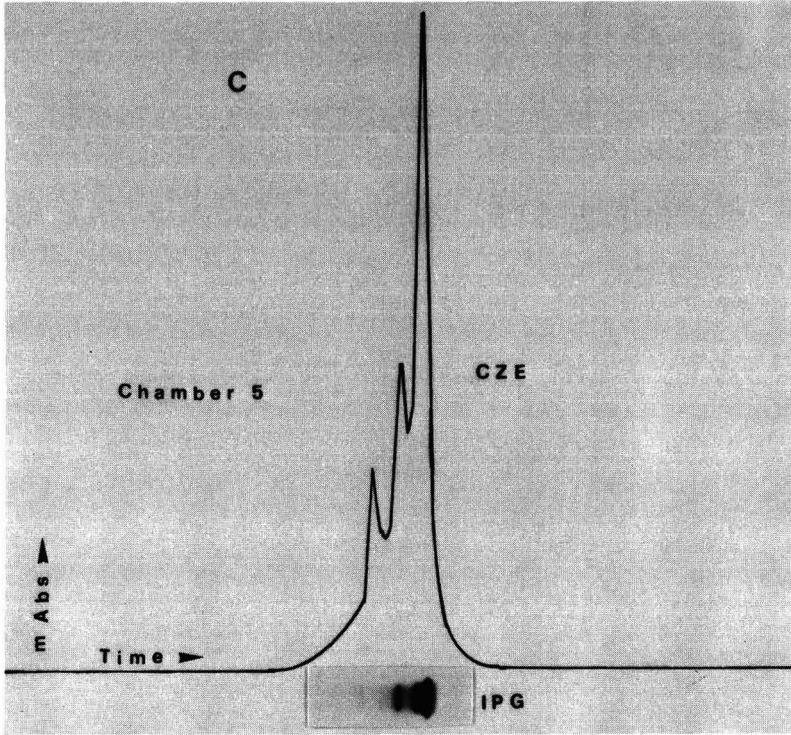


Fig. 2. Progress of purification of Mabs in a multi-compartment electrolyser. After running the electrolyser for 1 day at 1000 V/cm, the content of each chamber was analysed by CZE and IPG. (A) Comparative data for the content of chamber 3; (B) analysis of the content of chamber 4; (C) screening of the content of chamber 5. The purification progress can easily be compared with the same patterns shown in Fig. 1 (21 bands by analytical IPGs). All other conditions as in Fig. 1.

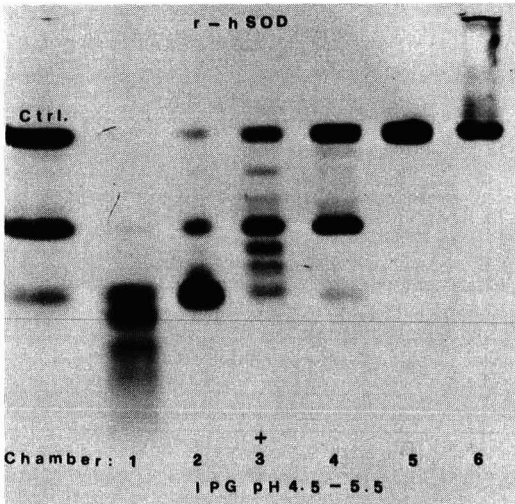


Fig. 3. Analytical IPG gel of a preparative r-hSOD run in the multi-compartment electrolyser. IPG gel: 5% T, 3% C, pH range 4.5–5.5, run for 20 000 V h at 10°C. Staining with Coomassie Brilliant Blue R-250 in Cu^{2+} . Ctrl. = Control, unfractionated r-hSOD. Tracks 1–6: content of chambers 1–6 in the electrolyser. The cathode is uppermost. Note that chamber 5 contains a single homogeneous SOD band.

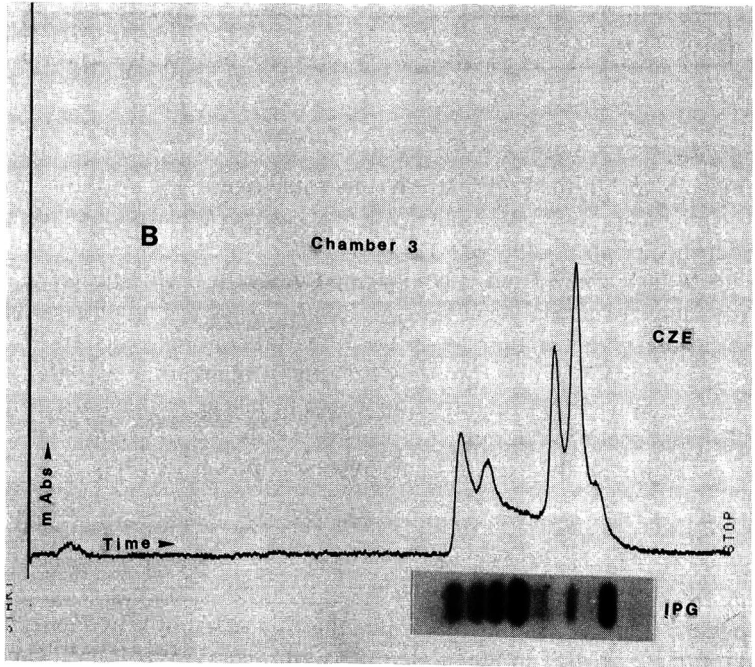
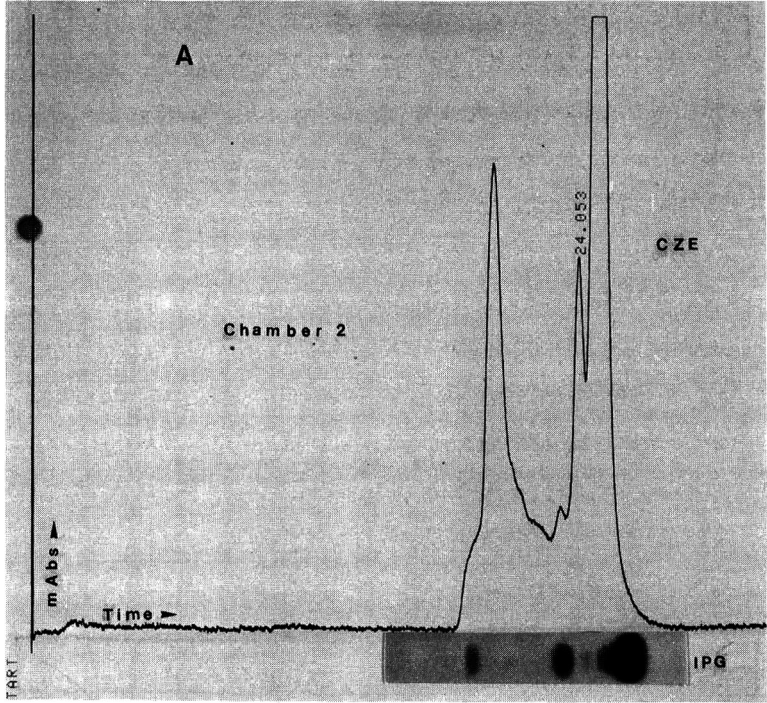


Fig. 4.

(Continued on p. 142)

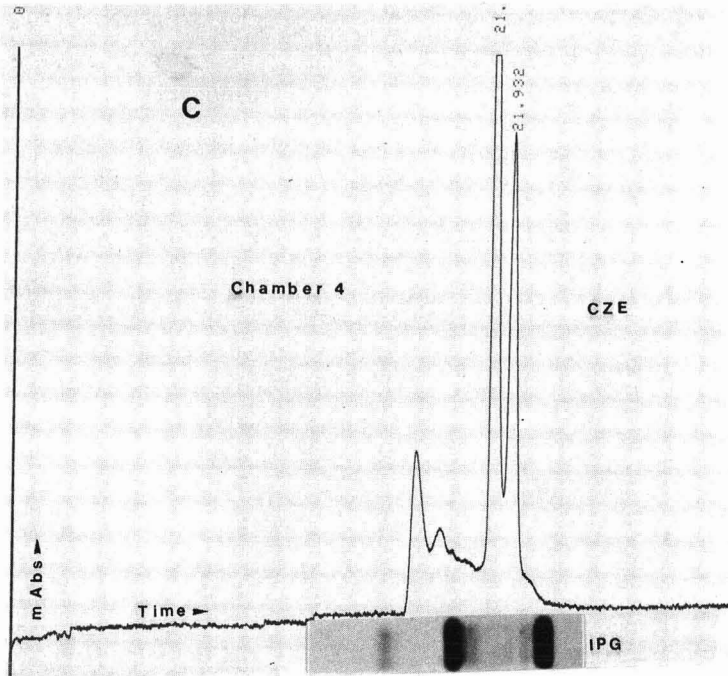


Fig. 4. Progress of purification of r-hSOD in a multi-compartment electrolyser. After running the electrolyser for 1 day at 200 V/cm, the contents of each chamber were analysed by CZE and IPG. (A) Comparative data for the content of chamber 2; (B) analysis of the content of chamber 3; (C) screening of the content of chamber 4. The purification progress can easily be compared with the same patterns shown in Fig. 3. Conditions for CZE: Applied Biosystems Model 270CE unit (standard 72-cm capillary) in 20 mM sodium citrate buffer (pH 4.0); sample loading: 2-s vacuum injection, run at 20 kV, 21 μ A, 25°C. All other conditions as in Fig. 1.

IPG profile, is completely lost in the CZE pattern (this could again be due to the fact that there is no baseline resolution between the two zones, or perhaps to the reversal of the mobility order in CZE as compared with IPG).

Our experience so far accumulated in comparing CZE with IPG indicates that CZE has a clear advantage over analytical IPGs in terms of speed of analysis (each CZE run takes *ca.* 20 min, whereas narrow-range IPGs take as many as 10 h to process) and also in zone quantification (but only because of the reading at 200–210 nm; with fluorescent or coloured tags, quantitation would be just as problematic as in conventional gel electrophoresis). However, in terms of resolution, it seems that at present no technique can match the extraordinary resolving power of IPGs.

DISCUSSION

Advantages and limitations of CZE

“Are the Russians Ten Feet Tall?” predicated the title of a book by Keller²¹ meant to destroy everything created in the modern Russian society. We do not want to be so vicious and unscrupulously hard as Mr. Keller, but we feel that a proper

assessment of the performance of CZE, especially with regard to protein analysis, is now due and we listing here a series of points worth examining.

Speed

There is no doubt that speed of separation is by far the greatest advantage of CZE, when compared to all other electrophoretic techniques. For example, both sodium dodecyl sulphate (SDS) electrophoresis and conventional isoelectric focusing²² take at least 2–3 h for the migration step alone (to this must be added the time for preparing the gel, staining, destaining and densitometry). In the case of IPGs, the situation is the same when running wide pH gradients, but in narrow and ultra-narrow pH ranges (*e.g.*, 1 pH unit or less) it might take up to 10 h to reach steady-state conditions¹⁷. The only system which can substantially reduce these times (and which also represents an instrumental approach to electrophoresis) is the Fast System of Pharmacia, where both SDS and IEF can be run in *ca.* 45 min and where gel staining and destaining have been completely automated. This has been made possible by an idea proposed long ago by Kinzkofer and Radola²³, *viz.*, running IEF in postage stamp-size gels. For example, in gels barely 1–3 cm long, equilibrium IEF is obtained in only 2 min in 1-cm long gels and in only 10 min in 3-cm long gels. In addition, in such miniature, ultra-thin (50–100 μm) gels, staining is accomplished in 5 min and destaining in 2–3 min. This compares favourably even with CZE, where protein run times as long as 20 min are required (in addition, in such miniature gels, at least ten samples can be run simultaneously, which further reduces the analysis time to *ca.* 1 min per sample).

Sensitivity

Here too CZE scores fairly high, as extremely high sensitivities have been reported. For example, Chung and Dovichi²⁴ reported the detection of 2–7 amol of eighteen fluorescein isothiocyanate derivatives of amino acids. In the best cases, they could detect as little as 0.05 amol of arginine, which corresponds to *ca.* 5700 molecules. This is almost frightening and one wonders if one day we could scrape the bottom of Avogadro's barrel and dig out the last remaining molecule. This compares favourably with the best detection conditions obtained in gel electrophoresis: by Coomassie Brilliant Blue staining the lowest detection limit for proteins is of the order of 10–15 ng per band²³ and by silver staining it is *ca.* 1 ng per spot²⁵.

Nevertheless, even this should be taken with caution, as in real-world detection at such minute levels may not be feasible as extreme care would be required with respect to sample manipulation to minimize losses due to adsorption and the effects of contaminants on the signal. In addition, such sensitivity levels have been obtained with the use of a highly sophisticated detection system, *e.g.*, an ultratrace laser detector, not available in any commercially available equipment. With the UV detection system currently available, such sensitivity in protein analysis is drastically reduced. With a universal conductivity detector (which does not require any sample derivatization) the limit of detection is *ca.* 10^{-6} M (ref. 26). As a last comment, it should be noted that, whereas the mass sensitivity is good, relatively high sample concentrations are needed because, in most electrophoretic loading systems, only a fraction of the sample injected into the electrolyte reservoir enters the capillary²⁷.

Quantification

One of the major drawbacks in the quantification of protein zones in conventional gel electrophoresis is that the colour yield varies greatly with different proteins, so that the slope of the colour intensity curve can differ by as much as one order of magnitude. This applies to both Coomassie Brilliant Blue²⁸ and silver-stained patterns²⁵. It has been claimed that only CZE offers correct quantification of the different protein zones, and this is very important when assessing the level of impurities in, *e.g.*, r-DNA proteins. Thus, Frenz *et al.*⁶ demonstrated that, when determining the extent of deamidation of recombinant human growth hormone (r-hGH), they could determine 2.6% deamidated r-hGH by anion-exchange high-performance liquid chromatography and 3.1% by CZE, which is fairly good, considering also that part of the difference could result from the electrophoretic sample loading procedure in CZE, which could allow relatively more loading in the capillary of the faster migrating deamidated r-hGH. We fully agree with these data, but only with the proviso that they apply to UV sample detection at 200–210 nm, where protein adsorption is largely due to the peptide bond. However, when this statement is extended to proteins labelled with fluorescent dyes or with any other coloured tag, it is hard to understand why the signal should be quantitative in CZE and not in, *e.g.*, SDS electrophoresis or IEF or IPG.

Reproducibility

There are three problems to be addressed in this respect: reproducibility in sample loading, in sample migration time and in total sample eluted from the capillary. Our main problem in protein analysis has been reproducibility in sample migration (or transit) time, as also reported by Frenz *et al.*⁶, as well as in sample elution. CZE equipment is generally “user-friendly”, *i.e.*, very easy to operate even by inexperienced technicians. In addition, in some systems, such as the Bio-Rad unit, the coating in the inner capillary wall greatly helps in reducing protein adsorption, and this has been found by us to be excellent for the analysis of alkaline monoclonal antibodies (*pI* values in the *pH* range 9.1–9.6). Our major problem, however, has been the lack of reproducibility in transit times: often, after a few runs, no further protein was eluted and the capillary became clogged. Perhaps one problem, as pointed out by Nelson *et al.*²⁹ and Terabe *et al.*³⁰, could be the lack of adequate cooling of the capillary. In contrast, IPGs afford unique reproducibility; *e.g.*, in two-dimensional maps, the uncertainty in spot position is reduced to a minute ellipse, with a variation in absolute spot location never greater than 1–3 mm, over a gel area of 14 × 16 cm (IPG × SDS dimensions)³¹.

Resolving power

This is perhaps the most ambiguous aspect of CZE. According to Bushey and Jorgenson¹⁰, in protein separations over 100 000 theoretical plates can be obtained, which seems reasonable. However, theoretically, Jorgenson and Lukacs² have predicted, in diffusion-limited cases, several million theoretical plates. In the case of DNA restriction fragments, Cohen *et al.*³² have obtained an effective plate count of 600 000 (for a capillary length of 13 cm). More recently, in separations of oligodeoxynucleotides, Karger *et al.*¹ have claimed plate numbers, in gel-filled capillaries, as high as 15·10⁶, for lengths of 50 cm. We do not understand the significance of all these

numbers, but a close inspection at Fig. 1 could be instructive. Our anti-gp-41 monoclonal antibodies (a pure family of isoforms) are separated in an IPG pH 8.5–10 gradient into 21 fully resolved and clearly visible zones. In the best run obtained by CZE, only fifteen peaks can be counted. In chromatofocusing, only ten peaks are visible. There is more to it: in order to detect minor components, the run has to be overloaded with respect to the major fractions; this results in CZE in spread-out peaks (Fig. 1A) with no baseline resolution in the central portion of the electropherogram. In the IPG gel profile (Fig. 1B), because there is a built-in force which counteracts diffusion in focusing techniques, there is ample resolution even among the major peaks, with clear gel zones in between.

However, there is even more to it: had we wanted, we could have further improved the resolution in IPGs by narrowing the pH gradient to about 1/2 (in fact, most of the zones are isoelectric between p.H 8.9 and 9.6, so a pH gradient between pH 8.5 and 10 is indeed much too wide). Thus, if we have to speak in terms of resolution, it is clear that the order should be IPG > CZE >> chromatofocusing. This could give a clue as to why the spreading of IPGs has been relatively slow: too much resolution can be just as hard to deal with as too little resolution. There is no problem in handling chromatofocusing (moderate resolution); there are already some problems in adapting to CZE (high resolution), but there are definitely major difficulties in accepting the extremely high resolution of IPGs.

CONCLUSIONS

CZE, when used for monitoring the progress of protein purification in multi-compartment electrolyzers, has the definite advantage of very short analysis times and good quantification of proteins bands via UV readings at 200–210 nm. However, the technique still lacks reproducibility and is definitely not a match for the very high resolving power of immobilized pH gradients.

ACKNOWLEDGEMENTS

P.G.R. is supported in part by grants from Agenzia Spaziale Italiana and by the FATMA project (CNR, Rome, Italy). H.K. is supported by a grant from the "Innovations und Technologiefond" from the Federal Ministry of Science and Research of the Austrian Government (Project No. 7/62). We thank Bio-Rad Italy for the kind loan of the HPE-100 unit and Applied Biosystems of Austria for lending the 270A unit.

REFERENCES

- 1 B. L. Karger, A. S. Cohen and A. Gutmann, *J. Chromatogr.*, 492 (1989) 585–614.
- 2 J. W. Jorgenson and K. D. Lukacs, *Science (Washington, D.C.)*, 222 (1983) 266–270.
- 3 M. J. Gordon, X. Hung, S. L. Pentaney, Jr. and R. N. Zare, *Science (Washington, D.C.)*, 242 (1988) 224–229.
- 4 B. L. Karger (Guest Editor), *1st International Symposium on High Performance Capillary Electrophoresis; J. Chromatogr.*, 480 (1989) 1–435.
- 5 G. O. Roberts, P. H. Rhodes and R. S. Snyder, *J. Chromatogr.*, 480 (1989) 35–67.
- 6 J. Frenz, S. L. Wu and W. S. Hancock, *J. Chromatogr.*, 480 (1989) 379–391.

- 7 H. H. Lauer and D. McManigill, *Anal. Chem.*, 58 (1986) 166–172.
- 8 Y. Walbrohel and J. W. Jorgenson, *J. Microcolumn Sep.*, 1 (1989) 41–50.
- 9 J. S. Green and J. W. Jorgenson, *J. Chromatogr.*, 478 (1989) 63–72.
- 10 M. M. Bushey and J. W. Jorgenson, *J. Chromatogr.*, 480 (1989) 301–310.
- 11 F. Kilar and S. Hjertén, *Electrophoresis*, 10 (1989) 23–27.
- 12 F. Kilar and S. Hjertén, *J. Chromatogr.*, 480 (1989) 351–357.
- 13 M. Faupel, B. Barzaghi, C. Gelfi and P. G. Righetti, *J. Biochem. Biophys. Methods*, 15 (1987) 147–162.
- 14 P. G. Righetti, B. Barzaghi, M. Luzzana, G. Manfredi and M. Faupel, *J. Biochem. Biophys. Methods*, 15 (1987) 189–198.
- 15 P. G. Righetti, E. Wenisch and M. Faupel, *J. Chromatogr.*, 475 (1989) 293–309.
- 16 P. G. Righetti, E. Wenisch, A. Jungbauer, H. Katinger and M. Faupel, *J. Chromatogr.*, 500 (1990) 681–696.
- 17 P. G. Righetti, *Immobilized pH Gradient: Theory and Methodology*, Elsevier, Amsterdam, 1990, pp. 117–180.
- 18 A. Jungbauer, C. Tauer, E. Wenisch, F. Steindl, M. Purtscher, M. Reiter, F. Unterluggauer, A. Buchacher, K. Uhl and H. Katinger, *J. Biochem. Biophys. Methods*, 19 (1989) 223–233.
- 19 R. Weselake, S. L. Chesney, A. Petkau and A. D. Friesen, *Anal. Biochem.*, 155 (1986) 193–200.
- 20 P. G. Righetti and J. W. Drysdale, *J. Chromatogr.*, 98 (1974) 271–321.
- 21 W. Keller, *Are the Russians Ten Feet Tall?*, Thames & Hudson, London, 1961.
- 22 P. G. Righetti, *Isoelectric Focusing: Theory, Methodology and Applications*, Elsevier, Amsterdam, 1983.
- 23 A. Kinzkofer and B. J. Radola, *Electrophoresis*, 2 (1981) 174–183.
- 24 Y. F. Chung and N. J. Dovichi, *Science (Washington, D.C.)*, 242 (1988) 562–564.
- 25 C. R. Merrill and D. Goldman, in J. E. Celis and R. Bravo (Editors), *Two Dimensional Gel Electrophoresis of Proteins*, Academic Press, Orlando, FL, 1984, pp. 93–109.
- 26 X. Huang, M. J. Gordon and R. N. Zare, *J. Chromatogr.*, 480 (1989) 285–288.
- 27 M. V. Pickering, *LC/GC Int.*, 2 (1989) 202–204.
- 28 S. Fazekas de St Groth, R. G. Webster and A. Datyner, *Biochim. Biophys. Acta*, 71 (1963) 377–391.
- 29 R. J. Nelson, A. Paulus, A. S. Cohen, A. Guttman and B. L. Karger, *J. Chromatogr.*, 480 (1989) 111–127.
- 30 S. Terabe, K. Otsuka and T. Ando, *Anal. Chem.*, 57 (1985) 834–838.
- 31 E. Gianazza, S. Astrua-Testori, P. Caccia, P. Giacon, L. Quaglia and P. G. Righetti, *Electrophoresis*, 7 (1986) 76–83.
- 32 A. S. Cohen, D. Najarian, J. A. Smith and B. L. Karger, *J. Chromatogr.*, 458 (1988) 323–330.

Static and scanning array detection in capillary electrophoresis–mass spectrometry

N. J. REINHOUD

Division of Analytical Chemistry, Centre for Bio-Pharmaceutical Sciences, P.O. Box 9502, 2300 RA Leiden (The Netherlands)

E. SCHRÖDER

Finnigan MAT GmbH, Barkhausenstrasse 2, 2800 Bremen 14 (F.R.G.)

U. R. TJADEN and W. M. A. NIESSEN*

Division of Analytical Chemistry, Centre for Bio-Pharmaceutical Sciences, P.O. Box 9502, 2300 RA Leiden (The Netherlands)

M. C. TEN NOEVER DE BRAUW

Section Instrumental Analysis, TNO CIVO Institutes, P.O. Box 360, 3700 AJ Zeist (The Netherlands)
and

J. VAN DER GREEF

Division of Analytical Chemistry, Centre for Bio-Pharmaceutical Sciences, P.O. Box 9502, 2300 RA Leiden, and Section Instrumental Analysis, TNO CIVO Institutes, P.O. Box 360, 3700 AJ Zeist (The Netherlands)

ABSTRACT

An array detection system based on position- and time-resolved ion counting was evaluated for capillary electrophoresis–mass spectrometry using continuous-flow fast atom bombardment and a liquid-junction coupling. Peptides with molecular masses up to 3200 were measured. A 100–1000-fold improvement over conventional detection was demonstrated by applying the array detector in scanning and static modes. Absolute detection limits in the range 1–5 fmol are achievable.

INTRODUCTION

The coupling of capillary electrophoresis (CE) with mass spectrometry (MS) yields an extremely powerful analytical tool, as it combines a very efficient separation method with a very selective detector. Interfacing CE with MS has been reported using existing high-performance liquid chromatographic (HPLC)–MS interfaces such as electrospray^{1,2}, ion spray³ or continuous-flow fast atom bombardment (CF-FAB)^{4–7}. These approaches are attractive because the “soft” ionization characteristics open up the possibility of analysing polar high-molecular-mass compounds. Further, the above interfaces have optimum flow-rates in the lower $\mu\text{l}/\text{min}$ range and are more compatible with CE than with conventional HPLC. However, a make-up flow is essential to increase the flow-rate from the nl/min range to the *ca.* 5–20 $\mu\text{l}/\text{min}$ needed for

successful operation of these interfaces. The post-capillary addition of a make-up flow is achieved either by a coaxial solvent flow^{2,7} or by means of a so-called liquid-junction coupling, which is in fact a low-dead-volume T-piece between the separation capillary and the transfer capillary³⁻⁶. The latter approach may result in a considerable loss of efficiency⁵.

In this study, a CF-FAB interface was applied in the coupling of CE and MS. The make-up flow is achieved by the application of a liquid-junction coupling. The make-up flow is also used to add the necessary non-volatile FAB matrix, *e.g.*, glycerol⁵.

Maintaining the efficiency during CE-MS coupling is an important goal which not only requires optimization of the liquid-junction coupling, but also demands extreme performance of the MS detection system with respect to sensitivity and scanning speeds. Moreover, the limited injection volume in CE, typically in the range 5-20 nl for a 1 m \times 75 μ m I.D. fused-silica capillary, requires detection at very low levels.

In principle, high efficiencies are beneficial for a mass-flow sensitive detector, although peak standard deviations of a few seconds require rapid scanning over a broad mass range. This makes the overall situation problematic. For sensitivity reasons array detection is an interesting approach in CE-MS. However, because the detection must be performed over a wide mass range, array detection in the scanning mode is of more general interest. Therefore, the application of a PATRIC (position- and time-resolved ion counting) detector⁸ in CE-MS has been evaluated. The PATRIC detector operates in the ion counting mode. For each event the current central mass, the ion arrival position and the ion arrival time at the focal plane detector are registered, thus permitting scanning operation⁸. Scanning is not possible with array detectors based on photodiodes^{8,9}.

EXPERIMENTAL

Capillary electrophoresis was performed with an 800 mm \times 75 μ m I.D. fused-silica capillary (SGE, Ringwood, Victoria, Australia) applying a potential of 20 kV, supplied by a Model RR100-1.5P power supply (Gamma High Voltage Research, Mt. Vernon, NY, U.S.A). A volume of typically 20 nl was injected hydrodynamically. A laboratory made liquid-junction coupling, described in detail elsewhere⁵, was used for the addition of the make-up fluid (0.025% trifluoroacetic acid and 16.6% glycerol in water) and for the coupling of the CE capillary with the CF-FAB interface. The transfer capillary between the liquid-junction coupling and the CF-FAB probe tip was an 840 mm \times 100 μ m I.D. fused-silica capillary, resulting in a flow-rate of *ca.* 14 μ l/min. A newly designed CF-FAB target was used with a gold-plated channel¹⁰, yielding almost instant stability under the described conditions.

A Finnigan MAT (Bremen, F.R.G.) Model 900 double-focusing mass spectrometer equipped with both a normal secondary electron multiplier (SEM) and a PATRIC detector was used. The array detector was used in the static and scanning modes. For the experiments comparing the different detection modes in the analysis of three β -endorphin fragments, the resolution was set at 1000. Resolutions of 1000 and 2000 were used in the measurements of 15 pmol of galanin and 2 pmol of magainin, respectively.

The β -endorphin fragments were a gift from Organon (Oss, The Netherlands). Galanin and maganin were purchased from Bachem Feinchemicalien (Bubendorf, Switzerland). Trifluoroacetic acid was purchased from Merck (Darmstadt, F.R.G.) and glycerol from Lamers and Pleuger ('s Hertogenbosch, The Netherlands). These solvents were of analytical-reagent grade.

RESULTS AND DISCUSSION

Comparison of different detection modes

The analysis of β -endorphin fragments by CE-MS using a liquid-junction coupling and a CF-FAB interface has been reported previously⁵. In this study, the three fragments 6-13, 8-15 and 10-17 with molecular masses of 857, 882 and 900, respectively, were selected for a comparative study of the different detection modes, *viz.*, conventional detection by means of an SEM detector, scanning array detection and static array detection by means of the PATRIC detector. In the last instance the ions in a fixed mass range of 8% around a central mass, in this case of m/z 875, are detected. The analysis was performed with 5 pmol of each β -endorphin fragment.

With the SEM detector, scanning over a broad mass range (m/z 300-1000) at the 5-pmol level was not successful. Therefore, the mass range in this mode was reduced to m/z 840-910 using a cycle time of 1 s. The reconstructed mass chromatograms of the m/z values of the protonated molecules are given in Fig. 1A together with a spectrum of the fragment 8-15 in Fig. 1B.

Scanning array detection was performed over a much wider mass range, *viz.* m/z 300-1000, with a cycle time of 1 s. The reconstructed mass chromatograms and the spectrum of the 8-15 fragments from this analysis are given in Fig. 1C and D.

Fig. 1E and F give the results obtained with static array detection using the full 8% window, *i.e.*, detecting over the mass range m/z 840-910, with an accumulation time of 1 s.

When the reconstructed mass chromatograms in Fig. 1A, C and E are compared, a considerable improvement in the signal-to-noise ratio is observed on going from scanning with SEM detection via scanning with array detection to the static array detection mode. In the last instance the three peaks are clearly observed in the trace of m/z 883. The last peak can be attributed to the 8-15 fragment; the protonated molecule of this peptide loses a molecule of water on FAB. One of the other peaks is the β -endorphin fragment 6-13, and the third peak at this m/z ratio is probably due to an impurity in the sample.

The improvement in the quality of the spectrum in the series Fig. 1B, D and F, which represent single spectra without averaging, is also evident from the signal-to-noise ratio and the isotope cluster. The number of ions detected for the peak at m/z 901 in a single spectrum of fragment 8-15 in the different modes is 16, 480 and 16 000, respectively. In evaluating these figures it must be kept in mind that in the scanning array detection mode a broader mass range was scanned (m/z 300-1000) than with the conventional detector (m/z 840-910). Taking this into account, a 100-fold improvement for the scanning array mode and a 1000-fold improvement for the static array mode are observed. The data compared are all based on one spectrum and a cycle time of 1 s. This means for the static array mode that the absolute detection limit for the peptides investigated is in the 1-5-fmol range, and even lower, if all spectra during a CE peak are averaged.

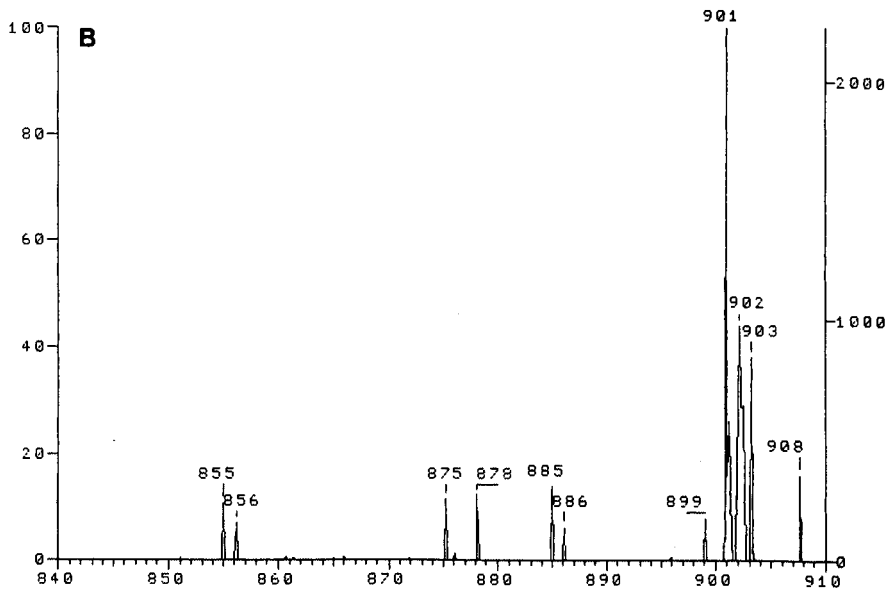
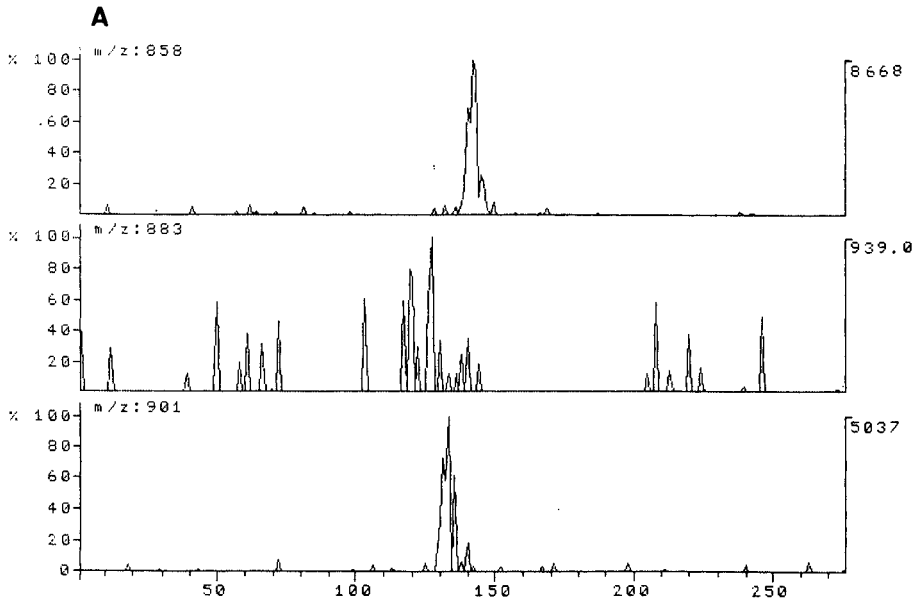


Fig. 1.

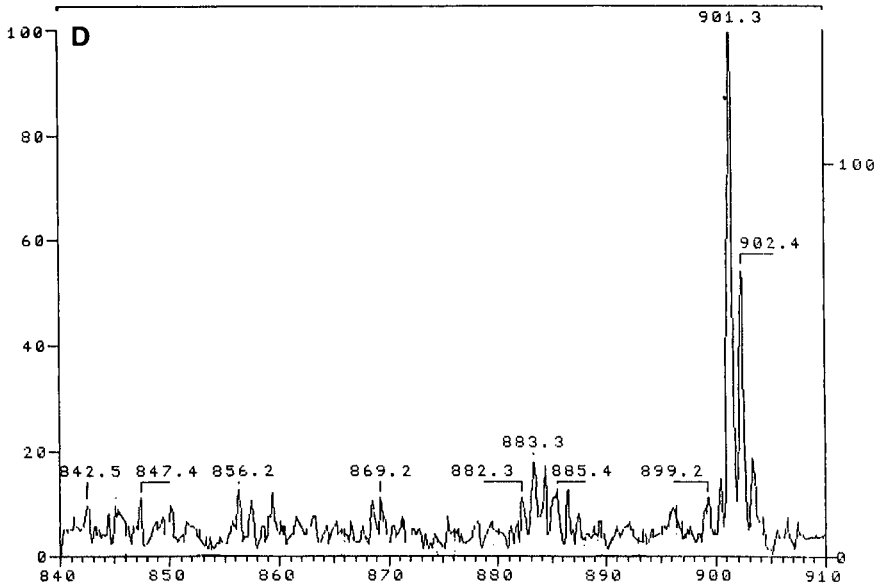
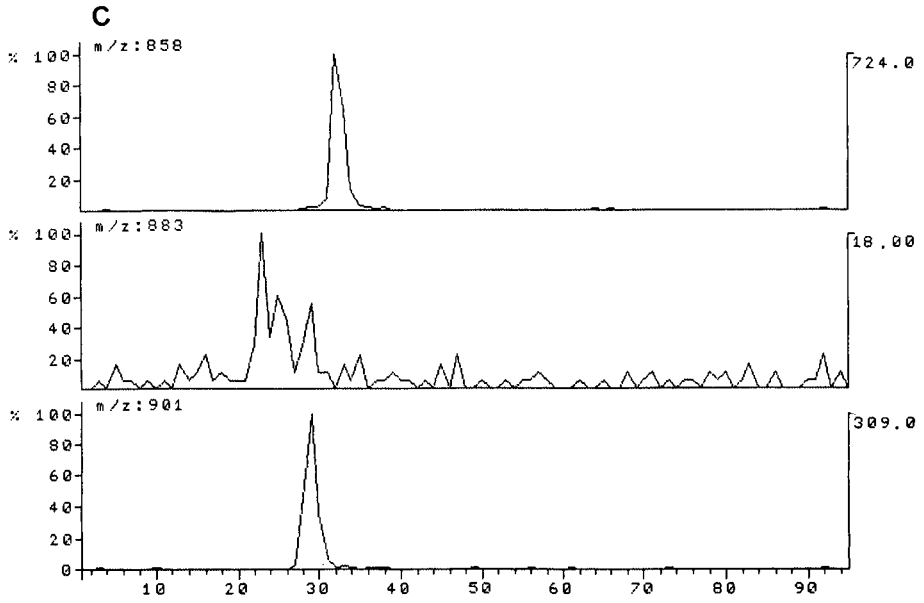


Fig. 1.

(Continued on p. 152)

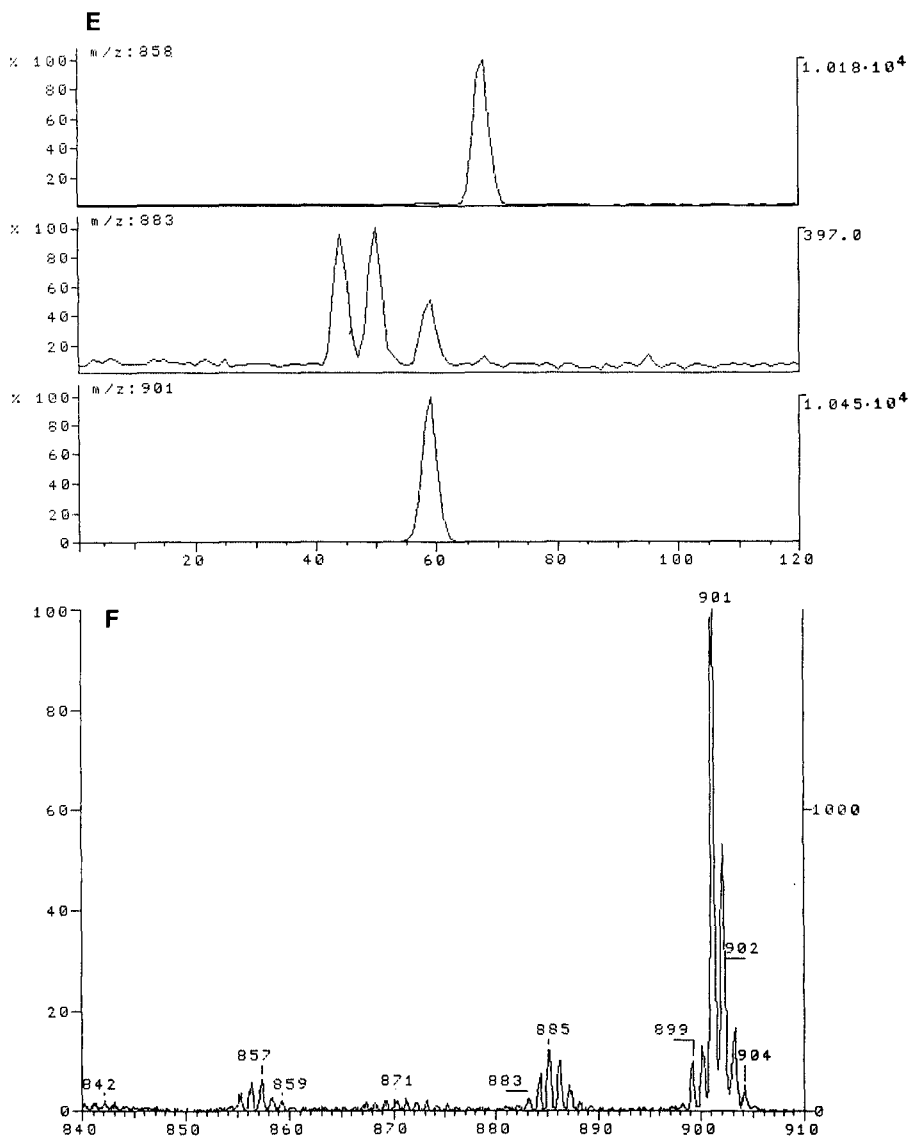


Fig. 1. (A, C and E) Reconstructed mass chromatograms (time in s) from the CE-MS analysis of the β -endorphin fragments 6-13, 8-15 and 10-17 and (B, D and F) CF-FAB mass spectra of the β -endorphin fragment 8-15. Data acquired with 1 s per scan. A and B, electron multiplier in scanning mode (m/z 840-910); C and D, scanning array detection (m/z 300-1000); E and F, static array detection with 8% window (m/z 840-910).

Static array detection of peptides with molecular mass 2000-3000

Continuous-flow FAB has been used very successfully in the detection of peptides in the mass range below 2000. Above this range hardly any data have been reported. From our own experiences the sensitivity at higher mass is lower than expected on the basis of comparing conventional FAB with CF-FAB at low mass. For

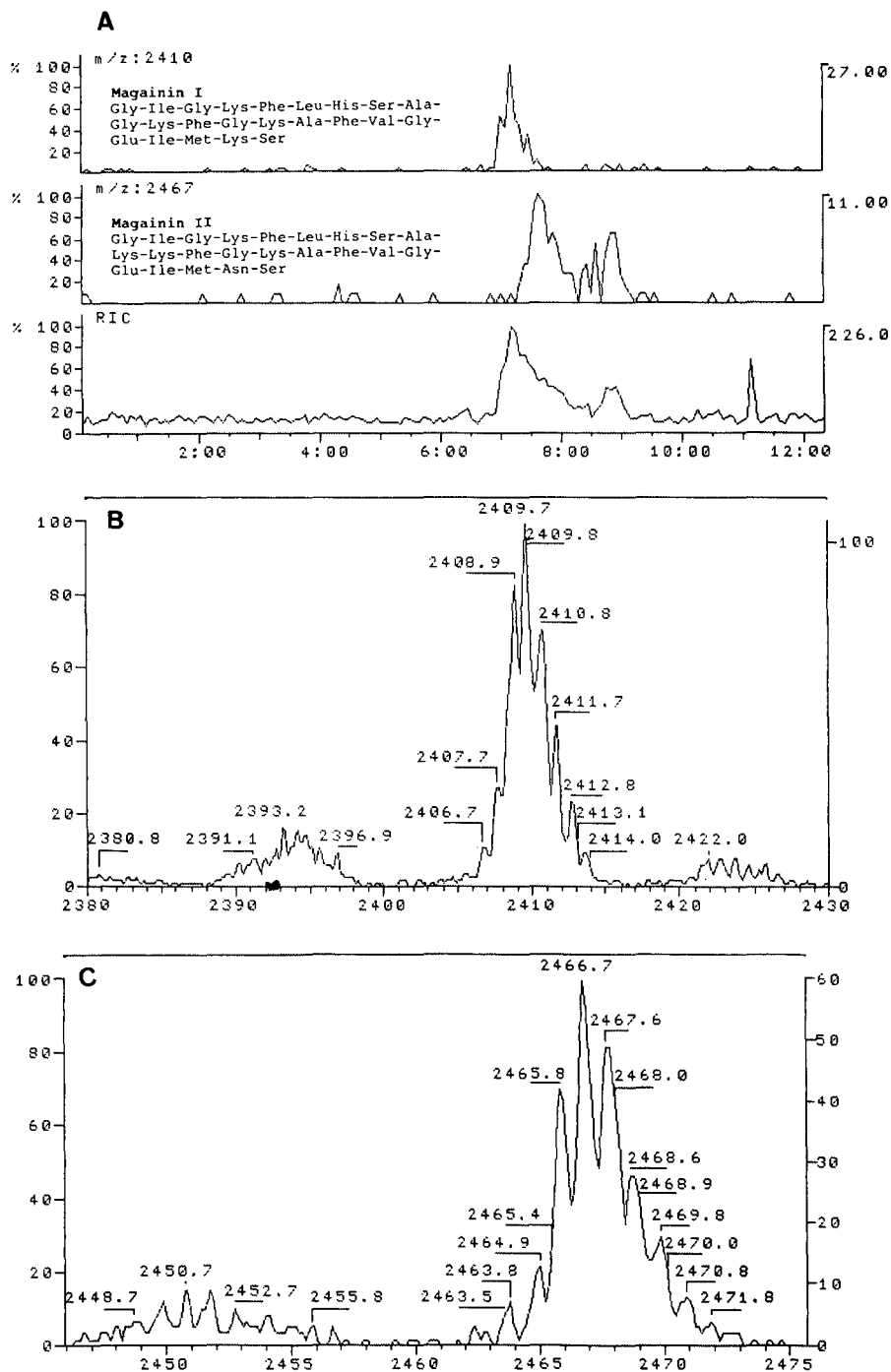


Fig. 2. (A) Reconstructed total ion and mass chromatograms (time in min) from CE-MS analysis of magainin I and II (static array detection). Data acquired with 1 s per scan. (B) CF-FAB mass spectrum of magainin I (average molecular mass of the protonated molecule = 2410.9). (C) CF-FAB mass spectrum of magainin II (average molecular mass of the protonated molecule = 2467.9).

this reason, static array detection was used to measure the performance of CF-FAB in combination with CE in the mass range 2000–3300.

The reconstructed total ion and the mass chromatograms for a CE-MS analysis of the two peptides magainin I and II are shown in Fig. 2A. Magainin I and II peptides, which originally were isolated from frog skin, have molecular masses of 2408.3 and 2465.3, respectively. Although the peptides differ in only 2 of the 23 amino acids, a separation is achieved in CE without any pretreatment of the separation capillary, and an impurity is also detected in the mass chromatogram of m/z 2467. The spectra obtained at the 2-pmol level with a resolution of 2000 are shown in Fig. 2B and C and are of good quality; a well defined isotope envelope is obtained.

In the analysis of the peptide galanin (average molecular mass 3211.6), the sensitivity is considerably lower. With a resolution of 1000 and injection of 15 pmol of the peptide, a good signal-to-noise ratio in the spectrum is observed, as shown in Fig. 3.

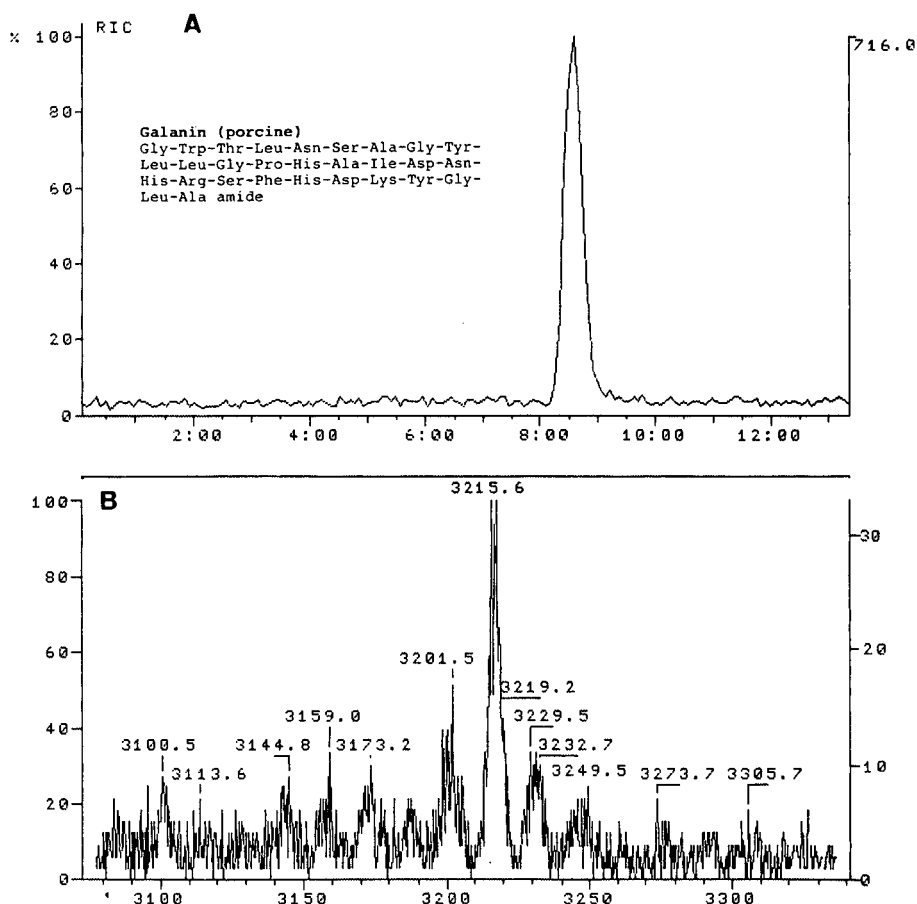


Fig. 3. (A) Reconstructed total ion chromatogram (time in min) and (B) CF-FAB mass spectrum of galanin (average molecular mass of the protonated molecule = 3211.6). Data acquired with 1 s per scan.

CONCLUSION

The PATRIC array detection method has been found to be an important tool for the improvement of the sensitivity in mass spectrometric detection in CE-MS. The static detection mode is useful in target compound analysis and results in sensitivities comparable to those obtained by single ion monitoring, but information over a mass range of 8% around a central mass is obtained. Scanning array detection is a universal detection approach of major importance, as the gain in sensitivity can be of the order of 10-100-fold over a conventional SEM detector in combination with scanning.

REFERENCES

- 1 J. A. Olivares, N. T. Nguyen, C. R. Yonker and R. D. Smith, *Anal. Chem.*, 59 (1987) 1230.
- 2 R. D. Smith, C. J. Barinaga and H. R. Udseth, *Anal. Chem.*, 60 (1988) 1948.
- 3 E. D. Lee, W. M. Mück, J. D. Henion and T. R. Covey, *Biomed. Environ. Mass Spectrom.*, 18 (1989) 844.
- 4 R. D. Minard, D. Luckenbill, P. Curry, Jr. and A. G. Ewing, *Adv. Mass Spectrom.*, 11 (1989) 436.
- 5 N. J. Reinboud, W. M. A. Niessen, U. R. Tjaden, L. G. Gramberg, E. R. Verheij and J. van der Greef, *Rapid Commun. Mass Spectrom.*, 3 (1989) 348.
- 6 R. M. Caprioli, W. T. Moore, M. Martin, B. B. DaGue, K. Wilson and S. Morning, *J. Chromatogr.*, 480 (1989) 247.
- 7 M. A. Moseley, L. J. Deterding, K. B. Tomer and J. W. Jorgenson, *Rapid Commun. Mass Spectrom.*, 3 (1989) 87.
- 8 C. Brunnée, R. Pesch and E. Schröder, *Rapid Commun. Mass Spectrom.*, 4 (1990) 173.
- 9 J. S. Cottrell and S. Evans, *Anal. Chem.*, 59 (1987) 1990.
- 10 P. Kokkonen, E. Schröder, W. M. A. Niessen, U. R. Tjaden and J. van der Greef, *Org. Mass Spectrom.*, submitted for publication.

Sensitivity considerations for large molecule detection by capillary electrophoresis–electrospray ionization mass spectrometry

RICHARD D. SMITH*, JOSEPH A. LOO, CHARLES G. EDMONDS, CHARLES J. BARINAGA
and HAROLD R. UDSETH

Chemical Methods and Separations Group, Chemical Sciences Department, Battelle, Pacific Northwest Laboratories, Richland, WA 99352 (U.S.A.)

ABSTRACT

The use of the electrospray ionization (ESI) method for interfacing capillary electrophoresis with mass spectrometry (CE–MS) is particularly well suited for the analysis of large molecules due to the multiple charging phenomenon. While ionization efficiency is very high, the available ion current is dispersed over more peaks so that the maximum peak intensity obtainable declines significantly for large molecules. Sensitivity with ESI can be improved by operation at very low flow-rates, an ideal situation for CE–MS. These and other considerations related to sensitivity are illustrated using ESI–MS measurements for cytochrome *c*.

INTRODUCTION

Capillary electrophoresis (CE) in its various manifestations (free solution, isotachopheresis, isoelectric focusing, polyacrylamide gel, micellar electrokinetic “chromatography”) is attracting growing attention as a method for rapid high resolution separations of very small sample volumes of complex mixtures. In combination with the sensitivity and selectivity of mass spectrometry (MS), CE–MS becomes a potentially powerful bioanalytical technique^{1–12}. The first CE–MS combination was based upon the electrospray ionization (ESI) approach^{1–10}. More recently continuous-flow fast atom bombardment interfaces have also been demonstrated^{11,12}. The ESI method has recently been demonstrated (off-line) for biomolecules exceeding 100 000 dalton⁴. The method provides extremely high ionization efficiencies [*i.e.*, very high (molecular ions produced)/(molecules consumed)] and precise molecular mass (M_r) measurements⁴. For the combined CE–MS of large biomolecules detection sensitivity becomes the overriding factor, often determining the success or failure of a particular electrophoretic method, buffer system, or application.

In this report, we consider the important subject of sensitivity, which defines the

ultimate potential of the CE-ESI-MS technique. Sensitivity is considered from the viewpoints of sample size, concentration and flow-rate, overall detection efficiency [*i.e.*, (ions detected)/(molecules introduced)], and actual ionization efficiency. The high charge state molecular ions produced by ESI allow tandem mass spectrometry to be extended to much higher M , than previously possible and places even greater demands upon the ionization method and instrumental performance. The development of combined CE-MS will be crucial for possible extension of ESI to the attomole (10^{-18} M) sample range.

EXPERIMENTAL

The ESI-MS instrumentation used in this study and typical operating conditions have been previously described^{4,8,9}. Cytochrome *c* in aqueous acidic buffer solutions, consisting of 5% glacial acetic acid, were introduced to the ESI source through a 100 μm I.D. fused-silica capillary at a rate of 1 $\mu\text{l}/\text{min}$. The flow mixes with a liquid sheath electrode, typically methanol, flowing at 3 $\mu\text{l}/\text{min}$, at the tip of the electrospray ionization source¹. Analyte and sheath flow are independently controlled by separate syringe pumps. A potential of +5 kV is applied to the sheath electrode, producing highly charged liquid droplets of *ca.* 1 μm diameter at atmospheric pressure in a flow of dry nitrogen to aid the desolvation process. The ESI source is mounted 1.5 cm from the entrance orifice of the quadrupole MS. Highly charged ions are sampled through a 1-mm nozzle orifice and 2-mm skimmer and are efficiently transported through a cryo-pumped region by the radio-frequency (rf) quadrupole lens to a quadrupole mass spectrometer for detection. For positive ions, the typical focusing lens voltage is +1 kV, with the nozzle at +200 V and the skimmer at ground potential. The mass spectrometer (EXTREL, Pittsburgh, PA, U.S.A.) used for these studies has an effective m/z range of 1700. The study of cytochrome *c* at various concentrations used slow 1.5-min scans to cover the entire m/z range. Peak abundances were collected only at integer m/z values using our current data system (Teknivent, St. Louis, MO, U.S.A.). Routine calibration of the m/z scale for ESI-MS was performed with low-molecular-mass polymers, such as polyethylene glycol (average molecular mass 1000), monitoring both the singly charged (singly sodiated) and doubly charged (doubly sodiated) molecular ion distributions. The horse heart cytochrome *c* was obtained from Sigma (St. Louis, MO, U.S.A.) and used without further purification.

RESULTS AND DISCUSSION

The electrospray ionization process

Although the use of ESI for MS is a relatively recent occurrence, it and related phenomena have been extensively investigated¹³⁻²⁴. Electrospray ion production requires two steps: dispersal of highly charged droplets at near atmospheric pressure, followed by conditions resulting in droplet evaporation. An electrospray is generally produced by application of a high electric field to a small flow of liquid (generally 1-10 $\mu\text{l}/\text{min}$) from a capillary tube. A potential difference of 3 to 6 kV is typically applied between the capillary and counter electrode located 0.5 to 2 cm away, where ions may be sampled by the mass spectrometer through a small orifice. The electric field results in charge accumulation on the liquid surface at the capillary terminus; thus

the liquid flow-rate, resistivity, and surface tension are important factors in droplet production. The high electric field results in disruption of the liquid surface and formation of highly charged liquid droplets. Positively or negatively charged droplets can be produced depending upon the capillary bias. (The negative ion mode requires the presence of an electron scavenger such as oxygen to inhibit electrical discharge²⁵.) While a wide range of liquids can be sprayed electrostatically into vacuum¹⁶, or with the aid of nebulizing gas^{15,26}, the use of only electric fields leads to some practical restrictions on the range of liquid conductivities and dielectric^{18,19}. Solution conductivities of $\lesssim 10^{-5} \Omega^{-1}$ are required for a stable electrospray at useful liquid flow-rates¹⁸, corresponding to an aqueous electrolyte solution of $\lesssim 10^{-4} N$. Typical ESI currents for water-methanol-5% acetic acid solution are in the range of 0.1–0.5 μA . In the mode found most useful for ESI-MS, an appropriate liquid flow-rate results in dispersion of the liquid as a fine mist. A short distance from the capillary the droplet diameter is often quite uniform and on the order of 1 μm ²¹. Of particular importance is that the total electrospray ion current increases only slightly for higher liquid flow-rates. Increasing flow-rates result in formation of larger droplets and ultimately electrical breakdown, although the use of a nebulizing gas can produce stable results at flow-rates as large as 100 $\mu l/min$ ²⁶. The use of higher voltages does not substantially increase the electrospray ion current until the onset of a corona discharge (generally at > 6 kV).

M_r measurements are obtainable since ESI-mass spectra generally consist of a distribution of molecular ion charge states without contributions due to dissociation. The envelope of charge states, for proteins arising generally from proton attachment, gives a distinctive pattern of peaks due to the quantum nature of electronic charge; *i.e.*, adjacent peaks appear always to vary by addition or subtraction of one charge. A striking feature of electrospray ionization mass spectra of many proteins is that the average charge state increases in an approximately linear fashion with M_r , although this observation is no doubt skewed by the nature of the MS "observational window". As first reported by Fenn and co-workers^{27,28} the M_r of a macromolecule may be immediately determined from spectra such as those in Fig. 1.

ESI-MS sensitivity of detection for macromolecules

The efficiency of ESI can be very high, providing the basis for extremely sensitive measurements. As shown in Table I, current instrumental performance can provide a total ion current at the detector of *ca.* $2 \cdot 10^{-12} A$, or *ca.* 10^7 counts/s for singly charged species. This is consistent with performance of instruments in our laboratory. For an analyte solution flow-rate of 1 $\mu l/min$, a $10^{-4} M$ solution of a singly charged species can account for the total electrospray ion current. At higher concentrations such analytes appear to "saturate" the mass spectrum and displace "normal" solvent-related peaks at low m/z . If the analyte carries more than one charge, the concentration which will saturate the ESI process decreases proportionately. On the basis of the instrumental performance given in Table I, concentrations as low as $10^{-10} M$, or *ca.* 10^{-18} mole/s, of singly charged species can be expected to yield detectable ion currents (*ca.* 10 counts/s) if the analyte is completely ionized. Indeed, we have obtained detection limits of $\ll 10^{-8} M$ in characterization of readily ionized ionic species in precipitation samples and low attomole detection limits for quaternary ammonium ions in conjunction with capillary zone electrophoresis^{2,3}.

TABLE I

TYPICAL ELECTROSPRAY ION SOURCE CHARACTERISTICS

Ionization: total current, $1-5 \cdot 10^{-7}$ A; unit charges/s, $0.6-3 \cdot 10^{12}$; droplet diameter^a, *ca.* 1–2 μm .

	<i>Ion sampling (nozzle-skimmer or capillary inlet-skimmer) efficiency^b</i>		
	<i>% of total ionization</i>	<i>Current (A)</i>	<i>Total ions/s^c</i>
Through nozzle ^d	$\approx 10^{-2}$	$\approx 2 \cdot 10^{-9}$	$\approx 10^{10}$
Focused into quadrupole	$\approx 10^{-4}$	$\approx 2 \cdot 10^{-11}$	$\approx 10^8$
Detected ^e	$\approx 10^{-5}$	$\approx 2 \cdot 10^{-12}$	$\approx 10^7$

^a Estimated at *ca.* 0.3 cm from capillary using 10^{-4} M electrolyte solution of water-methanol (50:50) solution. Droplets generally become too small to be visible ($< 0.3 \mu\text{m}$) at 0.5 cm from capillary.

^b Approximate performance measured using a quadrupole mass spectrometer described in ref. 1. We assume $2 \cdot 10^{-7}$ A total ESI current.

^c For a singly charged species.

^d 1-mm-diameter nozzle or a slightly larger capillary bore giving an equivalent gas flow.

^e At m/z 1000 based upon both direct Faraday cup current measurements and ion counting utilizing an electron multiplier.

Fig. 1 gives ESI-mass spectra obtained for aqueous solutions of horse heart cytochrome *c* (M_r 12 360) by direct infusion at 0.5 to 1 $\mu\text{l}/\text{min}$ using the sheath flow ESI interface¹. Spectra were acquired in 90-s scans for solution concentrations ranging from $1.5 \cdot 10^{-4}$ M (Fig. 1A) to $1.5 \cdot 10^{-8}$ M (Fig. 1F). For the most dilute solution a spectrum of quality adequate for M_r determination required only 23 fmol of cytochrome *c*. The mass spectra are dominated by the distribution of multiply protonated molecular ions, but other contributions are also evident. For example, Fig. 1B shows a scale expansion ($\times 36$) for the most concentrated solution (Fig. 1A). The spectrum shows a number of small peaks between m/z 550 and m/z 850 which may be due to small contributions of collisional dissociation in the nozzle-skimmer interface for the most highly charged species^{29,30}. For lower charge states small contributions which correspond to multiply charged dimers are also evident.

At cytochrome *c* concentrations below *ca.* $2 \cdot 10^{-5}$ M, two additional observations pertain. First, the relative intensities shifts of higher charge states increase and become nearly independent of solution concentration. Second, the lower charge states show contributions of adduct ions (of 98 ± 2 a.m.u.) giving a series of small peaks on the high m/z side of each molecular ion. At lower cytochrome *c* concentrations, the relative size of these adduct contributions is nearly constant. This is fortunate since the assumption of molecular ion protonation utilized for M_r determination (although strictly unnecessary²⁸) remains valid and unchanged at very low sample concentrations^{4,27,28}. Fig. 2 gives the peak intensity of the 10+ to 18+ charge states as a function of analyte flow-rate. Peak intensity increases nearly linearly with sample concentration. Such results suggest that high sample concentrations result in formation of ions *with reduced charge state rather than lower ionization efficiency*. Thus, although the peak intensity for the most abundant charge state is "saturated",

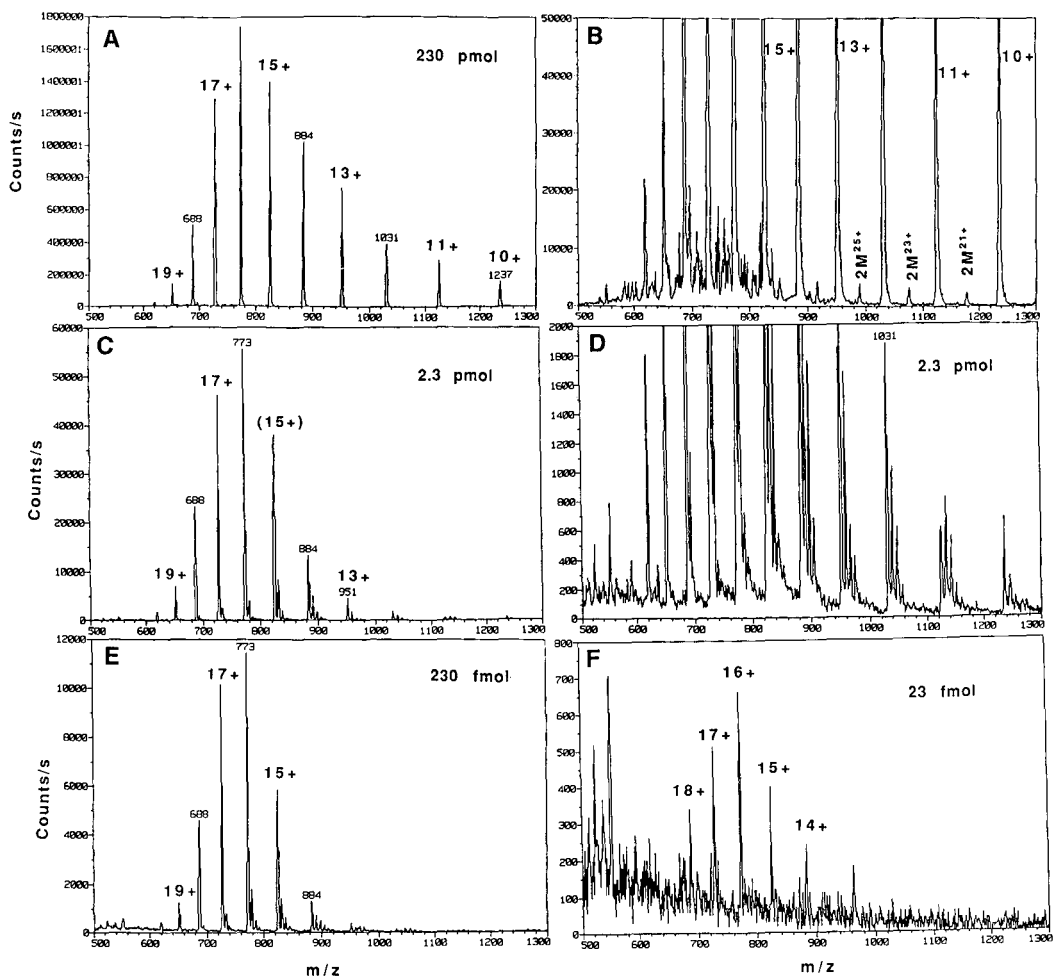


Fig. 1. ESI-MS spectra of cytochrome *c* obtained at sample flow-rates of $1 \mu\text{l}/\text{min}$ for sample concentrations ranging from $1.5 \cdot 10^{-4} M$ to $1.5 \cdot 10^{-8} M$, consuming from 230 pmol (A) to 23 fmol (F) during 90-s spectrum acquisition periods.

a nearly linear correlation between peak intensity and concentration is still obtained for the lower charge states.

One of the most striking aspects of the ESI process is that it appears to approach unit ionization efficiency. Even at *present levels* of instrument performance, it is conceivable that useful spectra of small proteins such as cytochrome *c* might be obtained with as little as 1 fmol. The “background” in Fig. 1F is likely due to trace impurities (in solvents, on capillary surfaces, etc.). The actual detector “noise” amounts to <4 counts/s. Thus, a more limited scan range (*e.g.*, m/z 600–1000) and reduced background might accomplish this goal. However, such a situation would be realistic only for very clean samples (unlikely for “real world” applications) or with on-line sample clean-up and separation using capillary electrophoresis. Since currently

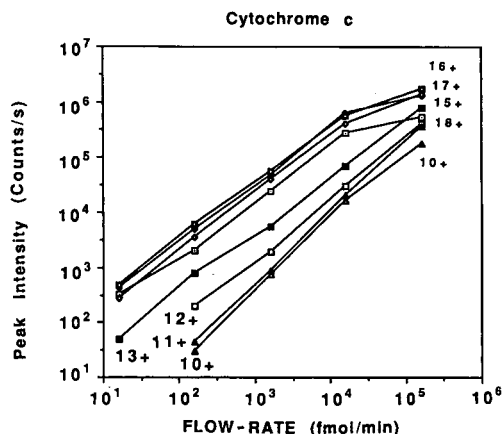


Fig. 2. Intensities of various charge states for ESI-MS of cytochrome *c* as a function of concentration (see Fig. 1).

only *ca.* 10^{-5} of all ions formed by ESI are typically detected, attention to the factors limiting instrument performance may provide a basis for extension of ESI-MS for proteins into the attomole regime.

The ability to obtain spectra for higher- M_r compounds is also crucially dependent upon instrument performance, but at very high M_r is ultimately limited due to the charge state distribution. As M_r increases, so does the average number of charges, the number of charge states, and the "peak width" as evident from our previous publications^{4,31}. The increased peak width is ascribed to currently unresolved contributions of solvent attachment, charge carrying adducts (either anionic or cationic), and, perhaps most importantly, sample heterogeneity⁴. As shown in Table II these factors reduce the maximum peak intensity obtainable. For example, we expect that a protein of M_r 10 000 would give a maximum peak intensity about a factor of 50 lower than for a singly charged species *at concentrations which saturate the ESI process*. Saturation of the ESI process will occur at *ca.* 10 times lower concentration for the larger protein due to its higher charge state; thus larger sample concentrations do not increase maximum peak intensity. Detection of a protein of M_r 100 000 would require instrumental performance *ca.* 10^4 better than necessary for singly charged species ionized with equal efficiency. Our experience to date with a wide range of proteins extending to over 200 000 M_r is consistent with these expectations³¹. The variable levels of success for analysis of larger proteins obtained at different laboratories may partially reflect this aspect of instrument performance.

Useful ESI-MS for very large proteins will require both more efficient mass spectrometers as well as a reduction in the "peak width" contribution. Studies in our laboratory³¹ with proteins of $M_r > 200\ 000$ have produced spectra with an unresolved "hump", consistent with expectations from Table II. Such a result is useless for M_r determination. Additionally, spectra of oligonucleotides suggest the maximum M_r addressable by ESI with current instrumentation may be somewhat lower (perhaps $< 100\ 000$) due to the slightly lower ion currents in the negative ion mode and the greater peak widths due to unresolved sodium attachment³¹.

TABLE II
DEPENDENCE OF SIGNAL INTENSITY UPON MOLECULAR MASS

M_r	Average number of charges ^a	Approximate number of charge states ^b	Peak "width" (m/z) ^c	Maximum intensity (ions/s) ^d
1000	1	1	1	10^{12}
10 000	10	5	1	$2 \cdot 10^{10}$
40 000	40	20	3	$4 \cdot 10^8$
100 000	100	50	6	$3 \cdot 10^7$
200 000	200	100	(6) ^e	$(8 \cdot 10^6)^f$

^a We assume the average number of charges increases linearly with M_r , and the distribution is centered about m/z 1000.

^b Estimated from existing data and assuming all charge states are equally intense. This approximation tends to somewhat underestimate maximum peak intensity.

^c Peak width due to sample micro heterogeneity (apparently typical of large biopolymers) and uncertain contributions of impurities, solvent adduction, etc. Approximated from available data.

^d ESI production before sampling losses and assuming *ca.* 80% ionization efficiency. Detected ion intensities for current MS instrumentation are at least 10^4 to 10^5 lower due to losses due to inefficiencies arising from ion sampling, transmission and detection (see Table I).

^e Peak width of 6 m/z units is too large for individual charge states to be resolved; a peak width of ≤ 4 would be required.

^f For a peak width of 6 m/z units (see note *e*).

Finally, the sample concentration necessary to "saturate" the ESI peak intensity decreases nearly linearly with the average charge state, from *ca.* 10^{-4} *M* for a singly charged species to 10^{-6} *M* for a protein of M_r 100 000 with an average of *ca.* 100 charges/molecule. Thus, an efficiently ionized peptide or protein will saturate the ESI signal at sample concentrations of *ca.* 0.1 $\mu\text{g}/\mu\text{l}$ for a 1 $\mu\text{l}/\text{min}$ flow-rate, if ions are produced efficiently with an average m/z of *ca.* 1000. A proportionally lower ionization efficiency and threshold for ESI saturation are obtained at higher flow-rates since ESI ion current is nearly independent of flow-rate.

CONCLUSIONS

Within the past year, ESI-MS has exploded onto the biochemical community, with new applications developing at an increasing pace, especially for peptide and protein analysis. Currently, well over 100 large polypeptides and proteins (a conservative estimate), with at least half of these materials having $M_r > 10$ 000, have been successfully analyzed³¹.

The correspondence between CE and ESI flow-rates and the fact that both are facilitated by (and primarily used for) ionic species in solution provide the basis for an extremely attractive combination^{6,8} based upon ESI-MS. Small peptides are easily amenable to capillary zone electrophoresis (CZE)-MS analysis with good reproducibility. High efficiency separations of a series of dynorphin and enkephalin peptides have been demonstrated, with over 250 000 theoretical plates obtained by CZE-ion spray-MS⁵. Complex mixtures of peptides generated from tryptic digestion of large proteins are well suited to CZE-MS analysis, as shown by Lee *et al.*⁷. Since trypsin

specifically cleaves peptide bonds C-terminally at lysine and arginine, the resulting peptides will tend to form doubly charged as well as singly charged molecular ions. This allows most large tryptic peptides to be within the m/z range of most quadrupole mass spectrometers. Lee *et al.*⁷ have demonstrated this approach for a tryptic digest from recombinant bovine somatotropin. Doubly charged molecular ions of the peptides dominate the mass spectrum. A CZE-MS daughter ion spectrum from one of the components was used to confirm the identity of a hexapeptide. Initial application of CZE-MS to proteins has been demonstrated at our laboratory³².

Capillary isotachopheresis (CITP) is an attractive complement to CZE, and is ideally suited for combination with mass spectrometry. We have demonstrated the feasibility of CITP-MS for quaternary phosphonium and ammonium salts, amino acids, and catecholamides⁶ and various polypeptides⁸. CITP is well suited to low concentration samples where the amount of solution is relatively large, whereas CZE is ideal for the analysis of minute quantities of solution. Sample size which can be addressed by CITP are much greater (>100-fold) than CZE. CITP results in concentration of analyte bands, which is in contrast to the inherent dilution with CZE. Electromigration injection allows effective sample volumes to be much larger still due to enrichment during migration into the capillary from low-ionic-strength samples⁶. Detection limits of approximately 10^{-11} M have been demonstrated for quaternary phosphonium salts, and substantial improvements appear feasible⁶. Analytes elute in CITP as bands where the length of the analyte band provides information regarding analyte concentration. Most importantly, however, is that CITP provides a relatively pure analyte band to the ESI source, without the large concentration of a supporting electrolyte demanded by CZE. Thus, CITP-MS has the potential of allowing much greater sensitivities (and analyte ion currents) than feasible with CZE-MS due to more efficient analyte ionization. The relatively wide and concentrated separated bands in CITP facilitates MS-MS experiments (which often requires more concentrated samples than tolerated by CZE). These characteristics make CITP-MS-MS well suited for characterization of enzymatic digests of proteins⁹. Recent results also suggest that useful sequence-related information may be obtained by direct MS-MS of proteins³³.

ACKNOWLEDGEMENTS

We thank the National Institute of General Medical Sciences (GM 42940) and the National Science Foundation (DIR 8908096) for support of this research.

REFERENCES

- 1 R. D. Smith, C. J. Barinaga and H. R. Udseth, *Anal. Chem.*, 60 (1988) 1948.
- 2 J. A. Olivares, N. T. Nguyen, C. R. Yonker and R. D. Smith, *Anal. Chem.*, 59 (1987) 1230.
- 3 R. D. Smith, J. A. Olivares, N. T. Nguyen and H. R. Udseth, *Anal. Chem.*, 60 (1988) 436.
- 4 J. A. Loo, H. R. Udseth and R. D. Smith, *Anal. Biochem.*, 179 (1989) 404.
- 5 E. D. Lee, W. Mück, J. D. Henion and T. R. Covey, *J. Chromatogr.*, 458 (1988) 313.
- 6 H. R. Udseth, J. A. Loo and R. D. Smith, *Anal. Chem.*, 61 (1989) 228.
- 7 E. D. Lee, W. Mück, J. D. Henion and T. R. Covey, *Biomed. Environ. Mass Spectrom.*, 18 (1989) 844.
- 8 R. D. Smith, J. A. Loo, C. J. Barinaga, C. G. Edmonds and H. R. Udseth, *J. Chromatogr.*, 480 (1989) 211.

- 9 R. D. Smith, S. M. Fields, J. A. Loo, C. J. Barinaga and H. R. Udseth, *Electrophoresis*, in press.
- 10 C. G. Edmonds, J. A. Loo, C. J. Barinaga, H. R. Udseth and R. D. Smith, *J. Chromatogr.*, 474 (1989) 21.
- 11 M. A. Moseley, L. J. Deterding, K. B. Tomer and J. W. Jorgenson, *J. Chromatogr.*, 480 (1989) 197.
- 12 R. M. Caprioli, W. T. Moore, M. Martin, B. B. DaGue, K. Wilson and S. Moring, *J. Chromatogr.*, 480 (1989) 247.
- 13 J. Zeleny, *Phys. Rev.*, 10 (1917) 1.
- 14 M. Dole, L. L. Mack, R. L. Hines, R. C. Mobley, L. D. Ferguson and M. B. Alice, *J. Chem. Phys.*, 49 (1968) 2240.
- 15 L. L. Mack, P. Kralik, A. Rheude and M. Dole, *J. Chem. Phys.*, 52 (1970) 4977.
- 16 J. J. Hogan, R. S. Carson, J. M. Schneider and C. D. Hendricks, *AIAA. J.*, 2 (1964) 1460.
- 17 E. W. Muller, *Phys. Rev.*, 102 (1956) 618.
- 18 V. G. Drozin, *J. Colloid. Sci.*, 10 (1955) 158.
- 19 D. Michelson and J. D. Shorey, *Nucl. Instrum. Methods*, 82 (1970) 295.
- 20 G. I. Taylor, *Proc. R. Soc. London, A*, 280 (1964) 383.
- 21 B. Vonnegut and L. Neubauer, *J. Colloid Sci.*, 7 (1952) 616.
- 22 V. E. Krohn, *J. Appl. Phys.*, 45 (1974) 1144.
- 23 A. G. Bailey, *Atomisation Spray Technol.*, 2 (1986) 95.
- 24 V. E. Krohn and G. R. Ringo, *Appl. Phys. Lett.*, 27 (1975) 479.
- 25 M. Yamashita and J. B. Fenn, *J. Phys. Chem.*, 88 (1984) 4671.
- 26 A. P. Bruins, T. R. Covey and J. D. Henion, *Anal. Chem.*, 59 (1987) 2642.
- 27 C. K. Meng, M. Mann and J. B. Fenn, *Z. Phys. D: At. Mol. Clusters*, 10 (1988) 361.
- 28 M. Mann, C. K. Meng and J. B. Fenn, *Anal. Chem.*, 61 (1989) 1702.
- 29 R. D. Smith, J. A. Loo, C. J. Barinaga, C. G. Edmonds and H. R. Udseth, *J. Am. Soc. Mass Spectrom.*, 1 (1990) 53.
- 30 R. D. Smith, C. J. Barinaga and H. R. Udseth, *J. Phys. Chem.*, 93 (1989) 5019.
- 31 R. D. Smith, J. A. Loo, C. G. Edmonds, C. J. Barinaga and H. R. Udseth, *Anal. Chem.*, 62 (1990) 882.
- 32 J. A. Loo, H. K. Jones, H. R. Udseth and R. D. Smith, *J. Microcolumn Sep.*, 1 (1989) 223.
- 33 J. A. Loo, C. G. Edmonds and R. D. Smith, *Science (Washington, D.C.)*, 248 (1990) 201.

CHROM. 22 557

Capillary zone electrophoresis–mass spectrometry using a coaxial continuous-flow fast atom bombardment interface

M. A. MOSELEY

Laboratory of Molecular Biophysics, National Institute of Environmental Health Sciences, P.O. Box 12233, Research Triangle Park, NC 27709, and Department of Chemistry, University of North Carolina at Chapel Hill, Chapel Hill, NC 27514 (U.S.A.)

L. J. DETERDING and K. B. TOMER*

Laboratory of Molecular Biophysics, National Institute of Environmental Health Sciences, Research Triangle Park, NC 27709 (U.S.A.)

and

J. W. JORGENSON

Department of Chemistry, University of North Carolina at Chapel Hill, Chapel Hill, NC 27514 (U.S.A.)

ABSTRACT

Mixtures of peptides have been analyzed by capillary zone electrophoresis in conjunction with mass spectrometry (MS) using an on-line coaxial continuous-flow fast atom bombardment interface. MS and MS–MS spectra have been acquired in electrophoretic real time from femtomole levels of the peptides, while maintaining separation efficiencies in excess of 100 000 theoretical plates.

INTRODUCTION

Capillary zone electrophoresis (CZE) has proven to be an exceptionally useful analytical tool for the analysis of mixtures of ionic analytes. The high separation efficiency of CZE permits the separation of complex mixtures, and its ability to analyze non-volatile and/or thermally labile species permits the study of biopolymers. The use of mass spectrometry (MS) as a detector for CZE is advantageous since qualitative information about the structure of the analytes can be obtained.

The first successful interface between CZE and MS was reported by Smith and co-workers^{1–3} consisting of an electrospray ionization (ESI) interface at atmospheric pressure in conjunction with a quadrupole mass spectrometer. Lee *et al.*^{4,5} have also reported the successful coupling of CZE with MS using another atmospheric pressure ionization source—an ion-spray interface (which is a variation of electrospray ionization) coupled with a triple quadrupole mass spectrometer.

In late 1988 work was begun in our laboratories on the coupling of CZE with MS using a modification of the coaxial system developed for coupling open tubular liquid chromatography with continuous-flow fast atom bombardment (coaxial CF-FAB)

MS^{6,7}. The online coaxial continuous-flow CZE-FAB-MS system has been shown^{8,9} to be capable of separating peptide mixtures with separation efficiencies of hundreds of thousands of plates, with limits of detection of less than 10 fmol. Caprioli *et al.*¹⁰ and Reinhold *et al.*¹¹ have also coupled CZE with CF-FAB-MS using a liquid junction interface.

Since the initial reports of the coupling of CZE with MS using coaxial CF-FAB^{8,9}, several design modifications have been made to the interface probe. These modifications are reported here, along with applications of the system to the analysis of chemotactic peptides and neuropeptides, under both positive and negative ionization conditions. An example of the suitability of the CZE-coaxial CF-FAB-MS interface for the acquisition of MS-MS data in electrophoretic real time is also given.

EXPERIMENTAL

The fundamentals of our CZE-coaxial CF-FAB-MS interface have been previously reported^{8,9}. In this coaxial interface the fused-silica CZE column (13 to 15 μm I.D., 150 μm O.D.) is inserted into the fused-silica sheath column (200 μm I.D., 350 μm O.D.) through which the FAB matrix solution is pumped via a syringe pump ($\mu\text{LC-500}$, Isco, Lincoln, NE, U.S.A.). All fused-silica capillary columns were obtained from Polymicro Technologies (Phoenix, AZ, U.S.A.). A 1/16-in. (1.59-mm) stainless-steel tee with vespel ferrules (400 μm I.D.) is used to couple the two capillaries. This tee is mounted in the plexiglass handle on the end of the FAB probe shaft. While in practice the CZE capillary can be threaded through the sheath column from either direction, it has been noted that threading from the 1/16-in. tee towards the FAB probe tip is preferred. Arcing between the inside and outside of the CZE capillary (leading to formation of a hole in the capillary wall) occurs more readily when the CZE column has been threaded from tip to tee.

The FAB matrix used with the CZE-FAB-MS system was glycerol-water (25:75), modified with either heptafluorobutyric acid (pH 3.5) or ammonium hydroxide (pH 9), at a flow-rate of approximately 0.5 $\mu\text{l}/\text{min}$. Proper flow-rate of the FAB matrix is readily determined by an observed lack of matrix ions in the mass spectrum (too little flow), or by CZE peak tailing (too much flow). The matrix solution transfer line from the pump to the tee incorporates a 0.5- μm in-line frit filter and a 3 m \times 25 μm I.D. fused-silica pressure restriction column to provide sufficient backpressure to the syringe pump for stable operation. The FAB matrix modifiers served both to provide ions for electrical contact between the FAB tip and the CZE column effluent, and to modify the pH of the solution on the FAB probe tip, increasing the production of protonated or deprotonated molecular ions for the MS detection of analytes. Note that this allows the analytes to be separated as either negative or positive ions within the CZE column and detected as either negative or positive ions by the mass spectrometer.

The two coaxial capillary columns terminate at the stainless-steel FAB probe tip (Fig. 1). An important feature of this CZE interface is that the FAB probe tip is used as the electrical "ground" of the CZE system. Thus, active electrophoretic transport of the analytes occurs through the CZE column to the FAB probe tip where ion desorption takes place. This arrangement obviates the use of a transfer line from the end of the CZE capillary to the FAB probe tip. This precludes any zone broadening

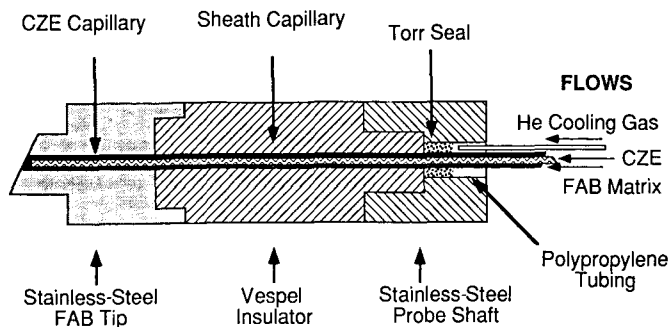


Fig. 1. On-line CZE-coaxial CF-FAB-MS probe tip.

that would occur within the transfer line used between the CZE column and the FAB probe tip, and in the connections between the CZE column and the transfer line. This FAB probe tip is electrically insulated from the probe shaft with a vespel insulator. The sheath column must fit very snugly within the FAB probe tip such that the FAB matrix solution cannot flow back inside the FAB tip. A loose fit between the sheath column and the probe tip will cause the ion source pressure to fluctuate, and consequently, ion intensities. Placement of a septum, teflon tape or Torr Seal in the probe tip helps prevent backflow.

The CZE high-voltage power supply (Glassman High Voltage, Princeton, NJ, U.S.A.) is maintained between -38 to $+38$ kV (depending upon the nature of the CZE-MS experiment), while the FAB probe tip is maintained at a potential of 8 kV for the detection of positive ions, and -8 kV for the detection of negative ions. The potential drop across the CZE column is ± 30 kV per meter. A safety interlock system incorporating a high-voltage relay (Model H-25, Kilovac, Santa Barbara, CA, U.S.A.) is used for operator safety, such that opening the lid of the sample/buffer box immediately shorts the CZE high-voltage electrode to ground potential. The high-voltage relay/safety interlock circuit incorporates a timer so that high-voltage switching can be performed for electromigration sample introductions.

Through the length of the FAB probe shaft, the two coaxial fused-silica capillary columns are contained within a polypropylene capillary (1.2 mm I.D., 1.9 mm O.D.), which serves to minimize the possibility of electrical shorts between the coaxial capillaries and the stainless-steel probe shaft. A fused-silica capillary column (200 μm I.D., 350 μm O.D.) is inserted into this polypropylene capillary from the plexiglass handle, terminating near the vespel insulator between the probe shaft and the FAB tip. This fused-silica capillary is used to purge the probe shaft with helium in order to cool the coaxial capillaries, and thus minimize the formation of temperature gradients within the capillaries.

Mass spectrometry

The mass spectrometer used in this work is a VG ZAB-4F (VG Analytical, Manchester, U.K.) four sector mass spectrometer of $B_1E_1E_2B_2$ geometry. An Ion Tech FAB gun was used with xenon as the FAB gas (8 kV at 1 mA). The desorbed ions were accelerated to 8 keV for analysis, and mass spectra were acquired by scanning MS-I (B_1E_1) and detecting the ions with a photomultiplier tube based detector located

in the third-field free region. MS-MS spectra were acquired by using MS-I to select the parent ions and focus them into the collision cell located in the third field-free region. Helium was used as the collision gas (50% parent ion beam suppression). Daughter ion spectra were acquired by a linked scan at constant B/E of MS-II (E_2B_2) with daughter ion detection in the fifth-field free region with a photomultiplier tube based detector. Nominal pressures were $2 \cdot 10^{-5}$ Torr in the ion source, and $5 \cdot 10^{-9}$ Torr in the analyzers.

Chemicals

The morphiceptin, proctolin, Phe-Leu-Glu-Glu-Ile (FLEEI), Met-Leu-Phe (MLF), Val-Gly-Val-Ala-Pro-Gly (VGVAPG), N-formyl Met-Leu-Phe (N-formyl MLF), and glycerol were obtained from Sigma (St. Louis, MO, U.S.A.) and were used as delivered. The water used in the preparation of all sample and buffer solutions had a resistance of $> 15 \text{ M}\Omega$ (Milli-Q System, Millipore, Bedford, MA, U.S.A.). Acetic acid, ammonium acetate, ammonium hydroxide and heptafluorobutyric acid were obtained from Aldrich (Milwaukee, WI, U.S.A.). Sample and buffer solutions are degassed and filtered ($0.2 \mu\text{m}$ pore size) immediately prior to use.

RESULTS AND DISCUSSION

The use of volatile buffers such as ammonium acetate has been found to be required for the long term stability of the CZE-MS analysis. The use of non-volatile buffers such as potassium phosphate leads to an unstable ion beam, as well as the formation of potassium adducts of the peptides, $(M + K)^+$, $(M + 2K - H)^+$ (ref. 9), which reduces the intensity of the protonated molecular ion, $(M + H)^+$. All data presented in this report were obtained using a 0.005 M ammonium acetate buffer, the pH of which was adjusted to 8.5 using ammonium hydroxide. At this pH all peptides had a net negative charge except for those peptides containing more than one arginine and/or lysine amino acid. Conversion of the negatively charged species to positive ions for MS detection was accomplished by using a FAB matrix acidified to pH 3.5 with heptafluorobutyric acid.

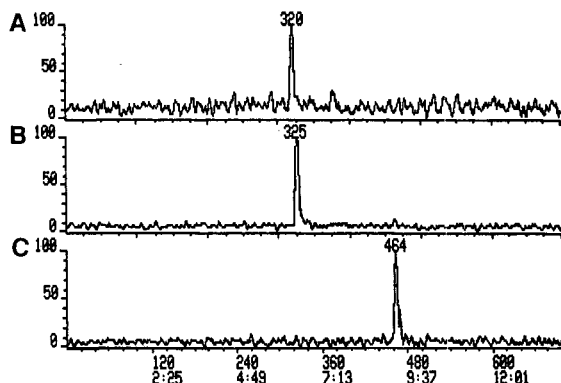


Fig. 2. Single ion electropherograms of the protonated molecular ions of (A) morphiceptin (30 fmol, number of plates $N = 91\ 000$), (B) proctolin (24 fmol, $N = 120\ 000$), and (C) FLEEI (24 fmol, $N = 190\ 000$). Time in min:s.

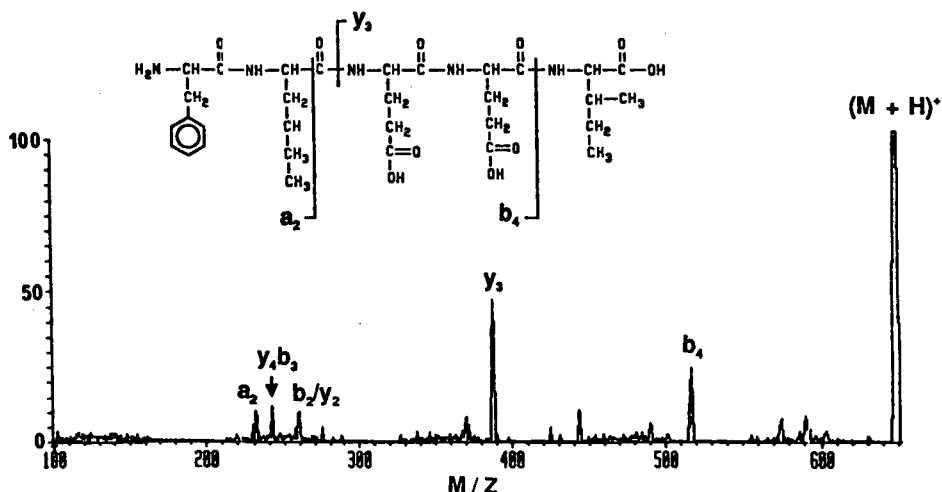


Fig. 3. On-line CZE-MS-MS spectrum of FLEEI.

The CZE-MS analysis of a mixture of three neuropeptides is given in Fig. 2. The sample ($2 \cdot 10^{-4} M$) was introduced onto the CZE column using an electromigration sample introduction for 2 s at a potential of 6 kV. This corresponds to the introduction of between 24 to 30 fmol per component, with separation efficiencies ranging from 91 000 plates for morphiceptin to 190 000 plates for FLEEI.

The CZE-coaxial CF-FAB-MS interface has been used for the acquisition of MS-MS data in electrophoretic real time. In order to acquire CZE-MS-MS data with our system multiple analysis are performed. The first analysis is used to identify the mass-charge ratios of the analytes (parent ions). The analysis is then repeated, with the parent ions being subjected to collisionally activated dissociation, yielding an MS-MS daughter ion spectrum. As an example, Fig. 3 gives the on-line CZE-coaxial FAB-MS-MS spectrum of the pentapeptide FLEEI, obtained from a peptide mixture at a concentration of $1.5 \cdot 10^{-4} M$. The MS-MS daughter ion spectrum contains sufficient structural information to confirm the identity of the parent ion.

The utility of CZE-MS for the analysis of low levels of peptides and their impurities is exemplified by the analysis of chemotactic peptides given in Fig. 4. This mixture of VGVAPG (14 fmol) and MLF (16 fmol) was found to contain an impurity peak, the mass-charge ratio of which is 16 units above that of MLF, suggesting the possibility of an oxidation product of MLF. MS-MS analysis of the impurity peak revealed that a fraction of the MLF in solution had been oxidized, with the site of oxidation being on the methionine side chain. The total amount of MLF injected onto the CZE column was approximately 16 fmol, and the signal-to-noise ratios of the two single ion electropherograms suggest that approximately 1/3 of the MLF had oxidized (assuming equivalent FAB-MS response factors for MLF and oxidized MLF).

In the majority of our applications, peptides are separated by CZE as negative ions but detected by MS as positive ions. The change in charge takes place on the tip of the FAB probe, where the basic CZE buffer mixes with the acidic FAB matrix (pH 3.5). Since the flow-rate of the FAB matrix solution is at least an order of magnitude higher than the CZE electroosmotic flow-rate, the buffer's capacity is exhausted, and the

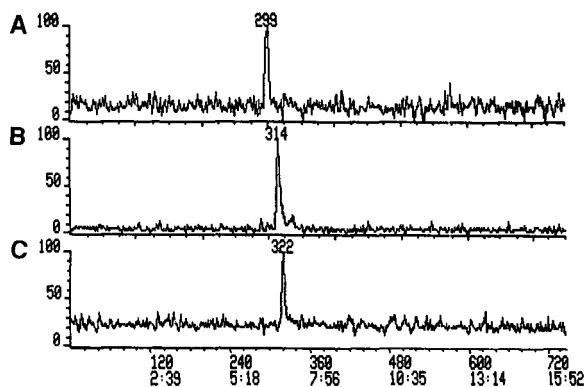


Fig. 4. Single ion electropherograms of the protonated molecular ions of (A) VGAPG (14 fmol, $N = 10\,000$), (B) MLF (<16 fmol, $N = 31\,000$), and (C) oxidized MLF (<16 fmol, $N = 32\,000$).

conversion to positive ion readily occurs. The CZE-coaxial CF-FAB-MS system can easily be used for the detection of negative ions by adding ammonium hydroxide to the FAB matrix (pH 9). This is illustrated by the CZE-MS analysis of MLF and N-formyl MLF as negative ions (Fig. 5). The detectivity of these negative ions (MLF, 150 fmol, N-formyl MLF, 46 fmol) with this system is within an order of magnitude of that observed when detecting them as positive ions.

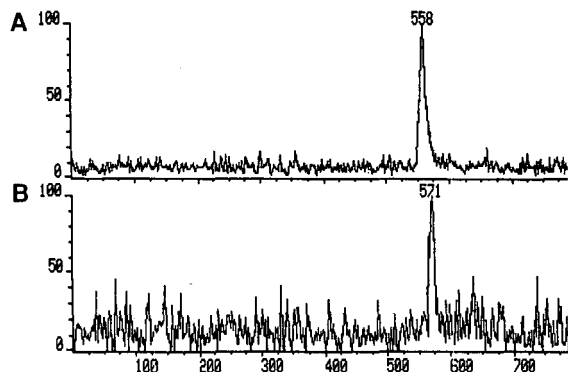


Fig. 5. Single ion electropherograms of the deprotonated molecular ions of (A) MLF (150 fmol) and (B) N-formyl MLF (46 fmol).

CONCLUSIONS

The on-line CZE-coaxial CF-FAB-MS system has been used for the acquisition of MS and MS-MS data in electrophoretic real time from femtomole levels of peptides, with separation efficiencies in excess of 100 000 plates. The ability of the coaxial interface to independently deliver the CZE effluent and the FAB matrix to the FAB probe tip permits the independent optimization of the composition and flow-rate of the two fluids, yielding experimental flexibility, as illustrated by the CZE separation of analytes as negative ions, with their MS detection as either positive or negative species.

REFERENCES

- 1 J. A. Olivares, N. T. Nguyen, C. R. Yonker and R. D. Smith, *Anal. Chem.*, 59 (1987) 1230.
- 2 R. D. Smith, C. J. Baringa and H. R. Udseth, *Anal. Chem.*, 60 (1988) 1948.
- 3 R. D. Smith, J. A. Olivares, N. T. Nguyen and H. R. Udseth, *Anal. Chem.*, 60 (1988) 436.
- 4 E. D. Lee, W. Mück, J. D. Henion and T. R. Covey, *J. Chromatogr.*, 458 (1988) 313.
- 5 E. D. Lee, W. Mück, J. D. Henion and T. R. Covey, *Biomed. Environ. Mass Spectrom.*, 18 (1989) 253.
- 6 J. S. M. DeWit, L. J. Deterding, M. A. Moseley, K. B. Tomer and J. W. Jorgenson, *Rapid Commun. Mass Spectrom.*, 2 (1988) 100.
- 7 M. A. Moseley, L. J. Deterding, K. B. Tomer, R. T. Kennedy, N. L. Bragg and J. W. Jorgenson, *Anal. Chem.*, 61 (1989) 1577.
- 8 M. A. Moseley, L. J. Deterding, K. B. Tomer and J. W. Jorgenson, *Rapid Commun. Mass Spectrom.*, 3 (1989) 87.
- 9 M. A. Moseley, L. J. Deterding, K. B. Tomer and J. W. Jorgenson, *J. Chromatogr.*, 480 (1989) 197.
- 10 R. M. Caprioli, W. T. Moore, M. Martin, B. B. DaGue, K. Wilson and S. Moring, *J. Chromatogr.*, 480 (1989) 247.
- 11 N. J. Reinhoud, W. M. A. Niessen, U. R. Tjaden, L. G. Gramberg, E. R. Verheij and J. van der Greef, *Rapid Commun. Mass Spectrom.*, 3 (1989) 348.

CHROM. 22 560

Identification of aprotinin degradation products by the use of high-performance capillary electrophoresis, high-pressure liquid chromatography and mass spectrometry

ANDERS VINTHER*

Department of Fermentation Physiology, Novo-Nordisk A/S, DK-2820 Gentofte (Denmark)

SØREN E. BJØRN

Protein Biochemistry, Novo-Nordisk A/S, DK-2880 Bagsværd (Denmark)

HANS HOLMEGAARD SØRENSEN

Analytical Development, Novo-Nordisk A/S, DK-2820 Gentofte (Denmark)

and

HENRIK SØBERG

Department of Chemical Engineering, The Technical University of Denmark, DK-2800 Lyngby (Denmark)

ABSTRACT

A preparation of bovine aprotinin, bovine pancreatic trypsin inhibitor, was subjected to high-performance capillary electrophoresis (HPCE) analysis and the purity was calculated to be approximately 80%. The two dominating contaminants were integrated to approximately 7% each as compared to the intact molecule. Characterization by high-pressure liquid chromatographic (HPLC) and mass spectrometric analysis was carried out on digests of the reduced and alkylated molecules. The contaminants were identified as truncated aprotinin, missing one and two amino acids, respectively, at the C-terminus. No such structures were identified in similar amounts in preparations of recombinant aprotinin by HPLC or HPCE.

INTRODUCTION

Aprotinin consists of 58 amino acids in a single polypeptide chain, which is cross-linked by three disulphide bridges¹ (Fig. 1). The molecular mass is 6512 and the isoelectric point close to 10.5. A very compact tertiary structure makes the molecule extremely stable against physical and chemical stress and proteolytic degradation. Aprotinin has a relatively broad inhibitory specificity¹, and has found use as a therapeutic agent based on its inhibition of serine proteases, *e.g.*, in the treatment of acute pancreatitis. It strongly inhibits trypsin as well as chymotrypsin, plasmin and kallikreins of different origin.

Since high-performance capillary electrophoresis (HPCE) was introduced by Mikkers *et al.*² and Jorgenson and Lukacs³ as an instrumental approach to

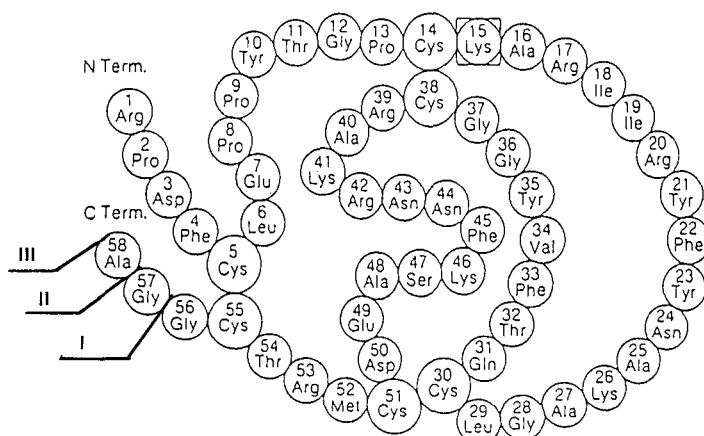


Fig. 1. Primary structure of aprotinin, bovine pancreatic trypsin inhibitor. The inhibitor consists of a single polypeptide chain of 58 amino acids cross-linked by three disulphide bridges. The molecular mass is 6512 and the isoelectric point is close to 10.5.

electrophoresis, the method has shown great promise for the high-resolution separation of charged species. Among the areas of special interest is the characterization of peptides and proteins⁴⁻⁹, *e.g.*, for purity control.

Polypeptides and proteins may adsorb to the fused-silica capillary column due to electrostatic interactions between the peptide and the negatively charged surface of the capillary. Dependent on the techniques available and the actual peptide preparations of interest, these interactions can be minimized/eliminated in four different ways. First, the peptide is repelled from the negatively charged capillary surface, when electrophoresis is performed at higher pH values than the isoelectric point of the peptide, due to the negative net charge of the peptide^{10,11}. Second, physical coating of the capillary wall, by *e.g.*, polyacrylamide¹² or via silane derivatization¹³ deactivates the capillary surface. Third, dynamic coating by the addition of ionic species to the buffer solution^{14,15} results in a competition between the peptide and the cationic species for the adsorption sites on the capillary surface. Finally, lowering the pH of the running buffer below the isoelectric point of the peptide results in a positively charged ion, but at the same time some of the negative charge will be titrated off the capillary wall, hence lowering the coulombic interactions between the capillary surface and the peptide^{11,13}. Due to the high isoelectric point of aprotinin and its high stability at low pH¹, we chose the latter approach by performing the electrophoresis at a pH value of 2.5, where most of the negative charge is titrated off the fused-silica capillary wall¹¹.

HPCE has a very high resolving power, but contaminants/degradation products are not identified directly with this technique. The standard analytical approach for characterization of the contaminants is fraction collection and further analysis. However, at present the amount of material that can be collected in HPCE is not sufficient for further analysis (*e.g.*, amino acid sequencing). Direct coupling of HPCE and another analytical method, *e.g.*, mass spectrometry¹⁶, is one way to circumvent this problem. Without direct coupling, characterization of the contaminants might be accomplished either by subjecting the samples to enzymatic or chemical treatment

prior to analysis, or by spiking with known structures. In order to identify the two dominating contaminants, bovine aprotinin preparations were spiked with fractions collected from reversed-phase high-performance liquid chromatography (HPLC) of bovine aprotinin and identified by plasma desorption mass spectrometry (PD-MS).

EXPERIMENTAL

Materials

Bovine and recombinant aprotinin were from Novo-Nordisk (Bagsværd, Denmark). *Armillaria mellea* protease was a gift from Lars Thim, Novo-Nordisk, and had been purified according to published procedures¹⁷. Ammonium sulphate, dithiothreitol (DTT), hydrochloric acid and ammoniumhydrogencarbonate were from Merck (Darmstadt, F.R.G.); acetonitrile was from Rathburn (Walkerburn, U.K.); trifluoroacetic acid (TFA), sequenal grade, was purchased from Pierce (Oud-Beijerland, The Netherlands); 4-vinylpyridine and Tris (Trizma Base) were from Sigma (St. Louis, MO, U.S.A.); guanidinium hydrochloride was from Serva (Heidelberg, F.R.G.); ethanol was from Danisco (Aalborg, Denmark) and citrate buffer for HPCE analysis was from Applied Biosystems (Foster City, CA, U.S.A.).

Methods

HPLC. An analytical Vydac C4 column (code 214TP54, The Separations Group, Hesperia, CA, U.S.A.) was used throughout at 1.5 ml/min with 0.1% TFA and 2% (w/w) ammonium sulphate as eluent A and 0.07% TFA in acetonitrile as eluent B. For HPLC of native aprotinin a linear gradient was run from 5–25% B in 20 min with detection at 220 nm. Three fractions of material were collected and desalted by use of the same system except that ammonium sulphate was omitted. For HPLC of pyridylethylated material a linear gradient was run from 5–45% B in 20 min with detection at 254 nm. For peptide mapping an isocratic elution with eluent A for 5 min was followed by elution with a linear gradient from 0–25% B in 25 min and detection at 214 nm.

Vinylpyridylethylation. Salt-free samples of approximately 50 nmol aprotinin were concentrated to nearly dryness in a vacuum centrifuge and 120 μ l of water, 40 μ l of 2 M Tris-HCl pH 7.5, 100 mg guanidinium hydrochloride and 2.2 mg of DTT were added. Reduction was carried out under nitrogen at 37°C for 2 h. Alkylation with 6 μ l of 4-vinylpyridine was then performed at room temperature in the dark. The reaction was stopped after 30 min with the addition of 5 mg solid DTT. The pyridylethyl derivatives were purified by HPLC.

Proteolytic digestion. The HPLC-purified pyridylethyl derivatives were concentrated in a vacuum centrifuge and 400 μ l of 0.1 M ammoniumhydrogencarbonate pH 7.9 was added. Half of the material (approximately 25 nmol) was incubated at 37°C for 4 h together with 1 nmol *Armillaria mellea* protease.

PD-MS. Fractions from HPLC containing peptides of the proteolytic digestions were dried by vacuum centrifugation and redissolved in 200 μ l 0.1% TFA. Aliquots were mixed with an equal volume of ethanol and 5 μ l samples, approximately 100 pmol peptide, were applied nitrocellulose coated targets (BIO-ION Nordic, Uppsala, Sweden) for mass analysis¹⁸. PD-MS analysis was carried out in positive mode on a ²⁵²Californium time of flight mass spectrometer (BIO-ION Nordic). PD-MS spectra were collected for 1 million fission events.

HPCE. Analysis was performed on Applied Biosystems Model 270A analytical capillary electrophoresis system. The fused-silica capillaries (Polymicro Technologies, Phoenix, AZ, U.S.A.) had an internal diameter of 50 μm , with a total length of 100 cm, and a distance of 75 cm to the detector. By applying a vacuum at the detector end of the capillary tube for 1 s, samples were introduced. The samples were diluted with distilled water to a concentration of 0.5 mg/ml. A 20 mM citrate buffer (pH 2.5) was used as running buffer. The applied potential was 20 kV and the temperature 27°C. The electropherograms were obtained at 200 nm with a risetime of 1.0 s.

RESULTS AND DISCUSSION

Fig. 2a and b shows the electropherograms of bovine and recombinant aprotinin, respectively. While the dominating peak could be integrated to more than 99% of the total area in the electropherogram of the recombinant aprotinin, the electropherogram of the bovine aprotinin revealed several contaminants/degradation products, and the full-length molecule, 1–58 (III, Fig. 2a) was integrated to approximately 80% of the total area. The two dominating contaminants (I and II, Fig. 2a) eluted non-resolved in front of the main peak. An area of 5–9% could be calculated for each of the peaks I and II. Areas were normalized to migration time to account for variable rates of movement through the detector. None of these two contaminants were present in similar amounts in the electropherogram of the recombinant aprotinin (Fig. 2b).

The running buffer had a pH value of 2.5. Electrophoresis at higher pH values, but below the isoelectric point of aprotinin, resulted in adsorption of the aprotinin

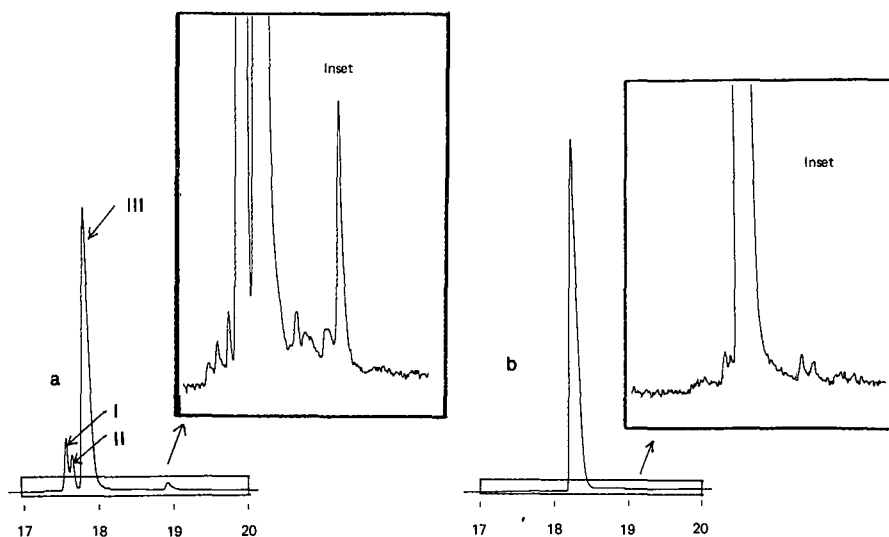


Fig. 2. HPCE electropherograms, obtained at 200 nm, of bovine and recombinant aprotinin. Samples were introduced by applying a vacuum for 1 s. A citrate buffer (pH 2.5) was used as running buffer. The field strength was 200 V/cm and the temperature 27°C. (a) Bovine aprotinin. I–III corresponds to HPLC fractions I–III (Fig. 3). (b) Recombinant aprotinin. All retention times are in minutes. The insets display the electropherograms at higher sensitivity for 17–20 min as indicated by the boxes in the figures.

molecules to the capillary wall. Hence, the results in Fig. 2 show that the charge density of the capillary surface is a very important factor in performing electrophoresis below the isoelectric point of the highly alkaline aprotinin peptide. At very low pH values, most of the negative surface charge is titrated off the fused-silica capillary wall, and the coulombic interactions between the positively charged aprotinin molecules and the capillary surface are minimized, thus avoiding aprotinin adsorption.

Analysis of bovine aprotinin by reversed-phase HPLC showed major resemblance with the corresponding HPCE electropherogram as shown in Fig. 3. Again the main peak was integrated to approximately 80% and preceded by the two dominating contaminants, which also in this analysis eluted as non-resolved peaks. Fractions I-III were collected for further analysis.

HPLC fractions I and II analyzed by HPCE indicated that they were heterogenous by being contaminated with material from at least one of the other fractions (Fig. 4b and c). Spiking analysis demonstrated that fractions I and II were detected in the same order in the HPCE analysis as they were eluted from the HPLC column (Fig. 4d and e). The reason for the relative differences in peak height of fractions I and II in Figs. 2a and 3 might be due to the better resolution of the two fractions in HPCE compared to HPLC. In the HPLC chromatogram (Fig. 3), the number of theoretical plates seems to be considerably lower for fraction I compared to fraction II. Hence, due to tailing of fraction I, the HPLC-collected fraction II is more contaminated with fraction I (Fig. 4c), than the opposite (Fig. 4b). The close elution of the material in the three fractions by HPLC and HPCE, two separation principles with high resolving power, indicates that the material is closely related.

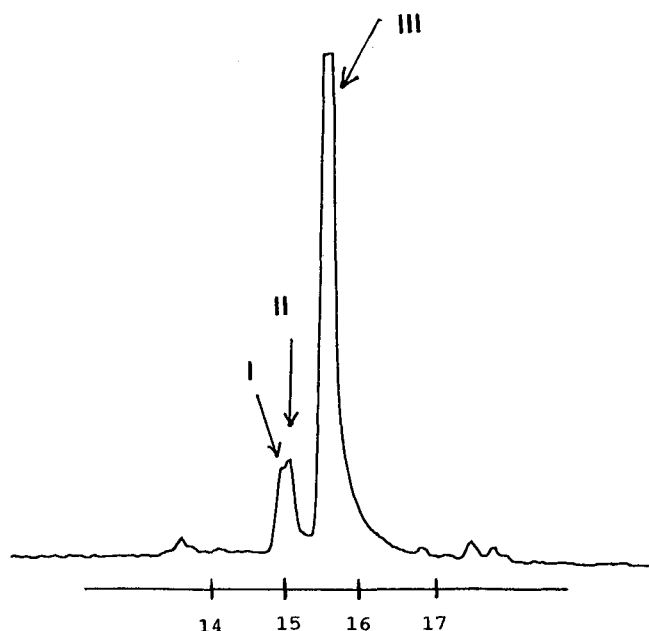


Fig. 3. Reversed-phase HPLC of bovine aprotinin. A linear gradient was run from 5–25% B in 20 min with detection at 220 nm. Eluent A: 0.1% TFA and 2% (w/w) ammonium sulphate, eluent B: 0.07% TFA in acetonitrile. Fractions I-III were collected for further analysis. The x-axis scaling is in minutes.

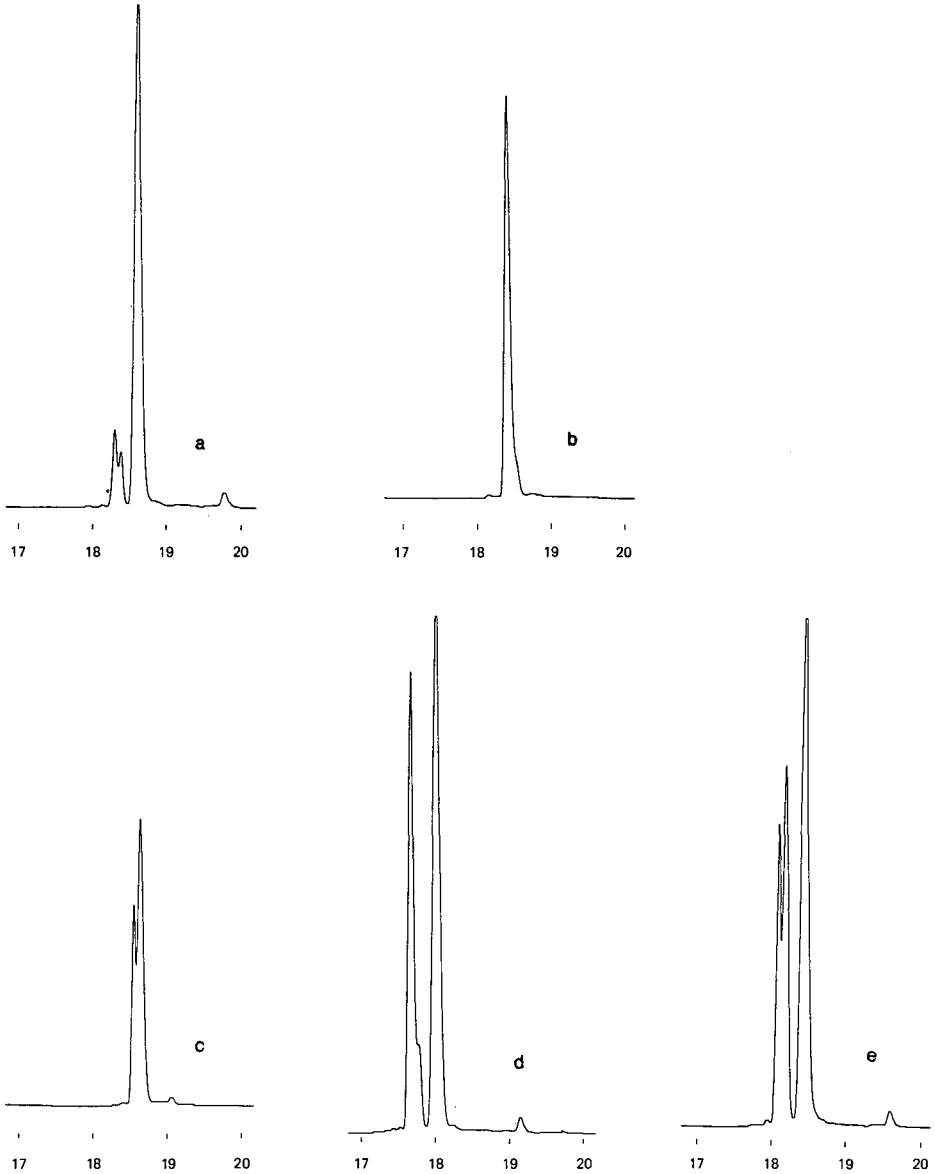


Fig. 4. Electropherograms of HPCE spiking analysis of fractions I and II. The experimental conditions are described in the legend to Fig. 2. a = Bovine aprotinin (1-58), b = fraction I (1-56), c = fraction II (1-57), d = bovine aprotinin spiked with fraction I, e = bovine aprotinin spiked with fraction II. All retention times are in minutes.

Equal amounts of the bovine material, collected as fractions I-III, were reduced and alkylated with 4-vinylpyridine. The derivatives were separated from reagent surplus by preparative reversed-phase HPLC.

Aliquots of the derivatives were digested with *Armillaria mellea* protease which cleaves selectively at the N-terminal side of the lysine residues. Reversed-phase HPLC of the digested, pyridylethylated material, originating from fractions I-III, gave

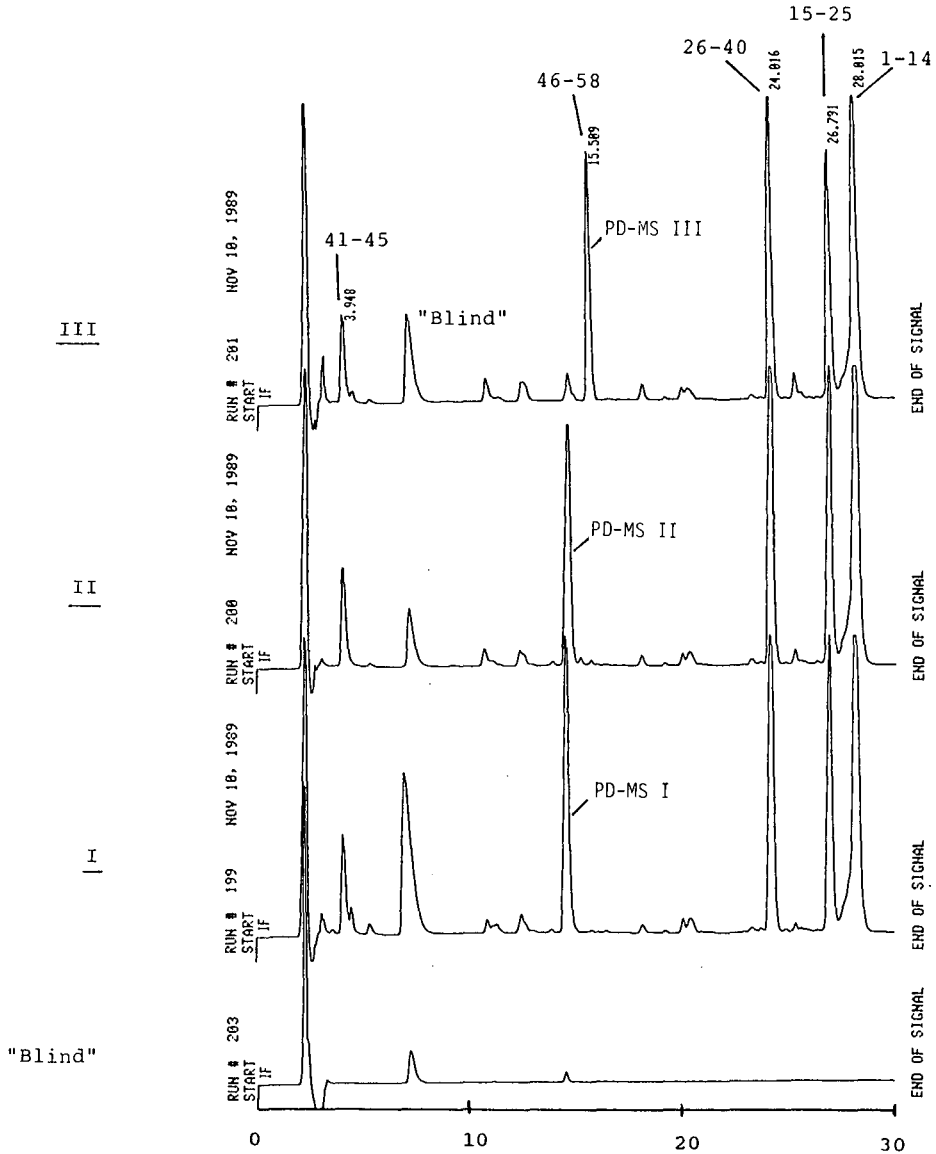


Fig. 5. Elution pattern from HPLC of pyridylethylated bovine aprotinin preparations I-III (Fig. 3) digested with *Armillaria mellea* protease. A "blind"-digest is shown for reference. An isocratic elution with eluent A for 5 min preceded elution with a linear gradient from 0-25% B in 25 min and detection at 214 nm. The eluents are described in the legend to Fig. 3. Fractions were collected for mass analysis (PD-MS) as indicated. The five peptides obtained after digestion of the bovine aprotinin are identified in chromatogram III by their amino acid residue numbers in the intact molecule. The four chromatograms are shown with the same x-axis scaling shown at the bottom line of the figure. All retention times are in minutes.

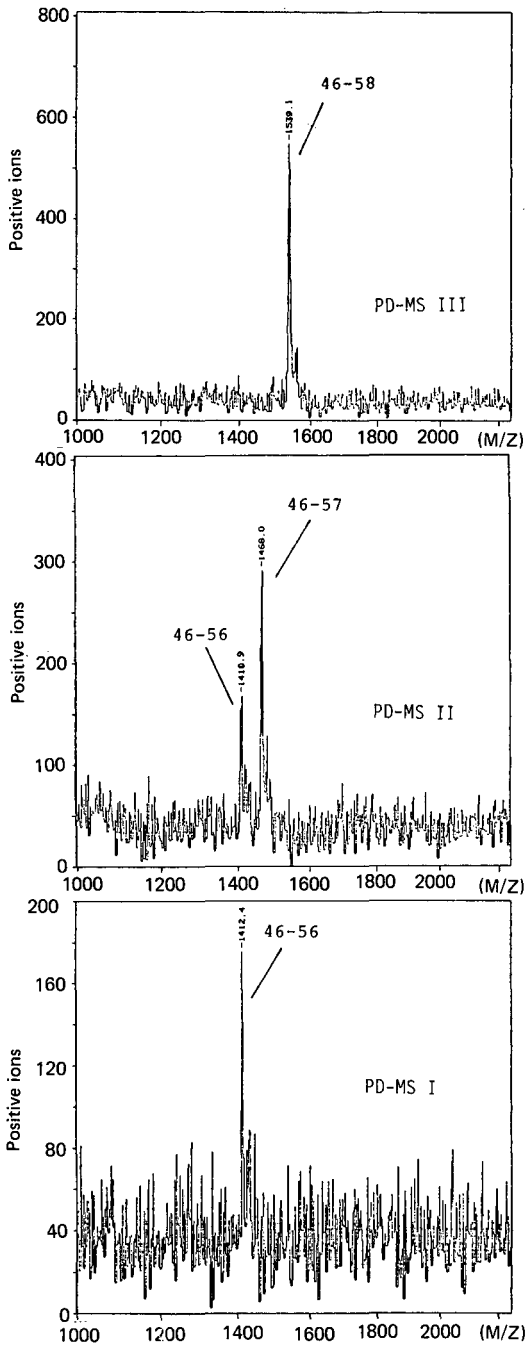


Fig. 6. PD-MS spectra of HPLC-purified carboxy-terminal fragments of pyridylethylated bovine aprotinin preparations I-III after digestion with *Armillaria mellea* protease. PD-MS spectra were collected for 1 million fission events. Fragments: Lys₄₆-Gly₅₆: 1410.7; Lys₄₆-Gly₅₇: 1456.7; Lys₄₆-Ala₅₈: 1538.8 dalton.

almost identical elution patterns (Fig. 5). This strongly indicates that the primary structure of the material collected in fractions I and II is very similar to the primary structure of full-length aprotinin (fraction III).

Primary sequence has unambiguously been assigned to the peaks in the corresponding HPLC chromatogram derived from the full-length aprotinin (fraction III). This was obtained by PD-MS analysis and amino acid sequencing. The corresponding chromatogram has been labeled accordingly (Fig. 5). No peak with a retention time corresponding to the C-terminal fragment Lys₄₆-Ala₅₈ was identified in the HPLC chromatograms derived from fractions I and II, but in both cases an earlier eluting peak of equal size was observed and the material collected (Fig. 5, PD-MS I and II). This peak was absent in the chromatogram derived from the digest of the derivatized full-length molecule. In addition the fraction containing the C-terminal fragment Lys₄₆-Ala₅₈ was collected (Fig. 5, PD-MS III).

PD-MS was used to assess the molecular masses of the fragments collected in fractions PD-MS I-III. Molecular ions, MH⁺, were assigned to C-terminal fragments for all three fractions (Fig. 6). As expected the intact C-terminal fragment, Lys₄₆-Ala₅₈, was assigned to the major molecular ion obtained for fraction PD-MS III. The two major molecular ions in the mass spectra of fractions PD-MS II and PD-MS I had lower molecular masses and were assigned to truncated C-terminal fragments of aprotinin missing one (Ala₅₈) and two (Ala₅₈, Gly₅₇) amino acids, respectively. It is observed, that the relative amounts of the two molecular ions in the two fractions (PD-MS I and PD-MS II) obtained in Fig. 6 are in accordance with the results obtained by HPCE (Fig. 4b and c).

It is most likely that the degradation products [des-Ala(58)-aprotinin and des-Ala-Gly(58,57)-aprotinin] detected in the electropherogram (Fig. 2a) and the chromatogram (Fig. 3) of bovine aprotinin are due to the presence of proteolytic enzymes during purification procedures, e.g., carboxypeptidases.

The resolution of the two truncated aprotinin molecules in these particular HPCE and HPLC systems was better in HPCE (Fig. 2a) than in HPLC (Fig. 3), though baseline separation was not obtained. Hence, HPCE can be used as an alternative to reversed-phase HPLC as a standard analytical procedure for aprotinin purity control.

The results as discussed above show how spiking of the bovine aprotinin starting material with species of known sequence, identified by the combined use of HPLC and PD-MS, can be accomplished as a method for the identification of some of the bovine aprotinin contaminants/degradation products.

ACKNOWLEDGEMENT

The Danish Academy of Technical Sciences is acknowledged for financial support.

REFERENCES

- 1 H. Fritz and G. Wunderer, *Arzneim. Forsch.*, 33 (1983) 479.
- 2 F. E. P. Mikkers, F. M. Everaerts and Th. P. E. M. Verheggen, *J. Chromatogr.*, 169 (1979) 11.
- 3 J. W. Jorgenson and K. D. Lukacs, *Anal. Chem.*, 53 (1981) 1298.
- 4 H. Lüdi, E. Gassmann, H. Grossenbacher and W. Märki, *Anal. Chim. Acta*, 213 (1988) 215.

- 5 P. Puma, P. Young, R. Karol and M. Fuchs, presented at *1st International Symposium on High-Performance Capillary Electrophoresis, Boston, MA, 1989*, paper MP126.
- 6 P. D. Grossmann, J. C. Colburn, H. H. Lauer, R. G. Nielsen, R. M. Riggin, G. S. Sittampalam and E. C. Rickard, *Anal. Chem.*, 61 (1989) 1186.
- 7 R. Palmieri and J. Rampal, presented at *1st International Symposium on High-Performance Capillary Electrophoresis, Boston, MA, 1989*, paper MP130.
- 8 J. Frenz, S.-L. Wu and W. S. Hancock, *J. Chromatogr.*, 480 (1989) 379.
- 9 R. G. Nielsen, R. M. Riggin and E. C. Rickard, *J. Chromatogr.*, 480 (1989) 393.
- 10 H. H. Lauer and D. McManigill, *Anal. Chem.*, 58 (1986) 166.
- 11 P. D. Grossmann, K. J. Wilson and H. H. Lauer, *Anal. Biochem.*, 173 (1988) 265.
- 12 S. Hjertén, *J. Chromatogr.*, 347 (1985) 191.
- 13 R. M. McCormick, *Anal. Chem.*, 60 (1988) 2322.
- 14 J. S. Green and J. W. Jorgenson, *J. Chromatogr.*, 478 (1989) 63.
- 15 M. M. Bushey and J. W. Jorgenson, *J. Chromatogr.*, 480 (1989) 301.
- 16 R. D. Smith, J. A. Loo, C. J. Barinaga, C. G. Edmonds and H. R. Udseth, *J. Chromatogr.*, 480 (1989) 211.
- 17 W. G. Lewis, J. M. Basford and P. L. Walton, *Biochim. Biophys. Acta*, 522 (1978) 551.
- 18 G. P. Jonson, A. B. Hedin, P. L. Håkansson, B. U. R. Sundqvist, B. G. S. Säve, P. F. Nielsen, P. Roepstorff, K. Johansson, I. Kamensky and M. S. L. Lindberg, *Anal. Chem.*, 58 (1986) 1084.

CHROM. 22 555

Continuous sample collection in capillary zone electrophoresis by coupling the outlet of a capillary to a moving surface

XIAOHUA HUANG^a and RICHARD N. ZARE*

Department of Chemistry, Stanford University, Stanford, CA 94305 (U.S.A.)

ABSTRACT

Use of an on-column frit structure, constructed by sintering a mixture of glass powders, makes it possible to ground a fused-silica capillary on its side prior to its outlet. Electroosmotic pressure permits convenient sample collection. We illustrate the use of this device by depositing the eluent in a continuous manner on a moving surface. This provides a permanent record of the separated species in a mixture.

INTRODUCTION

Capillary zone electrophoresis (CZE) is rapidly becoming a powerful separation method for the analysis of complex mixtures, particularly those involving biomolecules in aqueous media^{1–4}. Most applications involve on-column detection of the species of interest as a function of time to produce an electropherogram. Collection is made difficult because the capillary outlet is usually placed in a large reservoir containing milliliters of electrolyte and one of the electrodes. The volumes of the sample zones are typically nanoliters, so that the dilution factor is on the order of 10^6 . A second problem is the remixing of the separated species in the outlet reservoir.

Several different approaches have been taken to overcome these problems so that the eluent can be collected. Rose and Jorgenson⁵ move the capillary outlet from one small fraction collector to another in a programmed manner. A similar technique involving interruption of the applied voltage has been employed by Cohen *et al.*⁶. Both these methods have the disadvantage that the capillary outlet must contact electrolyte in the fraction collector to complete an electrical circuit. This causes some dilution of the sample as well as raises the problem of possible interference from electrochemical reaction at the outlet electrode inside the fraction collector. However, it is a simple matter to reconcentrate the fraction collected by evaporation, and electrochemical reactions are often minimal.

^a Present address: Genomix, 460 Point San Bruno Boulevard, South San Francisco, CA 94080, U.S.A.

Recently, we have developed an alternative approach for sample collection. In this method the electrical circuit is completed in the capillary prior to its outlet⁷. This is achieved by making a frit structure in the sidewall of the capillary about 1–2 cm before its outlet. This frit allows electrical connections to be made to the capillary so that the first segment of the capillary (inlet to frit) may be used for electrokinetic separations while the second segment (frit to outlet) may be used for field-free eluent collection because the electroosmotic flow in the first segment pumps eluent through the second segment. Measurements show that the leakage of eluent through the frit is nearly negligible; more than 90% of an injected sample can be collected⁷.

In this paper we illustrate the use of a capillary with an on-column frit for sample collections in which we couple the capillary outlet to a moving surface (filter paper placed on the periphery of a plastic disc). In this way we are able to deposit continuously the eluent along a track on the filter paper, which becomes a recording of the separation. This record may be subsequently read by some detection scheme, such as fluorescence, or it may be interfaced to another separation method, such as paper or thin-layer chromatography.

EXPERIMENTAL

Construction of apparatus

The description of how to fabricate the frit structure has been presented elsewhere⁷. Briefly, a focused CO₂ laser makes a slightly tapered hole about 40 μm in diameter on the side of the fused-silica capillary wall (75 μm I.D., 360 μm O.D., Polymicro Technologies, Phoenix, AZ, U.S.A.). Next, a mixture of glass powders is used to cover this hole and is sintered in place. Finally, a protective jacket is carefully attached, and the entire frit structure is surrounded by a reservoir of electrolyte containing a Pt electrode. The yield of acceptable frit structures is presently about 50%. Once an acceptable frit structure has been made, no degradation in performance has been observed during months of operation.

Fig. 1 shows how the capillary outlet is interfaced to a moving surface. The particular configuration we have chosen is a rotating wheel whose speed of revolution

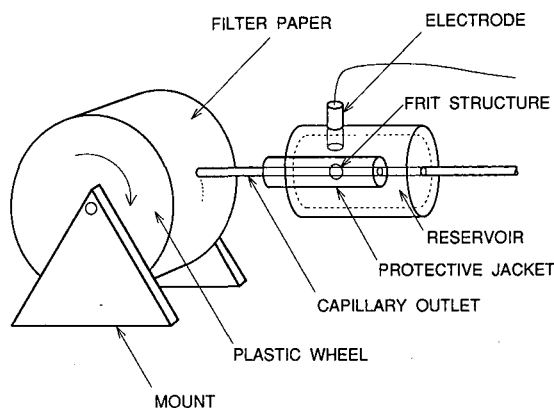


Fig. 1. Experimental setup for continuously depositing eluent onto a moving surface.

is controlled by a variable gear train attached to an electric motor. The periphery of the wheel is covered with a strip of filter paper (No. 41-01870; Schleicher & Schüll, Keene, NH, U.S.A.). The rate of linear displacement is variable but we typically operate at 0.1 mm/s. The position of the capillary outlet is adjusted so that it lightly touches the moving surface.

In order to view the capillary outlet during CZE separation, we use a 50 \times microscope (5 \times objective, 10 \times eyepiece) attached to a 35 mm SLR camera (Nikon FE). We also use UV fluorescence to view the eluent track on the filter strip. A photograph is made by irradiating the filter strip with a portable UV lamp (Model UV6-11; UVP, San Gabriel, CA, U.S.A.). For some runs it is convenient to use on-column detection. This is accomplished using UV absorption (Model UVIDEX-100 V; Japan Spectroscopic Co., Tokyo, Japan).

Chemicals

All chemicals are from Sigma (St. Louis, MO, U.S.A.) and are used without further purification. Buffer consists of 10 mM phosphate at a pH of 6.8. Water used to prepare solutions is freshly deionized and distilled with a water purifier (Model LD-2A coupled with a Mega-Pure automatic distiller, Corning Glassworks, Corning, NY, U.S.A.).

RESULTS AND DISCUSSION

Fig. 2. shows the droplet formation at the capillary outlet during CZE operation. The conditions were phosphate buffer with no sample injection. The electric field strength was 300 V/cm. Fig. 2a shows the capillary outlet before starting a run. Fig. 2b is a picture of the outlet *ca.* 1 s later, and Fig. 2c is *ca.* 3 s later. This last figure illustrates the formation of an eluent droplet with a volume of *ca.* 15 nl. Thus, we are able to visualize directly the pumping action of the electroosmotic flow in the first segment of the capillary (between the inlet and the ground through the frit structure).

In previous work⁷, we collected the eluent for a fixed period of time in a 0.5-ml disposable microcentrifuge tube. By weighing the contents of the microcentrifuge tube we were able to determine that the flow-rate is linear with time. Moreover, we could reinject the collected sample to demonstrate that we were able to collect separate fractions of a mixture. We investigated the reproducibility of this collection scheme and found a coefficient of variance of less than 11%.

In this paper we report the "direct writing" of the eluent onto a moving surface, using the experimental setup described in Fig. 1. A three-component mixture of dansylated amino acids, *ca.* $1 \cdot 10^{-3}$ M each, was injected by raising the inlet of the capillary about 7 cm higher than the outlet for 10 s. This procedure gives an injection volume of about 20 nl. The electric field strength was again 300 V/cm. Fig. 3 shows a picture of the resulting filter paper strip under UV irradiation. For convenience, a ruler has been placed in this picture the origin of which is located at the start of electrophoresis. Three fluorescent spots are clearly visible in Fig. 3. The spot at shortest distance from the origin is dansyl-Arg, the next spot is dansyl-Ser, and the last spot is dansyl-Glu. Each spot corresponds to a few picomoles of the dansylated amino acid.

In a subsequent study, we have cut out one of the three spots, eluted the spot with

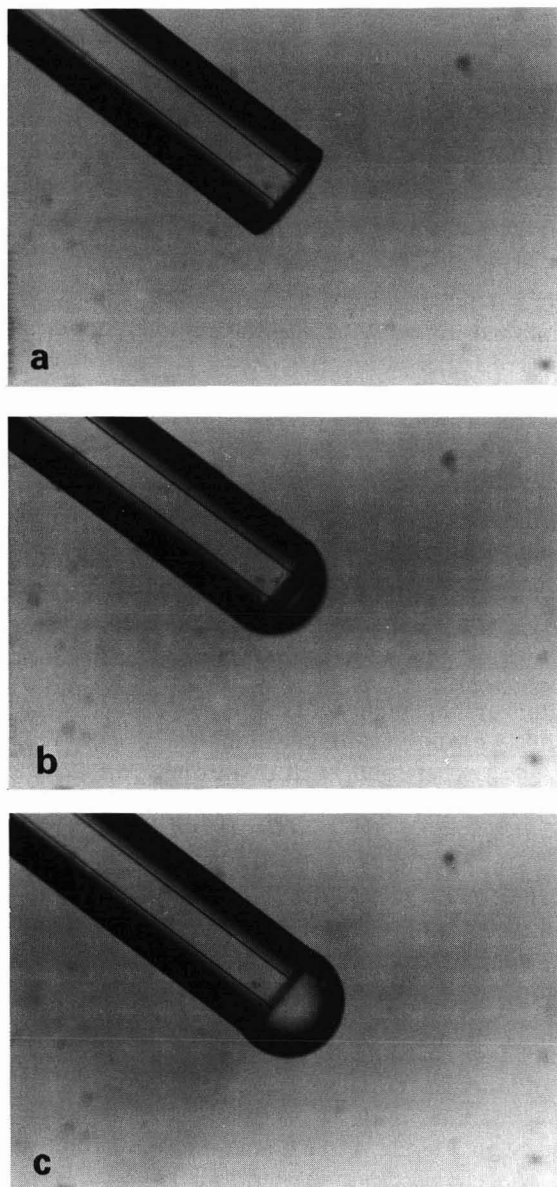


Fig. 2. Microphotographs ($50\times$) of droplet formation at the outlet of a capillary having an on-column frit structure: (a) at start of electrophoresis, (b) *ca.* 1 s after start of electrophoresis, and (c) *ca.* 3 s after start of electrophoresis.

methanol, dried the methanol extract, redissolved the residue with $1\ \mu\text{l}$ of buffer, and reinjected this sample. Using the on-column UV detector, we could easily see a single peak at a migration time corresponding to the dansyl amino acid injected. This simple procedure is able to recover more than 90% of the originally injected analyte.

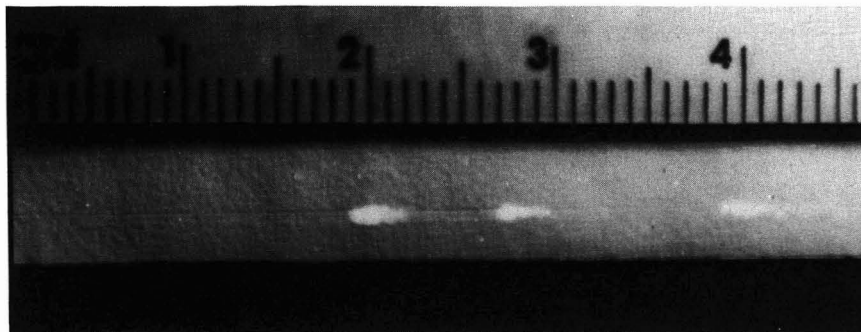


Fig. 3. Photograph of filter paper strip under UV irradiation (254 nm), showing fluorescence from the deposition of three dansylated amino acids. A ruler has been included to indicate length along track; the origin of the ruler is located at the start of the electrophoretic run.

This collection procedure has many advantages compared to writing with the outlet of a normal capillary on wet filter paper placed on a metal plate to complete the circuit. We found that the latter procedure suffered from the difficulty of maintaining the filter paper sufficiently wet to make good electrical contact but sufficiently dry to avoid extensive spreading of the spot. In addition to providing a convenient permanent record of the separated species in a mixture, the present device can also serve as the interface to another separation scheme, such as paper or thin-layer chromatography, so that "two-dimensional separations" are obtained. It is also possible to use this procedure to improve detection, such as taking autoradiographic exposures of the record track after radiolabels⁸ are used to tag components in the mixture.

ACKNOWLEDGEMENTS

We thank R.T. (Skip) Huckaby, Electrical Engineering Department, Stanford University, for assistance in constructing the frit structure. This work is supported by Beckman Instruments, Inc.

REFERENCES

- 1 J. Jorgenson and K. D. Lukacs, *Science (Washington, D.C.)*, 222 (1983) 266.
- 2 M. J. Gordon, X. Huang, S. L. Pentoney, Jr. and R. N. Zare, *Science (Washington, D.C.)*, 242 (1988) 224.
- 3 A. G. Ewing, R. A. Wallingford and T. M. Olefirowicz, *Anal. Chem.*, 61 (1989) 292A.
- 4 R. A. Wallingford and A. G. Ewing, *Adv. Chromatogr.*, 29 (1989) 1.
- 5 D. J. Rose and J. W. Jorgenson, *J. Chromatogr.*, 438 (1988) 23.
- 6 A. S. Cohen, D. R. Najarian, A. Paulus, A. Guttman, J. A. Smith and B. L. Karger, *Proc. Natl. Acad. Sci. U.S.A.*, 85 (1988) 9660.
- 7 X. Huang and R. N. Zare, *Anal. Chem.*, 62 (1990) 443.
- 8 S. L. Pentoney, Jr., J. F. Quint and R. N. Zare, in J. Nikelly and Cs. Horváth (Editors), *Separations in Analytical Biotechnology (ACS Symposium Series)*, American Chemical Society, Washington, DC, in press.

CHROM. 22 679

Thermal model of capillary electrophoresis and a method for counteracting thermal band broadening

WILLIAM A. GOBIE and CORNELIUS F. IVORY*

Department of Chemical Engineering, Washington State University, Pullman, WA 99164 (U.S.A.)

ABSTRACT

Thermal band broadening is known to be caused by the temperature dependence of ionic mobility. This dependence also strongly influences the temperature of the capillary by providing positive feedback between the temperature and power density. Previous thermal models of capillary electrophoresis have not fully considered this “autothermal effect”. We show that it always causes a capillary to run hotter than is predicted by a constant conductivity model; temperature excursions two times greater are typical.

We propose that the thermally induced parabolic distortion of the migration velocity can be countered with an opposing Poiseuille (pressure-driven) flow. Dispersion calculations indicate that it may be possible to obtain plate numbers in excess of 10^6 m^{-1} even in very large bore ($400 \mu\text{m}$) capillaries.

INTRODUCTION

Capillary electrophoresis (CE) is characterized by voltage gradients of 100–300 V/cm. Depending upon the buffer conductivity, power density can reach 1 kW/cm^3 . A significant radial temperature gradient arises as a consequence in the capillary lumen. Jorgenson and Lukacs¹ pointed out that such gradients may cause band broadening through thermal Taylor dispersion²: In the warmer region near the center of the lumen, the temperature dependence of electrophoretic mobility increases migration velocities relative to the wall region. The solute band is distorted in a parabolic fashion, as sketched in Fig. 1 (where we depict a solute that migrates opposite the direction of electroosmotic flow). Radial molecular diffusion tends to average out radial concentration variations, so that dispersion appears to proceed by a diffusive rather than convective mechanism. Grushka *et al.*³ have investigated this effect mathematically, and find that this mechanism can indeed produce significant band broadening.

It is known from large-scale electrophoresis⁴ that the temperature dependence of the buffer ions' mobility strongly influences the buffer temperature through the “autothermal effect”. As the buffer in an electrophoresis apparatus warms due to the passage of current, its conductivity rises. If the power supply is operated in

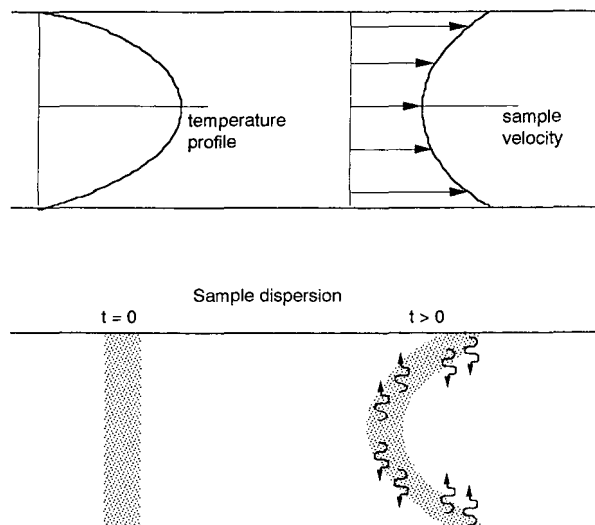


Fig. 1. Taylor dispersion in a heated capillary. The temperature profile in the lumen distorts the sample's electrophoretic velocity. Molecular diffusion ameliorates the effect by radially averaging the concentration. The sample is depicted migrating opposite the direction of electroosmotic flow. t = time.

a constant-voltage mode, the current will increase, thereby increasing the power dissipated in the buffer and warming the buffer further. The apparatus always runs hotter than a constant-conductivity model would predict. Further, there is a critical voltage above which a temperature increase produces a greater increase in Joule heating than in heat transfer to the coolant. Under such conditions the device experiences "autothermal runaway". This phenomenon places an absolute limit on the voltage which may be used, and is not predicted by a constant conductivity model.

Grushka *et al.*³ omitted the autothermal effect on the grounds that the difference between the autothermal and constant-conductivity temperature profiles is rather small in CE⁵ and does not justify the additional mathematical complexity. This is often the case. But since one of our purposes here is to examine modifications to CE which will permit operation with significant temperature gradients, we shall employ the more rigorous model.

Since thermal Taylor dispersion is due to a nearly parabolic variation in electrophoretic velocity, we realized that it might be possible to compensate for the variation by opposing it with a small Poiseuille flow, as depicted in Fig. 2. Hertén⁶ has used a Poiseuille flow to compensate for electroosmotic dispersion in closed-end tubes, where the goal was to flatten the hydrodynamic velocity profile by opposing a laminar flow with a second laminar flow. Our object is to distort the hydrodynamic flow in the capillary to compensate for the thermally induced distortion of the sample's velocity.

The band broadening model we present incorporates a laminar flow as well as our autothermal thermal model. We find that a small Poiseuille flow can dramatically improve column performance, although such improvement may be chimerical unless one can reduce the initial length of the sample to 1 mm or less. Our proposed method seems to hold the most promise for very large capillaries, *i.e.* those with internal

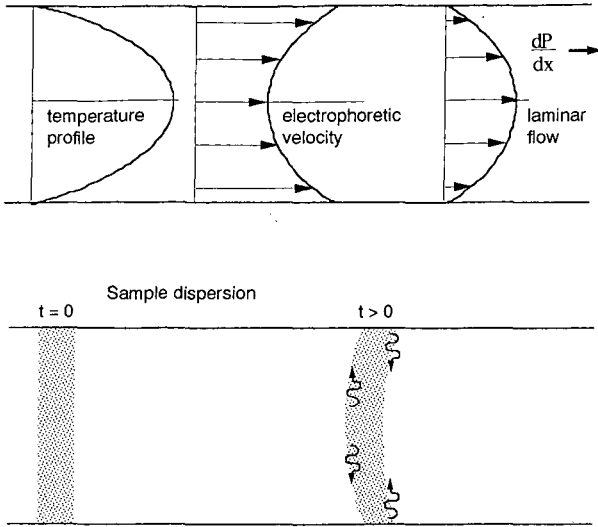


Fig. 2. By opposing the distortion of the sample's electrophoretic velocity with a laminar flow, it is possible to give the sample a nearly flat velocity profile.

diameters of 400 μm or more, for which it appears possible to obtain plate numbers of 10^6 m^{-1} or more. The ability to use such large capillaries could considerably ease detection problems; for the same sample length, sample loading in a 500- μm capillary is 100 times greater than in a 50- μm I.D. capillary.

THEORY

Thermal model

The theory of electrically heated cylindrical objects is well established (*e.g.*, see ref. 7). Hinkley⁸, and Coxon and Binder⁹ gave the first analyses specific to tubular electrophoresis equipment. Grushka *et al.*³ and Jones and Grushka⁵ have recently presented analyses specifically for CE. Our analysis considers in greater detail (i) the ramifications of the autothermal effect and (ii) the sensitivity of the capillary to heat transfer conditions.

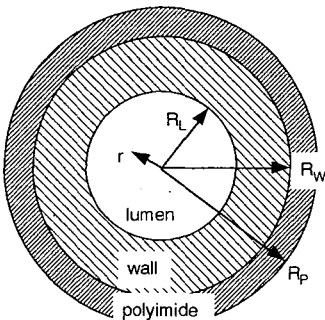


Fig. 3. Capillary cross section, showing the lumen, silica wall and polyimide coat.

Fig. 3. shows the geometry used for the capillary. The energy balance on the buffer in the lumen is

$$k \frac{1}{r} \frac{d}{dr} r \frac{dT}{dr} = -E^2 \kappa \quad (1)$$

Here r is the radial coordinate, T the buffer temperature, E the electric field, k the thermal conductivity of the buffer and κ the electrical conductivity.

At the centerline the temperature must be finite. Heat transfer from the capillary surface to the surroundings is described by an overall heat transfer coefficient h_{OA} . The boundary conditions are accordingly

$$-k \frac{dT}{dr} = \begin{matrix} T \text{ finite} & r = 0 \\ h_{OA}(T - T_C) & r = R_L \end{matrix} \quad (2)$$

In the second boundary condition T_C is the coolant temperature. The heat transfer coefficient is obtained by combining the thermal resistances of the silica wall, the polyimide coat, and the surface resistance according to the usual rule for cylindrical geometry⁷:

$$h_{OA} = \frac{1}{R_L \frac{1}{\ln \frac{R_W}{R_L}} + \frac{1}{\ln \frac{R_P}{R_W}} + \frac{1}{R_P h_s}} \quad (3)$$

The radii R_W , R_L and R_P are as shown in Fig. 3, k_w and k_p are the thermal conductivity of the wall and polyimide coat, and h_s is the surface heat transfer coefficient. For a liquid-cooled capillary, h_s will be so large that its term in eqn. 3 can be neglected. For an air-cooled capillary, h_s is a function of the surface temperature T_S , which can be found by equating the rates of heat transfer at the lumen surface and the outer capillary surface:

$$-R_L k \frac{dT}{dr} \Big|_{r=R_L} = R_P h_s (T_S - T_C) \quad (4)$$

As detailed below, h_s can be calculated from a correlation involving a low-order non-linearity in T_S .

A linear model of the electrical conductivity is mathematically convenient and is usually a good approximation over a 10–20°C temperature range:

$$\kappa = \kappa_0 [1 + \kappa_1 (T - T_0)] \quad (5)$$

Here T_0 is a reference temperature, κ_0 the conductivity at T_0 , and κ_1 the temperature coefficient. For mathematical convenience we will take $T_0 = T_C$ with no loss of generality.

Using the dimensionless variables defined in Table I puts the model in the form

TABLE I
DIMENSIONLESS VARIABLES

$\theta = \frac{T - T_0}{\Delta T_{ref}}$	Dimensionless temperature
$\eta = r/R_L$	Dimensionless radial coordinate
$\Delta T_{ref} = \frac{\kappa_0 E^2 R_L^2}{k}$	Characteristic temperature rise
$\lambda = \sqrt{\kappa_1 \Delta T_{ref}}$	Autothermal parameter
$Bi_{OA} = \frac{h_{OA} R_L}{k}$	Overall Biot number

$$\frac{1}{\eta} \frac{d}{d\eta} \eta \frac{d\theta}{d\eta} + \lambda^2 \theta = -1 \tag{6}$$

$$-\frac{d\theta}{d\eta} = \theta \text{ finite} \quad \eta = 0$$

$$\frac{1}{2} Bi_{OA} \theta \quad \eta = 1$$

Here k is the ‘‘autothermal parameter’’, the characteristic increase in electrical conductivity due to the characteristic temperature rise ΔT_{ref} . Bi_{OA} is the overall Biot number, a dimensionless heat transfer coefficient which compares the rate of heat conduction through the composite wall with the rate at which heat is removed by the coolant.

The scaled surface temperature θ_s is found from scaling eqn. 4

$$-\frac{d\theta}{d\eta} \Big|_{\eta=1} = \frac{1}{2} Bi_s \theta_s \tag{7}$$

where Bi_s is the surface Biot number, $h_s R_p / k$.

The dimensionless temperature inside the capillary is found to be

$$\theta = \frac{1}{\lambda^2} \frac{J_0(\lambda\eta) - J_0(\lambda) + \frac{2\lambda}{Bi_{OA}} J_1(\lambda)}{f(\lambda)} \tag{8}$$

J_0 and J_1 are Bessel functions of the first kind. The first two terms in the numerator give the temperature variation across the lumen radius, while the last term gives the temperature at the lumen surface. The function $f(\lambda)$ expresses the autothermal effect, *i.e.*, the additional temperature rise due to the feedback between temperature and power density. It is given by

$$f(\lambda) = J_0(\lambda) - \frac{2\lambda}{Bi_{OA}} J_1(\lambda) \tag{9}$$

For non-zero λ , $f(\lambda)$ is always less than unity, so the capillary always runs hotter than would be predicted by a constant-conductivity model. Further, at a critical value of the autothermal parameter, λ^* , $f(\lambda^*)$ vanishes, implying *autothermal runaway*. Under such conditions the capillary is unable to attain thermal equilibrium by increasing its temperature, and the temperature rises until a vapor bubble forms. The threshold for autothermal runaway establishes an absolute upper bound on the voltage one may apply. In practice the buffer usually boils before λ^* is reached.

The largest critical value of the autothermal parameter is obtained with perfect cooling, *e.g.*, by forced liquid cooling of a capillary with a vanishingly thin wall. Setting the overall Biot number Bi_{OA} to infinity in eqn. 9 shows that the maximum critical value is $\lambda^* \approx 2.4$, the first root of J_0 .

In general, the heat transfer resistance is quite significant. Fig. 4 shows how the overall Biot number depends on the temperature difference between the surface of the capillary and the surroundings for a 100×200 (I.D. \times O.D.) μm capillary cooled by natural convection in air. The method of calculation is described below. A typical value of Bi_{OA} for rough calculations can be taken as 0.055. For the same capillary with forced liquid cooling, the surface resistance can be neglected, giving a Bi_{OA} value of about 1.2. A similar result can be obtained with vigorous forced air cooling.

For $Bi_{OA} \leq 5$, $f(\lambda)$ can be well approximated by replacing the Bessel functions in eqn. 9 with the leading terms of their power series through $O(\lambda^4)$:

$$f(\lambda) = \frac{1}{8} \left[\frac{1}{Bi_{OA}} + \frac{1}{8} \right] \lambda^4 - \left[\frac{1}{Bi_{OA}} + \frac{1}{4} \right] \lambda^2 + 1 \tag{10}$$

From this one can obtain

$$\lambda^* = \sqrt{\frac{1}{\frac{1}{Bi_{OA}} + \frac{1}{8}}} \tag{11}$$

For natural convection air-cooled capillaries this expression shows that $\lambda^* \approx \sqrt{Bi_{OA}}$. The relative inefficiency of air cooling compared to liquid cooling can be gauged by using the rough values for Bi_{OA} of 0.055 and 1.2 in eqn. 11. Ignoring the question of when the buffer will boil, a factor of $\lambda^*_{\text{liquid}}/\lambda^*_{\text{air}} \approx 18$ times greater voltage can be applied to a $100 \times 200 \mu\text{m}$ capillary if it is liquid cooled.

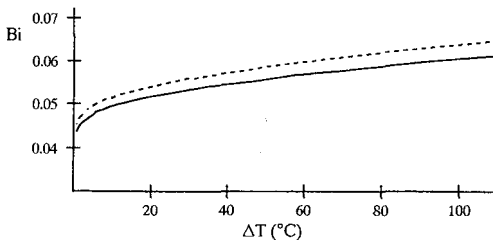


Fig. 4. Biot number for a $100 \times 200 \mu\text{m}$ air-cooled capillary as function of temperature difference between the surface and surroundings. Solid line is overall Biot number, dashed line is surface Biot number. Surface resistance dominates heat transfer for air cooled capillaries.

For natural convection air-cooled capillaries the small magnitude of λ permits us to replace the Bessel functions in eqn. 8 with the first few terms of their power series, giving

$$\theta \approx \frac{\frac{1}{4}(1 - \eta^2) + \frac{\lambda^2}{64}(\eta^4 - 1) + \frac{1}{Bi_{OA}}\left(1 - \frac{\lambda^2}{8}\right)}{f(\lambda)} \quad (12)$$

Taking the limit $\lambda \rightarrow 0$ in eqn. 12 while holding Bi_{OA} constant in $f(\lambda)$ gives the parabolic temperature profile of refs. 3 and 5. But since the critical value λ^* for air-cooled capillaries is quite small, the value of λ in practice will generally be an appreciable fraction of λ^* . Thus $f(\lambda)$ will be small and the autothermal effect pronounced. Therefore, while the temperature profiles obtained in refs. 3 and 5 give the correct shape, they may seriously underpredict the magnitude of the temperature variation.

Heat transfer coefficient

For capillaries cooled by forced convection of air or liquid, the surface heat transfer coefficient will generally be so large that the surface resistance will be negligible in eqn. 3. Cooling by natural convection in air is much less efficient, so the surface resistance cannot be neglected.

Heat transfer coefficient for natural convection air cooling

The surface resistance is the most significant resistance to heat transfer for a natural convection air-cooled capillary, although at higher temperatures radiation can account for 10–20% of the heat loss. If the capillary is shielded from drafts, the convective contribution can be calculated from standard correlations for natural convection from a horizontal cylinder. For the calculations reported here, we used the following slightly modified form of McAdams¹⁰ correlation for the convective Nusselt number:

$$Nu_c = 0.45 + 0.55 (GrPr)^{\frac{1}{4}} \quad (13)$$

The modification consisted of adding the asymptotic value 0.45 and adjusting the multiplicative constant to improve the fit to McAdams' recommended interpolation points. Gr and Pr are the Grashof and Prantl numbers.

The radiant heat transfer coefficient is calculated assuming equal emissivities for the polyimide and surroundings:

$$Nu_r = \frac{2R_p}{k_c} \frac{\sigma e(T_s^4 - T_c^4)}{T_s - T_c} \quad (14)$$

Here e is the emissivity, σ is the Stefan-Boltzmann constant, and k_c is the thermal conductivity of the coolant (air). A surface Nusselt number is obtained by adding the convective and radiative Nusselt numbers, $Nu_s = Nu_c + Nu_r$, and Nu_s is converted to a surface Biot number by

$$Bi_s = \frac{k_C R_P}{k R_L} Nu_s \quad (15)$$

Since the heat transfer coefficients and surface temperature are coupled non-linearly, iteration is required to determine the capillary temperature. However, the radiative component is relatively small, and the non-linearity of the convective component is low-order, so the calculation is not a difficult one.

Band spreading model

Band spreading in CE can be treated as a problem in Taylor dispersion², in which radial diffusion tends to average out radial concentration variations produced by convective dispersion. Whether such treatment is accurate depends upon the capillary dimensions and the substances being analysed. Gill and Sankarasubramanian¹¹ have shown that the residence time L/U must satisfy

$$\frac{L}{U} \gg 0.5 \frac{R_L^2}{D} \quad (16)$$

This criterion is easily satisfied for capillaries up to 100 μm inner radius and proteins with diffusion coefficients of $O(10^{-6} \text{ cm}^2/\text{s})$. For significantly larger capillaries the analysis loses rigor, because the residence time is not long enough to allow thorough radial mixing by diffusion. However, the result remains adequate for the purposes of gauging the effectiveness of adding a Poiseuille flow and of estimating the required magnitude of the flow.

Aris¹² formulation is the appropriate starting point. The mean velocity of a tracer pulse is given by

$$U = 2 \int_0^1 u\eta d\eta \quad (17)$$

Here u is the sample's velocity. It is determined by the material's electrophoretic mobility α , the electroosmotic mobility α' , and the Poiseuille flow. Each of these velocities depends on temperature through the variation of viscosity with temperature. In the most general form, the velocity is

$$u = E\alpha' + E\alpha - \frac{R_L^2}{4\mu} \frac{dP}{dx} (1 - \eta^2) \quad (18)$$

The rate at which the pulse spreads is characterized by the rate of growth of its second moment, given by¹²

$$\frac{dm_2}{dt} = 2 + 4 \frac{R_L}{D} \int_0^1 \eta c_1 \chi d\eta \quad (19)$$

where χ is the departure from the mean velocity¹²

$$\chi = u - U \quad (20)$$

and c_1 is the radial variation from the mean concentration¹²

$$c_1 = - \frac{R_L}{D} \int_0^{\eta'} \int_0^{\eta'} \chi \eta \frac{d\eta}{\eta'} d\eta' \quad (21)$$

From the second moment we obtain the effective, or Taylor, diffusion coefficient¹²:

$$D_T = \frac{1}{2} \frac{dm_2}{dt} \quad (22)$$

Evaluating eqns. 19 and 21 using the temperature profile of eqn. 8 and an exact formula for the viscosity¹³ is best done numerically. However, for air cooled capillaries, we can use the approximate temperature profile, eqn. 11, and express the temperature dependence of viscosity with the following linear perturbation:

$$\begin{aligned} \frac{1}{\mu} &= \mu_0 [1 + \omega^2 \theta(\eta)] \\ \omega &= \sqrt{\mu_1 \Delta T_{ref}} \end{aligned} \quad (23)$$

Here μ_0 is the reciprocal viscosity at T_0 , and μ_1 is the temperature coefficient. The integrands in eqns. 17, 19 and 21 are then polynomials, and after some tedium one finds

$$\begin{aligned} U = \left(- \frac{1}{8} R_L^2 \mu_0 \frac{dP}{dx} \right) & \left[\left(\frac{1}{Bi_{OA}} + \frac{1}{6} \right) \frac{\omega^2}{f(\lambda)} + 1 \right] + \\ & + \left[\left(\frac{\lambda^2}{Bi_{OA} f(\lambda)} + 1 \right) (\alpha_0 + \alpha'_0) + \frac{1}{8} \frac{\alpha_0 \lambda^2}{f(\lambda)} \right] E \end{aligned} \quad (24)$$

$$D_T = D \left\{ 1 + \frac{1}{3072} \frac{R_L^2}{D^2} \left[\left(\frac{\omega^2}{Bi_{OA} f(\lambda)} + 1 \right) R_L^2 \mu_0 \frac{dP}{dx} - \frac{E \alpha_0 \lambda^2}{f(\lambda)} \right]^2 \right\} \quad (25)$$

Only the dominant terms for small Bi_{OA} , λ and ω have been retained in these expressions. The factor enclosed in square brackets (eqn. 25) is the mean value of the velocity distortion. Here we see the desired effect: dP/dx can be adjusted to reduce the effective dispersion coefficient to the diffusive limit. We find

$$\frac{dP}{dx} = \frac{E \alpha_0 \lambda^2}{\left[\frac{\omega^2}{Bi_{OA} f(\lambda)} + 1 \right] R_L^2 \mu_0 f(\lambda)} \quad (26)$$

In using this equation it must be borne in mind that the mobility α_0 and electric field E are signed quantities. Because the pressure gradient affects the mean velocity,

eqn. 26 may not maximize the plate number. We investigate this question after defining the plate number.

The plate number is usually defined as

$$N = \frac{UL}{2D_T} \quad (27)$$

Eqn. 27 does not necessarily predict the plate numbers that would be deduced in practice from measurements of output peak widths. This because the increase in peak width may be so small in CE that the output peak width is substantially determined by the initial size of the sample. This effect can be quantified by adding the initial variance of the sample to the increase in variance produced in the column go give the "observed" plate number:

$$N_{\text{obs}} = \frac{1}{2\frac{D_T}{LU} + \frac{1}{12}\frac{z^2}{L^2}} \quad (28)$$

Here z is the initial length of the sample.

We can estimate the optimal pressure gradient by substituting eqns. 24 and 25 into eqn. 27, differentiating with respect to dP/dx , and setting the result to zero. A quadratic equation in dP/dx is obtained. One root is rejected since it leads to a negative value for N . The remaining root is quite complicated; for clarity we retain temperature dependence only in the terms involving the mobility of the sample:

$$\frac{dP}{dx} = 8 \frac{(\alpha_0 + \alpha'_0)E}{R_L^2 \mu_0} - \sqrt{3072 \frac{D^2}{R_L^6 \mu_0^2} + \frac{E^2}{R_L^4 \mu_0^2} \left[-8(\alpha_0 + \alpha'_0) + \frac{\alpha_0 \lambda^2}{f(\lambda)} \right]^2} \quad (29)$$

The first term under the root and the second term inside the square brackets are generally much smaller than the first term inside the brackets. Using the Taylor series approximation

$$a - \sqrt{c + (-a+b)^2} \approx b - \frac{1}{2} \frac{c}{a} \quad (30)$$

where $|a| \gg \{|b|, |c|\}$, we can estimate

$$\frac{dP}{dx} \approx -192 \frac{D^2}{(\alpha_0 + \alpha'_0)ER_L^4 \mu_0} + \frac{E\alpha_0 \lambda^2}{R_L^2 f(\lambda) \mu_0} \quad (31)$$

The first term is generally much smaller than the second, so we conclude that pressure gradients which minimize the effective dispersion coefficient little affect the mean velocity. Eqn. 26 adequately estimates the optimal pressure gradient.

EXPERIMENTAL

We used four untreated silica capillaries, donated by Polymicro Technologies. The capillary dimensions are given in Table II. The actual diameters of the ends of the capillaries were measured under a microscope. The power supply was a Spellman UHR-30, with a maximum output of 30 kV. Voltage was read from the power supply's front panel meter and current from a Hewlett-Packard 412A multimeter connected in series on the grounded side of the capillary.

The buffer used for all the experiments contained 10 mM sodium phosphate, adjusted to pH 7.0 by mixing 10 mM monobasic sodium phosphate and 10 mM dibasic sodium phosphate, and 50 mM KCl. The buffer was degassed immediately before experiments by agitating it while under a 600 mmHg vacuum. Upon heating, the degassed buffer began to outgas at 80–85°C.

The sodium phosphate–KCl buffer's conductivity has the desirable property of virtually linear variation with temperature, as shown in Fig. 5. The buffer conductivity was measured with a YSI Model 35 conductance meter and YSI 3417 conductivity cell.

In use, a capillary was positioned nearly horizontally, with its ends dipping into 50-ml beakers which served as buffer reservoirs. The capillary, supports, and beakers were enclosed in a plexiglass box 91 cm wide, 50 cm deep and 107 cm high (36 × 20 × 42 in.). The door of the box actuated interlock switches, which disabled the power supply when the door was open. In addition to providing operator safety, the box shielded the capillary from strong drafts.

An experiment consisted of measuring the current passed by the capillary at fixed voltages, and terminated when a vapor bubble formed in the capillary. Average temperature in the lumen was then inferred from the calibration shown in Fig. 5.

RESULTS

Temperature experiments and thermal model

Figs. 6–9 show comparisons of experiment and theory. The curves labeled "Autothermal theory" give the predicted average temperature obtained by radially averaging eqn. 10. The curves labeled " $\lambda = 0$ " show the temperatures predicted by a constant-conductivity model. The actual capillary dimensions given in Table II were used in the calculations. The heat transfer coefficient was calculated using eqns. 13–15.

For reasons discussed below, the autothermal model generally overpredicts the

TABLE II
CAPILLARY DIMENSIONS

Nominal dimensions (μm , I.D. × O.D.)	Actual lumen diameter (μm)	Actual wall diameter (μm)	Actual polyimide thickness (μm)	Length (cm)
250 × 350	263	313	21	91.7
250 × 530	257	510	15	101.2
100 × 200	98	172	18	100.3
75 × 150	78	133	8.5	146.8

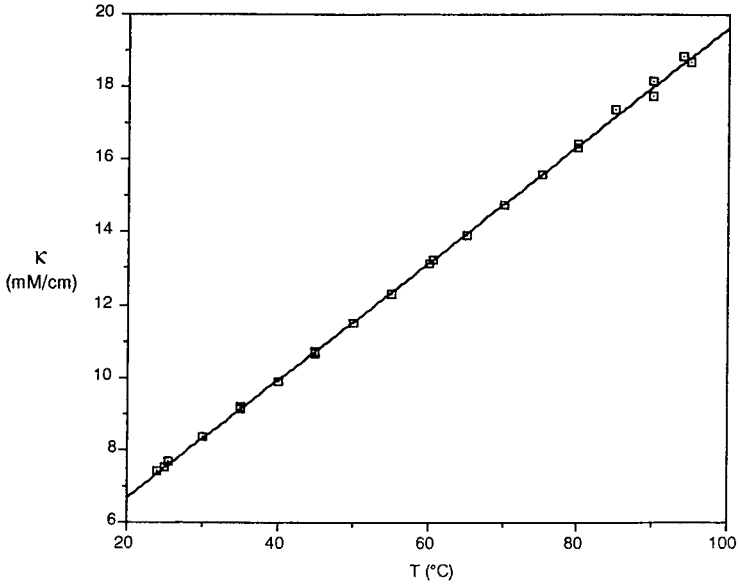


Fig. 5. Conductivity of the sodium phosphate-potassium chloride buffer used in the temperature experiments.

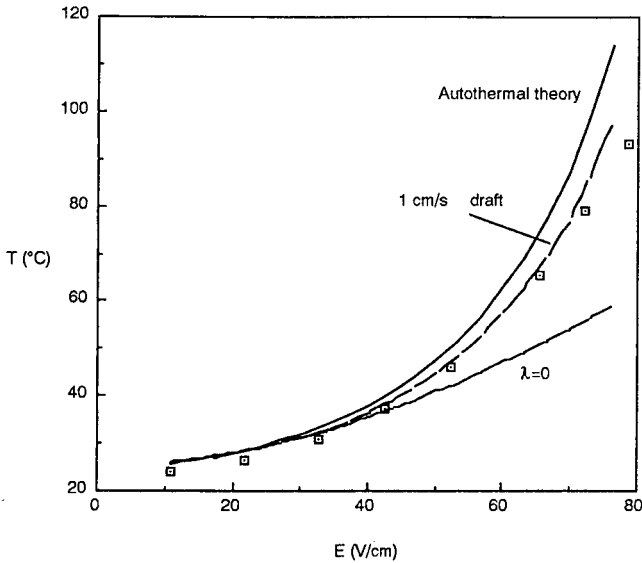


Fig. 6. Comparison of experimentally measured capillary temperature and theory for the $250 \times 350 \mu\text{m}$ capillary. This figure also shows the effect of a 1-cm/s draft on the predicted capillary temperature.

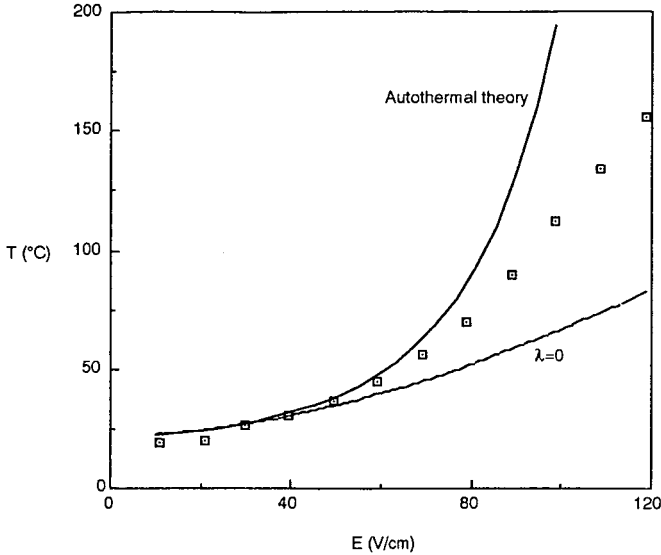


Fig. 7. Comparison of experimentally measured temperature and theory for the $250 \times 530 \mu\text{m}$ capillary. This capillary exhibited about 50°C superheating.

capillary temperature, while the constant-conductivity model underpredicts it. At higher voltages the discrepancy between the data and constant-conductivity model approaches 40°C .

The discrepancy between our data and the predictions of the autothermal model is most likely due to slow circulation of air inside the apparatus enclosure. We explored

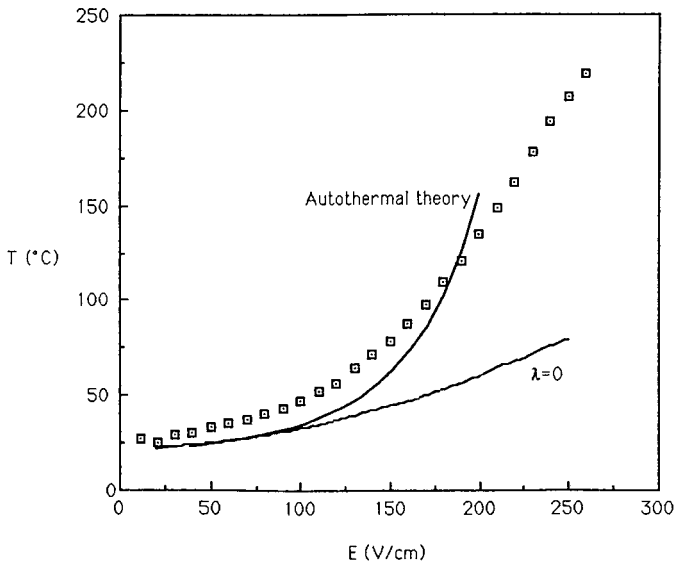


Fig. 8. Comparison of experimentally measured temperature and theory for the $100 \times 200 \mu\text{m}$ capillary. This capillary exhibited more than 100°C superheating.

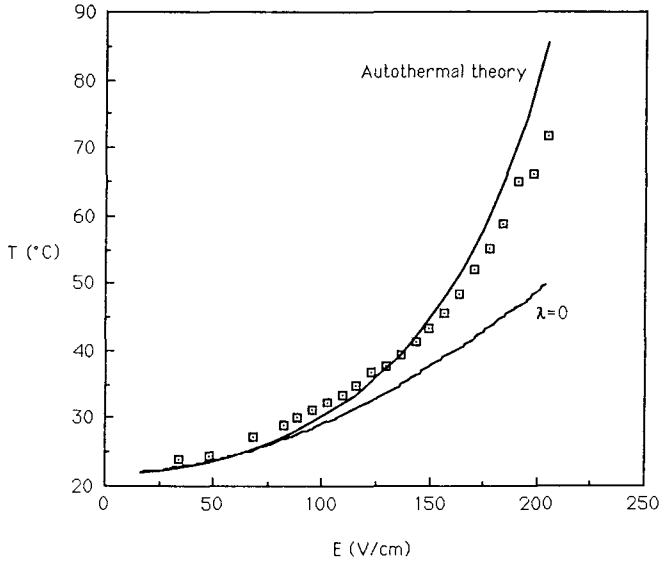


Fig. 9. Comparison of experimentally measured temperature and theory for the $75 \times 150 \mu\text{m}$ capillary.

this effect by incorporating a 1 cm/s draft into the surface heat transfer coefficient used for the $250 \times 350 \mu\text{m}$ capillary simulation. As shown in Fig. 6, this markedly improves the agreement with experiment. Because convection reduces the capillary temperature, adding a draft to the constant-conductivity simulations would only worsen the predictions of the constant-conductivity model.

A remarkable feature of Figs. 7 and 8 is the superheated temperatures achieved in these capillaries, some 50 and 120°C above the boiling point. A direct measurement of the temperature was made for the 100×200 capillary: a thermocouple, approximately 1 mm in diameter, was placed in contact with the capillary near the grounded end. Thermal contact was improved with a small amount of Omegatherm 201 thermally conductive paste (Omega Engineering). Although this arrangement gave only a crude measurement of the surface temperature, the thermocouple registered 107°C at the highest electric field, verifying the occurrence of superheating.

TABLE III
PARAMETERS USED FOR PLATE NUMBER SIMULATIONS

$\alpha_0 = 4 \mu\text{m cm/V s}$
$\alpha'_0 = 8 \mu\text{m cm/V s}$
$D = 1 \cdot 10^{-6} \text{ cm}^2/\text{s}$
$k = 6 \text{ mW/cm }^\circ\text{C}$
$\kappa_0 = 10 \text{ mS/cm}$
$\kappa_1 = 0.046 \text{ }^\circ\text{C}^{-1}$
$\mu_0 = 100 \text{ cm s/g}$
$\mu_1 = 0.011 \text{ }^\circ\text{C}^{-1}$

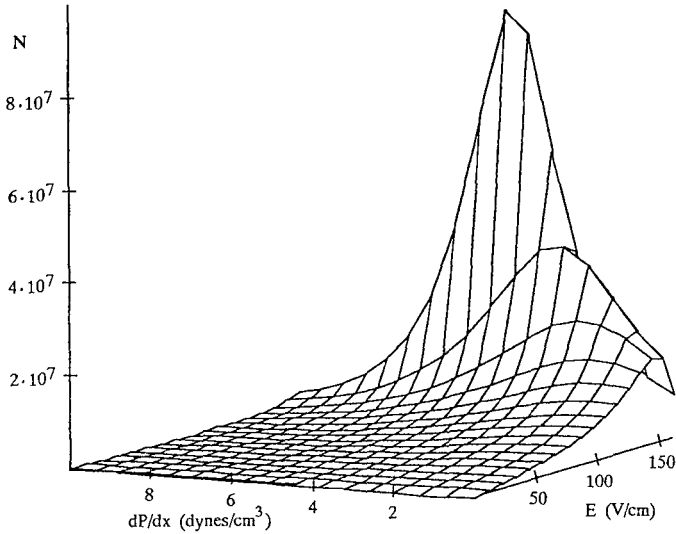


Fig. 10. Plate number for an air-cooled, 100 cm long, $100 \times 200 \mu\text{m}$ capillary. By applying a pressure gradient it is possible to increase N by as much as 10 times.

Dispersion model

Parameters used for the following calculations are given in Table III. Fig. 10 shows the plate number predicted for an air cooled, 100 cm long, $100 \times 200 \mu\text{m}$ capillary as a function of pressure gradient and electric field. With no pressure gradient, this capillary can achieve approximately 10^6 plates. When a pressure gradient is applied the plate number can be doubled at 150 V/cm, and increased to about 10^7 plates at higher voltages. The pressures required are modest: 5 dynes/cm² cm over

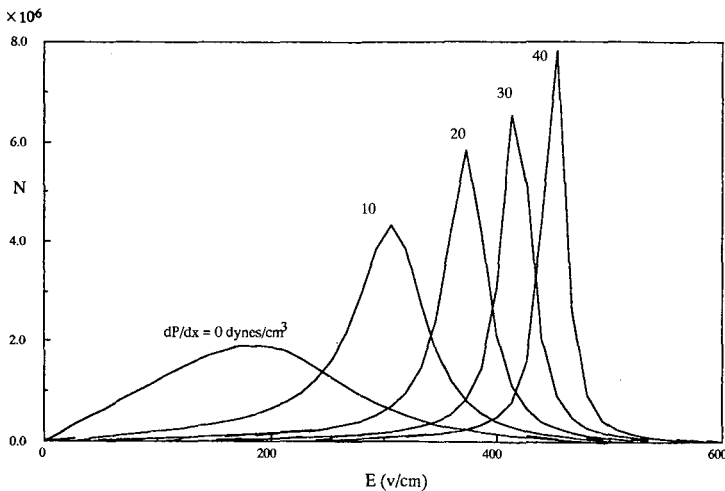


Fig. 11. Plate number for a liquid-cooled, 20 cm long, $100 \times 200 \mu\text{m}$ capillary as a function of electric field for various applied pressure gradients.

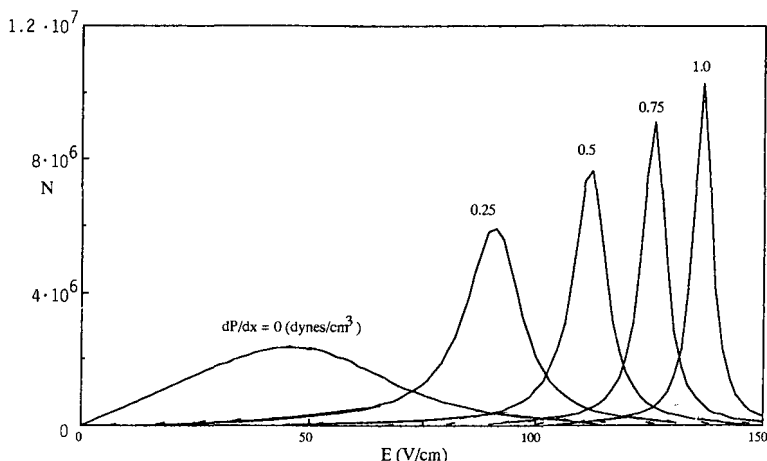


Fig. 12. Plate number for a liquid-cooled, 100 cm long, $400 \times 530 \mu\text{m}$ capillary. Remarkably high plate numbers can be obtained despite the large inner diameter.

a 100 cm capillary is equivalent to a difference in elevation of the buffer reservoirs of about 5 mm.

Fig. 11 shows the plate number predicted for a liquid cooled, 20 cm long, $100 \times 200 \mu\text{m}$ capillary. This capillary can also approach 10^7 plates when a pressure gradient is applied. Higher pressure gradients are required here than for the air cooled case because the temperature variation across the lumen is greater.

Fig. 12 shows the plate number predicted for a liquid-cooled, 100 cm long, 400

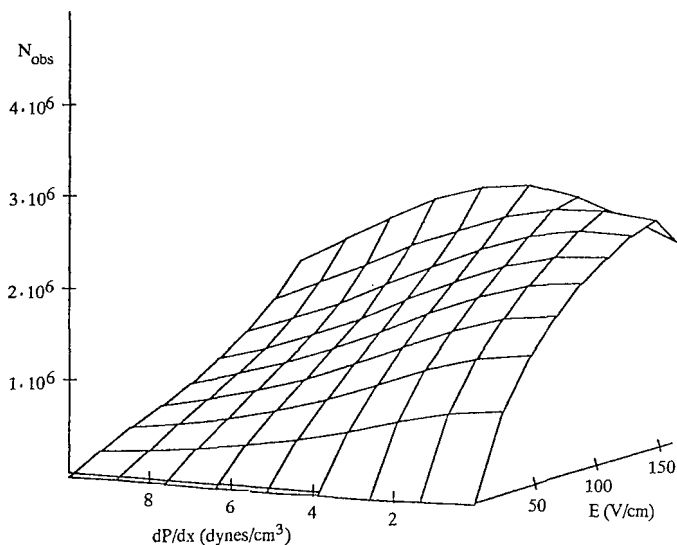


Fig. 13. Observed plate number for an air cooled 100 cm long, $100 \times 200 \mu\text{m}$ capillary assuming a 2-mm long sample. Performance is severely degraded in comparison with Fig. 8. There is little benefit in applying a pressure gradient.

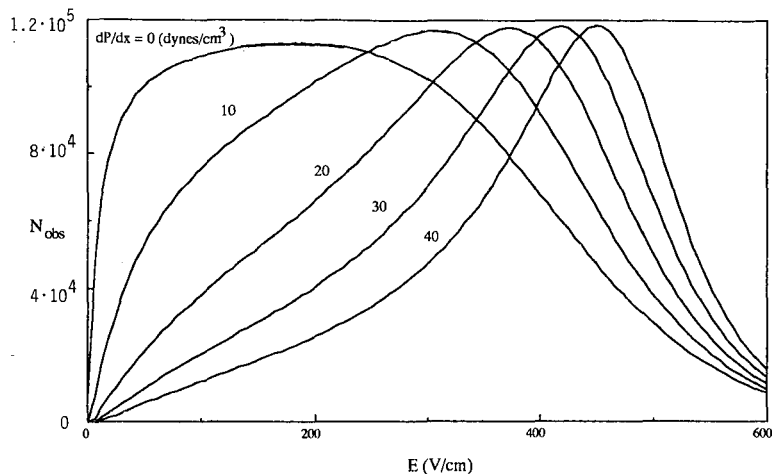


Fig. 14. Observed plate numbers predicted for a liquid cooled, 20 cm long, $100 \times 200 \mu\text{m}$ capillary, assuming a 2-mm long initial sample size. The sample size greatly degrades performance.

$\times 530 \mu\text{m}$ capillary. This large bore capillary can reach high plate numbers with the assistance of a pressure gradient.

For comparison, Figs. 13–15 show plate numbers predicted for these capillaries assuming an initial sample length of 2 mm. Such a sample size severely limits the performance of all the columns. Performance is most drastically reduced in the 20 cm long $100 \times 200 \mu\text{m}$ column because of its short length. In contrast, much less degradation occurs in the 100 cm long $400 \times 530 \mu\text{m}$ column.

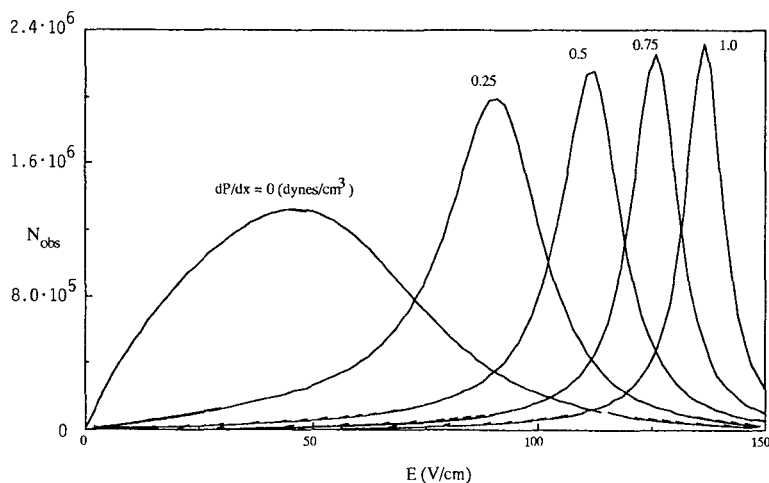


Fig. 15. Observed plate number predicted for a liquid cooled 100 cm long, $400 \times 530 \mu\text{m}$ capillary, assuming a 2-mm long initial sample. Good performance can be obtained without a pressure gradient, and the plate number can be roughly doubled by applying a pressure gradient.

DISCUSSION

Thermal model

The results show that a constant-conductivity model can seriously underpredict the temperature in a capillary at high power levels. This can adversely affect estimates of electrophoretic mobility, residence time, and plate number.

The simulation incorporating a 1 cm/s draft points up the extreme sensitivity of air cooled capillaries to drafts. Air cooled capillaries function rather like hot-wire anemometers. It is important to keep them carefully shielded from air currents.

Forced liquid cooling offers substantially better heat transfer. Liquid cooled capillaries can be operated at significantly higher voltages than air cooled ones. The increase in voltage may be as much as a factor of 20; in practice however, the autothermal effect probably limits the increase to a factor less than 10. But since the autothermal effect amplifies electrophoretic mobility, the increase in migration velocities may yet be as much as 20 times.

It is possible that the two capillaries which exhibited superheating possess very smooth lumen surfaces which provide no nucleation sites. The lumens are too large to interfere with bubble formation through capillary pressure; they would have to have radii of about 0.1 μm to give the observed superheating. This conclusion is supported by the smallest capillary (Fig. 7), which exhibited no superheating.

Superheating has no obvious application in CE. However, carefully selected capillaries could provide convenient vessels for studying phenomena in aqueous solutions above the boiling point without the need for high-pressure apparatus.

Band spreading model

In cases where column performance is limited by thermal effects rather than sample loading or other dispersive phenomena, it is possible to improve the plate number to near the limit set by sample size and molecular diffusion by imposing a pressure gradient. The simulations show that at a particular pressure gradient, the optimal electric field is narrowly defined. This is because of the autothermal effect's strong non-linearity. The theoretical relations given here can only be used to provide an initial guess of the best conditions, owing to the non-linear variation of viscosity and of the mobility of buffer and sample ions.

Large capillaries appear to benefit the most from application of a pressure gradient. Such capillaries suffer greatly from thermal Taylor dispersion because their large radii preclude efficient radial diffusive averaging. But by flattening the velocity profile with a pressure gradient, plate numbers in excess of 10^6 can be obtained. Larger capillaries would ease detection difficulties since sample capacity increases with the diameter squared. Wall interactions also would become less deleterious.

The dispersion simulations illustrate the constraint on column performance imposed by the initial length of the sample. This constraint can be overcome, to some degree, by lengthening the column. For example, the upper limit on plate number based on sample size for a 100-cm column and 2-mm sample pulse is $3 \cdot 10^6$ plates. Samples this small may pose a detection problem. However, if one uses a large diameter capillary, sample loading can be increased even while sample length is decreased, e.g., a 2-mm long sample in a 500- μm capillary contains 20 times more material than a 1-cm long sample in a 50- μm capillary.

CONCLUSIONS

The autothermal effect makes CE capillaries run significantly hotter than constant conductivity models predict. The autothermal model presented here is in substantial agreement with experimental measurements of capillary temperatures. The temperature simulations illustrate the sensitivity of air cooled capillaries to drafts. Forced liquid cooled capillaries offer better temperature control and allow higher operating voltages.

The method we have proposed to reduce thermal band broadening, by imposing a small Poiseuille flow, appears promising. Best results should be obtained with capillaries which are considered too large to be useful for CE: It appears possible to obtain plate numbers in excess of 10^6 in capillaries as large or larger than $400 \mu\text{m}$.

Performance of any CE column is limited by the initial length of the sample. Shorter samples improve plate number at the expense of detectability. Detectability can be maintained in large diameter capillaries, which offer the possibility of maintaining or increasing sample volume while decreasing sample length.

SYMBOLS

Bi_{OA}	overall Biot number, $h_{OA}R_L/k$
Bi_S	surface Biot number, $h_S R_P/k$
c_1	variation of concentration from mean value
c_p	heat capacity
D	diffusion coefficient
D_T	effective, or Taylor, diffusion coefficient
e	emissivity
E	electric field
$f(\lambda)$	autothermal function
g	gravitational acceleration
Gr	Grashof number, $D^3 \rho^2 \beta g \Delta T / \mu^2$
h_{OA}	overall heat transfer coefficient
h_S	surface heat transfer coefficient
J_0, J_1	Bessel functions
k	thermal conductivity of water
k_C	thermal conductivity of coolant
k_P	thermal conductivity of polyimide
k_W	thermal conductivity of capillary wall
L	length of capillary
m_2	second moment of concentration distribution
N, N_{obs}	plate number and observed plate number
Nu_C, Nu_R, Nu_S	convective, radiative and surface Nusselt numbers
P	pressure
Pr	Prandtl number, $c_p \mu / k$
r	radial coordinate
R_L	lumen radius
R_P	polyimide outer radius
R_W	silica wall outer radius

t	time
T	temperature in lumen
T_C	coolant temperature
T_S	surface temperature
T_0	reference temperature for electrical conductivity
u	sample velocity
U	mean velocity
x	axial coordinate
z	initial length of sample
α, α'	electrophoretic and electroosmotic mobility
α_0, α'_0	reference electrophoretic and electroosmotic mobility
α_1, α'_1	electrophoretic and electroosmotic mobility temperature coefficients
β	coefficient of thermal expansion
ΔT_{ref}	characteristic temperature rise
η	dimensionless radial coordinate, r/R_L
η'	variable of integration
κ	electrical conductivity
κ_0	reference electrical conductivity
κ_1	electrical conductivity temperature coefficient
λ	autothermal parameter
μ	viscosity
μ_0	reference reciprocal viscosity
μ_1	temperature coefficient of reciprocal viscosity
χ	departure from mean velocity
ρ	density
σ	Stephan-Boltzmann constant
θ	dimensionless temperature
ω	characteristic dimensionless variation of reciprocal viscosity

REFERENCES

- 1 J. W. Jorgenson and K. D. Lukacs, *Science (Washington, D.C.)*, 222 (1983) 266.
- 2 G. I. Taylor, *Proc. Roy. Soc.*, A219 (1953) 186.
- 3 E. Grushka, R. M. McCormick and J. J. Kirkland, *Anal. Chem.*, 61 (1989) 241.
- 4 E. Lynch and D. A. Saville, *Chem. Eng. Commun.*, 9 (1981) 201.
- 5 A. E. Jones and E. Grushka, *J. Chromatogr.*, 466 (1989) 219.
- 6 S. Hertén, *Chromatogr. Rev.*, 9 (1967) 122.
- 7 R. B. Bird, W. E. Stewart and E. N. Lightfoot, *Transport Phenomena*, Wiley, New York, 1960.
- 8 J. O. N. Hinkley, *J. Chromatogr.*, 109 (1975) 218.
- 9 M. Coxon and M. J. Binder, *J. Chromatogr.*, 101 (1974) 1.
- 10 W. H. McAdams, *Heat Transmission*, McGraw-Hill, New York, 3rd ed., 1954, p. 176.
- 11 W. N. Gill and R. Sankarasubramanian, *Proc. R. Soc. London, Ser. A*, 316 (1970) 341.
- 12 R. Aris, *Proc. R. Soc. London, Ser. A*, 235 (1956) 67.
- 13 R. C. Reid, J. M. Prausnitz and T. K. Sherwood, *The Properties of Gases and Liquids*, McGraw-Hill, New York, 3rd ed., 1977, p. 454.

Isotachopheresis in open-tubular fused-silica capillaries

Impact of electroosmosis on zone formation and displacement

W. THORMANN

Department of Clinical Pharmacology, University of Bern, Murtenstrasse 35, CH-3010 Berne (Switzerland)

ABSTRACT

Isotachopheresis (ITP) in untreated and coated open-tubular fused-silica capillaries of 25–50 μm I.D. was examined in order to elucidate the impact of electroosmosis on zone formation and displacement. Electroosmotic flow does not hinder the formation of cationic and anionic ITP zone structures. Having untreated capillaries and a single, on-column detector towards the cathodic column end (as in different commercial instruments) permits the execution of cationic and anionic ITP analyses with the same polarity, *i.e.*, with an electroosmotic flow towards the cathode. For cationic experiments, the leader is acting as catholyte and electrophoretic and electroosmotic displacement occur in the cathodic direction. For anionic analyses, the terminator is used as catholyte and ITP develops towards the anode. The net displacement within the capillary, however, is in the cathodic direction as long as electroosmosis exceeds electrophoresis, a situation which was true for all the systems tested.

INTRODUCTION

In isotachopheresis (ITP), sample zones stack between a leading and a displacing electrolyte, display a steady-state shape and all migrate at the same velocity which is given by the properties of the leading buffer and the current density applied. Theoretical treatments predict that (i) a small amount of sample focuses non-isoelectrically as Gaussian-like peak within the migrating boundary of the discontinuous buffer system, (ii) when a system-dependent sample size is reached the sample zone forms a plateau which lengthens linearly with additional sample, (iii) the velocity of the leading boundary is independent of sample composition and (iv) in the absence of buffer flow, the position of the leading boundary depends only upon the amount of charge which has passed^{1–4}. For the past 20 years, most ITP analyses were performed in narrow-bore plastic tubes of 200–500 μm I.D. or separation channels of rectangular cross-section (about 0.3 \times 1.0 mm) and with minimized electroosmosis. In

these systems a buffer flow required for co-flow, counter-flow and continuous sampling was generated with electrolyte pumps^{1,2}.

Modern capillary-type electrophoretic instrumentation features coated or uncoated open-tubular fused-silica capillaries of 25–75 μm I.D. together with a single, on-column detector placed toward one end of the capillary^{5,6}. With these types of apparatus the ITP configurations presented in Fig. 1 are considered. The negative surface charge of untreated fused silica causes an electroosmotic flow toward the cathode. The structure of the electroosmotic velocity field is strongly dependent on how the surface potential and the electric field vary along the column walls. In ITP, the electric field, composition of zones, pH, etc., are changing across the boundaries. Thus, electroosmosis is expected to cause a loss of separation quality. Little work has been done on the use of this new generation of capillary electrophoretic instruments for ITP^{7,8}. In this paper the formation and displacement of ITP zones in open-tubular fused-silica capillaries is described. The impact of electroosmosis and its consequences for cationic and anionic ITP analyses are elucidated. The ultimate goal is the use of automated electrophoretic capillary analysers for ITP determinations of drugs in body fluids.

EXPERIMENTAL

Capillary ITP in coated fused-silica capillaries was performed with an HPE 100 apparatus (Bio-Rad Labs., Richmond, CA, U.S.A.). This instrument features capillaries of 25 μm I.D. and 20 cm length whose inside walls are coated for minimization of electroosmosis and sample adsorption. Sample injection occurs by electromigration and detection via on-line monitoring of UV absorbance close to the capillary end. No special cooling capability is provided. For ITP, the capillary and the outlet reservoir were first filled with the leader. The sample (about 50–200 μl) was then introduced into the inlet compartment prior to application of a constant voltage for 2–32 s. Subsequently, the inlet reservoir was rinsed with the terminator and the running voltage of 6–8 kV was applied. The currents were of the order of 0.2–2 μA . Isotachopherograms were monitored with a strip-chart recorder.

Capillary ITP in untreated fused-silica capillaries was performed with a Model 270A (Applied Biosystems, Foster City, CA, U.S.A.). This automated instrument features untreated fused-silica capillaries of 50 μm I.D. and about 60–100 cm length, optical absorbance zone detection toward the capillary end and a thermostated capillary compartment. Samples are placed in a autosampler from which aliquots can be vacuum-aspirated or loaded electrokinetically (at a constant 5 kV) into the capillary. The autosampler mechanism operates by alternating from wash, buffer and sample positions in a carousel at the injection end of the capillary. Prior to all experiments the capillary was washed for 3 min with 0.1 *M* sodium hydroxide solution. For cationic ITP (configuration iii in Fig. 1) leader from buffer vial B1 was aspirated into the capillary for 3 min, the sample was inserted for a specified period of time (1–30 s), and the terminating electrolyte, placed in buffer vial B2, was connected to the capillary end. For anionic ITP (configuration iv in Fig. 1) the terminator solution (vial B1) was aspirated into the separation capillary whereas the leader was in buffer vial B2. In both instances a constant voltage of 20–30 kV was applied, which produced currents of the order of a few μA . Electropherograms were monitored with a strip-chart recorder.

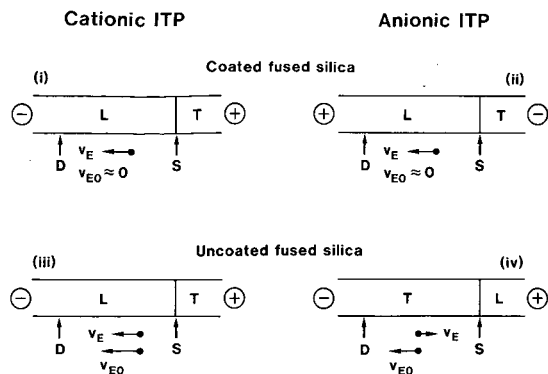


Fig. 1. Schematic representation of configurations for ITP in open-tubular fused-silica capillaries. L = Leading electrolyte; T = terminating electrolyte; S = sample inlet; D = detector position; v_{EO} = electroosmotic velocity; v_E = electrophoretic velocity.

RESULTS AND DISCUSSION

Fig. 2 depicts cationic ITP data for cycloserine (cser) between 10 mM sodium formate (the leader) and formic acid. This represents a model system which has been investigated previously using computer simulation and experimental validation in other instruments⁹. Fig. 2A presents data obtained with the HPE 100, the configuration with minimized or zero electroosmosis. A small amount of cser (2-s injection time) produces a peak-like zone within the sodium formate–formic acid boundary. With increasing amounts of sample, zones with a distinct plateau concentration and increasing length are established. Similar results were obtained using the ABI 270A. A typical response is shown in Fig. 2B, illustrating that electroosmosis in open tubes does not disturb the formation of this cationic ITP zone. This has also shown to be true for other cationic examples by Udseth *et al.*⁸.

Under normal operation of the HPE 100 (8 kV, 2 μ A for this example) and the ABI 270A (30 kV, 6 μ A), distorted cser plateaus are monitored. This is best seen with long sample zones (Fig. 2C). At the high current densities applied (3000–4000 A/m²) electrohydrodynamic forces similar to those observed in isoelectric focusing⁹ and zone electrophoresis¹⁰ could account for this behaviour. Decreasing the current density by about an order of magnitude results in an undistorted sample shape (Fig. 2D), which compares well with theoretical prediction and experimental data obtained in an instrument with a PTFE tube of 500 μ m I.D.⁹.

In Fig. 3 anionic ITP data for a three-component sample are shown using 10 mM HCl, adjusted with histidine to pH 6, as leader and 2-(N-morpholino)ethanesulphonic acid (MES) as terminator. The sample was composed of two dyes, amaranth red (A) and bromophenol bue (B), together with acetate as spacer (S). With coated capillaries (configuration ii in Fig. 1) the electropherograms shown in the upper panel are obtained. Having injection times > 5 s plateau zones were detected whose step lengths increased with additional sample. Components are detected in order of migration; A migrates ahead of S and B, as is customary in conventional capillary ITP¹¹. Performing the same experiment using untreated capillaries was found to be impos-

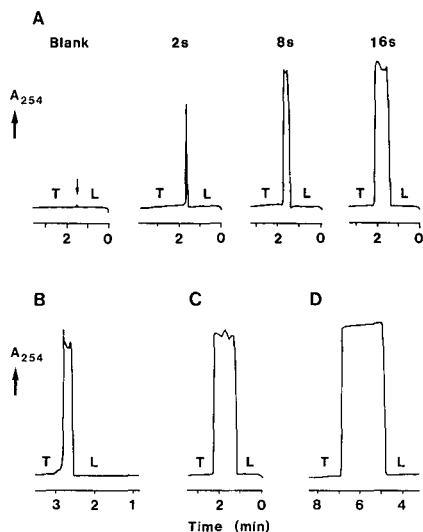


Fig. 2. Cationic capillary ITP data of cycloserine between 10 mM sodium formate, the catholyte (leader, L), and formic acid, the anolyte (terminator, T). A 12-mM sample solution was employed. The electropherograms presented were obtained in a coated capillary (HPE 100; A, C, D) and in an untreated capillary of 50 μm I.D. (ABI 270A; B). With the former instrument sample introduction occurred at 8 kV for (A) 0, 2, 8, 16 s, (C) 32 s and (D) 8 s. The running conditions were 8 kV (A and C, D during the first min only, current about 2 μA) and 0.8 kV (D, after 1 min of current flow, current about 0.2 μA). It is important to realize that the increased zone length in D originates from the small current during detection. For the experiment with electroosmosis (B), vacuum loading of the sample occurred for 30 s prior to application of a constant 30 kV (initial current, 10 μA ; current during sample detection, 6 μA). The capillary length was 70 cm and the temperature was 35°C. In both instruments sample detection occurred at 254 nm.

sible because the electroosmotic flow exceeds the electrophoretic displacement. Changing the polarity and exchanging the buffers, however, allowed the anionic analysis of this sample in the presence of electroosmosis (configuration iv in Fig. 1). The corresponding electropherograms are shown in the lower panel of Fig. 3. Note the reverse order of zone detection compared with the upper panel. In this configuration electrophoretic separation occurs in the anodic direction in the presence of a strong electroosmotic flow toward the cathode which does not appear to disturb the anionic ITP process. The net displacement within the capillary is in the cathodic direction because electroosmosis exceeds electrophoretic displacement. This is similar to the zone electrophoretic analysis of anions reported by Jorgenson and Lukacs⁵.

Fig. 4 displays data for an anionic ITP determination of *S*-carboxymethyl-L-cysteine (SCMC) in human urine using an untreated fused-silica capillary. The leader was 10 mM HCl, adjusted with histidine to pH 6, and the terminator was 30 mM MES adjusted with histidine to pH 6. This represents the same configuration as employed for the data shown in the lower panel of Fig. 3 and supplements the ITP analyses of this drug reported elsewhere¹². Again the sequence of zone detection is reversed compared with analyses in electroosmosis-free configurations. These data provide information on the magnitude of electroosmosis via detection of the "stationary" boundary which was formed electrophoretically at the location of the initial discontinuity (marked with an asterisk in A and B).

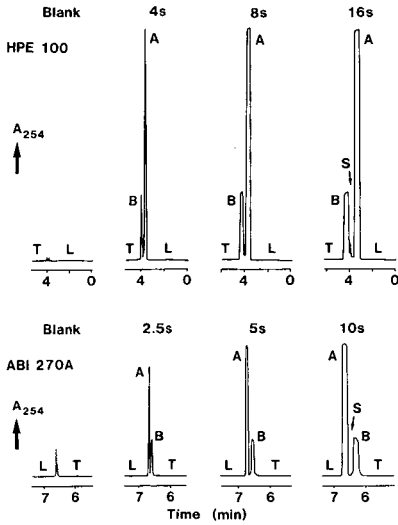


Fig. 3. Anionic capillary ITP of amaranth red (A, 1 mM), acetate (spacer, S, 2 mM) and bromphenol blue (B, 1 mM) between 10 mM HCl adjusted with histidine to pH 6 (leader) and MES-histidine at pH 6 (terminator). The electropherograms presented were obtained in a coated capillary of 20 cm length (HPE 100; upper panel; configuration ii in Fig. 1) and in an untreated capillary of 60 cm length (ABI 270A; lower panel; configuration iv in Fig. 1). In the first approach sample application occurred by electromigration at a constant 8 kV for 0 (blank), 4, 8 and 16 s. The running voltage was 8 kV and the current decreased from 2 to about 0.7 μ A. In the second instrument sample insertion occurred by vacuum aspiration at the time intervals indicated. The running voltage was 30 kV, the temperature 35°C and the current decreased from 6 to 4 μ A within the first 2 min of current flow and was again about 6 μ A during detection of sample zones. Detection was performed at 254 nm in both instruments. Note that the sequence of zone detection is different in the two approaches.

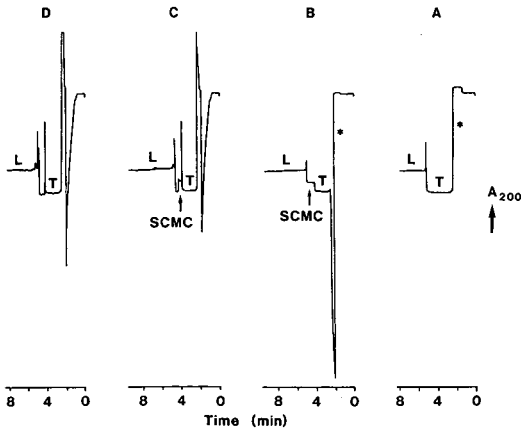


Fig. 4. Anionic ITP of S-carboxymethyl-L-cysteine (SCMC) in human urine in an untreated capillary of 60 cm length and 50 μ m I.D. (ABI 270A). The buffer configuration described for Fig. 3 was used. Volume injection occurred for 15 s by vacuum aspiration. The running voltage was 30 kV, the temperature was 35°C and the detector settings were at 200 nm and 0.5 A.U. The current decreased initially from about 6 to 4 μ A before increasing again to 6 μ A. Electropherograms for (A) the blank, (B) a 10-mM SCMC sample solution, (C) urine spiked with 20 mM SCMC and (D) control urine are shown. The urine samples were pretreated by filtration using Sep-Pak C₁₈ cartridges (Waters Assoc., Milford, MA, U.S.A.) as described elsewhere¹². The asterisks indicate the detection of the boundary formed at the location of the initial buffer discontinuity.

As reported earlier, there are electrolyte systems which are suitable for ITP analyses in both migrational directions (dual ITP)¹³. In principle, cationic and anionic sample trains could be monitored having a single detector placed toward the cathodic end of an untreated fused-silica capillary. Fig. 5 depicts an electropherogram using the operational configuration iii in Fig. 1 with 10 mM sodium formate as catholyte (cationic leader) and 2.5 mM HCl as anolyte (anionic leader). Cser and amaranth red were employed as sample components. The cationic ITP zone of cser was monitored within a short time but the anionic zone migrated too slowly to reach the detector within 10 min (and even 60 min in other runs) of current flow. In every instance, however, the amaranth red zone (A in Fig. 5) was moved across the point of detection during the subsequent wash of the capillary. This means that the electroosmotic flow at the low pH was stronger than the electrophoretic displacement. An additional hydrodynamic flow towards the cathode could be applied and used for the detection of this anionic zone pattern under current flow.

Important for quantification by zone length measurements with a stationary, single sensor is that the current does not change appreciably during detection. Therefore, ITP data obtained at constant current are simpler to evaluate than those monitored at constant voltage. Further, data generated with electrokinetic sample application at constant voltage (as provided with both instruments used in this work) are difficult to evaluate quantitatively. In all instances the current was observed to decrease considerably during that process, and therefore doubling of the injection time did not exactly double the detected sample zone length. However, with volume injection, as is provided in the ABI 270A, a linear relationship between the time of sample application and monitored zone length was obtained.

The data presented here show that open-tubular fused-silica capillaries of 25–50 μm I.D. are well suited for rapid high-resolution ITP analyses of low-molecular-mass

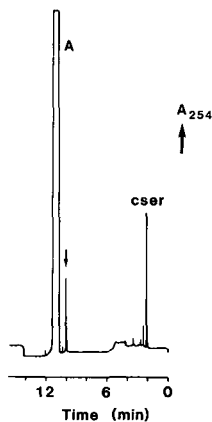


Fig. 5. "Dual" ITP with 10 mM sodium formate as catholyte and 2.5 mM HCl as anolyte. Electrophoresis took place in an untreated capillary of 70 cm length (ABI 270A). The sample was composed of cser and amaranth red, about 6 mM each. Sample application occurred for 6 s using vacuum aspiration, the temperature was 35°C and the monitoring was performed at 254 nm. A constant 30 kV was applied for 10 min. The current dropped from 9 to 2 μA within 7 min of power application. The cser zone (cationic ITP) passes the detector after about 2 min of current application. Amaranth red (A) passes through the detector cell during the wash cycle. The arrow marks the end of power application.

substances. Zone transitions are extremely sharp at the high current densities applied (3000–4000 A/m²). Some distortions of zone plateaux are observed at these high current densities. Electroosmosis in open-tubular, untreated, fused-silica capillaries does not hinder the formation of ITP zones. Anionic ITP analyses can be performed with a net zone displacement toward the cathode. This also represents a configuration which is potentially suitable for the evaluation of cationic and anionic ITP sample trains in a single experiment (dual ITP).

ACKNOWLEDGEMENTS

The generous loan of the HPE 100 by its manufacturer, Bio-Rad Labs., Richmond, CA, U.S.A., and of the ABI 270A by the Paul Bucher Company, Basle, Switzerland, is gratefully acknowledged. This work was supported in part by the Swiss National Science Foundation.

REFERENCES

- 1 F. M. Everaerts, J. L. Beckers and Th. P. E. M. Verheggen, *Isotachophoresis*, Elsevier, Amsterdam, 1976.
- 2 P. Boček, M. Deml, P. Gebauer and V. Dolník, *Analytical Isotachophoresis*, VCH, Weinheim, 1988.
- 3 W. Thormann, *Sep. Sci. Technol.*, 19 (1984) 455.
- 4 W. Thormann and R. A. Mosher, in A. Chrambach, M. J. Dunn, and B. J. Radola (Editors), *Advances in Electrophoresis*, Vol. 2, VCH, Weinheim, 1988, pp. 45–108.
- 5 J. W. Jorgenson and K. D. Lukacs, *Science (Washington, D.C.)*, 222 (1983) 266.
- 6 M. J. Gordon, X. Huang, S. L. Pentoney and R. N. Zare, *Science, (Washington, D.C.)*, 242 (1988) 224.
- 7 S. Hjertén, K. Elenbring, F. Kilår, J. Liao, A. J. C. Chen, C. J. Siebert and M. Zhu, *J. Chromatogr.*, 403 (1987) 47.
- 8 H. R. Udseth, J. A. Loo and R. D. Smith, *Anal. Chem.*, 61 (1989) 228.
- 9 W. Thormann and R. A. Mosher, in C. Schafer-Nielsen (Editor), *Electrophoresis '88*, Protein Laboratory, University of Copenhagen (Distributor: VCH, Weinheim), 1988, pp. 121–140.
- 10 P. H. Rhodes, R. S. Snyder and G. O. Roberts, *J. Colloid Interface Sci.*, 129 (1989) 78.
- 11 W. Thormann, R. A. Mosher and M. Bier, in C. J. King and J. D. Navratil (Editors), *Chemical Separations, Vol. 1, Principles*, Litarvan Literature, Denver, CO, 1986, pp. 153–168.
- 12 Y. Tanaka and W. Thormann, *Electrophoresis*, 11 (1990) in press.
- 13 W. Thormann, D. Arn and E. Schumacher, *Electrophoresis*, 6 (1985) 10.

Applicability of dynamic change of pH in the capillary zone electrophoresis of proteins

F. FORET

Institute of Analytical Chemistry, Kounicova 42, 61142 Brno (Czechoslovakia)

S. FANALI

Istituto di Cromatografia, P.O. Box 10, I-00016 Monterotondo Scalo (Italy)

and

P. BOČEK*

Institute of Analytical Chemistry, Kounicova 42, 61142 Brno (Czechoslovakia)

ABSTRACT

A method to extend the separation power of CZE is described. The method is based on the separation of sample components at two different pH values during one separation run, and involves dynamic buffering of the pH inside a separation capillary by controlling the flow of H^+ ions from the anodic electrode chamber. By changing the anolyte in the chamber, a dynamic pH step is generated, which proceeds rapidly along the capillary and establishes the required new pH value. The use of the method has been demonstrated by the cationic separation of a model mixture of proteins.

INTRODUCTION

In capillary zone electrophoresis (CZE), it is often very difficult to find a suitable buffer composition with which both complete separation of all analyte substances and their reasonably rapid migration may be achieved. With acids and bases possessing similar ionic mobilities and a wide range of pK values, the finding of a suitable pH value is often almost impossible. With protein mixtures possessing a wide range of pI values, very low (< 4)¹ or very high (> 10)² pH values are frequently required, which causes difficulties in finding a suitable background electrolyte (BGE). Recently, it was established³ that the buffering of pH may be effectively controlled by the regulated electromigratory flow of ions into the BGE in the capillary.

It has already been shown that various types of controlled changes are possible, namely, pH gradients⁴, pulses of counter ions⁵ and step changes of counter ions⁶. In previous work⁷, we described the programmable formation of pH gradients by means of time-controlled pH changes in the anodic electrode chamber. Here we demonstrate the utilization of dynamic step changes of H^+ serving as the co-ion, which lead to the possibility of using two different pH values during one analytical run.

Obviously, step changes of pH closely resemble the mobilization of substances after isoelectric focusing^{8,9}. The formation of pH gradients for the improvement of the separation of proteins has recently also been demonstrated in free-flow electrophoresis¹⁰.

The principle of the performance of stepwise changes of the pH of the BGE can be explained with the help of migration trajectories⁶ (see Fig. 1). It can be seen in Fig. 1 that substances A and B are not separated at pH_1 as their trajectories are identical. The pair of substances A and C cannot be separated at pH_2 as their trajectories show the same slopes (which reflects the same mobilities); however, once separated, these substances migrate in parallel and do not mix. Further, it can be seen from Fig. 1 that the change from pH_1 to pH_2 moves very fast and soon reaches and passes the substances to be analysed.

To fulfil the requirement that the change from pH_1 to pH_2 moves sufficiently fast along the migration path L, unbuffered BGE must be used, where the migration of H^+ is not hindered by the formation of reaction moving boundaries. These reaction boundaries are well known in isotachopheresis, where their existence is employed to create H^+ terminating zones in cationic systems¹¹.

EXPERIMENTAL

A Bio-Rad HPE 100 electrophoretic analyser equipped with a $20 \text{ cm} \times 25 \mu\text{m}$ I.D. coated fused-silica capillary was used in all experiments. All chemicals were of analytical-reagent grade from Serva (Heidelberg, F.R.G.). A mixture containing cytochrome *c* (horse heart), lysozyme (chicken egg), myoglobin (horse heart), carbonic anhydrase (bovine) and trypsinogen (bovine), all from Sigma (St. Louis, MO, U.S.A) was used as the model sample. All proteins were dissolved in 0.05 M Tris-HCl electrolyte at $\text{pH} 3.0$ and their concentration was 0.1 mg/ml .

The sample was introduced into the capillary by electromigration for 6 s at 7 kV and the analysis was performed at constant voltage of 8 kV.

RESULTS AND DISCUSSION

For the verification of the possibility of the dynamic control of pH, separations were performed at both a constant pH of the BGE and with pH changes during the

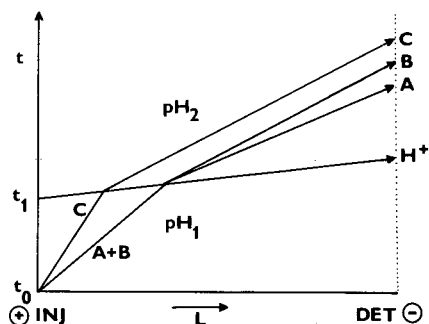


Fig. 1. Migration trajectories of cations A, B and C in CZE with a dynamic pH step. t = Time of migration; INJ = injection; DET = detection; L = migration path.

analysis. The separation records obtained at constant pH of the BGE (pH 3.0, 3.8 and 4.5) are shown in Fig. 2a, b and c, respectively.

It can be seen from Fig. 2a that at low pH (3.0) the proteins migrate rapidly and give symmetrical peaks; however, myoglobin, carbonic anhydrase and trypsinogen are separated only partially or not at all.

At pH 3.8 (Fig. 2b), carbonic anhydrase and trypsinogen are slower than myoglobin and they are separated from it, but their mutual separation is only partial.

At pH 4.5 (Fig. 2c), the mobility of lysozyme is reduced to a greater extent than that of myoglobin and the peaks of lysozyme and myoglobin are resolved only partially. The peaks of carbonic anhydrase and trypsinogen are fully resolved, but tailing of last three peaks is more pronounced. Obviously, for a good mutual separation of lysozyme and myoglobin, pH 3.0 or 3.8 should be selected, but this is not suitable for the mutual separation of carbonic anhydrase and trypsinogen. On the other hand, for a good separation of the last pair, pH 4.5 should be selected, but this is not suitable for the separation of myoglobin and lysozyme. Hence it is clear that any one of these pH values, if kept constant, does not provide a successful separation of the whole mixture.

For the reasons mentioned earlier, a step change of pH should be selected in such a way that $pH_2 < pH_1$ for cationic separations. Obviously, the propagation of the H^+ front is much faster than the migration of the sample zones. As is known from theory^{1,2}, when a front of a highly mobile cation penetrates electrophoretically into the BGE containing cations with a lower mobility, a moving concentration gradient is formed. Thus, in the case of an H^+ front a moving pH gradient is formed. This dynamic pH gradient also brings an inherent focusing effect which may decrease the tailing of the peaks.

The utilization of dynamically controlled pH is shown in Fig. 3, where a pH change from 4.5 to 3.0 was applied. Based on preliminary experiments, a period of

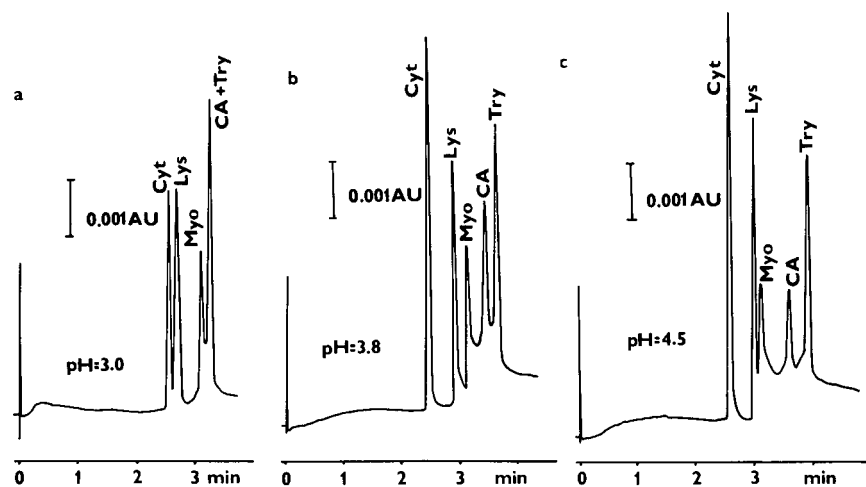


Fig. 2. Cationic separation of proteins at constant pH of the BGE: (a) pH 3.0 (8 kV, 13 μ A); (b) pH 3.8 (8 kV, 12 μ A); (c) pH 4.5 (8 kV, 12 μ A). UV detection at 206 nm. Cyt = cytochrome; Lys = lysozyme; Myo = myoglobin; Try = trypsinogen; CA = carbonic anhydrase.

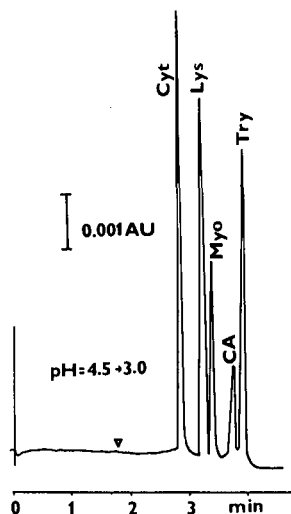


Fig. 3. Cationic separation of proteins using a dynamic pH step. pH change from 4.5 to 3.0. Other details as in Fig. 2.

2 min was elected as a suitable time interval for the first stage of separation at higher pH of the BGE. This combination resulted in complete separation and fairly symmetrical peaks.

We conclude that the use of a step change of pH in CZE can substantially improve the separation of protein mixtures. This improvement can be attributed both to the change in the selectivity during the separation and focusing of the rear boundary of migrating zones.

ACKNOWLEDGEMENT

The authors thank the Bio-Rad subsidiary in Rome, Italy, for the loan of the instrumentation used.

REFERENCES

- 1 R. McCormick, *Anal. Chem.*, 60 (1988) 2322.
- 2 H. H. Lauer and D. McManigill, *Anal. Chem.*, 58 (1986) 166.
- 3 J. Pospíchal, M. Deml, P. Gebauer and P. Boček, *J. Chromatogr.*, 470 (1989) 43.
- 4 P. Boček, M. Deml, J. Pospíchal and J. Sudor, *J. Chromatogr.*, 470 (1989) 309.
- 5 P. Boček, M. Deml and J. Pospíchal, *J. Chromatogr.*, 1990, in press.
- 6 J. Sudor, Z. Stránský, J. Pospíchal, M. Deml and P. Boček, *Electrophoresis*, 10 (1989) 802.
- 7 V. Šustáček, F. Foret and P. Boček, *J. Chromatogr.*, 480 (1989) 271.
- 8 Z. Buzás, L. M. Hjelmeland and A. Chrambach, *Electrophoresis*, 4 (1983) 27.
- 9 S. Hjertén, F. Kilár, L. Liao and M. Zhu, in M. J. Dunn (Editor), *Electrophoresis '86*, VCH, Weinheim, 1986, p. 451.
- 10 S. A. Shukun and V. P. Zavyalov, *J. Chromatogr.*, 496 (1988) 121.
- 11 P. Boček, P. Gebauer and M. Deml, *J. Chromatogr.*, 219 (1981) 21.
- 12 F. E. P. Mikkers, F. M. Everaerts and Th. P. E. M. Verheggen, *J. Chromatogr.*, 169 (1979) 1.

CHROM. 22 575

Influence of buffer concentration, capillary internal diameter and forced convection on resolution in capillary zone electrophoresis

HENRIK T. RASMUSSEN and HAROLD M. McNAIR*

Department of Chemistry, Virginia Polytechnic Institute and State University, Blacksburg, VA 24061 (U.S.A.)

ABSTRACT

The relative velocity difference ($\Delta U/U_{av}$) of two zones, separated by capillary zone electrophoresis, increased with increasing buffer concentration, but remained constant for a given concentration regardless of electric field strength. For diffusion-limited band broadening, the increase in $\Delta U/U_{av}$ offset a decrease in migration velocity to provide slightly better resolution. In practice, however, additional dispersion occurred as a result of Joule heating, especially when concentrated buffers, high electric field strengths and/or capillaries with large internal diameters were employed. To improve efficiency, under such conditions, forced air convection was investigated as a means for dissipating some of the Joule heat generated. In 100- μm capillaries, forced convection increased efficiency from $190\,000 \pm 3.1\%$ relative standard deviation (R.S.D.) to $226\,000 \pm 3.3\%$ R.S.D. theoretical plates. For comparison, 264 000 theoretical plates were observed in 50- μm capillaries under similar operating conditions. In the latter case the improved efficiency is, however, obtained at the expense of sample capacity.

INTRODUCTION

By Giddings¹ definition, the resolution (R_s) between two species migrating at different linear velocities is given as:

$$R_s = \frac{N^{1/2}}{4} \frac{\Delta U}{U_{av}} \quad (1)$$

where N is the number of theoretical plates, and $\Delta U/U_{av}$ the relative velocity difference between the two components. This relative velocity difference may, for capillary zone electrophoresis (CZE), be expressed² as:

$$\Delta U/U_{av} = \frac{v_{el.1} - v_{el.2}}{v_{el.av} + v_{co}} \quad (2)$$

where $v_{el.1}$ and $v_{el.2}$ are the electrophoretic velocities of the two species being separated, $v_{el.av}$ their average electrophoretic velocity and v_{eo} the velocity resulting from electroosmosis; v_{el} and v_{eo} may be further defined as:

$$v_{el} = \mu_{el}E \quad \text{and} \quad v_{eo} = \mu_{eo}E \quad (3)$$

where E is the electric field strength, μ_{el} the electrophoretic mobility and μ_{eo} the coefficient of electroosmotic flow. Combination of eqns. 1–3 yields:

$$R_s = \frac{N^{1/2}}{4} \frac{\mu_{el.1} - \mu_{el.2}}{\mu_{el.av} + \mu_{eo}} \quad (4)$$

which predicts that optimization of resolution is contingent on controlling the parameters that control μ_{eo} and μ_{el} .

Expressions for μ_{eo} and μ_{el} may be given as³:

$$\mu_{eo} = \varepsilon\zeta/4\pi\eta \quad (5)$$

and

$$\mu_{el} = ze/6\pi\eta r \quad (6)$$

where ε is the dielectric constant of the buffer employed, ζ the zeta potential at the buffer–capillary interface, η the buffer viscosity, z the charge of the analyte, e the charge of an electron and r the analyte's hydrodynamic radius.

As seen from eqns. 4 and 5, resolution in CZE may be optimized by changing the zeta potential. This may be achieved by varying the buffer pH^{4,5}, by coating the capillary^{6,7}, by means of buffer additives^{5,8} or, as will be discussed in this paper, by changing the buffer concentration⁹.

It should be noted from eqn. 4 however, that for resolution to be optimized, the procedure employed to control μ_{eo} must not significantly reduce N . Due to the flat flow profile provided by electroosmotic flow¹⁰, N may, in the absence of Joule heating and extra-column band broadening, be expressed as²:

$$N = (\mu_{eo} + \mu_{el})V/2D \quad (7)$$

where V is the applied voltage used to effect the separation and D the molecular diffusion coefficient of the analyte.

In the presence of Joule heating however, a radial viscosity gradient is established inside the capillary and as a result N may be decreased considerably^{2,11–14}. Temperature additionally affects μ_{el} , μ_{eo} and D , and as such the degree of Joule heating becomes an important parameter in determining resolution. The Joule heat generated increases as capillary I.D., or electric-field strength is increased. To provide a viable comparison of resolution for different buffer concentrations, the influence of these parameters must therefore also be examined.

This work focuses on determining the influence of buffer concentration on resolution and characterizes forced air convection as a method for controlling Joule heating.

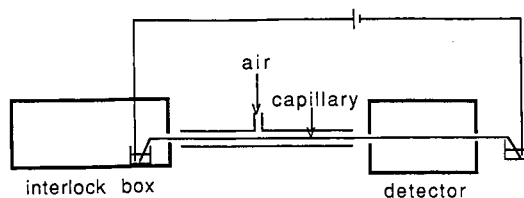


Fig. 1. Schematic of the apparatus for CZE employing forced convection.

EXPERIMENTAL

CZE was performed in $1\text{ m} \times 100\ \mu\text{m}$ I.D. (Chrompack, Raritan, NJ, U.S.A.) and $1\text{ m} \times 50\ \mu\text{m}$ I.D. (Polymicro, Phoenix, AZ, U.S.A.) fused-silica capillaries, using 0.01, 0.02 and 0.05 M Na_2HPO_4 , pH 7.00. To determine the influence of electric field strength on electroosmotic flow, phenol was dissolved in each operating buffer, introduced into the capillaries electrokinetically ($+3\text{ kV}/5\text{ s}$) and analyzed at operating voltages of $+10$ – $+25\text{ kV}$. In experiments where electrophoretic mobilities were additionally required, sodium toluenesulfonate (STS) was added to the above samples.

Voltages required for sample introduction and electrokinetic migration were provided by a Spellman Model RHR 30 high-voltage power supply (Spellman, Plainview, NY, U.S.A.). On capillary UV detection at 254 nm was effected 80 cm from the point of sample introduction, using an ISCO Model CV4 capillary electrophoresis absorbance detector (ISCO, Lincoln, NE, U.S.A.). To evaluate the effect of forced air convection, the capillary was inserted into a $50\text{ cm} \times 8\text{ mm}$ I.D. glass tube and air introduced through a sidearm in the tube at 3.5 l/min (Fig. 1).

RESULTS AND DISCUSSION

Due to the dependence of resolution on each of the operating parameters in CZE, optimization of resolution must be discussed with respect to all the variables. Consequently, to determine the influence of buffer concentration on resolution, the influence of capillary internal diameter and electric field strength must be evaluated. As shown by Boček *et al.*¹³, the relationship between Joule heating and μ_{eo} may be determined for a given capillary diameter by measuring μ_{eo} as a function of electric field strength.

In this study, μ_{eo} was determined from the migration times (t_R) of phenol, using the equation¹⁵:

$$\mu_{eo} = L/t_{R(\text{phenol})}E \quad (8)$$

where L is the distance along the capillary from the point of sample introduction to the detector (80 cm). The use of phenol as a μ_{eo} marker has been documented previously⁴. Phenol has a $\text{p}K_a$ of 10.0 at 25°C , and may thus be considered neutral at a pH of 7.00.

The influence of buffer concentration and electric field strength on μ_{eo} in a $50\ \mu\text{m}$ capillary is shown in Fig. 2. The use of more concentrated Na_2HPO_4 buffers decreased μ_{eo} (refs. 7 and 9). Additionally, as indicated by the increase in μ_{eo} with increasing

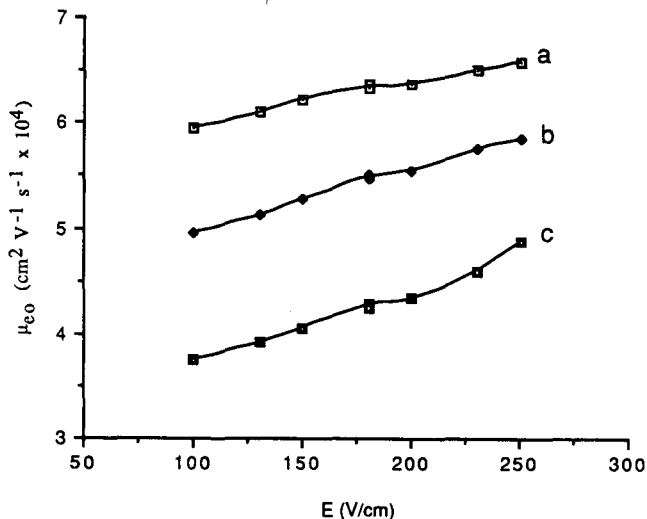


Fig. 2. Influence of buffer concentration and electric field strength (E) on the coefficient of electroosmotic flow (μ_{eo}) in 50- μm capillaries¹³. Na_2HPO_4 concentrations: a = 0.01 M ; b = 0.02 M ; c = 0.05 M .

electric field strength, Joule heating of the buffers occurred, which is in agreement with the results reported by Boček *et al.*¹³. In 100- μm capillaries (Fig. 3) the same relationship between buffer concentration and μ_{eo} was observed at lower electric field strengths. However, as expected, Joule heating was more pronounced in the larger capillary, especially when concentrated buffers were employed; as a result μ_{eo} increased markedly with electric field strength.

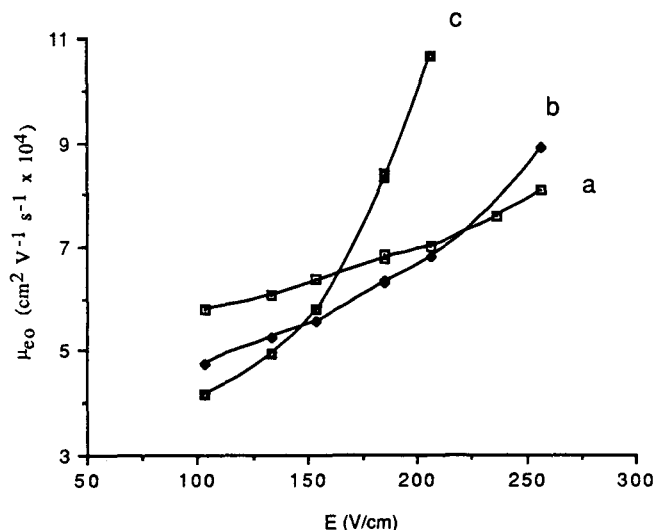


Fig. 3. Influence of buffer concentration and electric field strength (E) on the coefficient of electroosmotic flow (μ_{eo}) in 100- μm capillaries¹³. Na_2HPO_4 concentrations: a = 0.01 M ; b = 0.02 M ; c = 0.05 M .

As can be seen from eqns. 4 and 7, the effects observed in Figs. 2 and 3 make it difficult to determine the optimum experimental conditions for CZE. From eqn. 4, μ_{eo} is seen to be an important parameter in determining the relative velocity difference. From eqn. 7, the increase in both the applied voltage and μ_{eo} is predicted to have a favorable influence on N . The improvement in diffusion-limited efficiency is, however, potentially offset by the greater degree of Joule heating.

To better understand the influence of μ_{eo} and Joule heating on resolution, the various operating parameters were evaluated with respect to separation efficiency and the relative velocity difference. The relative velocity difference $(\mu_{el.1} - \mu_{el.2})/(\mu_{el.av} + \mu_{eo})$ was determined from the separation of phenol and STS. By virtue of its negative charge, toluenesulfonate eluted after phenol and its electrophoretic mobility was designated $\mu_{el.2}$; $\mu_{el.1}$ corresponds to the electrophoretic mobility of phenol and was assumed to be zero. Since the total linear velocity (v) of STS is governed by both electrophoresis and electroosmosis, its migration time is given as:

$$t_R = L/v = L/(-\mu_{el} + \mu_{eo})E \quad (9)$$

which, on rearrangement, gives μ_{el} in terms of experimentally measurable parameters as:

$$\mu_{el} = \mu_{eo} - L/t_R E \quad (10)$$

As shown in Fig. 4, the expression $(\mu_{el.1} - \mu_{el.2})/(\mu_{el.av} + \mu_{eo})$ was constant for a given buffer concentration, regardless of electric field strength. This was observed not only for a 0.01 M buffer in a 50- μm capillary, where Joule heating was minimal, but also for

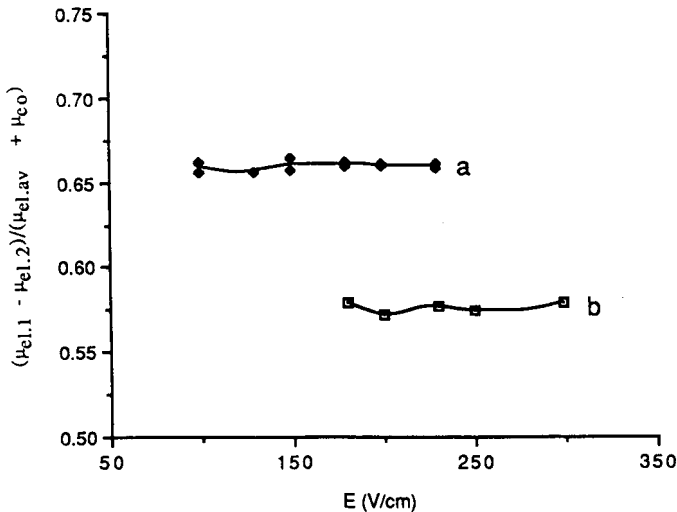


Fig. 4. Influence of buffer concentration and electric field strength (E) on the relative velocity difference $(\mu_{el.1} - \mu_{el.2})/(\mu_{el.av} + \mu_{eo})$. Conditions: a = 0.02 M buffer/100- μm capillary; b = 0.01 M buffer/50- μm capillary.

0.02 *M* Na₂HPO₄ in a 100- μ m capillary where appreciable Joule heating was observed at high electric field strengths. The independence of the relative velocity difference with Joule heating is presumably attributable to the both μ_{e1} and μ_{e0} having the same viscosity dependence (eqns. 5 and 6)⁶.

The average values of the relative velocity difference were 0.576 and 0.661 in the 0.01 and 0.02 *M* buffers, respectively. Thus, on the basis of the relative velocity difference alone, resolution was improved in 0.02 vs. 0.01 *M* buffer, by a factor of 1.15. The influence of efficiency must, however, also be explored.

If it is assumed that no Joule heating occurs, as is presumably the case when 50- μ m capillaries and low electric field strengths are employed, eqn. 7 may be rewritten to express resolution as a function of efficiency as:

$$R_s = f(v/2D)^{1/2} \quad (11)$$

If it can, additionally, be assumed that diffusion coefficients are the same in each buffer, resolution as a function of efficiency, in 0.02 vs. 0.01 *M* buffer, can be shown to be decreased by the ratio $(v_{0.02}/v_{0.01})^{1/2}$, where $v_{0.02}$ and $v_{0.01}$ are the linear velocities in 0.02 and 0.01 *M* buffer, respectively. At low electric field strengths (100 V/cm), the linear velocities of phenol were determined to be $4.96 \cdot 10^{-2}$ (0.02 *M*) and $5.96 \cdot 10^{-2}$ cm/s (0.01 *M*). Accordingly, the resolution as a function of efficiency ratio was 0.912.

Multiplication of the relative velocity difference and efficiency ratios yielded a value of 1.05. It is thus seen that the more concentrated buffer did not provide a significant improvement in resolution. Additionally, as higher electric field strengths or larger internal diameter capillaries were used, the degree of Joule heating increased to a greater extent in the 0.02 *M* buffer (Fig. 3). As shown in Fig. 5, Joule heating

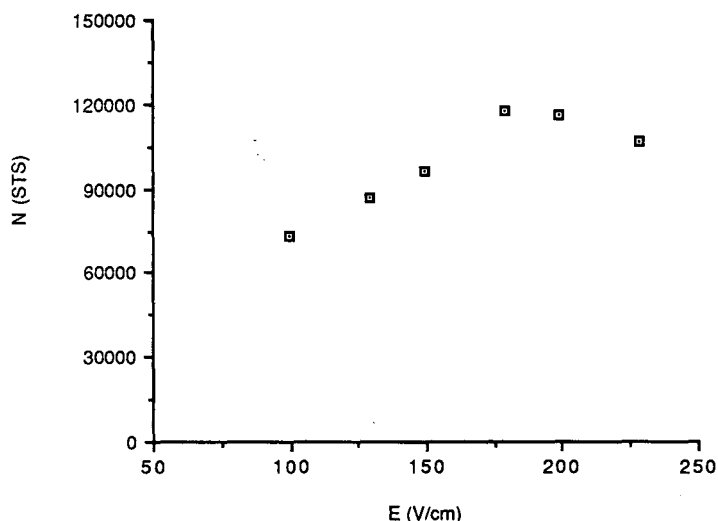


Fig. 5. Influence of electric field strength (*E*) on the efficiency (*N*) of STS. Conditions: buffer: 0.02 *M* Na₂HPO₄; capillary: 100 μ m.

actually decreased efficiency at high electric field strengths, when the separation was performed in a 100- μm capillary using 0.02 M buffer. When appreciable Joule heating occurs, the resolution as a function of efficiency ratio will, consequently, be reduced with respect to the ratio calculated in the diffusion-limited case and resolution is predicted to be improved in the less concentrated buffer.

By comparing Figs. 2 and 3, it can be seen that Joule heating was much less appreciable in 50- vs. 100- μm capillaries. To maximize resolution, the capillary internal diameter should, therefore, be minimized regardless of the buffer concentration used.

It may, however, be undesirable to use 50- μm capillaries in applications where detectability is a problem. Defining N as:

$$N = \frac{t_R^2}{\sigma^2} \quad (12)$$

where σ^2 , the total variance, is the summation of independent sources of zone dispersion; it is seen that each source of variance should be minimized. The variance contribution from sample volume, σ_S^2 , may be expressed as¹⁶:

$$\sigma_S^2 = \frac{\tau^2}{12} \quad (13)$$

where τ , the sampling time, is related to the sample volume, S , introduced. For a cylindrical capillary of internal diameter, d_c , the relationship is:

$$\tau = \frac{S}{v\pi(d_c/2)^2} \quad (14)$$

Combination of eqns. 13 and 14 allows for σ_S^2 to be expressed as:

$$\sigma_S^2 = \frac{S^2}{12 v^2 \pi^2 (d_c/2)^4} \quad (15)$$

which predicts that 16 times the sample volume may be introduced in 100- vs. 50- μm capillaries to yield the same σ_S^2 . Thus while the zone concentration in 50- μm capillaries is four times that obtained in 100- μm capillaries (assuming equal efficiencies and migration times), concentration detection limits are predicted to be improved in the larger capillaries by virtue of the larger sample volume allowed.

The latter prediction is, additionally, influenced by the specific design of the detector employed and the experimental values of N and t_R obtained in 50- and 100- μm capillaries. However, its validity can readily be shown to be upheld. For on-capillary UV detection, generating the same noise level for 50- and 100- μm capillaries, the detection limits are improved for the larger capillary as the result of a longer pathlength (the specific improvement is governed by the detector slit width and the capillary position in the light path).

The influence of t_R and N on the detection limit may be evaluated from the peak

area (A) of an eluting analyte. The area of a Gaussian peak may be described by the expression¹⁶:

$$A = 2.51\sigma h \quad (16)$$

where h is the height at the peak apex. Eqn. 16 may be combined with eqn. 12 and rearranged to yield:

$$h = \frac{AN^{1/2}}{2.51t_R} \quad (17)$$

Thus, for the same peak area, a larger peak height (signal) will result in the higher efficiency case. In practice however, the efficiency enhancement observed in 50- vs. 100- μm capillaries is minimal (as will be shown) and as a result does not offset the sample-size advantage obtained in the larger capillaries. Furthermore, as illustrated in Figs. 2 and 3, the decrease in efficiency resulting from Joule heating is countered by a smaller t_R value by virtue of increased electroosmotic flow.

From the foregoing, it may be concluded that improved concentration detection limits are obtained in 100- μm capillaries. This improvement is, however, accompanied by a decrease in efficiency which may be required to effect the separation. To achieve a compromise between detectability and resolution, it is therefore desirable to find a method of reducing Joule heating. The theoretical work of Knox¹² has predicted that the Joule heat generated may be dissipated by forced convection. This prediction is supported by the experimental work of Boček *et al.*¹³ and Nelson *et al.*¹⁷ and by these results, as shown in Fig. 6. When forced air convection at 3.5 l/min was applied to

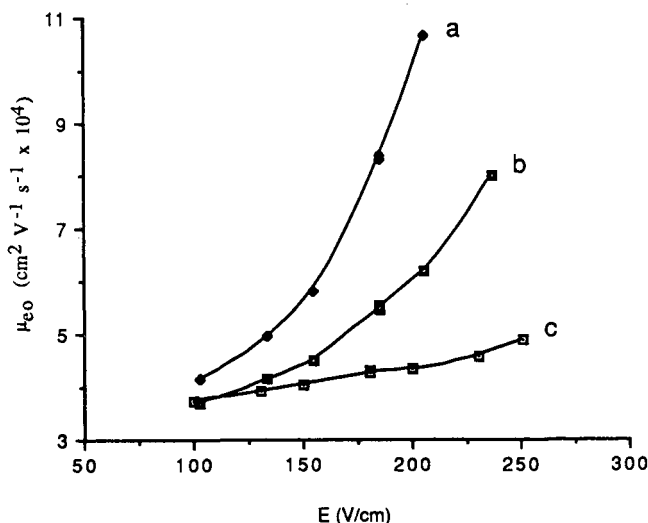


Fig. 6. Influence of forced convection on the coefficient of electroosmotic flow (μ_{eo}) in 0.05 M Na_2HPO_4 ¹³. Capillaries: a = 100 μm ; b = 100 μm with convection; c = 50 μm .

50 cm of the 100- μm capillary (Fig. 1), μ_{eo} as a function of electric field strength was reduced in comparison to the same capillary in the absence of forced convection.

As a result of the reduction in Joule heating, efficiency was improved. Initial results showed the efficiency for phenol in 0.05 M Na_2HPO_4 at 18 kV/m to increase from 112 000 to 117 000 theoretical plates when forced convection was employed¹⁸. In these initial studies however, high concentrations of phenol were employed and consequently an additional source of band broadening was incurred^{4,13,19}. When the analyses were repeated at 22.7 kV/m and a $2 \cdot 10^{-4}$ M phenol solution used as the sample, efficiencies were improved from $191\,000 \pm 3.1\%$ relative standard deviation (R.S.D.) to $226\,000 \pm 3.3\%$ R.S.D. theoretical plates (based on 4 determinations). For comparison, the efficiency obtained in 50- μm capillaries, under similar operating conditions, was approximately 264 000 theoretical plates.

As can be seen from Fig. 6, more effective forced convection is required to reduce μ_{eo} to approach the level observed in 50- μm capillaries. Work to achieve this via changes in the air flow-rate, changes in the chemical nature of the dissipant and convection along the entire length of the capillary, is currently ongoing.

ACKNOWLEDGEMENTS

H.T.R. wishes to thank the San Francisco Bay Area Chromatography Colloquium and the Barnett Institute of Northeastern University for a travel grant which made the presentation of this paper at HPCE '90 possible.

REFERENCES

- 1 J. C. Giddings, *Sep. Sci.*, 4 (1969) 181.
- 2 J. W. Jorgenson and K. D. Lukacs, *Anal. Chem.*, 53 (1981) 1298.
- 3 A. W. Adamson, *Physical Chemistry of Surfaces*, Wiley-Interscience, New York, 4th ed., 1981, Ch. 5.
- 4 K. D. Lukacs and J. W. Jorgenson, *J. High Resolut. Chromatogr. Chromatogr. Commun.*, 8 (1985) 407.
- 5 K. D. Altria and C. F. Simpson, *Chromatographia*, 24 (1987) 527.
- 6 S. Hjerten, *J. Chromatogr.*, 347 (1985) 191.
- 7 G. J. M. Bruin, J. P. Chang, R. H. Kuhlman, K. Zegers, J. C. Kraak and H. Poppe, *J. Chromatogr.*, 471 (1989) 429.
- 8 S. Fujiwara and S. Honda, *Anal. Chem.*, 59 (1987) 487.
- 9 K. D. Altria and C. F. Simpson, *Anal. Proc.*, 23 (1986) 453.
- 10 M. Martin, G. Guiochon, Y. Wahlbroehl and J. W. Jorgenson, *Anal. Chem.*, 57 (1985) 559.
- 11 E. Gruska, R. M. McCormick and J. J. Kirkland, *Anal. Chem.*, 61 (1989) 241.
- 12 J. H. Knox, *Chromatographia*, 26 (1988) 329.
- 13 F. Foret, M. Deml and P. Boček, *J. Chromatogr.*, 452 (1988) 601.
- 14 H. H. Lauer and D. McManigill, *Trends Anal. Chem.*, 5 (1986) 11.
- 15 K. D. Lukacs, *Thesis*, University of North Carolina, Chapel Hill, NC, 1983.
- 16 J. C. Sternberg, *Adv. Chromatogr.*, 2 (1966) 205.
- 17 R. J. Nelson, A. Paulus, A. S. Cohen, A. Guttman and B. L. Karger, *J. Chromatogr.*, 480 (1989) 111.
- 18 H. T. Rasmussen and H. M. McNair, presented at the 2nd International Symposium on High Performance Capillary Electrophoresis, San Francisco, CA, 1990, paper P-122.
- 19 F. E. P. Mikkers, F. M. Everaerts and Th. P. E. M. Verheggen, *J. Chromatogr.*, 169 (1979) 1.

CHROM. 22 649

Non-uniform electrical field effect caused by different concentrations of electrolyte in capillary zone electrophoresis

XIAOHUA HUANG* and J. I. OHMS

Research Department, Spinco Division, Beckman Instruments, Inc., Palo Alto, CA 94304 (U.S.A.)

ABSTRACT

Capillary zone electrophoresis is usually performed with uniform electrolyte concentrations in the electrolyte reservoirs and the capillary and a resultant uniform electrical field. Thus, the sample species migrates as the algebraic sum of electroosmotic flow mobility and ionic mobilities. A non-uniform electrical field can be formed by filling the capillary and outlet reservoir with electrolyte at a given concentration (initial electrolyte) and the inlet reservoir with a different electrolyte concentration of the same chemical species (replacement electrolyte). Application of an electrical field causes continuous entrance of the replacement electrolyte changing the conductivity consequent to electrolyte concentration. Therefore, the electrical field strength is not uniform along the capillary. In this paper we will discuss the effect of this non-uniform electrical field on migration rates of different sample ions as well as its application to model samples.

INTRODUCTION

Capillary electrophoresis (CE) methodology has developed rapidly^{1–3}. In capillary zone electrophoresis (CZE), generally, the same electrolyte solution is used in the inlet reservoir, outlet reservoir and capillary tube. When voltage is applied to this system, an electroosmotic flow is produced and moves from capillary inlet (usually at the anode) to the outlet (usually at the cathode). In other words, the electrolyte solution in the inlet reservoir (replacement electrolyte) will move continuously into the capillary and the electrolyte solution initially inside the capillary (initial electrolyte) will be replaced continuously by the replacement electrolyte. Since there is no difference in composition and concentration between replacement electrolyte and initial electrolyte, there are no differences in electrolytic conductivity. If it is assumed that the electrical disturbance from sample zone can be neglected, a uniform electrical field will be established along the capillary. The value of this uniform electrical field strength is constant along the capillary length (spatially uniform) and with time (temporally uniform). In some cases, different kinds of electrolyte solutions are employed in the capillary and electrolyte reservoirs such as in capillary isotachopheresis⁴, iso-electric focusing⁵ and CZE with gradient electrolyte⁶. Either the composition or con-

centration of one or both of replacement and initial electrolytes may be different. Under these conditions, the electrical field strength along the capillary is not uniform. In this paper, a simplified equation is presented to describe this non-uniform electrical field.

EXPERIMENTAL

All experiments were performed with a P/ACE™ 2000 instrument (Beckman, Palo Alto, CA, U.S.A.). For these studies the capillary was 75 μm in diameter, 66 cm in total length, 61 cm from inlet to detector with an applied voltage of 20 kV. UV detection was at 254 nm. Temperature was controlled at 20°C. Phosphate buffer (pH 6.8) was made at different concentration levels from a stock solution of 100 mM. Pyridoxamine, nucleosides and nucleotides were purchased from Sigma (St. Louis, MO, U.S.A.) and used without further purification. Samples were diluted from stock solution (20 mM) to 0.2 mM with phosphate buffers.

RESULTS AND DISCUSSION

Preparation and simplified description of non-uniform electrical field

The formation of a non-uniform electrical field along the capillary can be explained by a simple model (see Fig. 1). Before applying voltage, the capillary was filled with initial electrolyte which has the unit resistance $r(i)$ (where unit resistance is defined as total resistance divided by capillary length). Since only initial electrolyte exists at this time, a uniform electrical field is established along the capillary. This is true for most situations in zone electrophoresis which use uniform electrolyte and samples which are not overloaded. Assuming that electroosmotic flow moves toward the cathode, the replacement electrolyte in the anode reservoir will continuously enter the inlet of the capillary. If the unit resistance of the replacement electrolyte is differ-

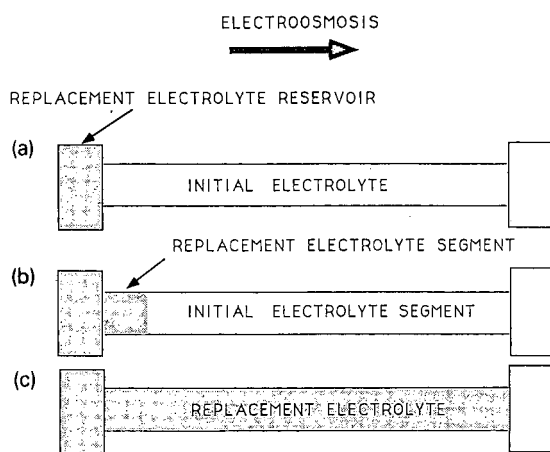


Fig. 1. Schematic model of non-uniform electrical field. (a) Uniform electrical field at the start of electrophoresis. (b) Non-uniform electrical field when the replacement electrolyte replaces some of the initial electrolyte. (c) Uniform electrical field after replacement electrolyte occupies the whole capillary.

ent from the initial electrolyte, for example at higher unit resistance, the electrical field along the capillary will not remain uniform.

There are two characteristics. First, at any moment prior to the front of replacement electrolyte reaching the capillary outlet, two different electrical field strengths exist along the capillary. The front of the replacement electrolyte acts as the boundary of these two levels of the electrical field. Under this condition, the replacement electrolyte at higher unit resistance has a greater electrical field and the initial electrolyte has lesser field. Second, this electrical field strength will continuously change with the rate of replacement electrolyte entering the capillary inlet and will establish a uniform electrical field strength after replacement electrolyte completely occupies the capillary.

A simple mathematical expression can be derived to describe the non-uniform electrical field along the capillary. In the beginning, the capillary is filled only with the initial electrolyte and the electrical field strength is constant:

$$E = V/L \quad (1)$$

Here, the E is electrical field strength (V/cm), V is applied voltage and L is total length of the capillary. Then, the replacement electrolyte moves into the capillary inlet and starts to replace the initial electrolyte inside the capillary. At time t the replacement electrolyte enters into the capillary to length l , then the total resistance R across the capillary is:

$$R = lr(r) + (L - l)r(i) \quad (2)$$

where $r(i)$ is the unit resistance of the initial electrolyte; $r(r)$ is the unit resistance of the replacement electrolyte; l is the length of segment of replacement electrolyte.

The voltage drop on l is:

$$V(l) = \frac{Vlr(r)}{lr(r) + (L - l)r(i)} \quad (3)$$

The electrical field strength on l is

$$E(l) = \frac{V(l)}{l} = \frac{Vr(r)}{lr(r) + (L - l)r(i)} \quad (4)$$

$$\frac{V}{l + (L - l)(r(i)/r(r))}$$

Letting $K = \frac{r(i)}{r(r)}$, eqn. 4 can be simplified to

$$E(l) = \frac{V}{l + (L - l)K} \quad (5)$$

Likewise, we can calculate electrical field strength on the initial electrolyte segment, $E(L-l)$

$$E(L-l) = \frac{V}{l/K + (L-l)} \quad (6)$$

From eqn. 5 we can see that:

(1) When $K = 1$, *i.e.*, there is no difference between initial and replacement electrolyte, the equation is simplified to $E(l) = V/L$, which is the same as the uniform electrical field situation.

(2) When $K \neq 1$, the electrical field strength along the capillary will not stay the same but will change with time. Fig. 2a shows the relationship between the electrical field strength and the length of replacement electrolyte at $K = 0.8$. Fig. 2b shows the relationship between electrical field strength and the length of initial electrolyte at $K = 1.25$.

(3) When the absolute value of K is close to 1, the difference between uniform and non-uniform electrical field is decreasing. Fig. 3 shows the relationship between K values and the changes of non-uniform fields.

Theoretically, K is the ratio of resistances of initial and replacement electrolyte. Since in CZE the ionic strength of electrolytes is quite small, we can probably use the ratio of concentrations without introducing significant errors in most cases.

Effect of non-uniform electrical field on the migration rates of different species

From Fig. 2, we can see that there are two different electrical field strengths along the capillary. For simplicity, we only discuss the $K < 1$ case (Fig. 2a), *i.e.*, the

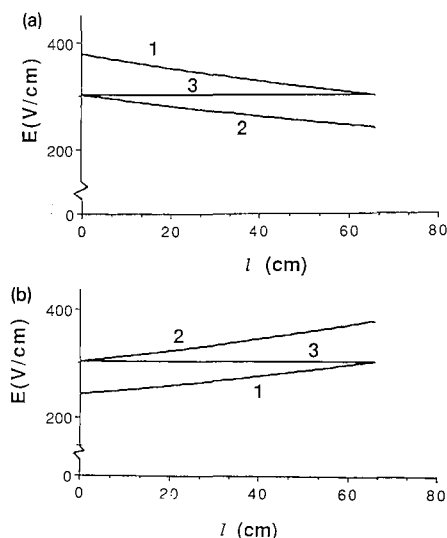


Fig. 2. Calculated electrical field strength in initial and replacement electrolyte segments. Parameters: Capillary length 66 cm. Applied voltage 20 kV. (a) $K = 0.8$; (b) $K = 1.25$. Curves: 1 = electrical field in replacement electrolyte segment; 2 = electrical field in initial electrolyte segment; 3 = in uniform electrical field.

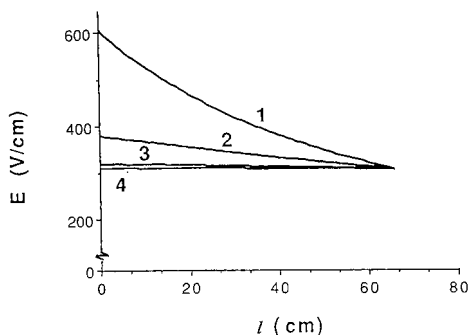


Fig. 3. The influence of K values to electrical field strength in replacement electrolyte segment. Parameters as in Fig. 2. Curves: (1) $K = 0.5$; (2) $K = 0.8$; (3) $K = 0.95$; (4) $K = 0.98$.

unit resistance of replacement electrolyte is higher than that of the initial electrolyte, in this case, the electrical field of the initial electrolyte is lower than the electrical field of the replacement electrolyte. For cations, the direction of electrophoretic mobility is the same as the electroosmotic flow. The total migration rate of a cation is:

$$v(\text{total}) = v(\text{eos}) + v(i) = v(\text{eos}) + E\mu(i) \quad (7)$$

were $v(i)$ and $\mu(i)$ are the migration rate and the mobility of the cation, respectively and $v(\text{eos})$ is the electroosmotic velocity. It should be noted that with a non-uniform field, the electroosmotic flow rate will not stay the same as it would under a uniform field conditions. For simplicity, here we use an overall electroosmotic velocity.

Since cations have greater total migration rate, they will migrate ahead of the front of the replacement electrolyte. In other words, they will migrate in the region of initial electrolyte. Since the electrical field is lower in initial electrolyte (when $K < 1$), the migration rate of cations will be lower than in uniform electrical field conditions. On the other hand, the direction of electrophoretic mobility of an anion is opposite to the electroosmotic flow. In this case the total migration rate is:

$$v(\text{total}) = v(\text{eos}) - v(i) = v(\text{eos}) - E\mu(i) \quad (8)$$

Since anions move slower than the electroosmotic flow, they migrate behind the front of replacement electrolyte, *i.e.*, they first migrate with a lower total velocity under a non-uniform electrical field and then migrate with a constant velocity under a newly-formed uniform electrical field after replacement electrolyte completely occupies the capillary. For less negatively charged anions, they will stay a shorter time in the later uniform electrical field. More negatively charged anions will stay longer in the later electrical field. Neutral molecules will migrate with the electroosmotic flow, *i.e.*, they will stay between the initial and replacement electrolyte. The difference of ionic strength and viscosity between the initial and replacement electrolyte will determine the migration rate of these neutral molecules. Fig. 4 is an example of the effects of a non-uniform electrical field on different species at different K values. Tables I and II give the calculated data of this effect. The ADP peak disappeared at $K = 0.5$.

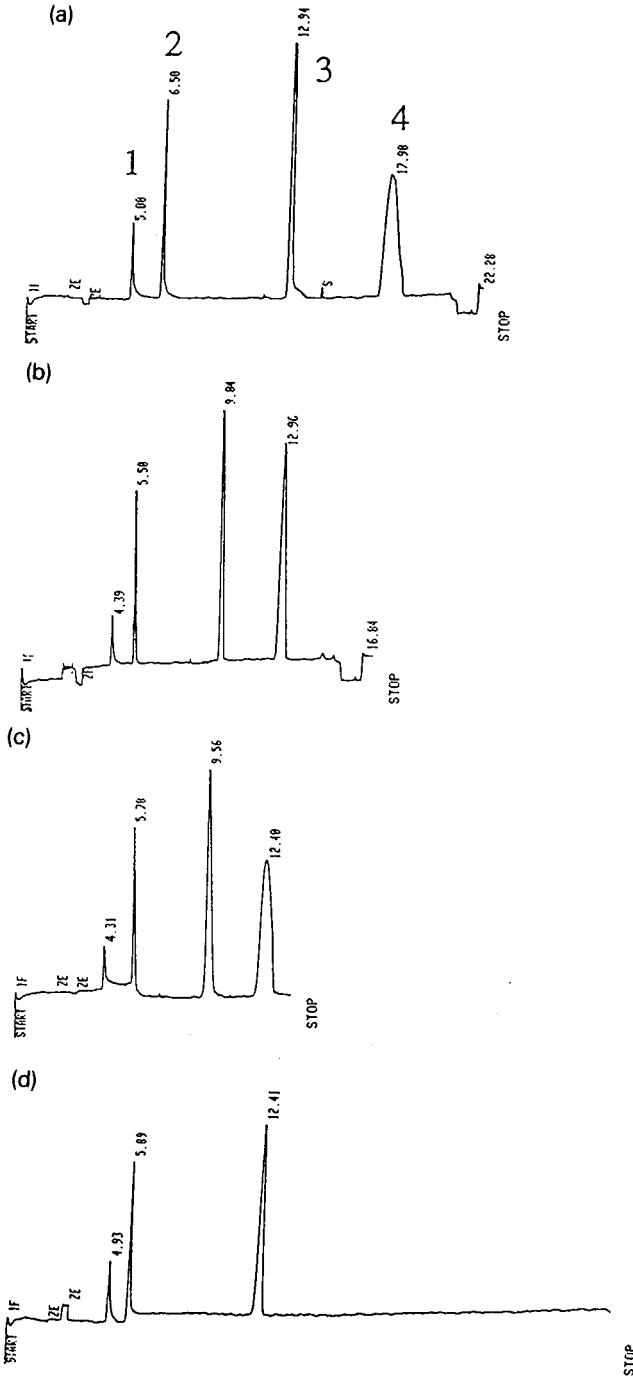


Fig. 4. Effect of non-uniform electrical field on the migration rates of different species. Capillary $75 \mu\text{m}$ I.D., 66 cm total length, 61 cm to detector. Applied voltage 20 kV. Phosphate buffer, pH 6.8. Sample: 1 = pyridoxamine; 2 = adenosine; 3 = AMP. 4 = ADP. (a) $K = 1$: Initial electrolyte 20 mM, replacement electrolyte 20 mM; (b) $K = 1$: Initial electrolyte 10 mM, replacement electrolyte 10 mM; (c) $K = 2$: Initial electrolyte 10 mM, replacement electrolyte 20 mM; (d) $K = 0.5$: Initial electrolyte 20 mM, replacement electrolyte 10 mM. Numbers at peaks indicate migration times in min.

TABLE I

MEAN OF MIGRATION RATE OF THREE SPECIES UNDER ELECTRICAL FIELD WITH DIFFERENT K VALUES.

Electrophoresis conditions as in Fig. 4. Pyr = pyridoxamine; Ado = adenosine; AMP = adenosine monophosphate.

K	Migration rate (mm/s)		
	Pyr	Ado	AMP
1.0 (20 mM)	0.47	1.54	-0.77
1.0 (10 mM)	0.47	1.83	-0.81
0.5	0.34	1.71	-0.90
2.0	0.59	1.75	-0.69

because ADP molecules have a higher negative charge. After injection the inlet of the capillary was placed in a higher unit resistance replacement electrolyte. When the replacement electrolyte enters the capillary, the ADP band will be in the replacement segment which has a higher electrical field strength. When $v(\text{eos})$ is less than $E\mu(\text{ADP})$; ADP will migrate backward and escape detection. As mentioned above, when K is close to 1, the effect will be reduced. At $K = 0.98$, this influence is insignificant.

Effects of non-uniform electrical field on sample injection

The simplified model of non-uniform electrical field can be used to explain the sampling bias in electrokinetic injection. When the conductivity of the sample solution is different from that of the running electrolyte in capillary zone electrophoresis, a non-uniform electrical field strength is formed along the capillary. This field will change the movement of the sample species in the sample solution. Here we assume that the sample concentration is at least 100 times less than the electrolyte concentration in which the sample is dissolved. Assuming the unit resistance of bulk sample solution is higher than the running electrolyte, *i.e.*, the local non-uniform electrical field of the sample zone which formed during sampling is higher than the uniform electrical field strength at the same applied voltage, the migration rate of both electroosmotic flow and ions will be altered. Thus the cation will enter the capillary inlet

TABLE II

RELATIVE CHANGE OF MIGRATION RATES SHOWN IN TABLE I

The values were obtained by comparison with the mean of these species in uniform electrical field ($K = 1$, in both of 10 mM and 20 mM conditions)

K	Relative change of migration rate (%)		
	Pyr	Ado	AMP
0.5	-28	<2	+12
2.0	+26	<4	-13

with a higher total velocity than in uniform electrical field strength conditions. Since the injection volume is proportional to the total velocity, more cations will be injected. A previous study discussed this kind of bias⁷. Anions have more complicated behavior. If the difference of electroosmotic mobility and ionic mobility does not suffer significant changes, the amount of anion injected is proportional to the local electrical field strength of the sample plug. In some cases, when non-uniform electrolyte is high enough due to high unit resistance of the sample solution, the product of E and $\mu(i)$ may be equal to or even larger than the electroosmotic flow-rate. Thus, the total velocities of anions will be equal to zero or a negative value. It means that these anions will not enter the capillary inlet during the sampling process, and as a result, these peaks will not appear in the electropherogram.

REFERENCES

- 1 J. Jorgenson and K. D. Lukacs, *Science (Washington, D.C.)* 222 (1983) 266.
- 2 M. J. Gordon, X. Huang, S. L. Pentoney, Jr. and R. N. Zare, *Science (Washington, D.C.)*, 242 (1988) 224.
- 3 A. G. Ewing, R. A. Wallingford and T. M. Olefirowicz, *Anal. Chem.*, 61 (1989) 292A.
- 4 F. M. Everaerts and P. E. M. Verheggen, in J. W. Jorgenson and M. Phillips (Editors), *New Directions in Electrophoretic Methods (ACS Symposium Series, No. 335)*, American Chemical Society, Washington, D.C., 1987, p. 199.
- 5 F. Kilar and S. Hjertén, *J. Chromatogr.* 480 (1989) 351.
- 6 P. Boček, M. Deml, J. Pospichal and J. Sudor, *J. Chromatogr.*, 470 (1989) 309.
- 7 X. Huang, M. J. Gordon and R. N. Zare, *Anal. Chem.*, 60 (1988) 375.

Free solution capillary electrophoresis and micellar electrokinetic resolution of amino acid enantiomers and peptide isomers with L- and D-Marfey's reagents

AN D. TRAN* and TIMOTHY BLANC

R.W. Johnson Pharmaceutical Research Institute at Ortho Pharmaceutical Corporation, Bioanalytical R&D, Biotech Division, Route 202, Raritan, NJ 08869 (U.S.A.)

and

ERIC J. LEOPOLD

Beckman Instruments Inc., 1117 California Avenue, Palo Alto, CA 94304 (U.S.A.)

ABSTRACT

Separation of amino acid enantiomers and peptide isomers has been made possible through the use of Marfey's reagent and high-performance capillary electrophoresis (HPCE). Samples of amino acids and peptides were first derivatized with Marfey's reagent and subsequently analyzed by HPCE. Different modes of separation were investigated including free solution and micellar electrokinetic chromatography.

The use of micellar electrokinetic chromatography in combination with L- and D-Marfey's reagent offered unequivocal means to confirm the presence of D-amino acid in an unknown sample. This method is also particularly useful for the analysis of peptide isomers.

INTRODUCTION

Chirality analysis of amino acids is of particular interest in both the food and pharmaceutical industries. In the food industry, the racemization of amino acids could occur during food processing such as roasting or treatment of food proteins under alkaline conditions¹. In the pharmaceutical industry, the interest ranges from control of racemization of amino acids during peptide synthesis to post-translational protein modification caused by deamidation during protein processing. Fig. 1 illustrates the well accepted mechanism of deamidation through the formation of a cyclic imide intermediate. The latter is a reactive species, readily undergoing hydrolysis to produce the corresponding deamidated peptide or isopeptide. During hydrolysis, racemization could occur at the C^α chiral center of asparagine (Asn) or glutamine (Gln)². A simple way to study the deamidation process is to detect the presence of D-aspartic acid (D-Asp) or D-glutamic acid (D-Glu) and the release of ammonia in the deamidated sample.

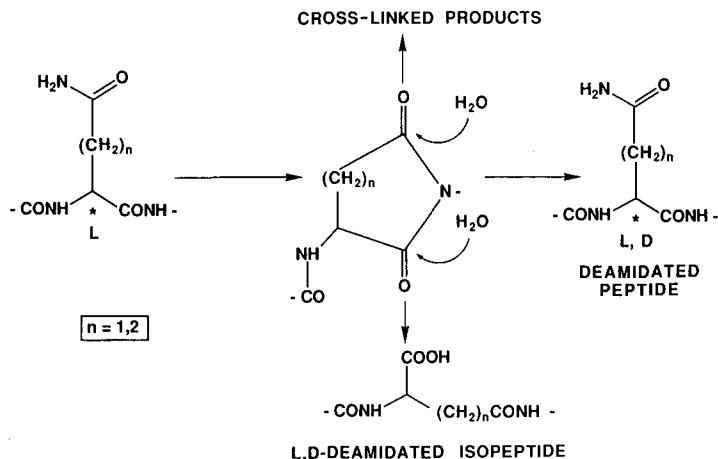
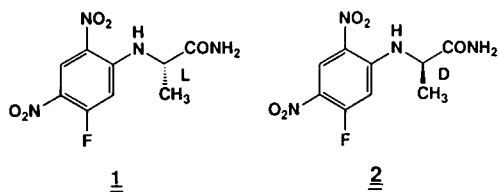


Fig. 1. Proposed mechanism for deamidation of asparaginyl and glutaminyl peptides and proteins.

Amino acid racemates are commonly resolved using high-performance liquid chromatography (HPLC) or gas chromatography (GC) and recently by capillary electrophoresis³⁻⁵. We report here the use of free solution capillary electrophoresis (FSCE), micellar electrokinetic capillary chromatography (MECC) in combination with *L*-Marfey's reagent (**1**), (1-fluoro-2,4-dinitrophenyl-5-*L*-alanine amide) and *D*-Marfey's reagent (**2**), (1-fluoro-2,4-dinitrophenyl-5-*D*-alanine amide)⁶ to provide a rapid and unambiguous technique for chiral analysis of amino acids and peptides.



EXPERIMENTAL

Apparatus

Separations were carried out on a capillary electropherograph P/ACETM system 2000 (Beckman, Palo Alto, CA, U.S.A.) equipped with a capillary cartridge 75 μm I.D. and 375 μm O.D.; the total length of the capillary was 57 cm (50 cm effective length) and was pretreated successively with 0.1 *M* hydrochloric acid and 0.1 *M* sodium hydroxide for 10 min each, then rinsed with water and electrolyte prior to use. The column temperature was maintained at $25 \pm 0.1^\circ\text{C}$ by means of a fluorocarbon liquid continuously circulated through the cartridge. A deuterium light source with a 214- or 340-nm bandpass filter was used and absorbance was monitored at a range of 0.02 a.u.f.s. Data collection was performed using the Beckman P/ACE system or Gold Chromatography data system version 4.0.

Materials

The phosphate buffer (pH 3.3) was prepared using 50 mM of ammonium phosphate monobasic from Fisher Scientific (Springfield, NJ, U.S.A.) and the pH of the solution was adjusted with a solution of orthophosphoric acid (0.05 M). The borate buffer (pH 8.0) was purchased from Beckman; sodium dodecyl sulfate (SDS) from Bio-Rad Labs. (Richmond, CA, U.S.A.); L-Marfey's **1** reagent from Pierce (Rockford, IL, U.S.A.); and acetonitrile from Baxter Health Care, a Burdick & Jackson Division (Muskegon, MI, U.S.A.). Dipeptides Ala-Ala-OH, Ala-Phe-OH and tripeptide Ala-Ala-Ala-OH isomers used in this study were purchased from Chemical Dynamics (Plainfield, NJ, U.S.A.). D-Marfey's reagent **2**, a new product, was synthesized in our laboratory following a similar procedure used for L-Marfey's reagent **1**⁶. The identity of this reagent was confirmed by ¹H-NMR, mass spectrometry, elemental analysis and optical rotation.

Derivatization methods

Method A. Marfey's reagent in acetonitrile (70 μ l, 1% solution) was added to an aqueous solution of amino acid or peptide (50 μ l, 0.05 M) in a 1-ml Reacti-VialTM from Pierce, containing a micromagnetic stirring bar. To this mixture was added a solution of sodium bicarbonate (20 μ l, 1 M). The vial was sealed with a screw cap and stirred at $35 \pm 1^\circ\text{C}$ for 90 min. After cooling to room temperature, the mixture was neutralized by addition of hydrochloric acid (20 μ l, 1 M). The resulting solution was degassed. The mixture was then diluted with sodium borate buffer, pH 8.5 (340 μ l, 0.1 M). Stock solutions of amino acids and peptides derivatized with Marfey's reagent are stable when stored at $25 \pm 5^\circ\text{C}$ in the dark. Electrophoresis was performed using solutions made by diluting the stock solutions with a running buffer (dilution 1:3). All running buffer solutions were filtered through an Acrodisc[®]-CR (1.0 μ m) from Gelman Sciences (Ann Harbor, MI, U.S.A.) before use.

*Method B*⁷. The procedure for method B was similar to method A with the exception that Marfey's reagent was dissolved in acetone (1% solution) and the stirring was done at $55\text{--}60^\circ\text{C}$ for 15 min. This method offered a much shorter reaction time when compared to method A.

RESULTS AND DISCUSSION

Determination of D,L-amino acids by free solution capillary electrophoresis

Amino acids are derivatized with Marfey's reagent as described under Experimental. The short reaction time at a moderate temperature (15 min, 50°C in acetone, method B) makes this method attractive. The derivatized amino acids have a strong absorbance at 340 nm ($\epsilon_M = 3.10^4 \text{ l mol}^{-1} \text{ cm}^{-1}$)⁶. Fig. 2 outlines the reaction sequence for the derivatization of racemic mixtures of amino acids with L-Marfey's reagent **1**. The resulting products are a pair of diastereoisomers L-1-aminylacid-2,4-dinitrophenyl-5-L-alanylamine (LL-**3**) and D-1-aminylacid-2,4-dinitrophenyl-5-L-alanylamine (DL-**4**).

If derivatization is achieved with D-Marfey's reagent **2**, the resulting products are a pair of diastereoisomers L-1-aminylacid-2,4-dinitrophenyl-5-D-alanylamine (LD-**5**) and D-1-aminylacid-2,4-dinitrophenyl-5-D-alanylamine (DD-**6**). Note that the two compounds **3** and **6** are enantiomers and the same holds true for compounds **4** and **5**.

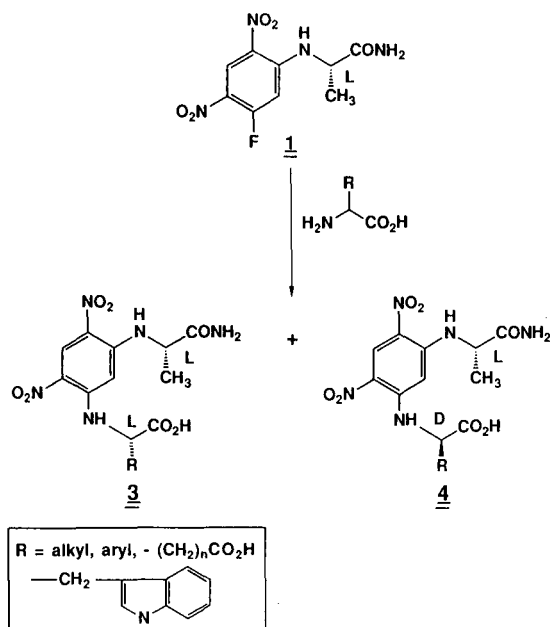


Fig. 2. Derivatization of racemic mixtures of amino acids with L-Marfey's reagent.

Fig. 3 represents a typical electropherogram of racemic mixtures of alanine (Ala), valine (Val), leucine (Leu), phenylalanine (Phe) and tryptophan (Trp) derivatized with L-Marfey's reagent **1**. The electropherogram was obtained by free solution capillary electrophoresis at 10 kV with sodium borate as the running buffer (pH 8.5). No separations were observed and the mixture of derivatized products coeluted as a single peak. When the same mixture was run at 30 kV, good separations were obtained

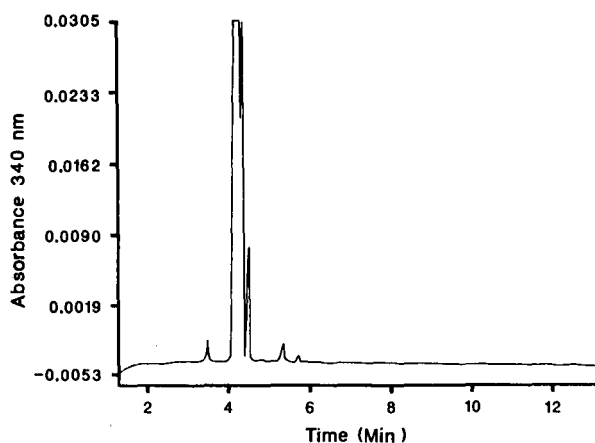


Fig. 3. Electropherogram of racemic mixtures of Ala, Val, Leu, Phe and Trp derivatized with L-Marfey's reagent. The electropherogram was obtained by free solution capillary electrophoresis using a 75 μm I.D. capillary; 100 mM sodium borate buffer, pH 8.5; 10 kV, 25 \pm 0.1°C; detection at 340 nm.

between different derivatized amino acids; however, the lack of separation between the pair of amino acid enantiomers could result from the remote location between the two chiral centers of the derivatized products. This hypothesis is corroborated by additional experiments showing that dipeptides L-Ala-L-Ala-OH and L-Ala-D-Ala-OH are well separated under similar conditions, using sodium borate buffer (pH 8.5), at 30 kV.

The separation of derivatized amino acids is not detected when a buffer with a low pH such as ammonium phosphate (pH 3.3) is used, and no bands elute through the detector. Since the electroosmotic flow is significantly reduced at low pH due to the protonation of the silanolate group of the capillary wall (pI of the silanol group is around 1.0, ref. 8), the electrophoretic migration of the negatively charged species overcomes the electroosmotic flow and migrates in an opposite direction towards the anode (+) where the inlet buffer reservoir is located. If the polarity of the electrodes is reversed after the injection is made, the derivatized amino acid will migrate towards the detector as illustrated in Fig. 4.

A typical electropherogram of Ala, Leu, Asp and Glu derivatized with L-Marfey's reagent **1** is represented in Fig. 5. All L-amino acids were eluted first when compared to the corresponding D-amino acids. The sequence of migration increased from Asp < Glu < Ala < Val < Leu < Trp in direct correlation with the increase in hydrophobicity of the side chain of the amino acid. It is of special interest to observe that the order of migration is reversed with D-amino acids eluting first when D-Marfey's reagent **2** is used for the derivatization step. Such reversal offers an unequivocal means to confirm the presence of D-amino acids in an unknown sample.

As expected, no separation was observed when enantiomers **3** and **6** or **4** and **5** are coinjected. The wide and asymmetrical peak shapes observed in the FSCE mode operated at low pH could result from differences in electrophoretic mobilities between the solute and the buffer constituents.

Determination of L,D-amino acids by micellar electrokinetic capillary chromatography using L- and D-Marfey's reagents

MECC was introduced by Terabe *et al.*⁹ for separations of neutral compounds. The technique involves the addition of an anion surfactant, particularly SDS, to the operating buffer at a concentration exceeding the critical micelle concentration (CMC). When a mixture of five pairs of diastereoisomers of Ala, Val, Leu, Phe and Trp

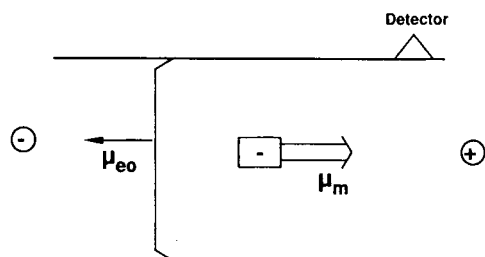


Fig. 4. Schematic representation of free solution capillary electrophoresis operated at low pH; polarity of the electrodes is reversed after the injection is made. Anionic species migrates towards the detector or the anode (+) in the opposite direction of the osmotic flow; μ_{eo} = electroosmotic flow factor, μ_m = electrophoretic mobility of the anionic species.

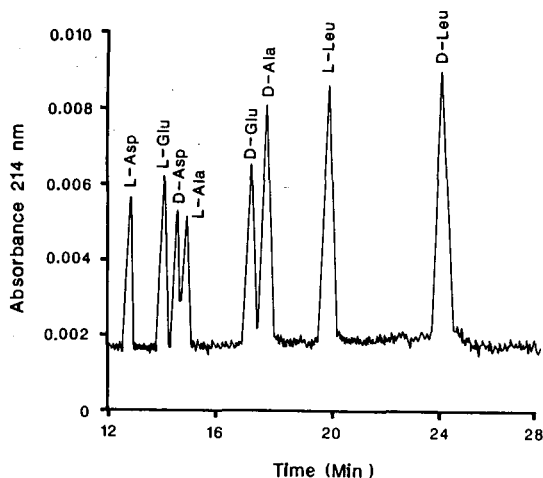


Fig. 5. Electropherogram of racemic mixtures of Ala, Asp, Glu and Leu derivatized with L-Marfey's reagent. The electropherogram was obtained by free solution capillary electrophoresis using a 75 μm I.D. capillary; 50 mM of ammonium phosphate, pH 3.3; 20 kV, 120 mA, $25 \pm 0.1^\circ\text{C}$; detection at 214 nm.

derivatized with L-Marfey's reagent **1** are separated under the MECC mode, good separations and peak shapes are observed as represented in Fig. 6. The presence of 5% acetonitrile in the running buffer is critical for good separation between L-Trp and D-Val; the level of SDS was selected at 200 mM because of the acceptable separation times and current values.

All L-amino acids of the five pairs of diastereoisomers migrated earlier from the capillary when compared to the corresponding D-amino acids. It is tempting to suggest that derivatized products of the DL-3 configuration are more hydrophobic and interact

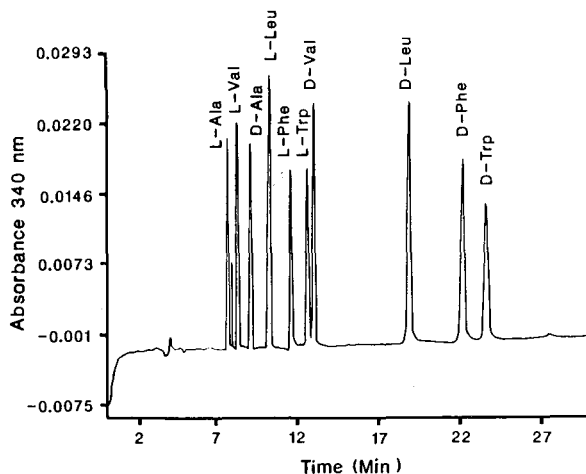


Fig. 6. Electropherogram of racemic mixtures of Ala, Val, Leu, Phe and Trp derivatized with L-Marfey's reagent. The electropherogram was obtained by micellar electrokinetic capillary chromatography using a 75 μm I.D. capillary; 100 mM sodium borate buffer, pH 8.5; 20 kV, 20 mA, $25 \pm 0.1^\circ\text{C}$; detection at 340 nm.

more strongly with the SDS micelle compared to their counterparts of LL-4 configuration. When D-Marfey's reagent **2** is used, the order of migration is reversed, with D-amino acids migrating first, suggesting that the product LD-5 binds more strongly to the micelle compared to the DD-6. As expected, no separation was observed when the pairs of enantiomers LD-5 and DL-4 are coinjected; the same holds true for compounds LL-3 and DD-6. The sequence and differences in migration times of the five diastereoisomers derivatized with L- or D-Marfey's reagents are in the following order: Ala (1.39 min) < Val (4.62 min) < Leu (8.62 min) < Phe (10.31 min) < Trp (10.90 min). It is clear that the migration times and resolutions increase with the increased hydrophobicity of the side chain.

Several consecutive runs with different concentrations of standard solutions of amino acids were made in order to study the reproducibility of elution times and the variation of the peak areas *versus* concentrations. The reproducibility of the elution times (1%) and the good correlation coefficients ($r = 0.99$) of the straight-line fits indicate that this method could be used as a quantitative analysis.

Under similar conditions no separation was observed for the pair of diastereoisomers of Asp or Glu. The extra negative charge of the side chain of these amino acids could be the origin for charge repulsion between micelle and amino acid, and so prohibit potential interactions between the two species.

When MECC is operated at low pH with ammonium phosphate (pH 3.3), no product was eluted through the detector, similar to the situation mentioned earlier for FSCE. Because of the significant reduction of the osmotic flow at low pH, the negative SDS micelle could now migrate in the opposite direction to the anode (+) or the inlet buffer. Good separations for neutral, basic and acidic amino acids were observed when the polarity was reversed after the injection was made, as illustrated in Fig. 7.

Fig. 8 illustrates a schematic representation of MECC mode operated at low pH. Similar to MECC operating at neutral and basic pH, the migration of the solute is based on its hydrophobicity. However, the order of migration is reversed with more

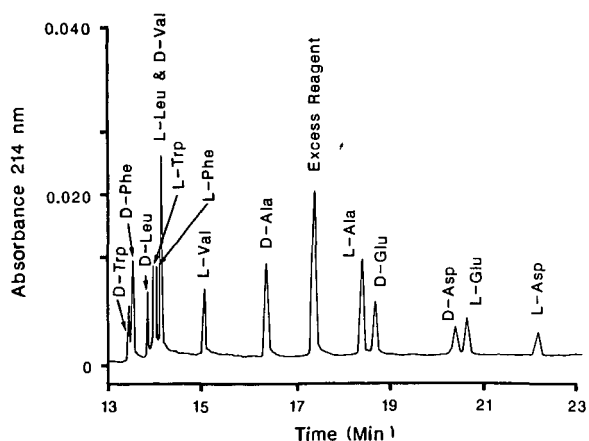


Fig. 7. Electropherogram of racemic mixtures of Ala, Asp, Glu, Val, Leu, Phe and Trp derivatized with L-Marfey's reagent. The electropherogram was obtained by micellar electrokinetic capillary chromatography using a 75 μm I.D. capillary; 50 mM ammonium phosphate buffer, pH 3.3; 10 kV, 60 mA, $25 \pm 0.1^\circ\text{C}$; detection at 214 nm.

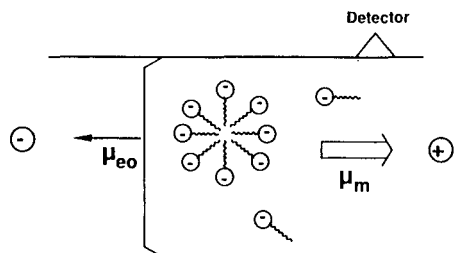


Fig. 8. Schematic representation of micellar electrokinetic capillary chromatography operated at low pH; polarity of the electrodes was reversed after the injection was made. The SDS micelle migrated towards the detector in the opposite direction of the osmotic flow; μ_{eo} = electroosmotic flow factor, μ_m = electrophoretic mobility of the micelle.

hydrophobic compounds eluted first, since the micelle migrates towards the detector. When D-Marfey's reagent **2** is used, the order of elution is reversed with L-amino acids eluted first compared to the corresponding D-amino acids. MECC mode operated at low pH is a complementary approach to MECC at basic pH. This method is especially useful for negatively charged products which may not separate under MECC at basic pH because of charge repulsion between product and micelle.

As with MECC, this method could be used for both qualitative and quantitative analysis since there appears to be good reproducibility of the elution times (1%) and good linearity curves between peak areas and concentrations ($r = 0.99$) of the straight-line fits of different standard amino acid solutions.

Determination of dipeptide and tripeptide isomers by micellar electrokinetic capillary chromatography using L- and D-Marfey's reagents

To further extend the use of Marfey's reagent to peptides, Ala-Ala-OH was

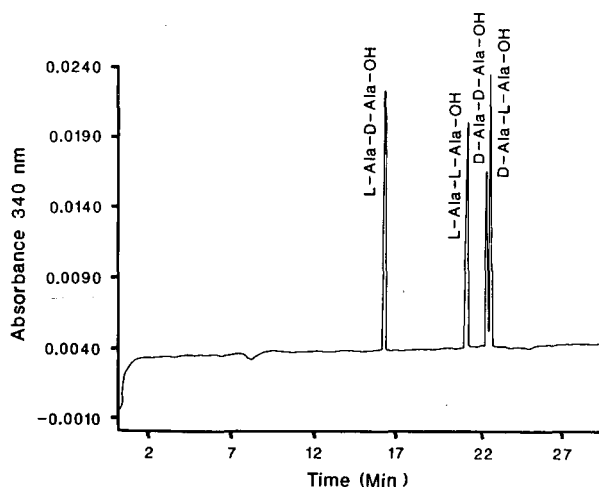


Fig. 9. Electropherogram of isomers of dipeptides Ala-Ala-OH derivatized with L-Marfey's reagent **1**. The electropherogram was obtained by micellar electrokinetic capillary chromatography using a 75 μm I.D. capillary; 100 mM sodium borate, pH 8.5; 12 kV, 10 mA, $25 \pm 0.1^\circ\text{C}$; detection at 340 nm.

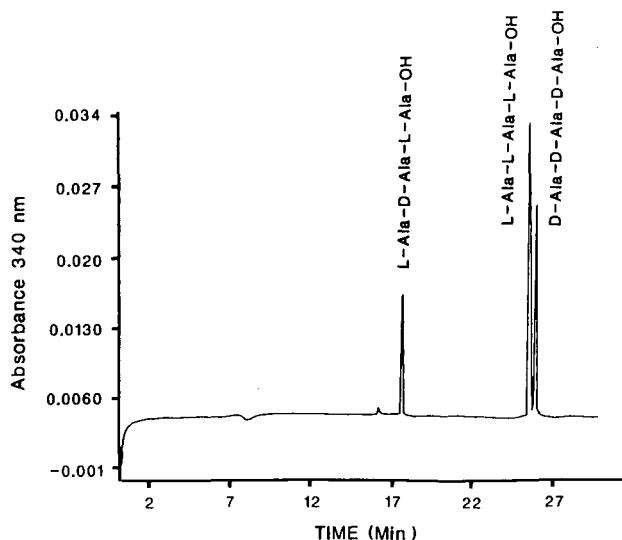


Fig. 10. Electropherogram of isomers of tripeptide Ala-Ala-Ala-OH derivatized with L-Marfey's reagent I. The electropherogram was obtained by micellar electrokinetic capillary chromatography using a 75 μm I.D. capillary; 100 mM sodium borate buffer, pH 8.5; 12 kV, 20 mA, $25 \pm 0.1^\circ\text{C}$; detection at 340 nm.

selected as a model substrate since all four dipeptide isomers are commercially available. As expected under MECC mode, the mixture of underivatized isomers separated as two bands, with enantiomeric pairs L-D and D-L or L-L and D-D coeluted as a single peak. However, when derivatized with L-Marfey's reagent I, all four isomers are diastereoisomers and are well separated as illustrated in Fig. 9. The sequence of migration increases from L-D < L-L < D-D < D-L and varied to DL < DD < LL < LD when D-Marfey's reagent is used for the derivatization step. Unlike amino acids, the sequence of migration of dipeptides is more difficult to predict. A different order of migration is obtained with Ala-Phe-OH increasing from L-D < D-D < D-L < L-L.

The isomers of tripeptide Ala-Ala-Ala-OH were also used to test the effect of chirality in remote parts of a peptide chain. Fig. 10 illustrates the separation of L-D-L, L-L-L and D-D-D isomers derivatized with L-Marfey's reagent.

REFERENCES

- 1 H. Bruckner, R. Wittner, M. Hausch and H. Godel, *Fresenius Z. Anal. Chem.*, 333 (1989) 775.
- 2 B. A. Johnson, *Biochem.*, 24 (1985) 2587.
- 3 J. Jacques, A. Collet and S. H. Wilen, *Enantiomers, Racemates and Resolutions*, Wiley, New York, 1981.
- 4 P. Gozel, E. Gassmann, H. Michelson and R. N. Zare, *Anal. Chem.*, 59 (1987) 44.
- 5 E. Gassmann, J. E. Kuo and R. N. Zare, *Science (Washington, D.C.)*, 230 (1985) 813.
- 6 P. Marfey, *Carlsberg Res. Commun.*, 49 (1984) 591.
- 7 P. Marfey, personal communication.
- 8 G. A. Parks, *Chem. Rev.*, 65 (1965) 177.
- 9 S. Terabe, K. Otsuka, K. Ichikawa, A. Isuchiya and T. Ando, *Anal. Chem.*, 56 (1984) 111.

Isotachophoretic separation of organic acids in biological fluids

PETER OEFNER*, ROBERT HÄFELE and GEORG BARTSCH

Department of Urology, University of Innsbruck, Anichstrasse 35, A-6020 Innsbruck (Austria)

and

GÜNTHER BONN

Institute of Radiochemistry, University of Innsbruck, Innrain 52a, A-6020 Innsbruck (Austria)

ABSTRACT

The operating conditions for the isotachophoretic separation of organic acids were evaluated. At pH values ranging from 2.90 to 4.25 both relative step heights and molar flow-rates were determined experimentally for 26 anions. Comparing the observed values with simulated data, highly significant ($p = 0.0001$) correlation coefficients of 0.993 and 0.920, respectively, were found at pH 3.50. Whereas the concentration of the leading electrolyte did not affect the relative step heights, it increased the molar flow-rates significantly. The same applied to the detection current. The time of analysis was observed to be a function of the concentration of the leading electrolyte. However, the time elapsed between injection of the analyte and its detection depended solely on the volume and not on the amount of analyte injected.

In isotachopheresis, incomplete separation of two compounds is indicated by the occurrence of a mixed zone which can hardly be distinguished from a pure zone. Thus, knowledge of the separation capacity is a prime prerequisite in optimizing the system for the analysis of biological fluids. The separability of nine equimolar pairs of anions was determined at pH values ranging from 2.90 to 4.25. Although two ionogenic constituents would separate only when their migration rates in the mixed state were different, no clear correlation was observed between separation capacity and difference in relative mobility. Separability, however, was found to increase with increasing concentration of the leading electrolyte. While the separation capacity was not influenced by the electric current, it was significantly affected by the volume injected. In subsequent analyses of serum, cerebrospinal fluid, seminal plasma and prostatic fluid, a variety of organic acids could be detected. Calibration graphs for the detected anions revealed a detection limit of 1 nmol and linearity over their biological concentration ranges. Further, the isotachophoretic results correlated well with high-performance liquid chromatographic and enzymatic analyses of citric acid and lactic acid in human seminal plasma and cerebrospinal fluid, respectively.

INTRODUCTION

The usually small volumes of human body fluids, such as seminal plasma and prostatic fluid, have always hampered their investigation. Although the analysis of pooled samples proved useful in the basic determination of the chemical composition of biological fluids, such a procedure did not fulfil the requirements for the evaluation of the biochemical nature of diseases in the individual patient, research usually being confined to the analysis of single known substances. In recent years, the call for analytical methods that can provide sensitive and selective information on a broad range of compounds has resulted in the development of new techniques that permit the separation, identification, quantification and even isolation of a great variety of solutes contained in biological fluids.

Regarding the analysis of organic acids, various techniques are available. Isotachopheresis is certainly a powerful method, as it meets the basic requirements for screening procedures, namely multi-component information, rapid completion, reliability and low cost. The separation of organic acids by capillary isotachopheresis has been the topic of many theoretical and experimental papers in the last 15 years. The main reason for the extensive theoretical evaluation may be attributed to the large knowledge of dissociation constants of organic acids in aqueous solution¹⁻³. Most publications dealing with the experimental evaluation of capillary isotachopheresis in the analysis of organic acids deal with their determination in food, microbiological samples, tissue and cell extracts, enzyme assays and in samples obtained during the hydrolytic degradation or oxidation of saccharides. Regarding human body fluids, most investigations have been restricted to the analysis of one specific organic acid, such as oxalic acid in urine⁴⁻¹⁰ or trifluoroacetic acid, which is a major metabolite of the anaesthetic halothane, in urine and serum^{11,12}. Only a limited number of papers have been published on the use of capillary isotachopheresis in obtaining profiles of organic acids in various body fluids¹³⁻²⁰.

In this study we investigated the experimental conditions for the determination of organic acids by means of capillary isotachopheresis, such as the influence of the pH and the concentration of the leading electrolyte on relative mobility, molar flow-rate and separation capacity. These data were then applied to the determination of organic acids in various biological fluids.

EXPERIMENTAL

Sample collection and pretreatment

Cerebrospinal fluid specimens were obtained by lumbar puncture. No pretreatment was required. Blood samples were taken from the cubital vein and deproteinized immediately by ultrafiltration, using the disposable micropartition system Centrisart I (Sartorius, Göttingen, F.R.G.), which was filled with small glass beads to avoid coagulation. Volumes of 200–300 μl of ultrafiltrate were obtained from 2 ml of blood centrifuged with a swing-head rotor at 2000 g for 15 min at 4°C. In order to avoid both haemolysis and build-up of blood cells at the membrane surface, which would restrict the solvent flow considerably, blood samples were precentrifuged for about 2–3 min before inserting the floater with the membrane. Spontaneously liquefied semen was centrifuged at 1000 g for 10 min to remove spermatozoa. The samples were then

deproteinized by ultrafiltration, for which the disposable micropartition system Centrifree (Amicon, Danvers, MA, U.S.A.) was used. Volumes of 100–200 μl of ultrafiltrate were obtained from 400–500 μl of seminal plasma centrifuged in a fixed-angle rotor (25°) at 1500 g for 15 min at 4°C. Prostatic fluid was collected on routine rectal examination. Volumes of 20–100 μl of prostatic fluid could be obtained per patient. The samples were diluted 1:2 or 1:5 with doubly distilled water prior to ultrafiltration according to the conditions used for deproteinization of seminal plasma. All samples were stored at -30°C prior to their analysis.

Isotachophoretic conditions

Isotachophoretic analyses were carried out on an LKB (Bromma, Sweden) Model 2127 Tachophor equipped with a 250-mm Teflon capillary of I.D. 0.5 mm.

The leading electrolyte was 10 mM hydrochloric acid (Merck, Darmstadt, F.R.G.) adjusted to pH values ranging from 2.90 to 4.25 by the addition of β -alanine (Merck). Triton X-100 (Serva, Heidelberg, F.R.G.) was added to the leader to sharpen the zone boundaries by depressing electroendosmosis. The terminating electrolyte was 10 mM propionic acid (Sigma, St. Louis, MO, U.S.A.).

The samples were injected through the inlet membrane into the leading electrolyte by means of 5- and 10- μl Hamilton syringes (Hamilton, Bonaduz, Switzerland). Separations were started at a current of 200–225 μA , which was gradually reduced to 25–125 μA shortly before the separated anions could be detected on account of their conductivity. All analyses were carried out at 20°C.

High-performance liquid chromatographic (HPLC) determination of citric acid

The HPLC system, which was used for the determination of citric acid in human seminal plasma, consisted of a Model 112 pump (Beckman, Berkeley, CA, U.S.A.), a sample injection valve (Beckman Model 210) with a 20- μl loop, a Shimadzu (Kyoto, Japan) CTO-2A column oven unit, a differential refractive index detector (Altex, Berkeley, CA, U.S.A.) and a Shimadzu C-R2A-X integration system.

As stationary phase a pre-packed Aminex HPX-87H strong cation-exchange resin column (8% cross-linked, 300 \times 7.8 mm I.D.) (Bio-Rad Labs., Richmond, CA, U.S.A.), fitted with an ion-exclusion micro-guard refill cartridge (Bio-Rad Labs.), was used. The eluent was 0.01 M sulphuric acid. The column temperature was maintained at 40°C. The flow-rate was adjusted to 0.6 ml/min^{21,22}.

Enzymatic determination of lactate

The L-lactate test provided by Boehringer (Boehringer, Mannheim, F.R.G.) was used for the enzymatic determination of lactate in human cerebrospinal fluid.

Colorimetric determination of inorganic phosphate

The inorganic phosphate test provided by Merck (Merckotest No. 3331) was used for the colorimetric determination of inorganic phosphate in human seminal plasma.

RESULTS

The relative step heights of 26 anions (Table I) in relation to propionic acid, which served as the terminating electrolyte, were obtained at seven pH values ranging

TABLE I

ZONE IDENTIFICATION OF THE INVESTIGATED COMPOUNDS AND THEIR pK VALUES¹⁻³

Zone No.	Compound	pK_1	pK_2	pK_3	pK_4
1	Pyrophosphate	0.85 ^a	1.49 ^a	5.77 ^a	8.22 ^a
2	2,3-Diphosphoglyceric acid				
3	Oxalic acid	1.27 ^b	4.26 ^b		
4	Maleic acid	1.97 ^c	6.24 ^c		
5	Pyruvic acid	2.49 ^c			
6	Adenosine 5'-triphosphate				
7	L-Cysteic acid	1.89 ^c	8.70 ^c		
8	Phosphoric acid	2.12 ^c	7.21 ^c	12.67 ^c	
9	2-Ketoglutaric acid	2.60 ^c			
10	Fumaric acid	3.02 ^c	4.38 ^c		
11	L(+)-Tartaric acid	3.03 ^c	4.37 ^c		
12	Glyoxylic acid	3.34 ^c			
13	Citric acid	3.14 ^b	4.77 ^b	6.39 ^b	
14	Malic acid	3.40 ^c	5.14 ^c		
15	Acetoacetic acid	3.61 ^a			
16	Glycolic acid	3.83 ^c			
17	L(+)-Lactic acid	3.86 ^b			
18	2-Hydroxybutyric acid	3.98 ^c			
19	Hippuric acid	3.80 ^c			
20	L-Aspartic acid	2.05 ^c	3.87 ^c	10.00 ^c	
21	Succinic acid	4.22 ^b	5.64 ^b		
22	Benzoic acid	4.20 ^b			
23	L-Ascorbic acid	4.17 ^b	11.56 ^b		
24	L-Glutamic acid	2.10 ^c	4.07 ^c	9.47 ^c	
25	3-Hydroxybutyric acid	4.70 ^c			
26	Acetic acid	4.76 ^b			

^a 18°C.^b 20°C.^c 25°C.

from 2.90 to 4.25 by injecting 15, 30 and 50 nmol of each anion. The observed relative step heights could be reproduced with intra- and inter-assay precisions of 0.37% and 3.84% R.S.D. ($n = 6$), respectively. Polynomial regression analysis was used to generate the curve fits through the data points. The relative step heights of almost all compounds increased gradually with increasing pH of the leading electrolyte, as shown in Fig. 1. However, as the change in mobility is not uniform, the analytical system may be adjusted to allow optimum separation of the organic acids of interest.

Molar flow-rates were evaluated under the same conditions as the relative step heights (Fig. 1). It is evident that the pH of the leading electrolyte does not exert a significant effect on the molar flow-rates for more than half of the investigated compounds within the pH range 3.3–4.0, indicating, that minor changes in pH will not influence the quantitative results. This is confirmed by the intra- and inter-assay precisions of 0.37% and 1.48% R.S.D. ($n = 5$), respectively.

Whereas the concentration of the leading electrolyte does not affect the relative step heights of various anions, the molar flow-rates were found to increase significantly with increasing concentration of hydrochloric acid in the leading electrolyte system

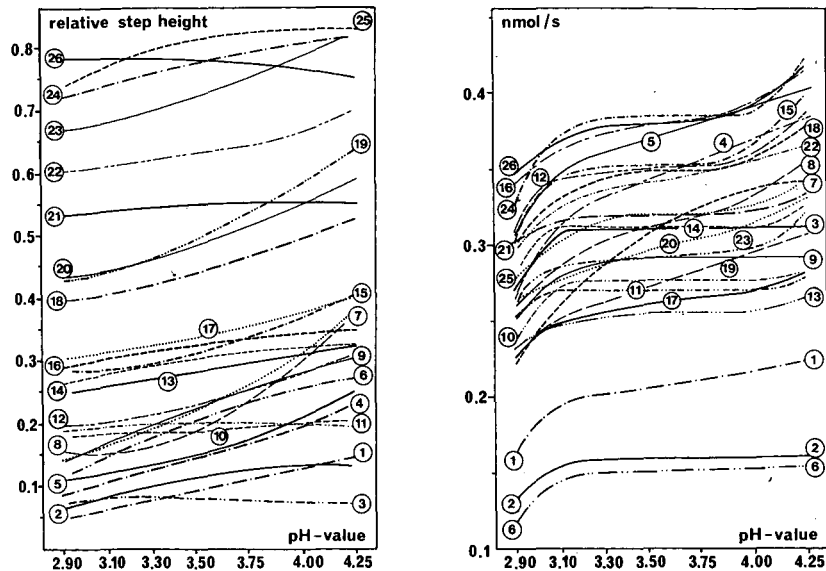


Fig. 1. Relative step heights (propionic acid = 1.0) and molar flow-rates (nmol/s) of 26 anions at pH values ranging from 2.90 to 4.25. Leading electrolyte: 10 mM HCl- β -alanine-0.1% Triton X-100. Terminating electrolyte: 10 mM propionic acid. For identification, see Table I.

(Fig. 2). As regards the driving current, there is a direct proportionality between molar flow-rate and the current fed through the system. The relative step heights, however, are not affected by the electric current.

From the results shown in Fig. 3, it is evident that the time elapsed between the injection of the analyte and its detection depends solely on the injection volume and not on the amount injected.

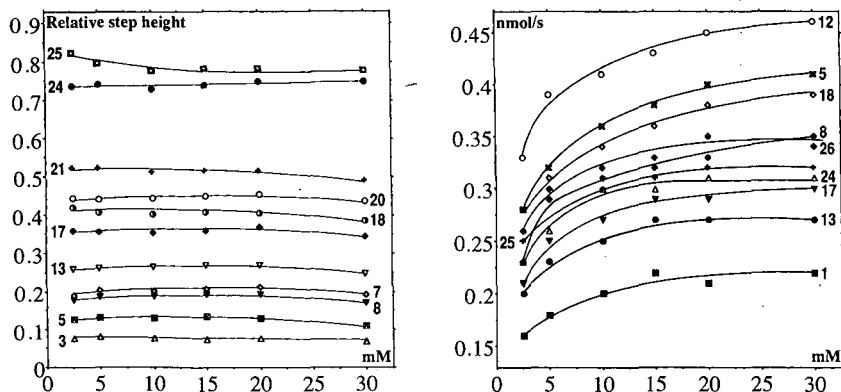


Fig. 2. Impact of the concentration of hydrochloric acid in the leading electrolyte system on relative step heights and molar flow-rates of different anions at pH 3.50. The concentration of the terminating electrolyte was the same as that of hydrochloric acid. Current: 75 μ A. For identification, see Table I.

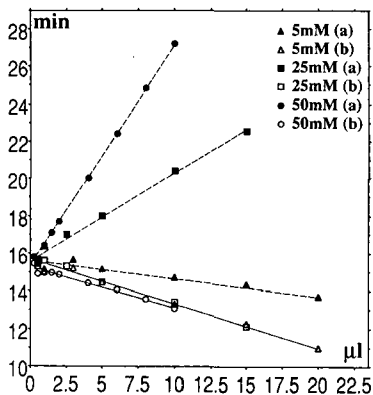


Fig. 3. Impact of injection volume and concentration of malonic acid on time of analysis: a = overall time of analysis; b = time elapsed between injection of the analyte and its detection. Leading electrolyte: 10 mM HCl- β -alanine-0.1% Triton X-100 (pH 3.50). Terminating electrolyte: 10 mM propionic acid. Current: 125 μ A.

In isotachopheresis, incomplete separation of two compounds is indicated by the occurrence of a mixed zone which can hardly be distinguished from a zone containing only one constituent (see Fig. 10b).

The data in Fig. 4 show the maximum separable amounts of nine equimolar pairs of anions within the pH range 2.90–4.25. As preliminary experiments had indicated that the separation capacity might vary with time, probably owing to changes in the composition of the leading electrolyte, determinations were carried out on five consecutive days for every pH value. This period was chosen because under routine conditions both leading and terminating electrolyte solutions would be prepared only once a week in amounts sufficient to allow the continuous analysis of samples from Monday to Friday. Triton X-100, the addition of which had been observed to make

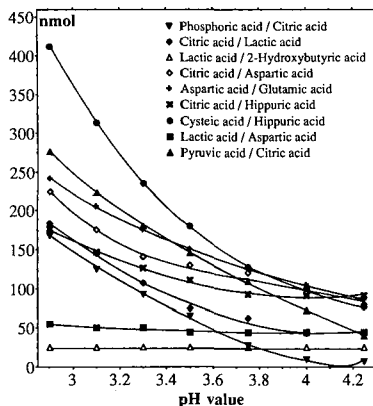


Fig. 4. Impact of the pH of the leading electrolyte on the separability of nine equimolar pairs of anions. Leading electrolyte: 10 mM HCl- β -alanine-0.1% Triton X-100. Terminating electrolyte: 10 mM propionic acid. Current: 75 μ A. The capillary tubing was 25 cm \times 0.5 mm I.D.

solutions visibly turbid within a few days depending on the amount added, was dissolved in the leading electrolyte approximately 1 h before the first isotachopheretic run on day one.

As illustrated in Fig. 5, the data obtained for an equimolar mixture of phosphoric acid and citric acid also apply to a non-equimolar mixture. Additionally, a linear relationship was observed between the concentration of hydrochloric acid in the leading electrolyte system and the separation capacity.

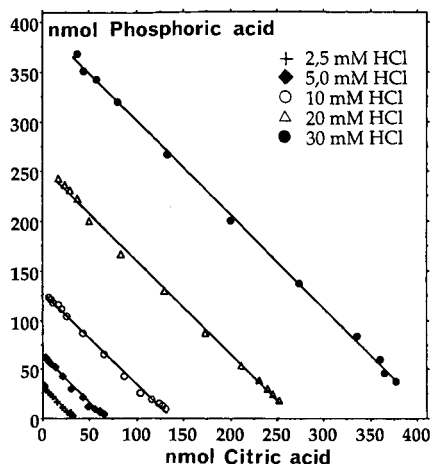


Fig. 5. Impact of the concentration of hydrochloric acid in the leading electrolyte system on the separability of phosphoric acid from citric acid, which were injected at different molar ratios. The concentration of the terminating electrolyte was the same as that of hydrochloric acid. pH of the leading electrolyte = 3.50. Current: 75 μ A. The capillary tubing was 25 cm \times 0.5 mm I.D.

Whereas the electric current chosen does not influence the separation capacity, the latter is affected by the sample volume injected. This was assessed by preparing mixtures of equal amounts of seven pairs of anions at concentrations of 5, 10, 20, 40, 60, 80 and 100 mM, respectively. The injected volumes of a certain concentration were then increased until mixed zones occurred and the maximum values defined the points in Fig. 6. The vertical axis denotes the maximum number of nanomoles of each of the sample ions which separated completely and the horizontal axis gives the total volume that was injected. It can be concluded that the injection volume should be as low as possible in order to avoid distortion and, thus, a reduced separation capacity by overloading.

Fig. 7a shows the isotachopheretic analysis of a sample of human seminal plasma that had been deproteinized by ultrafiltration prior to analysis. Phosphate, citric acid, lactic acid, aspartic acid and glutamic acid are the main constituents. Their identities were confirmed by the injection of an additional small amount of each compound, which resulted in an increase in the length of the respective zones. Further, the step heights were characteristic of the detected compounds.

Fig. 7b shows an isotachopherogram of ultrafiltered human prostatic fluid.

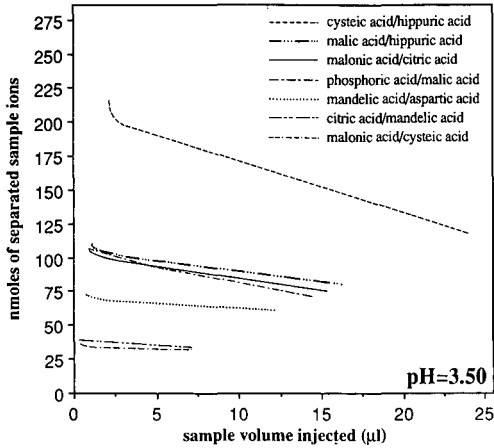


Fig. 6. Effect of sample volume injected on the separability of seven equimolar pairs of anions. Leading electrolyte: 10 mM HCl- β -alanine-0.2% Triton X-100 (pH 3.50). Terminating electrolyte: 10 mM propionic acid. Current: 75 μ A. The capillary tubing was 25 cm \times 0.5 mm I.D.

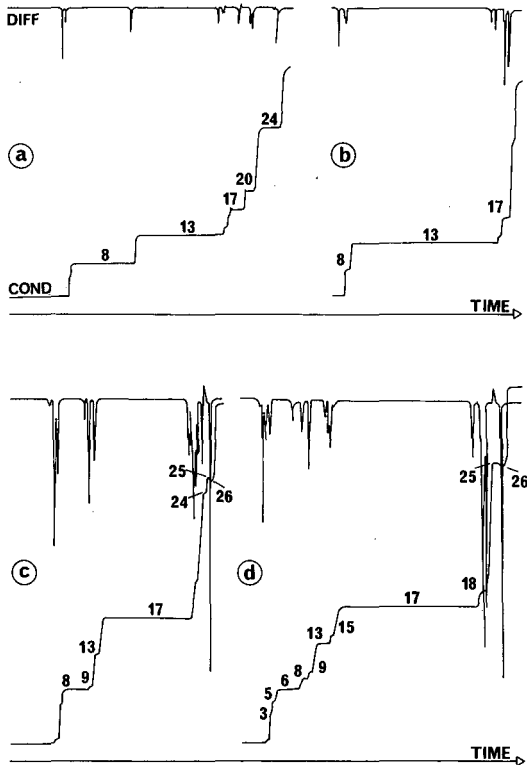


Fig. 7. Isotachopheretic analyses of (a) seminal plasma, (b) prostatic fluid, (c) serum and (d) cerebrospinal fluid. Leading electrolyte: 10 mM HCl- β -alanine-0.2% Triton X-100 (pH 3.30). Terminating electrolyte: 10 mM propionic acid. The capillary tubing was 25 cm \times 0.5 mm I.D. Detection: conductivity (COND) and differential conductivity (DIFF). Current: 75 μ A. Chart speed: 0.5 mm/s. Injection volumes: 2.5, 5, 10 and 10 μ l, respectively. For zone-identification, see Table I.

Citric acid is the main constituent, with concentrations ranging from 53 to 126 mM. In contrast to seminal plasma, only small amounts of phosphate could be detected. Based on the investigation of semen samples obtained from vasectomized patients, it can be concluded that phosphate is mainly derived from the seminal vesicles.

Phosphate, 2-ketoglutaric acid, citric acid, lactic acid, glutamic acid, 3-hydroxybutyric acid and acetic acid were detected routinely in ultrafiltered samples of serum (Fig. 7c). The isotachopherogram of cerebrospinal fluid shown in Fig. 7d reflects the significantly increased metabolic activity of cerebral tissue in a patient who had just experienced an epileptic seizure. As organic acids diffuse only slowly across the blood-brain barrier as long as it is intact, the prompt determination of organic acids in cerebrospinal fluid and blood is of great value in assessing the cerebral acid-base status and the integrity of the blood-brain barrier.

Quantitative information from isotachophoretic analyses was obtained by measuring the zone lengths. The calibration graphs for the detected anions revealed a detection limit of *ca.* 1 nmol and linearity over their biological concentration ranges. The reproducibility of the measurements was checked by at least seven repeated determinations for which different samples of biological fluids were used. A precision of 1.5% was obtained, the main errors resulting from the injection of the samples and the measurements of the zone lengths.

A linear relationship was found between isotachophoretic and HPLC determinations of citric acid in ultrafiltered human seminal plasma ($r = 0.998$, $p = 0.0001$). A comparison of the enzymatic assay of lactic acid in cerebrospinal fluid and the isotachophoretic results also showed a good correlation ($r = 0.997$, $p = 0.0001$). For phosphate, however, the zone length seen with seminal plasma was about three to five times greater than that expected based on colorimetric analyses of inorganic phosphate. This suggested that the phosphate zone contained additional components which had about the same mobility. No conditions could be found that caused a further separation of this zone, but several phosphorus-containing compounds commonly occurring in biological materials were observed to migrate within the respective zone.

DISCUSSION

Owing to their further metabolization, several organic acids are known to be unstable in blood and to a lesser extent in other body fluids after their collection. Therefore, immediate inhibition of enzyme activities is a prime prerequisite for accurate analyses. This is accomplished either by the addition of enzyme inhibitors, such as sodium fluoride, or through protein-precipitating agents, such as organic solvents and anions. However, both fluoride and anionic precipitants, such as perchloric acid, trichloroacetic acid and metaphosphoric acid, interfere with the isotachophoretic determination of organic acids, as they exhibit similar migration behaviours to the compounds under investigation. Moreover, low-molecular-mass constituents of the sample may be trapped in the precipitate. With blood, the addition of the anticoagulants most often used in clinical laboratories, such as citrate, oxalate and heparin, again results in a large increase in the time of analysis and in a considerable reduction in separation capacity. Further, these compounds may also mask constituents of the sample under investigation. Recently, ultrafiltration has been

established to be a reliable and convenient method for the preparation of protein-free samples^{18–20,22,23}. As the concentration of the sample solutes remains constant and none of the ultrafilterable constituents are partially or totally coprecipitated, deproteinization can be accomplished within a few minutes with an efficiency of more than 99.5%²⁴. Moreover, organic acid have been shown to be stable in protein-free ultrafiltrates²⁵.

For several years, computer simulation of isotachophoretic equilibria has been used for the determination of qualitative and quantitative indices and as for the establishment of optimum separation conditions for organic acids^{26–29}. Therefore, it was considered of interest to compare the observed values of relative mobility and time-based zone length with simulated data. For this purpose, the indices evaluated by Hirokawa *et al.*²⁹ for 287 anionic substances in the pH range 3.0–10.0 were used. Prior to simple regression analysis, the R_E values, which define the ratio of the potential gradient of the sample zone to that of the leading zone, had to be converted into the indices given in this paper using the R_E values of the sample, $R_E(S)$, and terminating ion, $R_E(T)$:

$$\text{relative step height} = [R_E(S) - 1]/[R_E(T) - 1]$$

Highly significant ($p = 0.0001$) correlation coefficients of 0.993 and 0.920 were found between observed and simulated values of relative step height and molar flow-rate at pH 3.50, respectively (Figs. 8 and 9).

For the identification of unknown sample zones, the addition of standards has usually been employed. However, this may prove cumbersome if possible candidates are not known. Based on data in this paper and published by Hirokawa *et al.*²⁹, qualitative identification may also be achieved by comparing the observed and simulated values. At least the possible candidates for the components detected in

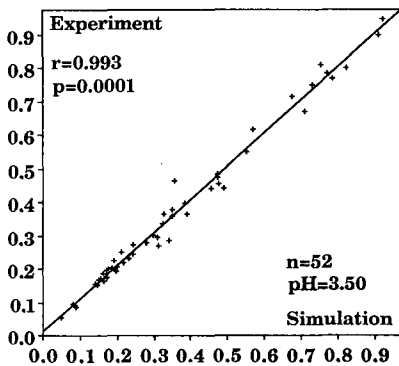


Fig. 8. Correlation between simulated and experimentally obtained values for the relative step heights of 52 anions at pH 3.50. The solid line was generated by simple linear regression analysis. The leading electrolyte system was 10 mM HCl, the pH having been adjusted by the addition of β -alanine.

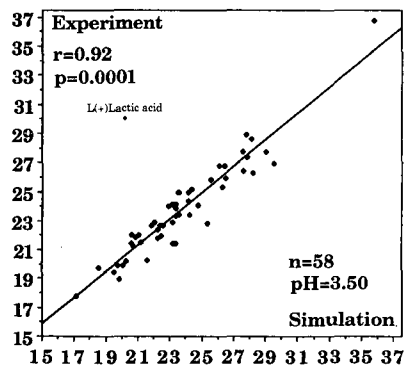


Fig. 9. Correlation between simulated and experimentally obtained values for the time-based zone lengths of 10-nmol samples of 58 anions at pH 3.50. The solid line was generated by simple linear regression. The leading electrolyte was 10 mM HCl. The pH was adjusted by the addition of β -alanine. Current: 100 μ A. Capillary length: 25 cm \times 0.5 mm I.D.

actual samples can be limited to several kinds, and their number may be reduced further by considering the relative mobilities measured at other pH values. The identification may even be made easier and more accurate if the time-based zone lengths are measured at different pH values.

As it is difficult to establish whether two compounds have been separated completely or not, it is important to know the maximum separable amounts of two analytes under the conditions used. However, the values obtained for equal amounts of two compounds do not necessarily apply to a more complex mixture of organic acids, as is shown in Fig. 10. By injecting equimolar amounts of phosphoric acid and citric acid, for instance, it was possible to separate a maximum amount of 65 nmol of each anion (Fig. 10a and b), but when aspartic acid and glutamic acid were added to the mixture, only 40 nmol of phosphoric acid and citric acid could be separated (Fig. 10c and d). As regards the separability of aspartic acid and glutamic acid, however, the separation capacity was not affected by the addition of other analytes (Fig. 10h–j).

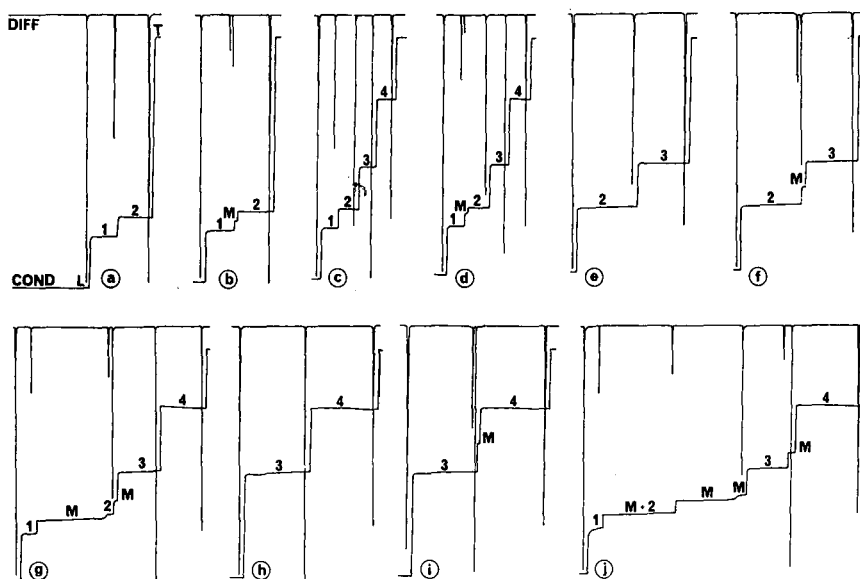


Fig. 10. Evaluation of the separability of equimolar amounts of (1) phosphoric acid, (2) citric acid, (3) aspartic acid and (4) glutamic acid. The appearance of a mixed zone (M) indicates the end of separability under the conditions used. (a) 65, (b) 72.5, (c) 40, (d) 45, (e) 120, (f) 125, (g) 105, (h) 150, (i) 155 and (j) 155 nmol. Leading electrolyte (L): 10 mM HCl- β -alanine-0.1% Triton X-100 (pH 3.50). Terminating electrolyte (T): 10 mM propionic acid. Capillary: 25 cm \times 0.5 mm I.D. Detection: conductivity (COND) and differential conductivity (DIFF).

The separation capacity can be enhanced in various ways, such as by increasing the concentration of the leading electrolyte or the length of the capillary. All these measures, however, result in proportional increase in the time of analysis. Therefore, it will be necessary to adjust the experimental conditions to the requirements of a specific analysis in order to permit the separation of analytes with a maximum resolution and separability within the shortest period possible.

By allowing the rapid and reproducible determination of a vast range of organic acids in body fluids, isotachopheresis may serve as a valuable technique in the diagnosis, prognosis and monitoring of various pathological conditions.

ACKNOWLEDGEMENT

The authors express their appreciation to Miss Monika Trebo for valuable assistance in preparing the manuscript.

REFERENCES

- 1 G. G. Grau, in J. Bartels, P. Ten Bruggencate, H. Hausen, K. H. Hellwege, K. Schäfer and E. Schmidt (Editors), *Landolt-Börnstein, Zahlenwerte und Funktionen*, Springer, Berlin, 1960, p. 839.
- 2 G. Kortüm, W. Vogel and K. Andrussov, *Dissociation Constants of Organic Acids in Aqueous Solution*, Butterworths, London, 1961.
- 3 A. Albert and E. P. Serjeant, *Ionization Constants of Acids and Bases*, Methuen, London, 1962.
- 4 K. Schmidt, G. Bruchelt and V. Hagmaier, *J. Clin. Chem. Clin. Biochem.*, 17 (1979) 187.
- 5 F. M. Everaerts, F. E. P. Mikkers and Th. P. E. M. Verheggen, in B. J. Radola (Editor), *Electrophoresis '79*, Walter de Gruyter, Berlin, New York, 1980, p. 255.
- 6 K. Schmidt, V. Hagmaier, G. Bruchelt and G. Rutishauser, *Urol. Res.*, 8 (1980) 177.
- 7 W. Tschöpe, R. Brenner, A. Baldesten and E. Ritz, in A. Adam and C. Schots (Editors), *Biochemical and Biological Applications of Isotachopheresis*, Elsevier, Amsterdam, 1980, p. 117.
- 8 K. H. Schmidt, V. Hagmaier, D. H. Hornig, J. P. Vuilleumier and G. Rutishauser, *Am. J. Clin. Nutr.*, 34 (1981) 305.
- 9 W. Tschöpe, R. Brenner and E. Ritz, *J. Chromatogr.*, 222 (1981) 41.
- 10 N. Schwendtner, W. Achilles, W. Engelhardt, P. O. Schwille and A. Sigel, *J. Clin. Chem. Clin. Biochem.*, 20 (1982) 833.
- 11 M. Morio, K. Fujii, R. Takiyama, F. Chikasue, H. Kikuchi and L. Ribaric, *Anesthesiology*, 53 (1980) 56.
- 12 T. Hirokawa, H. Takemi, Y. Kiso, R. Takiyama, M. Morio, K. Fujii and H. Kikuchi, *J. Chromatogr.*, 305 (1984) 429.
- 13 J. Sollenberg and A. Baldesten, *J. Chromatogr.*, 132 (1977) 469.
- 14 W. Zschiesche, K. H. Schaller and K. Gossler, *Fresenius' Z. Anal. Chem.*, 290 (1978) 115.
- 15 J. S. van der Hoeven and H. C. M. Franken, in A. Adam and C. Schots (Editors), *Biochemical and Biological Applications of Isotachopheresis*, Elsevier, Amsterdam, 1980, p. 69.
- 16 F. Mikkers and S. Ringoir, in A. Adam and C. Schots (Editors), *Biochemical and Biological Applications of Isotachopheresis*, Elsevier, Amsterdam, 1980, p. 127.
- 17 V. Dolnik and P. Bocek, *J. Chromatogr.*, 225 (1981) 455.
- 18 P. J. Oefner, G. Bonn and G. Bartsch, *Fresenius' Z. Anal. Chem.*, 320 (1985) 175.
- 19 P. J. Oefner, P. Pohl and G. Bonn, *Ann. N.Y. Acad. Sci.*, 529 (1988) 193.
- 20 P. J. Oefner, S. Wongyai, G. Bonn and G. Bartsch, in D. S. Coffey and W. Gardner (Editors), *Cytopathology/Flow Cytometry and Prognostic Indicators of Prostate Cancer*, Elsevier, New York, 1988, p. 374.
- 21 R. Pecina, G. Bonn, E. Burtscher and O. Bobleter, *J. Chromatogr.*, 287 (1984) 245.
- 22 P. Oefner, G. Bonn and G. Bartsch, *J. Liq. Chromatogr.*, 8 (1985) 1009.
- 23 G. Bonn, P. J. Oefner and O. Bobleter, *Fresenius' Z. Anal. Chem.*, 331 (1988) 46.
- 24 J. Blanchard, *J. Chromatogr.*, 226 (1981) 455.
- 25 M. Yamakawa, T. Yamamoto, T. Kishimoto, Y. Mizutani, M. Yatsuboshi, H. Nishitani, S. Hirata, N. Horiuchi and M. Maekawa, *Nephron*, 32 (1982) 155.
- 26 T. Hirokawa, M. Nishino and Y. Kiso, *J. Chromatogr.*, 252 (1982) 49.
- 27 T. Hirokawa and Y. Kiso, *J. Chromatogr.*, 257 (1983) 197.
- 28 T. Hirokawa and Y. Kiso, *J. Chromatogr.*, 260 (1983) 225.
- 29 T. Hirokawa, M. Nishino, N. Aoki, Y. Kiso, Y. Sawamoto, T. Yagi and J.-I. Akiyama, *J. Chromatogr.*, 271 (1983) D1.

Retention of eleven priority phenols using micellar electrokinetic chromatography

C. P. ONG, C. L. NG, N. C. CHONG, H. K. LEE and S. F. Y. LI*

Department of Chemistry, National University of Singapore, Kent Ridge, Singapore 0511 (Singapore)

ABSTRACT

The use of micellar electrokinetic chromatography (MECC) for the separation of eleven substituted phenols listed by the United States Environmental Protection Agency as priority pollutants was investigated. Solutions of potassium and sodium dodecyl sulphate in phosphate–borate buffer of pH 6.6, 7.0 and 7.5 were used as the electrophoretic media. Satisfactory separation of the eleven phenols was obtained using a 180- μm capillary at 10 kV and pH 6.6 with a solution containing both sodium and potassium dodecyl sulphate. Observations on the retention behaviour of the phenols in MECC were related to their physico-chemical properties.

INTRODUCTION

Capillary zone electrophoresis (CZE) and micellar electrokinetic chromatography (MECC) have become popular separation techniques owing to their inherently high separation efficiency^{1–4}. The analysis of a series of chlorophenols using MECC has been reported⁵. However, the application of these techniques to the analysis of environmental pollutants has rarely been investigated.

Substituted phenols are of great environmental concern owing to their high toxicity. The United States Environmental Protection Agency (USEPA) lists the eleven phenols shown in Fig. 1 as priority pollutants⁶. Some of these phenols, which originate from such diverse sources as pesticide application, industrial wastes, water supplies and automobile exhausts, are highly toxic even at low concentrations. A widely used technique for the analysis of phenols is high-performance liquid chromatography (HPLC) with either reversed-phase isocratic or gradient elution^{7–10}. However, owing to the inherent limited resolving power of conventional HPLC techniques, optimization of the separation of the phenols often involves complicated procedures or a large number of experiments¹¹. In this work, the use of MECC for the separation of the eleven priority phenols was investigated. For this purpose, two types of micellar solutions were used to examine the selectivity. The retention behaviour of these compounds in MECC at various pH values is discussed.

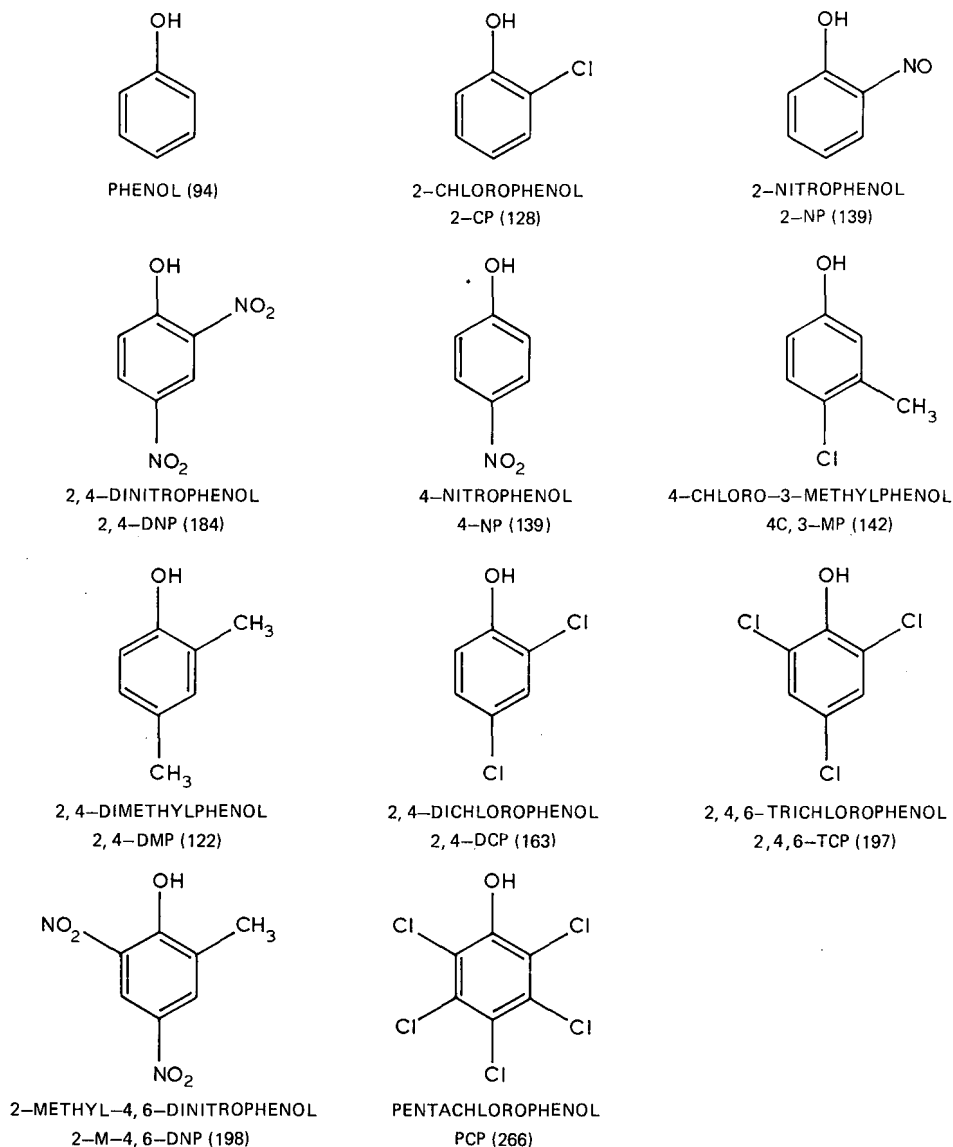


Fig. 1. Structures of the eleven phenols studied (molecular masses in parentheses).

EXPERIMENTAL

The experiments were performed on a laboratory-built MECC system. A Spellman (Plainview, NY, U.S.A.) Model RM15P10KD (15 kV maximum) power supply was used to maintain the high voltage. The columns used were fused-silica capillary tubes of 180 and 50 μm I.D. (J & W Scientific, Folsom, CA, U.S.A.) with effective lengths of 1 and 0.85 m, respectively. Peaks were detected with a micro-UV-VIS

detector (Carlo Erba, Milan, Italy) with the wavelength set at 254 nm. The detection cell for on-column detection was formed by removing the polyimide coating of a small section of the fused-silica tubing used for electrophoresis.

Chromatographic data were collected and analysed on a Hewlett Packard (Palo Alto, CA, U.S.A.) Model 3390A integrator. A Linear Instruments (Irvine, CA, U.S.A.) Model 252A/MM chart recorder was also used to record the chromatograms. Samples were introduced manually by gravity feed: sample solution was introduced into one end of the capillary tube by siphoning from sample solution at a level higher than that of the electrophoretic solution in which the other end of the tube was immersed. An injection time of 5 s at a height difference of 5 cm was used. A schematic diagram of the experimental set-up is shown in Fig. 2.

Two types of electrophoretic media were used. Both were phosphate-borate buffer solutions prepared as described previously⁵. For the solution containing only sodium dodecyl sulphate (SDS), sodium dihydrogenphosphate and sodium tetraborate were used, whereas for the solution containing potassium dodecyl sulphate (KDS), potassium dihydrogenphosphate and sodium tetraborate was used in preparing the buffer. For brevity, the two solutions are henceforth referred to as solutions 1 and 2, respectively. In both instances the pH of the buffer solution was adjusted by mixing phosphate and borate in an appropriate ratio. The pH was measured using a Hanna (Limena, Italy) Model H18417 pH meter. SDS of analytical-reagent grade was dissolved in the buffer. For solution 2, as the Kraff point of KDS is higher than room temperature, precipitation of some of the KDS would be expected. The solution was therefore filtered before use to remove any precipitate formed during mixing. A sample mixture of the eleven priority phenols and Sudan III was prepared in methanol. The concentration of each phenol in the sample mixture was 1000 ppm. Sudan III was used to obtain the retention time of the micelles and its concentration was 100 ppm.

RESULTS AND DISCUSSION

Preliminary experiments using the conditions listed in Table I were performed with the two types of solutions at pH 6.6 and at a voltage of either 10 or 15 kV for the

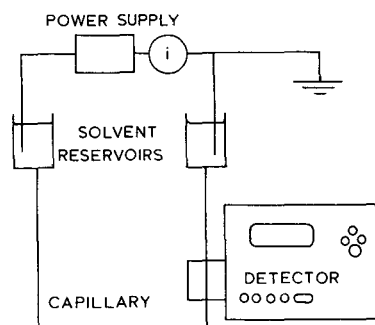


Fig. 2. Schematic diagram of MECC instrument.

TABLE I

EXPERIMENTAL CONDITIONS FOR THE PRELIMINARY EXPERIMENTS AND THE t_0 , t_{mc} , t_0/t_{mc} AND v_{eo} VALUES OBTAINED

Parameter	Experiment 1	Experiment 2	Experiment 3	Experiment 4
Tubing I.D. (μm)	180	180	50	50
Electrophoretic solution	1	2	1	2
Power (kV)	10	10	15	15
Current (μA)	54	130	7.2	15
t_0 (min)	12.6	9.0	9.6	15.3
t_{mc} (min)	37.2	45.6	36.7	41.5
t_0/t_{mc}	0.34	0.20	0.26	0.36
v_{eo} (mm s^{-1})	1.32	1.85	1.48	0.93

180- and 50- μm I.D. capillary tubings. The results obtained are listed in Table II. The apparent capacity factors k' were calculated according to the equation⁵:

$$k' = \frac{t_R - t_0}{t_0 [1 - (t_R/t_{mc})]} \quad (1)$$

were t_R , t_0 and t_{mc} are the elution times of the solute, the insolubilized solute and the micelle, respectively. In the experiments, t_0 was regarded as the retention time of methanol and t_{mc} that of Sudan III.

From the results in Table II, it can be seen that among the four sets of conditions, the combination of the 180- μm I.D. capillary tubing with solution 2 (experiment 2) provides superior selectivity for the phenols. In fact, all eleven phenols were satisfactorily separated using this set of conditions. The variation in selectivity could be explained in terms of the t_0/t_{mc} ratio and the electroosmotic velocity, v_{eo} . The

TABLE II

CAPACITY FACTORS OF THE PHENOLS AT pH 6.6 USING THE EXPERIMENTAL CONDITIONS IN TABLE I

No.	Solute	Capacity factor			
		Experiment 1	Experiment 2	Experiment 3	Experiment 4
2	4-NP	0.95	2.76	0.20	0.05
3	2,4-DCP	1.15	3.23	0.22	0.08
4	2-NP	0.95	3.76	0.33	0.15
5	2-CP	1.15	4.67	0.34	0.18
6	TCP	1.15	6.82	0.35	0.22
7	PCP	1.22	8.98	0.44	0.22
8	DNOC	1.22	10.39	0.44	0.83
9	2,4-DNP	1.70	11.64	0.44	1.25
10	Phenol	0.83	13.11	0.18	1.47
11	4C,3-MP	1.70	40.72	0.47	1.47
12	2,4-DMP	2.55	46.44	0.88	8.27

values of t_0/t_{mc} and v_{eo} obtained for the four experiments are included in Table I. As shown by Otsuka *et al.*¹², a smaller t_0/t_{mc} ratio would result in better resolution between peaks. From Table I, it can be seen that the t_0/t_{mc} ratio obtained for experiment 2 was the smallest among the four sets of experiments. Consequently, better separation and selectivity could be obtained using this set of conditions. Another reason for the difference in selectivity could be attributed to the v_{eo} values. As shown by the results of Terabe *et al.*¹³, obtained for a range of v_{eo} values up to 2 mm/s, the HETP for most of the phenols decreased with increasing v_{eo} in the range studied. Similar results were obtained in this work, as is evident by the large v_{eo} value obtained for experiment 2 which favours better separations.

Another observation was that the capacity factors calculated using eqn. 1 for experiment 2 were much larger than those for the other experiments. This could be due to the difference in the t_0 values obtained for each set of experiments. As indicated in Table I, the t_0 value obtained for experiment 2 was the smallest among the four experiments. From eqn. 1, it can be seen that a small t_0 would result in larger capacity factors. This is in agreement with the results obtained.

It is also worth noting that with different solutions slight changes in the retention order were observed. One notable example is the retention order for phenol. In experiments 1 and 3, the retention order seems to be similar to that obtained by Terabe and co-workers.^{3,5} However, in the other two instances, the phenol peak was observed much later. The reason could be that even though the fused-silica capillary tubing was deactivated, there is a possibility that some free OH groups are not completely removed. These free OH groups would be susceptible to the formation of hydrogen bonds with solutes having suitable substituent groups. As a result, these solutes would be retained much longer in the column. Among the eleven compounds, only phenol seems to be substantially affected. Consequently, phenol was retained much longer despite its low hydrophobicity. On the other hand, for most of the larger phenols, such as PCP and TCP, because of steric hindrance by the substituent groups, formation of hydrogen bonds with the free OH groups is not favourable. With solu-

TABLE III

CAPACITY FACTORS OF THE PHENOLS AT pH 7.0 AND 7.5 AND THEIR LOG P AND pK_a VALUES USING THE 180- μm I.D. FUSED-CAPILLARY TUBING AND SOLUTION 2

Solute	$\log P$	pK_a	Capacity factor	
			pH 7.0	pH 7.5
4-NP	1.96	7.16	0.359	0.310
2,4-DCP	3.08	7.89	1.838	1.100
2-NP	1.79	7.23	0.083	0.107
2-CP	2.15	8.55	0.083	0.107
TCP	3.77	6.23	1.838	1.174
PCP	5.85	4.50	1.838	0.711
DNOC	2.77	4.70	0.841	0.711
2,4-DNP	2.29	4.07	0.355	0.447
Phenol	1.46	11.00	0.841	0.711
4C,3-MP	2.95	9.54	1.838	1.100
2,4-DMP	2.42	10.59	0.841	0.711

tion 1, as no precipitation occurs, the higher surfactant concentration is probably able to protect the phenol molecules from interaction with the free OH groups on the silica tubing. Hence, phenol was eluted in the usual retention order, which is governed by the hydrophobicity.

As experiment 2 provided better selectivity, subsequent experiments were carried out using this set of conditions; pH 7 and 7.5 were also investigated. The results obtained and the pK_a and $\log P$ values for the phenols are given in Table III. As pH 6.6 gave the best separation, the order of elution at this pH was used as the reference for discussion. A typical electropherogram obtained using pH 6.6 is shown in Fig. 3. The eleven compounds were divided into three groups on the basis of their retention characteristics. The apparent capacity factors for the eleven phenols are plotted in Fig. 4, which illustrates that in general the capacity factors for pH 6.6 were much larger than those at higher pH. It was noted that compounds in group I (peaks 2–5) have fairly high pK_a values (6.23–8.55) and therefore at pH 6.6 these compounds would either be neutral or partially ionized. For the compounds in group II (peaks 7–9), the pK_a values were smaller and these compounds would be expected to be completely ionized at pH 6.6. Therefore, the compounds in group II would be less solubilized by the micelles and the capacity factors should be smaller than those of group I. However, the opposite trend was observed. The reason could be that the compounds in group II, being ionized and thus negatively charged, would have a tendency to migrate to the positive electrode (electrophoretic flow). Owing to this electrophoretic pull in the direction opposite to the electroosmotic flow, group II compounds reached the detector at relatively longer times than those of group I and

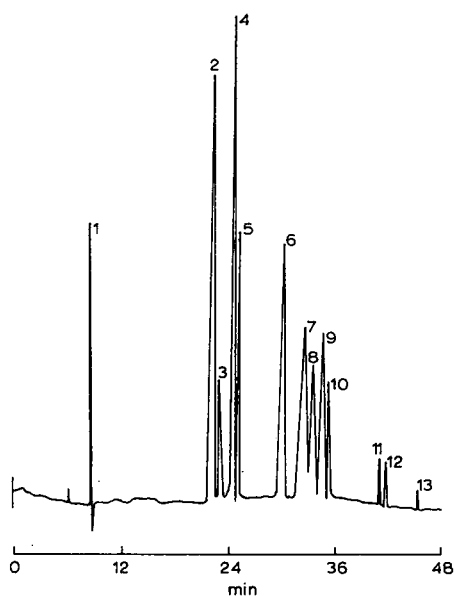


Fig. 3. Electrokinetic chromatogram of the eleven phenols with solution 2. Buffer, SDS (0.05 *M*) in phosphate (0.005 *M*)–borate (0.01 *M*); pH, 6.6; separation tube, 1 m \times 180 μ m I.D. fused-silica capillary; voltage, 10 kV; current, 130 μ A; detector wavelength, 254 nm. Peaks: 1 = methanol; 13 = Sudan III; other peak numbers as in Table II.

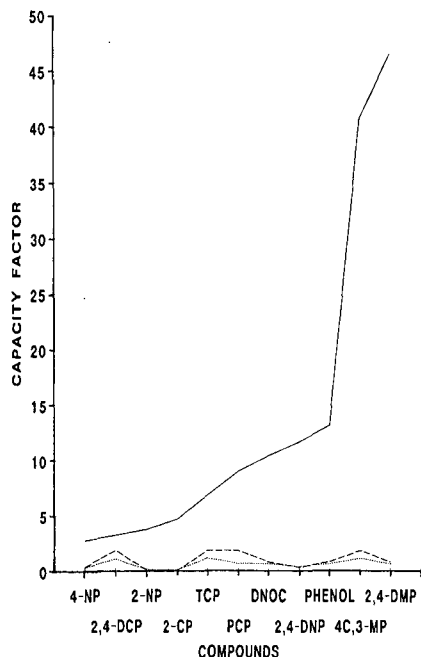


Fig. 4. Variation of capacity factors of phenols with pH. Solid line, pH 6.6; darkened line, pH 7.0; dotted line, pH 7.5.

hence have higher capacity factors. The compounds in group III (peaks 10–12), having fairly high pK_a values, are in the neutral form and therefore, they would be solubilized more easily by the micelles. It was also noted that the two compounds that were eluted last (4-chloro-3-methylphenol and 2,4-dimethylphenol) contain one or two methyl groups. This may account for the fact that the two compounds have exceptionally high capacity factors, as SDS and KDS contain long alkyl chains and their interaction with the methyl groups on the two compounds would be stronger, tending to enhance solubilization.

From the results in Table III, it was found that for pH 7.0 and 7.5, the trend in the capacity factors appeared to be governed by the trend in the partition coefficients, $\log P$, *i.e.*, an increase in capacity factor with increase in $\log P$ was observed. The exceptions to the general trend are phenol and pentachlorophenol. Phenol has a small size and hence a greater tendency for partition with the micelles. Further, because of the possibility of forming hydrogen bonds with the free OH groups on the silica tubing, its capacity factor was found to be exceptionally high. With pentachlorophenol, which has a large $\log P$ value but a small pK_a , there is a greater tendency for it to be ionized and thus less solubilized by the micelles. Despite the high $\log P$ value, its capacity is lower than those of 2,4-dichlorophenol and trichlorophenol.

In Fig. 4, it is also noted that in general the capacity factors decrease with increase in pH. The differences in capacity factors between the eleven phenols were not very significant at pH 7 and 7.5, whereas larger differences were observed at pH 6.6. The reason is that as the pH increases, more of the phenols would ionize to the

anionic form, resulting in a higher electrostatic repulsion between the ionized solutes and the SDS micelles. Despite the increased interaction of the anions with the positive electrode, the effect of the stronger electrostatic repulsion with the micelles dominates, which tends to suppress micellar solubilization. Consequently the net effect is that the capacity factors decrease at higher pH. As the capacity factors for all the phenols are small under these conditions, the differences between them are also relatively small. This observation is in agreement with that of Otsuka *et al.*⁵ At pH 6.6 the differences were more obvious because at this pH most neutral compounds are highly solubilized by micelles. Hence they would be retained for a longer time and larger capacity factors and greater differences were observed.

The results obtained show that MECC is a relatively simple yet powerful technique that can be used for the analysis of priority phenols. To achieve satisfactory separation in this study, a very simple instrument was used, *i.e.*, the high-pressure pumps and chromatographic columns normally used for HPLC were not required. Satisfactory separation of a relatively complicated mixture can be easily achieved owing to the inherently high resolving power of the technique. Therefore, further investigations on the use of capillary electrophoretic techniques for the analysis of environmental pollutants would be an interesting area of development.

ACKNOWLEDGEMENT

The authors thank Mr. Edgardo Biado, Morgal Scientific, for his help in setting up the instrument.

REFERENCES

- 1 F. E. P. Mikkers, F. M. Everaerts and Th. P. E. M. Verheggen, *J. Chromatogr.*, 169 (1979) 11.
- 2 J. W. Jorgenson and K. D. Lukacs, *Anal. Chem.*, 53 (1981) 1298.
- 3 S. Terabe, K. Otsuka, K. Ichikawa, A. Tsuchiya and T. Ando, *Anal. Chem.*, 56 (1984) 111.
- 4 S. Terabe, K. Otsuka and T. Ando, *Anal. Chem.*, 57 (1985) 834.
- 5 K. Otsuka, S. Terabe and T. Ando, *J. Chromatogr.*, 348 (1985) 39.
- 6 *Sampling and Analysis Procedures for Screening of Industrial Effluents for Priority Pollutants*, U.S. Environmental Protection Agency, Environment Monitoring and Support Laboratory, Cincinnati, OH, 1977.
- 7 N. G. Buckman, J. O. Hill, R. J. Magee and M. J. McCormick, *J. Chromatogr.*, 284 (1984) 441.
- 8 F. P. Bigely and R. L. Grob, *J. Chromatogr.*, 350 (1985) 407.
- 9 S. F. Y. Li and H. K. Lee, *Chromatographia*, 25 (1988) 515.
- 10 K. Abrahamsson and T. M. Xie, *J. Chromatogr.*, 279 (1983) 199.
- 11 C. P. Ong, H. K. Lee and S. F. Y. Li, *J. Chromatogr.*, 464 (1989) 405.
- 12 K. Otsuka, S. Terabe and T. Ando, *J. Chromatogr.*, 332 (1985) 219.
- 13 S. Terabe, K. Otsuka and T. Ando, *Anal. Chem.*, 61 (1989) 251.

Capillary electrophoresis of urinary porphyrins with absorbance and fluorescence detection

ROBERT WEINBERGER* and EDWIN SAPP

Applied Biosystems, Inc., 170 Williams Drive, Ramsey, NJ 07446 (U.S.A.)

and

STEPHEN MORING

Applied Biosystems, Inc., 3745 North First Street, San Jose, CA 95131 (U.S.A.)

ABSTRACT

Urinary porphyrins are separated in a 72 cm × 50 μm I.D. fused-silica capillary by micellar electrokinetic capillary chromatography with 100 mM sodium dodecyl sulfate and 20 mM 3-(cyclohexylamino)-1-propanesulfonic acid at pH 11. Detection is accomplished by absorbance at 400 nm or fluorescence with excitation at 400 nm and emission at wavelengths above 550 nm. Substantial trace enrichment is found for porphyrins in urine samples or for porphyrin standards prepared without surfactant in the injection buffer. Limits of detection are in the 100 pmol/ml concentration range with an optimized fluorescence system. The method is shown suitable for the determination of porphyrins in clinical urine specimens. Comparisons are made between electrophoretic and chromatographic methods for the separation and detection of urinary porphyrins.

INTRODUCTION

The separation of urinary porphyrins by chromatographic methods of analysis have been thoroughly reviewed in recent years^{1,2}. The chromatographic methods, in particular liquid chromatography (LC), give relatively rapid separations that are well suited for clinical determinations.

Modern high-performance capillary electrophoresis (CE) is a relatively new technique. The vast majority of published work has dealt with separations, instrumentation and detection^{3–5}. There has been little work reported dealing with the handling of biological fluids in CE, particularly with regard to matrix effects.

Urinary porphyrins appear to be ideal compounds for separation by electrophoresis. These compounds have between two and eight carboxylic acid groups and in alkaline buffers should be so negatively charged. Electrophoretic migration of the ionized porphyrins will be towards the positive electrode. Since electroosmotic flow will direct the bulk flow towards the negative electrode⁶, a counter-migration technique must be employed. Both free solution capillary electrophoresis (FSCE) and

micellar electrokinetic capillary chromatography (MECC) were studied to determine methodology appropriate for this application.

FSCE separations are performed with a homogeneous buffer medium. The separation is based on the combination of molecular charge and size⁷.

MECC employs surfactants in the run buffer. Above the critical micelle concentration (CMC) hydrophobic aggregation of surfactant molecules produce micelles which migrate countercurrent to the electroosmotic flow. The micelles provide a heterogeneous and hydrophobic "pseudo-phase" which can impart reversed-phase properties to the separation^{8,9}. Separations of phenols⁸, phenylthiohydantoin amino acids¹⁰, *o*-phthalaldehyde amino acids¹¹ and nucleosides¹² have been reported.

In the present study, the potential for CE to measure porphyrins in a biologically relevant matrix is investigated. Detection is optimized and comparisons are made with LC. If sufficiently selective, sensitive, and reproducible, the instrumental simplicity of automated CE might be advantageous in the clinical setting.

EXPERIMENTAL

Apparatus

An automated CE instrument [Model 270A; Applied Biosystems (ABI), San Jose, CA, U.S.A.] was used, unmodified for MECC separations with absorption detection employing tungsten and deuterium lamps. A 72 cm × 50 μm I.D. capillary (ABI part No. 0602-0014) was used for all separations except for the work described in Fig. 2 where a 55 cm capillary was employed. Vacuum injection at a preset vacuum of 127 mmHg was used for the MECC work. Both electrokinetic and vacuum injection were used for FSCE.

The following modifications were performed to permit the use of fluorescence detection. The "flow-cell assembly" was removed and machined to permit the insertion of two optical fibers oriented at right angles to the separation capillary. The fibers were routed to a filter assembly. Emitted light was measured with a Hamamatsu R1527 photomultiplier tube (PMT) located as close to the filter as possible. The PMT leads were routed outside of the instrument to the photometer of an LC fluorometer (Model 980; ABI, Ramsey, NJ, U.S.A.). The fluorescence wavelengths were selected with a 550 nm longwave filter (Corion, Holliston, MA, U.S.A.).

To adapt the instrument to accept a xenon arc lamp, the following modifications were made. The lamp cradle at the rear of the monochromator was removed and replaced with a lamp mount assembly (ABI part No. 1400-0159). A 75-W xenon arc lamp (ABI part No. 2450-0193) was fitted onto the lamp hub assembly. An external 150-W power supply with an automatic starter (Model LPS 200X, Photon Technologies) was set at 13 V, 5.6 A to run the lamp.

Data were collected on either a strip chart recorder (Kipp and Zonen) or integrator (Model 4290, Spectra-Physics, San Jose, CA, U.S.A.).

Chemicals

A chromatographic marker kit containing a mixture of mesoporphyrin, coproporphyrin, pentacarboxyl porphyrin, hexacarboxyl porphyrin, heptacarboxyl porphyrin and uroporphyrin, 10 nmol each was purchased from Porphyrin Products (part No. CMK-1A; Logan, UT, U.S.A.). The individual porphyrins, as well as

uroporphyrin III and coproporphyrin III were also purchased in pure form from the same source. Sodium dodecyl sulphate (SDS) was Sequanol grade from Pierce (Rockford, IL, U.S.A.). 3-Cyclohexylamino-1-propanesulfonic acid (CAPS) buffer and sodium hydroxide were from Sigma (St. Louis, MO, U.S.A.). Water was provided by an in-house reverse osmosis, ion-exchange system (Hydro, Research Triangle Park, NC, U.S.A.). LC grade methanol was from J. T. Baker (Phillipsburgh, NJ, U.S.A.).

Buffer preparation

The MECC run buffer was prepared as follows. A 2.88-g amount of SDS plus 442 mg CAPS was dissolved in about 95 ml water. The pH was adjusted to 11.0 with 1 M sodium hydroxide and the volume brought up to 100 ml. The solution was filtered through a 0.2- μ m filter. This gave a working concentration of SDS and CAPS of 100 and 20 mM, respectively. Other buffers were prepared in a similar fashion. A 15% methanolic buffer was prepared by mixing 17 ml of the above described buffer with 3 ml methanol.

Standard preparation

Standards were prepared by adding 250–1000 μ l buffer to culture tubes containing 10 nmol each of the six different porphyrins and sonicating for about a minute. Further dilutions were made as required. Since porphyrins are photosensitive, they were kept in the dark as much as possible. To minimize light exposure, the autosampler illuminator within the Model 270A was disconnected and the autosampler viewing window was covered to exclude room light.

Urine samples

A 24-h pooled sample of urine from a patient suffering from porphyria cutanea tarda was used. About 0.5 ml urine was centrifuged for a few minutes prior to injection and the supernatant transferred into a 0.5-ml micro-centrifuge tube. Samples of normal urines were obtained from a volunteer and treated as noted above. To aid in peak identification, the normal urine was spiked with 300 pmol/ml of each porphyrin.

Capillary conditioning

A new capillary was flushed by vacuum for 30 min with 1 M sodium hydroxide followed by 10 min 0.1 M sodium hydroxide and then 30 min with run buffer. After that sequence, the detector-side buffer reservoir was rinsed and filled with run buffer.

Routine operation

The programming features of the Model 270A include the following sequential steps: WASH, BUFFER, MARKER, INJECTION, DETECTOR, TIME1, TIME2, TIME3 and TIME4. After the initial conditioning step described above, the WASH cycle was not used. BUFFER wash was set for 3 min to fill the capillary with the run buffer. The MARKER, which could be used for adding a neutral unretained marker or an internal standard was not used. INJECTION was set for vacuum at selected times from 1- to 20-s injections. The DETECTOR was set for 400 nm with a rise time of 0.5 s. TIME1 conditions were: voltage, 20 kV; polarity, +; temperature, 45°C; run time, 17 min. The current draw was 30 μ A under these conditions with the 100 mM SDS, 20 mM CAPS, pH 11 MECC buffer. Conditions that deviate from the above are so indicated on the figure captions.

Electroendosmotic velocity measurement

The electroendosmotic velocity (V_{eo}) was measured in 3 buffers: (1) 20 mM CAPS, pH 11, (2) 20 mM CAPS, 100 mM SDS, pH 11 and (3) 20 mM CAPS, 150 mM SDS, pH 11. V_{eo} was measured using a neutral marker that does not partition into the micelle; 1 part methanol plus 9 parts of the respective buffer. The V_{eo} was calculated by dividing the capillary length (mm) by the migration time (s) of the methanol. The voltage was 20 kV and the capillary temperature was 45°C.

Theoretical plate calculation

Theoretical plates (N) were calculated for uroporphyrin using the formula: $N = 5.54(t_m)^2/w_{1/2}^2$ where t_m = the migration time and $w_{1/2}$ = the peak width at half height. A chart speed of 5 cm/min was used to enable accurate measurements to be made.

LC conditions

An Econosphere C₁₈ column, 25 cm × 4.6 mm I.D. packed with 5- μ m particles (Alltech) was used. A Spectroflow 430 gradient former and a Spectroflow 400 (Kratos, Ramsey, NJ, U.S.A.) pumping system was employed. The mobile phase was a binary gradient: solvent A: methanol-potassium phosphate, monobasic buffer, 6.9 g/l, pH 3.5 (50:50); solvent B: 100% methanol. The gradient was a ramp from 100% A to 100% B in 10 min, hold at 100% B for 10 min followed by reequilibration to initial conditions in 5 min. The detector, a Kratos FS 970 equipped with a xenon arc was set at 400 nm excitation. The wavelengths of emission were selected with a 600-nm bandpass filter, 70 nm bandwidth. The loop size was 20 μ l.

RESULTS AND DISCUSSION

Free solution capillary electrophoresis

A separation employing free solution, counter migration capillary electrophoresis is shown in Fig. 1A. The elution order is consistent with the charge on each porphyrin for a counter migration mechanism. The least charged solute elutes first and the elution continues in the order of increasing negative charge. While the most negatively charged solute has the greatest electrophoretic mobility, it is directed towards the positive electrode away from the detector. Since electroosmosis results in the bulk flow being directed towards the detector, the solute with the greatest electrophoretic mobility elutes last. This elution order is exactly the opposite of reversed-phase LC (Fig. 1B¹³).

Two peaks are found for hexacarboxyl porphyrin that were not resolved in the above cited LC separation. The presence of two peaks is an artifact of the synthetic procedure¹⁴. According to the manufacturer, adjacent and opposite decarboxylation can occur during the synthesis. The adjacent isomer is about two times more likely to decarboxylate and this is represented in Fig. 1A by the peak height ratio for the two peaks of hexacarboxyl porphyrin. In the naturally occurring biological system, only one of the isomers is found. It is probable that these isomers could be separated by LC in a 1 M acetate buffer^{1,2}.

The run buffer for the Fig. 1A separation contained 10% methanol. Without the methanol, an asymmetric peak was found for coproporphyrin, presumably due to its poor solubility. The sample was dissolved in 50% methanol. Without such a high

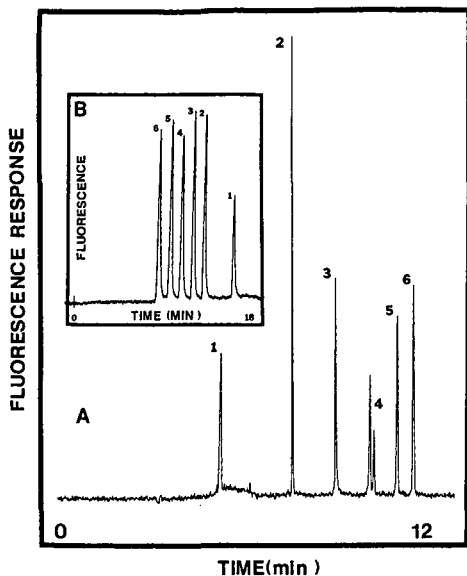


Fig. 1. (A) Free solution separation of urinary porphyrins. Buffer: 20 mM CAPS, pH 11 with 10% methanol. Sample: porphyrin mixture, 5 nmol/ml dissolved in methanol-20 mM CAPS (50:50). Injection: electrokinetic, 12 s at 10 kV. Run voltage: 30 kV. Temperature: 30°C. Detection: fluorescence, excitation wavelength 400 nm, emission wavelengths > 595 nm, with xenon arc source. Peaks: 1 = mesoporphyrin (dicarboxyl); 2 = coproporphyrin (tetracarboxyl); 3 = pentacarboxyl porphyrin; 4 = hexacarboxyl porphyrin positional isomers (two peaks); 5 = heptacarboxyl porphyrin; 6 = uroporphyrin (octacarboxyl). (B) Reversed-phase high-performance LC separation of urinary porphyrins.

concentration of methanol, mesoporphyrin is insoluble and did not appear on the electropherogram. Mesoporphyrin is not naturally occurring but was added to the test mix by the manufacturer as a typical dicarboxylic acid porphyrin.

During the course of running the system, loss of resolution and peak broadening was sometimes noticed. Regeneration of the capillary through base or acid washing did not always restore the separation. It appeared that adsorption of porphyrins was occurring at the capillary wall. Perhaps this was mediated by the marginal solubility of mesoporphyrin and coproporphyrin. Because of this problem, a more robust system was required for this separation to be useful.

MECC of urinary porphyrins

The rationale for employing MECC for this separation was not to provide for a pseudo-reversed-phase mechanism but to control wall adsorption of the analytes. Since both the porphyrins and the surfactant, SDS, are anionic at pH 11, electrostatic repulsion was expected. The elution order was expected to remain the same as in the free solution experiments. Rather than contribute to the separation mechanism, the anionic surfactant was used to bind any electrostatic or hydrophobic sites on the capillary wall that might interact with the anionic analyte.

The non-interaction hypothesis is not totally correct. As Fig. 2A and B indicates, mesoporphyrin (peak 1) shows a shift in selectivity. At 100 mM SDS, it elutes between

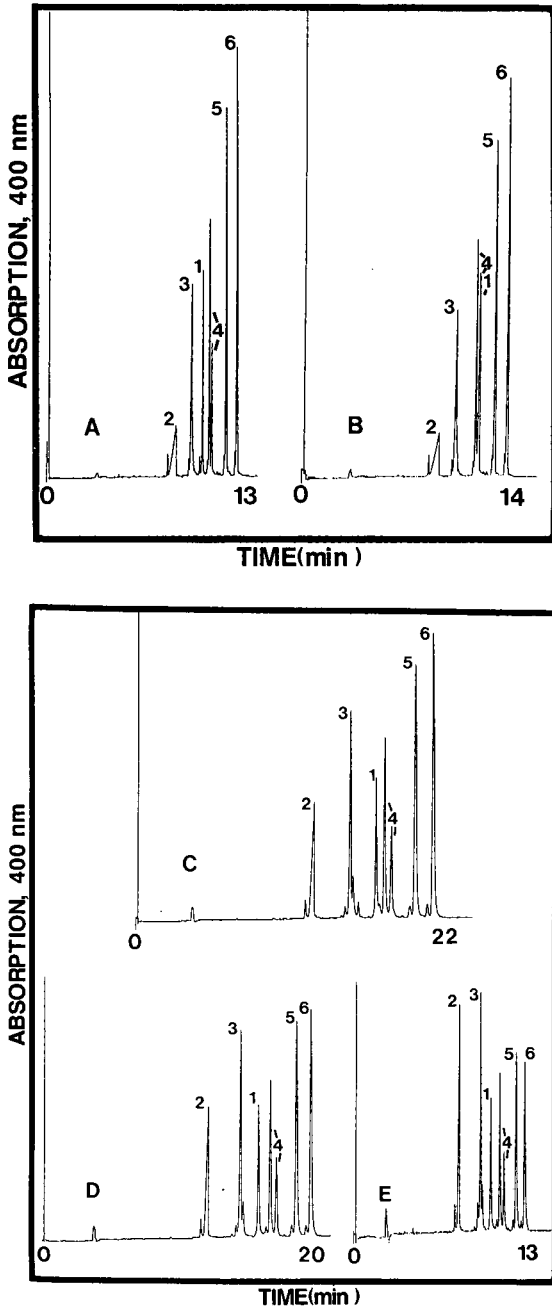


Fig. 2. MECC separation of urinary porphyrins. Sample: porphyrin mixture, 20 nmol/ml in 20 mM CAPS, pH 11. Injection, 3 s vacuum. Capillary: 55 cm \times 50 μ m I.D. Detection: absorbance, 400 nm with tungsten lamp. Sensitivity: 0.064 absorbance units full scale. (A) Run buffer: 100 mM SDS, 20 mM CAPS, pH 11; 20 kV; 45°C. (B) Run buffer: 150 mM SDS, 20 mM CAPS, pH 11; 20 kV; 45°C. (C) Run buffer: 17 ml of 100 mM SDS, 20 mM CAPS, pH 11, plus 3 ml of methanol; 20 kV; 45°C. (D) Run buffer: 17 ml of 100 mM SDS, 20 mM CAPS, pH 11, plus 3 ml of methanol; 20 kV; 55°C. (E) Run buffer: 17 ml of 100 mM SDS, 20 mM CAPS, pH 11, plus 3 ml of methanol; 30 kV; 45°C. Peaks as in Fig. 1.

the penta- and hexa-species. At 150 mM SDS, mesoporphyrin coelutes with the latter hexacarboxyl porphyrin isomer.

The other porphyrins did not show any changes in elution order that would be suggestive of an MECC separation mechanism. The migration times for the porphyrins are somewhat longer at the higher surfactant concentration. This is consistent with conventional MECC where longer migration times are expected as the surfactant concentration is increased. Measurement of V_{eo} gave values of 1.79 and 1.81 mm/s for 100 and 150 mM SDS solutions, respectively. The difference between these results is probably not significant therefore electroosmotic flow is not responsible for the differences in migration time *versus* surfactant concentration. Otsuka *et al.*¹⁰ have defined the velocity of the micelle, $v_{mc} = V_{eo} + v_{ep}(mc)$ where $v_{ep}(mc)$ = the electrophoretic velocity of the micellar aggregate. The micellar velocity, v_{mc} is more profoundly influenced by the surfactant concentration¹⁰. v_{mc} decreases rapidly with increasing surfactant concentration. This is a consequence of the enhanced $v_{ep}(mc)$ of the micelle towards the positive electrode due to the reduction in viscosity from Joule heating at the higher surfactant concentration. In a similar fashion, the electrophoretic mobility of the porphyrins is expected to increase with surfactant concentration.

It is unlikely that the porphyrins, excepting mesoporphyrin are interacting hydrophobically with the micelle. The anionic charge is well distributed in all four molecular quadrant for the porphyrins having four or more $-COOH$ groups. Electrostatic repulsions of porphyrins from the anionic micellar aggregate is most likely responsible for the free solution mechanism of separation.

In free solution, the porphyrins elute somewhat faster than in the MECC mode. The electroosmotic flow is 2.1 mm/s at 20 kV with 20 mM CAPS buffer at pH 11 and the current draw is only 10 μA . Under these conditions, there is minimal Joule heating and it is likely that the electrophoretic mobility is reduced due to the higher viscosity.

The explanation for the behavior of mesoporphyrin is clear. Mesoporphyrin has both of its carboxyl groups located on adjacent indoles. For this substance, the anionic charge is highly localized. The opposite side of the molecule is free to interact hydrophobically with SDS without experiencing electrostatic repulsion. The other porphyrins have a more uniform distribution of carboxyl groups throughout their structures. This is a further evidence for the free solution mechanism. Coproporphyrin, which contains four $-COOH$ groups would be better solubilized if an MECC mechanism were occurring.

The surfactant-wall interaction hypothesis proposed above may indeed have some merit. Separations were always successful on both new and aged capillaries.

Coproporphyrin gave a peak that exhibited fronting. This effect was reduced but not eliminated by running at elevated temperatures. A temperature of 45°C was selected as a compromise between peak sharpness and loss of resolution due to the increase in electroosmotic flow. The improvement in peak sharpness may be due to increasing the solubility of the solute in the buffer. Adding 15% methanol to the buffer solubilizes the coproporphyrin and a sharp peak is obtained (Fig. 2C). A 55-cm capillary was used for these experiments to better manage the run time. The longer run time can also be compensated by increasing the temperature to 55°C (Fig. 2D) or the voltage to 30 kV (Fig. 2E). The use of the methanolic buffer was not pursued at this time because of expectation that even modest solvent evaporation would produce migration time drift. A non-ionic surfactant may yet prove a better choice to solubilize marginally soluble compounds.

Detection

Urinary porphyrins have major absorption maxima between 395 and 405 nm. Intense fluorescence occurs between 600 and 700 nm. The selection of the appropriate light source profoundly influences the limits of detection (LOD) found either with absorption or fluorescence detection. Table I lists the LOD values found for free solution separations with electrokinetic injection, MECC separations with vacuum injection and for comparative purposes, LC with a 20- μ l loop injection.

The optimal lamp source differs depending on whether fluorescence or absorption is employed. Not surprising, the deuterium lamp was the least sensitive since a wavelength of 400 nm was used. This wavelength is in a spectral region where the deuterium lamp has little energy. For fluorescence, the xenon arc is optimal due to its substantial power for visible excitation. For absorption measurements, the tungsten lamp is superior. While less powerful than the xenon lamp, a filament based lamp is generally more stable than a gas discharge plasma.

The comparison with LC illustrates one of the limiting problems in CE, *i.e.* substantially lower concentration limits of detection (CLOD). The LC method has a CLOD 80–90 times lower than found for CE. The mass limit of detection (MLOD) for CE is superior to that found with LC. With an injection size of approximately 4 nl (1 s at 127 mmHg), the amount of material injected at the LOD is calculated as $0.1 \text{ nmol/ml} \cdot (4 \cdot 10^{-6} \text{ ml}) = 0.4 \text{ fmol}$. To contrast this loading factor with LC, the calculation gives $1 \text{ pmol/ml} \cdot 0.02 \text{ ml} = 20 \text{ fmol}$. For CE, the MLOD is 50-fold lower than found in LC for the porphyrins. The LC flow cell had a volume of 5 μ l. The on-capillary optical window for CE had a volume of less than 0.2 nl.

The advantage of CE over LC in a clinical application is ease of use and low operating costs. The LC separation requires gradient elution, expendable columns and relatively large amounts of solvents, the disposal of which is costly in light of environmental regulations.

Trace enrichment

Trace enrichment, or peak compression will always occur in chromatographic or

TABLE I

LIMITS OF DETECTION OF URINARY PORPHYRINS BY CE AND LC

Please refer to the Experimental section for the detection conditions for both CE and LC measurements. NM = Not measured.

Lamp	Limit of detection (nmol/ml)				
	Free solution CE ^a		MECC ^b		High-performance LC ^c , fluorescence
	Absorbance	Fluorescence	Absorbance	Fluorescence	
Deuterium	0.7–1.7	>5	NM	NM	0.01–0.02
Tungsten	0.4–1.1	>5	0.3–1.4	NM	NM
Xenon	NM	0.08–0.2	1.1–2.5	0.1–0.4	0.001–0.002

^a Electrokinetic injection, 6 s at 6 kV.

^b Vacuum injection, 1 s at 127 mmHg.

^c 20- μ l loop.

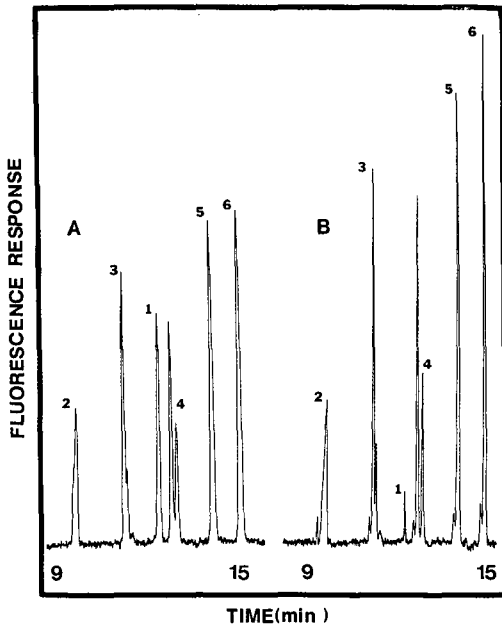


Fig. 3. Impact of injection buffer on resolution. Sample: porphyrin mixture, 5 nmol/ml in (A) run buffer (100 mM SDS, 20 mM CAPS, pH 11) and (B) 20 mM CAPS, pH 11. Injection: 1 s vacuum. Run voltage: 20 kV. Detection: fluorescence, excitation wavelength 400 nm, emission wavelengths > 550 nm with xenon arc. Temperature: 45°C. Peaks as in Fig. 1.

electrophoretic separations whenever the solute's velocity is greater in the injection medium than in the separation medium. In electrophoresis, this phenomenon is known as stacking.

This effect was observed during the course of injecting urine directly into the instrument during an MECC separation. The resulting peaks were substantially sharper than found for standards injected in micellar media. This is illustrated in Fig. 3 where a standard porphyrin mixture was injected in 20 mM CAPS buffer and compared to the same mixture injected in run buffer which contained 100 mM SDS. Note the improvement in resolution, particularly with regard to the minor components (photodegradation products). The increase in resolution and theoretical plates, even for a short 1-s injection is substantial. The mesoporphyrin signal is much lower with a non-micellar injection solvent due to poor solubility. At lower concentrations, that solubility problem is overcome.

The impact of the injection buffer on peak compression can be substantial. When using an injection buffer with a low conductivity (high resistance) relative to the run buffer, the voltage drop differential can be substantial. For example, the 100 mM SDS, 20 mM CAPS run buffer draws 30 μA at 20 kV in a 72-cm capillary. The injection buffer, 20 mM CAPS draws only 10 μA under equivalent conditions. Then the resistance of these buffers is 9.2 and 27.8 M Ω , respectively. If a 5-cm zone of injection buffer is introduced, the voltage drop is 243 V/cm for the run buffer and 736 V/cm for the injection buffer. Since both V_{eo} and v_{ep} are proportional to the voltage drop and/or

the current, the impact on peak compression can be visualized in a qualitative fashion. Computation of the actual amount of peak compression is complex and beyond the scope of this paper.

A study was performed to determine the degree of trace enrichment at various injection times and the sacrifice in resolution that occurs. The electropherograms are shown in Fig. 4 with some of the figures of merit illustrated in Fig. 5.

It is possible to perform vacuum injections of up to 5 s without substantial loss in resolution. The plate count, measured by peak width at half-height declines from 373 000 to 336 000 for 1- and 5-s injections, respectively. Both peak height and area are linear within this range after which peak height, as expected begins to deviate. Peak

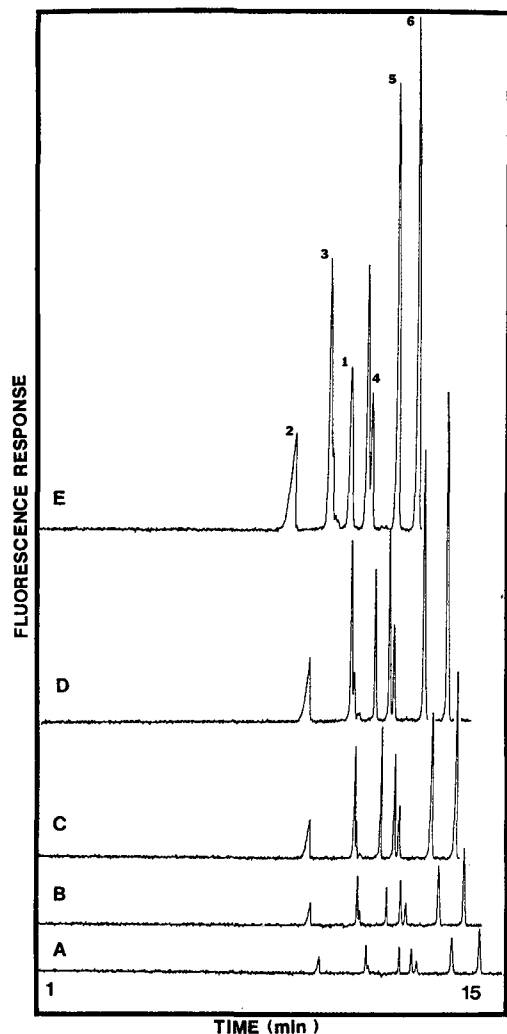


Fig. 4. Impact of injection time on resolution, migration time and response. (A) 1 s; (B) 2 s; (C) 5 s; (D) 10 s; (E) 20 s. Other conditions as in Fig. 3. Peaks as in Fig. 1.

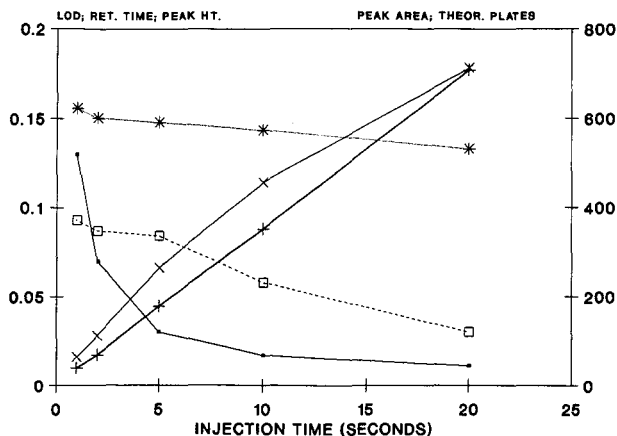


Fig.5. Impact of injection time on LOD, peak area, peak height, migration time and theoretical plate count for uroporphyrin. Key: *---* = migration time ($\times 0.01$ min); \times — \times = peak height; +—+ = peak area; \square --- \square = plate count; \blacksquare — \blacksquare = LOD (ng/ml). Values for theoretical plates should be multiplied by 10^3 .

areas were linear for injection times up to 20 s. The limit of detection was improved from 130 pmol/ml to 30 pmol/ml for uroporphyrin, a 4.3-fold decrease between 1- and 5-s injections. In contrast, going from 5 to 20 s produced an LOD improvement of only $2.7\times$ because of the increased band broadening; the plate count was reduced to 120 000 theoretical plates.

The disadvantage of large-volume injections in non-micellar media is a shifting of migration time that is dependent on the size of the injection. With a 20-s injection, the migration time for uroporphyrin decreases by 15%. The decrease for a 5-s injection is only 5%. The decrease in migration time is due to two factors: (1) the analytes migrate faster in the free solution injection buffer due to the increased field strength as described above and (2) the injection occupies a finite space in the capillary, the length of which is dependent on the size of the injection. A 20-s injection occupies about 50 mm of capillary length. That factor alone would provide for a 10% reduction in migration time.

Matrix effects

It is desirable to inject untreated urine directly into the instrument to avoid sample handling. Unfortunately, the matrix can severely perturb the separation. This is illustrated in Fig. 6 where electropherograms of normal urine and urine spiked with 300 pmol/ml of porphyrins are shown. Injection times of 2, 3 and 5 s were used.

Based on the dramatic sharpening of the uroporphyrin peak (peak 6), it appears that urine or some urine samples may have stacking properties, at least for uroporphyrin. The uroporphyrin was positively identified by standard addition (Fig. 6B). Buffering the urine to 20 mM CAPS had no perceptible effect on the separation compared to unbuffered urine.

The source of this unusual peak compression has not been positively identified. As per comments at an international meeting¹⁵, isotachophoretic focusing is a possibility. Perhaps some component or components in a urine specimen can serve as

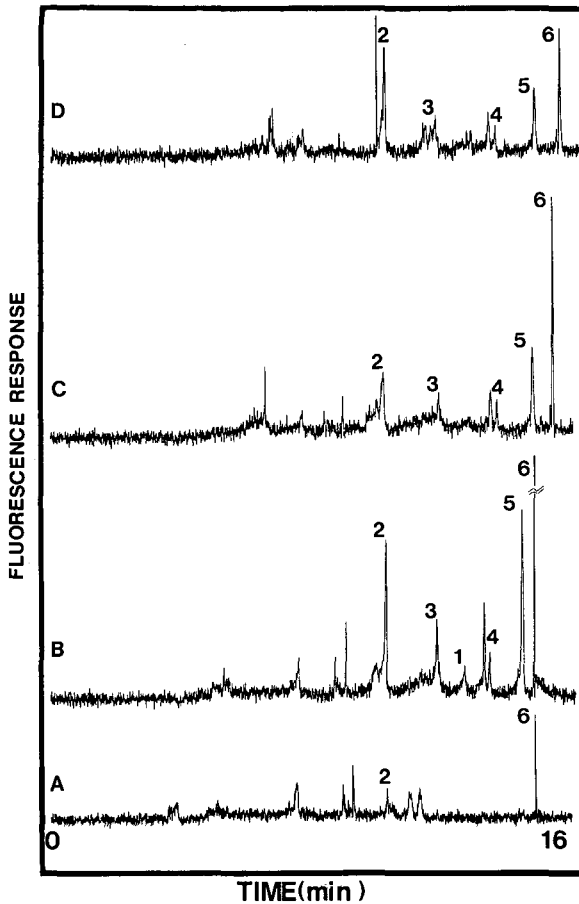


Fig. 6. Impact of injection time of a urine sample on the electropherogram. (A) Urine from a normal patient, 5-s injection; (B–D) urine spiked with 300 pmol/ml porphyrins; (B) 5-s injection; (C) 3-s injection; (D) 2-s injection. Other conditions as in Fig. 3. Peaks as in Fig. 1.

a terminating buffer, then it might be possible that an isotachophoretic zone might overlap and compress an electrophoretic peak. On a 55-cm capillary, peak compression of pentacarboxyl porphyrin was observed with the same urine specimen as employed in Fig. 6. Elevating the temperature eliminated the peak compression. This indicates that whatever the phenomenon, it can be regulated and if controllable, might be useful from the analytical perspective.

There are several important issues that can be extracted from these data: (1) migration time, peak height and peak width can be related to the injection time, the dependence of which can be influenced by the sample matrix; (2) 1–2-s injection times have only a modest impact on the electropherogram; (3) the use of such short injection times will limit detectability of the porphyrins to 100–200 pmol/ml.

For positive peak identification, standard addition techniques may be necessary to confirm the identity of unusual peaks when large volume injections are made.

Alternatively, sample preparation techniques such as solvent or solid-phase extraction may be employed to minimize matrix effects. An additional benefit of these techniques is the potential to improve the sensitivity of the method through off-line trace enrichment.

Precision and linearity

Peak area linearity was assessed at concentrations of 0.64, 1.4, 4 and 10 nmol/ml. The calibration curves were linear ($r^2 > 0.9994$) for all natural porphyrins and passed close to the origin. Mesoporphyrin, showed a modest loss of linearity at the higher concentrations ($r^2 = 0.9593$), presumably due to low solubility in the non-micellar injection buffer.

Peak height precision was assessed at three concentration levels. The following data excludes coproporphyrin which will be discussed later. At the 40 nmol/ml level, injecting with micellar buffer, the relative standard deviations (R.S.D.) ranged from 0.9–2.5% ($n = 5$). At 4 nmol/ml, injecting with CAPS buffer, the R.S.D. values were from 2.8–4.6% ($n = 9$). At 1 nmol/ml, injecting with CAPS buffer, the R.S.D. values were 3.6–8.5% ($n = 9$).

Coproporphyrin was not as well-behaved electrophoretically, presumably due to solubility problems. Occasionally, peak shape changes were noted. Injecting with micellar solvent may help here as an R.S.D. of 1.9% was calculated at the 40 nmol/ml concentration level. At 1 and 4 nmol/ml, the R.S.D. values were 18 and 14%, respectively. When coproporphyrin must be determined, the previously described methanolic buffer should give superior results.

Migration time precision was not calculated owing to a reproducible bias due to variations in the electroosmotic-flow. Run-to-run variation measured for each of the 7 peaks was 1.2–2.5 s/run. This corresponds to a relative migration drift of 0.2–0.3%. Replenishment of the buffers after several runs restored the migration times to the initial values. The cause of the drift is probably depletion of one or more of the buffer components.

Patient sample

An electropherogram of a urine specimen from a patient suffering from porphyria cutanea tarda is shown in Fig. 7A. Splitting of the peaks in the uro- and hepta-areas was noted. Spiking experiments with pure porphyrins indicated that the second peak of each doublet was the correct signal. Suspecting separation of uro(I) and uro(III) isomers a mixture of the two was injected and coelution was obtained. This method will not discriminate between uro(I) and uro(III), nor copro(I) and copro(III).

The urine sample was an aliquot from a 24-h collection. Although it was stored frozen, the sample was a few months old. Since porphyrins are known to degrade photochemically, a standard mixture was exposed to fluorescent room light for an hour. The ensuing electropherogram is shown in Fig. 7B. Photodegradation of all of the porphyrins were noted. In particular, the splitting pattern for uro- and hepta- very closely matched that found for the standard.

The highly elevated uro- and heptaporphyrins found in the patient sample is consistent with porphyria cutanea tarda.

These results suggest that CE may be useful in the clinical setting. While less concentration sensitive than LC, the instrumental simplicity, minimal sample usage,

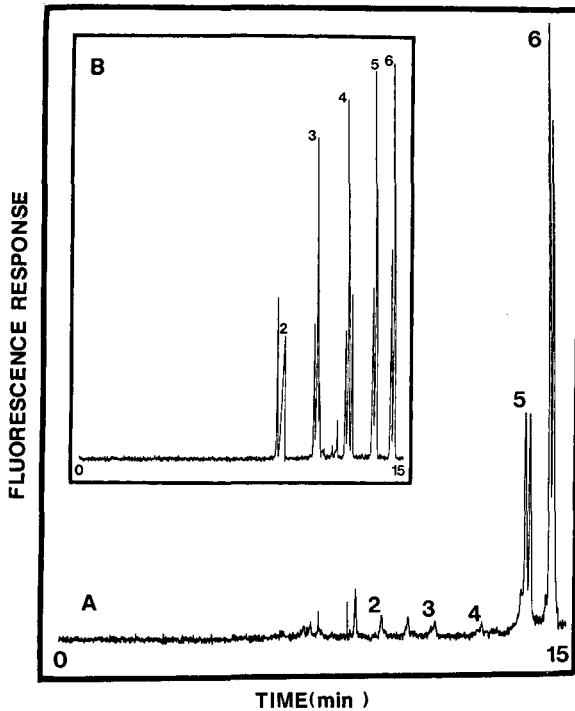


Fig. 7. (A) Electropherogram of a urine sample from a patient with porphyria cutanea tarda. Sample preparation: centrifugation for 1 min. Injection: 2 s vacuum. Other conditions as in Fig. 3. (B) Electropherogram of a partially decomposed porphyrin standard. Initial sample concentration, 5 nmol/ml. Conditions as in Fig. 3. Peaks as in Fig. 1.

low reagent consumption and freedom from organic solvents should be attractive to clinical chemists. If the general detection problem in CE can be solved, this technique will have unequivocal advantages over LC for this application.

ACKNOWLEDGEMENTS

The authors wish to thank Edith Zaider of the New York Medical College, Department of Dermatology, Porphyrin Laboratory, Vahalla, NY, U.S.A. for providing the patient sample. We are grateful to Joel Colburn of Applied Biosystems Inc., San Jose, CA, U.S.A. for his helpful discussions. We also acknowledge the anonymous reviewer of this paper for an outstanding critique.

REFERENCES

- 1 E. Rossi and D. H. Curnow, in C. K. Lim (Editor), *HPLC of Small Molecules*, IRL Press, Oxford, 1986, pp. 261-303.
- 2 C. K. Lim, F. Li and T. J. Peters, *J. Chromatogr.*, 429 (1988) 123.
- 3 N. A. Guzman, L. Hernandez and B. G. Hoebel, *BioPharm*, 2 (1989) 22; and references cited therein.
- 4 A. G. Ewing, R. A. Wallingford and T. M. Olefirowicz, *Anal. Chem.*, 61 (1989) 292A; and references cited therein.

- 5 S. E. Moring, J. C. Colburn, P. D. Grossman and H. H. Lauer, *LC·GC*, 8 (1990) 34; and references cited therein.
- 6 J. W. Jorgenson and K. D. Lukacs, *Science (Washington, D.C.)*, 222 (1983) 266.
- 7 P. D. Grossman, J. C. Colburn, H. H. Lauer, R. G. Nielsen, R. M. Riggan, G. S. Sittampalam and E. C. Rickard, *Anal. Chem.*, 61 (1989) 1186.
- 8 S. Terabe, K. Otsuka, K. Ichikawa, A. Tsuchiya and T. Ando, *Anal. Chem.*, 56 (1984) 111.
- 9 S. Terabe, K. Otsuka and T. Ando, *Anal. Chem.*, 57 (1985) 834.
- 10 K. Otsuka, S. Terabe and T. Ando *J. Chromatogr.*, 332 (1985) 219.
- 11 J. Liu, K. A. Cobb and M. Novotny, *J. Chromatogr.*, 468 (1988) 55.
- 12 A. S. Cohen, S. Terabe, J. A. Smith and B. L. Karger, *Anal. Chem.*, 59 (1987) 1021.
- 13 R. Weinberger and V. Coniglione, *LC Mag.*, 2 (1984) 766.
- 14 J. C. Bommer, Porphyrin Products, Logan, UT, personal communication.
- 15 F. Everaerts, comments at *2nd International Symposium on High-Performance Capillary Electrophoresis, San Francisco, CA, January 29–31, 1990*.

Separation and partial characterization of Maillard reaction products by capillary zone electrophoresis

ZDENEK DEYL*, IVAN MIKSIK and RUDOLF STRUZINSKY

Institute of Physiology, Czechoslovak Academy of Sciences, Videnska 1083, 142 00 Prague 4 (Czechoslovakia)

ABSTRACT

Capillary zone electrophoresis proved useful for separating small amounts of both charged and uncharged solutes that are otherwise difficult to analyse. A typical complex mixture that had previously resisted all analytical approaches, including reversed-phase separations, is the products arising from the reaction of free amino acids with aldehydic sugars (Maillard reaction products). By using capillary zone electrophoresis [untreated capillary 50 cm × 75 μm I.D., 18 kV, 0.02 mol/l phosphate buffer (pH 7.5)], a number of products resulting from the reaction of glucose or ribose with glycine, alanine and isoleucine were separated and partially characterized. They were separated (1) without derivatization (and profiles of compounds absorbing at 220 nm were obtained), (2) as phenylthiocarbamyl derivatives in a search for reactive amino groups and (3) after derivatization with 2,4-dinitrophenylhydrazine in a search for a method for compounds with a free aldehydic group. Phenylthiocarbamyl derivatives were separated in 0.005 mol/l borate buffer (pH 9.6) at 20 kV and 25 μA. Separation of 2,4-dinitrophenylhydrazones was effected by electrokinetic micellar chromatography in the same apparatus using a 50 cm × 75 μm I.D. capillary at 10 kV in 0.01 mol/l Na₂HPO₄–0.006 mol/l tetraborate, 0.050 mol/l with respect to sodium dodecyl sulphate. The results are compared with those given by high-performance liquid and thin-layer chromatography.

INTRODUCTION

In a previous study¹ we attempted to separate reactive 2,4-dinitrophenylhydrazine compounds arising during the Maillard reaction. It was emphasized that Maillard reaction products represent complex mixtures which are very difficult to analyse. On the other hand, their importance is considerable: they represent a traditional topic in food chemistry² and more recently they have been shown to be involved in cross-linking of proteins³ and even nucleic acids⁴, influencing the metabolic turnover of these biopolymers. Biologically they are undesirable side-products of metabolism and their role in ageing is a matter of discussion⁵. Briefly, in the reaction of D-glucose and L-glycine after an Amadori rearrangement D-fruc-

toseglycine was found which, in the next step, may react to give di-D- fructoseglycine. At weakly acidic pH and at elevated temperature the compound is rapidly split into 3-deoxy-D-erythrohexosulose and unsaturated side-products. Dicarbonyl intermediates are prone to reactions with available free amino groups with the formation of brownish and/or polymeric products⁶.

Within the Maillard products obtained some individual compounds were identified and a rough estimate of over 150 compounds present was reported⁷. Some of the *in vivo* occurring compounds that were identified were later shown to be preparative artifacts⁸.

From the analytical point of view, it is evident that new approaches have to be applied because, *e.g.*, high-performance liquid chromatographic (HPLC) procedures did not give satisfactory results in spite of testing a wide variety of separation conditions. Moreover, a profiling technique would help considerably in obtaining orientation information on the reaction products as it has to be kept in mind that not only are the products numerous but also their nature is likely to depend on the nature of the sugar and amino acid involved.

In this work we have tried to exploit the high separating power of capillary zone electrophoresis (CZE); the profiles were obtained on the basis of UV (220 nm) absorbance and additional information was gained by reacting the products with 2,4-dinitrophenylhydrazine and phenyl isothiocyanate using simple amino acid-sugar mixtures as model systems.

EXPERIMENTAL

Chemicals

All chemicals used were of analytical-reagent grade, *i.e.*, glycine (Reanal, Budapest, Hungary), β -alanine (Loba, Wien-Fischamend, Austria), isoleucine (Calbiochem, San Diego, CA, U.S.A.), glucose monohydrate, ribose and 2,4-dinitrophenylhydrazine (Lachema, Brno, Czechoslovakia). Solvents for the Maillard products preparation and derivatization were used without further purification. Methanol for chromatography (Merck, Darmstadt, F.R.G.), acetonitrile of spectrometric grade (Janssen, Beerse, Belgium) and doubly distilled water were used in chromatographic separations. For sterilization filters of 0.2- μ m pore size (Sigma, St. Louis, MO, U.S.A.) were used. All chemicals used in the preparation of electrophoretic buffers were of analytical-reagent grade and were purchased from Lachema.

Preparation of Maillard products

Glucose-glycine Maillard products were prepared by the following procedure⁹: 0.018 mol of glycine (1.35 g) were reacted with 0.0045 mol of glucose monohydrate (0.9 g) in 60 ml of ethanol with 20 drops of glacial acetic acid under reflux. After boiling for 24 h the reaction mixture was filtered and the filtrate was dried and reconstituted in doubly distilled water (*ca.* 10 mg/ml). Maillard reaction products with other amino acids were prepared in a similar way (alternatively 2.36 g of isoleucine or 1.50 g of alanine were used in the reaction).

Long-term incubation of ribose and glycine was performed by the following procedure: 0.0015 mol of glycine (0.113 g) and 0.003 mol of ribose (0.450 g) were incubated at 37°C in 15 ml of 0.2 mol/l phosphate buffer (pH 7.4). Sterilization was

effected by filtration through a 0.2- μm pore size filter. Samples of 2 ml were taken at 2, 6 and 36 days.

Preparation of 2,4-dinitrophenylhydrazones

The reagent was prepared as a saturated solution of 2,4-dinitrophenylhydrazine in 2 mol/l hydrochloric acid¹⁰. Reaction was performed by addition of 6 ml of reagent solution to 1 ml of the solution of the Maillard products. After 1 h at room temperature the sediment was filtered off and washed with distilled water on the filter. 2,4-Dinitrophenylhydrazones obtained in this way were dissolved in ethyl acetate (ca. 5 mg/ml).

Preparation of phenylthiocarbamyl (PTH) derivatives

Derivatization of Maillard products with phenyl isothiocyanate followed the procedure recommended in the Operator's Manual for the Waters Assoc. PICO-TAG system¹¹.

Electrophoretic apparatus

Capillary zone electrophoresis was effected in a laboratory-assembled apparatus (described in detail elsewhere¹²) resembling the set-up published by Jorgenson and De Arman-Lukacs¹³. An untreated fused-silica capillary protected on the external surface with a silicone-rubber layer (Institute of Physics, Slovak Academy of Sciences, Bratislava, Czechoslovakia) was used for separation. The capillary was 50 cm long (to the detector) with an additional 10 cm to the cathode and had an inside diameter of 75 μm . Before analysis the capillary was washed with 1 ml each of methanol, chloroform, methanol, 1 mol/l sodium hydroxide solution and 3 mol/l hydrochloric acid. Finally, the capillary was washed with 2 ml of the running buffer, attached to the high-voltage source and left running at 10 kV until the current dropped to 20 μA .

The light beam generated by a deuterium lamp at 220 nm passed a slit and entered the capillary. This was conditioned so that a 1-cm long piece of the plastic covering sheet was removed near the cathodic end and this part was used as a cuvette. The outcoming light was then measured with a UV detector.

The capillary was attached to a variable-voltage source. If the current exceeded 70 μA , the voltage automatically decreased to avoid overheating. The sample was applied electrophoretically (0.05 min, 10 kV).

Electrophoretic operating conditions

Samples for the analysis of underivatized Maillard products were run in 0.02 mol/l phosphate buffer (pH 7.4) at 18 kV and 60 μA . Separation of phenyl isothiocyanate-derivatized Maillard reaction products was effected in 0.005 mol/l borate buffer (pH 9.6) at 20 kV and 25 μA . Electrokinetic chromatography of 2,4-dinitrophenylhydrazones was carried out in 0.01 mol/l Na_2HPO_4 -0.006 mol/l tetraborate which was 0.05 mol/l with respect to sodium dodecyl sulphate (SDS). The applied potential was 10 kV. Owing to the higher conductivity, the current limit was set at 80 μA .

Reversed-phase chromatography

All separations except those of phenylthiocarbamyl derivatives were carried out

on a Spectra-Physics (San Jose, CA, U.S.A.) SP 8100 liquid chromatograph connected to a Spectra-Physics SP 4100 computing integrator. The eluent was monitored at 270 nm (underivatized Maillard products) or at 360 nm (2,4-dinitrophenylhydrazones) using a Waters Assoc. (Milford, MA, U.S.A.) 490E programmable multi-wavelength detector. A glass column (150 × 3.3 mm I.D.) packed with Separon SGX C₁₈ (7 μm) (Tessek, Prague, Czechoslovakia) was mounted in the instrument. Separation of phenylthiocarbamyl derivatives of Maillard reaction products was done on the PICO-TAG Amino Acid Analysis System (Millipore, Milford, MA, U.S.A.).

Separation of underivatized Maillard reaction products. The column was conditioned with acetonitrile for 15 min before every analysis. The flow-rate was maintained at 1.0 ml/min. At time zero (100% acetonitrile) the sample (10 μl) was applied to the column and was eluted by decreasing the proportion of acetonitrile to give acetonitrile-methanol-water (70:28:2, v/v/v) at 2 min. Then the elution was isocratic with acetonitrile-methanol-water (70:28:2) from 2 to 10 min and acetonitrile-methanol-water (70:20:10) from 10.1 to 20 min. From 20 min the sample was eluted with an increasing proportion of water in the mobile phase, reaching 100% at 30 min. Finally the column was eluted for 10 min with water. The temperature was maintained at 40°C.

Separation of 2,4-dinitrophenylhydrazine-reactive products. The column was conditioned with methanol-water (30:70, v/v) for 15 min before every analysis. The flow-rate was 1.0 ml/min. The sample was applied to the column in ethyl acetate (ca. 5 mg/ml) and elution was started with methanol-water (30:70, v/v) followed by a linear gradient reaching 65% methanol in 15 min after application; isocratic elution with methanol-water (65:35, v/v) followed for another 15 min. The column was washed with methanol for another 10 min. The temperature was maintained at 30°C. Preparative separations were done with the same system and corresponding fractions were pooled.

Separation of phenylthiocarbamyl derivatives. Analysis of these derivatives was done on a PICO-TAG Amino Acid Analysis System¹¹ with standard derivatization. Briefly, samples were separated by reversed-phase HPLC using two eluents: (A) 19.0 mg/l of sodium acetate trihydrate, 0.5 ml/l of triethylamine, titrated to pH 6.40 with glacial acetic acid and subsequently 60 ml of acetonitrile being added to 940 ml of this buffer and (B) 400 ml of water added to 600 ml of acetonitrile. The column was conditioned with 100% eluent A for 18 min before each analysis at a flow-rate of 1.5 ml/min. During analysis the flow-rate was 1.0 ml/min. Elution was started with 100% eluent A followed by a linear gradient reaching 46% eluent B at 10 min and 100% eluent B at 10.5 min. Between 10.5 to 12.0 min elution was isocratic with 100% eluent B. The temperature was maintained at 38°C and the effluent was monitored at 254 nm.

Affinity chromatography

A Glyco-gel boronate-agarose column (Pierce, Rockford, IL, U.S.A.), which is cross-linked 6% beaded agarose prepacked with 1.0 ml of immobilized *m*-aminophenylboronic acid, was equilibrated with 10 ml of wash buffer (0.25 mol/l ammonium acetate, 0.05 mol/l magnesium chloride, 0.003 mol/l sodium azide, pH 8.5). The sample in wash buffer (0.4 ml) was applied to the column and allowed to soak the gel. Then 5 ml of wash buffer were added to the column and allowed to drain into the gel. This non-bound fraction was collected. The bound fraction was eluted with 4 ml of elution

buffer (0.2 mol/l sorbitol, 0.05 mol/l Na_2EDTA , 0.003 mol/l sodium azide, pH 8.5). The column was regenerated by washing with 5 ml of water and then 10 ml of 0.1 mol/l acetic acid.

High-performance thin-layer chromatography (HPTLC)

Silica gel 60 F_{254} HPTLC plates (10 × 10 cm) for nano-TLC (Merck) were used. Samples were developed twice with carbon tetrachloride–ethanol–*n*-butanol (90:5:5),

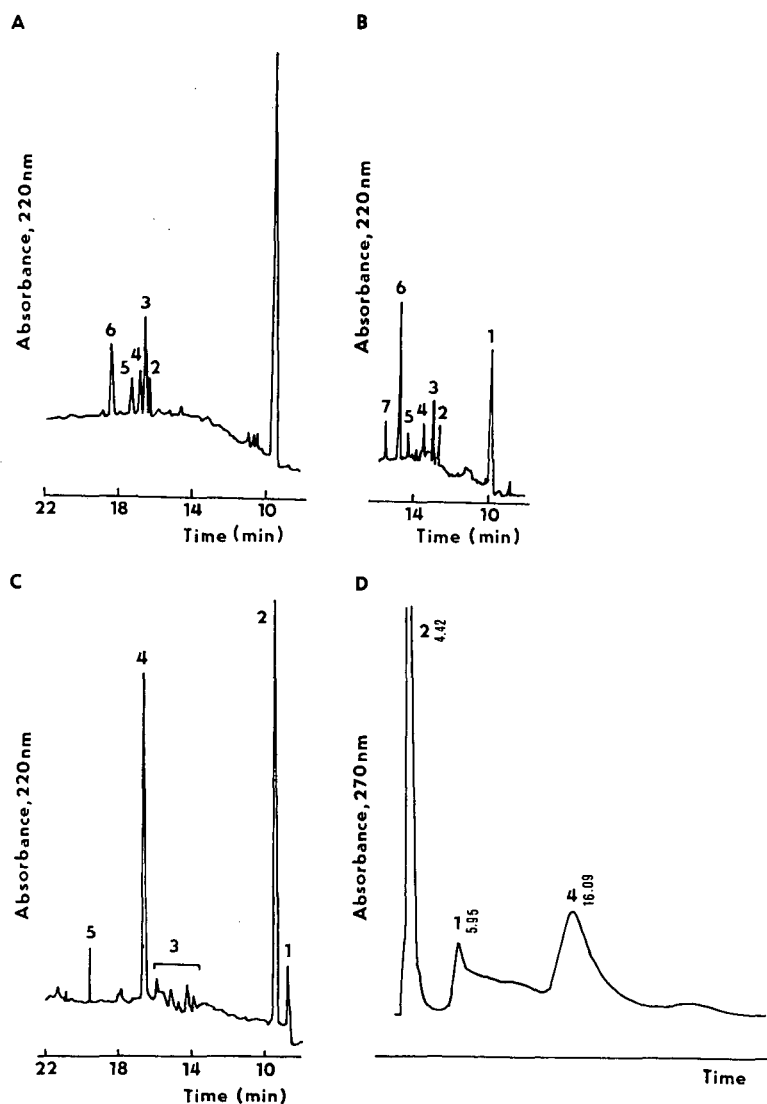


Fig. 1. Electrophoretic profiles of Maillard reaction products during the reaction of different amino acids and glucose. (A) Glycine; (B) isoleucine; (C) alanine. (D) Reversed-phase HPLC separation of products arising during the reaction of glucose and alanine.

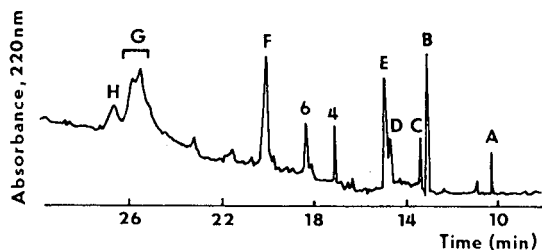


Fig. 2. Electrophoretic patterns of products arising during the reaction of glycine with glucose after hydrolysis.

v/v/v). The compounds were detected as quenching spots under UV light at 254 nm (Min UVIS; Desaga, Heidelberg, F.R.G.).

RESULTS

UV absorbance (220 nm) profiles of Maillard reaction products arising during the reaction of glucose with glycine, alanine and isoleucine by CZE are presented in Fig. 1A-C. Fig. 1D shows a comparative separation obtained by reversed-phase

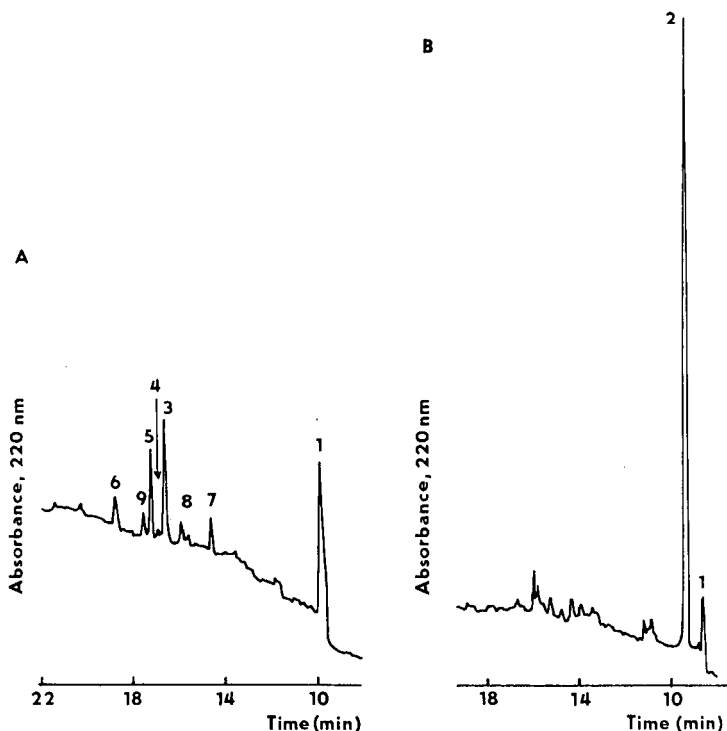


Fig. 3. Electrophoretic patterns of products arising from the reactions of (A) glucose with glycine (B) glucose with alanine after removal of 2,4-dinitrophenylhydrazine-reactive products.

chromatography of the glucose–alanine Maillard products. Five to seven peaks can be distinguished in individual CZE separations. The results clearly show that the composition of the mixture formed differs according to the amino acid component of the starting mixture. For glycine and alanine the profile is typical in containing two prominent peaks present at comparable concentrations, one of which moves much faster than the other in the electric field. Most of the separated peaks are unstable during acid hydrolysis in 6 mol/l hydrochloric acid (Fig. 2); this indicates that the types of compounds present in the unstable peaks are precluded from being detected in naturally occurring samples of glycated (non-enzymatically glycosylated) proteins. Thus, *e.g.*, the main peak of the glucose–glycine profile disappears completely and only peaks 4 and 6 (Fig. 2) withstand routine protein treatment for amino acid analysis.

When the glucose–glycine reaction mixture is reacted with 2,4-dinitrophenylhydrazine to eliminate components possessing oxo groups, the profile presented in Fig. 3A is obtained, showing a distinct decrease in peaks 1 and 6 and complete disappearance of peaks 2 and 4. The same treatment of the alanine–glucose mixture (Fig. 3B) shows the complete disappearance of peak 4 emerging in the untreated sample at 16.4 min.

If the glucose–glycine reaction products are prepared by long-term incubation at 37°C rather than by boiling, the profile obtained is considerably simplified (Fig. 4). Both main peaks (1 and 2) are virtually eliminated after 2,4-dinitrophenylhydrazine treatment.

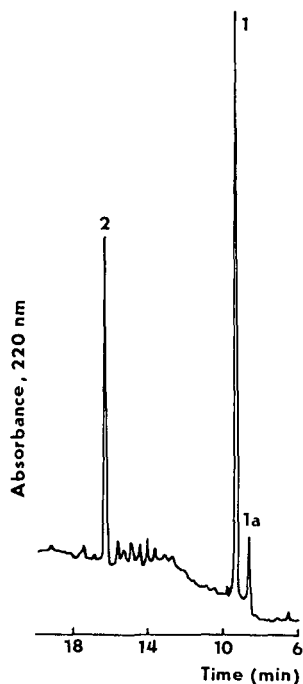


Fig. 4. Electrophoretic profiles of glucose–glycine Maillard reaction products obtained after incubation for 36 days at 37°C.

TABLE I

PROPERTIES OF THE INDIVIDUAL PEAKS OF MAILLARD REACTION PRODUCTS OBTAINED DURING THE GLUCOSE–GLYCINE REACTION

Six peaks can be distinguished after PTH derivatization, indicating the possibility that all the separated peaks may possess a reactive amino group.

<i>Peak No.</i>	<i>Susceptible to acid hydrolysis (6 mol/l HCl)</i>	<i>Susceptible to reaction with 2,4-dinitrophenylhydrazine (oxo-group possessing)</i>	<i>Retained during boronate affinity chromatography (possessing vicinal diol)</i>
1	Yes	Yes (partly)	No
2	Yes	Yes	Yes
3	Yes	No	Yes
4	No	Yes	Yes
5	Yes	No	Yes
6	No	Yes (partly)	Yes

When the glucose–glycine Maillard product mixture obtained at high temperature is subjected to boronate–agarose affinity chromatography, the whole profile is clearly split into two parts: the compound(s) present in the first peak of the electrophoretic profile pass unretained through the column, indicating that it is devoid of vicinal OH groups, whereas the compounds present in the remainder of the electrophoretic profile are bound to the column. A survey of the properties of individual peaks is presented in Table I.

So far the experiments were oriented only to the analysis of products arising by the reaction of glucose. If ribose is used as the sugar component for the preparation of Maillard reaction products a different profile is obtained, indicating that the nature of the products depends on both the carbohydrate and the amino acid component of the reaction mixture. Fig. 5 shows the profiles obtained after incubation of glycine with ribose for 2, 6 and 36 days: the profile consists of a cluster of rapidly emerging peaks (with low electrophoretic mobility) followed by a series of rapidly electrophoresed peaks at the longest incubation time. Within the rapidly emerging cluster of peaks, that designated as 2 is split into 2a and 2b at longer incubation times. Comparative HPLC separations are presented on the right-hand side.

Fig. 6 demonstrates the attempt to separate the 2,4-dinitrophenylhydrazine-reactive products (oxo-containing) arising during the Maillard reaction between glycine and glucose. It is evident that all the three methods used, *i.e.*, CZE (electrokinetic chromatography in the presence of 0.5 mol/l SDS), reversed-phase (RP) HPLC and normal-phase TLC yielded reasonable separations of the main five peaks. Similarly to RP-HPLC, in micellar electrokinetic chromatography the more hydrophobic solutes interact more strongly with the hydrophobic (micellar) phase and, consequently, should be retained longer than hydrophilic compounds. In other words, the order of elution of individual peaks should be similar to that for reversed-phase separation. Further, the order of eluted peaks during normal-phase TLC separation should be the reverse of that in both RP-HPLC and micellar electrokinetic chromatography. It is evident that this is not completely true. On comparing electrokinetic chromatography with RP-HPLC, particularly the retention time of peak

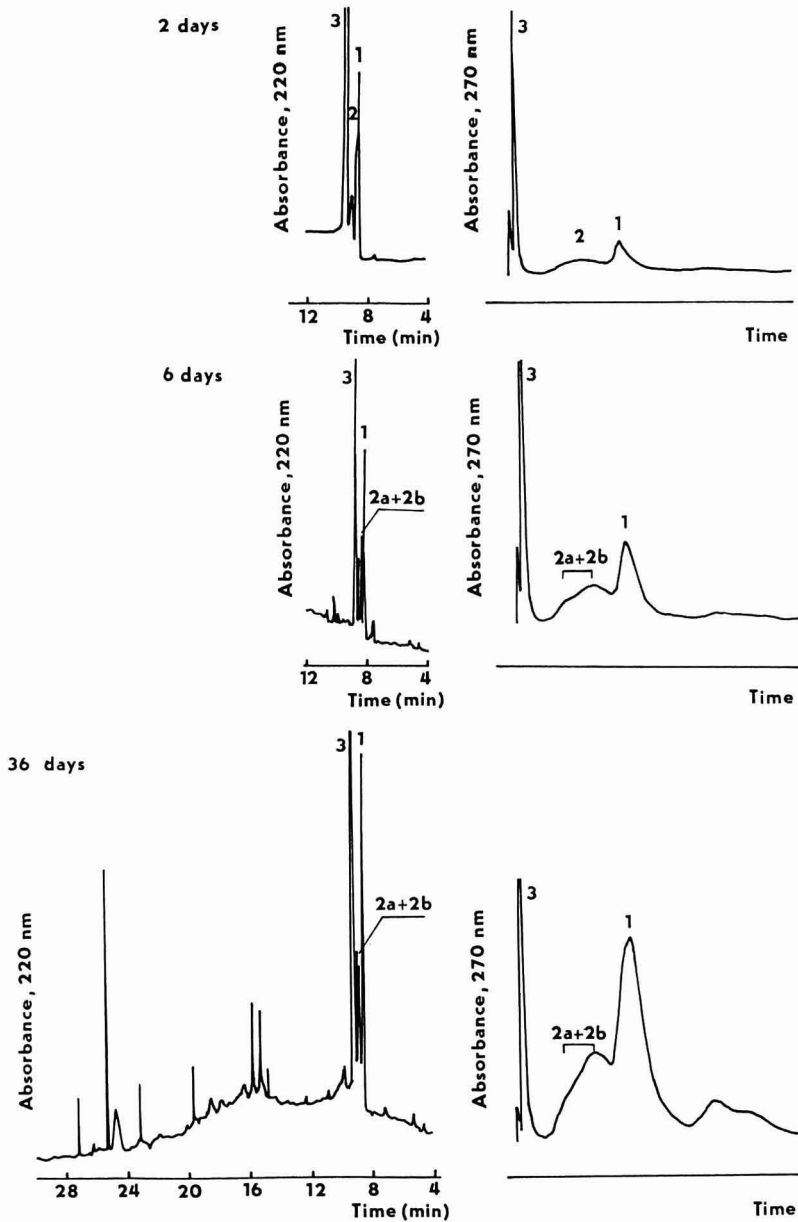


Fig. 5. Profiles of ribose-glycine Maillard reaction products obtained after incubation for 2, 6 and 36 days at 37°C. Capillary zone electrophoresis runs are on the left and RP-HPLC separations on right.

3 is unexpectedly prolonged in the former instance. The normal-phase TLC separation does not follow any theoretical predictions at all. Peaks 1a and 3 were identified by comparison with standards and by mass spectra as formaldehyde and acetaldehyde, respectively.

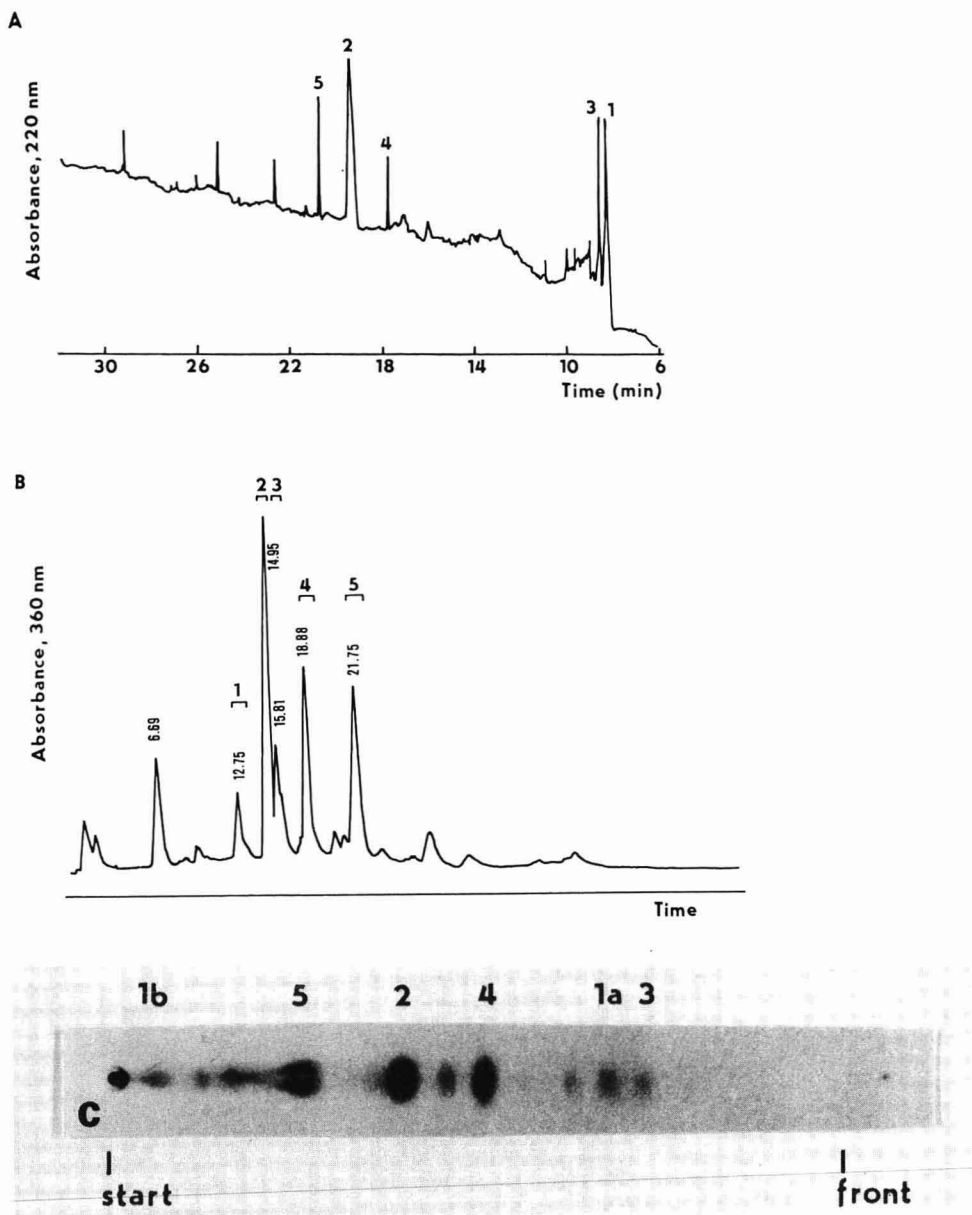


Fig. 6. Comparison of (A) CZE, (B) RP-HPLC and (C) TLC of the separation of 2,4-dinitrophenylhydrazones of the glycine-glucose Maillard reaction products.

DISCUSSION

Capillary zone electrophoresis offers new possibilities for separating complex mixtures that are otherwise difficult to separate. Maillard reaction products represent

a typical example: in liquid column chromatographic separations in both the normal- and reversed-phase modes and under a wide variety of experimental conditions the Maillard products yield broad incompletely resolved peaks. Application of gas chromatographic techniques suffers from problems regarding the low volatility of most of the products; this is particularly true for polymeric Maillard products arising at a later stage of the reaction when coloured polymers are formed. For these reasons we applied CZE to separate Maillard reaction products arising during the reaction of glucose and ribose with glycine, alanine and isoleucine.

As demonstrated, it was possible to separate a number of differently charged peaks in any particular model Maillard system. It was easily possible to follow, *e.g.*, the resistance of individual peaks towards acid hydrolysis, the susceptibility of the products formed towards reaction with 2,4-dinitrophenylhydrazine or phenyl isothiocyanate and the content of vicinal diols. Finally, it was possible to obtain at least general information about the types of compounds formed (Table I).

Separation of the phenylthiocarbamyl derivatives of glycine-glucose Maillard reaction products is shown in Fig. 7. Six main peaks were obtained both by CZE and with the PICO-TAG Amino Acid Analysis System.

If we consider next the general profile of glycine-glucose products, of the six peaks present (Fig. 1a), four contain 2,4-dinitrophenylhydrazine-reactive compounds. At least some of these four peaks are not homogeneous, as revealed by the

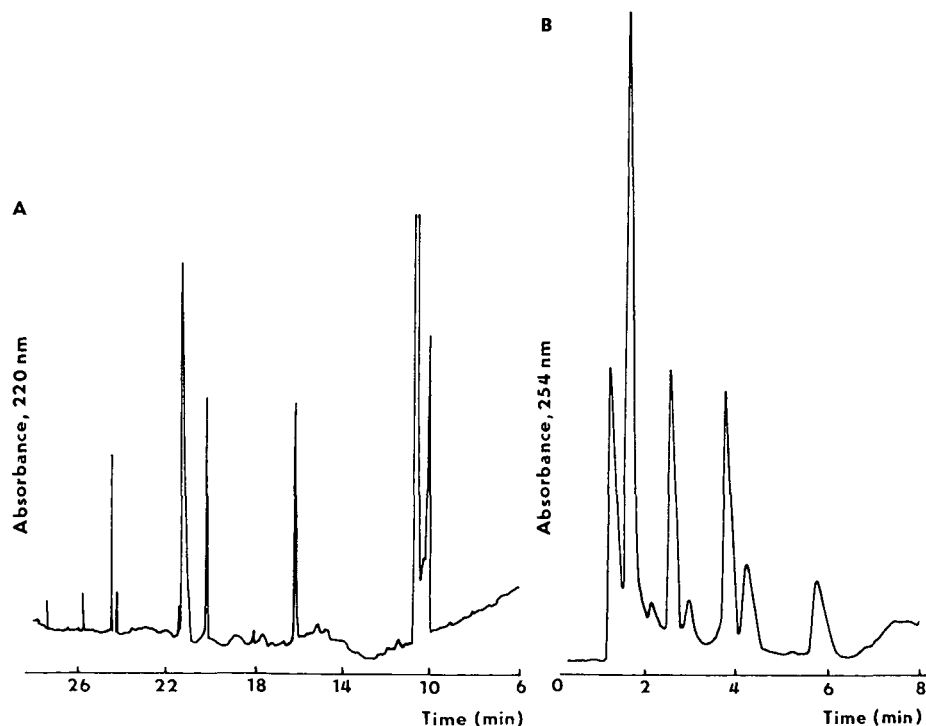


Fig. 7. Capillary zone electrophoresis profile in comparison with the RP-HPLC pattern of glycine-glucose Maillard reaction products after PTH derivatization.

electrokinetic micellar chromatography in the next step. Electrochromatographic separation resulted in five distinct peaks, two of which were identified as formaldehyde and acetaldehyde and one of which can be further separated into two zones by normal-phase TLC. Individual peaks in the electrochromatographic separation of components possessing oxo groups as 2,4-dinitrophenylhydrazones were (except for peak 1) obviously homogeneous and their number was coincident with the number of peaks obtained during RP-HPLC and normal-phase TLC. Two of these peaks were identified, on the basis of their migration in three different separation systems, as acetaldehyde and formaldehyde. By comparing the individual profiles (the original mixture and the mixture of 2,4-dinitrophenylhydrazine-reactive products), at least eight products originate during the Maillard reaction between glucose and glycine.

On reacting the Maillard reaction mixture of glucose and glycine with phenyl isothiocyanate, six peaks can be discerned both in CZE and RP-HPLC, indicating that there are six compounds with a reactive amino group present in the mixture, provided that none of the compounds present yields more than one phenyl isothiocyanate derivative.

The products arising during the glycine–glucose Maillard reaction are neither of clearly polar nor distinctly hydrophobic nature, which causes most of the problems in their separation. These unfavourable properties are preserved even after derivatization, as clearly demonstrated by comparing the different techniques applied to 2,4-dinitrophenylhydrazones (Fig. 6). The separation mechanisms involved are apparently of the multiple-mode type. Consequently, theoretical predictions for the electromigration (and also chromatographic) separations of Maillard products are very difficult indeed.

Regarding the main product(s) arising in all the model systems used at both low and high temperatures, our present knowledge of its properties can be summarized as follows: it is a poorly charged compound (or a category of compounds) at pH 7.4 (or higher), susceptible to acid hydrolysis, which does possess 2,4-dinitrophenylhydrazine-reacting groups and is devoid of vicinal diols.

REFERENCES

- 1 I. Miksik, R. Struzinsky, K. Macek and Z. Deyl, *J. Chromatogr.*, 500 (1990) 607.
- 2 M. Namiki, *Adv. Food Res.*, 32 (1988) 115.
- 3 M. Brownlee, A. Cerami and H. Vlassara, *N. Engl. J. Med.*, 318 (1988) 1315.
- 4 R. Bucala, P. Model and A. Cerami, *Proc. Natl. Acad. Sci. U.S.A.*, 81 (1984) 105.
- 5 J. J. Harding, H. T. Beswick, R. Ajiboye, R. Huby, R. Blakytyn and K. C. Rixon, *Mech. Age Dev.*, 50 (1989) 7.
- 6 H. Paulsen and K.-W. Pflughaupt, in W. Pigman, D. Horton and J. D. Wander (Editors), *The Carbohydrates, Chemistry and Biochemistry*, Vol. 1B, Academic Press, New York, 1980, p. 881.
- 7 W. Boltes and L. Mewissen, *Z. Lebensm.-Unters.-Forsch.*, 187 (1988) 209.
- 8 F. G. Njoroge, A. A. Fernandes and V. M. Monnier, *J. Biol. Chem.*, 263 (1988) 10646.
- 9 M. Sengl, F. Ledl and T. Severin, *J. Chromatogr.*, 463 (1989) 119.
- 10 R. H. Brandenberger and H. Brandenberger, in K. Blau and G. King (Editors), *Handbook of Derivatives for Chromatography*, Heyden, London, 1978, p. 234.
- 11 Waters Assoc., *PICO-TAG Amino Acid Analysis System, Operator's Manual*, Millipore, Milford, MA, 1984.
- 12 V. Rohlicek and Z. Deyl, *J. Chromatogr.*, 494 (1989) 87.
- 13 J. W. Jorgenson and K. De Arman-Lukacs, *Science (Washington, D.C.)*, 222 (1983) 266.

END OF SPECIAL ISSUE

journal of
chromatography news section

SHORT CONFERENCE REPORT

SECOND INTERNATIONAL SYMPOSIUM ON HIGH PERFORMANCE CAPILLARY ELECTROPHORESIS (HPCE '90), SAN FRANCISCO, CA, U.S.A., JANUARY 29-31, 1990

The obvious success of this meeting, following the much praised Boston 1989 symposium (see J. Chromatogr., Vol. 480) resulted in a decision to hold the third one on February 3-6, 1991 in San Diego.

We present here some photographs to give some impression of the atmosphere. Informal discussions went on even during the social events and the coffee breaks, all helping to contribute to the overall restrained excitement of the meeting.



Fig. 1. The opening of the symposium. Professors Hjertén, Karger and Jorgenson presiding.



Fig. 2. A general impression of the audience during one of the lectures. A centrally-situated Frans Everaerts listens keenly whilst Dr. Wenisch appears to be either deeply in thought or even utterly transported to higher spheres.



Fig. 3. Professor Ossicini, Dr. Fanali and Dr. Boček with Professor Westerlund on their left hand — the last studying a poster apparently with tongue in cheek.



Fig. 4. At one of the many evening events during the meeting. A happy group composed of Milos Novotny, Dr. Bushey and Jim Jorgenson.

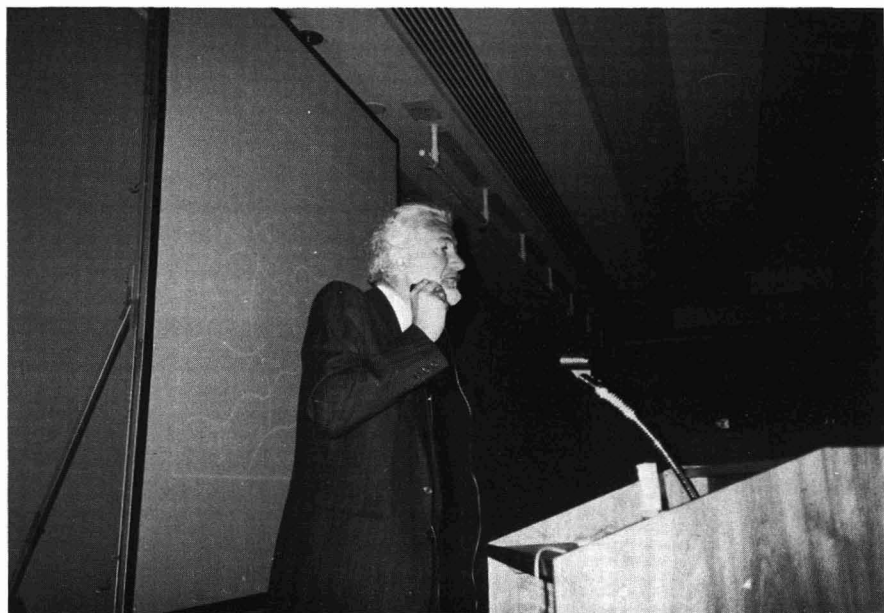


Fig. 5. Professor Righetti — lecturing with Italian enthusiasm.



Fig. 6. Where the manuscripts for the proceedings were collected: Herman Frank and Bob Goodman brightly illuminated at the Elsevier desk.



Fig. 7. Professor Karger, clearly delighted with the way the meeting has gone, and an equally satisfied Professor Zare.

PUBLICATION SCHEDULE FOR 1990

Journal of Chromatography and Journal of Chromatography, Biomedical Applications

MONTH	J	F	M	A	M	J	J	A	S	O	N	D ^a
Journal of Chromatography	498/1 498/2 499	500 502/1	502/2 503/1 503/2 504/1	504/2 505/1	505/2 506 507 508/1	508/2 509/1 509/2 510	511 512 513	514/1 514/2 515	516/1 516/2 517 518/1	518/2 519/1	519/2 520 521/1 521/2	
Cumulative Indexes, Vols. 451–500		501										
Bibliography Section		524/1		524/2		524/3		524/4		524/5		
Biomedical Applications	525/1	525/2	526/1	526/2 527/1	527/2	528/1 528/2	529/1	529/2 530/1	530/2	531 532/1	532/2 533	

^aThe publication schedule for further issues will be published later.

INFORMATION FOR AUTHORS

(Detailed *Instructions to Authors* were published in Vol. 513, pp. 413–416. A free reprint can be obtained by application to the publisher, Elsevier Science Publishers B.V., P.O. Box 330, 1000 AH Amsterdam, The Netherlands.)

Types of Contributions. The following types of papers are published in the *Journal of Chromatography* and the section on *Biomedical Applications*: Regular research papers (Full-length papers), Notes, Review articles and Letters to the Editor. Notes are usually descriptions of short investigations and reflect the same quality of research as Full-length papers, but should preferably not exceed six printed pages. Letters to the Editor can comment on (parts of) previously published articles, or they can report minor technical improvements of previously published procedures; they should preferably not exceed two printed pages. For review articles, see inside front cover under Submission of Papers.

Submission. Every paper must be accompanied by a letter from the senior author, stating that he is submitting the paper for publication in the *Journal of Chromatography*. Please do not send a letter signed by the director of the institute or the professor unless he is one of the authors.

Manuscripts. Manuscripts should be typed in double spacing on consecutively numbered pages of uniform size. The manuscript should be preceded by a sheet of manuscript paper carrying the title of the paper and the name and full postal address of the person to whom the proofs are to be sent. As a rule, papers should be divided into sections, headed by a caption (*e.g.*, Abstract, Introduction, Experimental, Results, Discussion, etc.). All illustrations, photographs, tables, etc., should be on separate sheets.

Introduction. Every paper must have a concise introduction mentioning what has been done before on the topic described, and stating clearly what is new in the paper now submitted.

Abstract. Full-length papers and Review articles should have an abstract of 50–100 words which clearly and briefly indicates what is new, different and significant. (Notes and Letters to the Editor are published without an abstract.)

Illustrations. The figures should be submitted in a form suitable for reproduction, drawn in Indian ink on drawing or tracing paper. Each illustration should have a legend, all the legends being typed (with double spacing) together on a *separate sheet*. If structures are given in the text, the original drawings should be supplied. Coloured illustrations are reproduced at the author's expense, the cost being determined by the number of pages and by the number of colours needed. The written permission of the author and publisher must be obtained for the use of any figure already published. Its source must be indicated in the legend.

References. References should be numbered in the order in which they are cited in the text, and listed in numerical sequence on a separate sheet at the end of the article. Please check a recent issue for the layout of the reference list. Abbreviations for the titles of journals should follow the system used by *Chemical Abstracts*. Articles not yet published should be given as "in press" (journal should be specified), "submitted for publication" (journal should be specified), "in preparation" or "personal communication".

Dispatch. Before sending the manuscript to the Editor please check that the envelope contains four copies of the paper complete with references, legends and figures. One of the sets of figures must be the originals suitable for direct reproduction. Please also ensure that permission to publish has been obtained from your institute.

Proofs. One set of proofs will be sent to the author to be carefully checked for printer's errors. Corrections must be restricted to instances in which the proof is at variance with the manuscript. "Extra corrections" will be inserted at the author's expense.

Reprints. Fifty reprints of Full-length papers, Notes and Letters to the Editor will be supplied free of charge. Additional reprints can be ordered by the authors. An order form containing price quotations will be sent to the authors together with the proofs of their article.

Advertisements. Advertisement rates are available from the publisher on request. The Editors of the journal accept no responsibility for the contents of the advertisements.



In the fast-moving field of capillary electrophoresis, only the Model 270A puts you in the lead.

Harness the power of capillary electrophoresis (CE) with high performance instrumentation. For meaningful quantitation and reliable analysis, CE's inherent selectivity and resolution must be complemented with accuracy and precision.

The Model 270A Analytical Capillary Electrophoresis System is the first fully integrated system designed to meet the stringent demands of quantitative CE. The system you need when every minute, every result, counts.

The human serum albumin digest was provided courtesy of Delta Biotechnology Ltd., Nottingham, U.K.

True quantitation begins with precision and accuracy in both sample injection and column temperature control. The Applied Biosystems Model 270A combines automation with a unique injector design, a thermostatted capillary compartment and proven detector technology to achieve unsurpassed reproducibility of peak areas and electrophoretic mobility.

Count on your first results within minutes after installing the Model 270A. Select a preprogrammed separation protocol,

or create and store your own methods using the interactive display and keypad. The Model 270A is designed for both the novice and the seasoned user of analytical instrumentation.

Contact Applied Biosystems today, and join the leaders in advancing capillary electrophoresis from theory to application.

 **Applied
Biosystems**

U.S.A. 850 Lincoln Centre Drive, Foster City, CA 94404. Tel: (415) 570-6667, (800) 874-9868, in California (800) 831-3582. Telex: 470052 APBIO UL. Fax: (415) 572-2743.
Mississauga, Canada. Tel: (416) 821-8183. Fax: (416) 821-8246.
Warrington, U.K. Tel: 0925-825650. Telex: 629611 APBIO G. Fax: 0925-828196.
Weiterstadt, West Germany. Tel: 06151-87940. Telex: 4197318 Z ABI D. Fax: 06151-84899.
Paris, France. Tel: (1) 48 63 24 44. Telex: 230458 ABIF. Fax: (1) 48 63 22 82.
Milan, Italy. Tel: 02-835 4920. Fax: 02-832 1655.
Rotterdam, The Netherlands. Tel: (0) 10 452 35 11. Telex: 26249. Fax: (0) 10 452 91 57.
Burwood, Australia. Tel: (03) 288-7777. Fax: (03) 887-1469.
Tokyo, Japan. Tel: (03) 699-0700. Fax: (03) 699-0733.